PERGAMON

NEURO PHARMACOLOGY

Neuropharmacology 38 (1999) 199–207

Neuroprotective activity of the potent and selective mGlu1a metabotropic glutamate receptor antagonist, (+)-2-methyl-4 carboxyphenylglycine (LY367385): comparison with LY357366, a broader spectrum antagonist with equal affinity for mGlu1a and mGlu5 receptors

V. Bruno [a], G. Battaglia [a], A. Kingston [b], M.J. O'Neill [b], M.V. Catania [c], R. Di Grezia [a], F. Nicoletti [a,d,*]

[a] *I.N.M. Neuromed, Pozzilli, Italy*
[b] *Eli Lilly, Lilly Research Centre, Windlesham, UK*
[c] *I.B.F.S.N.C., C.N.R., Catania, Italy*
[d] *Institute of Pharmacology, School of Pharmacy, University of Catania, Viale A. Doria, 6, 95125 Catania Italy*

Accepted 17 July 1998

Abstract

(+)-2-Methyl-4-carboxyphenylglycine (LY367385), a potent and selective antagonist of mGlu1a metabotropic glutamate receptors, was neuroprotective in the following in vitro and in vivo models of excitotoxic death: (i) mixed cultures of murine cortical cells transiently exposed to *N*-methyl-D-aspartate (NMDA); (ii) rats monolaterally infused with NMDA into the caudate nucleus; and (iii) gerbils subjected to transient global ischemia. We have compared the activity of LY367385 with that of the novel compound (±)-α-thioxantylmethyl-4-carboxyphenylglycine (LY367366), which antagonizes both mGlu1a and -5 receptors at low micromolar concentrations, but also recruits other subtypes at higher concentrations. Although LY367366 was neuroprotective, it was in general less efficacious than LY357385, suggesting that inhibition of mGlu1 receptors is sufficient to confer significant neuroprotection. We conclude that endogenous activation of mGlu1a receptors (or perhaps other mGlu1 receptor splice variants) contributes to the development of neuronal degeneration of excitotoxic origin.

Keywords: Group-I metabotropic glutamate receptors; LY367385; LY367366; *N*-methyl-D-aspartate toxicity; Global ischemia; Neuroprotection

1. Introduction

Recent evidence suggests that metabotropic glutamate (mGlu) receptors are potential targets for neuroprotective drugs. In particular, activation of group-II (mGlu2 and -3) or group-III (mGlu4, -7 and -8) mGlu receptor subtypes is protective against excitotoxicity or other form of neuronal degeneration (Nicoletti et al., 1996). The role of group-I mGlu receptors (i.e. mGlu1 and -5) in neurodegeneration/neuroprotection has recently been examined by using subtype-selective agonists or antagonists. Results obtained with agonists are controversial. In murine cortical cells in culture, the group-I mGlu receptor agonists (*R,S*)-3,5-dihydroxyphenylglycine, quisqualate, *trans*-azetidine-2,3-dicarboxylic acid, and 3-hydroxyphenylglycine amplify neuronal degeneration induced by submaximal concentrations of *N*-methyl-D-aspartate (NMDA) or by mild conditions of hypoxia combined with glucose deprivation (Bruno et al., 1995; Buisson and Choi, 1995). In contrast, group-I mGlu receptor agonists are neuroprotective in cultured cerebellar granule cells or in brain slice preparations (Pizzi et al., 1996a,b). Inhibition of group-I mGlu receptors consistently results into neuroprotection. Thus, intracerebroventricular injection of

* Corresponding author. Tel.: +39-95-337167; fax: +39-865-927575.

0028-3908/99/$ - see front matter
PII: S0028-3908(98)00159-2

antisense oligonucleotides directed against mGlu5 receptors protects striatal neurons against malonic acid lesions (Cha et al., 1996), whereas a series of mGlu1 receptor antagonists, including aminoindandicarboxylic acid (AIDA), 4-carboxyphenylglycine (4CPG) and 4-carboxy-3-hydroxyphenylglycine (4C3HPG), reduce NMDA toxicity in cultured cortical cells (Buisson and Choi, 1995; Strasser et al., 1997). AIDA can also attenuate the delayed degeneration of vulnerable neurons in gerbils subjected to transient global ischemia (Cozzi et al., 1997), suggesting that activation of mGlu1a receptors contributes to the development of ischemic neuronal damage. It is important to confirm these promising results by using more selective and potent group-I mGlu receptor antagonists. We have examined the neuroprotective activity of (+)-2-methyl-4-carboxyphenylglycine (LY367385), a highly potent and selective mGlu1a receptor antagonist (Clark et al., 1997). In addition, we have compared the activity of LY367385 with that of the novel compound, (±)-α-thioxantylmethyl-4-carboxyphenylglycine (LY367366), which antagonizes mGlu1a and -5 receptors with equal affinity.

2. Materials and methods

2.1. Assessment of excitotoxic neuronal death in culture

Mixed cortical cell cultures containing both neurons and astrocytes were prepared from fetal mice at 14–16 day of gestation, as described by Rose et al. (1992). In brief, dissociated cortical cells were plated in 15-mm multiwell vessels (Falcon Primaria, Lincoln Park, NY) on a layer of confluent astrocytes (Rose et al., 1992), using a plating medium of MEM-Eagle's salts (supplied glutamine-free) supplemented with 5% heat-inactivated horse serum, 5% fetal bovine serum, glutamine (2 mM), glucose (21 mM), and $NaHCO_3$ (25 mM). After 3–5 days in vitro (DIV), non neuronal cell division was halted by a 1-3 day exposure to 10 μM cytosine arabinoside, and cultures were shifted to a maintenance medium identical to plating medium, but lacking fetal bovine serum. Subsequent partial medium replacement was carried out twice a week. Cultures at 13–14 DIV were used.

We have exposed the cultures to NMDA for 10 min at room temperature in a HEPES-buffered salt solution containing (in mM): 120 NaCl, 5.4 KCl, 0.8 $MgCl_2$, 1.8 $CaCl_2$, 20 HEPES, 15 glucose. Afterwards, the cultures were extensively washed and incubated in MEM-Eagle's (supplemented with 25 mM $NaHCO_3$ and 21 mM glucose) at 37°C. Neuronal injury was estimated by examining the cultures with phase-contrast microscopy 24 h after the insult, when the process of cell death was largely complete. Neuronal damage was quantitatively assessed by trypan-blue staining. Stained neurons were counted from three random fields per well.

2.2. Assessment of in vivo neuronal injury

Male Sprague-Dawley rats (250–300 g, b.w.) were anesthesized with pentobarbital (50 mg/kg, i.p.) and infused with NMDA (100 nmol/0.5 μl/2 min) or NMDA + mGlu receptor antagonists (200 nmol in the same volume) in the left corpus striatum, at +2.0 mm AP, 2.6 mm L, and 5 mm V, according to the Pellegrino and Cushman atlas. The injection was repeated at a second site (+1 mm AP, 2.6 mm L, and 5 mm V) to obtain a more consistent loss of striatal neurons. Animals were killed by decapitation 7 days later. Neuronal toxicity was evaluated either by histological analysis or by measuring striatal glutamate decarboxylase (GAD) activity as a marker for GABAergic neurons. For histological analysis, the brains were removed, rapidly frozen in isopentan at −40°C, and then stored at −80°C. Twenty micrometre cryostat sections were Nissal-stained and examined in light microscopy. For measurements of GAD activity, the corpus striatum was dissected bilaterally and homogenized in 5 mM imidazol buffer containing 0.2% Triton X-100 and 10 mM dithiothreitol. An aliquot of the homogenate was incubated in 400 μl of 10 mM phosphate buffer (pH 7.0) containing 10 mM 2-mercaptoethanol, 0.02 mM pyridoxalphosphate, and 1 μCi of [^{3}H]-glutamate (Amersham, sp. act. 46 Ci/mmol) for 1 h at 37°C; the reaction was stopped with 15 μl of ice-cold 11.8 N $HClO_4$. After centrifugation in a microfuge at maximal speed, 10 μl of the supernatant were diluted 4 with 0.01 N HCl and derivatized with *O*-phthalaldehyde and mercaptoethanol for 1 min at room temperature before injection into a HPLC. The HPLC apparatus consisted of a programmable solvent module 126 (Beckman Instrument, Fullerton CA), an analytical C-18 reverse phase column kept at 30°C (Ultrasphere ODS 5 μm Spherical, 80 A pore, 2 mm × 15 cm, Beckman Instrument) and a RF-551 spectrofluorometric detector (Shimadzu). Excitation and emission were set at 360 and 450 nm, respectively. The mobile phase consisted of (A) 50 mM sodium phosphate/10% methanol, pH 7.2, and (B) 50 mM sodium phosphate/70% methanol, pH 7.2. After 8 min of isocratic conditions with 98% (A) and 2% (B), (B) was increased up to 40% in 30 min and then to 98% in 1 min and maintained at 98% for 11 min before returning to the initial conditions. The radioactivity coeluting with GABA was collected and counted by scintillation spectrometry. Protein concentrations in the original samples were determined by using a commercially available kit (BIO-RAD protein assay, BIO-RAD Laboratories, Munchen).

2.3. Assessment of ischemic neuronal death in gerbils

Male Mongolian gerbils (Bantin and Kingman, Hull, UK) at least 3-months-old and weighing an excess of 60 g were used. The animals were maintained at a constant temperature of 21 ± 1°C with standard lighting conditions and food and water ad libitum. The animals were anaesthesized by inhalation of 5% halothane/oxygen in anaesthetic mixture and maintained with 2% halothane delivered with oxygen at 1 l/min via a face mask throughout the operation and placed on a thermostatically controlled heating blanket to maintain body temperature within the range of 37–38°C. The animals were then placed in a stereotaxic apparatus and the scalp incised so as to uncover the parietal bones. Two small holes were drilled in the skull and cannulae stereotaxically implanted in the lateral ventricle (coordinates: 2 mm AP, ±2 mm L, and −1.2 mm V to bregma). LY367385 (100 nmol/2.5 μl/5 min, to obtain a final brain concentration of 250 μM) or vehicle (2.5 μl over 5 min) was infused, the cannulae were then withdrawn and the wound sutured. After 30 min, a small midline cervical incision was made to expose both common carotid arteries. In animals to be rendered ischaemic, both carotid arteries were clamped for 5 min. At the end of the occlusion blood was re-established. In sham operated animals, the arteries were exposed but not occluded. The wound was then sutured and the animals allowed to recover. The temperature was maintained at 37°C throughout surgery using a 'K-temp' temperature controller/heating pad (International Market Supply, Chershire, UK) and rectal temperatures were measured. The animals were allowed to recover in a thermacage (Beta Medical and Scientific, UK), which consisted in a 4-compartmental chamber in which the environmental temperature was maintained at 28°C and rectal temperatures were monitored for 6 h post-occlusion.

Five days after surgery, the animals were perfused transcardially with 30 ml of 0.9% saline followed by 100 ml of 10% buffered formalin solution. The brains were removed and placed in 10% formalin for 2 days, processed and embedded in paraffin wax. Five micrometers coronal sections were taken at 1.5, 1.7 and 1.9 mm caudal to the bregma in the anterior hippocampus using a sledge (Leitz 1400) microtome. The slices were stained with haematoxylin and eosin and the neuronal density in the CA1 subfield of the hippocampus was measured using a microscope with grid lines (0.05 × 0.05 mm).

2.4. Materials

LY367385 and LY367366 (Fig. 1) were synthesized by Lilly Research Laboratories. Synthesis of LY367385 is described by Clark et al. (1997). LY367366 was synthesized according to the method described by Clark et al. (manuscript submitted). A comparative pharmacological profile of LY367385 and LY367366 at different mGlu receptor subtypes or ionotropic Glu receptors is shown in Table 1. Note that LY367385 is a highly selective antagonist of mGlu1a receptors; LY367366 is equally potent at mGlu1 a and -5 receptors, but may also interact with other mGlu subtypes at concentrations > 10 gM; LY367385 and LY367366 fail to interact with AMPA, NMDA or kainate binding sites.

(*S*)-3,5-Dihydroxyphenylglycine (DHPG), 1-aminocyclopentane-1 *S*,3*R*-dicarboxylic acid (1*S*,3*R*-ACPD) and NMDA were purchased from Tocris Cookson, Langford, Bristol, UK. All other drugs or chemicals were purchased from Sigma, Milano, Italy.

3. Results

3.1. Neuroprotective activity of mGlu receptor antagonists in culture

In mixed cortical cultures, a 10-min pulse with 100 μM NMDA led to necrotic death of about 70–80% of the neuronal population. LY367385 or LY367366 combined with NMDA during the toxic pulse attenuated neuronal degeneration in a concentration-dependent fashion, with a maximal reduction of NMDA toxicity ranging from 40 to 60% (Fig. 2). LY367385 showed greater efficacy than LY367366 and neither of these compounds influenced neuronal viability per se (results not shown). Given that activation of group-I mGlu receptors ampilfies NMDA toxicity in cortical cultures (Bruno et al., 1995; Buisson and Choi, 1995), we have

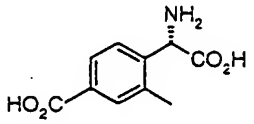

LY367385: (+)-2-methyl-4-carboxyphenylglycine

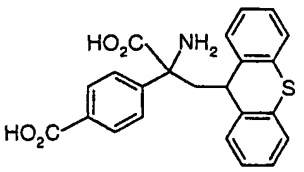

LY367366: (±)-α-thioxanthylmethyl-4-carboxyphenylglycine

Fig. 1. Structures of the group-I mGlu receptor antagonists, LY367385 and LY367366.

Table 1
Pharmacological profile of LY367385 and LY367366 at different mGlu or ionotropic Glu receptor subtypes[a]

	LY367385	LY367366
Group-I mGlu receptors		
mGlu1	8.8 ± 3.9	5.7 ± 2.9
mGlu5	>200	3.4 ± 1.5
Group-II mGlu receptors ACPD-sensitive		
[^{3}H]glutamate binding	>>100	>10
Group-III mGlu receptors mGlu4/8	>10	>10
[^{3}H]AMPA binding	>10 000	>10 000
[^{3}H]Kainate binding	>10 000	>10 000
[^{3}H]CGP39653 binding	>10 000	>10 000

[a] IC_{50} values are reported in μM (mean ± SD, $n = 3$). The potencies of LY367385 and LY367366 at mGlu1a or -5 receptors were determined by measuring quisqualatestimulated polyphosphoinositide hydrolysis in AV-12 cells expressing either of these subtypes (Kingston et al., 1995). ACPD-sensitive [^{3}H]glutamate binding to adult rat forebrain membranes was carried out according to the method described by Wright et al. (1994). The effect of compounds at mGlu4 and mGlu8 receptors was estimated by measuring the reduction of cAMP formation by L-2-amino-4-phosphonobutanoate in cells overexpressing mGlu4 receptors, as described by Schoepp et al., (1997). In experiments measuring cAMP formation in mGlu2 and mGlu4 expressing cells, neither LY367385 nor LY367366 produced agonist effects (data not shown). Measurement of [^{3}H]AMPA, [^{3}H]kainate and [^{3}H]CGP39653 binding was carried out as described by Schoepp et al. (1995). [^{3}H]AMPA (5 nM) binding was undertaker) with washed crude rat forbrain membranes in the presence of KSCN (100 mM). Non specific binding was determined with 10 μM AMPA. Binding of [^{3}H]CGP39653 (10 nM), a selective NMDA receptor ligand, was performed with Triton-X100 treated rat forebrain synaptosomal membranes, and non-specific binding was determined with 10 μM glutamate. [^{3}H]Kainate (5 nM) binding was performed at 4°C using washed rat forbrain synaptosomal membranes, and non-specific binding was determined with kainate (100 μM). In all cases, bound and free ligands were separated by filtration.

examined the effect of LY367385 or LY367366 on the potentiation of NMDA toxicity by the selective mGlu1/5 receptor agonist, DHPG (Ito et al., 1992). DHPG was combined with a lower concentration of NMDA (60 μM), which killed only 30–40% of the neuronal population (Bruno et al., 1995). LY367385 and LY367366 showed potent neuroprotective effects, with both compounds causing a 50% reduction in DHPG potentiation at a concentration of 10 nM. Moreover, under these experimental conditions at higher concentrations of antagonist, both LY367385 and LY367366 completely antagonized the amplification of NMDA toxicity by DHPG. At 10 μM, LY367385 brought the extent of degeneration below the levels observed with NMDA alone. In contrast, increasing the concentration of LY367366 to 10 μM produced a lesser neuroprotective effect than observed at 1 μM (Fig. 3). This inverse trend in the dose-response curve of LY367366 has also been observed for similar experiments carried out with pure cultures of rat cortical neurons (results not shown).

3.2. Neuroprotective activity of mGlu receptor antagonists against excitotoxic striatal lesions

In animals infused with NMDA (100 nmol/0.5 μl/2 min; double injection) in the left caudate nucleus, histological analysis showed a central core of necrosis, surrounded by an area of extensive neuronal loss, reactive gliosis and oedema. Neuronal loss and picnosis were still visible in the remote periphery of the lesion, about 3 mm posterior to the injection sites (Fig. 4A). In animals coinfused with NMDA and LY367385 (200 nmol/0.5 μl/2 min; double injection), the central area of necrosis was much smaller, although oedema and reactive gliosis were still substantial. Outside the necrotic area, neurons were spared and exhibited a regular shape. The extension of the lesion was much more limited in animals infused with NMDA + LY367385 than in those infused with NMDA alone (Fig. 4A,B). In animals infused with NMDA + LY367366 (200 nmol/0.5 μl/double injection), the size of the necrotic area and the extension of the lesion was intermediated between those observed in animals infused with NMDA and NMDA + LY367385 (Fig. 4C–E). Oedema was however, less pronounced in animals infused with NMDA + LY367366 than in animals infused with NMDA or NMDA + LY367385.

To quantify the neuroprotective activity of LY367385 and LY367366 we have measured striatal GAD activity, which reflects the number of spared

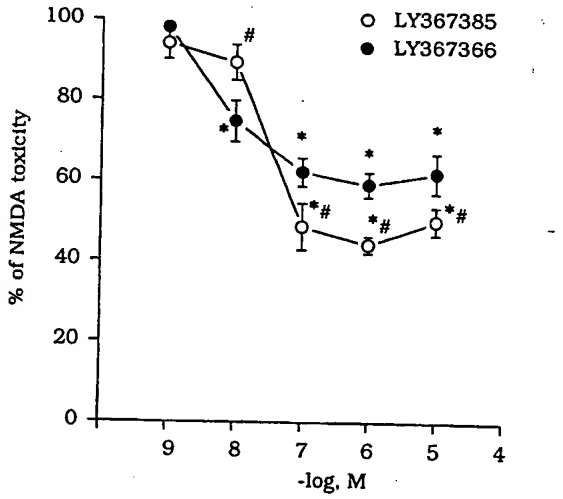

Fig. 2. Concentration-dependent neuroprotection by LY367385 or LY367366 applied in combination with 100 μM NMDA to mixed cortical cultures. Values are means ± S.E.M. of four–12 determinations and are expressed as per cent of NMDA toxicity. Basal values (trypan blue-positive neurons in three random microscopic fields): 18 ± 3.1; NMDA: 140 ± 7.4. Neither LY367385 not LY367366 influenced neuronal viability per se (not shown). * $P < 0.01$ (One-way ANOVA + Fisher PLSD), if compared with NMDA alone. # $P < 0.01$ (Student's t-test), if compared with the corresponding LY367366 values.

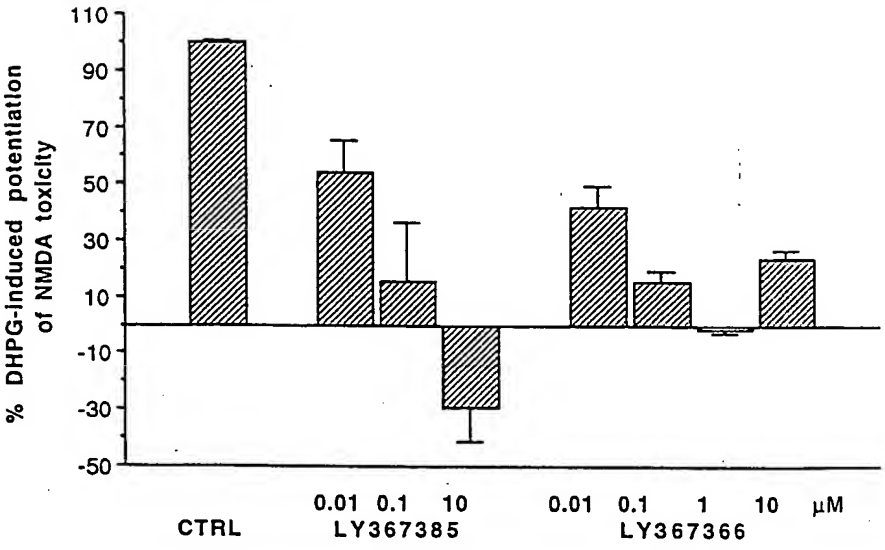

Fig. 3. LY367385 and LY367366 counteract the potentiation of NMDA toxicity induced by DHPG in mixed cultures of cortical cells. Values are means ± SEM. of four determinations and are expressed as per cent of DHPG-induced potentiation of NMDA toxicity. Basal values (trypan blue-positive neurons in three random fileds): 44 ± 1; NMDA, 60 μM: 70 ± 4; NMDA + DHPG, 100 μM: 145 ± 5. All values are significantly different from controls (CTRL) ($P < 0.01$, One-way ANOVA + Fisher PLSD).

GABAergic neurons. GAD activity in the injected caudate nucleus was always related to the respective unlesioned controlateral site. Infusion of NMDA alone reduced striatal GAD activity by about 50%. The extent of this reduction was significantly smaller in the striatum injected with NMDA + LY367385 or NMDA + LY367366. As opposed to what observed by histological analysis, there was no difference between the effects of LY367385 and LY367366 on striatal GAD activity (Fig. 5).

3.3. Effect of LY367385 on ischemic neuronal death

To establish whether LY367385 was protective against ischemic neuronal damage in vivo, we have injected the coumpound i.c.v. (100 nmol/2.5 μl/5 min; calculated to obtain a final brain concentration of 250 gM) 30 min before a 5-min bilateral carotid artery occlusion in gerbils. In control gerbils, ischemia induced a substantial loss (95%) of pyramidal neurons in the CA1 region of the hippocampus. In animals injected with LY367385 around 40% of CA1 neurons were protected against ischemic degeneration (Fig. 6).

4. Discussion

Group-I mGlu receptors include mGlu1 (splice variants: a–e, g) and mGlu5 (splice variants: a, b), which are coupled to polyphosphoinositide (PPI) hydrolysis (with the exception of mGlu1e) in heterologous expression systems (Abe et al., 1992; Nakanishi, 1994; Pin and Duvoisin, 1995). At subcellular level, both mGlu1a and -5 receptors are localized at the periphery of postsynaptic densities and, therefore, respond to concentrations of glutamate that are sufficiently high to spread away from the central region of the synapsis (Baude et al., 1993; Shigemoto et al., 1996). However, group-I mGlu receptor agonists are reported to amplify glutamate release (Herrero et al., 1992), suggesting a possible presynaptic localization of either mGlu1 or mGlu5 receptors. A role for group-I mGlu receptors in neuronal degeneration has originally been inferred by the neurotoxic effect of the mixed agonist, 1*S*,3*R*-ACPD, locally infused into the rat hippocampus or caudate nucleus (McDonald and Schoepp, 1992; Sacaan and Schoepp, 1992; McDonald et al., 1993). 1*S*,3*R*-ACPD is particularly effective in producing neuronal death in newborn animals (McDonald et al., 1993), which respond to mGlu receptor agonists with a substantial stimulation of PPI hydrolysis (Nicoletti et al., 1986). Hence, it has been suggested that stimulation of PPI hydrolysis is potentially neurotoxic as a result of either the release of intracellular Ca^{2+} or the activation of protein kinase C (Schoepp and Conn, 1993). The subsequent discovery of more selective group-I mGlu receptor agonists, such as DHPG or 3-hydroxyphenylglycine, has facilitated a closer examination of the function of mGlu1 or -5 receptors. Activation of group-I mGlu receptors amplifies NMDA toxicity, as well as neurodegeneration induced by mild conditions of oxygen-glucose deprivation in cultured cortical cells (Bruno et al., 1995; Buisson and Choi, 1995). However, group-I mGlu receptor agonists are neuroprotective in cultured cerebellar granule cells, where they reduce the delayed increase of cytosolic

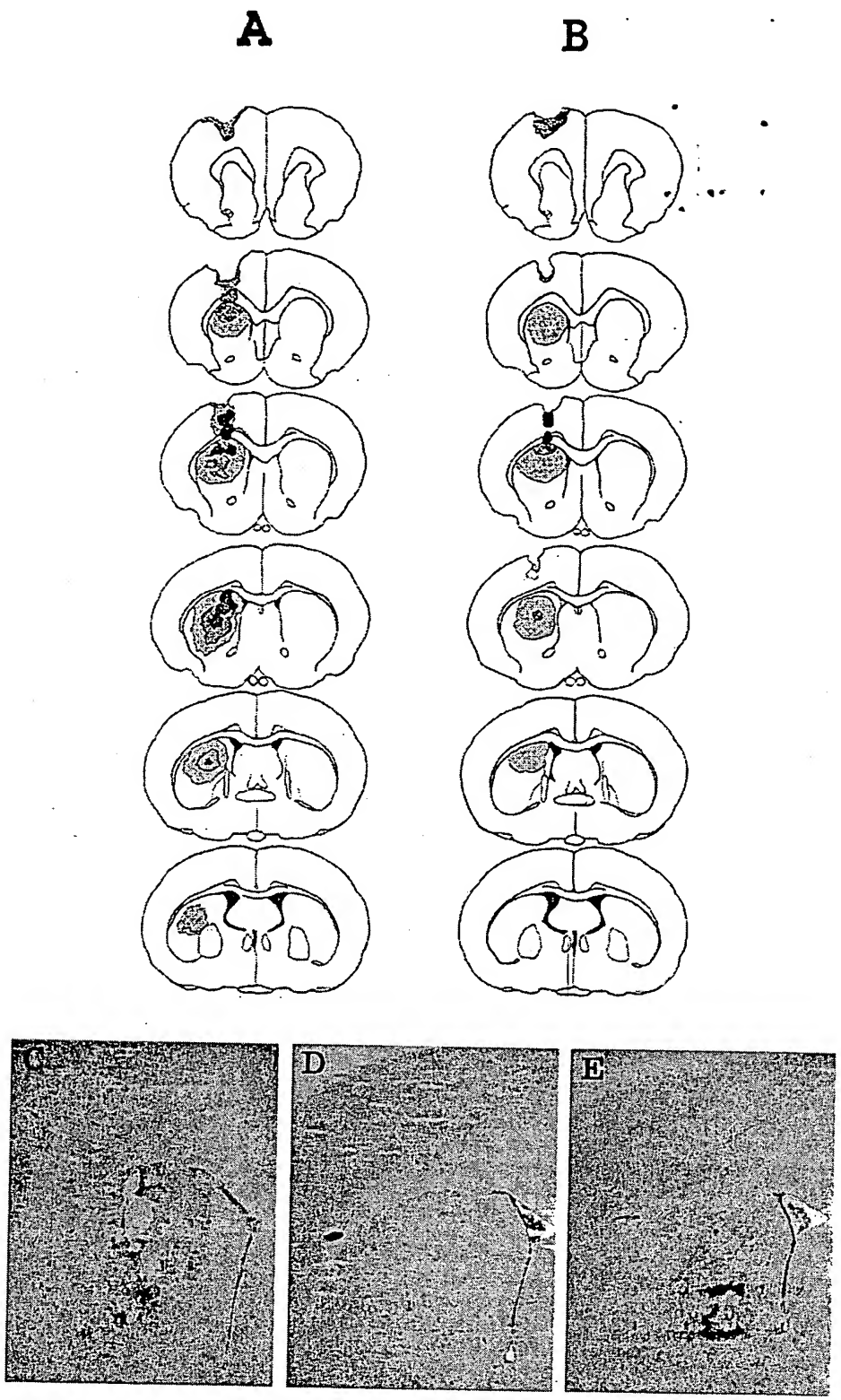

Fig. 4. Serial frontal sections across the extension of the caudate nucleus from a representative animal locally infused with NMDA (A) or NMDA + LY367385 (B). Necrotic areas are in black, whereas the grey shadow represents the surrounding oedema. Microphotographs at the injection sites of animals infused with NMDA, NMDA + LY367385 and NMDA + LY367366 are shown in (C), (D) and (E), respectively. Note that the size of the necrotic area is reduced in (E) and no macroscopic loss of tissue, but only oedema is present in (D).

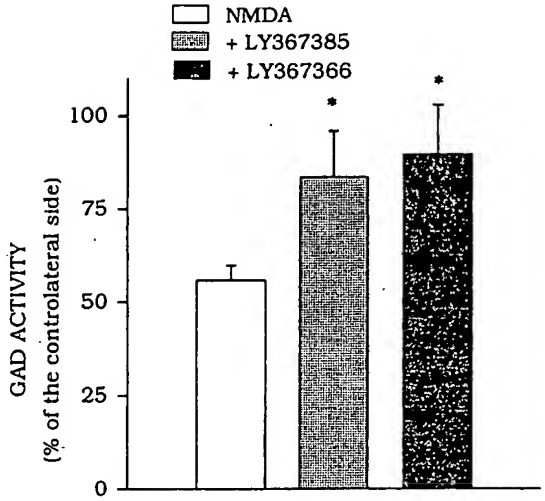

Fig. 5. LY367385 or LY367366 prevent the reduction of GAD activity induced by monolateral infusion of NMDA into the left caudate nucleus. Results are expressed as per cent of the of the respective controlateral unlesioned site for each individual determination. GAD activity was calculated as c.p.m. of authentic [^{3}H]GABA/μg pros. Means ± S.E.M. of GAD activity in the ipsilateral and controlateral sites from the various groups of animals ($n = 4–6$) were the following. Monolateral infusion of NMDA alone: controlateral site = 209 ± 7; ipsilateral site = 125 ± 16; infusion of NMDA + LY367385: controlateral site = 170 ± 11; ipsilateral site: 144 ± 25; infusion of NMDA + LY367366: controlateral site = 192 ± 17; ipsilateral site: 171 ± 15. * $P < 0.05$ (One-way ANOVA + Fisher PLSD).

free Ca^{2+} resulting from a sustained activation of NMDA receptors (Pizzi et al., 1993). Thus, pharmacological activation of group-I mGlu receptors may either amplify or attenuate neuronal degeneration depending on the cell type and/or the paradigm of toxicity. More recently, attention has been focused on how endogenous activation of group-I mGlu receptors affects the development of neuronal degeneration. Based on the assumption that perisynaptic mGlu1 or -5 receptors are recruited by the high levels of glutamate that are released during ischemia, it has been predicted that group-I mGlu receptor antagonists attenuate ischemic neuronal damage. Accordingly, in the gerbil model of transient global ischemia the mGlu1a receptor antagonist, AIDA, reduces the delayed degeneration of pyramidal cells in the hippocampal CA1 region (Cozzi et al., 1997). We have confirmed these results with LY367385, which behaves as a potent and highly selective mGlu1a receptor antagonist. LY367385 was also neuroprotective against excitotoxic death induced by infusion of NMDA into the caudate nucleus, as well as against NMDA toxicity in cultured cortical cells. The latter effect is in agreement with the reported neuroprotection by AIDA, 4CPG or α-methyl-4-carboxyphenylglycine (a mixed group I/II mGlu receptor antagonist) in cultured cortical cells exposed to submaximal concentrations of NMDA (Strasser et al., 1997). A possible explanation for the protective effect of LY367385 against NMDA toxicity is that activation of mGlu1a receptors by the endogenously released glutamate plays a permissive role in the induction of excitotoxic death. The substantial neuroprotection observed at 100 nM LY367385 (as well as at 10–100 nM LY367366) was unexpected because both drugs antagonize group-I mGlu receptors with IC_{50} values > 1 μM. It cannot be excluded that LY367385 displaces more efficiently DHPG or the endogenous glutamate from mGlu1 a receptors in cortical cells than quisqualate in heterologous expression systems, and that, therefore, the real potency of LY367385 is underestimated.

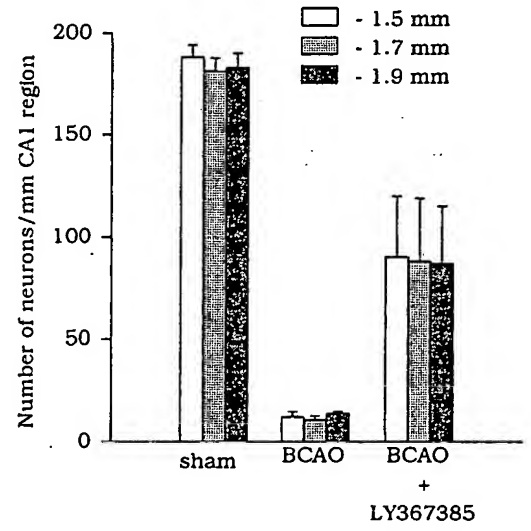

Fig. 6. Neuroprotective activity of LY367385 infused i.c.v. 30 min before a 5-min bilateral carotid artery occlusion (BCAO) in gerbils. Histological results are expressed as means ± SEM of neurons/mm of hippocampal CA1 region (three sections at −1.5, −1.7 and −1.7 mm distance from bregma) from four animals per group.

In CA1 pyramidal cells, striatal GABAergic neurons and cultured cortical neurons, mGlu5 receptors predominate over mGlu1a receptors (Bruno et al., 1995; Pin and Duvoisin, 1995). To examine to what extent mGlu5 receptors contributed to the development of excitotoxic death, we compared the activity of the mGlu1 selective antagonist LY367385 with that of LY367366, a compound which antagonizes both mGlu1a and -5 receptors in the low micromolar range. In cortical cultures, LY367366 was neuroprotective at low micromolar concentrations, but appeared to be less efficacious than LY 367385. The protective activity of LY 367366 against striatal toxicity in vivo was less pronounced than that of LY 367385, at least when evaluated by histological examination. Although antagonism of group-II or -III mGlu receptors by high concentrations of LY367366 might have counterbalanced its neuroprotective activity, these results indicate that inhibition of mGlu1a receptors (or perhaps other mGlu1 receptor splice variants) is sufficient to confer significant neuroprotection. However, complete assessment of the relative contribu-

tions of the group I mGlu receptor subtypes to the development of excitotoxic death awaits the discovery of a specific mGlu5 antagonist.

mGlu1a receptors stimulate PPI hydrolysis and inhibit K^+ channels in heterologous expression systems (Aramori and Nakanishi, 1992; Ikeda et al., 1995). Any of these transduction pathways may contribute to amplify excitotoxic death, although native mGlu1a receptors are less efficiently coupled to PPI hydrolysis than mGlu5 receptors (Casabona et al., 1997). The protective activity of LY367385 in the gerbil model of global ischemia are difficult to explain, because CA1 pyramidal cells apparently lack mGlu1a receptors. These receptors, however, are expressed by a subset of GABAergic neurons in the CA1 hippocampal region (Baude et al., 1993; Hampson et al., 1994), where application of group-I mGlu receptor agonists reduces transmission at inhibitory synapses (Desai and Conn, 1991; Desai et al., 1994; Gereau IV and Conn, 1995). Thus, LY367385 might facilitate GABA release (and therefore attenuate the excitotoxic degeneration of CA1 pyramidal cells) by removing the inhibitory action of mGlu1a receptors at GABAergic nerve terminals. Whether this represents a general mechanism mediating the neuroprotective activity of mGlu1a receptor antagonists remains to be established.

Acknowledgement

Supported by the BIOMED grant VEBHH4-CT96-085.

References

Abe, T., Sugihara, H., Nawa, H., Shigemoto, R., Nakanishi, S., 1992. Molecular characterization of a novel metabotropic glutamate receptor, mGluR5 coupled to inositol phosphate/Ca^{2+} signal transduction. J. Biol. Chem. 267 (13), 361–368.

Aramori, I., Nakanishi, S., 1992. Signal transduction and pharmacological characteristics of a metabotropic glutamate receptor, mGluR1, in transfected CHO cells. Neuron 8, 757–765.

Baude, A., Nusser, Z., Robert, J.D.B., Mulvihill, E., Mcilhinney, R.A.J., Somogyi, P., 1993. The 1a form of metabotropic glutamate receptor (mGluR1a) is concentrated at extra and perisynaptic membrane of discrete subpopulations of neurons as detected by immunogold reaction in the rat. Neuron 11, 771–787.

Bruno, V., Copani, A., Knopfel, T., et al., 1995. Activation of metabotropic glutamate receptors coupled to inositol phospholipid hydrolysis amplifies NMDA-induced neuronal degeneration in cultured cortical cells. Neuropharmacology 34, 1089–1098.

Buisson, A., Choi, D.W., 1995. The inibitory mGluR agonist, *S*-4-carboxy-3-hydroxyphenylglycine selectively attenuates NMDA neurotoxicity and oxygen-glucose deprivation-induced neuronal death. Neuropharmacology 3 (4), 1081–1087.

Casabona, G., Knopfel, T., Kuhn, R., et al., 1997. Expression and coupling to polyphosphoinositide hydrolysis of group I metabotropic glutamate receptors in early postnatal and adult rat brain. Eur. J. Neurosci. 9, 12–17.

Cha, J.J., Talati, A., Kerner, J.A., Lichtenbaum, R.A., Young, A.B., 1996. Antisense oligodeoxynucleotides directed against MELURS glutamate receptors protect against malonic acid legions in rat striatum. Neuropharmacol. 35, 87.

Clark, B.P., Baker, S.R., Goldsworthy, J., Harris, J.R., Kingston, A.E., 1997. 2-Methyl-4-carboxyphenylglycine (LY367385) selectively antagonises metabotropic glutamate mGluR1 receptors. Biorg. Med. Chem. Lett. 7, 2777–2780.

Cozzi, A., Lombardi, G., Leonardi, P., Attucci, S., Peruginelli, F., Pellicciari, R., Moroni, F., 1977. AIDA, a group I metabotropic glutamate receptor antagonist reduces the ischemia-induced neuronal loss. Soc. Neurosci. Abs. 23, 788.

Desai, M.A., Conn, P.J., 1991. Excitatory effects of ACPD receptor activation in the hippocampus are mediated by direct effects on pyramidal cells and blockade of synaptic inhibition. J. Neurophysiol. 66, 40–52.

Desai, M.A., McBain, C.J., Kauer, J.A., Conn, P.J., 1994. Metabotropic glutamate receptor-induced disinhibition is mediated by reduced transmission at excitatory synapses onto interneurons and inhibitory synapses onto pyramidal cells. Neurosci. Lett. 181, 78–82.

Gereau IV, R.W., Conn, P.J., 1995. Multiple presynaptic metabotropic glutamate receptors modulate excitatory and inhibitory synaptic transmission in hippocampal area CAT. J. Neurosci. 15, 6879–6889.

Hampson, D.R., Theriault, E., Huang, X.-P., et al., 1994. Characterization of two alternative spliced forms of a metabotropic glutamate receptor in the central nervous system of the rat. Neuroscience 60, 325–336.

Herrero, I., Miras-Portugal, M.T., Sanchz-Prieto, J., 1992. Positive feed-back of glutamate of glutamate exocytosis by metabotropic presynaptic receptor stimulation. Nature 360, 163–166.

Ikeda, S.R., Lovinger, D.M., McCool, B.A., Lewis, D.L., 1995. Heterologous expression of metabotropic glutamate receptors in adult rat sympathetic neurons: subtype-specific coupling to ion channels. Neuron 14, 1029–1038.

Ito, I., Kohda, A., Tanabe, S., Hirose, E., Hayashi, M., Mitsunaga, A., Sugiyama, H., 1992. 3,5-Dihydroxyphenylglycine: a potent agonist of metabotropic glutamate receptors. Neuro Report 3, 1013–1016.

Kingston, A.E., Burnett, J.P., Mayne, N.G., Lodge, D., 1995. Pharmacological analysis of 4-carboxyphenylglycine derivatives: comparison of the effects of mGlu1a and mGlu5 subtypes. Neuropharmacology 34, 887–894.

McDonald, J.W., Schoepp, D.D., 1992. The metabotropic glutamate receptor agonist 1*S*,3*R*-ACPD selectively potentiates *N*-methyl-D-aspartate-induced brain injury. Eur. J. Pharmacol. 215, 353–354.

McDonald, J.W., Fix, A.S., Tizzano, I.P., Schoepp, D.D., 1993. Seizures and brain injury in neonatal rats induced by 1*S*,3*R*-ACPD, a metabotropic glutamate receptor agonist. J. Neurosci. 13, 4445–4455.

Nakanishi, S., 1994. Metabotropic glutamate receptors: synaptic transmission, modulation and plasticity. Neuron 13, 1031–1037.

Nicoletti, F., Ladarola, M.J., Wroblewski, J.T., Costa, E., 1986. Excitatory amino acid recognition sites coupled with inositol phospholipid metabolism: developmental changes and interaction with α1-adrenoceptors. Proc. Natl. Acad. Sci. USA 83, 1931–1935.

Nicoletti, F., Bruno, V., Copani, A., Casabona, G., Knoepfel, T., 1996. Metabotropic glutamate receptors: a new target for the therapy of neurodegenerative disorders? Trends Neurosci. 1 (9), 267–271.

Pin, J.-P., Duvoisin, R., 1995. The metabotropic glutamate receptors: structure and functions. Neuropharmacology 3 (4), 1–26.

Pizzi, M., Fallacara, C., Arrighi, V., Memo, M., Spano, P.F., 1993. Attenuation of excitatory amino acid toxicity by metabotropic glutamate receptor agonists and aniracetam in primary cultures of cerebellar granule cells. J. Neurochem. 61, 683–689.

Pizzi, M., Gallic, P., Consolandi, O., Arrighi, V., Memo, M., Spano, P.F., 1996a. Metabotropic and ionotropic transducers of glutamate signal inversely control cytoplasmic Ca^{2+} concentration and exitotoxicity in cultured cerebellar pranule cells: pivotal role of protein kinase C. Mol. Pharmacol. 49 (4), 586–594.

Pizzi, M., Consolandi, O., Memo, M., Spano, P.F., 1996b. Activation of multiple metabotropic glutamate receptor subtypes prevents NMDA-induced excitotoxicity in rat hippocampal slices. Eur. J. Neurosci. 8 (2), 1516–1521.

Rose, K., Goldberg, M.P., Choi, D.W., 1992. Cytotoxicity in murine neocortical cell culture. In: Tyson, C.A., Frazier, J.M. (Eds.), Methods in Toxicology, vol. 1. Academics, San Diego, pp. 46–60.

Sacaan, A.I., Schoepp, D.D., 1992. Activation of hippocampal metabotropic excitatory amino acid receptors leads to seizures and neuronal damage. Neurosci. Lett. 139, 7782.

Schoepp, D.D., Conn, P.J., 1993. Metabotropic glutamate receptors in brain function and pathology. Trends Pharmacol. Sci. 14, 13–20.

Schoepp, D.D., Johnson, B.G., Wright, R.A., et al., 1997. LY354740 is a potent and highly selectivegroup 2 metabotropic glutamate receptor agonist in cells expressing human glutamate receptors. Neuropharmacology 36, 1–11.

Schoepp, D.D., Lodge, D., Bleakman, D., et al., 1995. In vitro and in vivo antagonism of AMPA receptor activation by 3*S*,4a*R*,6*R*,8a*R*)-6-[2-(1(2)H-tetrazole-5-yl)ethyl]decahydroisoquinaline-3-carboxylic acid. Neuropharmacology 34, 1159–1168.

Shigemoto, R., Kulik, A., Roberts, J.D.B., Ohishi, H., Nusser, Z., Kaneko, T., Somogyi, P., 1966. Target-cell-specific concentration of a metabotropic glutamate receptor in the presynaptic active zone. Nature 381, 523–525.

Strasser, U., Lobner, D., Behrens, M.M., Dugan, L.L., Choi, D.W., 1977. Block of group I mGluRs attenuates NMDA-induced neuronal death in cortical cultures. Soc. Neurosci. Abs. 23, 899.

Wright, R.A., McDonald, J.W., Schoepp, D.D., 1994. Distribution and ontoeny of 1*S*,3*R*-1 -amino-cyclopentane-1,3-dicarboxylic acid sensitive and quisqualate insensitive [^{3}H]-glutamate binding sites in the rat brain. J. Neurochem 63, 938–945.

EXHIBIT B

PERGAMON

NEURO PHARMACOLOGY

Neuropharmacology 38 (1999) 209–216

Protective effect of group I metabotropic glutamate receptor activation against hypoxic/hypoglycemic injury in rat hippocampal slices: timing and involvement of protein kinase C

Ulrich H. Schröder [a,*], Thoralf Opitz [a], Tino Jäger [a], Clemens F. Sabelhaus [a], Jörg Breder [a], Klaus G. Reymann [a,b]

[a] *Department of Neurophysiology, Federal Institute for Neurobiology, P.O Box 1860, D-39008 Magdeburg, Germany*
[b] *Research Institute for Applied Neurosciences, D-39008 Magdeburg, Germany*

Abstract

Excessive release of glutamate during ischemia leads to sustained neuronal damage. In this study we investigated the influence of metabotropic glutamate receptor (mGluR) activation on neuronal recovery from a hypoxic/hypoglycemic event in hippocampal slices from rats. The slices were transiently exposed to an oxygen- and glucose-free environment in an interface chamber and the synaptically evoked population spike in the CA1 region was taken as a measure of neuronal viability. Under control conditions the population spike amplitude recovered to 41.4% of baseline value within 1 h after hypoxia/hypoglycemia. The specific mGluR group I agonist 3,5-dihydroxyphenylglycine (DHPG, 10 μM) increased the recovery rate to 88.3% of baseline value when applied from 20 min before until 10 min after the event. Similar recovery rates were obtained when DHPG was present only 10 or 20 min before hypoxia/hypoglycemia (89.3% and 79.3% of baseline value, respectively). However, when applied later, DHPG had no protective effect. Co-application of the protein kinase C (PKC) inhibitors staurosporine (100 nM) or chelerythrine (30 μM) prevented the protective effect of DHPG. Our data suggest that group I mGluR agonists are only protective when present prior to the onset of the hypoxic/hypoglycemic event and that the activation of PKC is a critical step of the protective mechanism.

Keywords: 3,5-Dihydroxyphenylglycine; Hypoxia; Ischemia; Metabotropic glutamate receptors; Neuroprotection; Protein kinase C; Rat hippocampal slices

1. Introduction

The loss of high energy compounds (e.g. ATP, creatine phosphate) during hypoxia and ischemia results in a massive depolarization of the neuronal membrane and an excessive release of glutamate (Benveniste et al., 1984; Mitani et al., 1991; Hara et al., 1993) which in turn activates ionotropic (iGluRs) and metabotropic (mGluRs) glutamate receptors and initiates a chain of intracellular events that eventually lead to sustained neuronal damage.

The activation of iGluRs induces calcium overload and loss of cation homeostasis, crucial mechanisms leading to neuronal degeneration (Hartley et al., 1993; Urenjak and Obrenovitch, 1996). Many investigations have shown that iGluR antagonists may protect neurons from such degeneration (Choi and Rothman, 1990; Meldrum, 1992).

The mGluRs, which are coupled to various effector systems via GTP-binding proteins (G-proteins), are also activated during hypoxia and ischemia, but little is known about their contribution to cell death. Based on their amino acid sequence homology, pharmacology and transduction mechanisms the eight mGluRs that are known to date can be divided into three main groups. The subtypes mGluR1 and mGluR5 which couple primarily to phospholipase C (PLC) constitute group I, whereas the subtypes mGluR2-3 and mGluR4-6-7-8 which inhibit adenylyl cyclase constitute group II and group III, respectively (Nakanishi 1994; Pin and Duvoisin 1995). The application of mGluR agonists and antagonists in models of NMDA neurotoxicity and hypoxia/hypoglycemia has yielded conflicting results.

* Corresponding author. Tel.: +49-391-6263431; fax: +49-391-6263438; e-mail: schroede@ifn-magdeburg.de.

0028-3908/99/$ - see front matter
PII: S0028-3908(98)00180-4

The activation of group I and group II mGluRs has been reported in different studies to either contribute to, or protect against, cell death (Koh et al., 1991; Chiamulera et al., 1992; Sacaan and Schoepp, 1992; Birrell et al., 1993; Opitz and Reymann, 1993; Tizzano et al., 1993; Buisson and Choi, 1995; Opitz et al., 1995; Pizzi et al., 1996a). In addition, it has been shown that both the group I and group II mGluR agonist 1-aminocyclopentane-1,3-dicarboxylic acid (ACPD) and the group I and group II mGluR antagonist (+)-α-methyl-4-carboxyphenylglycine ((+)-MCPG) reduce the extent of injury in the CA1 region of the hippocampus in the same in vitro model of hypoxia/hypoglycemia (Opitz et al., 1995). These apparent contradictions led us to hypothetize that distinct mGluR subtypes may be differentially involved in hypoxic/ischemic cell death and that the timing of activation of a specific mGluR subtype may influence recovery. The aim of this study was to evaluate the influence of group I mGluRs on neuronal recovery from hypoxia/hypoglycemia with the highly selective agonist 3,5-dihydroxyphenylglycine (DHPG) (Ito et al., 1992; Schoepp et al., 1994). We investigated whether the timing of group I mGluR activation influences recovery and whether protein kinase C (PKC) is involved in the protective mechanism.

2. Materials and methods

2.1. Hippocampal slice preparation

Seven to 8-week-old male Wistar rats (Institute breeding stock) were killed by a blow to the neck. After decapitation, the brain was quickly removed and placed into ice-cold Ringer solution with the following composition (in mM): NaCl 124, KCl 4.9, $MgSO_4$ 1.3, $CaCl_2$ 2, KH_2PO_4 1.2, $NaHCO_3$ 25.6, D-glucose 10, bubbled to pH 7.4 with carbogen (95% O_2/5% CO_2). Both hippocampi were isolated and transverse hippocampal slices (400 μm) were prepared using a tissue chopper with a cooled stage. The slices were transferred to an interface type recording chamber, where they were allowed to recover for at least 1 h before the experiment started. The chamber was constantly perfused with Ringer solution at a rate of 1 ml/min. The surface of the slices was exposed to a moist carbogen atmosphere, which was exchanged at a rate of 20 l/h. The temperature of the chamber was maintained at 34 ± 1°C.

2.2. Electrophysiological recordings

Population spike (PS) responses were evoked by stimulation of the Schaffer collateral/commissural fibers with stainless steel electrodes in the stratum radiatum and recorded with glass microelectrodes (1–4 MΩ) in the stratum pyramidale of the CA1 region. Test stimuli (biphasic constant voltage pulses, 0.1 ms per half wave) were adjusted to elicit a population spike of about 60% of its maximum amplitude. The PS amplitude was evaluated by calculating the voltage difference between the negative peak and the positive one preceding it. Since the amplitude of the PS correlates over a wide range with the number of firing neurons (Andersen et al., 1971), the PS may serve as a measure of neuronal functional integrity.

2.3. Induction of hypoxia/hypoglycemia

Hypoxia/hypoglycemia was induced by changing the carbogen atmosphere of the chamber to a gas mixture containing 95% N_2/5% CO_2 in the presence of a Ringer solution in which glucose was replaced by mannitol. Evoked extracellular responses were recorded every 20 s during the hypoxic/hypoglycemic period in the hippocampal CA1 region. After 4 min of hypoxia/hypoglycemia normal oxygen and glucose supply was re-established. The recovery of field potentials was monitored every 5 or 15 min for at least 1 h (the responses of four test stimuli with a frequency of 0.2 Hz were averaged).

2.4. Pharmacological tools

In this study DHPG was employed as a highly specific agonist for group I mGluRs. DHPG activates mGluR1 and mGluR5 and stimulates phosphatidylinositol-4,5-bisphosphate ($PtdInsP_2$) hydrolysis, but it does not inhibit the forskolin-stimulated cAMP formation and has no direct effect on ionotropic glutamate receptors (Ito et al., 1992; Schoepp et al., 1994; Gereau IV and Conn, 1995). We used (+)-MCPG to antagonize effects of DHPG. However, (+)-MCPG is not solely a competitive antagonist for group I mGluRs but is also an antagonist for group II mGluRs (Hayashi et al., 1994). The PKC inhibitors staurosporine and chelerythrine were applied in order to assess whether DHPG effects resulted from the activation of PKC. Staurosporine is the most potent inhibitor of PKC. However, it inhibits other protein kinases, including cAMP-dependent protein kinase (PKA), as well (Tamaoki 1991; Hidaka and Kobayashi 1992). Chelerythrine on the contrary is highly specific for PKC with only a marginal effect at high concentrations on PKA, but is less potent than staurosporine (Herbert et al., 1990). The effect of PKC activation on PS recovery was examined using 12-*O*-tetradecanoylphorbol-13-acetate (TPA) as PKC activator. All substances were bath applied during the intervals stated in the respective figure legends. DHPG and (+)-MCPG were obtained from Tocris Neuramin (Bristol, UK), staurosporine and TPA were purchased from Sigma (Deisenhofen, Ger-

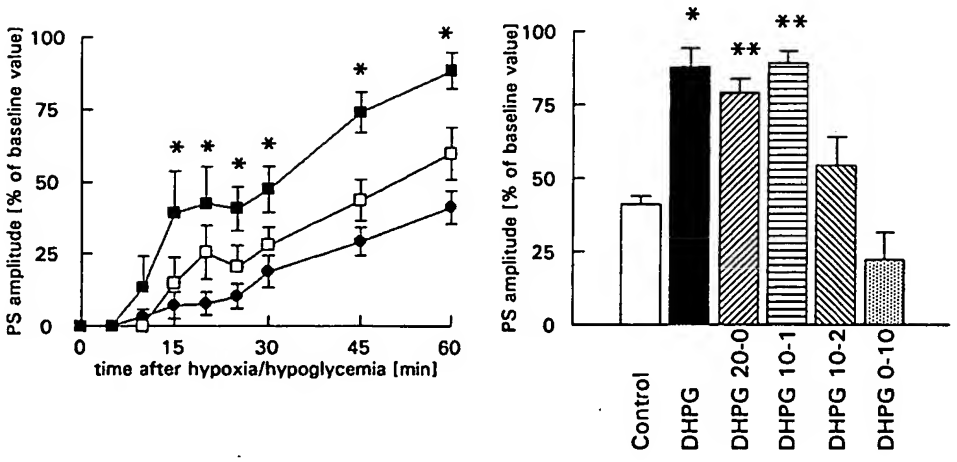

Fig. 1. DHPG protects hippocampal neurons against hypoxic/hypoglycemic injury. Left side, 10 μM DHPG (■, $n = 7$) significantly improved PS recovery when present 20 min before until 10 min after the hypoxic/hypoglycemic event whereas 1 μM DHPG (□, $n = 6$) affected PS recovery only marginally. * Significant protection ($P \leq 0.05$, Mann–Whitney U-Test). ●, no drug ($n = 11$). Right side, DHPG (10 μM) was neuroprotective when present 20 min before until 10 min after the hypoxic/hypoglycemic event ($n = 7$, $P \leq 0.05$), when applied for 20 min until immediately before hypoxia/hypoglycemia (DHPG 20-0; $n = 7$, $P \leq 0.01$) or when given for 10 min and washed out 1 min before the onset of hypoxia/hypoglycemia (DHPG 10-1; $n = 9$, $P \leq 0.01$). DHPG did not improve PS recovery when given for 10 min and washed out 2 min before the onset of hypoxia/hypoglycemia (DHPG 10-2; $n = 7$) or when washed in immediately before and washed out 10 min after hypoxia/hypoglycemia (DHPG 0-10; $n = 6$). Control: no drug ($n = 52$). * Significant protection (* $P \leq 0.05$, ** $P \leq 0.01$, Mann–Whitney U-Test).

many) and chelerythrine from Biomol (Hamburg, Germany).

3. Statistics

All values are given as mean ± SEM. The Mann–Whitney U-test was used to compare the field potential recovery between two groups of differentially treated slices (i.e. control vs. drug treatment).

4. Results

4.1. Activation of group I mGluRs protects neurons from hypoxic/hypoglycemic injury

In our model the interruption of the oxygen- and glucose supply resulted in a complete loss of the evoked electrophysiological response 1–2 min after the onset of hypoxia/hypoglycemia. When the oxygen and glucose supply was re-established after 4 min the PS amplitude in untreated control slices recovered to 41.4 ± 2.8% ($n = 52$) of baseline value within 1 h (Fig. 1). No further improvement of recovery was observed during the next hour (Fig. 2). This indicates that the hypoxic/hypoglycemic event was sufficient to cause sustained damage to CA1 neurons.

In order to assess the role of group I mGluRs in hypoxia/hypoglycemia we applied the specific agonist DHPG at different concentrations. When bath applied 20 min before hypoxia/hypoglycemia and washed out 10 min after the oxygen and glucose supply was re-established, 10 μM DHPG significantly improved the recovery of the PS amplitude to 88.3% of baseline value (Figs. 1 and 2), whereas 1 μM DHPG had no effect. DHPG (10 μM) did not alter the baseline PS amplitude during 80 min of application (101.5% of pre-DHPG value) in control experiments. In addition, the PS of DHPG-treated slices disappeared at approximately the same time after the onset of hypoxia/hypoglycemia as in untreated control slices (after about 100 s, $n = 6$), implying that DHPG does not affect the onset of anoxic depolarization of the neuronal membranes.

4.2. The neuroprotection by group I mGluRs depends on the timing of activation

Recently we reported that both the group I and group II mGluR agonist ACPD and the group I and group II mGluR antagonist (+)-MCPG reduced the extent of injury in our in vitro model of hypoxia/hypoglycemia, whereas the co-application of both substances abolished the protective effects (Opitz et al., 1995). These apparently conflicting results led us to hypothetize that the timing of activation of the mGluR subtypes may determine their effect on recovery after a hypoxic/hypoglycemic event. Thus, in another set of experiments we investigated when DHPG had to be present to exert a protective effect. DHPG (10 μM) was protective when present from 20 min before until 10 min after hypoxia/hypoglycemia, but had no protective effect when applied only immediately before the onset of hypoxia/hypoglycemia and washed out 10 min thereafter (Fig. 1). However, when DHPG was present 20 min before until the onset of hypoxia/hypoglycemia it

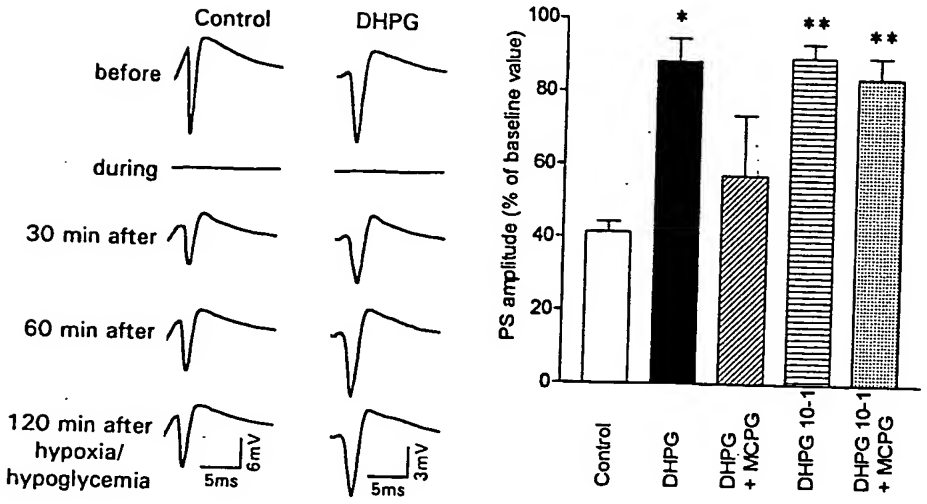

Fig. 2. Neuroprotection by DHPG. Electrophysiological time course and effect of MCPG. Left side; The representative traces show evoked population spikes recorded immediately before, during, and at different time points after hypoxia/hypoglycemia. Right side; Neuroprotection by DHPG (10 μM) present 20 min before until 10 min after the hypoxic/hypoglycemic event (DHPG, $n = 7$) was abolished when the competitive antagonist (+)-MCPG (500 μM) was co-applied (DHPG + MCPG, $n = 5$). The protective effect of DHPG given for 10 min and washed out 1 min before the onset of hypoxia/hypoglycemia (DHPG 10-1; $n = 9$, $P \leq 0.01$) was not attenuated when in addition (+)-MCPG (500 μM) was washed in immediately before and was washed out 10 min after hypoxia/hypoglycemia (DHPG 10-1 + MCPG, $n = 7$, $P \leq 0.01$). Control, no drug ($n = 52$); * Significant protection (* $P \leq 0.05$, ** $P \leq 0.01$, Mann–Whitney U-Test).

enhanced the PS recovery to about 79% of the baseline value (Fig. 1). The PS amplitude recovered to a similar extent (to about 89%, Fig. 1) when DHPG was applied only for 10 min and washed out 1 min before the hypoxic/hypoglycemic event. These data indicate that group I mGluRs promote neuroprotection only when activated prior to the onset of the hypoxic/hypoglycemic insult. When DHPG was given for 10 min and was withdrawn 2 min before the insult, the PS amplitude recovered to only about 54.6% of the baseline values (Fig. 1), which is similar to the value reached by untreated control slices. This suggests that the group I mGluR agonists must be applied until shortly before the hypoxic/hypoglycemic incident in order to exert a neuroprotective effect.

4.3. Effect of MCPG on neuroprotection by DHPG

In order to establish whether DHPG exerts its protective effect by activating mGluRs, we employed a mGluR antagonist. Since highly selective group I mGluR antagonists were not available at the time the experiments were performed we tested whether the group I and group II mGluR antagonist (+)-MCPG would diminish the protective effect of DHPG. Indeed, when (+)-MCPG (500 μM) and DHPG (10 μM) were co-applied the PS amplitude only recovered to about 57% of baseline value (Fig. 2). This was not significantly different from the value reached by untreated control slices and corroborated the hypothesis that DHPG exerted its neuroprotective effect by activation of group I mGluRs. However, in the above experiments both DHPG and (+)-MCPG were present from 20 min before to 10 min after the hypoxic/hypoglycemic incident. In a previous study (Opitz et al., 1994) we established a protective effect of (+)-MCPG itself when applied during hypoxia/hypoglycemia, a result that we were able to confirm in the present investigation (data not shown); and DHPG protects neurons only when present before the insult. To examine if both effects are independent from each other we applied DHPG and (+)-MCPG successively. When DHPG was present for 10 min and washed out 1 min before the hypoxic/hypoglycemic event and MCPG was applied only immediately before the onset of hypoxia/hypoglycemia and washed out 10 min after the incident the neuroprotective effect of DHPG prevailed (Fig. 2).

4.4. Influence of protein kinase inhibitors on neuroprotection by DHPG

Group I mGluRs couple to G-proteins which activate PLC (Pin and Duvoisin 1995). This enzyme catalyses the hydrolysis of phosphatidylinositol-4,5-bisphosphate to generate diacylglycerol (DAG) and inositol-1,4,5-trisphosphate ($InsP_3$), leading to the activation of PKC and to the mobilization of intracellular calcium (Rhee and Choi 1992). However, besides activating PLC G-proteins can regulate ion channels in a phosphorylation-independent fashion (Nicoll, 1988; Lester and Jahr, 1990; Yu et al., 1997), which also might result in neuroprotection. In order to elucidate whether the protective

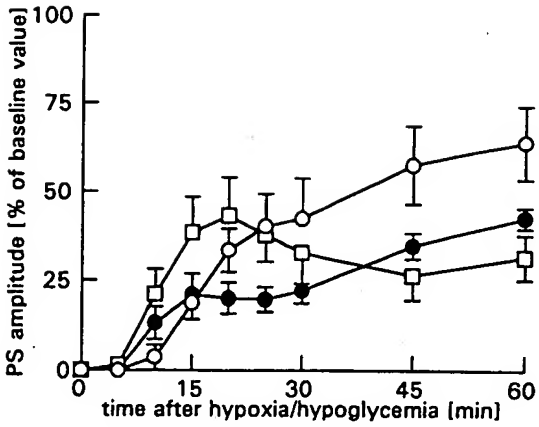

Fig. 3. Protein kinase inhibitors do not affect PS recovery after hypoxia/hypoglycemia. Neither staurosporine, given for 20 min and washed out 1 min before the onset of hypoxia/hypoglycemia (□, $n = 11$), nor chelerythrine (○, 30 μM, $n = 7$), present 20 min before until 10 min after the insult, significantly influenced the recovery of the PS amplitude 60 min after the event. ●, no drug ($n = 35$).

effect of DHPG (10 μM) was phosphorylation-dependent we co-applied the relatively non-selective protein kinase inhibitor staurosporine (100 nM). Staurosporine did not alter baseline PS amplitude during 20 min of application (97.3% of baseline value, $n = 12$) but it slightly decreased the PS recovery 1 h after hypoxia/hypoglycemia to 31.4 ± 6.2% of baseline value (Fig. 3). When staurosporine and DHPG were co-applied the PS amplitude reached only 39.9 ± 7.1% of baseline value ($n = 7$) 1 h after the insult, a value not significantly different from that of control slices (Fig. 4). This implies that protein kinase activation is indispensably involved in the protective mechanism triggered by

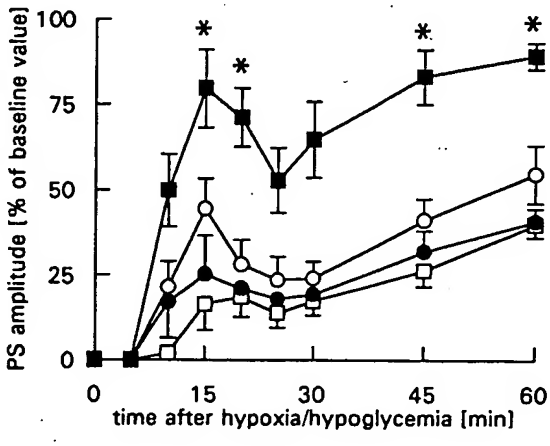

Fig. 4. Effect of protein kinase inhibitors on neuroprotection by DHPG. The protective effect of 10 μM DHPG applied from 10 min before until 1 min before the onset of hypoxia/hypoglycemia (■, $n = 9$) was abolished by co-application of 100 nM staurosporine (□, $n = 5$ $P \leq 0.001$) and 30 μM chelerythrine (○, $n = 7$; $P \leq 0.01$). Both drugs were given for 20 min and were washed out 1 min before the onset of hypoxia/hypoglycemia. ●, no drug ($n = 25$). * Significantly different from control (Mann–Whitney U-Test).

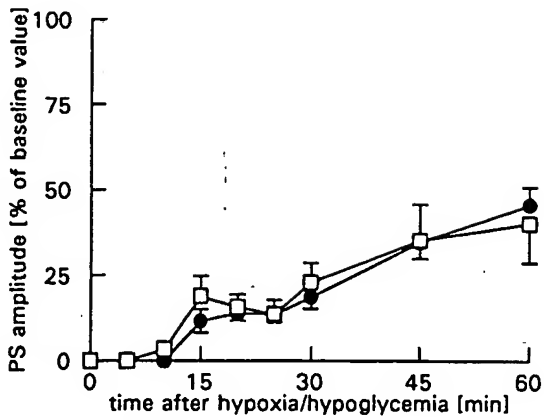

Fig. 5. Application of phorbol ester is not neuroprotective. The phorbol ester TPA (1 μM, □, $n = 6$) did not improve the recovery of the PS amplitude. TPA was applied for 10 min until 1 min before the onset of hypoxia/hypoglycemia. ●, No drug ($n = 15$).

group I mGluRs. Since DAG production and calcium mobilization rendered PKC the most likely candidate to be involved in the protective mechanism we examined whether the highly specific PKC inhibitor chelerythrine was able to block the protective effect of DHPG. Chelerythrine (30 μM) did not significantly affect PS recovery when applied from 20 min before to 10 min after the hypoxic/hypoglycemic event (Fig. 3). When chelerythrine and DHPG were co-applied the recovery 1 h after the insult was comparable to that of untreated control slices (Fig. 4). It reached only 54.7% of the prehypoxic/hypoglycemic values and indicates, that the activation of PKC is a critical step of the protective mechanism triggered by group I mGluRs. In order to find out whether the activation of PKC alone is sufficient to elicit neuroprotection we added the phorbol ester TPA (1 μM) which was shown to activate PKC in hippocampal slices (Genazzani et al., 1994). However, the application of TPA did not increase recovery of the PS amplitude (Fig. 5).

5. Discussion

In previous studies (Opitz and Reymann, 1993; Opitz et al., 1995) we have shown that ACPD and *trans*-azetidine-2,4-dicarboxylic acid (*t*-ADA) are able to protect CA1 neurons in rat hippocampal slices from hypoxic/hypoglycemic injury. However, uncertainty remained about the mGluR subtypes involved in the protective mechanism, because both drugs might have activated multiple groups of mGluRs simultaneously. Besides activating both group I and group II mGluRs, ACPD has also been found to stimulate phospholipase D in hippocampal slices, presumably via a novel, as yet unidentified mGluR subtype (Boss and Conn, 1992; Holler et al., 1993; Pellegrini-Giampietro et al., 1996).

Similarly, although many reports suggest that *t*-ADA is a selective group I mGluR agonist (Favaron et al., 1993; Kozikowski et al., 1993; Bruno et al., 1995b; Manahan-Vaughan et al., 1996), it has been reported to activate human mGluR2 expressed in Xenopus oocytes (Knöpfel et al., 1995). Thus, in the present study, we addressed the question of whether the activation of group I mGluRs suffices to afford neuroprotection in hippocampal slices subjected to hypoxia/hypoglycemia, utilizing the specific group I mGluR agonist DHPG. It has been shown in a number of expression systems that this drug activates group I mGluRs, but unlike ACPD or *t*-ADA, does not affect group II mGluRs and does not stimulate phospholipase D (Ito et al., 1992; Schoepp et al., 1994; Brabet et al., 1995; Gereau IV and Conn, 1995; Pellegrini-Giampietro et al., 1996; Sekiyama et al., 1996). Therefore, we attribute the protective effects of DHPG demonstrated in this study to its ability to activate group I mGluRs.

When co-applied with DHPG, the competitive mGluR antagonist (+)-MCPG was able to abolish the protective effect of DHPG. However, in our model of hypoxia/hypoglycemia, (+)-MCPG has been found to be neuroprotective itself when applied alone (Opitz et al., 1994). This produces the contradictory situation that both an agonist and an antagonist exhibit the same effect. Since we still observed neuroprotection when (+)-MCPG was applied after DHPG, the conflicting results may best be explained by assuming that antagonist and agonist act in different time windows. Alternatively, a yet unknown mGluR subtype might also be involved in the protective mechanism. In line with this interpretation, it has been observed that (+)-MCPG is an agonist and DHPG is an antagonist of an unidentified mGluR subtype coupled to phospholipase D (Pellegrini-Giampietro et al., 1996).

Our data suggest that the activation of group I mGluRs is sufficient to rescue hippocampal neurons from hypoxic/hypoglycemic damage. It is likely that neuronal injury in our model is mainly due to excessive Ca^{2+} influx through NMDA receptor channels. Thus, reduction of Ca^{2+} entry through NMDA receptor channels may be one of the neuroprotective mechanisms of group I mGluR activation. This interpretation is in line with a number of reports showing that group I mGluR agonists protect cultured neurons and hippocampal slices from NMDA and glutamate excitotoxicity (Koh et al., 1991; Birrell et al., 1993; Pizzi et al., 1996a,b; Montoliu et al., 1997), downregulate NMDA receptor channels (Yu et al., 1997) and reduce NMDA receptor mediated Ca^{2+} influx (Pizzi et al., 1996b). It was, however, shown by several groups (Aniksztein et al., 1992; Fitzjohn et al., 1996; Pisani et al., 1997) that the activation of group I mGluRs can reversibly enhance NMDA responses which in turn might have an aggravating effect during hypoxia/hypoglycemia. Our results indicate that group I mGluR agonists are protective only when applied before an insult and therefore also before ischemic glutamate release. If there is a potentiating effect of DHPG on NMDA responses, which we could not detect in our experiments (Opitz et al., 1995), it might be reversed by the time of ischemic NMDA receptor activation.

The neuroprotective effect of (+)-MCPG in our studies contrasts other findings that activation, not inhibition, of group II mGluRs prevents neurodegeneration induced by glutamate, NMDA (Bruno et al., 1995a; Buisson et al., 1996; Pizzi et al., 1996a) or hypoxia/hypoglycemia (Buisson and Choi, 1995) in neuronal and organotypic cultures. This discrepancy can not be readily explained. It is difficult to compare results from acutely isolated hippocampal slices with those from neuronal cultures because mGluR expression, mGluR responses and subsequent signalling cascades in neuronal cultures may depend on the origin of the neurons and the state of maturation of the cultures (Aronica et al., 1993; Blanc et al., 1995; Pizzi et al., 1996b). However, recent evidence indicates that group I and group II mGluRs may both act on the same protective mechanism (Pizzi et al., 1996b) in a time window that appears to be different from the neuroprotective window of (+)-MCPG. In that study, the attenuation of glutamate induced $(Ca^{2+})_i$ rise by ACPD was fully mimicked by a group I and partially by a group II mGluR agonist. Group II mGluR agonists have also been shown to mediate neuroprotection by a pathway that involves interaction between neurons and astrocytes (Bruno et al., 1997). Since this pathway requires new protein synthesis, it may be important in neuronal cultures but less likely affect acute recovery of synaptic transmission in hippocampal slices.

Further contrasting our results, intracerebral injections of ACPD (Sacaan and Schoepp, 1992; Tizzano et al., 1993) or DHPG (Tizzano et al., 1995) have been reported to induce limbic seizures and the loss of hippocampal CA1 neurons (Sacaan and Schoepp, 1992; Tizzano et al., 1993) in rodents in vivo. However, these seizures might have been initiated by higher concentrations of the drugs since DHPG did not induce epileptiformic activity in our slices. Conversely, ACPD has been reported to reduce infarct volume following middle cerebral artery occlusion in mice when administered systemically (Chiamulera et al., 1992).

Group I mGluRs stimulate PLC, which generates $InsP_3$, which releases intracellularly stored Ca^{2+}, and DAG, both of which can activate PKC. Thus we considered PKC to be a likely candidate for involvement in this protective mechanism. The observation that both the highly potent PKC inhibitor staurosporine and the highly selective inhibitor chelerythrine were able to attenuate DHPG-mediated neuroprotection corroborates our hypothesis. These

findings are in agreement with other studies suggesting that PKC activation can promote neuronal survival (Koh et al., 1991; Pizzi et al., 1996b; Durkin et al., 1997).

Perhaps most interestingly, DHPG exerted its neuroprotective effect only when present before, but not during, a hypoxic/hypoglycemic insult. The very dramatic difference between withdrawing DHPG, 2 and 1 min before the insult is most surprising, showing that the protective mechanism can be readily and rapidly switched off. Since it seems unlikely that PKC inactivation would occur in that short an interval, our data suggest that mGluR occupancy plus PKC activation may be needed to provide neuroprotection. Consistent with this hypothesis, PKC activation alone by TPA did not result in neuroprotection. However, failure of TPA to induce protection may also be related to the age of the animal since phorbol esters have been reported to be sufficient to elicit neuroprotection in slices from younger rats (Pizzi et al., 1996b; Small et al., 1996).

In summary, our study demonstrates that the selective activation of group I mGluRs by DHPG is sufficient to protect CA1 neurons in rat hippocampal slices from hypoxic/hypoglycemia-induced loss of synaptic transmission. In order to exert neuroprotection, group I mGluRs must be activated immediately before or right at the onset of the hypoxic/hypoglycemic event. The protective mechanism involved depends on both activation of PKC and occupancy of either mGluR or another DHPG-sensitive receptor.

Acknowledgements

The authors wish to thank Sabine Hartmann and Heidi Herold for expert technical assistance. This research was supported by the German Ministry for Science and Technology (BMBF) grant BEO 21-0319998B and a BIOMED 2 grant (PL95-0228).

References

Andersen, P., Bliss, T.V.P., Skrede, K.K., 1971. Unit analysis of hippocampal population spikes. Experimental Brain Research 13, 208–221.

Aniksztein, L., Otani, S., Ben-Ari, Y., 1992. Quisqualate metabotropic glutamate receptors modulate NMDA currents and facilitate induction of long-term potentiation through protein kinase C. European Journal of Neuroscience 4, 500–505.

Aronica, E., Dell'Albani, P., Condorelli, D.F., Nicoletti, F., Hack, N., Balazs, R., 1993. Mechanisms underlying developmental changes in the expression of metabotropic glutamate receptors in cultured cerebellar granule cells: homologous desensitization and interactive effects involving *N*-methyl-D-aspartate receptors. Molecular Pharmacology 44, 981–989.

Benveniste, H., Drejer, J., Schousboe, A., Diemer, N.H., 1984. Elevation of the extracellular concentrations of glutamate and aspartate in rat hippocampus during transient cerebral ischemia monitored by intracerebral microdialysis. Journal of Neurochemistry 43, 1369–1374.

Birrell, G.J., Gordon, M.P., Marcoux, F.W., 1993. (1*S*,3*R*)-1-aminocyclopentane-1,3-dicarboxylic acid attenuates *N*-methyl-D-aspartate-induced neuronal cell death in cortical cultures via a reduction in delayed Ca^{2+} accumulation. Neuropharmacology 32, 1351–1358.

Blanc, E., Vignes, M., Recasens, M., 1995. Protein kinase C differently regulates quisqualate- and 1*S*,3*R*-*trans* aminocyclopentane dicarboxylate-induced phosphoinositide hydrolysis during in vitro development of hippocampal neurons. Neurochemistry International 26, 623–633.

Boss, V.K., Conn, P.J., 1992. Metabotropic excitatory amino acid receptor activation stimulates phospholipase D in hippocampal slices. Journal of Neurochemistry 59, 2340–2343.

Brabet, I., Mary, S., Bockaert, J., Pin, J.-P., 1995. Phenylglycine derivatives discriminate between $mGluR_1$- and $mGluR_5$-mediated responses. Neuropharmacology 34, 895–903.

Bruno, V., Battaglia, G., Copani, A., Giffard, R.G., Raciti, G., Raffaele, R., Shinozaki, H., Nicoletti, F., 1995a. Activation of class II and class III metabotropic glutamate receptors protects cultured cortical neurons against excitotoxic degeneration. European Journal of Neuroscience 7, 1906–1913.

Bruno, V., Copani, A., Knopfel, T., Kuhn, R., Casabona, G., Dell'Albani, P., Condorelli, D.F., Nicoletti, F., 1995b. Activation of metabotropic glutamate receptors coupled to inositol phospholipid hydrolysis amplifies NMDA-induced neuronal degeneration in cultured cortical cells. Neuropharmacology 34, 1089–1098.

Bruno, V., Sureda, F.X., Storto, M., Casabona, G., Caruso, A., Knopfel, T., Kuhn, R., Nicoletti, F., 1997. The neuroprotective activity of group-II metabotropic glutamate receptors requires new protein synthesis and involves a glial-neuronal signaling. Journal of Neuroscience 17, 1891–1897.

Buisson, A., Yu, S.P., Choi, D.W., 1996. DCG-IV selectively attenuates rapidly triggered NMDA-induced neurotoxicity in cortical neurons. European Journal of Neuroscience 8, 138–143.

Buisson, A., Choi, D.W., 1995. The inhibitory mGluR agonist, s-4-carboxy-3-hydroxyphenyglycine selectively attenuates NMDA neurotoxicity and oxygen-glucose depriviation induced neuronal death. Neuropharmacology 34, 1081–1087.

Chiamulera, C., Albertini, P., Valerio, E., Reggiani, A., 1992. Activation of metabotropic receptors has a neuroprotective effect in a rodent model of focal ischaemia. European Journal of Pharmacology 216, 335–336.

Choi, D.W., Rothman, S.M., 1990. The role of glutamate neurotoxicity in hypoxic-ischemic neuronal death. Annual Review of Neuroscience 13, 171–182.

Durkin, J.P., Tremblay, R., Chakravarthy, B., Mealing, G., Morley, P., Small, D., Song, D., 1997. Evidence that the early loss of membrane protein kinase C is a necessary step in the excitatory amino acid-induced death of primary cortical neurons. Journal of Neurochemistry 68, 1400–1412.

Favaron, M., Manev, R.M., Candeo, P., Arban, R., Gabellini, N., Kozikowski, A.P., Manev, H., 1993. *Trans*-azetidine-2,4-dicarboxylic acid activates neuronal metabotropic glutamate receptors. NeuroReport 4, 967–970.

Fitzjohn, S.M., Irving, A.J., Palmer, M.J., Lodge, D., Collingridge, G.L., 1996. Activation of group I mGluRs potentiates NMDA response in rat hippocampal slices. Neuroscience Letters 203, 211–213.

Genazzani, A.A., L'Episcopo, M.R., Casabona, G., Shinozaki, H., Nicoletti, F., 1994. (2*S*,1'*R*,2'*R*,3'*R*)-2-(2,3-dicarboxycyclopropyl) glycine positively modulates metabotropic glutamate receptors coupled to polyphosphoinositide hydrolysis in rat hippocampal slices. Brain Research 659, 10–16.

Gereau IV, R.W., Conn, P.J., 1995. Roles of specific metabotropic glutamate receptor subtypes in regulation of hippocampal CA1

pyramidal cell excitability. Journal of Neurophysiology 74, 122–129.

Hara, H., Sukamoto, T., Kogure, K., 1993. Mechanisms and pathogenesis of ischemia-induced neuronal damage. Progress in Neurobiology 40, 645–670.

Hartley, D.M., Kurth, M.C., Bjerkness, L., Weiss, J.H., Choi, D.W., 1993. Glutamate-receptor induced $^{45}Ca^{2+}$ accumulation in cortical cell culture correlates with subsequent neuronal degeneration. Journal of Neuroscience 13, 1993–2000.

Hayashi, Y., Sekiyama, N., Nakanishi, S., Jane, D.E., Sunter, D.C., Birse, E.F., Udvarhelyi, P.M., Watkins, J.C., 1994. Analysis of agonist and antagonist activities of phenylglycine derivatives for different cloned metabotropic glutamate receptor subtypes. Journal of Neuroscience 14, 3370–3377.

Herbert, J.M., Augereau, J.M., Gleye, J., Maffrand, J.P., 1990. Chelerythrine is a potent and specific inhibitor of protein kinase C. Biochemical and Biophysical Research Communications 172, 993–999.

Hidaka, H., Kobayashi, R., 1992. Pharmacology of protein kinase inhibitors. Annual Review of Pharmacology and Toxicology 32, 377–397.

Holler, T.E., Cappel, E., Klein, J., Löffelholz, K., 1993. Glutamate activates phospholipase D in hippocampal slices of newborn and adult rats. Journal of Neurochemistry 61, 1569–1572.

Ito, I., Kohda, A., Tanabe, S., Hirose, E., Hayashi, M., Mitsunaga, S., Sugiyama, H., 1992. 3,5-dihydroxyphenylglycine: a potent agonist of metabotropic glutamate receptors. NeuroReport 3, 1013–1016.

Knöpfel, T., Sakaki, J., Flor, P., Baumann, P., Sacaan, A.I., Velicebeli, G., Kuhn, R., Allgeier, H., 1995. Profiling of *trans*-azetidine-2,4-dicarboxylic acid at the human metabotropic glutamate receptors hmGluR1b, 2, 4a, and 5a. European Journal of Pharmacology 288, 389–392.

Koh, J., Palmer, E., Cotman, C.W., 1991. Activation of the metabotropic glutamate receptor attenuates *N*-methyl-D-aspartate neurotoxicity in cortical cultures. Proceedings of the National Academy of Sciences of the United States of America 88, 9431–9435.

Kozikowski, A.P., Tückmantel, W., Reynolds, I.J., Wroblewski, J.T., 1993. Synthesis and bioactivity of a new class of rigid glutamate analogues. Modulators of the *N*-methyl-D-aspartate receptor. Journal of Medical Chemistry 33, 1561–1571.

Lester, R.A.J., Jahr, C.E., 1990. Quisqualate receptor-mediated depression of calcium currents in hippocampal neurons. Neuron 4, 741–749.

Manahan-Vaughan, D., Reiser, M., Pin, J.-P., Wilsch, V., Bockaert, J., Reymann, K.G., Riedel, G., 1996. Physiological and pharmacological profile of *trans*-azetidine-2,4-dicarboxylic acid: metabotropic glutamate receptor agonism and effects on long-term potentiation. Neuroscience 72, 999–1008.

Meldrum, B., 1992. Protection against ischemic brain damage by excitatory amino acid antagonists. In: Bazan, N.G., Braquet, P., Ginsberg, M.D. (Eds.), Advances in Neurochemistry 7. Plenum Press, New York, pp. 245–263.

Mitani, A., Kadoya, F., Nakamura, Y., Kataoka, K., 1991. Visualization of hypoxia-induced glutamate release in gerbil hippocampal slice. Neuroscience Letters 122, 167–170.

Montoliu, C., Llansola, M., Cucarella, C., Grisolia, S., Felipo, V., 1997. Activation of the metabotropic glutamate receptor mGluR5 prevents glutamate toxicity in primary cultures of cerebellar neurons. Journal of Pharmacology and Experimental Therapeutics 281, 643–647.

Nakanishi, S., 1994. Metabotropic glutamate receptors: synaptic transmission, modulation and plasticity. Neuron 13, 1031–1037.

Nicoll, R.A., 1988. The coupling of neurotransmitter receptors to ion channels in the brain. Science 240, 545–551.

Opitz, T., Richter, P., Reymann, K.G., 1994. The metabotropic glutamate receptor antagonist (+)-α-methyl-4-carboxyphenylglycine protects hippocampal CA1 neurons of the rat from in vitro hypoxia/hypoglycemia. Neuropharmacology 33, 715–717.

Opitz, T., Richter, P., Carter, A.J., Kozikowski, A.P., Shinozaki, H., Reymann, K.G., 1995. Metabotropic glutamate receptor subtypes differentially influence neuronal recovery from in vitro hypoxia/hypoglycemia in rat hippocampal slices. Neuroscience 68, 989–1001.

Opitz, T., Reymann, K.G., 1993. (1*S*, 3*R*)-ACPD protects synaptic transmission from hypoxia in hippocampal slices. Neuropharmacology 32, 103–104.

Pellegrini-Giampietro, D.E., Torregrossa, S.A., Moroni, F., 1996. Pharmacological characterization of metabotropic glutamate receptors coupled to phospholipase D in the rat hippocampus. British Journal of Pharmacology 118, 1035–1043.

Pin, J.-P., Duvoisin, R., 1995. The metabotropic glutamate receptors: structure and function. Neuropharmacology 34, 1–26.

Pisani, A., Calabresi, P., Centonze, D., Bernardi, G., 1997. Enhancement of NMDA responses by group I metabotropic glutamate receptor activation in striatal neurons. British Journal of Pharmacology 120, 1007–1014.

Pizzi, M., Consolandi, O., Memo, M., Spano, P., 1996a. Activation of multiple metabotropic glutamate receptor subtypes prevents NMDA-induced excitotoxicity in rat hippocampal slices. European Journal of Neuroscience 8, 1516–1521.

Pizzi, M., Galli, P., Consolandi, O., Arrighi, V., Memo, M., Spano, P.F., 1996b. Metabotropic and ionotropic transducers of glutamate signal inversely control cytoplasmic Ca^{2+} concentration and excitotoxicity in cultured cerebellar granule cells: pivotal role of protein kinase C. Molecular Pharmacology 49, 586–594.

Rhee, S.G., Choi, K.D., 1992. Regulation of inositol phospholipid-specific phospholipase C isozymes. Journal of Biological Chemistry 267, 12393–12396.

Sacaan, A.I., Schoepp, D.D., 1992. Activation of hippocampal metabotropic excitatory amino acid receptors leads to seizures and neuronal damage. Neuroscience Letters 139, 77–82.

Schoepp, D.D., Goldsworthy, J., Johnson, B.G., Salhoff, C.R., Baker, S.R., 1994. 3,5-Dihydroxyphenylglycine is a highly selective agonist for phosphoinositide-linked metabotropic glutamate receptors in rat hippocampus. Journal of Neurochemistry 63, 769–772.

Sekiyama, N., Hayashi, Y., Nakanishi, S., Jane, D.E., Tse, H.W., Birse, E.F., Watkins, J.C., 1996. Structure-activity relationships of new agonists and antagonists of different metabotropic glutamate receptor subtypes. British Journal of Pharmacology 117, 1493–1503.

Small, D.L., Monette, R., Chakravarthy, B., Durkin, J., Barbe, G., Mealing, G., Morley, P., Buchan, A.M., 1996. Mechanisms of 1*S*,3*R*-ACPD-induced neuroprotection in rat hippocampal slices subjected to oxygen and glucose deprivation. Neuropharmacology 35, 1037–1048.

Tamaoki, T., 1991. Use and specificity of staurosporine, UCN-01, and calphostin C as protein kinase inhibitors. Methods in Enzymology 201, 340–347.

Tizzano, J.P., Griffey, K.I., Johnson, J.A., Fix, A.S., Helton, D.R., Schoepp, D.D., 1993. Intracerebral 1*S*, 3*R*-1-aminocyclopentane-1,3-dicarboxylic acid (1*S*,3*R*-ACPD) produces limbic seizures that are not blocked by ionotropic glutamate receptor antagonists. Neuroscience Letters 162, 12–16.

Tizzano, J.P., Griffey, K.I., Schoepp, D.D., 1995. Induction or protection of limbic seizures in mice by mGluR subtype selective agonists. Neuropharmacology 34, 1063–1067.

Urenjak, J., Obrenovitch, T.P., 1996. Pharmacological modulation of voltage-gated Na^+ channels: a rational and effective strategy against ischemic brain damage. Pharmacological Reviews 48, 21–67.

Yu, S.P., Sensi, S.L., Canzoniero, L.M., Buisson, A., Choi, D.W., 1997. Membrane-delimited modulation of NMDA currents by metabotropic glutamate receptor subtypes 1/5 in cultured mouse cortical neurons. Journal of Physiology (London) 499, 721–732.

Pergamon

Neuropharmacology 40 (2001) 1–9

NEURO PHARMACOLOGY

www.elsevier.com/locate/neuropharm

Metabotropic glutamate receptor subtype 5 (mGlu5) and nociceptive function
I. Selective blockade of mGlu5 receptors in models of acute, persistent and chronic pain

K. Walker [a, b,*], M. Bowes [a, b], M. Panesar [a, b], A. Davis [a, b], C. Gentry [a, b], A. Kesingland [a, b], F. Gasparini [a], W. Spooren [a], N. Stoehr [a], A. Pagano [a, d], P.J. Flor [a], I. Vranesic [a], K. Lingenhoehl [a], E.C. Johnson [c], M. Varney [c], L. Urban [a, b], R. Kuhn [a]

[a] *Nervous System Research, Novartis Pharma AG, CH-4002 Basle, Switzerland*
[b] *Novartis Institute for Medical Sciences, Novartis Pharma AG, 5 Gower Place, London WC1E 6BN, UK*
[c] *SIBIA Neurosciences, 505 Coast Boulevard South, La Jolla, CA 92037-4631, USA*
[d] *Departimento di Scienze Chimiche, Universita di Catania, Catania, Italy*

Received 22 February 2000; received in revised form 14 June 2000; accepted 20 June 2000

Abstract

The excitatory neurotransmitter, glutamate, is particularly important in the transmission of pain information in the nervous system through the activation of ionotropic and metabotropic glutamate receptors. A potent, subtype-selective antagonist of the metabotropic glutamate-5 (mGlu5) receptor, 2-methyl-6-(phenylethynyl)-pyridine (MPEP), has now been discovered that has effective anti-hyperalgesic effects in models of inflammatory pain. MPEP did not affect rotarod locomotor performance, or normal responses to noxious mechanical or thermal stimulation in naïve rats. However, in models of inflammatory pain, systemic administration of MPEP produced effective reversal of mechanical hyperalgesia without affecting inflammatory oedema. In contrast to the non-steroidal anti-inflammatory drugs, indomethacin and diclofenac, the maximal anti-hyperalgesic effects of orally administered MPEP were observed without acute erosion of the gastric mucosa. In contrast to its effects in models of inflammatory pain, MPEP did not produce significant reversal of mechanical hyperalgesia in a rat model of neuropathic pain.

Keywords: Metabotropic glutamate receptor; mGlu5 antagonist; MPEP; Pain; Inflammatory hyperalgesia

1. Introduction

Glutamate has long been recognised to play a principal role in the transmission of pain within the nervous system (Dickenson et al., 1997). The actions of glutamate are mediated either through interaction with ionotropic glutamate (iGlu) receptor channels or by G protein-coupled metabotropic glutamate (mGlu) receptors that are linked to the modulation of second messenger systems (Salt, 1986; Baranauskas and Nistri, 1998). A specific role for group I mGlu receptors (mGlu1 and mGlu5 receptors) in nociceptive processing has been demonstrated by pharmacological, immunohistochemical and in situ hybridisation (Vidnyanszky et al., 1994; Romano et al., 1995, 1996; Valerio et al., 1997; Fisher and Coderre, 1998; Boxall et al., 1998a; Berthele et al., 1999; Jia et al., 1999). A role of dorsal horn group I mGlu receptors, particularly the mGlu1 receptor, in acute nociception has been described in behavioural (Fisher and Coderre, 1996a,b; Young et al., 1997; Fisher et al., 1998) and electrophysiological studies in vitro (Boxall et al., 1998b) or in vivo (Neugebauer et al., 1999). Both mGlu1 and mGlu5 receptor subtypes are functionally expressed in the rat ventrobasal thalamus (Salt et al., 1999a,b). mGlu1 receptor antagonists have been shown to reduce responses of single rat thalamic somatosensory neurones excited by the application of a

* Corresponding author. Tel.: +44-20-7333-2143; fax: +44-20-7387-4116.
E-mail address: kath.walker@pharma.novartis.com (K. Walker).

0028-3908/01/$ - see front matter
PII: S0028-3908(00)00113-1

noxious thermal stimulus to the receptive field (Salt and Turner, 1998).

Nevertheless, the lack of subtype-selective agonists and antagonists has made it difficult to further define the respective roles of mGlu1 and particularly mGlu5 receptors in nociceptive processes. Recently, the use of screening assays based on agonist-induced changes in intracellular calcium concentrations or phosphoinositide (PI) hydrolysis in a cell line expressing the human mGlu5a (hmGlu5a) receptor led to the discovery of 2-methyl-6-(phenylazo)-pyridin-3-ol, a selective antagonist of the human mGlu5 receptor (Daggett et al., 1995; Veliçelebi et al., 1998; Varney et al., 1999). Derivatisation of this compound produced the more potent antagonist, 2-methyl-6-(phenylethynyl)-pyridine (MPEP), with an IC_{50} of 32 nM on the human mGlu5a receptor in the PI hydrolysis assay (Gasparini et al., 1999). MPEP inhibited dihydroxyphenylglycine (DHPG)-stimulated PI hydrolysis in neonatal rat brain slices with potency and selectivity similar to that observed for human mGlu5 receptors (Gasparini et al., 1999).

In this study we have examined the effects of selective antagonism of the mGlu5 receptor in rat models of pain. Chronic pain syndromes, such as those associated with persistent inflammation or nerve injury, have been shown to differ dramatically in terms of their receptor pharmacology and their therapeutic response to different pharmaceutical agents (Walker et al., 1999). Therefore, we tested the effects of systemic mGlu5 antagonist treatment in a variety of rat pain models, including acute, inflammatory and neuropathic pain, where it was compared to drugs with proven efficacy in comparable human chronic pain syndromes. Systemic mGlu5 antagonist treatment produced significant reversal of inflammatory hyperalgesia in the absence of locomotor side effects, as measured in the rat rotarod assay. Acute gastric erosion is a side effect of many non-steroidal anti-inflammatory drugs (NSAIDs) used for the clinical treatment of inflammatory pain (Allison et al., 1992). Therefore, we compared the acute gastric erosion produced following oral administration of NSAIDs or MPEP in the rat.

2. Methods

2.1. Drugs

MPEP was synthesised as described previously (Gasparini et al., 1999), and was used in all experiments as its hydrochloride salt (molecular weight=229.7). MPEP, lamotrigine (kindly supplied by Glaxo Wellcome), indomethacin (Sigma; molecular weight = 357.8) or diclofenac (Novartis; molecular weight = 318.1) were administered orally (p.o.) in 0.5% methylcellulose (vol.=0.5 ml) and administered by gastric gavage. Morphine SO_4 (molecular weight=758.8) was administered subcutaneously (s.c.) in 0.9% saline (1 ml/kg).

2.2. Models of pain

All animal procedures were carried out in accordance with the UK Animals (Scientific Procedures) Act 1986 and associated guidelines. Male Sprague–Dawley rats (180–220 g; Charles River, UK), six per group, were used in all experiments. Animals were housed in groups of six and had free access to food and water at all times, except prior to oral administration of drugs when food was removed for 12 h before and returned 1 h after dosing. For comparison with compound-treated groups, animals treated with the appropriate drug vehicle were included in each experiment. The volume of administration was identical for vehicle- and compound-treated rats. Vehicle-treated rats were identical to compound-treated rats with respect to all other experimental procedures.

To assess the actions of drugs on acute nociception, the rat tail flick and paw pressure tests were employed. For the tail flick test (D'Amour and Smith, 1941), rats were placed inside a cotton pouch and the tail exposed to a focused beam of radiant heat at a point 3 cm from the tip using a tail flick unit (7360, Ugo Basile, Italy). Tail flick latencies were defined as the interval between the onset of the thermal stimulus and the flick of the tail. Animals not responding within 15 s were removed from the tail flick unit and assigned a withdrawal latency of 15 s. Tail flick latencies were measured immediately before (pre-treatment) and 1, 3 and 6 h following drug administration. Data were expressed as tail flick latency (s), and the percentage of the maximal possible effect (15 s) was calculated as follows:

$$\%MPE=[(\text{post-drug latency}-\text{pre-drug latency})/(15\text{ s}-\text{pre-drug latency})]\times 100.$$

Hind paw withdrawal threshold (PWT) to a noxious mechanical stimulus was determined using the paw pressure technique (Stein et al., 1988). The analgesymeter (7200, Ugo Basile, Italy) employed a wedge-shaped probe (area 1.75 mm^2). Cut off was set at 250 g and the end point was taken as paw withdrawal. PWTs were measured before (pre-treatment) and 1, 3 and 6 h following drug administration. Data analysis was performed on the untransformed latency or PWT data by analysis of variance (ANOVA) with repeated measures, and followed by Tukeys HSD post hoc analysis.

The Freund's complete adjuvant (FCA) model of inflammatory pain was used to measure effects of drugs on established inflammatory hyperalgesia in rats. FCA-induced inflammation of the rat hind paw is associated

with the development of persistent inflammatory mechanical hyperalgesia (decrease in PWT) and provides reliable prediction of the anti-hyperalgesic effects of clinically useful analgesic drugs (Bartho et al., 1990). The left hind paw of each animal was injected, subplantar, with 25 μl of Freund's complete adjuvant (Sigma). PWT were determined prior to FCA treatment (pre-treatment) and then again 24 h following FCA treatment (pre-dose). PWT were then measured 1, 3 and 6 h after drug administration. Percentage reversal of hyperalgesia for each animal was defined as:

[(post-dose PWT−pre-dose PWT)/(baseline−pre−dose PWT)]×100.

The carrageenin model of inflammation has been commonly used to examine the effects of drugs on the development of inflammatory hyperalgesia and oedema (Perrot et al., 1998). Carrageenin lambda (0.25 ml of a 1% solution; Sigma) was injected directly into the rat left hind paw. Oedema was measured as the change in hind paw volume (ml), measured using a plethysmemometer (Ugo Basile, Milan). Hind paw volume and PWT were measured, as described above, before carrageenin treatment (baseline), 2 h following carrageenin treatment (pre-dose) and 1, 3 and 6 h following drug administration.

The partial sciatic nerve ligation model of neuropathic pain was used to produce neuropathic hyperalgesia in rats (Seltzer et al., 1990). Rats weighed 140 g at time of nerve ligation. Partial ligation of the left sciatic nerve was performed under enflurane/O_2 inhalation anaesthesia. The left thigh of the rat was shaved and the sciatic nerve exposed at high thigh level through a small incision. The nerve was carefully cleared of surrounding connective tissues at a site near the trocanther just distal to the point at which the posterior biceps semitendinosus nerve branches off the common sciatic nerve. A 7-0 silk suture was inserted into the nerve with a 3/8 curved, reversed-cutting mini-needle, and tightly ligated so that the dorsal 1/3 to 1/2 of the nerve thickness was held within the ligature. The wound was closed with a single muscle suture (7-0 silk) and a Michelle clip. Following surgery the wound area was dusted with antibiotic powder. Sham-treated rats underwent identical surgical conditions except that the sciatic nerve was not manipulated. Experiments were carried out 11–15 days following ligation. The anti-epileptic drug, lamotrigine (30 mg/kg, p.o.), was used as a positive control (Hunter et al., 1997). PWT were measured, as described above, immediately prior to and 1, 3 and 6 h after drug administration. Percentage reversal of neuropathic hyperalgesia was defined as:

100−[(right pre-dose PWT−left post−dose PWT)/(right pre-dose PWT−left pre-dose PWT)]×100.

Data analysis was performed on the untransformed PWT data by ANOVA with repeated measures, and followed by Tukeys HSD post hoc analysis.

2.3. Locomotor activity

The accelerating rotarod (7750, Ugo Basile, Italy) was used to assess the effects of compounds on locomotor activity (Bristow et al., 1997). The initial rotarod speed was 4 rev/min, accelerating to 40 rev/min over 5 min. The duration of time spent on the rotarod was measured in seconds. Animals remaining on the rotarod for 300 s were removed from the apparatus and assigned a latency of 300 s. Rats were given a training trial on the rotarod 24 h prior to drug testing. Rotarod latencies were measured immediately prior to and 1, 3 and 6 h following drug administration. Percentage disruption was defined as:

100−(post-dose latency/pre−dose latency)×100.

In all experiments data analysis was performed on the untransformed latency data by ANOVA with repeated measures, and followed where appropriate by Tukeys HSD post hoc analysis. D_{50} was defined as the dose that produced 50% disruption of performance in the rotarod assay.

2.4. Acute gastric erosion

Gastrointestinal erosion is a common side effect of NSAID use (Allison et al., 1992). Rats received a single dose of MPEP, indomethacin, diclofenac or vehicle (0.5% methylcellulose). The dose (30 mg/kg) produced significant anti-hyperalgesic effects for all three compounds in the rat FCA model of inflammatory pain [Fig. 2(b)]. Rats were killed by cervical dislocation 4 h following administration. The stomach was removed, dissected along the greater curvature, rinsed with 0.9% saline (4°C) and gastric mucosal tissue was examined with a Nikon SMZ 10 Binocular Microscope. NSAID-induced acute gastric damage (Allison et al., 1992), which is usually presented as mucosal erosions (an erosion being defined as surface epithelial damage that does not penetrate the muscularis mucosa), was assessed on a severity scale of 0 to 8 (the acute gastric lesion index), where:

0	no morphological damage
1	one mucosal erosion
2	up to three mucosal erosions
3	up to six mucosal erosions
4	up to 10 mucosal erosions
5	up to 20 mucosal erosions

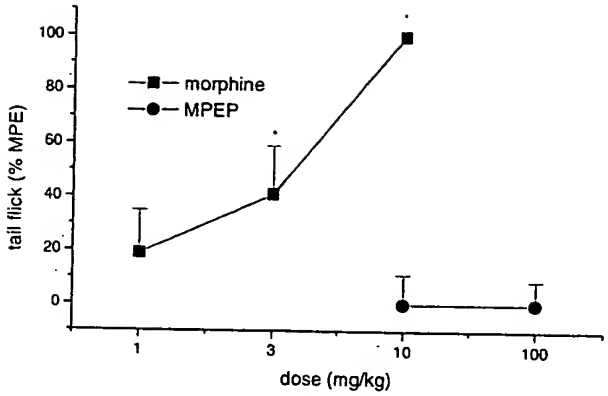

Fig. 1. MPEP does not affect tail flick latencies to noxious thermal stimulation in naïve rats (n=6/group). Tail flick latencies (%MPE; mean±SEM) were measured 1 h following treatment with morphine (1–10 mg/kg, s.c.) or MPEP (10 and 100 mg/kg, p.o.). An asterisk denotes a significant difference from vehicle-treated control ($P<0.05$).

6 up to 40 mucosal erosions
7 large haemorrhagic streaks up to 1 cm in length
8 the presence of one or more ulcers (an ulcer being defined as epithelial damage extending beyond the mucosa into the muscularis mucosa).

Statistical analysis was performed using the Mann–Whitney test ($P<0.05$).

3. Results

3.1. Tests of acute nociception

MPEP did not affect behavioural responses to noxious thermal or mechanical stimulation in naïve rats. The tail flick latencies of naïve rats were unaffected by p.o. administration of MPEP (10 and 100 mg/kg) or the vehicle, whereas morphine (1–10 mg/kg, s.c.) produced a dose-dependent increase in tail flick latency (Fig. 1). MPEP (3–100 mg/kg, p.o.) did not affect the PWT of rats at 1 or 3 h following administration compared with the vehicle group (Table 1).

3.2. Inflammatory hyperalgesia

FCA treatment produced a significant reduction in PWT [mean±standard error of the mean (SEM)] in all animals 24 h following treatment (55.3±4.1 g) compared with their baseline PWT (145.5±3.3 g). Administration of MPEP (1–100 mg/kg, p.o.) dose-dependently reversed established mechanical hyperalgesia in the FCA-inflamed rat hind paw [Fig. 2(a) and (b)]. Reversal of mechanical hyperalgesia was produced between 1 and 5 h following p.o. administration of MPEP; however, all animals displayed their pre-drug paw withdrawal thresholds by 24 h following administration [Fig. 2(a)]. At the highest dose tested (100 mg/kg, p.o.) MPEP produced a maximal 70% reversal of mechanical hyperalgesia (3 and 5 h following administration), making the overall efficacy of MPEP in this model superior to that of the NSAIDs, indomethacin and diclofenac [Fig. 2(b)]. Morphine (s.c.) produced the most potent anti-hyperalgesic effects in FCA-treated rats, with an ED_{50} value of 4.4 mg/kg 3 h following s.c. administration. However, estimation of morphine's efficacy was prevented by the appearance of severe sedation that interfered with behavioral measurements at the highest dose (10 mg/kg, s.c., see Section 3.4). Although MPEP produced effective reversal of inflammatory hyperalgesia, it was much less potent than morphine, with an ED_{50} value of 29 mg/kg 3 h following oral administration.

MPEP (3–100 mg/kg, p.o.) or diclofenac (1–30 mg/kg) reversed carrageenin-induced mechanical hyperalgesia with similar efficacy (Fig. 3). Diclofenac was 10 times more potent than MPEP against mechanical hyperalgesia. Diclofenac produced significant inhibition of carrageenin-induced oedema (increased paw volume) in the same rats that showed anti-hyperalgesic effects. In contrast, although MPEP reversed carrageenin-induced hyperalgesia, it did not affect hind paw oedema in the same rats (Fig. 3).

3.3. Neuropathic hyperalgesia

Mechanical hyperalgesia was observed in all rats 11–15 days following partial ligation of the sciatic nerve, as previously described (Seltzer et al., 1990). PWT for

Table 1
Mean PWT of naïve rats 1 and 3 h following oral administration of MPEP (n=6/group)

MPEP dose (mg/kg, p.o.)	PWT (g), 1 h	SEM	PWT (g), 3 h	SEM
0	110	1.4	111.6	1.8
3	110	2	110.8	1.6
10	111.6	1.8	111.6	1.1
30	112.5	2.7	110.8	3.7
100	110.8	1.6	111.6	1.1

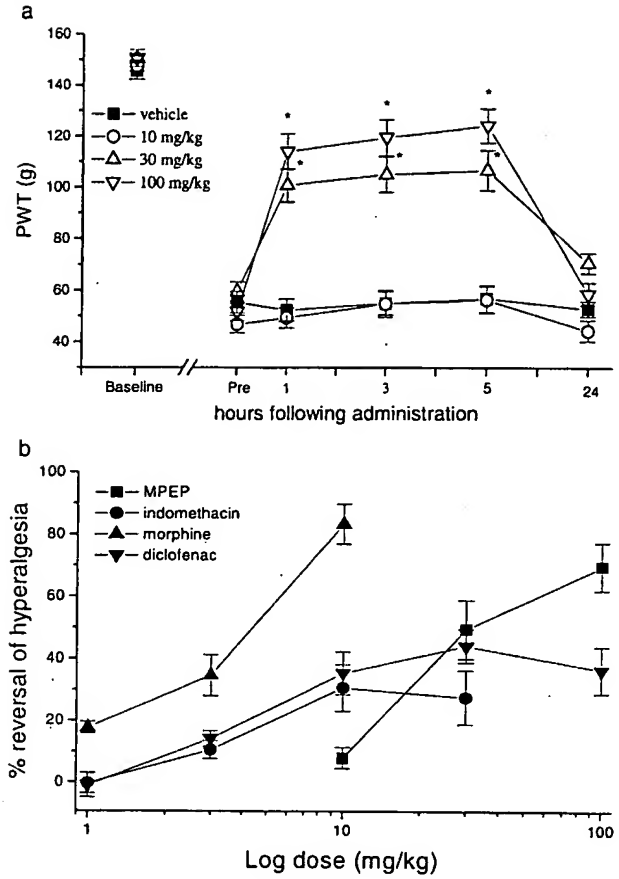

Fig. 2. (a) Reversal of FCA-induced mechanical hyperalgesia (mean±SEM) in the inflamed rat hind paw following a single oral dose of vehicle or MPEP (n=6/group). An asterisk denotes a significant difference from control (P<0.05). (b) Comparison of the effects of morphine (1–10 mg/kg, s.c.), indomethacin (1–30 mg/kg, p.o.), diclofenac (1–100 mg/kg, p.o.) and MPEP (10–100 mg/kg, p.o.) on the reversal of mechanical hyperalgesia (mean±SEM) in the FCA-inflamed rat hind paw 3 h following a single dose. Sedation was observed in all rats following treatment with morphine (10 mg/kg, s.c.).

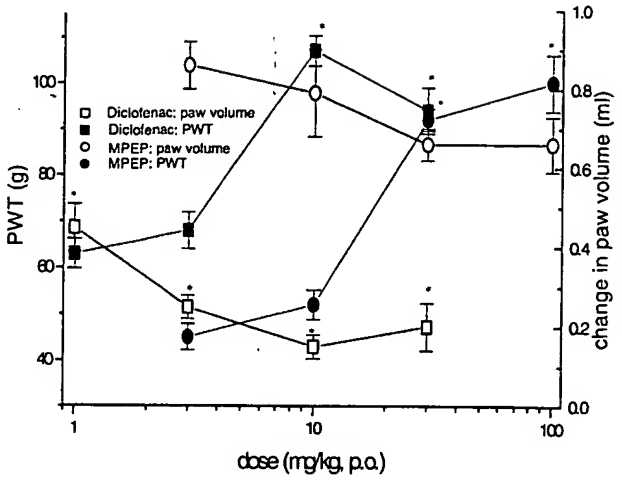

Fig. 3. Inhibition (mean±SEM) of carrageenin-induced mechanical hyperalgesia (closed symbols) or increased paw volume (open symbols) in the inflamed rat hind paw following administration of diclofenac (squares; 1–30 mg/kg, p.o.) or MPEP (circles; 3–100 mg/kg, p.o.). The same animals were used for mechanical hyperalgesia and paw volume measurements (n=6/group). An asterisk denotes a significant difference from vehicle-treated control (P<0.05).

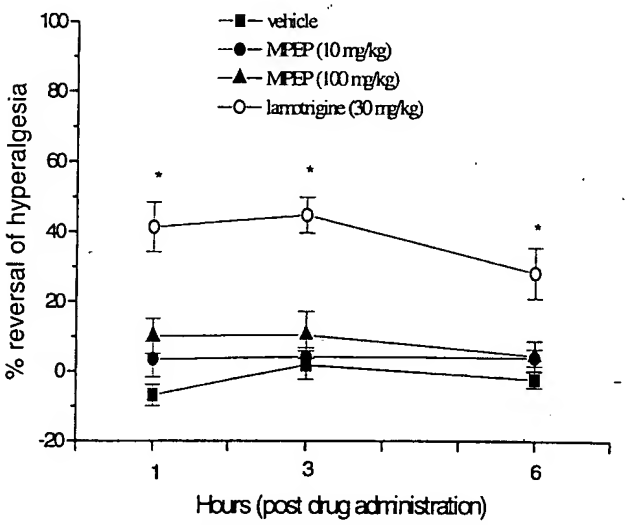

Fig. 4. Reversal (mean±SEM) of neuropathic hyperalgesia in rats by single p.o. administration of lamotrigine, but not MPEP, 14 days following partial ligation of the sciatic nerve (n=6/group). An asterisk denotes a significant difference from vehicle-treated control (P<0.05).

sham-treated rats 11–15 days following treatment ranged from 100 to 105 g, and did not differ significantly from those of age-matched naïve rats (105–112 g). The PWT (mean±SEM) of the partially denervated hind paw prior to drug administration was 66.6±2.4 g, whereas the PWT of the non-ligated hind paw was 103.3±2.1 g. The non-selective sodium channel blocker, lamotrigine (30 mg/kg, p.o.), produced significant reversal of mechanical hyperalgesia (PWT in ligated hind paw=81.6±2.4 g, 1 h following administration) in the partially denervated hind paw, from 1 to 6 h following a single administration 14 days following partial ligation of the sciatic nerve. MPEP (10 and 100 mg/kg, p.o.) had no effect on mechanical hyperalgesia following a single administration, 14 days following partial ligation of the rat sciatic nerve (Fig. 4).

3.4. Locomotor activity

Although morphine is well known as a potent analgesic drug, behavioural assessment of the anti-hyperalgesic effects of morphine in rodents is often impaired by the appearance of severe sedation within the analgesic dose range. The sedative effects of morphine have also been shown to interfere with locomotor performance in the rotarod assay (Kissin et al., 1990). In this study morphine (1–10 mg/kg, s.c.) dose-dependently disrupted per-

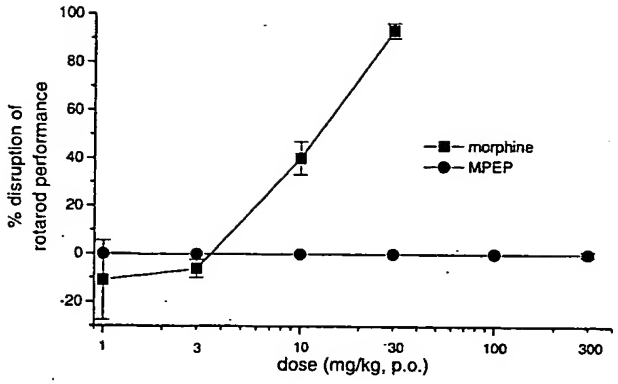

Fig. 5. Disruption (mean±SEM) of rotarod performance in rats (n=6/group) 1 h following treatment with morphine (1–30 mg/kg, s.c.). Rats treated with MPEP (1–300 mg/kg, p.o.) showed no disruption of rotarod performance. An asterisk denotes a significant difference from vehicle-treated control (P<0.05).

formance in the rotorod assay with a D_{50} value of 12.3 mg/kg; however, rats treated with MPEP (1–300 mg/kg, p.o.) all performed the maximal duration of the rotarod assay without disruption of performance at any dose (Fig. 5).

3.5. Acute gastric erosion

All rats treated with a single oral dose of indomethacin or diclofenac (30 mg/kg) showed evidence of acute damage to the mucosa (Fig. 6). This damage consisted of more than six mucosal erosions and in several rats large haemorrhagic lesions and evidence of blood in the stomach were noted. Single administration of MPEP (30 mg/kg, p.o.) did not produce evidence of acute gastric erosion; however, one rat treated with vehicle alone was found to have a single mucosal erosion (intensity "1" on the lesion index).

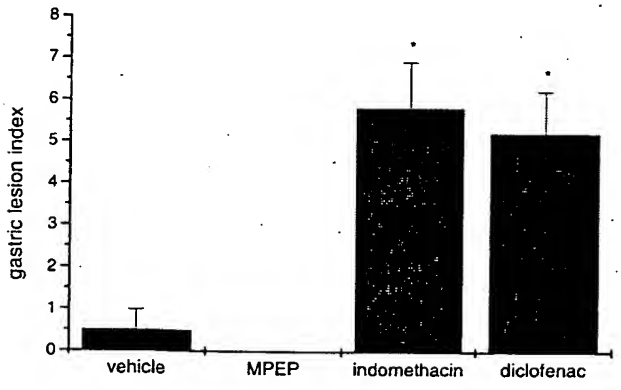

Fig. 6. Induction of acute gastric erosion (mean±SEM) in rats 4 h following single p.o. administration of MPEP (30 mg/kg, n=6), indomethacin (30 mg/kg, n=6) or diclofenac (30 mg/kg, n=6). None of the rats treated with MPEP showed evidence of acute gastric damage. An asterisk denotes a significant difference from vehicle-treated control (P<0.05).

4. Discussion

Traditional therapies for chronic pain are based on two well-established classes of analgesics, opioids and non-steroidal anti-inflammatory drugs. Both of these classes have significant shortcomings, particularly with respect to their undesirable side effects. The use of opioid analgesics is limited by their sedative, respiratory and gastrointestinal side effects as well as their abuse potential, whereas chronic NSAID use is restricted by serious gastrointestinal or renal side effects. These problems have led to new approaches focusing on the discovery of novel molecular and pharmacological mechanisms of nociceptive modulation that will allow the development of new classes of pain-relieving drugs, without such undesirable side effects.

In this study we show that systemic administration of MPEP produced reversal of inflammatory hyperalgesia. In contrast to its effects on inflammatory hyperalgesia, mGlu5 receptor antagonist treatment has no effect on normal responses to noxious stimulation. In this respect an mGlu5 receptor antagonist does not produce an opioid-like profile in assays of acute nociception, and therefore cannot be considered as a true analgesic drug. Instead, MPEP acted solely against the pain that accompanies inflammatory pathology, as defined by the dose-dependent reversal of both FCA- and carrageenin-induced hyperalgesia. It is notable that MPEP was equally effective against hyperalgesia whether it was associated with acute inflammatory processes, as in the case of the carrageenin model, or when animals were treated with MPEP 24 h following FCA treatment, when inflammation is established.

In contrast to the potent anti-inflammatory effects of diclofenac, MPEP did not affect inflammatory oedema formation. These findings are consistent with those of Fiorentino et al. (1999), who demonstrated that a peripheral injection of glutamate induced behavioural responses associated with pain but did not induce inflammation or plasma extravasation. These results suggest that although excitatory amino acids play a role in the sensitisation of primary afferent neurones during inflammation, they may not play as important a role in other aspects of inflammation.

In contrast to its efficacy in models of inflammatory pain, MPEP did not affect hyperalgesia associated with nerve injury. In this respect the role of mGlu5 receptors in nociception may differ from that proposed for the mGlu1 receptor. Antisense ablation of the mGlu1 receptor has been shown to reduce cold allodynia associated with nerve injury in the rat (Young et al., 1998).

A particular role of mGlu5 receptors in pain modulation is supported by pharmacological studies using group I mGlu receptor agonists and antagonists. In the brain, the use of phenylglycine antagonists has demonstrated that group I mGlu receptors are involved in

nociceptive responses of neurones of the ventrobasal thalamus (Eaton et al., 1993; Salt and Eaton, 1994; Salt and Turner, 1998). Glutamate is the main excitatory neurotransmitter at the first modulatory site in the spinal dorsal horn and plays a critical role in the transmission of nociceptive sensory information to the brain. The exact role of dorsal horn mGlu receptors in this process is still poorly understood, but there is an emerging consensus that they may be involved in the modulation of ionotropic glutamate receptor-mediated responses (Boxall et al., 1998a,b; Alagarsamy et al., 1999a,b). Activation of metabotropic receptors has been shown to potentiate *N*-methyl-D-aspartate (NMDA) and α-amino-3-hydroxy-5-methyl-4-isoxazole propionic acid (AMPA) responses in the rat dorsal horn and co-activation of AMPA and mGlu receptors in the dorsal horn produces mechanical hyperalgesia in the rat (Bleakman et al., 1992; Cerne and Randic, 1992; Fisher and Coderre, 1996b). Group I selective mGlu agonists, such as DHPG and (R5)-2-chloro-5-hydroxyphenylglycine (CHPG) (Schoepp et al., 1999), have been used to show that activation of spinal group 1 mGlu receptors, particularly the mGlu1 receptor, produces behaviours indicative of nociception (Fisher and Coderre, 1996a, 1998) or potentiates the behavioural and electrophysiological responses associated with inflammation in rats (Neugebauer et al., 1994; Young et al., 1997; Neugebauer et al., 1999). The ability of systemically administered MPEP to cross the blood–brain barrier has been demonstrated using in vivo electrophysiological approaches in which the effects of centrally applied mGlu receptor agonists were antagonised by intravenously administered MPEP (Gasparini et al., 1999; Salt et al., 1999a,b).

In addition to the location of mGlu5 receptors within spinal and brain components of the nociceptive pathway, mGlu5 antagonists may have potential to exert effects on nociceptive transmission at the level of peripheral primary afferent neurons (see Walker et al., accompanying manuscript). Crawford et al. (2000) have recently demonstrated the stimulation of increases in intracellular calcium concentrations in rat cultured dorsal root ganglion neurons by the mGlu5 agonist, CHPG. Furthermore, the endogenous agonist, glutamate, is known to evoke mechanical hyperalgesia following injection to the naïve rat hind paw (Coggeshall et al., 1997). We have found that the injection of a selective mGlu5 agonist into the naïve rat hind paw also produces mechanical hyperalgesia and that both agonist-induced and inflammatory hyperalgesia can be inhibited by pre-treatment of the rat hind paw with MPEP (see Walker et al., accompanying manuscript). These and other pharmacological, electrophysiological and immunohistochemical experiments indicate that perpherally expressed mGlu5 receptors play an important role in the development of inflammatory hyperalgesia in the rat (see Walker et al., accompanying manuscript).

In our experiments MPEP produced reversal of inflammatory hyperalgesia with similar efficacy to both NSAIDs and morphine, but in the absence of locomotor side effects or acute gastric toxicity. Compounds that can selectively antagonise mGlu5 receptors may provide a new mechanistic approach for the management of pain associated with inflammatory syndromes that avoids the potential for adverse side effects on the central nervous system and acute gastrointestinal toxicity.

Acknowledgements

We gratefully acknowledge the assistance of R. Brom, M. Heinrich, W. Inderbitzin, T. Leonhardt, S. Litschig, S. Lukic, H.P. Mueller, D. Rüegg and C. Stierlin. We also thank Dr Stuart Bevan and Professor Humphrey Rang for their help during the preparation of this manuscript. The anti-epileptic drug, lamotrigine, was kindly supplied by Glaxo Wellcome.

References

Alagarsamy, S., Marino, M.J., Rouse, S.T., Gereau, R.W., Heinemann, S.F., Conn, P.J., 1999a. Activation of NMDA receptors reverses desensitization of mGluR5 in native and recombinant systems. Nature Neuroscience 2, 234–240.

Alagarsamy, S., Rouse, S.T., Gereau, R.W., Heinemann, S.F., Smith, Y., Conn, P.J., 1999b. Activation of *N*-methyl-D-aspartate receptors reverses desensitization of metabotropic glutamate receptor, mGluR5, in native and recombinant systems. Annals of the New York Academy of Sciences 868, 526–530.

Allison, M.C., Howatson, A.G., Torrance, C.J., 1992. Gastrointestinal damage associated with the use of non-steroidal anti-inflammatory drugs. New England Journal of Medicine 327, 749–754.

Baranauskas, G., Nistri, A., 1998. Sensitization of pain pathways in the spinal cord: cellular mechanisms. Progress in Neurobiology 54, 349–365.

Bartho, L., Stein, C., Herz, A., 1990. Involvement of capsaicin-sensitive neurones in hyperalgesia and enhanced opioid antinociception in inflammation. Naunyn-Schmiedeberg's Archives of Pharmacology 342, 666–670.

Berthele, A., Boxall, S.J., Urban, A., Anneser, J.M.H., Zieglgansberger, W., Urban, L., Tolle, T.R., 1999. Distribution and developmental changes in metabotropic glutamate receptor messenger RNA expression in the rat lumbar spinal cord. Developmental Brain Research 112, 39–53.

Bleakman, D., Rusin, K.I., Chard, P.S., Glaum, S.R., Miller, R.J., 1992. Metabotropic glutamate receptors potentiate ionotropic glutamate receptors in the rat dorsal horn. Molecular Pharmacology 42, 192–196.

Boxall, S.J., Berthele, A., Laurie, D.J., Sommer, B., Zieglgansberger, W., Urban, L., Tolle, T.R., 1998a. Enhanced expression of metabotropic glutamate receptor 3 messenger RNA in the rat spinal cord during ultraviolet irradiation induced peripheral inflammation. Neuroscience 82, 591–602.

Boxall, S.J., Berthele, A., Tolle, T.R., Zieglgansberger, W., Urban, L., 1998b. mGluR activation reveals a tonic NMDA component in inflammatory hyperalgesia. Neuroreport 9, 1201–1203.

Bristow, L.J., Collinson, N., Cook, G.P., Curtis, N., Freedman, S.B., Kulagowski, J.J., Leeson, P.D., Patel, S., Ragan, C.I., Ridgil, M.,

Saywell, K.L., Tricklebank, M.D., 1997. L-745,870, a subtype selective dopamine D4 receptor antagonist, does not exhibit a neuroleptic profile in a rodent behavioural test. The Journal of Pharmacology and Experimental Therapeutics 233, 1256–1263.

Cerne, R., Randic, M., 1992. Modulation of AMPA and NMDA responses in rat spinal dorsal horn neurons by *trans*-1-aminocyclopentane-1,3-dicarboxylic acid. Neuroscience Letters 144, 180–184.

Coggeshall, R.E., Zhou, S., Carlton, S.M., 1997. Opioid receptors on peripheral sensory axons. Brain Research 764, 126–132.

Crawford, J.H., Wainwright, A., Heavens, R., Pollock, J., Duncan, M.J., Scott, R.H., Seabrook, G.R., 2000. Mobilization of intracellular Ca^{2+} by mGluR5 metabotropic glutamate receptor activation in neonatal rat cultured dorsal root ganglia neurones. Neuropharmacology 39, 621–630.

D'Amour, F.E., Smith, D.L., 1941. A method for determining loss of pain sensation. The Journal of Pharmacology and Experimental Therapeutics 72, 74–79.

Daggett, L.P., Sacaan, A.I., Akong, M., Rao, S.P., Hess, S.D., Liaw, C., Urrutia, A., Jachec, C., Ellis, S.B., Dreessen, J., Knopfel, T., Landwehrmeyer, G.B., Testa, C.M., Young, A.B., Varney, M., Johnson, E.C., Velicelebi, G., 1995. Molecular and functional characterization of recombinant human metabotropic glutamate receptor subtype 5. Neuropharmacology 34, 871–886.

Dickenson, A.H., Chapman, V., Green, G.M., 1997. The pharmacology of excitatory and inhibitory amino acid-mediated events in the transmission and modulation of pain in the spinal cord. General Pharmacology 28, 633–638.

Eaton, S.A., Birse, E.F., Wharton, B., Sunter, B., Udvarhelyi, P.M., Watkins, J.C., Salt, T.E., 1993. Mediation of thalamic sensory responses in vivo by ACPD-activated excitatory amino acid receptors. European Journal of Neuroscience 5, 186–189.

Fiorentino, M., Cairns, B.E., Hu, J.W., 1999. Development of inflammation after application of mustard oil or glutamate to the rat temporomandibular joint. Archives of Oral Biology 44, 27–32.

Fisher, K., Coderre, T.J., 1996a. The contribution of metabotropic glutamate receptors (mGluRs) to formalin-induced nociception. Pain 68, 255–263.

Fisher, K., Coderre, T.J., 1996b. Comparison of nociceptive effects produced by intrathecal administration of mGluR agonists. Neuroreport 7, 2743–2747.

Fisher, K., Coderre, T.J., 1998. Hyperalgesia and allodynia induced by intrathecal (*RS*)-dihydroxyphenylglycine in rats. Neuroreport 9, 1169–1172.

Fisher, K., Fundytus, M.E., Cahill, C.M., Coderre, T.J., 1998. Intrathecal administration of the mGluR compound, (*S*)-4CPG, attenuates hyperalgesia and allodynia associated with sciatic nerve constriction injury in rats. Pain 77, 59–66.

Gasparini, F., Lingenhoehl, K., Stoehr, N., Flor, P.J., Heinrich, M., Vranesic, I., Biollaz, M., Allgeier, H., Heckendorn, R., Urwyler, S., Varney, M.A., Johnson, E.C., Hess, S.D., Rao, S.P., Sacaan, A.I., Santori, E., Veliçelebi, G., Kuhn, R., 1999. 2-Methyl-6-(phenylethynyl)-pyridine (MPEP), a potent, selective and systemically active mGlu5 receptor antagonist. Neuropharmacology 38, 1493–1504.

Hunter, J.C., Gogas, K.R., Hedley, L.R., Jacobson, L.O., Kassotakis, L., Thompson, J., Fontana, D.J., 1997. The effect of novel anti-epileptic drugs in rat experimental models of acute and chronic pain. European Journal of Pharmacology 324, 153–160.

Jia, H., Rustioni, A., Valtschanoff, J.G., 1999. Metabotropic glutamate receptors in superficial laminae of the rat dorsal horn. Journal of Comparative Neurology 410, 627–642.

Kissin, I., Brown, P.T., Bradley, E.L., 1990. Sedative and hypnotic midazolam–morphine interactions in rats. Anesthesia and Analgesia 71, 137–143.

Neugebauer, V., Lucke, T., Schaible, H.G., 1994. Requirement of metabotropic glutamate receptors for the generation of inflammation-evoked hyperexcitability in rat spinal cord neurons. European Journal of Neuroscience 6, 1179–1186.

Neugebauer, V., Chen, P.S., Willis, W.D., 1999. Role of metabotropic glutamate receptor subtype mGluR1 in brief nociception and central sensitization of primate STT cells. Journal of Neurophysiology 82, 272–282.

Perrot, S., Idanpaan Heikkila, J.J., Guilbaud, G., Kayser, V., 1998. The enhancement of morphine antinociception by a CCKB receptor antagonist in the rat depends on the phase of inflammation and the intensity of carrageenin-induced hyperalgesia. Pain 74, 269–274.

Romano, C., Sesma, M.A., McDonald, C.T., O'Malley, K., Van den Pol, A.N., Olney, J.W., 1995. Distribution of metabotropic glutamate receptor mGluR5 immunoreactivity in rat brain. Journal of Comparative Neurology 355, 455–469.

Romano, C., Van den Pol, A.N., O'Malley, K., 1996. Enhanced early developmental expression of the metabotropic glutamate receptor mGluR5 in rat brain: protein, mRNA splice variants and regional distribution. Journal of Comparative Neurology 367, 403–412.

Salt, T.E., 1986. Mediation of thalamic sensory input by both NMDA receptors and non-NMDA receptors. Nature 322, 263–265.

Salt, T.E., Eaton, S.A., 1994. The function of metabotropic excitatory amino acid receptors in synaptic transmission in the thalamus: studies with novel phenylglycine antagonists. Neurochemistry International 24, 451–458.

Salt, T.E., Turner, J.P., 1998. Reduction of sensory and metabotropic glutamate receptor responses in the thalamus by the novel metabotropic glutamate receptor-1-selective antagonist *S*-2-methyl-4-carboxy-phenylglycine. Neuroscience 85, 655–658.

Salt, T.E., Binns, K.E., Turner, J.P., Gasparini, F., Kuhn, R., 1999a. Antagonism of the mGlu5 agonist 2-chloro-5-hydroxyphenylglycine by the novel selective mGlu5 antagonist 6-methyl-2(phenylethynyl)-pyridine (MPEP) in the thalamus. British Journal of Pharmacology 127, 1057–1059.

Salt, T.E., Turner, J.P., Kingston, A.E., 1999b. Evaluation of agonists and antagonists acting at Group I metabotropic glutamate receptors in the thalamus in vivo. Neuropharmacology 38, 1505–1510.

Schoepp, D.D., Jane, D.E., Monn, J.A., 1999. Pharmacological agents acting at subtypes of metabotropic glutamate receptors. Neuropharmacology 38, 1431–1476.

Seltzer, Z., Dubner, R., Shir, Y., 1990. A novel behavioral model of neuropathic pain disorders produced in rats by partial sciatic nerve injury. Pain 43, 205–218.

Stein, C., Millan, M.J., Herz, A., 1988. Unilateral inflammation of the hindpaw in rats as a model of prolonged noxious stimulation: alterations in behavior and nociceptive thresholds. Pharmacology Biochemistry and Behavior 31, 451–455.

Valerio, A., Rizzonelli, P., Paterlini, M., Moretto, G., Knopfel, T., Kuhn, R., Memo, M., Spano, P., 1997. mGluR5 metabotropic glutamate receptor distribution in rat and human spinal cord: a developmental study. Neuroscience Research 28, 49–57.

Varney, M., Cosford, N.D.P., Jachec, C., Rao, S.P., Sacaan, A.I., Lin, F.F., Bleicher, L., Santori, E., Flor, P.J., Allgeier, H., Gasparini, F., Kuhn, R., Hess, S.D., Veliçelebi, G., Johnson, E.C., 1999. SIB-1757 and SIB-1893: selective, non-competitive antagonists of metabotropic glutamate receptor type 5 (mGluR5). The Journal of Pharmacology and Experimental Therapeutics 290, 170–181.

Veliçelebi, G., Stauderman, K.A., Varney, M.A., Akong, M., Hess, S.D., Johnson, E.C., 1998. Fluorescence techniques for measuring ion channel activity. Methods in Enzymology 294, 20–47.

Vidnyanszky, Z., Hamori, J., Negyessy, L., Ruegg, D., Knopfel, T., Kuhn, R., Gorcs, T.J., 1994. Cellular and subcellular localization of the mGluR5a metabotropic glutamate receptor in rat spinal cord. Neuroreport 6, 209–213.

Walker, K., Fox, A., Urban, L., 1999. Animal models for pain research. Molecular Medicine Today 5, 319–321.

Young, M.R., Blackburn-Munro, G., Dickinson, T., Johnson, M.J., Anderson, H., Nakalembe, I.F., Feetwood-Walker, S.M., 1998.

Antisense ablation of type I metabotropic glutamate receptor mGluR(1) inhibits spinal nociceptive transmission. Journal of Neuroscience 18, 10180–10188.

Young, M.R., Fleetwood Walker, S.M., Dickinson, T., Blackburn Munro, G., Sparrow, H., Birch, P.J., Bountra, C., 1997. Behavioural and electrophysiological evidence supporting a role for group I metabotropic glutamate receptors in the mediation of nociceptive inputs to the rat spinal cord. Brain Research 777, 161–169.

Pergamon

Neuropharmacology 40 (2001) 10–19

NEURO PHARMACOLOGY

www.elsevier.com/locate/neuropharm

mGlu5 receptors and nociceptive function II. mGlu5 receptors functionally expressed on peripheral sensory neurones mediate inflammatory hyperalgesia

K. Walker [a, b,*], A. Reeve [a, b], M. Bowes [a, b], J. Winter [a, b], G. Wotherspoon [a, b], A. Davis [a, b], P. Schmid [c], F. Gasparini [a], R. Kuhn [a], L. Urban [a, b]

[a] *Novartis Pharma AG, Nervous System Research, CH-4002 Basle, Switzerland*
[b] *Novartis Institute for Medical Sciences, 5 Gower Place, London WC1E 6BN, UK*
[c] *Novartis Pharma AG, Dermatology Research, CH-4002 Basle, Switzerland*

Received 22 February 2000; received in revised form 15 June 2000; accepted 20 June 2000

Abstract

Previous studies have demonstrated that the metabotropic glutamate receptor subtype 5 (mGlu5 receptor) is expressed in the cell bodies of rat primary afferent neurones. We have further investigated the function and expression of mGlu5 receptors in primary afferent neurones, and their role in inflammatory nociception. Freund's complete adjuvant-induced inflammatory hyperalgesia of the rat hind paw was significantly reduced by intraplantar, but not by intracerebroventricular or intrathecal microinjection of the selective mGlu5 receptor antagonist, 2-methyl-6-(phenylethynyl)-pyridine (MPEP). Pharmacological comparison in vivo of the nociceptive effects of glutamate, and ionotropic and metabotropic glutamate (mGlu) receptor agonists applied to the rat hind paw, indicated that group I mGlu receptor agonists induce a dose-dependent decrease in paw withdrawal threshold (mechanical hyperalgesia). Group I mGlu agonist-induced hyperalgesia was inhibited by co-microinjection of MPEP, but not by the mGlu1 receptor antagonist (*S*)-4-carboxy-phenylglycine (4-CPG). Carrageenan-induced inflammatory hyperalgesia was inhibited by pre-treatment of the inflamed hind paw with MPEP, but not following MPEP injection into the contralateral hind paw. Dorsal horn neurones receiving peripheral nociceptive and non-nociceptive afferent input were recorded in anaesthetized rats following microinjection of CHPG into their peripheral receptive fields. CHPG significantly increased the frequency and duration of firing of dorsal horn wide dynamic range (WDR) neurones and this activity was prevented by co-administration of CHPG and MPEP into their receptive fields. Immunohistochemical experiments revealed the co-expression of mGlu5 receptor protein and βIII tubulin in skin from naive rats, indicating the constitutive expression of mGlu5 receptors on peripheral neurones. Double-labelling of adult rat DRG cells with mGlu5 receptor and vanilloid receptor subtype 1 antisera also supports the expression of mGlu5 receptors on peripheral nociceptive afferents. These results suggest that mGlu5 receptors expressed on the peripheral terminals of sensory neurones are involved in nociceptive processes and contribute to the hyperalgesia associated with inflammation.

Keywords: Metabotropic glutamate receptor; Ionotropic glutamate receptor; MPEP; Inflammation; Pain

1. Introduction

The actions of glutamate are mediated either through interaction with ionotropic glutamate (iGlu) receptor channels or by G protein-coupled metabotropic glutamate (mGlu) receptors that are linked to the modulation of second messenger systems (Salt, 1986; Knopfel et al., 1995; Conn and Pin, 1997). A specific role for group I mGlu receptors (mGlu1 and mGlu5) in nociceptive processing has been demonstrated by pharmacological, immunohistochemical and in situ hybridization studies (Fisher and Coderre, 1998; Salt and Turner, 1998; Boxall et al., 1998a; Jia et al., 1999). In addition to a role in pain transmission within the central nervous system, glutamate also excites peripheral nociceptive neurones

* Corresponding author. Tel.: +44-207-333-2143; fax: +44-207-387-4116.
E-mail address: kath.walker@pharma.novartis.com (K. Walker).

0028-3908/01/$ - see front matter
PII: S0028-3908(00)00114-3

(Carlton et al., 1995; Jackson et al., 1995; Lawand et al., 1997; Fiorentino et al., 1999). This effect has been attributed to the activation of peripherally expressed ionotropic glutamate receptors (Carlton et al., 1995; Jackson et al., 1995; Zhou et al., 1996; Davidson et al., 1997; Lawand et al., 1997).

In our first study (see Walker et al., 2001), we examined the effects of the selective mGlu5 receptor antagonist, 2-methyl-6-(phenylethynyl)-pyridine (MPEP: Gasparini et al., 1999) in models of pain. These experiments demonstrated that systemic administration of MPEP produced effective reversal of the hyperalgesia associated with inflammation, without affecting the normal behavioural responses to noxious stimulation in naive rats (see Walker et al., 2001).

The expression of the mGlu5 receptor in various regions of the brain and spinal cord has been studied in detail (Shigemoto et al., 1993; Romano et al., 1995; Valerio et al., 1997; Boxall et al., 1998b). Interestingly, Valerio and colleagues have shown that mGlu5 receptor protein is also expressed in small diameter rat DRG cells, and the superficial layers of the rat dorsal horn, suggesting that mGlu5 receptors are expressed at the central terminals of nociceptive afferents (Valerio et al., 1997). However, we hypothesized that mGlu5 receptors might also be functionally expressed at the peripheral terminals of primary nociceptive afferent neurones.

In this study we carried out pharmacological, electrophysiological and immunohistochemical experiments to further explore the possible site and mechanism of mGlu5 receptor-mediated antihyperalgesia. The purpose of these experiments was to: (1) determine the local CNS or peripheral site of action of MPEP that produces the most effective reversal of inflammatory hyperalgesia; (2) provide pharmacological evidence for the function of mGlu5 receptors, and their role in nociceptive processes, outside the CNS; and (3) provide immunohistological evidence for the expression of mGlu5 receptors by neurones in rat skin.

2. Methods

2.1. Drugs

MPEP was synthesized as described previously (Gasparini et al., 1999), and was used in all experiments as its hydrochloride salt (MW=229.7). (*RS*)-2-chloro-5-hydroxyphenylglycine (CHPG, MW=201.61), 3,5-dihydroxyphenylglycine (DHPG, MW=183.16), α-amino-3-hydroxy-5-methyl-4-isoxazolepropionic acid (AMPA, MW=186.17), *N*-methyl-D-aspartic acid (NMDA, MW=147.13), (*S*)-4-carboxy-phenylglycine (4-CPG, MW=195.17) and L-(+)-2-amino-4-phosphonobutyric acid (L-AP4, MW=183.1) are all described by Schoepp and colleagues (Schoepp et al., 1999) and were purchased from Tocris. LY314582 (MW=185.2) was synthesized according to the procedure described by Monn et al. (1997). L-Glutamate (Sigma), CHPG, DHPG, AMPA, LY3 14582, 4-CPG and morphine SO_4 were administered in 0.9% saline, whereas L-AP4 was administered in 30% DMSO/0.9% saline. MPEP was administered in 10% ethanol, 10% Tween 80 in saline. All compounds were microinjected at pH 7.0.

2.2. Animals and drug administration

All animal procedures were carried out in accordance with the UK Animals (Scientific Procedures) Act 1986 and associated guidelines. Male Sprague–Dawley rats (180–220 g; Charles River, UK), were used in all experiments. Animals were housed in groups of six and had free access to food and water at all times. Microinjections were made in rats briefly anaesthetized with enflurane (maximal duration of anaesthesia=10 min) via subdermal intraplantar (i.pl.), intrathecal (i.t.) and intracerebroventricular (i.c.v.) routes. I.pl. injections (10 μl bolus) were sub-dermal into the plantar surface of either naive or FCA-treated rat hind paws using a 26 gauge needle attached to a Hamilton syringe. For i.t. injections (10 μl bolus), the lumbar back of the anaesthetized rat was shaved, and the injections were made via a 26 gauge needle inserted into the tissue to one side of the L5 or L6 spinous process, as described previously (Hylden and Wilcox, 1980). I.c.v. (5 μl/2 min) microinjections were made using standard stereotaxic surgical techniques, as described previously (Walker et al., 1996). Following anaesthesia, rats were fixed to a Kopf stereotaxic frame and solutions were injected via a sterile glass microcapillary pipette (Sigma, No. P-0549), drawn to a fine point. The tip of the injector was placed at co-ordinates: 0.8 mm posterior to bregma, 1.4 mm lateral to the sagittal suture and 3.7 mm below the surface of the skull in the right lateral ventricle. Following the removal of the injector the skull was sealed with sterile bone wax and the scalp was sutured. Following the microinjection procedures described above, animals were placed on a warm pad until they had recovered from the anaesthetic.

2.3. Models of inflammatory pain

Hind paw withdrawal thresholds (PWT) to a noxious mechanical stimulus were determined using the paw pressure technique (Stein et al., 1988). The analgesymeter (7200, Ugo Basile, Italy) employed a wedge shaped probe (area 1.75 mm^2). Cut off was set at 250 g and the end point was taken as paw withdrawal. PWT were measured before and following drug administration, as indicated. Data analysis was performed on the untransformed latency or PWT data by ANOVA with repeated measures, and followed by Tukey's HSD post hoc analysis.

The Freund's complete adjuvant (FCA) model of inflammatory pain was used to measure effects of drugs on established inflammatory hyperalgesia in rats. FCA-induced inflammation of the rat hind paw is associated with the development of persistent inflammatory mechanical hyperalgesia (decrease in PWT; Bartho et al., 1990). The left hind paw of each animal was injected, sub-plantar, with 2.5 μl of Freund's complete adjuvant (Sigma). PWT were determined prior to FCA treatment (baseline) and then again 24 h following FCA treatment (pre-dose). PWT were then measured 1 and 3 h after drug administration. As a positive control for the i.t. and i.c.v. experiments, an additional group of FCA-treated rats received administration of morphine (10 nmole) via these routes.

The carrageenan model of inflammation has been commonly used to examine the effects of drugs on the development of inflammatory hyperalgesia (Perrot et al., 1998). MPEP was microinjected into a rat hind paw, as described above. Thirty minutes following MPEP administration, carrageenan lambda (0.25 ml of a 1% solution; Sigma) was injected directly into the same hind paw. PWT were measured, as described above, before carrageenan treatment (baseline), and 1 and 3 h following carrageenan administration.

2.4. In vivo electrophysiology

Recordings from dorsal horn neurones were made using the techniques described by Dickenson and colleagues (Dickenson and Sullivan, 1987). Male Sprague–Dawley rats (200–220 g) were anaesthetized with enflurane in a gaseous mixture of N_2O and O_2 (66 and 33%, respectively) throughout the experiment. The animal was held in a stereotaxic frame and a laminectomy performed over the lumbar segments L_1–L_3 to expose the spinal cord. Single wide dynamic range (WDR) neurones located in the deep (500–1000 μm) dorsal horn, with receptive fields in the rat hind paw, were isolated by inserting a praylene-coated tungsten electrode (A-M Systems, Inc., USA) into the spinal dorsal horn. The electrode was progressively moved through the dorsal horn, using a Significat, Scat-01 Ultrastepper (Digitimer, UK).

WDR neurones were identified for recording based on the existence of inputs from both high- and low-threshold sensory afferents. This was evaluated by, first, characterizing the responses of the neurone following mechanical stimulation to the peripheral receptive field in the hind paw with innocuous (light touch) and noxious (pinch) stimuli. Once a neurone was located in this way, further confirmation of its nociceptive afferent input was carried out by determining whether that the neurone received input from Aβ-, Aδ- and C-fibres. This was carried out by characterizing the responses evoked by transcutaneous electrical stimulation of the peripheral receptive field. This test consisted of 16 stimuli at 0.5 Hz with a 2 ms wide pulse, at three times C-fibre threshold (0.8–3 mA) to ensure activation of all categories of peripheral afferents. These responses were identified on the basis of latency and threshold: the responses to Aβ-fibre inputs were attributed to the 0–20 ms post-stimulus latency band, the Aδ-fibre responses to the 20–90 ms latency band, and the C-fibre evoked responses to the 90–300 ms latency band. Post-discharge of the neurone was attributed to the firing occurring in the latency band between 300 and 800 ms. Once this basic characterization of the WDR neurone was complete, electrodes were removed from the skin and either CHPG (51 μl bolus) or a mixture of CHPG and MPEP (5 μl bolus) was administered intracutaneously into the receptive field by injection via a 26 gauge needle attached to a Hamilton syringe. Action potentials were recorded over time as a rate recording in response to either of the above drug combinations. Responses of WDR neurones to the drug administration were measured as change of frequency of neuronal firing and the duration of altered firing rate after drug application (see Fig. 3). Student's *t*-test (paired, two-tailed) was used to test for significance for drug effects compared to vehicle effects ($P<0.05$).

2.5. Immunohistochemistry

Cryostat sections of 20 μm, taken from unfixed glabrous skin of the adult rat hind paw, or 10 μm sections of DRG from perfusion fixed animals, were thaw mounted onto Superfrost Plus microscope slides (BDH/Merck). Skin sections were air dried and fixed for 10 min at room temperature in acetone. Antibodies were all diluted in PBS (Sigma) plus 0.1% Triton X 100 (BDH/Merck) and all incubations were carried out at room temperature. Skin sections were co-incubated with a mixture of affinity purified rabbit anti-mGlu5 raised to the C-terminal peptide of the rat mGlu5 sequence (Valerio et al., 1997) at a final concentration of 5 μg/ml, and a monoclonal anti-neuronal βIII tubulin (Promega) at a final concentration of 1 μg/ml. Rabbit antibody was visualized with anti-rabbit antibodies conjugated to TRITC (Sigma), 1–200 final concentration, and mouse antibody with an anti-mouse FITC at 1–200 (Sigma). Secondary antibodies were applied for 2 h at room temperature. Appropriate controls showed that the secondary antibodies were specific for either rabbit or mouse antisera (data not shown). Images were collected using a Leica confocal microscope equipped with appropriate filters.

Sections of 10 μm of perfusion fixed (4% paraformaldehyde) rat DRG were double labelled for mGlu5 and VR1. The rat VR1 C-terminal sequence (KPEDAEVFKDSMVPGEK) was conjugated to thyroglobulin via an amino-terminal cysteine and used to immunize rabbits (Severn Biotech). Anti-VR1 at 1–10,000 labelled only one band at approximately 90 kDa

in Western blots of DRG extracts (not shown). VR1 immunolabelling on tissue sections or on blots was eliminated by preabsorption of the antiserum with free peptide used as the immunogen.

Sections were processed using a modification of the tyramide signal amplification (TSA) indirect method for immunofluorescence (NEN). This enables double labelling with antibodies raised in the same host species. Briefly, sections were blocked for 1 h with 10% goat serum and incubated overnight with a 1:100,000 dilution of rabbit anti-VR1. Sections were then washed in PBS, incubated for 1 h with goat anti-rabbit biotin (1:400 dilution), 30 min in a 1:5 dilution of ABC (avidin biotin complex, Vector Labs) and 7 min in biotinyl tyramide solution (NEN). PBS washes were performed between all steps. Sections were then incubated for 2 h with 1:400 ex-Avidin FITC (Sigma), mounted and viewed using a Nikon Eclipse fluorescence microscope. (For controls, a 1:100,000 dilution VR1-like immunoreactivity was applied to some sections but the TSA protocol was omitted. Other sections were submitted to the TSA protocol but had no primary VR1 antibody.) Labelled sections were then further incubated overnight with 5 μg/ml rabbit anti-mGlu5 followed by anti-rabbit TRITC (Sigma).

3. Results

3.1. Effects of central vs. peripherally administered MPEP in rat models of inflammatory pain

The central vs. peripheral effects of MPEP were compared by examining the reversal of FCA-induced mechanical hyperalgesia produced by the local microinjection of MPEP via i.c.v., i.t. or i.pl. routes. I.c.v. or i.t. administration of morphine (10 nmole) reversed FCA-induced hyperalgesia 1 h following administration (Fig. 1(a)). In contrast, neither i.t. nor i.c.v. microinjection of MPEP (10–300 nmole) produced a significant effect on paw withdrawal thresholds in the inflamed rat hind paw 1 or 3 h following administration. However, when administered directly to the inflamed hind paw, MPEP produced significant reversal of mechanical hyperalgesia by 1 h following administration (Fig. 1(a)). Nevertheless, in these experiments MPEP was injected into the swollen hind paw, 24 h following FCA treatment, and we could not accurately estimate its efficacy due to some leakage from the site of injection. Therefore, we tested whether pre-treatment of the hind paw with MPEP could also prevent the development of inflammatory hyperalgesia. In these experiments we used the carrageenan model of inflammation, due to the rapid onset of mechanical hyperalgesia and other signs of inflammation (e.g. paw oedema) in this model (Perrot et al., 1998). As a further control, to determine whether intraplantar microinjection could lead to systemic effects, we included a group of

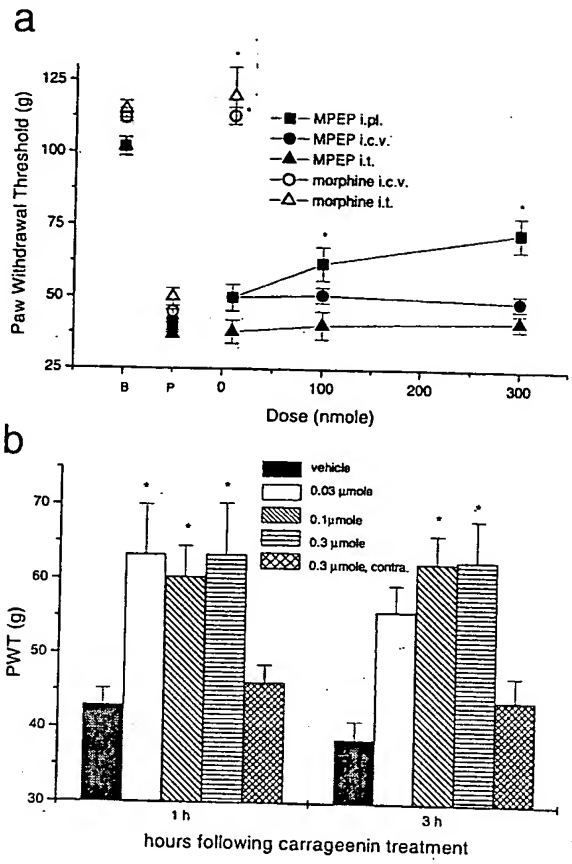

Fig. 1. (a) Reversal of mechanical hyperalgesia (mean±SEM) in the FCA-inflamed rat hind paw 1 h following i.t., i.c.v. or i.pl. administration of MPEP. PWT were measured before FCA treatment (B), and 24 h after FCA treatment, prior to MPEP administration (P). An asterisk denotes a significant difference from pre-MPEP administration PWT ($P<0.05$). (b) Inhibition of the development of mechanical hyperalgesia 1 and 3 h following i.pl. injection of carrageenan, as described above, by i.pl. microinjection (5 μl) of vehicle, 0.03–0.3 μmole of MPEP. PWT in the inflamed hind paw were unaffected following microinjection of 0.3 μmole MPEP into the contralateral (contra.) hind paw. An asterisk denotes a significant difference from the vehicle-treated group ($P<0.05$).

rats that had received pre-treatment with the highest dose of MPEP into the hind paw contralateral to the carrageenan-treated paw. Pre-treatment of the rat hind paw by intraplantar microinjection of MPEP 30 min before carrageenan treatment significantly inhibited the development of mechanical hyperalgesia (Fig. 1(b)). In contrast, pre-treatment of the hind paw contralateral to the inflamed hind paw with MPEP did not affect the development of mechanical hyperalgesia.

3.2. Hyperalgesic effects of peripherally applied glutamate receptor agonists

In order to provide pharmacological evidence for the functional expression of mGlu5 receptors in the periphery, we compared the ability of various ionotropic and

metabotropic glutamate receptor agonists to produce mechanical hyperalgesia when microinjected into the non-inflamed rat hind paw (Fig. 2(a)). The rank order of potency of glutamate receptor agonists (L-glutamate > CHPG = DHPG > NMDA = AMPA > LY314582 > L-AP4) indicated that the endogenous ligand, L-glutamate (1–100 nmole), produced the most potent hyperalgesic effect with a 50% decrease in paw withdrawal threshold at the earliest test, 30 min following i.pl. microinjection. NMDA, AMPA, the group I mGlu receptor agonist DHPG and the selective mGlu5 receptor agonist, CHPG (Schoepp et al., 1999), all produced mechanical hyperalgesia when microinjected into the rat hind paw. However, the group III mGlu receptor agonist, L-AP4 (Schoepp et al., 1999), did not produce a significant decrease in paw withdrawal threshold, and the group II mGlu receptor agonist, LY314582 (100 nmole; Monn et al., 1997), produced only a slight decrease in paw withdrawal threshold (Fig. 2(a)). Co-microinjection of MPEP with either glutamate, DHPG or CHPG resulted in a dose-dependent inhibition of agonist-induced mechanical hyperalgesia (Fig. 2(b)), whereas the mechanical hyperalgesia produced by DHPG was not affected by co-administration of the mGlu 1 receptor antagonist 4-CPG (Schoepp et al., 1999; fig. 2(b)). However, when MPEP was microinjected into the contralateral paw there was no effect on DHPG-induced mechanical hyperalgesia (Fig. 2(b)), thereby ruling out a possible systemic effect following i.pl. administration.

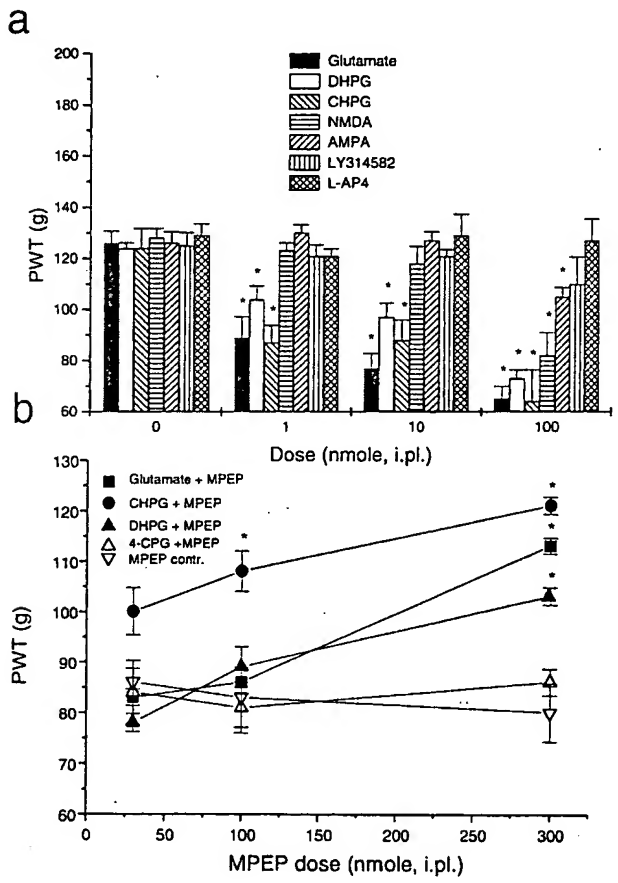

Fig. 2. Naive rats were used to examine the hyperalgesic effects of glutamate receptor agonists. The baseline PWT was measured and then each rat received an i.pl. microinjection (10 µl) of a glutamate receptor agonist. (a) Decreases in naive rat PWT (mean±SEM) were measured 30 min following i.pl. administration of 0.001–0.1 µmole of different excitatory amino acid receptor agonists. An asterisk denotes a significant difference from the vehicle-treated group ($P<0.05$). (b) Inhibition of CHPG (0.1 µmole), glutamate (0.1 µmole) or DHPG (0.1 µmole) induced mechanical hyperalgesia (mean±SEM) 30 min following i.pl. co-administration of 0.03, 0.1 or 0.3 µmole MPEP. DHPG-induced mechanical hyperalgesia was not inhibited following co-administration of 0.03, 0.1 or 0.3 µmole 4-CPG, or following injection of MPEP (0.03, 0.1 or 0.3 µmole) into the contralateral (contra.) hind paw. An asterisk denotes a significant difference from the vehicle-treated group ($P<0.05$).

3.3. *In vivo measurements of spinal cord neuronal activity*

If stimulation of mGlu5 receptors on the peripheral terminals of primary afferent neurons results in primary afferent activation, then it should be possible to measure changes in the activity of WDR dorsal horn neurons following application of a mGlu5 receptor agonist to the peripheral receptive field. To demonstrate this, dorsal horn neurons receiving peripheral nociceptive (high-threshold) and non-nociceptive (low-threshold) afferent input were recorded in anaesthetized rats following microinjection of the mGlu5 receptor agonist, CHPG, to their peripheral receptive fields. Peripheral microinjection of CHPG produced spontaneous firing of dorsal horn WDR neurons at a frequency and duration significantly above that produced by the vehicle control (Fig. 3(a,c)). This activation was inhibited by the co-microinjection of MPEP (Fig. (a,c)). MPEP microinjected into the receptive field on its own did not produce a significant effect on dorsal horn WDR neuron activity. These data demonstrate that an mGlu5 receptor agonist acting in the periphery is capable of evoking long lasting activation of WDR neurons in the spinal cord, and this can be prevented by the mGlu5 receptor antagonist MPEP.

3.4. *mGlu5 receptor-like immunoreactivity in rat DRG and skin*

Staining with a specific polyclonal antiserum raised against the mGlu5 receptor, as described previously by Valerio et al. (1997), revealed immunoreactivity in peripheral nerve fibres in glabrous skin from naive rat hind paw (Fig. 4B–D). Nerve fibres were identified by co-staining with a neurone specific anti-βIII tubulin antibody (Fig. 4(A,C,D)).

Fig. 5 shows double staining using TSA of a DRG section from a naive animal, co-stained for mGlu5 receptor and VR1 (vanilloid receptor 1) which is expressed

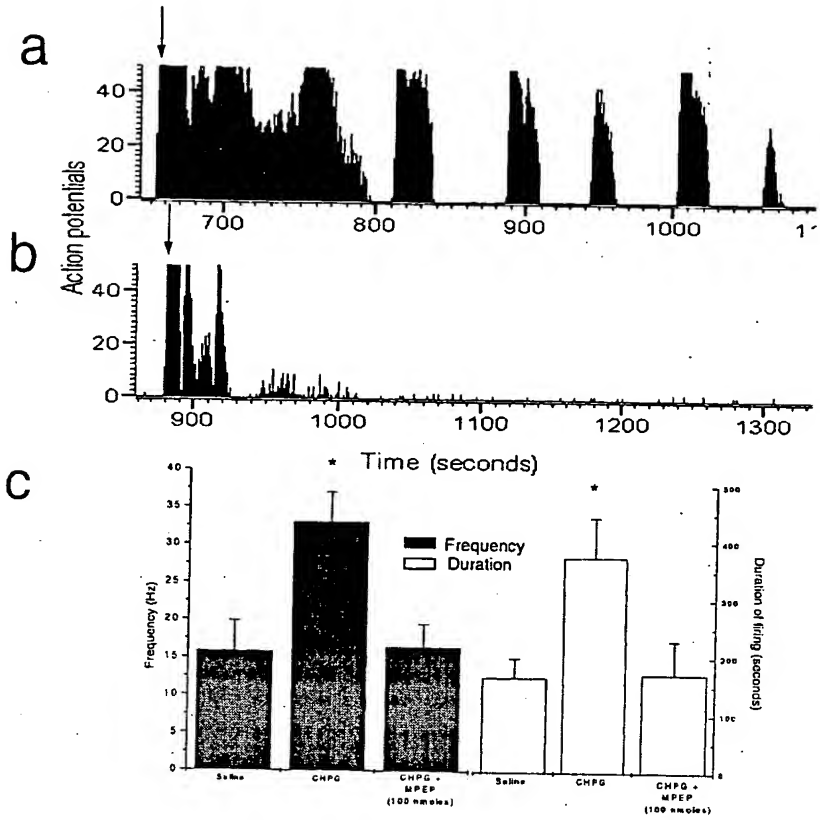

Fig. 3. Injection of CHPG, an mGlu5 receptor agonist, into the peripheral receptive field of identified WDR dorsal horn neurons produces firing (action potentials) of the neurons. (a) Post-stimulus histogram of action potentials evoked by intraplantar bolus injection of CHPG (100 nmole; indicated by arrow) into the peripheral receptive field of a single WDR neuron (see Section 2). (b) Post-stimulus histogram of action potentials evoked following i.pl. bolus co-administration of CHPG (100 nmole)+MPEP (500 nmole; indicated by arrow). (Histograms in (a) and (b) represent the same neuron.) (c) Increase in the (mean±SEM) frequency of action potentials (solid bars) and the duration of activity (open bars) of dorsal horn WDR neurons following i.pl. injections of saline (n=6); 100 nmole CHPG (n=9); 100 nmole CHPG+100 nmole MPEP (n=9) into their receptive field. An asterisk denotes a significant difference from both control groups and CHPG compared to CHPG+MPEP (P<0.05).

on many nociceptors (Tominaga, et al., 1998). Many of the neuron cell bodies express both of these receptors. (Controls without the VR1 or without the TSA step showed no VR1 staining.) Together, the mGlu5 distribution by immunohistochemistry suggests that mGlu5 receptor protein is constitutively expressed on a subpopulation of peripheral sensory neurons, some of which are nociceptors, and their axons.

4. Discussion

The expression of the mGlu5 receptor in various regions of the brain and spinal cord has been studied in detail (Shigemoto et al., 1993; Romano et al., 1995; Valerio et al., 1997; Boxall et al., 1998a). In the rat spinal cord mGlu5 receptors are predominantly expressed in the superficial layers of the dorsal horn where nociceptive primary afferent neurons terminate (Valerio et al., 1997; Berthele et al., 1999; Jia et al., 1999). We compared the central vs. peripheral effects of MPEP by examining the reversal of inflammation-induced mechanical hyperalgesia by the local microinjection of MPEP into the rat hind paw. Interestingly, neither i.t. nor i.c.v. microinjection of MPEP produced a significant effect on paw withdrawal thresholds in the inflamed rat hind paw. However, when administered directly to the inflamed hind paw the same doses of MPEP produced significant reversal of mechanical hyperalgesia. The lack of effect of MPEP when administered via central routes was unpredicted, as previous studies have indicated a role of dorsal horn group I mGlu receptors in acute nociception (Fisher and Coderre, 1996a,b; Young et al., 1997). Nevertheless, several of these studies have indicated that these intrathecal anti-nociceptive effects are likely mediated by the blockade of mGlu1 receptors (Boxall et al., 1998b; Salt and Turner, 1998; Neugebauer et al., 1999) or ablation of mGlu1 receptors by intrathecal antisense administration (Young et al., 1998). The role of dorsal horn mGlu5 receptors in inflammatory nociception is more controversial (see Stanfa and Dickenson, 1998; Jia et al., 1999) and intrathecal application of

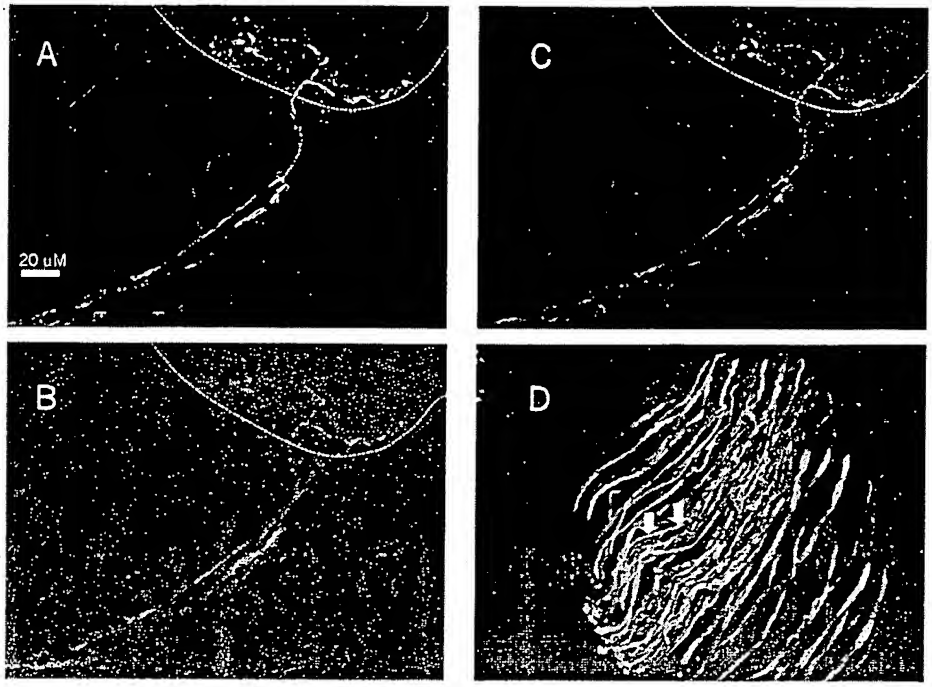

Fig. 4. Immunohistochemical staining of rat skin sections with a rabbit polyclonal antibody recognizing themGlu5a receptor (bar=20 μm for all panels). (A–C) Different representations of a nerve fibre arborizing in the epidermal layer of glabrous skin (dotted line marks the border between the dermis and epidermis). (A, B) Separate images from (C). (A) Neuronal βIII tubulin (green) staining, while (B) is the separate image of the red fluorescence (mGlu5 receptor). The two colours show overlap over the neuronal profile in (C). (D) Photomicrograph of a peripheral nerve trunk in the dermis (below the dotted line) of the rat skin. Green fluorescence represents neuronal tubulin, and red, mGlu5 receptor staining. Note that mGlu5a receptors are expressed only in a certain fraction of the nerve fibres. All photomicrographs were processed with a Leica confocal microscope with a 60× oil immersion objective.

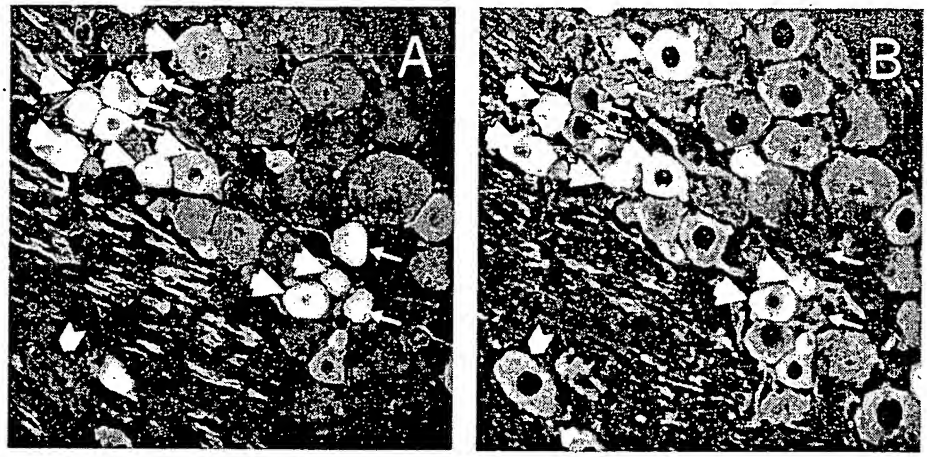

Fig. 5. Cryostat section (bar=10 μm for each panel) of adult rat DRG co-labelled with rabbit antibodies recognizing (A) mGlu5 and (B) VR1 (see Section 2). Many neurons label with both antibodies. Thick arrows mark neuronal cell bodies that label strongly with both mGlu5 and VR1 antibodies. Thin arrows mark neurons expressing only mGlu5 and the chevron labels a neuron expressing only VR1.

mGlu5 receptor antagonists has failed to reduce inflammatory hyperalgesia in rats in previous reports (Zahn and Brennan, 1998).

The exact role of dorsal horn mGlu5 receptors in nociceptive processes is still poorly understood, but there is an emerging consensus that they may be involved in the modulation of ionotropic glutamate receptor-mediated responses (Boxall et al., 1998a; see also Alagarsamy et al., 1999a,b). Interestingly, the activity of individual neurones can either be facilitated or inhibited by the activation of group I mGlu receptors (Stanfa and Dickenson, 1998). The diverse nature of the activation

of individual cell types by group I agonists may be explained, in part, by the complex pattern of mGlu5 receptor expression by different types of neurons in the dorsal horn. (Valerio et al., 1997; Jia et al., 1999). One population of cells showing mGlu5 receptor immunoreactivity have been characterized as inhibitory interneurones by double-labelling immunofluorescence (Jia et al., 1999). It is possible that at least some of these cells are GABAergic inhibitory interneurones, as the activation of mGlu receptors has been shown to facilitate the inhibitory effects of GABA in the spinal cord in vivo (Bond and Lodge, 1995). This complex configuration of mGlu5 receptor expression may contribute to induction of inhibitory and excitatory events during primary afferent activation (Stanfa and Dickenson, 1998).

Regardless of the role of mGlu5 receptors in spinal nociceptive processes, our results suggest that mGlu5 receptors expressed by primary afferent neurons are also involved in nociception, particularly that associated with inflammation. The functional expression of mGlu5 receptors by primary afferent neurons is consistent with the results of Crawford and colleagues, who recently demonstrated that increases in intracellular calcium concentration could be stimulated in rat cultured dorsal root ganglion neurons by the mGlu5 agonist CHPG (Crawford et al., 1999).

Previous studies have established that excitatory amino acids, including glutamate, are released at the site of inflammation in the periphery, and that glutamate itself causes hyperalgesia when injected into the rat skin (Lawand et al., 1997; Omote et al., 1998; Fiorentino et al., 1999). There are several possible cellular sources of glutamate in peripheral tissues, including the release from peripheral terminals of primary afferent neurons (Omote et al., 1998; De Groot and Carlton, 1998). By extending the comparison of the dose–response relationships for the hyperalgesic effects of different ionotropic and metabotropic glutamate receptor agonists we found that, in addition to the endogenous agonist, L-glutamate, significant hyperalgesia was also produced by the mGlu5 receptor agonist, CHPG. These agonist-induced hyperalgesic effects could be antagonized by local administration of the mGlu5 antagonist, MPEP. In contrast, 4-CPG did not affect the development of DHPG-induced hyperalgesia. Although 4-CPG is neither a highly selective nor a highly potent mGlu1 receptor antagonist (Salt et al., 1999; Kingston et al., 1995), it has been shown to discriminate between mGlu1 and mGlu5 receptor-mediated activity in cultured rat neurons (Brabet et al., 1995). The lack of effect of 4-CPG on DPHG-induced hyperalgesia does not provide evidence of a local mGlu1 receptor-mediated component. Nevertheless, it is possible that the lack of effect of 4-CPG might have been due to its poor potency or distribution following local administration to the hind paw and therefore we cannot completely rule out the possibility that mGlu1 or other mGlu receptors are also functionally expressed on peripheral neurons.

These pharmacological studies were further supported by the results of electrophysiological investigations which showed that intraplantar microinjection of CHPG induced an increase in the spontaneous firing of dorsal horn WDR neurons. Together these in vivo studies demonstrate that a mGlu5 receptor agonist acting in the periphery is capable of evoking mechanical hyperalgesia and long lasting activation of WDR neurons in the spinal cord, and that these effects can be prevented by peripheral application of a selective mGlu5 receptor antagonist.

Immunohistochemical investigations supported the localization of mGlu5 receptor protein by neurons in skin sections taken from the plantar surface of hind paws from untreated rats. This would suggest that mGlu5 receptors are expressed constitutively at both the central and peripheral terminals of a subset of primary afferent neurons. Moreover, a proportion of the mGlu5 expressing neurons also express the capsaicin receptor, VR1, which is associated with nociceptive sensory neurons. These results are consistent with those of Valerio et al. (1997), who have previously demonstrated that mGlu5 receptor protein is predominantly expressed in a subset of DRG neurone cell bodies, particularly those of small diameter. Taken together, these results provide strong evidence for a functional role of peripheral mGlu5 receptors in inflammatory hyperalgesia, and support the hypotheses raised by Carlton, Westlund and colleagues, for the involvement of excitatory amino acids in peripheral nociceptive transmission (Carlton et al., 1995; Davidson et al., 1997; Lawand et al., 1997).

To date, only two classes of drugs are available for the treatment of inflammatory pain, non-steroidal anti-inflammatory analgesics and opioids. However, chronic use of both NSAIDs and opioids for the treatment of persistent inflammatory pain is hampered by toxicity or CNS side-effects. The discovery of peripherally expressed mGlu5 receptors supports a role for excitatory amino acids in peripheral nociceptive processes. Compounds that can selectively antagonize mGlu5 receptor activity at peripheral neurones may provide a new mechanistic approach for the management of persistent inflammatory pain that avoids the potential for adverse CNS side-effects.

Acknowledgements

We would like to thank Prof. Roderick Scott, University of Aberdeen, for his help during the preparation of this manuscript.

References

Alagarsamy, S., Marino, M.J., Rouse, S.T., Gereau, R.W., Heinemann, S.F., Conn, P.J., 1999a. Activation of NMDA receptors reverses desensitization of mGluR5 in native and recombinant systems. Nature Neuroscience 2, 234–240.

Alagarsamy, S., Rouse, S.T., Gereau, R.W., Heinemann, S.F., Smith, Y., Conn, P.J., 1999b. Activation of N-methyl-D-aspartate receptors reverses desensitisation of metabotropic glutamate receptor mGluR5, in native and recombinant systems. Annals of the New York Academy of Science 868, 526–530.

Bartho, L., Stein, C., Herz, A., 1990. Involvement of capsaicin-sensitive neurones in hyperalgesia and enhanced opioid antinociception in inflammation. Naunyn Schmiedebergs Archives of Pharmacology 342, 666–670.

Berthele, A., Boxall, S.J., Urban, A., Anneser, J.M.H., Zieglgansberger, W., Urban, L., Tolle, T.R., 1999. Distribution and developmental changes in metabotropic glutamate receptor messenger RNA expression in the rat lumbar spinal cord. Developmental Brain Research 112, 39–53.

Bond, A., Lodge, D., 1995. Pharmacology of metabotropic glutamate receptor-mediated enhancement of responses to excitatory and inhibitory amino acids on rat spinal neurones in vivo. Neuropharmacology 34, 1015–1023.

Boxall, S.J., Berthele, A., Laurie, D.J., Sommer, B., Zieglgansberger, W., Urban, L., Tolle, T.R., 1998a. Enhanced expression of metabotropic glutamate receptor 3 messenger RNA in the rat spinal cord during ultraviolet irradiation induced peripheral inflammation. Neuroscience 82, 591–602.

Boxall, S.J., Berthele, A., Tolle, T.R., Zieglgansberger, W., Urban, L., 1998b. MGluR activation reveals a tonic NMDA component in inflammatory hyperalgesia. Neuroreport 9, 1201–1203.

Brabet, I., Mary, S., Brokaert, J., Pin, J.-P., 1995. Phenylglycine derivatives discriminate between mGluR1 and mGluR5-mediated responses. Neuropharmacology 34, 895–903.

Carlton, S.M., Hargett, G.L., Coggeshall, R.E., 1995. Localization and activation of glutamate receptors in unmyelinated axons of rat glabrous skin. Neuroscience Letters 197, 25–28.

Conn, P.J., Pin, J.P., 1997. Pharmacology and functions of metabotropic glutamate receptors. Annual Review of Pharmacology and Toxicology 37, 205–237.

Crawford, J.H., Wainwright, A., Heavens, R., Pollock, J., Martin, D.J., Scott, R.H., Seabrook, G.R., 1999. Mobilization of intracellular Ca2+ by mGluR5 metabotropic glutamate receptor activation in neonatal rat cultured dorsal root ganglia neurones. Neuropharmacology 39, 621–630.

Davidson, E.M., Coggeshall, R.E., Carlton, S.M., 1997. Peripheral NMDA and non-NMDA glutamate receptors contribute to nociceptive behaviors in the rat formalin test. Neuroreport 8, 941–946.

De Groot, J.F., Carlton, S.M., 1998. Sciatic nerve stimulation releases glutamate in the rat hindpaw. Society of Neuroscience Abstracts 24, 742–744.

Dickenson, A.H., Sullivan, A.F., 1987. Evidence for a role of the NMDA receptor in the frequency dependent potentiation of deep rat dorsal horn nociceptive neurones following C fibre stimulation. Neuropharmacology 26, 1235–1238.

Fiorentino, P.M., Cairns, B.E., Hu, J.W., 1999. Development of inflammation after application of mustard oil or glutamate to the rat temporomandibular joint. Archives of Oral Biology 44, 27–32.

Fisher, K., Coderre, T.J., 1996a. The contribution of metabotropic glutamate receptors (mGluRs) to formalin-induced nociception. Pain 68, 255–263.

Fisher, K., Coderre, T.J., 1996b. Comparison of nociceptive effects produced by intrathecal administration of mGluR agonists. Neuroreport 7, 2743–2747.

Fisher, K., Coderre, T.J., 1998. Hyperalgesia and allodynia induced by intrathecal (RS)-dihydroxyphenylglycine in rats. Neuroreport 9, 1169–1172.

Gasparini, F., Lingenhoehl, K., Stoehr, N., Flor, P.J., Heinrich, M., Vranesic, I., Biollaz, M., Allgeier, H., Heckendorn, R., Urwyler, S., Varney, M.A., Johnson, E.C., Hess, S.D., Rao, S.P., Sacaan, A.I., Santori, E., Veliçelebi, G., Kuhn, R., 1999. 2-Methyl-6-(phenylethynyl)-pyridine (MPEP) a potent selective and systemically active mGlu5 receptor antagonist. Neuropharmacology 38, 1493–1504.

Hylden, J.L.K., Wilcox, G.L., 1980. Intrathecal morphine in mice: a new technique. European Journal of Pharmacology 67, 313–316.

Jackson, D.L., Graff, C.B., Richardson, J.D., Hargreaves, K.M., 1995. Glutamate participates in the peripheral modulation of thermal hyperalgesia in rats. European Journal of Pharmacology 284, 321–325.

Jia, H., Rustioni, A., Valtschanoff, J.G., 1999. Metabotropic glutamate receptors in superficial laminae of the rat dorsal horn. Journal of Comparative Neurology 410, 627–642.

Kingston, A.E., Burnett, J.P., Mayne, N.G., Lodge, D., 1995. Pharmacological analysis of 4-carboxyphenylglycine derivatives: comparison of effects on mGluRla and mGluR5α subtypes. Neuropharmacology 34, 887–894.

Lawand, N.B., Willis, W.D., Westlund, K.N., 1997. Excitatory amino acid receptor involvement in peripheral nociceptive transmission in rats. European Journal of Pharmacology 324, 169–177.

Knopfel, T., Kuhn, R., Allgeier, 1995. Metabotropic glutamate receptors novel targets for drug development. Journal of Medicinal Chemistry 38, 1417–1426.

Monn, J.A., Valli, M.J., Massey, S.M., Wright, R.A., Salhoff, C.R., Johnson, B.G., Howe, T., Alt, C.A., Rhodes, G.A., Robey, R.L., Griffey, K.R., Tizzano, J.P., Kallman, M.J., Helton, D.R., Schoepp, D.D., 1997. Design, synthesis, and pharmacological characterization of (+)-2-aminobicyclo[3.1.0]hexane-2,6-dicarboxylic acid (LY354740): a potent, selective, and orally active group 2 metabotropic glutamate receptor agonist possessing anticonvulsant and anxiolytic properties. Journal of Medicinal Chemistry 40, 528–537.

Neugebauer, V., Chen, P.S., Willis, W.D., 1999. Role of metabotropic glutamate receptor subtype mGluR1 in brief nociception and central sensitization of primate STT cells. Journal of Neurophysiology 82, 272–282.

Omote, K., Kawamata, T., Kawamata, M., Namiki, A., 1998. Formalin-induced release of excitatory amino acids in the skin of the rat hindpaw. Brain Research 787, 161–164.

Perrot, S., Idanpaan Heikkila, J.J., Guilbaud, G., Kayser, V., 1998. The enhancement of morphine antinociception by a CCKB receptor antagonist in the rat depends on the phase of inflammation and the intensity of carrageenin-induced hyperalgesia. Pain 74, 269–274.

Romano, C., Sesma, M.A., McDonald, C.T., O'Malley, K., Van den Pol, A.N., Olney, J.W., 1995. Distribution of metabotropic glutamate receptor mGluR5 immunoreactivity in rat brain. Journal of Comparative Neurology 355, 455–469.

Salt, T.E., 1986. Mediation of thalamic sensory input by both NMDA receptors and non-NMDA receptors. Nature 322, 263–265.

Salt, T.E., Turner, J.P., 1998. Reduction of sensory and metabotropic glutamate receptor responses in the thalamus by the novel metabotropic glutamate receptor-1-selective antagonists 2-methyl-4-carboxy-phenylglycine. Neuroscience 85, 655–658.

Salt, T.E., Binns, K.E., Turner, J.P., Gasparini, F., Kuhn, R., 1999. Antagonism of the mGlu5 agonist 2-chloro-5-hydroxyphenylglycine by the novel selective mGlu5 antagonist 6-methyl-2-(phenylethynyl)-pyridine (MPEP) in the thalamus. British Journal of Pharmacology 127, 1057–1059.

Schoepp, D.D., Jane, D.E., Monn, J.A., 1999. Pharmacological agents acting at subtypes of metabotropic glutamate receptors. Neuropharmacology 38, 1376–1431.

Shigemoto, R., Nomura, S., Ohishi, H., Sugihara, H., Nakanishi, S., Mizuno, N., 1993. Immunohistochemical localization of a meta-

botropic glutamate receptor, mGluR5, in the rat brain. Neuroscience Letters 163, 53–57.

Stanfa, L.C., Dickenson, A.H., 1998. Inflammation alters the effects of mGlu receptor agonists on spinal nociceptive neurones. European Journal of Pharmacology 347, 165–172.

Stein, C., Millan, M.J., Herz, A., 1988. Unilateral inflammation of the hindpaw in rats as a model of prolonged noxious stimulation: alterations in behavior and nociceptive thresholds. Pharmacology Biochemistry and Behavior 31, 451–455.

Caterina, M.J., Malmberg, A.B., Rosen, T.A., Gilbert, H., Skinner, K., Raumann, B.E., Basbaum, A.I., Julius, D., 1998. The cloned capsaicin receptor integrates multiple pain producing stimuli. Neuron 21, 531–543.

Valerio, A., Rizzonelli, P., Paterlini, M., Moretto, G., Knopfel, T., Kuhn, R., Memo, M., Spano, P., 1997. mGluR5 metabotropic glutamate receptor distribution in rat and human spinal cord: a developmental study. Neuroscience Research 28, 49–57.

Walker, K., Bowes, M., Panesar, M., Davis, A., Gentry, C., Kesingland, A., Gasparini, F., Spooren, W., Stoehr, N., Pagano, A., Flor, P.J., Vranesic, I., Lingenhoehl, K., Johnson, E.C., Varney, M., Urban, L., Kuhn, R., 2001. Metabotropic glutamate receptor subtype 5 (mGlu5) and nociceptive function I. Selective blockade of mGlu5 receptors in models of acute, persistent and chronic pain. Neuropharmacology, 40, 1–9.

Walker, K., Dray, A., Perkins, M., 1996. Development of hyperthermia following intracerebroventricular administration of endotoxin in the rat: effect of kinin B1 and B2 receptor antagonists. British Journal of Pharmacology 117, 684–688.

Young, M.R., Blackburn-Munro, G., Dickinson, T., Johnson, M.J., Anderson, H., Nakalembe, I.F., Feetwood-Walker, S.M., 1998. Antisense ablation of type I metabotropic glutamate receptor mGluR(1) inhibits spinal nociceptive transmission. Journal of Neuroscience 18, 10180–10188.

Young, M.R., Fleetwood Walker, S.M., Dickinson, T., Blackburn Munro, G., Sparrow, H., Birch, P.J., Bountra, C., 1997. Behavioural and electrophysiological evidence supporting a role for group I metabotropic glutamate receptors in the mediation of nociceptive inputs to the rat spinal cord. Brain Research 777, 161–169.

Zahn, P.K., Brennan, T.J., 1998. Intrathecal metabotropic glutamate receptor antagonists do not decrease mechanical hyperalgesia in a rat model of postoperative pain. Anesthesia and Analgesia 87, 1354–1359.

Zhou, S., Bonasera, L., Carlton, S.M., 1996. Peripheral administration of NMDA, AMPA or KA results in pain behaviors in rats. Neuroreport 7, 895–900.

British Journal of Pharmacology (2001) 132, 1423–1430

www.nature.com/bjp

Potential anxiolytic- and antidepressant-like effects of MPEP, a potent, selective and systemically active mGlu5 receptor antagonist

[1]Ewa Tatarczyńska, [1]Aleksandra Kłodzińska, [1]Ewa Chojnacka-Wójcik, [1]Agnieszka Pałucha, [2]Fabrizio Gasparini, [2]Rainer Kuhn & *[,1,3]Andrzej Pilc

[1]Institute of Pharmacology, Polish Academy of Sciences, 31-343 Kraków, Smetna 12, Poland; [2]Novartis Pharma AG, Therapeutic Area Nervous System, Basle, Switzerland and [3]Institute of Public Health, Collegium Medicum, Jagiellonian University, Kraków, Poland

1 Several lines of evidence suggest a crucial involvement of glutamate in the mechanism of action of anxiolytic and/or antidepressant drugs. The involvement of group I mGlu receptors in anxiety and depression has also been proposed. Given the recent discovery of a selective and brain penetrable mGlu5 receptor antagonists, the effect of 2-methyl-6-(phenylethynyl)-pyridine (MPEP), i.e. the most potent compound described, was evaluated in established models of anxiety and depression.

2 Experiments were performed on male Wistar rats or male Albino Swiss or C57BL/6J mice. The anxiolytic-like effects of MPEP was tested in the conflict drinking test and the elevated plus-maze test in rats as well as in the four-plate test in mice. The antidepressant-like effect was estimated using the tail suspension test in mice and the behavioural despair test in rats.

3 MPEP (1–30 mg kg^{-1}) induced anxiolytic-like effects in the conflict drinking test and the elevated plus-maze test in rats as well as in the four-plate test in mice. MPEP had no effect on locomotor activity or motor coordination. MPEP (1–20 mg kg^{-1}) did shorten the immobility time in a tail suspension test in mice, however it was inactive in the behavioural despair test in rats.

4 These data suggest that selective mGlu5 receptor antagonists may play a role in the therapy of anxiety and/or depression, further studies are required to identify the sites and the mechanism of action of MPEP.

British Journal of Pharmacology (2001) **132**, 1423–1430

Keywords: mGlu5 receptors; MPEP; conflict drinking test; four-plate test; plus-maze test; tail suspension test; anxiety; depression

Abbreviations: S-4C3H-PG, (S)-4-Carboxy-3-hydroxyphenylglycine; CNS, central nervous system; GABA, γ-aminobutyric acid; L-5-HTP, L-5-hydroxytryptophan; mGluR, metabotropic glutamate receptors; MPEP, 2-methyl-6-(phenylethynyl)-pyridine; NMDA, N-methyl-D-aspartic acid

Introduction

Glutamate is the major excitatory neurotransmitter in the brain, and as such involved in several physiological and pathological conditions (Wroblewski & Danysz, 1989; Danysz *et al.*, 1996). Glutamate acts at two classes of receptors, the ionotropic and the metabotropic glutamate receptors (mGlu receptors) (Monaghan *et al.*, 1989; Conn & Pin, 1997). Metabotropic glutamate receptors are a family of eight G-protein coupled receptors which are classified into three groups according to their sequence homology, effector coupling and pharmacology. Group I mGlu receptors (mGlu1 and mGlu5) are positively coupled to phospholipase C; group II mGlu receptors (mGlu2 and mGlu3) and group III mGlu receptors (mGlu4, mGlu6, mGlu7 and mGlu8) are negatively coupled to adenylate cyclase (Conn & Pin, 1997). Activation of group I mGlu receptors leads to a transient increase in intracellular calcium *via* the production of inositol-trisphosphates (Conn & Pin, 1997). Generally, it has been shown that activation of group I receptors enhances or facilitates the excitatory effects of glutamate by modulation of ion channel activity (Conn & Pin, 1997). Antagonists of group I mGlu receptors have been proposed to exhibit potential positive therapeutic effects (Bruno *et al.*, 1994; Conn & Pin, 1997) in CNS disorders related to excessive excitatory neurotransmission such as epilepsy, ischaemia and pain (Nicoletti *et al.*, 1996; Conn & Pin, 1997).

Several lines of evidence suggest an important role for glutamate in anxiety and depression (Wiley *et al.*, 1995; Skolnick *et al.*, 1996; Danysz & Parsons, 1998; Skolnick, 1999). Involvement of group I mGlu receptors in psychiatric conditions such as depression and anxiety has also been proposed. It has been shown that antagonists of group I mGlu receptors exert anxiolytic-like effects after intrahippocampal injection in rats (Chojnacka-Wójcik *et al.*, 1997); and that antidepressant treatment influences group I mGlu receptors in the hippocampus (Bajkowska *et al.*, 1999; Pilc *et al.*, 1998).

Up to now studies concerning involvement of mGlu5 receptors in CNS functions were largely based on compounds which have only limited selectivity between mGlu1 and mGlu5 receptor subtypes (Nicoletti *et al.*, 1996; Conn & Pin,

*Author for correspondence at: Institute of Pharmacology, Polish Academy of Sciences, 31-343 Kraków, Smetna 12, Poland; E-mail: nfpilc@cyf-kr.edu.pl

1997) and which do not penetrate into the brain. Only recently, novel, selective and systemically active compounds have been described (Varney *et al.*, 1999; Gasparini *et al.*, 1999). The most potent of this series is 2-methyl-6-(phenylethynyl)-pyridine (MPEP), a noncompetitive antagonist with an IC_{50} of 36 nM at the human mGlu5a receptor in the PI hydrolysis assay but no significant effect at other metabotropic or ionotropic glutamate receptors (Gasparini *et al.*, 1999). To evaluate whether MPEP has anxiolytic-or antidepressant-like effects, we studied its effects in several models of anxiety or depression in rats and mice.

Methods

Animals and housing

The experiments were performed on male Wistar rats (200–250 g) and male Albino Swiss or male C57BL/6J mice (22–26 g). The animals were kept on a natural day–night cycle at a room temperature of 19–21°C, with free access to food and water. Each experimental group consisted of 6–10 naïve animals/dose. In rats, all injections were given in a volume of 2 ml kg^{-1}, and in mice in a volume of 10 ml kg^{-1}. Experiments were performed by an observer blind to the treatment. All experimental procedures were approved by Animal Care and Use Committee at the Institute of Pharmacology, Polish Academy of Sciences in Kraków.

Drugs

2-Methyl-6-(phenylethynyl)-pyridine (MPEP) was synthesized as described previously (Gasparini *et al.*, 1999). MPEP and diazepam (Polfa-Poznań, Poland) were suspended in a 1% aqueous solution of Tween 80. Imipramine hydrochloride (Polfa-Starogard Gdański, Poland) and L-5-hydroxytryptophan (L-5-HTP; Sigma, St. Louis, MO, U.S.A.) were dissolved in sterile saline. MPEP was administered intraperitoneally (i.p.) or perorally (p.o.), diazepam, imipramine and L-5-HTP were administered i.p. All compounds were given at 60 min before the tests.

Conflict drinking test (Vogel test)

A modification of the method of (Vogel *et al.*, 1971) described below was used. On the first day of the experiment, the rats were adapted to the test chamber for 10 min. It was a plexiglass box (27 × 27 × 50 cm), equipped with a grid floor of stainless steel bars and a drinking bottle containing tap water. After the adaptation period, the animals were deprived of water for 24 h, and were then placed in the test chamber for another 10 min adaptation period, during which they had a free access to the drinking bottle. Afterwards, they were allowed a 30 min free-drinking session in their home cage. After another 24 h water deprivation period, the rats were again placed in the test chamber and were allowed to drink for 30 s. Immediately afterwards, drinking attempts were punished with an electric shock (0.5 mA). The impulses were released every 2 s (timed from the moment when a preceding shock was delivered), between the grid floor and the spout of the drinking bottle. Each shock lasted for 1 s and if the rat was drinking when an impulse was released, it received a shock. The number of shocks accepted throughout a 5 min experimental session was recorded. MPEP (0.3, 1 and 10 mg kg^{-1}, i.p.) and diazepam (10 mg kg^{-1}, i.p.) were administered 60 min before the test.

Shock threshold and free-drinking tests

To control the possibility of drug-induced changes in the perception of a stimulus or in the thirst drive, which might have contributed to the activity in the conflict drinking test, stimulus threshold measurements and a free-drinking experiment were also carried out. In both cases, the rats were treated before the experiment in the same manner as described in the conflict drinking test, including two 24 h water deprivation periods separated by 30 min of water availability. In the shock threshold test, the rats were placed individually in the box, and electric shocks were delivered through the grid floor. The shock threshold was determined stepwise with 15 s shock free intervals by manually increasing the current (0.1, 0.2, 0.3, 0.4, 0.5 mA). The shock lasted for 1 s and was delivered through the grid-floor until a rat showed an avoidance reaction (jump or jerk) to the electric stimulus.

In the free-drinking test, each animal was allowed to drink from the water spout. Licking was not punished. The total amount of water (ml), consumed in 5 min, was recorded for each rat. MPEP (1 and 10 mg kg^{-1}, i.p.) was administered 60 min before the test.

Water intake test

The rats were housed and tested in individual cages (40 × 27 × 15 cm), with free access to food and water at all times. On the day of the test, water bottles were weighed at the time of drug administration. Water was presented immediately after drug injection. Water intake (ml) was recorded at 1, 2, 4, 6 and 24 h time points. L-5-hydroxytryptophan (L-5-HTP) was used as a reference drug (Rowland *et al.*, 1987). MPEP (1 and 10 mg kg^{-1}, i.p.) and L-5-HTP (20 mg kg^{-1}, i.p.) were administered immediately before the test.

Elevated plus-maze test

The construction and the testing procedure of the elevated plus-maze were based on a method described by Pellow & File (1986). Each rat was placed in the centre of the plus-maze, facing one of the enclosed arms immediately after a 5 min adaptation in a wooden box (60 × 60 × 35 cm). During a 5 min test period, two experimenters, who were sitting in the same room approximately 1 m from the end of the open arms, recorded the number of entries into the closed or the open arm, as well as the time spent in each type of arms. The entry with all four feet put onto one arm was defined as an arm entry. At the end of each trial the maze was wiped clean. MPEP (1, 3 and 10 mg kg^{-1}, i.p. or 10 and 30 mg kg^{-1}, p.o.) and diazepam (1.25, 2.5 and 5 mg kg^{-1}, i.p.) were administered 60 min before the test.

Four-plate test

The box is made of an opaque plastic and has the shape of a rectangle (25 × 18 × 16 cm). The floor is covered with four

rectangular metal plates (11.3 × 7.7 cm) separated by a gap of 4 mm. The plates are connected to a source of direct current and the 180 V difference of potential between two adjacent plates occurs for 0.5 s when the experimenter presses a switch. Single mice were placed gently onto the plate, and allowed to explore for 15 s. Afterwards, each time a mouse passed from one plate to another, the experimenter electrified the whole floor, which evoked a visible flight reaction of the animal. If the animal continued running, it received no new shocks for the following 3 s. The number of punished crossings was counted for 60 s (Aron *et al.*, 1971). MPEP (3, 10 and 30 mg kg^{-1}, i.p.) and diazepam (2 mg kg^{-1}, i.p) were administered 60 min before the test.

Rota-rod test

Mice were preselected 1 h before the test on the rotating rod (3 cm in diameter, 6 r.p.m). Those staying on the rotating road for 2 min (approximately 95% of animals) were placed again on the same rotating rod after drug administration and were observed for 2 min. The number of animals falling from the rota-rod within 2 min was recorded. MPEP (30 mg kg^{-1}, i.p.) was administered 60 min before the test.

Open field test

The studies were carried out with rats according to a slightly modified method of Janssen *et al.* (1960). The centre of the open arena (1 m in diameter), divided into six symmetrical sectors without walls, was illuminated with a 75 W electric bulb hung directly 75 cm above it. During all the experiments the laboratory room was dark. Individual control or drug-injected animals were placed gently in the centre of the arena and were allowed to explore freely. The time of walking, ambulation (the number of crossing of sector lines) and the number of rearing and peeping episodes (looking under the edge of the arena) were recorded for 3 min. MPEP (3 and 10 mg kg^{-1}, i.p.) was administered 60 min before the test.

Behavioural despair test

The studies were carried out on rats according to the method of Porsolt *et al.* (1978). Briefly, the rats were placed individually into a glass cylinder (height 40 cm; diameter 18 cm) containing 15 cm of water, maintained at 25°C. After 15 min they were removed to a drying room (30°C) for 30 min. They were replaced in the cylinder 24 h later and the total duration of immobility was measured during a 5 min test. MPEP (0.1, 1 and 10 mg kg^{-1}, i.p.) and imipramine (30 mg kg^{-1}, i.p.) were administered 60 min before the test.

Tail suspension test

Immobility was induced by tail suspension according to the procedure of Steru *et al.* (1985). C57BL/6J mice were hung individually on a plastic string, 75 cm above the table top with an adhesive tape placed *ca.* 1 cm from the tip of the tail. Duration of immobility was recorded for 8 min. Mice were considered immobile only when they hung passively and completely motionless. MPEP (0.1, 1, 10 and 20 mg kg^{-1}, i.p.) and imipramine (20 mg kg^{-1}, i.p.) were administered 60 min before the test.

Analysis of the data

The data obtained were presented as means ± s.e.mean and evaluated using one-way ANOVA, followed by Dunnett's *post hoc* determination, using GraphPad Prism version 3.00 for Windows 97 (Graph Pad Software, San Diego CA, U.S.A.).

Results

Conflict drinking test in rats

MPEP, which at a dose of 0.3 mg kg^{-1} was not effective, at doses of 1 and 10 mg kg^{-1} i.p. significantly ($F(3,30) = 11.193$, $P < 0.001$), increased the number of shocks (by 330 and 507%, respectively) accepted during the experimental session in the Vogel test (Figure 1). The maximal effect of MPEP at a dose of 10 mg kg^{-1} was comparable to that seen with diazepam at a dose of 10 mg kg^{-1}. At the effective doses in the conflict drinking test, neither the threshold current (0.4 ± 0.04 mA) nor the water intake (10.6 ± 0.6 ml) were changed compared to vehicle treatment (Table 1). As a control water intake in non-deprived rats was also evaluated. MPEP tested at doses effective in the conflict drinking test (1 or 10 mg kg^{-1}) had no significant effect on water consumption, while L-5-HTP (20 mg kg^{-1}) used as a standard drug (Rowland *et al.*, 1987) significantly increased the water intake (Table 2).

Plus-maze test in rats

The total number of entries (open + closed arm entries) observed with control rats during the 5 min test session was about six in the present set of experiments and was taken as 100%. In control rats 32.7, 34,4 and 38.5% of the entries were made into the open arms (Table 3), and 8.7, 9.0 and 10.9% of the total time (255 s) spent in the arms (either type) was spent in the open arms. MPEP administered at a dose of 1 mg kg^{-1} i.p. did not change the entries into and time spent

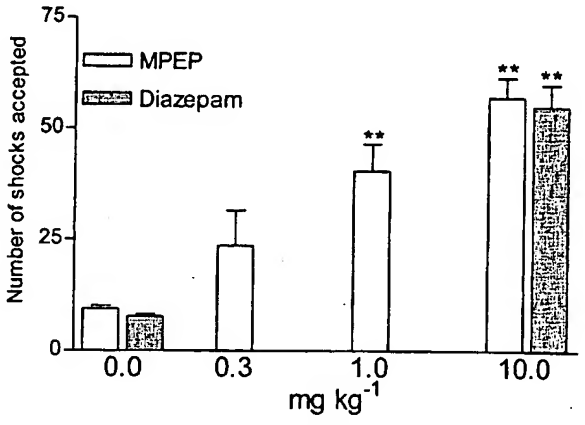

Figure 1 Effects of MPEP and diazepam in the conflict drinking test in rats. MPEP and diazepam were administered i.p. at 60 min before the test. The given values represent the mean ± s.e.mean of the number of shocks accepted during a 5 min experimental session, $n = 7-9$, ** $P < 0.01$ vs control group.

Table 1 The effect of MPEP on the shock threshold and the amount of water consumed in water deprived rats

Compound	Dose mg kg^{-1}	Shock threshold (mA)	Water consumption (ml)
Vehicle	–	0.4±0.04	10.6±0.6
MPEP	1	0.4±0.03	11.4±0.3
	10	0.3±0.01	9.9±0.6

MPEP was administered i.p. 60 min before tests. Values are the means±s.e.mean, $n=7$.

Table 2 Effects of MPEP and L-5-HTP on the amount of water intake in water non-deprivated rats

Compound	Dose mg kg^{-1}	Water consumption (ml) 1 h	2 h	4 h	6 h	24 h
Vehicle	–	1.0±0.4	2.1±0.5	2.4±0.6	2.7±0.6	35.4±2.1
MPEP	1	0.8±0.5	1.4±0.4	1.6±0.6	1.8±0.6	32.3±1.1
MPEP	10	0.6±0.1	1.5±0.5	1.7±0.5	1.8±0.6	33.1±2.7
L-5-HTP	20	2.8±0.8*	3.8±0.8*	4.0±0.9*	4.1±0.9*	39.4±3.3

MPEP and L-5-HTP were administered i.p. immediately before the test. The values are the means±s.e.mean, $n=6$. *$P<0.05$ vs vehicle group.

Table 3 The effects of MPEP and diazepam in the plus-maze test in rats

Compound	Dose mg kg^{-1}	% of time in open arms	% of open arm entries
Vehicle	–	8.7±0.5	32.7±5.2
MPEP	1 i.p.	16.2±5.8	38.7±8.2
	3 i.p.	45.1±7.1**	48.3±2.2
	10 i.p.	73.8±8.3**	67.7±6.7**
Vehicle	–	9.0±1.9	34.4±3.9
MPEP	10 p.o.	15.0±2.4	29.1±4.4
	30 p.o.	63.7±12.3**	62.6±9.2*
Vehicle	–	10.9±1.1	38.5±3.1
Diazepam	1.25 i.p.	20.3±5.5	45.2±8.9
	2.5 i.p	47.2±5.3*	73.8±4.2*
	5 i.p.	70.4±10.9**	76.2±8.8**

MPEP was administered i.p. or p.o. and diazepam i.p. 60 min before the test. Values are the means±s.e.mean, $n=6-7$, *$P<0.05$, **$P<0.01$ vs respective vehicle group.

in the open arms. When given at doses of 3 and 10 mg kg^{-1} i.p. it significantly (F (3,24)=22.978, $P<0.001$) dose-dependently increased the time spent in the open arms (up to 45 and 74%, respectively), and the percentage of entries into the open arms (up to 48 and 68%, respectively, F (3,24)=5.678, $P<0.01$) (Table 3). MPEP at doses of 3 and 10 mg kg^{-1} i.p. significantly increased (by 64%) the total number of entries and reduced (by about 25%) the total time spent (data not shown) in the arms (either type). After p.o. administration higher doses of MPEP were required to induce significant behavioural changes: at the dose of 30 mg kg^{-1} (but not 10 mg kg^{-1}) MPEP significantly (up to 64%, F (2,16)=14.249, $P<0.001$) increased the percentage of the time spent in the open arms and the percentage of entries into the open arms (up to 63%, F (2,16)=7.295, $P<0.01$). MPEP given p.o. in both doses used did not change the total number of entries nor the total time spent in the arms (either type). Diazepam, i.e. the positive standard, administered in a dose of 1.25 mg kg^{-1} i.p. was ineffective in that test, however when given at doses of 2.5 and 5 mg kg^{-1} i.p. it significantly (F (3,22)=14.52, $P<0.001$) increased the percentage of the time spent in the open arms (up to 47 and 70%, respectively), as well as the percentage of entries into the open arms (up to 74 and 76%, respectively (F (3,22)=5.871, $P<0.01$) (Table 3). Diazepam at a dose of 5 mg kg^{-1} (but not lower) significantly reduced (by 52%) the total number of entries (data not shown).

Open field test in rats and rota-rod test in mice

MPEP at doses of 3 and 10 mg kg^{-1} i.p. did not change exploratory locomotor activity in rats (F (2,18)=2; 0.273; 0.011, n.s.), as evaluated by the open field test (Table 4). MPEP at a dose of 30 mg kg^{-1} i.p. did not disturb endurance performance on the rotating rod in mice (data not shown).

Four-plate test in mice

MPEP administered at 30 mg kg^{-1} i.p. slightly but significantly increased (by 39%) the number of punished crossings in the four-plate test (Figure 2), lower doses of the compound (3 and 10 mg kg^{-1}) did not affect the number of punished crossings in that test (F (3,36)=3.240, $P<0.05$). Diazepam, i.e. the positive standard, in a dose of 2 mg kg^{-1} increased the number of crossings by 70%.

Table 4 The effect of MPEP on the exploratory activity in the open field test in rats

Compound	Dose mg kg^{-1}	Exploratory activity: Time of walking (s)	Exploratory activity: Ambulation	Exploratory activity: Peeping + rearing
Vehicle	–	44.9±2.7	14.6±1.4	9.9±1.2
MPEP	3	44.3±1.7	15.1±0.5	10.4±0.8
	10	44.9±4.3	18.3±2.0	11.1±1.5

MPEP was administered i.p. 60 min before the test. Values are means±s.e.mean, $n=6$.

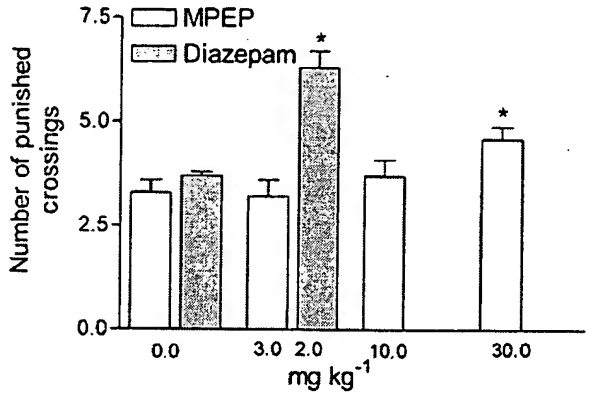

Figure 2 Effects of MPEP and diazepam in the four-plate test in mice. MPEP and diazepam were administered i.p. 60 min before the test. The given values represent the mean±s.e.mean of the number of shocks accepted during a 1 min experimental session, $n=10$. *$P<0.05$ vs control group.

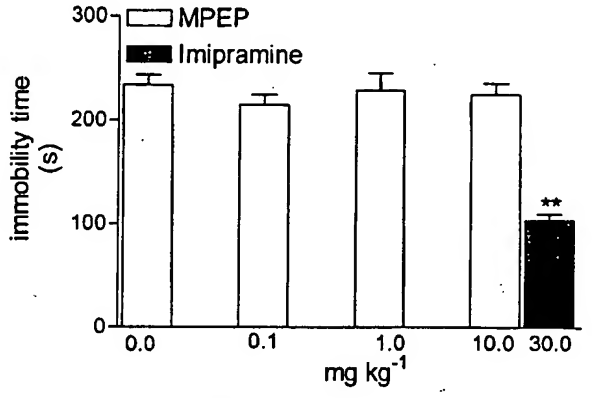

Figure 3 The effects of MPEP and imipramine on the total duration of immobility in the forced swimming test in rats. MPEP and imipramine were administered i.p. at 60 min before the test. Values represent the mean±s.e.mean of the immobility time during a 5 min experimental session, $n=9-10$. ** $P<0.01$ vs control group.

Behavioural despair test in rats and tail suspension test in mice

MPEP in doses of 0.1, 1 and 10 mg kg^{-1} i.p. did not change the behaviour of rats in the behavioural despair test, while imipramine, 30 mg kg^{-1}, used as standard drug, significantly ($F(6,49)=25.02$, $P<0.001$) decreased the immobility time in that test (Figure 3).

MPEP used in doses of 1, 10 and 20 mg kg^{-1} significantly (by 55% after the highest dose), ($F(3,28)=15.47$, $P<0.001$) decreased the immobility time of mice in the tail suspension test. Its efficacy was similar to that of imipramine (20 mg kg^{-1}), used as the positive standard (Figure 4).

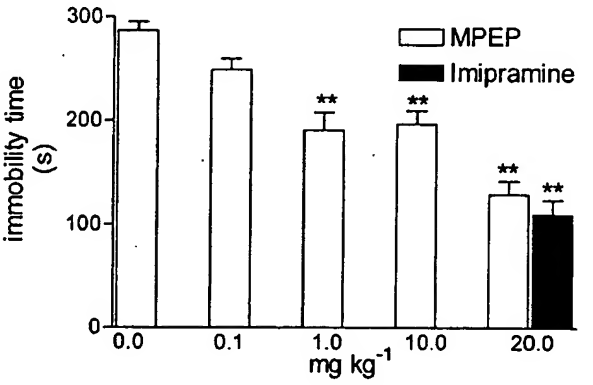

Figure 4 The effects of MPEP and imipramine on the total duration of immobility in the tail suspension test in mice. MPEP and imipramine were administered i.p. at 60 min before the test. Values represent the mean±s.e.mean of the immobility time during a 8 min experimental session, $n=9-10$. ** $P<0.01$ vs control group.

Discussion

Anxiolytic-like effects of MPEP

Benzodiazepines which are the most commonly used anxiolytic drugs, act *via* facilitation of the inhibitory GABA-ergic transmission. Benzodiazepines are effective agents, but disadvantageous side effects such as sedation, ataxia and abuse liability are associated with their administration. Decreased glutamatergic transmission, which leads to overall inhibitory effects in the central nervous system may have consequences similar to the effect of increased GABA-ergic transmission. Hence substances which inhibit stimulatory glutamatergic neurotransmission may possess anxiolytic effects. Indeed, antagonists of ionotropic glutamate receptors exhibit an anxiolytic-like activity in animal models (Stephens *et al.*, 1986; Bennett *et al.*, 1989; Jessa *et al.*, 1996), however the potential clinical utility of competitive and noncompetitive NMDA antagonists is strictly limited by their undesirable side effects (Danysz & Parsons, 1998).

Substances which influence mGlu receptors, including agonists of group II mGluR and antagonists of group I mGluR, can also exert an inhibitory function in the brain

(Conn & Pin 1997). Our earlier data have shown that (S)-4-carboxy-3-hydroxyphenylglycine (S-4C3H-PG), an antagonist of group I mGluR, exhibits anxiolytic-like activity in animals (Chojnacka-Wójcik *et al.*, 1997). However, S-4C3H-PG is also an agonist of group II mGluR (Sekiyama *et al.*, 1996) and agonists of group II mGluR exert anxiolytic-like effects in animals (Helton *et al.*, 1998; Kłodzińska *et al.*, 1999).

In order to further investigate the involvement of group I mGlu receptors in anxiety, we decided to evaluate the action of the selective antagonist of the mGlu5 receptor MPEP, which is devoid of agonist activity on group II mGlu receptors and which penetrates into the brain (Gasparini *et al.*, 1999). An anxiolytic-like effect of MPEP was evaluated in three behavioural tests: the rat Vogel test (Vogel *et al.*, 1971), the elevated plus-maze test (Pellow & File, 1986), and the four-plate test in mice (Aron *et al.*, 1971). In the elevated plus-maze test the total number of entries (open + closed arm entries/test session) is taken as an index of drug effect on the locomotor activity, but this is a relatively insensitive measure (Dawson & Tricklebank, 1995). MPEP caused a small but significant increase in the total number of entries into the arms of the maze, but did not change the exploratory activity of rats in the open field test. Therefore, the increase in the percentage of the open arm entries/time spent on the open arms induced by MPEP is likely to reflect a specific anti-anxiety effect and can not be explained by competing behaviour such as exploration. This is further supported by the anxiolytic-like effects of MPEP in two conditioned response paradigms, i.e. the Vogel test and the four-plate test. In the Vogel test in rats the action of MPEP was not related to reduced perception of the stimulus or to an increased thirst drive. Preliminary findings of anxiolytic-like effects of MPEP in unconditioned response tests (social exploration test, stress-induced hyperthermia and marble burying test (Spooren *et al.*, 2000), suggest, that MPEP exhibits anxiolytic effects in various rodent models of anxiety. Taken together, all the data suggests that MPEP produces potential anti-anxiety effects and indicate an involvement of mGlu5 receptors in anxiety.

The hippocampus is involved in anxiety (Gray, 1982) and effects of different anxiolytics, including a variety of agents acting upon the glutamatergic system (e.g. Przegalinski *et al.*, 1997). In the hippocampus, a high expression of mRNA for group I mGlu receptors (see Testa *et al.*, 1998), as well as the high immunoreactivity of group I mGlu receptors (Shigemoto *et al.*, 1997; Blumcke *et al.*, 1996) were found. That structure is also intensely immunolabelled by mGluR5 antibody (Lujan *et al.*, 1996). The ability of S-4C3H-PG, an antagonist of group I mGlu receptors to produce anxiolytic responses in the Vogel test after intrahippocampal administration (Chojnacka-Wójcik *et al.*, 1997), further suggests that this structure might be related to anxiolytic effects of group I mGlu receptor antagonists including MPEP. To verify that hypothesis experiments with intra-hippocampal injections of the MPEP are in progress.

Antidepressant-like effects of MPEP

The antidepressant-like effects of MPEP were evaluated in two behavioural tests, the tail suspension test in mice and the Porsolt test in rats. While MPEP did shorten the immobility time in one model of depression in mice, a tail suspension test, it was inactive in the behavioural despair test. The tail suspension test shows a higher predictive validity for identifying potentially useful pharmacotherapies for depression, compared to the behavioural despair test, e.g. it detects the antidepressant effects of specific serotonin reuptake inhibitors (Ali-Kodja *et al.*, 1986), and as shown by the above results, an action of the mGlu5 receptor antagonist. Earlier data indicate that the excitatory effect of an agonist of the group I mGlu receptor system is influenced by prolonged treatment with an antidepressant drug imipramine or by chronic electroconvulsive (ECS) treatment (Palucha *et al.*, 1997; Pilc *et al.*, 1998). In those experiments performed in the CA1 area of the hippocampus, the (R,S)-3,5-dihydroxyphenylglycine-mediated increase of the population spike, was attenuated both by chronic imipramine and ECS (Palucha *et al.*, 1997; Pilc *et al.*, 1998). It can be speculated therefore, that it is the inhibition of group I mGlu receptor mediated neurotransmission which can contribute to the antidepressant-like effects of both MPEP and imipramine or ECS.

The preclinical data indicate that compounds which reduce transmission at NMDA receptors behave like antidepressants (Skolnick, 1999). Glutamatergic transmission *via* stimulation of group I mGlu receptors has also been shown to potentiate the ionotropic glutamate responses in various preparations (Glaum & Miller, 1994), including potentiation of NMDA currents (Fitzjohn *et al.*, 1996; Ugolini *et al.*, 1999). The blockade of group I mGlu receptors by MPEP may therefore lead to a decrease in NMDA-receptor-mediated neurotransmission and might contribute to the antidepressant-like effect of MPEP. It can be speculated that MPEP, which neither causes sedation nor disturbs the rota-rod performance, might be free of side effects produced by antagonists of NMDA receptors.

In conclusion, MPEP is a selective, systematically active antagonist of mGlu5 receptors. It produced anxiolytic-like effects in several tests such as the Vogel test in rats, the elevated plus-maze test in rats as well as the four-plate test in mice. MPEP also exerted antidepressant-like effects in the tail suspension test in mice. It was also found that MPEP did not induce sedation nor disturb motor coordination in animals. The above results indicate that antagonists of mGlu5 receptors may play a role in the therapy of anxiety and/or depression. Identification of the sites of action of MPEP and of the mechanism of these effects still requires further studies.

The study was supported by the Institute of Pharmacology, Polish Acad. Sci., and by the KBN grants No 4.P05A.091.17 to A. Pilc.

References

ALI-KODJA, F., BOUGARD, M., PERRAULT, G. & ZIVKOVIC, B. (1986). Effect of serotonin uptake inhibitors on the immobility of mice in the tail suspension test. *Br. J. Pharmacol.*, **87**, 130P.

ARON, C., SIMON, P., LAROUSSE, C. & BOISSIER, J.R. (1971). Evaluation of a rapid technique for detecting minor tranquilizers. *Neuropharmacology*, **10**, 459–469.

BAJKOWSKA, M., BRAŃSKI, P., ŚMIAŁOWSKA, M. & PILC, A. (1999). Effect of chronic antidepressant or electroconvulsive shock treatment on mGLuR1a immunoreactivity expression in the rat hippocampus. *Pol. J. Pharmacol.*, **51**, 539–541.

BENNETT, D.A., BERNARD, P.S., AMRICK, C.L., WILSON, D.E., LIEBMAN, J.M. & HUTCHISON, A.J. (1989). Behavioral pharmacological profile of CGS 19755, a competitive antagonist at N-methyl-D-aspartate receptors. *J. Pharmacol. Exp. Ther.*, **250**, 454–460.

BLUMCKE, I., BEHLE, K., MALITSCHEK, B., KUHN, R., KNOPFEL, T., WOLF, H.K. & WIESTLER, O.D. (1996). Immunohistochemical distribution of metabotropic glutamate receptor subtypes mGluR1b, mGluR2/3, mGluR4a and mGluR5 in human hippocampus. *Brain Res.*, **736**, 217–226.

BRUNO, V., COPANI, A., BATTAGLIA, G., RAFFAELE, R., SHINOZAKI, H. & NICOLETTI, F. (1994). Protective effect of the metabotropic glutamate receptor agonist, DCG-IV, against excitotoxic neuronal death. *Eur. J. Pharmacol.*, **256**, 109–112.

CHOJNACKA-WÓJCIK, E., TATARCZYŃSKA, E. & PILC, A. (1997). The anxiolytic-like effect of metabotropic glutamate receptor antagonists after intrahippocampal injection in rats. *Eur. J. Pharmacol.*, **319**, 153–156.

CONN, P.J. & PIN, J.P. (1997). Pharmacology and functions of metabotropic glutamate receptors. *Ann. Rev. Pharmacol. Toxicol.*, **37**, 205–237.

DANYSZ, W. & PARSONS, C.G. (1998). Glycine and N-methyl-D-aspartate receptors: Physiological significance and possible therapeutic applications. *Pharmacol. Rev.*, **50**, 597–664.

DANYSZ, W., PARSONS, C.G., BRESNIK, I. & QUACK, G. (1996). Glutamate in CNS Disorders. *Drug News & Perspectives*, **8**, 261–277.

DAWSON, G.R. & TRICKLEBANK, M.D. (1995). Use of the elevated plus maze in the search for novel anxiolytic agents. *Trends. Pharmacol. Sci.*, **16**, 33–36.

FITZJOHN, S.M., IRVING, A.J., PALMER, M.J., HARVEY, J., LODGE, D. & COLLINGRIDGE, G.L. (1996). Activation of group I mGluRs potentiates NMDA responses in rat hippocampal slices. *Neurosci. Lett.*, **203**, 211–213.

GASPARINI, F., LINGENHOHL, K., STOEHR, N., FLOR, P.J., HEINRICH, M., VRANESIC, I., BIOLLAZ, M., ALLGEIER, H., HECKENDORN, R., URWYLER, S., VARNEY, M.A., JOHNSON, E.C., HESS, S.D., RAO, S.P., SACAAN, A.I., SANTORI, E.M., VELICELEBI, G. & KUHN, R. (1999). 2-Methyl-6-(phenylethynyl)-pyridine (MPEP), a potent, selective and systemically active mGlu5 receptor antagonist. *Neuropharmacology*, **38**, 1493–1503.

GLAUM, S.R. & MILLER, R.J. (1994). Acute Regulation of Synaptic Transmission by Metabotropic Glutamate Receptors. In: *The Metabotropic Glutamate Receptors*. ed. Conn, P.J. and Patel, J. pp. 147–172. Totowa, NJ: Humana Press.

GRAY, J.A. (1982). Precis of the neuropsychology of anxiety:an enquiry into the functions of the septo-hippocampal system. *Behav. Brain Sci.*, **5**, 469–534.

HELTON, D.R., TIZZANO, J.P., MONN, J.A., SCHOEPP, D.D. & KALLMAN, M.J. (1998). Anxiolytic and side-effect profile of LY354740: a potent, highly selective, orally active agonist for group II metabotropic glutamate receptors. *J. Pharmacol. Exp. Ther.*, **284**, 651–660.

JANSSEN, P.A., JAGENEAU, A.H. & SCHELLEKENS, K.H. (1960). Chemistry and pharmacology of compounds related to 4-(4-hydroxy-4-phenyl-piperidino)-butyrophenone. IV. Influence of haloperidol (R 1625) and of chlorpromazine on the behaviour of rats in an unfamiliar 'open field' situation. *Psychopharmacologia.*, **1**, 389–392.

JESSA, M., NAZAR, M., BIDZINSKI, A. & PŁAŹNIK, A. (1996). The effects of repeated administration of diazepam, MK-801 and CGP 37849 on rat behavior in two models of anxiety. *Eur. Neuropsychopharmacol.*, **6**, 55–61.

KŁODZIŃSKA, A., CHOJNACKA-WÓJCIK, E., PAŁUCHA, A., BRAŃSKI, P., POPIK, P. & PILC, A. (1999). Potential anti-anxiety, anti-addictive effects of LY 354740, a selective group II glutamate metabotropic receptors agonist in animal models. *Neuropharmacology*, **38**, 1831–1839.

LUJAN, R., NUSSER, Z., ROBERTS, J.D.B., SHIGEMOTO, R. & SOMOGYI, P. (1996). Perisynaptic location of metabotropic glutamate receptors mGluR1 and mGluR5 on dendrites and dendritic spines in the rat hippocampus. *Eur. J. Neurosci.*, **8**, 1488–1500.

MONAGHAN, D.T., BRIDGES, R.J. & COTMAN, C.W. (1989). The excitatory amino acid receptors: their classes, pharmacology, and distinct properties in the function of the central nervous system. *Annu. Rev. Pharmacol. Toxicol.*, **29**, 365–402.

NICOLETTI, F., BRUNO, V., COPANI, A., CASABONA, G. & KNOPFEL, T. (1996). Metabotropic glutamate receptors: A new target for the therapy of neurodegenerative disorders? *Trends Neurosci.*, **19**, 267–271.

PAŁUCHA, A., BRAŃSKI, P., TOKARSKI, K., BIJAK, M. & PILC, A. (1997). Influence of imipramine treatment on the group I of metabotropic glutamate receptors in CA1 region of hippocampus. *Pol. J. Pharmacol.*, **49**, 495–497.

PELLOW, S. & FILE, S.E. (1986). Anxiolytic and anxiogenic drug effects on exploratory activity in an elevated plus-maze: a novel test of anxiety in the rat. *Pharmcol. Biochem. Behav.*, **24**, 525–529.

PILC, A., BRANSKI, P., PALUCHA, A., TOKARSKI, K. & BIJAK, M. (1998). Antidepressant treatment influences group I of glutamate metabotropic receptors in slices from hippocampal CA1 region. *Eur. J. Pharmacol.*, **349**, 83–87.

PORSOLT, R.D., ANTON, G., BLAVET, N. & JALFRE, M. (1978). Behavioural despair in rats: a new model sensitive to antidepressant treatments. *Eur. J. Pharmacol.*, **47**, 379–391.

PRZEGALIŃSKI, E., TATARCZYŃSKA, E., DEREŃ-WESOŁEK, A. & CHOJNACKA-WÓJCIK, E. (1997). Antidepressant-like effects of a partial agonist at strychnine-insensitive glycine receptors and a competitive NMDA receptor antagonist. *Neuropharmacology*, **36**, 31–37.

ROWLAND, N.E., CAPUTO, F.A. & FREGLY, M.J. (1987). Water intake induced in rats by serotonin and 5-hydroxytryptophan: different mechanisms? *Brain Res. Bull.*, **18**, 501–508.

SEKIYAMA, N., HAYASHI, Y., NAKANISHI, S., JANE, D.E., TSE, H.W., BIRSE, E.F. & WATKINS, J.C. (1996). Structure-activity relationships of new agonists and antagonists of different metabotropic glutamate receptor subtypes. *Br. J. Pharmacol.*, **117**, 1493–1503.

SHIGEMOTO, R., KINOSHITA, A., WADA, E., NOMURA, S., OHISHI, H., TAKADA, M., FLOR, P.J., NEKI, A., ABE, T., NAKANISHI, S. & MIZUNO, N. (1997). Differential presynaptic localization of metabotropic glutamate receptor subtypes in the rat hippocampus. *J. Neurosci.*, **17**, 7503–7522.

SKOLNICK, P., LAYER, R.T., POPIK, P., NOWAK, G., PAUL, I.A. & TRULLAS, R. (1996). Adaptation of N-methyl-D-aspartate (NMDA) receptors following antidepressant treatment: Implications for the pharmacotherapy of depression. *Pharmacopsychiatry*, **29**, 23–26.

SKOLNICK, P. (1999). Antidepressants for the new millennium. *Eur. J. Pharmacol.*, **375**, 31–40.

SPOOREN, W.P., VASSOUT, A., NEIJT, H.C., KUHN, R., GASPARINI, F., ROUX, S., PORSOLT, R.D. & GENTSCH, C. (2000). Anxiolytic-like effects of the prototypical metabotropic glutamate receptor 5 antagonist 2-methyl-6-(phenylethynyl)pyridine in rodents. *J. Pharmacol. Exp. Ther.*, **295**, 1267–1275.

STEPHENS, D.N., MELDRUM, B.S., WEIDMANN, R., SCHNEIDER, C. & GRUTZNER, M. (1986). Does the excitatory amino acid receptor antagonist 2-APH exhibit anxiolytic activity? *Psychopharmacology (Berl.)*, **90**, 166–169.

STERU, L., CHERMAT, R., THIERRY, B. & SIMON, P. (1985). The tail suspension test: A new method for screening antidepressants in mice. *Psychopharmacology*, **85**, 367–370.

TESTA, C.M., FRIBERG, I.K., WEISS, S.W. & STANDAERT, D.G. (1998). Immunohistochemical localization of metabotropic glutamate receptors mGluR1a and mGluR2/3 in the rat basal ganglia. *J. Comp. Neurol.*, **390**, 5–19.

UGOLINI, A., CORSI, M. & BORDI, F. (1999). Potentiation of NMDA and AMPA responses by the specific mGluR(5) agonist CHPG in spinal cord motoneurons. *Neuropharmacology*, **38**, 1569–1576.

VARNEY, M.A., COSFORD, N.D.P., JACHEC, C., RAO, S.P., SACAAN, A., LIN, F.-F., BLEICHER, L., SANTORI, E.M., FLOR, P.J., ALLGEIER, H., GASPARINI, F., KUHN, R., HESS, S.D., VELIÇE-LEBI, G. & JOHNSON, E.C. (1999). SIB-1757 and SIB-1893: Selective, non-competitive antagonists of metabotropic glutamate receptor type 5 (mGluR5). *Mol. Pharmacol.*, **290**, 170–181.

VOGEL, J.R., BEER, B. & CLODY, D.E. (1971). A simple and reliable conflict procedure for testing anti-anxiety agents. *Psychopharmacologia.*, **21**, 1–7.

WILEY, J.L., CRISTELLO, A.F. & BALSTER, R.L. (1995). Effects of site-selective NMDA receptor antagonists in an elevated plus-maze model of anxiety in mice. *Eur. J. Pharmacol.*, **294**, 101–107.

WRÓBLEWSKI, J.T. & DANYSZ, W. (1989). Modulation of glutamate receptors: molecular mechanisms and functional implications. Modulation of glutamate receptors: molecular mechanisms and functional implications. *Ann. Rev. Pharmacol. Toxicol.*, **29**, 441–474.

(Received July 11, 2000
Revised January 2, 2001
Accepted January 5, 2001)

0022-3565/00/2953-1267$03.00/0
THE JOURNAL OF PHARMACOLOGY AND EXPERIMENTAL THERAPEUTICS

JPET 295:1267–1275, 2000

Vol. 295, No. 3
2949/864946
Printed in U.S.A.

Anxiolytic-Like Effects of the Prototypical Metabotropic Glutamate Receptor 5 Antagonist 2-Methyl-6-(phenylethynyl)pyridine in Rodents

WILL P. J. M. SPOOREN, ANNICK VASSOUT, HANS C. NEIJT, RAINER KUHN, FABRIZIO GASPARINI, SILVAIN ROUX, ROGER D. PORSOLT, and CONRAD GENTSCH

Novartis Pharma AG, Nervous System Research, Basel, Switzerland (W.P.J.M.S., A.V., H.C.N., R.K., F.G., C.G.); and Porsolt and Partners Pharmacology, Boulogne-Billancourt, France (S.R., R.D.P.)

Accepted for publication August 24, 2000 This paper is available online at http://www.jpet.org

ABSTRACT

Recently, selective and systemically active antagonists for the metabotropic glutamate 5 receptor ($mGlu_5$) were discovered, and the most potent derivative was found to be MPEP (2-methyl-6-(phenylethynyl)pyridine). Given the high expression of $mGlu_5$ receptors in limbic forebrain regions, it was decided to evaluate the anxiolytic potential of MPEP. After an acute oral administration, MPEP attenuated the anxiety-dependent variable in a variety of well established anxiety test paradigms. In rats, MPEP (10, 30, and 100 mg/kg) increased punished responses in the Geller-Seifter test, but none of these effects reached statistical significance. MPEP significantly increased the ratio (open/total arm entries; 0.1, 1, and 10 mg/kg), the number of open arm entries (0.1, 1, and 10 mg/kg), as well as time spent on open arm (0.1 and 1 mg/kg) in the elevated plus maze test. Furthermore, MPEP (0.3 and 1 mg/kg) significantly increased the time spent in social contact in the social exploration test. In mice, MPEP attenuated stress-induced hyperthermia (15 and 30 mg/kg) and decreased the number of buried marbles in the marble burying test (7.5 and 30 mg/kg). Finally, MPEP (0.01, 0.1, 1, 10, and 100 mg/kg) was tested on spontaneous locomotor activity in mice, and only a dose of 100 mg/kg significantly reduced vertical activity; no effect was seen on horizontal activity. MPEP (7.5, 15, and 30 mg/kg) was ineffective on *d*-amphetamine-induced (2.5 mg/kg) locomotor activity in mice and prepulse inhibition in rats (1, 3, or 10 mg/kg). Thus, these findings indicate that MPEP exhibits anxiolytic-like effects and low risks for sedation and psychotomimetic side-effects in rodents.

It is widely accepted that glutamate is the main excitatory neurotransmitter in the brain (McGeer et al., 1987). Glutamate mediates its effect via two distinct types of receptors, i.e., the ionotropic receptors and the metabotropic receptors (Monaghan et al., 1989; Conn and Pin, 1997). The family of the metabotropic receptors (mGlu) contains of, at present, eight different subtypes (Conn and Pin, 1997). On the basis of sequence homology, effector coupling, and pharmacology, mGlu receptors are divided into three subgroups. The group I mGlu receptors ($mGlu_1$ and $mGlu_5$) are positively coupled to phospholipase C, and the group II mGlu receptors ($mGlu_2$ and $mGlu_3$) and the group III receptors ($mGlu_4$, $mGlu_6$, $mGlu_7$, and $mGlu_8$) are negatively coupled to adenylate cyclase (Pin and Duvoisin, 1995; Conn and Pin, 1997).

Drugs targeting ionotropic receptors have so far failed to qualify as therapeutics, not because of lack of efficacy but mainly due to the induction of severe and persistent side-effects, i.e., most prominently psychotomimetic effects (Danysz et al., 1996). Currently, agonists or antagonists of metabotropic glutamate receptors are believed to have a milder side effect profile and, accordingly, compounds specifically interacting at these receptors have been proposed as potential new therapeutics for a number of neurological and psychiatric disorders (Knöpfel et al., 1995; Conn and Pin, 1997; Nicoletti et al., 1997). However, these hypotheses originate from speculations based on the expression pattern of distinct mGlu-subtype receptors in the central nervous system and on the effects of nonselective compounds, which do not discriminate between distinct mGlu-receptor subtypes.

After the discovery of selective and systemically active antagonists for the $mGlu_5$ receptor, it is now possible to study the potential role of this receptor subtype in behavior and disease models (Gasparini et al., 1999). In cells expressing the human $mGlu_5$ receptor, the most potent derivative, 2-methyl-6-(phenylethynyl)pyridine (MPEP), completely inhibited quisqualate-stimulated phosphoinositide hydrolysis

Received for publication May 26, 2000.

ABBREVIATIONS: mGlu, metabotropic glutamate receptor; MPEP, 2-methyl-6-(phenylethynyl)pyridine; SIH, stress-induced hyperthermia; PPP, prepulse pulse; PA, pulse alone; PPI, prepulse inhibition; (+)-MK801, (5*R*,10*S*)-(+)-5-methyl-10,11-dihydro-5*H*-dibenzo[*a*,*d*]cyclohepten-5,10-imine hydrogen maleate.

with an IC_{50} value of 36 nM. When tested at group II and III receptors, MPEP did not show agonist or antagonist activity at 100 μM on human $mGlu_2$, $mGlu_3$, $mGlu_{4a}$, $mGlu_{7b}$, and $mGlu_{8a}$ receptors nor at 10 μM on the human $mGlu_6$ receptor. Electrophysiological recordings in *Xenopus laevis* oocytes demonstrated no significant effect at 100 μM on human NMDA (NMDA1A/2A), rat AMPA [Glu3-(flop)], and human kainate [Glu6-(IYQ)] receptor subtypes nor at 10 μM on the human NMDA1A/2B receptor (Gasparini et al., 1999). MPEP was also tested in a binding battery of receptors containing representatives of monoamine receptor subtypes (adrenaline, dopamine, serotonine), muscarinic, nicotinic, neurokinin, GABA-A, GABA-B, and adenosine receptors. MPEP did not show significant binding affinity for any of the receptors tested up to a concentration of 10 μM (F. Gasparini, manuscript in preparation). Furthermore, when tested for oral bioavailability and blood-brain barrier penetration, MPEP was found to be well absorbed and to readily penetrate the brain 1 h after administration (F. Gasparini, manuscript in preparation).

$mGlu_5$ receptors are widely expressed in the central nervous system with a particularly high expression in the hippocampus, the nucleus accumbens, and the striatum but also in the internal and external pallidal segments and the substantia nigra pars reticulata (Shigemoto et al., 1993; Testa et al., 1994; Romano et al., 1995). These brain areas are well known to represent key elements in the so-called cortico-basal ganglia-cortico circuitry (Albin et al., 1989; Chesselet and Delfs, 1996), i.e., circuits involved in emotional processes such as anxiety (Duncan et al., 1996). Thus, given the high expression of $mGlu_5$ receptors in limbic forebrain regions, it was decided to evaluate the potential of MPEP in a multiplicity of well established animal models of anxiety as recently reviewed by Olivier et al. (2000) and Rodgers (1997), that included a variety of nonconditioned and conditioned anxiety models with a wide range of different behaviors and motivations. In addition, the effect of MPEP on locomotion was studied to obtain an index of the specificity of anxiolytic action as well as its effect on *d*-amphetamine-induced locomotor activity to explore the mechanism of action of MPEP-mediated effects. Finally, to investigate also the potential for psychotomimetic side-effects, MPEP was tested on prepulse inhibition (PPI).

Materials and Methods

Social Exploration

Animals. Adult male Sprague-Dawley rats (="resident" rats; OFA/IC, Iffa Crédo, Les Oncins, France; 350–400 g) and young Lister Hooded rats (="intruder" rats; LI/HO, Harlan, Horst, The Netherlands; 100–120 g) were used. Intruder rats were housed in pairs and resident rats were individually housed in macrolon cages (42 × 26 × 15 cm) for 2 weeks before the test. All animals were housed in the same room. The housing facility was temperature- and humidity-controlled and equipped with artificial illumination (6:00 AM to 6:00 PM, lights on). The animals had access to water and food (Ecosan, Eberle Nafag AG, Gossau, Switzerland), ad libitum. All rats were experimentally naïve.

Drug Treatment and Experimental Procedure. Animals received MPEP [doses: 0.003, 0.3, or 1 mg/kg (experiment 1) or 1 or 10 mg/kg (experiment 2); the results of the first experiment suggested a bell-shaped dose-response effect and the second experiment was used to further explore these findings], chlordiazepoxide-HCl (5 mg/kg, p.o.; CDZ, Research Biochemicals International, Natick, MA), i.e., the reference compound, or vehicle (0.5% methylcellulose; Animed). The injection volume was 2 ml/kg. Oral treatment was given to the intruder rat only, and the test was performed 1 h after drug administration. All observations were made during the light phase (8:00 AM to 1:00 PM) in the home cage of the resident rat (see above). The floor of the cage was covered with sawdust. Pairs consisting of one intruder rat and one resident rat were assigned at random to one of the experimental or the control groups. The duration of active approach behaviors (=time spent in social activity) of the intruder rat (sniffing, anogenital exploration, nosing, grooming, licking, playing) toward the resident was manually scored and cumulatively recorded over a period of 5 min.

Statistics. The statistical evaluation was performed on pooled data of two independent experiments [dependent variable: time spent in social contact (see above)] using a one way ANOVA followed by Dunnett's test for comparison of multiple dose levels against vehicle (SigmaStat 2.03; SPSS, Chicago, IL).

Elevated Plus Maze

Animals. Male adult Sprague-Dawley rats (Iffa Crédo, Les Oncins, France; 180–220 g) were housed in groups of four in macrolon cages (42 × 26 × 15 cm) for at least 3 days before the experiment. The housing facility was temperature- and humidity-controlled and equipped with artificial illumination (6:00 AM to 6:00 PM, lights on). The animals had access to water and food (Ecosan, Eberle Nafag AG), ad libitum. All animals were experimentally naïve.

Apparatus. The elevated plus-maze consists of two open arms (40 × 12 cm) and two enclosed arms (40 × 12 × 20 cm), which all extend from a common central platform (12 × 12 cm). The configuration forms the shape of a plus sign, with similar arms arranged opposite to each another, and the apparatus is elevated 60 cm above the floor on a central pedestal. The maze is made from gray Plexiglas. The grip on the open arms is facilitated by inclusion of a small raised edge (0.25 cm) around their perimeter.

Drug Treatment and Experimental Procedure. The method was adopted from Handley and Mithani (1984). Rats were randomly allocated to one of the various treatments. Animals were transported from the housing room to the laboratory at least 1 h before testing. After oral drug administration, rats were individually housed in macrolon cages (22 × 16 × 14 cm), and after 60 min placed onto the central platform facing an enclosed arm. An 8-min trial was performed, and the maze was thoroughly cleaned between subjects. Direct registrations were made by an observer sitting close to the maze, and the following conventional parameters were used: number of open and closed arm entries (arm entry defined as all four paws entering an arm) and time spent on open arms (excluding the central platform). Animals from the different treatment groups were alternatively tested, and trials were performed between 8:30 AM and 12:30 PM, i.e., within the first half of the light phase.

Rats were treated with MPEP [doses: 0.1, 1, or 10 mg/kg, p.o. (n = 15 per group)], chlordiazepoxide-HCl (10 mg/kg, p.o.; Research Biochemicals International), i.e., the positive control, or vehicle (0.5% methylcellulose; Animed).

Statistics. For each behavioral parameter a separate ANOVA was performed followed by Dunnett's multiple comparison test to compare different dose levels against vehicle (SYSTAT 8.0; SPSS).

Stress-Induced Hyperthermia and Marble Burying

Animals. Male mice (OF1/IC; Iffa Crédo, Les Oncins, France; 18–20 g) were housed in macrolon cages (42 × 26 × 15 cm; n = 15 per cage) in the laboratory in which the animals were later tested. The room was temperature-controlled and equipped with artificial illumination (6:00 AM to 6:00 PM, lights on). The animals had free access to water and food (Ecosan, Eberle Nafag AG), ad libitum. All mice were experimentally naïve.

Stress-Induced Hyperthermia. The test procedure for stress-induced hyperthermia (SIH) was adopted with minor modification from the original description by Lecci et al. (1990). Briefly, rectal temperature was measured to the nearest 0.1°C by a thermometer (ELLAB instruments, Copenhagen, Denmark) via a lubricated thermistor probe (2-mm diameter) inserted 20 mm into the rectum while the mouse was hand-held near the base of the tail. The probe was left in place until steady readings were obtained (within 15 s).

Drug Treatment and Experimental Procedures. Fifteen animals were housed per macrolon cage (42 × 26 × 15 cm). At least 24 h before the experiment animals within a cage were marked on their fur with color for later identification. Sixty minutes before taking the rectal temperature all individuals within a given cage were consecutively treated at 1-min intervals with MPEP (doses: 1.5, 7.5, 15, or 30 mg/kg, p.o.; injection volume: 10 ml/kg), chlordiazepoxide-HCl (10 mg/kg, p.o.; Research Biochemicals International), i.e., the positive control, or vehicle (0.5% methylcellulose; Animed). Exactly 60 min later the mice were consecutively removed from the cage (again at 1-min intervals), and rectal temperature was determined and noted. Once temperature had been recorded, the animals were placed in a different (adjacent) cage. The dependent variable, i.e., the stress-induced hyperthermia, was defined as the delta of the median rectal temperature within the six initially removed mice and the median rectal temperature within the six last removed mice within a cage. This delta was calculated for six to eight cages depending on the specific treatment group (see Fig. 3 legend), whereas in the final representation the mean of these six to eight values was used. The rectal temperature of the very first animal was used, in addition, to evaluate the compound's potential effect on basal body temperature, per se.

Marble Burying. The test procedure for marble burying was adopted with minor modifications from the original description of Broekkamp et al. (1986). Briefly, the first two mice removed from the cage while assessing stress-induced hyperthermia were used in the marble burying test. The animals were individually placed in small cages (22 × 16 × 14 cm) in which 10 marbles had been equally distributed on top of a 5-cm sawdust bedding. The mice were left undisturbed in these cages for 60 min; after removal of the mouse the number of visible, nonburied marbles (i.e., less than two-thirds covered by sawdust) was counted and this number served as the dependent variable.

Statistics. Stress-induced hyperthermia (delta of rectal temperature) and marble burying (number of visible marbles) were statistically evaluated using a Kruskal-Wallis one-way ANOVA followed by a post hoc one-tailed Mann-Whitney *U* test, Bonferroni corrected (SYSTAT 8.0).

Geller-Seifter Conflict Test in Rats

Animals. Male Wistar rats (Elevage Janvier, Le Genest-Saint-Isle, France; 180–240 g) were housed in macrolon cages (41 × 25 × 14 cm; $n = 5$ per cage). The animal room was temperature-controlled and equipped with artificial illumination (6:00 AM to 6:00 PM, lights on). The animals had access to water and food (UAR, Villemoisson-sur-Orge, France), ad libitum. All rats were experimentally naïve.

Drug Treatment and Experimental Procedures. The method applied here was adopted from Geller and Seifter (1960) and included the modification put forward by Davidson and Cook (1969). Animals were trained in sound-attenuated standard Skinner boxes (23 × 21 × 18 cm; MED Associates, St. Albans, VT), which were fitted with a white house light, a red signal light, a lever (force necessary to depress lever: 25 g), and a food pellet dispenser. The lever was positioned on the right side of the food receptacle, which was itself connected to the pellet dispenser. The Skinner boxes were connected to a MED-PC programming system that controlled the experiment and automatically collected the data.

Training Procedure. Rats were submitted to daily training sessions (15 min) according to a variable interval, 15-s reinforcement schedule. In this schedule, only those responses occurring after variable intervals (mean value: 15 s) were rewarded. These reinforced responses consisted of the delivery of a 45-mg food pellet (Noyes, Lancaster, UK). The rats were then submitted to three nonpunished periods of 3 min each, signaled by the presence of the white house light, alternated with two punished periods of 3 min each, signaled by the presence of a red signal light, during which lever pressing was simultaneously reinforced and punished with electric foot-shock according to a variable ratio reinforced schedule (punished periods). Reinforcement and shocks were given after a variable number of responses (mean value: 10) and foot-shocks (0.4 mA, 0.5 s) were delivered by a scrambled shock generator (model E1308; Coulbourn Instruments, San Diego, CA). Daily sessions lasted 15 min. The animals received a p.o. administration of distilled water 60 min before each session. In addition to the food pellets consumed in the Skinner box, animals received a 15-g food ration in their home cages. This amount of food was given after the last animal was tested and represented around 80% of the unlimited daily food intake.

Three dependent variables were used: 1) The number of punished responses—the total number of presses on the lever during the punished periods; 2) The number of shocks—the total number of shocks the animal received during the punished periods; and 3) The number of nonpunished responses—the total number of lever-presses during the nonpunished periods.

Drug Testing Procedure. Drug testing was started once the rats showed stable baseline performance and had demonstrated a positive response to the reference anxiolytic chlordiazepoxide-HCl (16 mg/kg, p.o.; CDZ, Research Biochemicals International). Sessions with MPEP (doses: 10, 30, or 100 mg/kg, p.o.) were run twice weekly with at least one drug-free training session (oral treatment with distilled water) in between. During the training phase, drug sessions lasted 15 min and the food regime was similar to the training period. Each animal was used as its own control and received all treatments in a randomized order to ensure even distribution of the different treatments in time. Test drug or vehicle (0.5% methylcellulose) was administered 60 min before the test. Each of the eight rats was always tested in the same Skinner box and at the same time of day.

Statistics. Data were analyzed using a paired Student's *t* test, which was Bonferroni-corrected.

Spontaneous Locomotor Activity Test

Animals. Male OF1/IC mice (Iffa Crédo, Les Oncins, France; 18–20 g) were housed in macrolon cages (42 × 26 × 15 cm, $n = 10$ per cage) in a temperature-controlled room under artificial illumination (6:00 AM to 6:00 PM, lights on) and had access to water and food (Ecosan, Eberle Nafag AG), ad libitum.

Drug Treatment and Experimental Procedures. Mice received an oral injection of MPEP (doses: 0.01, 0.1, 1, 10, or 100 mg/kg, p.o. (experiment 1), or 7.5, 15, or 30 mg/kg, p.o. (experiment 2)) or vehicle (0.5% methylcellulose; Animed). Subsequently, the animals were individually placed into locomotor activity cages (17 × 32 × 20 cm; Motron motility, Novartis AG), and the number of beam interruptions at two different heights (2.5 and 11 cm) was registered for 120 min and used to quantify horizontal and vertical activity, respectively.

Statistics. A separate one-way ANOVA was used to evaluate total horizontal or vertical activity counts in a 120-min period of registration (SYSTAT 8.0).

d-Amphetamine-Induced Locomotor Activity

Animals. Male OF1/IC mice (Iffa Crédo, Les Oncins, France; 18–20 g) were housed in macrolon cages (42 × 26 × 15 cm, $n = 10$ per cage) in a temperature-controlled room under artificial illumination (6:00 AM to 6:00 PM, lights on) and had access to water and food (Ecosan, Eberle Nafag AG), ad libitum.

Drug Treatment and Experimental Procedures. Horizontal locomotor activity was assessed in transparent Plexiglas boxes (dimensions: 19 × 31 × 16 cm), and activity was detected and registered

using the TSE Moti system (TSE, Bad Homburg, Germany), which is based on the registration of infrared light beam interruptions along the x, y, and z axes, as caused by an animal's movements; data were directly stored in a computer. Mice were individually placed in the Plexiglas boxes and allowed to habituate for 45 min. Then the animals were removed from the boxes and injected with MPEP (7.5, 15, or 30 mg/kg, p.o.) or its solvent (methylcellulose, 0.5%) and then immediately returned to their respective boxes. Fifteen minutes later the animals were again removed from the boxes and injected with *d*-amphetamine (2.5 mg/kg, i.p.) or its solvent (distilled water). The animals were again immediately returned to their respective locomotor boxes, and the horizontal locomotor activity was registered for the next 120 min. The dose of *d*-amphetamine was chosen to allow either inhibition or potentiation to be seen.

Statistics. A separate two-way ANOVA (factors: MPEP and *d*-amphetamine) was used to evaluate total horizontal or vertical activity counts during 120 min of registration (SYSTAT 8.0).

Prepulse Inhibition

Animals. Male adult Brown Norway rats (Iffa Crédo, L'Arbresle, France; 214–245 g) were housed in groups of four in macrolon cages (42 × 26 × 15 cm) for at least 3 days before the experiment. The housing facility was temperature- and humidity-controlled and equipped with artificial illumination (6:00 AM to 6:00 PM, lights on). The animals had access to water and food (Ecosan, Eberle Nafag AG), ad libitum. All animals were experimentally naïve.

Apparatus. PPI was measured with a commercially available Coulbourn startle system (Coulbourn Instruments), modified such that all acoustic stimuli were presented to the animals via a single Visaton (Germany) wide range tweeter (type DHT 9 AW-NG) in the center of the ventilated, sound-attenuated test chamber. White noise was used for background, prepulse, and startle pulse stimuli with a frequency range of the tweeter around 4 kHz. Sound pressure levels were calibrated on the db-A scale using a Bruel and Kjaer (Copenhagen, Denmark) 4133 microphone and 2209 type meter (Naerum, Denmark). The startle response was recorded with a quartz force sensor for measuring dynamic and quasistatic forces (Kistler Instruments AG, Winterthur, Switzerland; type 9203; connected to a Kistler charge amplifier type 5011, with low pass filter at 300 Hz and high pass at 100 s). The sensor was mounted directly below the animal enclosure (plastic box covered with metal grid; 16 × 8 × 8 cm) and calibrated using weights in the range between 10 and 1500 g. The output signal of the charge amplifier was digitized (sample rate, 1 kHz for 200 ms, 8-bit) and stored on a microcomputer.

Drug Treatment and Experimental Procedures. Animals were pretreated with MPEP (1, 3, or 10 mg/kg, p.o.) or vehicle (0.5% methylcellulose, 2 ml/kg). Alternatively, animals were injected with (+)-MK801 (0.1 mg/kg, s.c.) or saline (1 ml/kg). 30 min after the administration of (+)-MK801, or 60 min after MPEP treatment, animals were positioned in the startle test chamber, such that at least one subject from each treatment group was included in each session. From session to session, the different treatment groups were assigned to different startle sensors (clockwise rotation). This procedure was used to rule out artifacts related to sensor and/or session differences. Background noise was continuous at a level of 62 db. Acoustic stimuli consisted of a startle-eliciting stimulus of 105 db for 40 ms and prepulses of 4, 8, or 16 db above background with a duration of 20 ms. The startle-eliciting stimulus was presented either alone (pulse alone, PA) or in combination with a prepulse presented 100 ms earlier (prepulse pulse, PPP). A startle session included an adaptation time of 3 min and subsequently of 63 stimuli. The first three stimuli were PA stimuli that were not included in the analysis; these merely served to achieve a stable baseline in startle reactivity. Subsequently, three blocks of 10 PA stimuli were presented (PA1, PA2, and PA3, respectively). The second block included in addition 30 PPP stimuli (10 of each type), whereby stimuli in this block were presented in randomized order. The interval between stimuli was randomized between 9 and 21 s. Startle peak amplitudes (g) were estimated for each animal averaged over the 10 stimuli of one type. Prepulse inhibition was computed according the formula, %PPI = 100 − 100 × [(PA2 − PPP)/PA2].

Statistics. For each stimulus type, results were statistically evaluated using ANOVA with one factor dose, e.g., 0, 1, 3, and 10 mg/kg for MPEP or 0 and 0.1 mg/kg for (+)-MK801 (SYSTAT 8.0). One animal (treated with vehicle) was detected as an outlier, independent of the stimulus type used. The data for this animal were excluded from the final analysis.

Results

Unconditioned Response Tests

Social Exploration. Chlordiazepoxide (5 mg/kg, p.o.), used here as a positive standard, significantly increased the time the "intruder" rat spent in active social contact when confronted with a "resident" rat (Fig. 1). Similarly, after an oral administration, MPEP in doses of 0.3 and 1 mg/kg significantly increased the duration of active social contact (Fig. 1). After 10 mg/kg MPEP, the effect was less pronounced and did not reach the level of statistical significance, potentially indicative of a bell-shaped dose-response relation. MPEP was ineffective at the very low dose of 0.003 mg/kg (p.o.).

Elevated Plus Maze. Chlordiazepoxide (10 mg/kg, p.o.), used here as a positive standard, exhibited the well known anxiolytic pattern: the time spent on open arms and the number of open arm entries was significantly increased as compared with vehicle-treated controls and this led to a significantly elevated ratio (Fig. 2, a–c). MPEP also exhibited this typical anxiolytic pattern and increased the ratio (0.1, 1, and 10 mg/kg), the number of open arm entries (0.1, 1, and 10 mg/kg), and the time spent on open arms (0.1 and 1 mg/kg, Fig. 2, a–c). However, chlordiazepoxide as well as MPEP (0.1, 1, and 10 mg/kg) increased the total number of arm entries (Fig. 2d).

Stress-Induced Hyperthermia. In the vehicle-treated cages, stress-induced hyperthermia was quantitatively comparable to the values reported in literature (+1.0°C; Fig. 3a). Chlordiazepoxide (10 mg/kg, p.o.), used here as a positive standard, significantly attenuated stress-induced hyperthermia (SIH; Fig. 3a). MPEP also induced a clear reduction in the stress-induced hyperthermia: already a dose of 7.5 mg/kg,

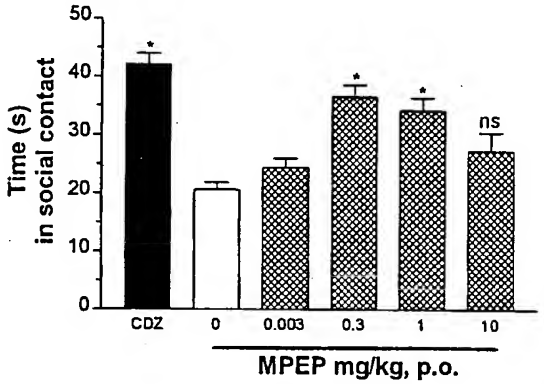

Fig. 1. Social exploration test: bars represent the mean time (seconds per 5-min trial; ± S.E.M.) during which the intruder rat actively explored the resident rat. Only the intruder rats were treated, receiving injections of MPEP [doses: 0.003 (n = 11), 0.3 (n = 11), 1 (n = 22), or 10 mg/kg; p.o. (n = 11)], chlordiazepoxide (CDZ; 5 mg/kg, p.o., n = 21) or vehicle (0 mg/kg; 0.5% methylcellulose, n = 23). Pretreatment time was 60 min. *P < .05 versus the vehicle-treated group (Dunnett's test).

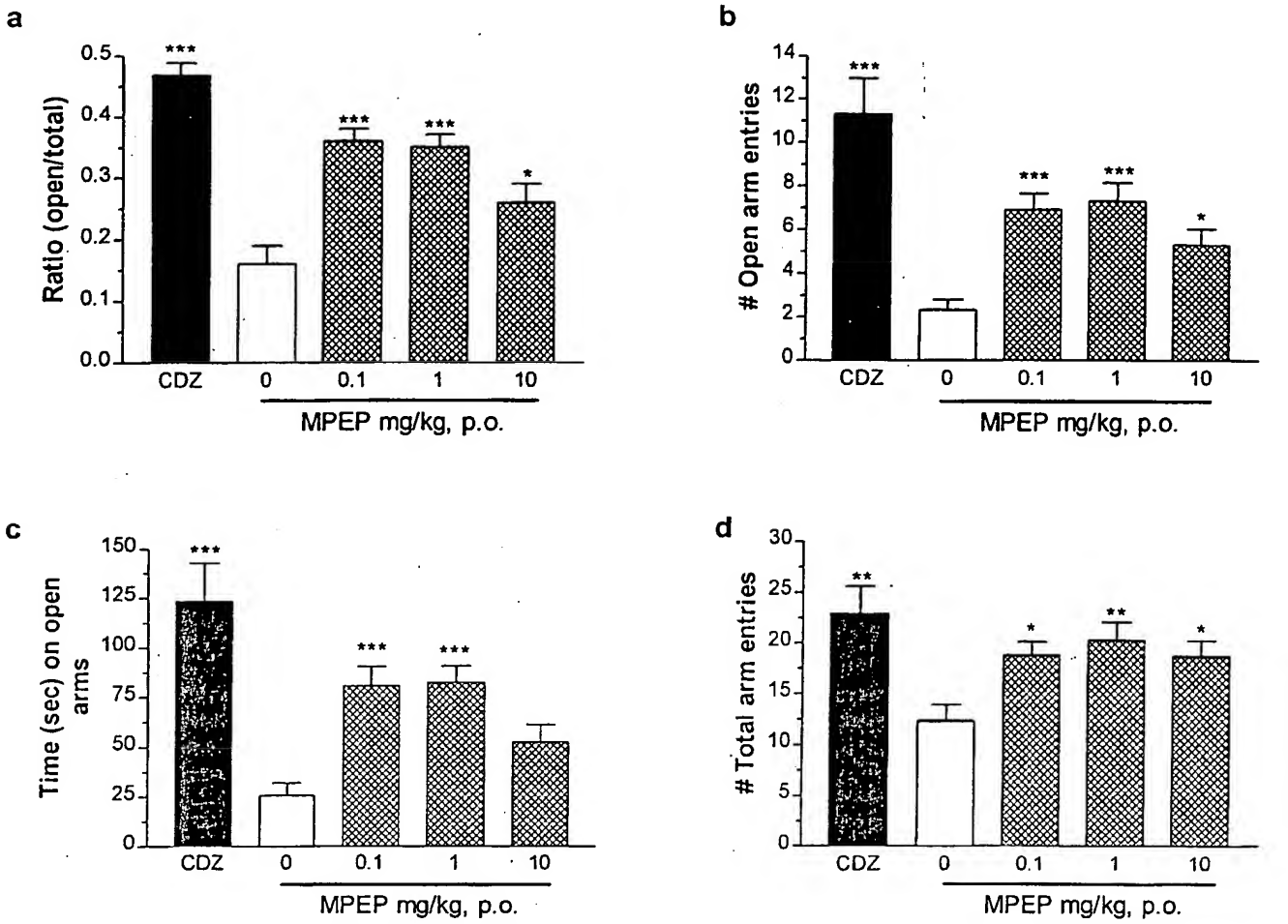

Fig. 2. Elevated plus maze: bars represent means (±S.E.M.) for the ratio (open/total arm entries) (a), the number of open arm entries (b), time (s) on open arm (c), and the total number of arm entries following treatment with MPEP (d) (doses: 0.1, 1, or 10 mg/kg, p.o.), chlordiazepoxide (CDZ; 10 mg/kg, p.o.) or vehicle (0 mg/kg; 0.5% methylcellulose). $n = 15$ per treatment group. $^*P < .05$, $^{**}P < .01$, or $^{***}P < .001$ versus the control-group (Dunnett's test).

p.o. tended to attenuate SIH ($P = .051$), but after a treatment with 15 and 30 mg/kg, p.o., MPEP attenuated SIH significantly (Fig. 3a). When tested at a dose of 1.5 mg/kg, p.o. (separate experiment, data not shown) MPEP was found to be ineffective. Note that none of the treatments significantly affected basal core body temperature (Fig. 3b).

Marble Burying. Mice treated with chlordiazepoxide (10 mg/kg, p.o.) buried significantly less marbles than those treated with vehicle (Fig. 4). Mice treated with MPEP also buried significantly less marbles (Fig. 4). Although the effects after treatment with 7.5 or 30 mg/kg MPEP reached the level of significance, the effect of 15 mg/kg failed to reach the level of significance (Fig. 4). Note that a low dose of 1.5 mg/kg, p.o. MPEP, which was tested in a separate experiment (data not shown), was found to be ineffective.

Conditioned Response Test

Geller-Seifter Test. Chlordiazepoxide (16 mg/kg, p.o.), i.e., the positive standard, significantly increased both the number of punished responses and the number of shocks (Fig. 5, a and b, respectively). MPEP (doses: 10, 30, or 100 mg/kg, p.o.) induced an increase in both the number of punished responses (Fig. 5a) and the number of shocks (Fig. 5b). Although the effects approached those seen with chlordiazepoxide, the response rate within the MPEP groups was too variable and, therefore, the level of statistical significance was not reached. Note that neither MPEP (10, 30, or 100 mg/kg, p.o.) nor chlordiazepoxide (16 mg/kg, p.o.) affected the number of nonpunished responses as compared with vehicle (Fig. 5c).

Locomotor Activity

Spontaneous Locomotor Activity. MPEP (doses: 0.01, 0.1, 1, 10, or 100 mg/kg, p.o.) had no effect on horizontal locomotor activity (Fig. 6a) and significantly reduced vertical activity at a dose of 100 mg/kg, p.o. only (Fig. 6b). In a separate experiment, when tested at those doses used in the SIH and marble burying study, i.e., 7.5, 15, or 30 mg/kg, p.o., MPEP was devoid of any significant effect on horizontal or vertical locomotor activity (data not shown; see also below).

***d*-Amphetamine-Induced Locomotor Activity.** Statistical significance was only found for horizontal *d*-amphetamine-induced locomotor activity (2.5 mg/kg, i.p.): all groups treated with *d*-amphetamine exhibited a significantly increased horizontal locomotor activity as compared with vehicle only (Table 1). However, no statistical significance was

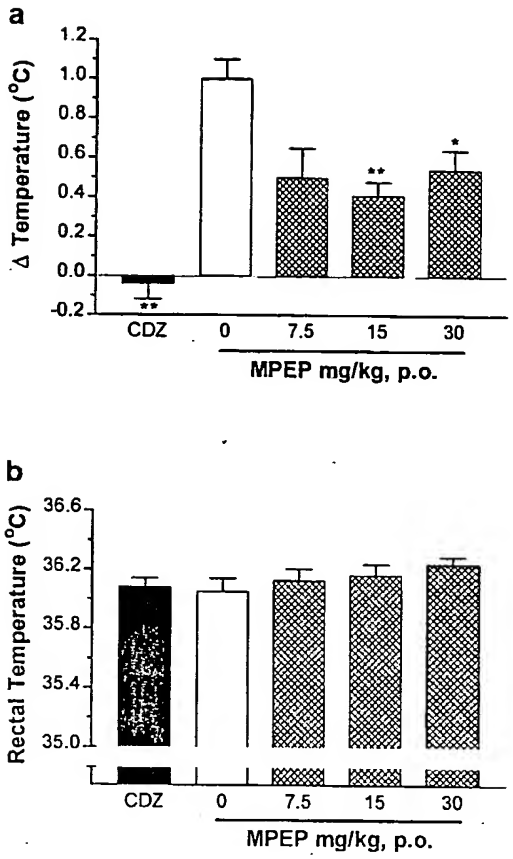

Fig. 3. Stress-induced hyperthermia: a, bars represent the mean of the Δ of the rectal temperature (±S.E.M.) per cage of 15 mice 60 min after treatment with MPEP (doses: 7.5, 15, or 30 mg/kg, p.o.; $n = 8$ per group), vehicle (0 mg/kg; 0.5% methylcellulose; $n = 6$), or chlordiazepoxide (CDZ; 10 mg/kg, p.o., $n = 6$). $^*P < .05$, $^{**}P < .01$ versus vehicle (Mann-Whitney U test). b, bars represent the mean rectal temperature (±S.E.M.) of the first mouse within the cage 60 min after treatment with MPEP (doses: 7.5, 15 or 30 mg/kg, p.o.; $n = 8$ per treatment group), vehicle (0.5% methylcellulose; $n = 6$) or chlordiazepoxide (CDZ; 10 mg/kg, p.o.; $n = 6$).

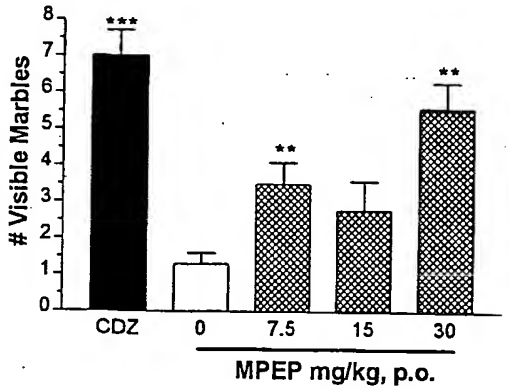

Fig. 4. Marble burying: bars represent the mean (±S.E.M.) number of marbles that were visible at the end of the 60-min trial. Mice were treated with MPEP (doses: 7.5, 15, or 30 mg/kg, p.o.; $n = 16$ per group), chlordiazepoxide (CDZ; 10 mg/kg, p.o.; $n = 12$ mice), or vehicle (0 mg/kg; 0.5% methylcellulose; $n = 12$ mice). $^{**}P < .01$, $^{***}P < .001$ versus vehicle (0 mg/kg; Mann-Whitney U test).

found for MPEP (7.5, 15, or 30 mg/kg, p.o.) or the interaction between d-amphetamine and MPEP on horizontal or vertical locomotor activity (Table 1).

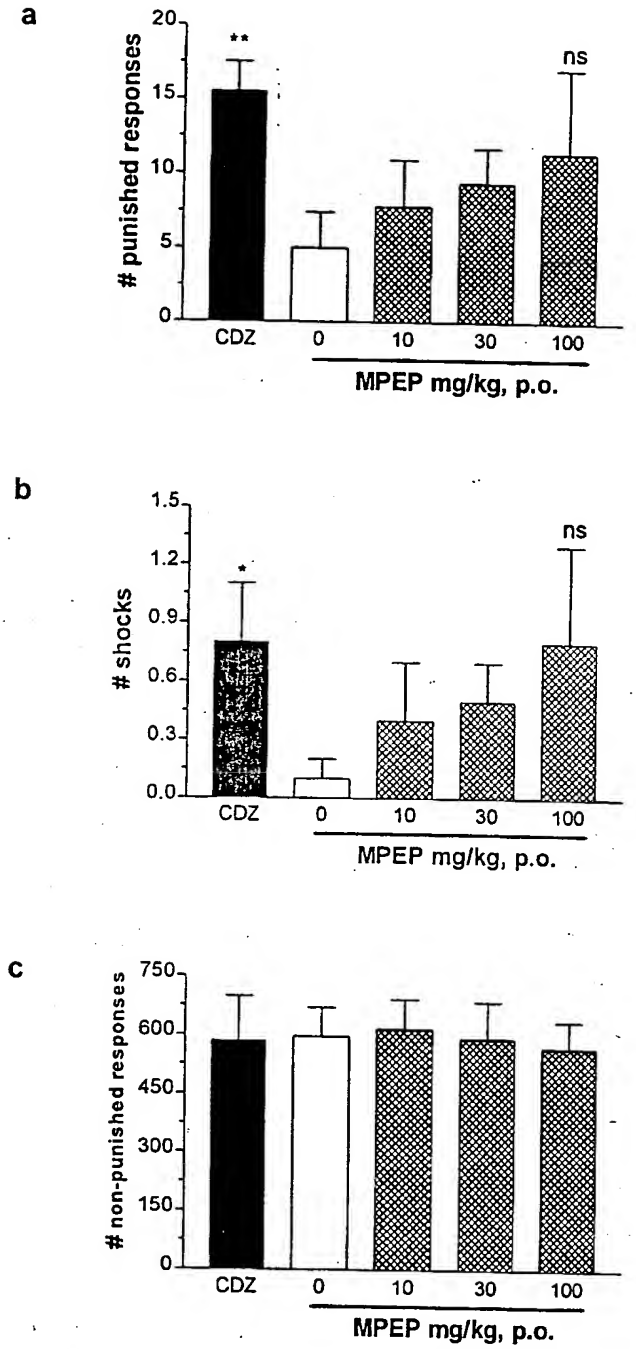

Fig. 5. Geller-Seifter test in rats: bars represent the mean number of punished responses (±S.E.M.; Fig. 1a), received shocks (Fig. 1b) and nonpunished-responses (Fig. 1c). Rats were treated with MPEP (doses: 10, 30, or 100 mg/kg, p.o.), chlordiazepoxide (CDZ; 10 mg/kg, p.o.) or vehicle (0 mg/kg; 0.5% methylcellulose). Each of the eight rats received each of the five different treatments (pretreatment time, 60 min) in a randomized order. $^*P < .05$, $^{**}P < .01$ (paired t test versus control values). ns, not significant.

Prepulse Inhibition. As expected, the ANOVA indicated a highly significant effect for (+)-MK801 (0.1 mg/kg, s.c.) on startle amplitude ($P < .001$) and on PPI ($P < .01$, $P < .001$, and $P < .001$ for prepulses of 8, 12, and 16 db above background noise, respectively). In contrast, statistical signifi-

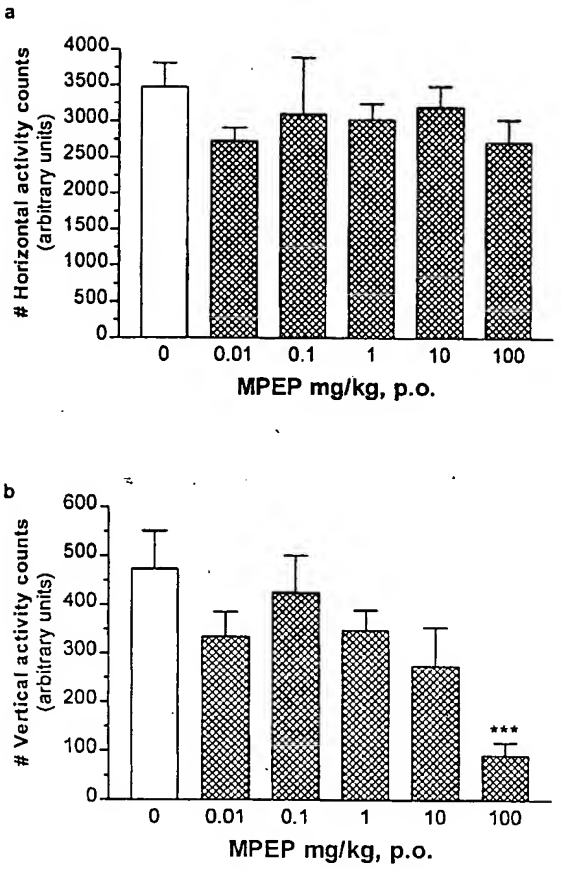

Fig. 6. Locomotor activity: bars represent the mean (±S.E.M.) number of horizontal (a) and vertical (b) activity counts in 120 min of registration after treatment with MPEP (doses: 0.01, 0.1, 1, 10, or 100 mg/kg, p.o.) or vehicle (0 mg/kg; 0.5% methylcellulose). $n = 15$ per treatment group.

TABLE 1

d-Amphetamine-induced locomotor activity

Values represent the mean (±S.E.M.) number of total horizontal and vertical activity counts (arbitrary units) in 120 min of registration after treatment with MPEP (doses: 7.5, 15, and 30 mg/kg, p.o.), vehicle only (methylcellulose, 0.5%), or in their respective combination with *d*-amphetamine (2.5 mg/kg, i.p.).

Treatment		n	Activity Counts ± S.E.	
MPEP (p.o.)	*d*-Amphetamine (i.p.)		Horizontal	Vertical
mg/kg			*arbitrary units*	
0	0	15	14.7 ± 3.2	95.5 ± 29.7
7.5	0	15	20.0 ± 4.5	123.5 ± 33.5
15	0	15	15.5 ± 3.1	59.4 ± 20.8
30	0	15	32.8 ± 10.6	220.7 ± 90.5
0	2.5	15	83.1 ± 15.1***	123.1 ± 27.0
7.5	2.5	15	69.1 ± 8.5***	77.3 ± 20.9
15	2.5	15	90.5 ± 14.9***	71.5 ± 24.7
30	2.5	15	80.6 ± 14***	103.2 ± 45.6

*** $P < .001$ versus vehicle only.

cance was found for MPEP (1, 3, or 10 mg/kg, p.o.) neither on startle amplitude ($P > .05$) nor the PPI ($P > .05$; Table 2).

Discussion

The recently identified selective and systemically active antagonists for the $mGlu_5$ receptor have made possible the experimental study of the consequences of a blockade of this receptor subtype in behavior as well as the effect of high affinity ligands as a potential treatment of disease states (Gasparini et al., 1999; Varney et al., 1999). Because MPEP is one of the most potent derivatives within this series of drugs, this compound was tested in various rodent models of anxiety. These animal models of anxiety can be differentiated into two main categories, the so-called conditioned response and the so-called unconditioned response paradigms (Rodgers, 1997; Rodgers and Dalvi, 1997; Olivier et al., 2000). MPEP was tested in several unconditioned response tests (social exploration test, elevated plus maze, stress-induced hyperthermia, and marble burying) and in one conditioned response test (Geller-Seifter test). The present data indicate that MPEP can exhibit anxiolytic-like activity in several rodent models of anxiety.

To test the prototypical representative of this new class of compounds as thoroughly as possible, MPEP was tested in a variety of standard, unconditioned test paradigms (Olivier et al., 2000). The tests used here can be differentiated and described as a model of "social anxiety" (assessed in the social exploration test in rats), a model of "novelty-induced" anxiety (assessed in the marble burying test), a model of anxiety in an "approach-avoidance conflict" (assessed in the elevated plus maze), and finally a model of "anticipatory anxiety" (assessed in the stress-induced hyperthermia paradigm in mice). In all these unconditioned paradigms, MPEP significantly and positively modulated the "anxiety"-dependent variable: anxiolytic-like effects were seen in the social exploration test and in the elevated plus maze in rats. The latter findings could also be confirmed in mice (C. Gentsch, unpublished observation). Given that MPEP, at doses between 0.01 and 30 mg/kg, p.o., did not alter horizontal or vertical activity in mice when exposed to a novel environment, it is unlikely that an effect on activity induced by MPEP has biased these findings. However, it is important to note that MPEP significantly increased the total number of arm entries, i.e., an indication of increased activity, although the effect was less pronounced as that seen for chlordiazepoxide. Accordingly, the effect of MPEP, as seen in these animal models, is indeed most likely to reflect anxiolysis. The same line of argumentation can be used in the SIH paradigm in mice. The principle, i.e., hyperthermia induced by anticipatory anxiety, is also a recognized and well described phenomenon in humans (Reeves et al., 1985), and autonomic (dys)function is one of the items in the diagnosis of generalized anxiety disorders (*Diagnostic and Statistical Manual of Mental Disorders, Fourth Edition*). The effect of MPEP on stress-induced hyperthermia can be considered as specific, because the compound did not affect the core temperature per se: obviously, MPEP selectively counteracted the anxiety-dependent variable. It is worthwhile to note that this particular test differs from the other "behavioral" unconditioned response tests in that SIH is hypothesized to model autonomic reflexes, which are triggered by emotional activation. It is suggested that such reflexes exist in various forms of anxiety and potentially represent a relatively common expression of anxiety (Lecci et al., 1990).

In the conditioned response paradigm, i.e., the Geller-Seifter test, an increase was found for the number of punished responses and shocks but, in contrast to the effect found after treatment with chlordiazepoxide, the effect of MPEP failed to reach significance in both variables; obviously, the higher variability in those groups treated with

TABLE 2

Prepulse inhibition

Values represent the mean (±S.E.M.) effect of a treatment with MPEP (1, 3, or 10 mg/kg; pretreatment time, 60 min), (+)-MK801 (0.1 mg/kg; pretreatment time, 30 min), or their respective vehicles, i.e. 0.5% methylcellulose or saline, on startle amplitude (g) and prepulse inhibition (%).

Compound	Dose	Startle Amplitude			Prepulse Inhibition			
		PA1	PA2	PA3	PPP, 8 db	PPP, 12 db	PPP, 16 db	N
	mg/kg		g			%		
MPEP (p.o., 60 min)	0	196 ± 19	154 ± 25	147 ± 32	38 ± 6	60 ± 2	83 ± 4	7
	1	180 ± 22	172 ± 20	141 ± 28	47 ± 2	61 ± 5	90 ± 2	8
	3	199 ± 22	200 ± 15	168 ± 20	39 ± 7	57 ± 4	88 ± 2	8
	10	197 ± 23	196 ± 26	166 ± 12	43 ± 4	57 ± 6	90 ± 3	8
P		>.05	>.05	>.05	>.05	>.05	>.05	
(+)-MK801 (s.c., 30 min)	0	202 ± 28	186 ± 26	140 ± 35	31 ± 5	53 ± 4	86 ± 3	8
	0.1	579 ± 29	526 ± 20	497 ± 22	7 ± 5	18 ± 5	33 ± 5	8
P		<.001	<.001	<.001	<.01	<.001	<.001	

MPEP (particularly at the 100 mg/kg dose) was fundamental to these statistical findings. The reasons for the higher variability as compared with their reaction to chlordiazepoxide are at present unclear but might be explained by the fact that the animals were preselected per se on their positive response to chlordiazepoxide (see *Materials and Methods*) in combination with the relatively low number of rats per group. Preliminary findings in two other conditioned response tests, i.e., fear potentiated startle (M. Koch et al., oral communication) and the Vogel test (A. Pilc et al., oral communication), suggest that MPEP exhibits anxiolytic effects in this type of tests. It should be mentioned, however, that MPEP has analgesic effects in inflammatory pain models in rats (Walker et al., 2000a,b), and, accordingly, differences in shock perception may (partially) influence the behavioral response in conditioned test paradigms.

Given the high affinity and selectivity of MPEP for $mGlu_5$ receptors as outlined in the introduction, it is safe to assume that the effects are indeed mediated by inhibition at this glutamate receptor. The mechanism of action of MPEP in relation to its anxiolytic effect is at present unclear. The fact that MPEP neither potentiated nor inhibited *d*-amphetamine-induced locomotor activity (this study) or apomorphine-induced climbing (W. P. J. M. Spooren, unpublished observation) may indicate that the effect does not involve directly or indirectly dopamine or one of its receptors, at least in the nonlesioned brain (however, see also Spooren et al., 2000). This latter observation is, for example, in contrast to buspirone, which has been shown to have a dopaminergic (antagonistic) component (Koek et al., 1998). Obviously, the exact function of $mGlu_5$ receptors in behavior and anxiety remains to be further elucidated in future, additional studies.

The present study used a variety of different paradigms, each of which is known to model or reflect different forms/aspects of anxiety. These different behavioral components are known to be modulated by anxiolytic drugs, as reported in their respective pharmacological validation. With regard to active doses, it is a well known fact that the same compound may act at different dose ranges in distinct models (Olivier et al., 2000). The effect of MPEP is in this respect no exception: anxiolytic doses of MPEP were variable in distinct models. However, given the variety of tests and dose ranges used here, a relatively good estimation on the optimal anxiolytic dose range has been obtained and can be proposed for future experimental as well as for clinical studies.

Two final points: 1) All tests described here were performed after a single administration. Given the fact that in humans anxiolytic drugs are administered repeatedly it remains to be determined as to whether the MPEP-induced effects will be retained after subchronic administration. 2) From clinical experience it is well known that some of the widely used anxiolytics induce unwanted side effects such as amnesia, interaction with alcohol, or unfavorable withdrawal symptoms after an abrupt cessation of a long-term treatment. At present it is unknown whether MPEP can be favorably distinguished with regard to its efficacy and/or its side effect profile from the most frequently used anxiolytics. However, the present study indicated that MPEP up to a dose of 100 mg/kg induced no marked sedation in mice. In addition, MPEP had no effect on PPI, which is indicative for the absence of psychotomimetic side effects, i.e., one of the major drawbacks that plagued the ionotropic *N*-methyl-D-aspartate receptor antagonists (Danysz et al., 1996).

In summary, this present set of data is clearly indicative of a potential anxiolytic activity of $mGlu_5$ receptor antagonists. The novel mechanism and the potential absence of sedation and psychotomimetic effects as assessed in the spontaneous locomotor activity and PPI paradigm, suggest that $mGlu_5$ receptor antagonists may indeed represent a new and safe approach for the treatment of anxiety.

Acknowledgments

We sincerely thank H. Buerki, C. Hunn, S. Imobersteg, R. Mayer, R. Meyerhofer, and M. Zingg for excellent technical assistance.

References

Albin RL, Young AB and Penney JB (1989) The functional anatomy of basal ganglia disorders. *Trends Neurosci* 12:366–375.

Broekkamp CL, Rijk HW, Joly-Gelouin D and Lloyd KL (1986) Major tranquillizers can be distinguished from minor tranquilizers on the basis of effects on marble burying and swim-induced grooming in mice. *Eur J Pharmacol* 126:223–229.

Chesselet MF and Delfs JM (1996) Basal ganglia and movement disorders; an update. *Trends Neurosci* 19:417–422.

Conn PJ and Pin JP (1997) Pharmacology and functions of metabotropic glutamate receptors. *Ann Rev Pharmacol Toxicol* 37:205–237.

Danysz W, Parsons CG, Bresnik I and Quack G (1996) Glutamate in CNS disorders. *Drugs News Perspect* 8:261–277.

Davidson AB and Cook L (1969) Effects of combined treatment with trifluoperazine-HCL and amobarbital on punished behavior in rats. *Psychopharmacologia* 15: 159–168.

Duncan GE, Knapp DJ and Breese GR (1996) Neuroanatomical characterization of FOS induction in rat behavioral models of anxiety. *Brain Res* 713:79–91.

Gasparini F, Lingenhöhl K, Stoehr N, Flor PJ, Heinrich M, Vranesic I, Biollaz M, Allgeier H, Heckendorn R, Urwyler S, Verney MA, Johnson EC, Hess SD, Rao SP, Sacaan AI, Santori EM, Velicelebi G and Kuhn R (1999) 2-Methyl-6-(phenylethynyl)-pyridine (MPEP), a potent, selective and systemically active mGlu5 receptor antagonist. *Neuropharmacology* 38:1493–1503.

Geller I and Seifter J (1960) The effects of meprobromate, barbiturates, d-amphetamine and promazine on experimentally induced conflict in the rat. *Psychopharmacologia* 1:482–492.

Handley SL and Mithani S (1984) Effects of alpha-adrenoceptor agonists and antagonists in a maze exploration model of "fear"-motivated behaviour. *Naunyn-Schmiedeberg's Arch Pharmacol* 327:1–5.

Knöpfel T, Kuhn R and Allgeier H (1995) Metabotropic glutamate receptors: Novel targets for drug development. *J Med Chem* 38:1417–1426.

Koek W, Patoiseau J-F, Assie M-B, Cosi C, Kleven MS, Dupont-Passelaigue E, Carilla-Durand E, Palmier C, Valentin J-P, John G, Pauwels P-J, Tarayre J-P and Colpaert FC (1998) F 11440, a potent, selective, high efficacy 5-HT_{1A} receptor agonist with marked anxiolytic and antidepressant potential. *J Pharmacol Exp Ther* 287:266–283.

Lecci A, Borsini F, Volterra G and Meli A (1990) Pharmacological validation of a novel animal model of anticipatory anxiety in mice. *Psychopharmacology* 101:255–261.

McGeer PL, Eccles JC and McGeer EG (1987) *Molecular Neurobiology of the Mammalian Brain*. Plenum Press, New York.

Monaghan DT, Bridges RJ and Cotman CW (1989) The excitatory amino acid receptors: Their classes, pharmacology, and distinct properties in the function of the central nervous system. *Annu Rev Pharmacol Toxicol* 29:365–402.

Nicoletti F, Bruno V, Copani A, Casaboni G and Knöpfel T (1997) Metabotropic glutamate receptors: A new target for the therapy of neurodegenerative disorders. *Trends Neurosci* 19:267–271.

Olivier B, van Wijngaarden I and Soudijn W (2000) 5HT3 receptor antagonists and anxiety; a preclinical and clinical review. *Eur Neuropsychopharmacol* 10:77–95.

Pin JP and Duvoisin R (1995) The metabotropic glutamate receptors: Structure and functions. *Neuropharmacology* 34:1–26.

Reeves DL, Levinson DM, Justesen DR and Lubin B (1985) Endogenous hyperthermia in normal human subjects: Experimental study of emotional states (II). *Int J Psychosom* 32:18–23.

Rodgers RJ (1997) Animal models of 'anxiety' where next? *Behav Pharmacol* 8:477–496.

Rodgers RJ and Dalvi A (1997) Anxiety, defense and the elevated plus-maze. *Neurosci Biobehav Rev* 21:801–810.

Romano C, Sesma MA, McDonald CT, O'Malley K, van den Pol AN and Olney JW (1995) Distribution of metabotropic glutamate receptor mGluR5 immunoreactivity in rat brain. *J Comp Neurol* 355:455–469.

Shigemoto R, Nomura S, Ohishi H, Sugihara H, Nakanishi S and Mizuno N (1993) Immunohistochemical localization of a metabotropic glutamate receptor, mGluR5, in the brain. *Neurosci Lett* 163:53–57.

Spooren WPJM, Gasparini F, Bergmann R and Kuhn R (2000) Effect of the prototypical $mGlu_5$ receptor antagonist 2-methyl-6-(phenylethyl)-pyridine (MPEP) on motor behaviour: Rotarod, locomotor activity and rotational responses in the unilateral 6-OHDA-lesioned rat. *Eur J Pharm* 406:403–410.

Testa CM, Standaert DG, Young AB and Penney JB (1994) Metabotropic glutamate receptor mRNA expression in the basal ganglia of the rat. *J Neurosci* 14:3005–3018.

Varney MA, Cosford NDP, Jachec C, Rao SP, Sacaan A, Lin F-F, Bleicher L, Santori EM, Flor PJ, Allgeier H, Gasparini F, Kuhn R, Hess SD, Veliçelebi G, Johnson EC (1999) SIB-1757 and SIB-1893: Selective, non-competitive antagonists of metabotropic glutamate receptor type 5 (mGluR5). *Mol Pharmacol* 290:170–181.

Walker K, Gasparini F, Bowes N, Stoehr N, Reeve AJ, Pagano AP, Flor PJ, Vranesic I, Lingenhoehl K, Winter J, Schmid P, Johnson EC, Varney M, Urban L and Kuhn R (2000a) Selective blockade of peripheral mGlu5 receptors offers a novel and effective relief of inflammatory pain. *Neuropharmacology* 40:1–9.

Walker K, Reeve A, Bowes M, Winter J, Wotherspoon G, Davis A, Schmid P, Gasparini F, Kuhn R and Urban L (2000b) mGlu5 receptors and nociceptive function. II. mGlu5 receptors functionally expressed on peripheral sensory neurones mediate inflammatory hyperalgesia. *Neuropharmacology* 40:10–19.

Send reprint requests to: Dr. W. P. J. M. Spooren, Novartis Pharma AG, Nervous System Research, WKL-126.3.64, CH-4002 Basel, Switzerland. E-mail: willibrordus.spooren@pharma.novartis.com

Molecular Psychiatry (2004) 9, 35–41

www.nature.com/mp

IMMEDIATE COMMUNICATION

Assessment of a prepulse inhibition deficit in a mutant mouse lacking mGlu5 receptors

SA Brody[1], SC Dulawa[1,*], F Conquet[2,†] and MA Geyer[1,3]

[1]*Department of Neuroscience, University of California, San Diego, La Jolla, CA, USA;* [2]*GlaxoWellcome Experimental Research, IBCM, University of Lausanne, Lausanne, Switzerland;* [3]*Department of Psychiatry, University of California, San Diego, La Jolla, CA, USA*

The glutamate hypothesis of schizophrenia derived from evidence that phencyclidine, a noncompetitive *N*-methyl-D-aspartate (NMDA) antagonist, produces schizophrenia-like symptoms in healthy humans. Sensorimotor gating, measured by prepulse inhibition (PPI), is a fundamental form of information processing that is deficient in schizophrenia patients and rodents treated with NMDA antagonists. Hence, PPI is widely used to study the neurobiology of schizophrenia. As the use of PPI as a model of gating deficits in schizophrenia has become more widespread, it has become increasingly important to assess such deficits accurately. Here we identify a possible role of mGluR5 in PPI by using wild type (WT) and mGluR5 knockout (KO) mice of two different background strains, 129SvPasIco and C57BL/6. In both strains, PPI was disrupted dramatically in the mGluR5 KO mice throughout a range of interstimulus intervals and sensory modalities. The present findings further support the glutamate hypothesis of schizophrenia and identify a functional role for mGluR5 in sensorimotor gating.
Molecular Psychiatry (2004) 9, 35–41. doi:10.1038/sj.mp.4001404

Keywords: PPI; metabotropic glutamate; mGluR5; startle; prepulse inhibition; knockout mouse

Prepulse inhibition of the startle response (PPI) provides an operational measure of sensorimotor gating, a process by which an organism filters extraneous information from the internal and external milieu.[1,2] In healthy humans, rodents, or nonhuman primates, the prepulse stimulus serves to attenuate the motor response to the pulse.[3] PPI deficits are found in a number of psychiatric populations, most notably patients with schizophrenia, obsessive–compulsive disorder, and Tourette's syndrome.[4] As a model of the gating deficits in schizophrenia, PPI is believed to have face, construct, and predictive validity.[5,6] In humans, PPI is measured via electromyographic recordings of the eyeblink response at the orbicularis oculi below the eye.[7] In rodents, startle can be measured as the whole-body flinch. Glutamate, dopamine, and serotonin have been implicated both in the etiology of schizophrenia and the modulation of PPI.[5] Effective antipsychotic agents appear to ameliorate PPI deficits in some patients with schizophrenia and in rodents given psychotomimetic compounds.[4,5]

The glutamate hypothesis of schizophrenia is derived from evidence that phencyclidine (PCP) and ketamine, noncompetitive *N*-methyl-D-aspartate (NMDA) antagonists, produce schizophrenia-like symptoms in healthy humans.[8,9] Administration of these same compounds to rodents[10,11] or nonhuman primates[12] reduces PPI. The actions of glutamate, however, are mediated by both ionotropic and metabotropic receptors (mGluRs; activating second messenger system cascades involving GTP-binding proteins). Molecular cloning has identified eight metabotropic receptor subtypes, known as mGluR1-8.[13] These receptor subtypes are divided into three groups based on sequence homologies and pharmacological properties.[13] Group I includes mGluR1 and mGluR5, which are coupled positively to phospholipase C[13] and are among the mGluRs[14] concentrated in brain regions that regulate PPI.[15]

Specifically, mGluR5 is concentrated in the striatum, nucleus accumbens, olfactory tubercle, hippocampus, deep cerebellar nuclei, and cerebral cortex.[16] Many of these structures, including the striatum, nucleus accumbens, and hippocampus, are known to modulate PPI.[15] Furthermore, it has recently been noted that there is increased neuronal mGluR5 in pyramidal layers of area 11 in the prefrontal cortex of patients with schizophrenia.[17] It has also been

Correspondence: Dr MA Geyer, PhD, Department of Psychiatry, University of California, San Diego, 9500 Gilman Drive, La Jolla, CA 92093-0804, USA.
E-mail: mgeyer@ucsd.edu
*Current address: Center for Neurobiology & Behavior, Columbia University, New York, NY 10032, USA.
†Current address: Addex Pharmaceuticals, 1228 Plan les Ouates, Geneva, Switzerland.

suggested that the mGluR5 gene on chromosome 11 might be relevant to an abnormal translocation linked to schizophrenia[18] and other disorders such as Down syndrome.[19] On the basis of this existing evidence, we hypothesized that a mouse lacking mGlu5 receptors (mGluR5 knockout (KO)) would exhibit an alteration in PPI.

Methods

Gene targeting

mGluR5 KO mice were generated as previously described.[20] The absence of mGluR5 was confirmed with an mGluR5 antibody (Upstate Biotech). Mutants were detected by Southern blot by cutting the genomic DNA with *Eco*RI resulting in a wild type (WT) band of 5.1 kb and a mutated band of 2.2 kb after hybridization with an internal probe.

Subjects

Subjects were mGluR5 KO (between 21 and 31 g, mean weight: 27 g) and WT (between 21 and 28 g, mean weight: 24 g) mice of two different background strains. All mice were bred homozygously at IFFA CREDO (a Charles River facility) in France and shipped to San Diego, CA. Upon arrival in San Diego, mice were housed by genotype in groups of one to four per cage with access to food and water and a reversed 12L:12D schedule (lights off at 0900). A minimum of 1 week acclimation to the San Diego facility preceded behavioral testing. All experiments were carried out in accordance with the NIH guide for the care and use of laboratory animals (NIH Publication No. 8023). All efforts were made to minimize animal suffering and to reduce the number of animals used.

Male GluR5 WT and KO mice were tested at N5, 92% 129SvPasIco and 8% C57BL/6 ('129SvPasIco') or 92% C57BL/6 and 8% 129SvPasIco ('C57BL/6'). A total of 17 KO (nine 129SvPasIco and eight C57BL/6) and 20 WT mice (10 of each background), 9–11 weeks old were first tested for PPI. At 13–15 weeks old, the same mice were tested with multiple pulse intensities followed 3 weeks later by a test involving multiple interstimulus intervals. Additionally, the 129SvPasIco mice were tested with multiple modalities three more weeks later.

Apparatus

Behavioral testing used four startle chambers (San Diego Instruments, San Diego, CA, USA), as described previously.[11,21] Briefly, each ventilated, illuminated chamber contained a clear, nonrestrictive Plexiglas cylinder resting on a platform and a high-frequency loudspeaker that produced both a continuous background noise of 65 dB and the various acoustic stimuli. Whole-body startle responses of the mouse caused vibrations of the Plexiglas cylinder. These vibrations were converted to analog signals by a piezoelectric transducer attached to the underside of the platform, and then digitized and stored by a computer. Monthly calibrations were performed on the chambers to ensure the accuracy of all acoustic stimuli and measurements.

Test sessions

Test sessions began with a 5-min acclimation period during which the background noise (a 65-dB white noise) was presented alone. Presentation of the 65-dB background noise then continued throughout the remainder of the test session. The initial acclimation period was followed by two to four blocks of trials, with an average intertrial interval of 15 s (and a range of intertrial intervals of 7–23 s). Block one consisted of six STARTLE (a 40-ms 120-dB broadband burst) trials; block(s) two (and, where presented, three) contained six trials of each type described below. When presented, block four consisted of six STARTLE trials.

Basic characterization

Four trial-types were presented during blocks two and three in a pseudorandomized sequence with six of each trial type per block. These trial types included: a 40-ms broadband 120-dB burst (STARTLE) and three distinct intensities of PREPULSE trials in which 20-ms-long prepulses (consisting of broadband bursts of 69, 73, or 77 dB) preceded the startle stimulus by an interstimulus interval of 100 ms (prepulse onset to pulse onset). The test session lasted for a total of 23 min and contained 72 trials.

Pulse intensities

To determine startle threshold and to verify that none of the mice were startling to the prepulses, mice were exposed to startle stimuli ranging from 65 to 120 dB. Each of nine distinct trial-types was presented six times in the course of this session. Following the first block of six STARTLE stimuli (40 ms long bursts of 120-dB broadband white noise), all trial types were presented in a pseudorandom order during the second block. Each trial consisted of a 40-ms broadband burst of one of the following intensities: 65, 69, 73, 77, 85, 90, 100, 110, or 120 dB. The session contained a total of 60 trials and lasted 20 min.

Interstimulus intervals

In humans, PPI is elicited at interstimulus intervals of 50–500 ms (onset of prepulse to onset of pulse[3,7]). In mice, PPI is typically examined using a similar interstimulus interval range with an optimum of 100 ms (see eg Varty *et al*[22]). To examine whether the WT and mGluR5 KO mice exhibited maximal PPI on the same timescale, PPI was observed across a range of interstimulus intervals. Eight trial-types were presented in four blocks. As described above, blocks one and four consisted of six STARTLE trials. Blocks two and three each contained six presentations of the following trials in a pseudorandom order: the 120 dB STARTLE; and seven distinct PREPULSE trials in which 20-ms 73-dB stimulus preceded the STARTLE by 50, 100, 200, 250, 300, 400, or 500 ms from prepulse onset to the onset of the STARTLE stimulus.

Equal startle

Owing to the fact that the mGluR5 WT and KO mice exhibit markedly different startle levels from one another, it was necessary to determine whether the observed PPI deficit was a function of startle magnitude. The data from Experiment 2 were used to determine the dB level at which the startle magnitude of the 129SvPasIco KO mice was equivalent to the startle magnitude of the 129SvPasIco WT mice elicited by a 120-dB PULSE. Only the 129SvPasIco mice were used in this experiment because the exaggerated startle in the C57BL/6 KO mice was so great that equivalent magnitudes could not be achieved by adjusting the stimulus intensity. Examination of the data from the multiple pulse intensities revealed that the response of the KO mice to a 105-dB stimulus was equivalent to that produced by the WT mice to a 120-dB stimulus. Therefore, four trial-types were presented: either a 40-ms broadband 120-dB burst (presented to the mGluR5 WT mice) or a 40-ms broadband 105-dB burst (presented to the mGluR5 KO mice) (STARTLE); three PREPULSE trials in which 20-ms 69, 73, or 77 dB prepulses preceded the startle stimulus by 100 ms.

Multimodal

The experiments described thus far all utilized auditory stimuli. PPI, however, is a multimodal phenomenon.[3] To ensure that the KO mice were not experiencing a simple hearing deficit, we examined PPI across a variety of modalities by utilizing a mixture of visual prepulses (using a light cue), tactile pulses (using an airpuff), and auditory stimuli. Trial-types were: the 120-dB STARTLE; a 30-ms 40-psi airpuff delivered through a tube inserted into one end of the Plexiglas cylinder; a 20-ms 73-dB prepulse followed by one of 120 dB; a 77-dB prepulse followed by the airpuff after 100 ms; a 100-W light on for 100 ms and then off for 100 ms prior to the airpuff; the same light stimulus followed by a 120-dB STARTLE.

Data analysis

Startle magnitude was calculated as the average response to the STARTLE trials presented during blocks two and/or three of the session. PPI was calculated as both percentage and difference scores.[21] In 129SvPasIco mice, both measures of PPI yielded similar results; in C57BL/6 mice, the marked increases in startle made difference scores uninterpretable. All scores are therefore presented as percentage scores. Appropriate two-way ANOVAs (with gene and, where present, strain as between subjects factors and trial type as a within subjects factor) were followed, when significant, by Student–Newman–Keul *post hoc* tests. Significance was determined by exceeding an alpha level of less than 0.05.

Results

Experiment 1—basic characterization

PPI: A main effect of genotype ($F[1,33]=31.32$, $P<0.0001$) indicated that the PPI of the KO mice was severely disrupted, while a main effect of strain ($F[1,33]=4.78$, $P<0.05$) indicated that the C57BL/6 mice had elevated PPI relative to the 129SvPasIco mice (Figure 1). Although there was a significant interaction between prepulse intensity and genotype ($F[2,66]=19.12$, $P<0.0001$), further analysis using the Student–Newman–Keul test revealed that the PPI of the mGluR5 KO was significantly less than the WT at all three prepulse intensities (pp4, pp8, and pp12). A separate Student–Newman–Keul test revealed that a

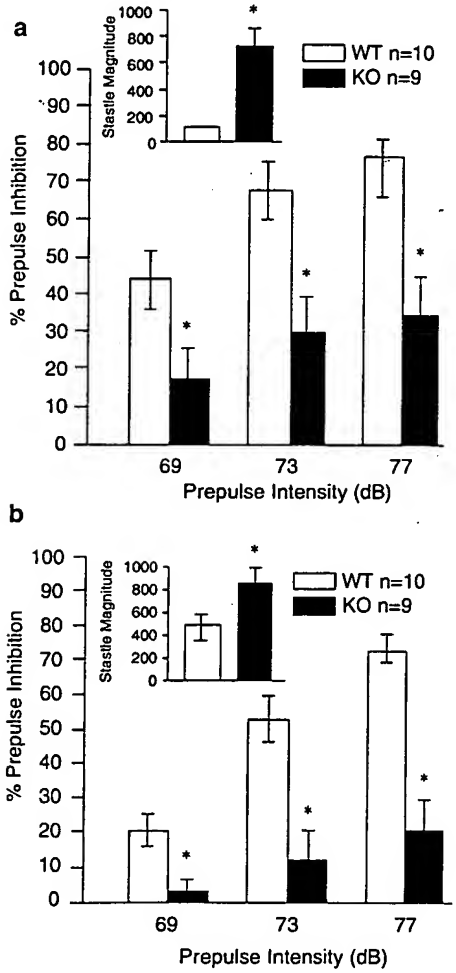

Figure 1 PPI and startle magnitude. (a) Graph depicts PPI values for mGluR5 WT and KO mice on a C57B1/6J background at three different prepulse intensities (69, 73, and 77 dB). Inset shows the startle magnitude of the same mice. White bars denote WT values, black bars denote KO values. Values are means ± SEM. *$P<0.05$ (b) Graph depicts PPI values for mGluR5 WT and KO mice on a 129SvPasIco background at three different prepulse intensities (69, 73, and 77 dB). Inset shows startle magnitude for the same mice.

significant interaction between intensity and strain ($F[2,66]=3.67$, $P<0.05$) was due to the fact that the PPI of the C57BL/6 mice was higher than that of the 129SvPasIco mice at a prepulse of 4 dB above background.

Startle: Main effects of genotype ($F[1,33]=37.88$, $P<0.0001$) and strain ($F[1,33]=12.54$, $P<0.005$) were found (Figure 1, inset). These results indicated that the KO mice had a larger startle response to the 120-dB pulse than did the WT mice. In addition, the 129SvPasIco mice exhibited a higher startle response than the C57BL/6 mice. The strain by genotype interaction approached but did not reach statistical significance ($F[1,33]=3.16$, $P=0.0845$).

Experiment 2—multiple pulse intensities

Although the deficit in PPI observed in mGluR5 KO mice is consistent with a reduction in sensorimotor gating, alternative explanations needed to be considered. The elevated startle reactivity in the KO mice could signify a reduced threshold for startle elicitation such that the KO mice might have startled in response to the prepulse stimuli. We therefore measured startle responses elicited by various acoustic intensities. Main effects of both genotype ($F[1,31]=25.92$, $P<0.0001$) and strain ($F[1,31]=6.64$, $P<0.05$) were found. A marginal strain by genotype interaction ($F[1,31]=4.10$, $P<0.0515$) was also evident, as were an intensity-by-gene interaction ($F[9,279]=18.76$, $P<0.0001$), an intensity by strain interaction ($F[9,279]=5.52$, $P<0.0001$), and an intensity-by-strain-by-gene interaction ($F[9,279]=3.87$, $P<0.001$). A Student-Newman-Keul analysis revealed that when presented with the background noise of 65 dB, the C57BL/6 mice showed higher basal motor activity than did the 129SvPasIco mice. Nevertheless, the KO and WT mice reacted comparably to the background noise and startled comparably to all of the stimuli 4–25 dB above background. Beginning at 90 dB (ie 25 dB above background), the KO mice of both strains show a higher startle response than do the WT mice. Since the most intense prepulses used in the above experiments were 77 dB, it does not appear that the KO mice were startling in response to the prepulse stimuli. The 129SvPasIco mice exhibited a higher startle response than the C57BL/6 mice beginning at 100 dB (Figure 2).

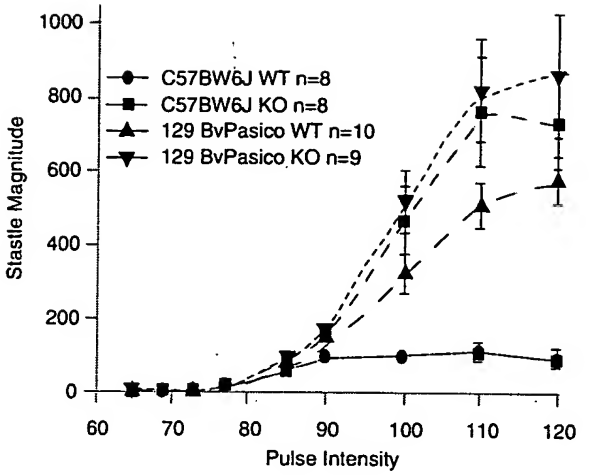

Figure 2 Pulse intensities. Startle magnitude at multiple pulse intensities ranging from 65 to 120 dB. Circles denote C57B1/6J WT, squares denote C57B1/6J KO, upward triangles denote 129SvPasIco WT, and downward triangles denote 129SvPasIco KO mice. Values are means ± SEM. $^*P<0.05$.

Experiment 3—interstimulus intervals

PPI exhibits temporal specificity in terms of the optimal interval between prepulse and pulse onsets. To determine whether the deficit in PPI in the KO mice reflected a shift in a timing function, we used a single prepulse intensity (73 dB, 8 dB above background) and a range of interstimulus intervals. A main effect of genotype ($F[1,31]=13.71$, $P<0.001$) indicated that, as expected, the PPI of the KO mice was severely disrupted (data not shown). An intensity-by-strain-by-gene interaction ($F[6,186]=3.67$, $P<0.005$) was also observed. Student–Newman–Keul analyses revealed that the KO mice exhibited impaired PPI (as compared to WT mice) at all interstimulus intervals examined. In addition, the 129SvPasIco mice exhibited significantly worse PPI than the C57BL/6 mice when the interval between the prepulse and the pulse was 300 ms or longer. As in schizophrenia patients,[23] no shift from the 100 ms optimum was observed in the KO mice. Thus, the PPI deficit in mGluR5 KO mice is not due to an abnormality in the temporal function characteristic of PPI.

Experiment 4—equal startle

PPI is calculated for each animal using the startle magnitude values obtained on the STARTLE trials. It is therefore possible, despite the numerous reports of dissociations between PPI and startle magnitude (see eg Paylor and Crawley[24]), that the putative PPI deficit of the mGluR5 KO mice is in fact a reflection of their exaggerated startle magnitude. We therefore sought to equalize the startle magnitude of the responses of the WT and KO mice. To do so, we utilized the data from Experiment 2, determining the decibel level at which the startle response of the 129SvPasIco KO mice most closely resembled that of the 129SvPasIco WT mice to the 120-dB stimulus. As anticipated based on the design of the experiment, the mGluR5 WT and KO mice did not differ in their startle magnitude ($F[1,15]<1$; Figure 3). Nevertheless, the mGluR5 KO mice exhibited lower PPI than their WT counterparts ($F[1,15]=10.60$, $P<0.01$; Figure 3).

Experiment 5—multimodal

In schizophrenia, deficits are observed in both intramodal and cross-modal PPI.[25] The studies presented above rely solely on acoustic stimuli. As such, the observed deficit might be due to an abnormality in

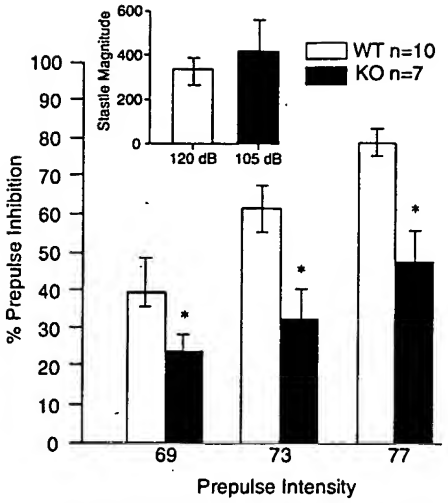

Figure 3 PPI with equal startle magnitudes. PPI values for WT and KO mice on a 129SvPasIco background. All mice received prepulses of 69, 73, and 77 dB. WT mice received pulses of 120 dB and KO mice received pulses of 105 dB. Startle magnitudes at these intensities are shown in the inset. White bars denote WT values, black bars denote KO values. Values are means ± SEM. $^*P<0.05$.

auditory processing as opposed to sensorimotor gating. Accordingly, 129SvPasIco mice were tested with different modalities of prepulses and pulses. In addition to an acoustic prepulse (8 dB above background), a light prepulse was presented. Acoustic and tactile (airpuff) startle stimulus intensities were adjusted to produce similar startle magnitudes, which did not differ between WT and KO mice in this study (Figure 4). Again, the mGluR5 KO mice exhibited less acoustic–acoustic PPI ($F[1,17]=5.80$, $P<0.05$). Similar deficits in PPI were observed when an acoustic prepulse preceded a tactile pulse ($F[1,17]=10.34$, $P<0.005$; Figure 4) and when a light prepulse preceded an acoustic pulse ($F[1,17]=17.22$, $P<0.001$). In the latter case, a negative mean value for PPI was observed, suggestive of prepulse facilitation, but this result cannot be considered facilitation due to the size of the error bars. When a light prepulse preceded a tactile pulse, not only was PPI highly variable, but the WT mice exhibited lower PPI than in the other modalities and the apparent deficit in the KO mice was not significant. Nevertheless, as in schizophrenia patients,[25] the demonstration of deficient light-induced PPI confirms that the mGluR5 KO mice exhibit deficits in sensorimotor gating rather than hearing.

Discussion

The results from this battery of experiments lead us to conclude that mGluR5 KO mice, as hypothesized, exhibit a deficit in sensorimotor gating as reflected in reduced PPI. The decrease in PPI observed in the mGluR5 KO mice is not due to alteration in the startle threshold (Experiment 2) or startle magnitude (Experiment 4). Furthermore, as in schizophrenia,[25,26] the decrease in PPI is observed across both multiple modalities (Experiment 5) and multiple prepulse intensities, and occurs at a range of interstimulus intervals (Experiment 3). The reduced PPI observed in the mGluR5 KO mice was not due to differences in reactivity to the prepulse stimuli, since none of the mice responded more to the prepulses than to the 65-dB background noise (Experiment 2). The PPI deficit of the mGluR5 KO mice is robust when the mutation is introduced into two different mouse strains (Experiment 1) and is replicable both within and across cohorts (data not shown). The combination of the results from this entire constellation of experiments allows us to state with confidence that the deficit observed in the mGluR5 KO mice is indeed a deficit in sensorimotor gating. In addition, our observation of a PPI deficit in mGluR5 KO mice is consistent with previously published abstracts[27,28] as well as a recent report by Kinney *et al*[29] that appeared after these studies were completed.

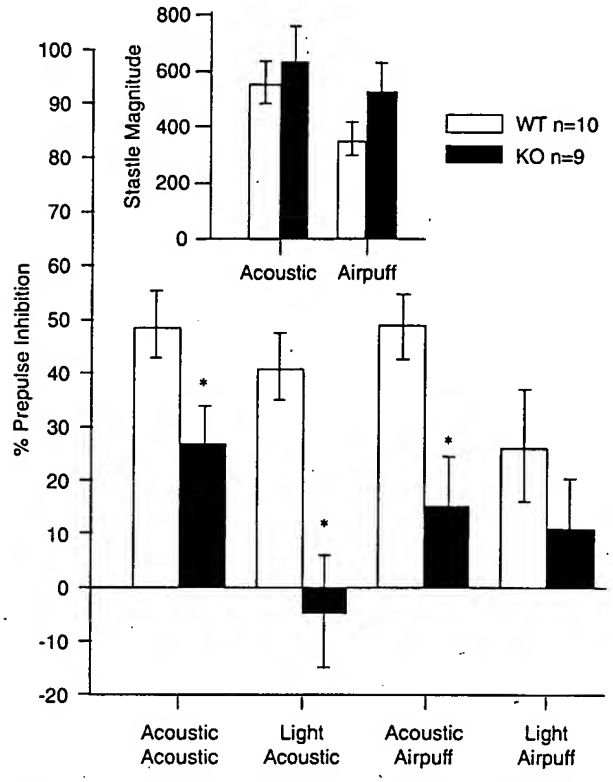

Figure 4 Multimodal PPI. PPI values for mGluR5 WT and KO mice on a 129SvPasIco background using a variety of stimulus modalities for the pulse and the prepulse. Prepulse modalities are listed below the *X*-axis. Pulse modalities are listed below the prepulses. White bars denote WT values, black bars denote KO values. Values are means ± SEM. $^*P<0.05$.

It should be noted, however, that the robustness of the PPI deficit of the mGluR5 KO mice appears to depend on which of the two currently available constructs for generating an mGluR5 KO is

utilized.[20,30] It has been observed[28] that the PPI deficit of the mGluR5 KO mice generated in the lab of Dr François Conquet[20] is more robust than that seen in the mice generated by Dr John Roder *et al*.[30] Nevertheless, mGluR5 mice generated by both groups do exhibit deficits in PPI relative to their respective WTs (this report, Henry *et al*[27,28] and Kinney *et al*[29]). The two groups backcrossed their respective mGluR5 KO mice onto different strains, one onto an outbred mouse strain,[30] the other onto both C57BL/6 and 129SvPasIco, as reported here. Insofar as these background strains have been shown to vary widely in both startle magnitude and PPI levels,[24] it is likely that the robustness of differences in startle and PPI due to deletion of mGluR5 is influenced by the background, as has been described for other phenotypes.[31]

In addition to the deficient PPI seen in both 129SvPasIco and C57BL/6 mGluR5 KO mice, the C57BL/6 mice, and to a lesser degree the 129SvPasIco mice, exhibited increases in startle magnitude. While the hyper-reactivity in the C57BL/6 mice was very striking, the 129SvPasIco mGluR5 KO mice exhibited a less pronounced exaggeration in startle magnitude than the C57BL/6 mGluR5 KO mice. Indeed, when small samples were involved, this increase in startle in the 129SvPasIco mGluR5 KO was not always statistically significant and was not evident with tactile stimuli (eg Experiment 5). Both the mGluR5 WT and the mGluR5 KO mice of both strains exhibited significant startle responses at the same dB level (85–90 dB), indicating no shift in the threshold for startle in the KO mice. To verify that the effects of the 129SvPasIco mGluR5 KO on startle magnitude could be dissociated from the effects on PPI, startle magnitude was held constant across groups (through the use of different startle stimulus intensities, one of 105 dB and one of 120 dB), and PPI measured under these conditions. The fact that the mGluR5 KO mice exhibited impaired PPI compared to their WT counterparts while concurrently exhibiting comparable startle magnitude strongly suggests both that the two measures are dissociable, as reported by others (eg Paylor and Crawley[24]), and that the deficit of the mGluR5 KO mice is not due to an alteration in startle magnitude or startle thresholds.

Although the similar startle thresholds implies that the WT and KO mice did not differ in hearing sensitivity, hearing deficits could still influence PPI. Indeed, C57BL/6 mice have been shown to exhibit high-frequency hearing loss beginning as early as 3 months old (eg Willot[32]). The broadband stimulus utilized in these studies minimizes the impact of selective high-frequency hearing loss. Furthermore, we elicited PPI using a variety of sensory modalities for both the prepulses and the pulses and found that the mGluR5 KO mice exhibited deficient PPI independently of the modality of stimulation.

The present findings of deficient PPI in mGluR5 KO mice are consistent with both human and rodent literature suggesting a contribution of mGluR5 to the etiology or treatment of schizophrenia or related psychiatric disorders that are characterized by deficits in sensorimotor gating. Pharmacological studies have shown that a metabotropic glutamate mixed Group I/II agonist injected directly into the nucleus accumbens or the striatum produces a PPI deficit.[33] Systemic administration of the more specific Group II mGluR2/3 agonist LY314582, or its racemate (+)-2-aminobicyclo[3.1.0]hexane-2,6-dicarboxylic acid (LY354740)[34] did not alter PPI alone nor did it alter the effects of the NMDA antagonist PCP.[35,36] In contrast, while the mGluR5 antagonist MPEP had no effect on PPI by itself even when administered at doses reported to attain at least 90% receptor occupancy,[29,36–38] it was shown to exacerbate the PPI deficit produced by PCP administration.[29,36] Thus, although MPEP alone does not appear to disrupt PPI in rodents, the influence of this mGluR5 antagonist on PPI in PCP-treated animals is consistent with the phenotypic difference in PPI in the mGluR5 KO mice. Furthermore, administration of an mGluR5 agonist reversed the PPI deficit induced by administration of amphetamine.[29] An mGluR5 agonist therefore has the anticipated opposite effect of an antagonist or other manipulation resulting in the unavailability of the mGlu5 receptors. Taken together, these pharmacological studies point towards a role of the Group I mGluRs, and more specifically, mGluR5 in the modulation of PPI.

The pharmacological data from the rodents are consistent with data from patients with schizophrenia in implicating a role of mGluR5 in the etiology or treatment of this disease. Just as drug administration produces changes in levels of available mGlu5 receptors in rodent brains, so too does schizophrenia in the human brain. In fact, several changes in glutamatergic markers have been noted in the brains of schizophrenia patients. Among these alterations in glutamatergic markers is an increase in neuronal mGluR5 found in the pyramidal layers of area 11 in prefrontal cortex of schizophrenia patients.[17] In addition, gene linkage studies have also implicated the mGluR5 gene on chromosome 11 as being abnormal in schizophrenia.[18] This abnormality of the mGluR5 gene in schizophrenia may be functionally similar to the absence of this gene in the mGlu5 KO mice and may partially explain why mice missing the mGluR5 gene exhibit PPI deficits such as those seen in patients with schizophrenia. We therefore believe that the work presented here indicates an important role for mGluR5 in the modulation of sensorimotor gating and perhaps even the etiology of schizophrenia, a psychiatric disorder associated with a deficit in PPI.

Acknowledgements

SAB was supported by MH12961. SCD was supported by MH12249. This work was supported by DA02925 and MH42228 to MAG. MAG holds an equity interest in San Diego Instruments.

References

1 Braff DL, Geyer MA. Sensorimotor gating and schizophrenia: human and animal model studies. *Arch Gen Psychiatry* 1990; **47**: 181–188.

2 Ison JR, Hoffman HS. Reflex modification in the domain of startle: II. The anomalous history of a robust and ubiquitous phenomenon. *Psychol Bull* 1983; **94**: 3–17.

3 Hoffman HS, Ison JR. Reflex modification in the domain of startle: 1. Some empirical-findings and their implications for how the nervous-system processes sensory input. *Psychol Rev* 1980; **87**: 175–189.

4 Braff DL, Geyer MA, Swerdlow NR. Human studies of prepulse inhibition of startle: normal subjects, patient groups, and pharmacological studies. *Psychopharmacology* 2001; **156**: 234–258.

5 Geyer MA, Krebs-Thomson K, Braff DL, Swerdlow NR. Pharmacological studies of prepulse inhibition models of sensorimotor gating deficits in schizophrenia: a decade in review. *Psychopharmacology* 2001; **156**: 117–154.

6 Swerdlow NR, Braff DL, Taaid N, Geyer MA. Assessing the validity of an animal model of deficient sensorimotor gating in schizophrenic patients. *Arch Gen Psychiatry* 1994; **51**: 139–154.

7 Graham FK, Putnam LE, Leavitt LA. Lead-stimulation effects on human cardiac orienting and blink reflexes. *J Exp Psychol—Hum Percept Perform* 1975; **104**: 161–169.

8 Allen RM, Young SJ. Phencyclidine-induced psychosis. *Am J Psychiatry* 1978; **135**: 1081–1084.

9 Karper LP, Grillon C, Abi-Saab D, Morgan CAI, Charney DS, Krystal J. The effect of ketamine on pre-pulse inhibition and attention. *Schizophr Res* 1995; **15**: 180.

10 Mansbach RS, Geyer MA. Effects of phencyclidine and phencyclidine biologs on sensorimotor gating in the rat. *Neuropsychopharmacology* 1989; **2**: 299–308.

11 Dulawa SC, Geyer MA. Psychopharmacology of prepulse inhibition in mice. *Chin J Physiol* 1996; **39**: 139–146.

12 Linn GS, Javitt DC. Phencyclidine (PCP)-induced deficits of prepulse inhibition in monkeys. *NeuroReport* 2001; **12**: 117–120.

13 Conn PJ, Patel J. *The Metabotropic Glutamate Receptors*. Humana Press, Inc.: Totowa, NJ, 1994.

14 Bordi F, Ugolini A. Group I metabotropic glutamate receptors: implications for brain diseases. *Prog Neurobiol* 1999; **59**: 55–79.

15 Swerdlow NR, Geyer MA, Braff DL. Neural circuit regulation of prepulse inhibition of startle in the rat: current knowledge and future challenges. *Psychopharmacology* 2001; **156**: 194–215.

16 Abe T, Sugihara H, Nawa H, Shigemoto R, Mizuno N, Nakanishi S. Molecular characterization of a novel metabotropic glutamate receptor mGluR5 coupled to inositol phosphate/Ca^{2+} signal transduction. *J Biol Chem* 1992; **267**: 13361–13368.

17 Ohnuma T, Augood SJ, Arai H, McKenna PJ, Emson PC. Expression of the human excitatory amino acid transporter 2 and metabotropic glutamate receptors 3 and 5 in the prefrontal cortex from normal individuals and patients with schizophrenia. *Mol Brain Res* 1998; **56**: 207–217.

18 Devon RS, Porteous DJ. Physical mapping of a glutamate receptor gene in relation to a balanced translocation associated with schizophrenia in a large Scottish family. *Psychiatr Genet* 1997; **7**: 165–169.

19 Oka A, Takashima S. The up-regulation of metabotropic glutamate receptor 5 (mGluR5) in Down's syndrome brains. *Acta Neuropathol* 1999; **97**: 275–278.

20 Chiamulera C, Epping-Jordan MP, Zocchi A, Marcon C, Cottiny C, Tacconi S *et al*. Reinforcing and locomotor stimulant effects of cocaine are absent in mGluR5 null mutant mice. *Nat Neurosci* 2001; **4**: 873–874.

21 Geyer MA, Swerdlow NR. Measurement of the startle response, prepulse inhibition, and habituation. In: Crawley JN, Skolnick P (eds). *Current Protocols in Neuroscience*. J Wiley: New York, 1998, pp. 8.7.1–8.7.15.

22 Varty GB, Walters N, Cohen-Williams M, Carey GJ. Comparison of apomorphine, amphetamine and dizocilpine disruptions of prepulse inhibition in inbred and outbred mice strains. *Eur J Pharmacol* 2001; **424**: 27–36.

23 Braff DL, Stone C, Callaway E, Geyer MA, Glick ID, Bali L. Prestimulus effects on human startle reflex in normals and schizophrenics. *Psychophysiology* 1978; **15**: 339–343.

24 Paylor R, Crawley JN. Inbred strain differences in prepulse inhibition of the mouse startle response. *Psychopharmacology* 1997; **132**: 169–180.

25 Braff DL, Grillon C, Geyer MA. Gating and habituation of the startle reflex in schizophrenic patients. *Arch Gen Psychiatry* 1992; **49**: 206–215.

26 Grillon C, Ameli R, Charney DS, Krystal J, Braff DL. Startle gating deficits occur across prepulse intensities in schizophrenic patients. *Biol Psychiatry* 1992; **32**: 939–943.

27 Henry SA, Dulawa SC, Conquet F, Geyer MA. Severe disruption of prepulse inhibition (PPI) in mice lacking mGluR5. *Soc Neurosci Abstr* 1999; **25**: 449.

28 Henry SA, Conquet F, Geyer MA. Prepulse inhibition (PPI) deficit in mGluR5 knockout mice after multiple manipulations. *Soc Neurosci Abstr* 2001; **27**, 983.14.

29 Kinney GG, Burno M, Campbell UC, Hernandez LM, Rodriguez D, Bristow LJ *et al*. Metabotropic glutamate subtype 5 receptors (mGluR5) modulate locomotor activity and sensorimotor gating in rodents. *J Pharmacol Exp Ther* 2003; **306**: 116–123.

30 Lu YM, Jia Z, Janus C, Henderson JT, Gerlai R, Wojtowicz JM *et al*. Mice lacking metabotropic glutamate receptor 5 show impaired learning and reduced CA1 long-term potentiation (LTP) but normal CA3 LTP. *J Neurosci* 1997; **17**: 5196–5205.

31 Crawley JN, Belknap JK, Collins A, Crabbe JC, Frankel W, Henderson N *et al*. Behavioral phenotypes of inbred mouse strains: implications and recommendations for molecular studies. *Psychopharmacology* 1997; **132**: 107–124.

32 Willott JF. Changes in frequency representation in the auditory-system of mice with age-related hearing impairment. *Brain Res* 1984; **309**: 159–162.

33 Grauer SM, Marquis KL. Intracerebral administration of metabotropic glutamate receptor agonists disrupts prepulse inhibition of acoustic startle in Sprague–Dawley rats. *Psychopharmacology* 1999; **141**: 405–412.

34 Monn JA, Valli MJ, Massey SM, Wright RA, Salhoff CR, Johnson BG *et al*. Design, synthesis, and pharmacological characterization of (+)-2-aminobicyclo[3.1.0]hexane-2,6-dicarboxylic acid (LY354740): a potent, selective, and orally active group 2 metabotropic glutamate receptor agonist possessing anticonvulsant and anxiolytic properties. *J Med Chem* 1997; **40**: 528–537.

35 Schreiber R, Lowe D, Voerste A, De Vry J. LY354740 affects startle responding but not sensorimotor gating or discriminative effects of phencyclidine. *Eur J Pharmacol* 2000; **388**: R3–R4.

36 Henry SA, Lehmann-Masten V, Gasparini F, Geyer MA, Markou A. The mGluR5 antagonist MPEP, but not the mGluR2/3 agonist LY314582, augments PCP effects on prepulse inhibition and locomotor activity. *Neuropharmacology* 2002; **43**: 1199–1209.

37 Anderson JJ, Rao SP, Rowe B, Giracello DR, Holtz G, Chapman DF *et al*. H-3]methoxymethyl-3-[(2-methylyl-1,3-thiazol-4-yl)ethynyl]-pyridine binding to metabotropic glutamate receptor subtype 5 in rodent brain: *in vitro* and *in vivo* characterization. *J Pharmacol Exp Ther* 2002; **303**: 1044–1051.

38 Spooren WP, Gasparini F, van der Putten H, Koller M, Nakanishi S, Kuhn R. Lack of effect of LY314582 (a group 2 metabotropic glutamate receptor agonist) on phencyclidine-induced locomotor activity in metabotropic glutamate receptor 2 knockout mice. *Eur J Pharmacol* 2000; **397**: R1–R2.

THIS PAGE BLANK (USPTO)

EXHIBIT H

PERGAMON

Progress in Neurobiology Vol. 59, pp. 55 to 79, 1999

Printed in Great Britain
0301-0082/99/$ - see front matter

PII: S0301-0082(98)00095-1

GROUP I METABOTROPIC GLUTAMATE RECEPTORS: IMPLICATIONS FOR BRAIN DISEASES

FABIO BORDI* and ANNAROSA UGOLINI

Pharmacology Department, GlaxoWellcome Medicine Research Centre, 37100 Verona, Italy

(*Received* 26 *October* 1998)

Abstract—Glutamate is the major excitatory neurotransmitter in the brain and plays a unique role in a variety of central nervous system (CNS) functions. The discovery of the metabotropic receptors (mGluRs), a family of G-protein coupled receptors than can be activated by glutamate, has led to an impressive number of studies in recent years aimed at understanding their biochemical, physiological and pharmacological characteristics.

The eight mGluRs now known are divided into three groups according to their sequence homology, signal transduction mechanisms, and agonist selectivity. Group I mGluRs include $mGluR_1$ and $mGluR_5$, which are linked to the activation of phospholipase C; Groups II and III include all others and are negatively coupled to adenylyl cyclases.

The availability in recent years of agents selective for Group I mGluRs has made possible the study of the physiological roles of these receptors in the CNS. In addition to mediating glutamatergic neurotransmission, Group I mGluRs can modulate other neurotransmitter receptors, including GABA and the ionotropic glutamate receptors.

Group I mGluRs are involved in many CNS functions and may participate in a variety of disorders such as pain, epilepsy, ischemia, and chronic neurodegenerative diseases. This class of receptor may provide important pharmacological therapeutic targets and elucidating its functions will be relevant to develop new treatments for neurological and psychiatric disorders in which glutamatergic neurotransmission is abnormally regulated.

In this review anatomical, physiological and pharmacological results are presented with a special emphasis on the role of Group I mGluRs in functional and pathological processes.

CONTENTS

1. Introduction 56
2. Pharmacology of the Group I mGluRs 56
3. Distribution of Group I mGluRs in the mammalian brain 58
4. Neurophysiological role of Group I mGluRs 58
   4.1. Neuronal excitability 58
   4.2. Modulation of synaptic transmission 60
      4.2.1. Presynaptic inhibition 60
      4.2.2. Modulation of GABA 60
      4.2.3. Modulation of other neurotransmitters 60
      4.2.4. Modulation of ionotropic GluRs 61
   4.3. Long-term regulation of synaptic efficacy 62
      4.3.1. LTP and memory 62
      4.3.2. LTD 66
5. Group I mGLURs in pathological conditions 66
   5.1. Role of Group I mGluRs in nociception 66
   5.2. Role of Group I mGluRs in epilepsy 68
   5.3. Role of Group I mGluRs in neurodegeneration 69
      5.3.1. Brain ischemia 69
      5.3.2. Huntington's and Parkinson's diseases 70
      5.3.3. Alzheimer's disease 71
   5.4. Role of Group I mGluRs in psychiatry disorders 71
6. Conclusions 71
   Acknowledgements 72
   References 72

* Corresponding author. Tel.: +39/045/921-8845; Fax: +39/045/921-8153; e-mail: fb23261@GlaxoWellcome.co.uk

ABBREVIATIONS

4CPG	(*S*)-4-Carboxyphenilglycine
4C3HPG	(*S*)-4-Carboxy-3-hydroxyphenylglycine
AC	Adenylyl cyclase
ACPD	1*S*,3*R*-1-Amino-1,3-cyclopentanedicarboxylate
AIDA	(*RS*)-1-Aminoindan-1,5-dicarboxylic acid
AMPA	(*S*)-α-Amino-3-hydroxy-5-methyl-4-isoxazole propionic acid
CHPG	(*RS*)-2-Chloro-5-hydroxyphenylglycine
DAG	Diacylglycerol
DHPG	3,5-Dihydroxyphenylglycine
EPSC	Excitatory postsynaptic current
EPSP	Excitatory postsynaptic potential
iGluR	Ionotropic glutamate receptor
IP_3	Inositol triphosphate
LTD	Long-term depression
LTP	Long-term potentiation
mGluR	Metabotropic glutamate receptor
MCPG	α-Methyl-4-carboxyphenilglycine
NMDA	*N*-Methyl-D-aspartate
PKC	Protein kinase C
PLC	Phospholipase C

1. INTRODUCTION

Glutamate is the major excitatory neurotransmitter in the mammalian central nervous system (CNS) and plays an important role in a number of CNS functions (Monaghan *et al.*, 1989; Hollmann and Heinemann, 1994). The receptors that mediate its action have been divided into two broad categories, termed ionotropic receptors, which contain glutamate-gated cation channels, and metabotropic receptors, which are coupled to GTP-binding proteins (G proteins) and linked to the activation of phospholipase C (PLC) or the inhibition or activation of adenylyl cyclases (AC).

The metabotropic receptors (mGluRs) were discovered only in the 1980s when it was shown that glutamate and other excitatory amino acids like quisqualate and ibotenate could stimulate phosphoinositide (PI) turnover (Sladeczek *et al.*, 1985; Nicoletti *et al.*, 1986; Sugiyama *et al.*, 1987) or lead to mobilization of intracellular Ca^{2+} in different cell types of the CNS (Mayer and Miller, 1990; Irving *et al.*, 1990). Soon after, the first cDNA clone of a mGluR subtype was isolated by functional expression cloning (Masu *et al.*, 1991; Houamed *et al.*, 1991). This subtype is now known as $mGluR_1$. In the following years the cloning effort rapidly led to the discovery of seven more different subtypes, termed $mGluR_2$ to $mGluR_8$ [Tanabe *et al.* (1992); Abe *et al.* (1992); Nakanishi and Masu (1994) for a review]. Based on sequence homology, signal transduction mechanisms and agonist selectivity, the eight mGluRs can be divided into three groups (Nakanishi, 1994; Pin and Duvoisin, 1995). Group I includes $mGluR_1$ (with its splice variants a, b, c and d) and $mGluR_5$ (a and b), which are positively coupled to PLC and lead to an increase in diacylglycerol (DAG) and inositol triphosphate (IP_3), and in some cases to an activation of AC (Aramori and Nakanishi, 1992); Groups II and III include all others and lead to a decrease in forskolin-stimulated AC [Conn and Pin (1997) for review].

Over the recent years the Group I mGluRs have been extensively studied in experimental animals, leading to an appreciation of their great importance in the CNS. Both $mGluR_1$ and $mGluR_5$ are present in a number of key CNS structures including the hippocampus, cortex, thalamus and cerebellum and the involvement of these receptors in a variety of disorders including epilepsy, ischemia, pain and neurodegenerative diseases is beginning to emerge. Drugs that act through the mGluRs may have the capability to modulate glutamatergic synapses in a selective manner without the potential side-effects that had limited the clinical usefulness of the ionotropic glutamate agents (Olney, 1994). This new class of receptors could provide unique opportunities for designing more selective therapies.

Trans-amino-cyclopentane-dicarboxylate (*trans*-ACPD) was the first compound shown to activate mGluRs selectively (Palmer *et al.*, 1989) but lack of mGluR subtype-specific drugs made it difficult to draw conclusions about the physiological roles of the various metabotropic receptor groups. Thanks to the synthesis of new selective agonists and antagonists in recent years it is becoming possible to distinguish among the mGluR groups and much improvement has been made in the understanding of the biochemical, physiological and pharmacological properties of the Group I mGluRs (Watkins and Collingridge, 1994; Roberts, 1995; Conn and Pin, 1997). In this review we will examine this new and still somewhat controversial topic, emphasising the role of Group I mGluRs in functional and pathological processes.

2. PHARMACOLOGY OF THE GROUP I mGLURs

Group I mGluRs stimulate PLC and PI hydrolysis [see Conn and Pin (1997) for a review], and in some cases these receptors can couple to AC (Aramori and Nakanishi, 1992).

Cloned mGluRs expressed in heterologous mammalian systems have been used to characterize the activity of selective compounds on mGluR subtypes. Using predominately $mGluR_{1a}$ or $mGluR_{5a}$ splice variants, the pharmacological profile of Group I mGluRs has been determined (Conn and Pin, 1997). In every cell line tested, quisqualate is the most potent agonist of these receptors followed by ibotenate and glutamate, the presumed endogenous transmitter (Aramori and Nakanishi, 1992; Nakanishi *et al.*, 1994; Joly *et al.*, 1995). The rank of potency of the agonists for Group I mGluRs was found to be: quisqualate > 3,5-dihydroxyphenylglycine (DHPG) = glutamate > 1*S*,3*R*-1-amino-1,3-cyclopentanedicarboxylate (ACPD) = ibotenate > (2*S*,1′*S*,2′*S*)-2-(carboxycyclopropyl)glycine (L-CCG-I) > 3-hydroxyphenylglycine (3-HPG) > *trans*-azetidine-2,4-dicarboxylate (*t*-ADA) (Pin and Duvoisin,

1995; Conn and Pin, 1997). The Group I mGluR specific agonists are DHPG, 3-HPG and *t*-ADA, which are devoid of activity in other mGluR groups (Ito *et al.*, 1992; Schoepp *et al.*, 1994; Brabet *et al.*, 1995; Hayashi *et al.*, 1994). A new phenylglycine derivative, (*RS*)-2-chloro-5-hydroxyphenylglycine (CHPG), has been recently reported to activate only $mGluR_5$, but not $mGluR_1$ in transfected cells. This is the first compound available to distinguish pharmacologically the two members of the Group I class, although it is not very potent (Doherty *et al.*, 1997).

The discovery in 1993 of phenylglycine compounds as antagonists of mGluRs made possible to test the selectivity of the various mGluRs in both heterologous and neuronal systems. The first antagonist described for Group I mGluRs was α-methyl-4-carboxyphenilglycine (MCPG) (Birse *et al.*, 1993; Eaton *et al.*, 1993a; Watkins and Collingridge, 1994). MCPG, however, is also an antagonist of Group II mGluRs (Hayashi *et al.*, 1994). Substances related to phenylglycine have been synthesized since then, with (*S*)-4-carboxyphenilglycine (4CPG) and (*S*)-4-carboxy-3-hydroxyphenylglycine (4C3HPG) found to be the most potent Group I mGluRs antagonists, although they also have agonist effects on Group II receptors (Hayashi *et al.*, 1994; Thomsen *et al.*, 1994). Some of these compounds were found to be selective for $mGluR_1$ over $mGluR_5$, like LY367385 (Clark *et al.*, 1997). Even MCPG and 4CPG show a much better sensitivity for $mGluR_1$ than $mGluR_5$ in transfected cells (Joly *et al.*, 1995). Very recently, other compounds with an improved potency for the Group I mGluRs have been synthetized. These include (*RS*)-1-aminoindan-1,5-dicarboxylic acid (AIDA) (Pellicciari *et al.*, 1995; Moroni *et al.*, 1997), (*S*)-(+)-2-3′-carboxybicyclo[1.1.1]pentyglycine (CBPG) (Pellicciari *et al.*, 1996), and ethyl 7-(hydroxyimino)cyclopropan[b]chromen-1a-carboxylate (EtCCC) (Annoura *et al.*, 1996).

Most of the results obtained in clonal cell lines have been confirmed in native neuronal systems, such as brain slices or cultured cells, where the stimulation of PI hydrolysis is measured, or in spinal cord, where the depolarization induced in motoneurons by specific agonists can be inhibited by selective antagonists. Table 1 shows the potency of the agonists and antagonists that act at the Group I mGluRs measured in transfected cell lines or in native systems.

Since $mGluR_1$ is highly expressed while $mGluR_5$ is almost absent in the cerebellum [Masu *et al.* (1991); Shigemoto *et al.* (1993) see below], this structure is particularly suitable for distinguishing between the two Group I mGluRs (Toms *et al.*, 1995; Chavis *et al.*, 1995; Batchelor *et al.*, 1997). Cultured granule cells from rat cerebellum appear to be an excellent system for investigating selective compounds in a native environment. Using this system to assay $mGluR_1$ responses coupled to PI hydrolysis, Toms *et al.* (1995) obtained similar pharmacological results to those reported for cloned $mGluR_1$. The pharmacological characteristics of $mGluR_1$ can also be studies in the intact cerebellar slice, where mGluR-mediated excitatory postsynaptic potentials (EPSP) are recorded from Purkinje cells (Batchelor *et al.*, 1994, 1997).

Another useful preparation for characterizing Group I mGluRs is the neonatal rat spinal cord. Postsynaptic depolarization of motoneurons induced by specific agonists can be recorded electrophysiologically from the ventral roots (Watkins and Collingridge, 1994). This depolarization is insensitive to ionotropic glutamate receptor (iGluR) antagonists, but it is inhibited in a dose-dependent fashion by specific Group I mGluR antagonists (Birse *et al.*, 1993; Jane *et al.*, 1993; Ugolini *et al.*, 1997).

Table 1.

	Cloned cells		Neuronal systems		
	mGluR1	mGluR5	Hippocampal or cortical cells	Cerebellar granule cells	Neonatal spinal cord
Agonist (EC_{50} values in mM)					
Glutamate	9–13	3–10		50‡‡	
Quisqualate	0.2–3	0.03–0.3		2‡‡	
(1*S*,3*R*)-ACPD	10–80	5–7	47.2¶	102‡‡	58.1§§
DHPG			27.6¶		
3-HPG	68–100	14–35	98**		
t-ADA	190	30			
CHPG	Not active*	750*			
Antagonist (IC_{50} or K_D values in mM)					
MCPG	40–200	> 200	130††	243‡‡	341¶¶; 243§§
4CPG	15–65	> 500	35††	51‡‡	208¶¶
4C3HPG	10–40	?	345**	41‡‡	
AIDA	214†	> 1000†			
EtCCC	23‡		40††		
LY367385	8.8§	> 100§			

Values are taken from the following references: *Doherty *et al.* (1997); †Moroni *et al.* (1997); ‡Annoura *et al.* (1996); §Clark *et al.* (1997); ¶Schoepp *et al.* (1994); **Birse *et al.* (1993); ††Batchelor *et al.* (1997); ‡‡Toms *et al.* (1995); §§Boxall *et al.* (1996); ¶¶Jones *et al.* (1993). All other values are taken from Conn and Pin (1997).

3. DISTRIBUTION OF GROUP I mGLURs IN THE MAMMALIAN BRAIN

With the isolation of the first cDNA for a mGluR, the $mGluR_1$, it became possible to study the expression of these receptors in the CNS (Masu *et al.*, 1991). Distribution of the mRNA for $mGluR_1$ by *in situ* hybridization revealed an abundant expression of this receptor in hippocampal neurons and cerebellar Purkinje cells (Shigemoto *et al.*, 1992; Fotuhi *et al.*, 1993). In the cerebellum, $mGluR_1$ is distributed in cell bodies and dendrites of Purkinje, stellate and some Golgi cells, as described by immunoreactivity for $mGluR_{1a}$ (Martin *et al.*, 1992; Baude *et al.*, 1993; Hampson *et al.*, 1994). No $mGluR_5$, on the other hand, is found in the cerebellum (Shigemoto *et al.*, 1993), except for a small signal in the granule cell layer but not in the Purkinje cells (Romano *et al.*, 1995). The strong presence of $mGluR_1$ in the cerebellum correlates well with the severe motor coordination syndrome characterized by ataxia and tremor and with the neurophysiological abnormalities obtained with the $mGluR_1$-deficient mice (Conquet *et al.*, 1994; Aiba *et al.*, 1994b).

Other areas of expression of $mGluR_1$ are the olfactory bulb, the amygdala, the thalamus, and the basal ganglia (Martin *et al.*, 1992; Baude *et al.*, 1993; Hampson *et al.*, 1994). The presence of this receptor in these areas has inspired study of the potential role of Group I mGluRs in extrapyramidal motor diseases like Hungtington Chorea or Parkinson's Disease (see later).

In the hippocampus, both CA1 and CA3 fields are heavily labeled by antibodies to $mGluR_{1a}$, but this immunoreactivity is present in 'non-principal' neurons and is concentrated in the postsynaptic membrane at the periphery of synaptic junctions (Baude *et al.*, 1993). Unlike antibodies to glutamate ionotropic receptors that label sites within the synaptic junctions (Nusser *et al.*, 1994, 1995), the antibodies to $mGluR_{1a}$ label sites that are at the edge of the synapse (Baude *et al.*, 1993). Because of the special segregation of ionotropic receptors and mGluRs, it has been suggested that they may respond differently to glutamate stimulation; the ionotropic receptors respond to glutamate under normal presynaptic stimulation, whereas the perisynaptic $mGluR_1$ is involved in excitatory responses evoked only by strong presynaptic stimulation. This anatomical distribution suggests a role for the mGluRs in synaptic function that is different from that of the ionotropic receptors which, mediating fast signals at glutamergic synapses, are close to release sites. The postsynaptic metabotropic receptors situated at the periphery would appear to have a role of delayed activation (Baude *et al.*, 1993). Although these observations have been made using the $mGluR_{1a}$ splice variant, the regional pattern of the immunoreactivity for this splice variant suggests that its distribution correlates with the mRNA coding for all $mGluR_1$ (Shigemoto *et al.*, 1992). Interestingly, recent studies have confirmed this perisynaptic location in the hippocampus also for $mGluR_5$ and it may be a general feature of all G-protein receptors (Luján *et al.*, 1996).

The hippocampus of the rat (Shigemoto *et al.*, 1993; Romano *et al.*, 1995) and the human (Blümcke *et al.*, 1996) contain many neurons that express $mGluR_5$. In the CA1 region of the rat, $mGluR_5$ is present in both pre- and postsynaptic membranes (Romano *et al.*, 1995). However, while most CA3 pyramidal and granule cells express both $mGluR_5$ and $mGluR_1$, CA1 pyramidal cells express only $mGluR_5$ (Luján *et al.*, 1996). This finding fits nicely with the neurophysiological results demonstrating that LTP can be induced in CA1 region in mice lacking $mGluR_1$ (Conquet *et al.*, 1994), but not in mice lacking $mGluR_5$ [Lu *et al.* (1997); see later].

Group I mGluRs are also abundant in the spinal cord (Vidnyánszky *et al.*, 1994; Valerio *et al.*, 1997a,b). $mGluR_{5a}$ antibody staining is heavy in laminae I–II of the dorsal horn of the rat at the level of dendrites and perikaria and is found around the postsynaptic membrane in a peri- or extrasynaptic location similar to that seen in the hippocampus (Vidnyánszky *et al.*, 1994). This distribution of $mGluR_5$ is also seen in the human spinal cord (Valerio *et al.*, 1997a). Rat spinal cord expresses high levels of mRNA encoding $mGluR_{1a}$ as well (Valerio *et al.*, 1997b). The presence of both $mGluR_1$ and $mGluR_5$ in the dorsal laminae of the spinal cord strongly suggests an important role for these receptors in the control of nociceptive transmission [Corsi *et al.* (1997) see later].

4. NEUROPHYSIOLOGICAL ROLE OF GROUP I mGLURs

Metabotropic glutamate receptor agonists have a wide variety of actions in the CNS that can be mediated by voltage- and ligand-gated ion channels. Substances that activate Group I mGluRs cause neuronal depolarization and excitation while antagonists of these receptors inhibit depolarization and excitation. In addition, activation of these receptors can modulate synaptic transmission by regulating GABA release or by interfering with iGluRs. Recent evidence has also shown the importance of Group I mGluRs in modulating other brain neurotransmitter systems.

4.1. Neuronal Excitability

Application of the broad spectrum mGluR agonist ACPD produces an array of physiological effects, both inhibitory and excitatory (Schoepp *et al.*, 1990; Conn and Pin, 1997). Group I mGluRs, however, seem to involve primarily postsynaptic excitatory effects. In the CA1 area of the hippocampus, activation of mGluRs with ACPD leads to depolarization, increase of input resistance, and reduction in spike frequency adaptation (Charpak *et al.*, 1990; Desai and Conn, 1991; Desai *et al.*, 1992). These effects have been attributed to activation of Group I mGluRs because they are also produced by the specific agonist DHPG (Gereau and Conn, 1995a) and are blocked by the antagonists MCPG and 4CPG (Davies *et al.*, 1995). In neocortical neurons, the reduction in spike frequency adaptation caused by ACPD or quisqualate and blocked by

MCPG is not prevented by protein kinase C (PKC) or protein kinase A (Burke and Hablitz, 1996).

The increase in neuronal excitability caused by activation of Group I mGluRs is produced primarily by modulation of potassium channels [for review, Gerber and Gähwiler (1994); Glaum and Miller (1994)]. ACPD induces net inward currents by inhibiting K^+ conductances in neurons in hippocampus (Charpak *et al.*, 1990; Crépel *et al.*, 1994; Gereau and Conn, 1995a), amygdala (Womble and Moises, 1994), nucleus of the tractus solitarius (Glaum and Miller, 1992), and hypothalamus (Schrader and Tasker, 1997). This effect is blocked by Group I mGluR selective antagonists (Guérineau *et al.*, 1995; Gereau and Conn, 1995a; Schrader and Tasker, 1997). In the CA3 region of the hippocampus the reduction of K^+ conductance in response to mGluR activation is not mediated by PKC or protein kinase A and it exhibits a pronounced voltage sensitivity which could be important in physiological processes such as long-lasting changes in cellular excitability or persistent modification of synaptic efficacy (Gerber and Gähwiler, 1994; Lüthi *et al.*, 1997).

Interestingly, a decrease in K^+ conductance has been hypothesized to account for the control of corticothalamic activation mediated by mGluRs. This effect is thought to be important in facilitating sensory transmission to activate arousal and cognitive processes (McCormick and von Krosigk, 1992).

Activation of mGluRs can also produce inward currents separate from inhibition of potassium channels (Glaum and Miller, 1992; Mercuri *et al.*, 1993; Crépel *et al.*, 1994; Guérineau *et al.*, 1995). These inward currents vary in different types of cells and sometimes involves a Ca^{2+}-activated non-specific cation (CAN) current (Crépel *et al.*, 1994; Guérineau *et al.*, 1995; Congar *et al.*, 1997), or an activation of a Na^+/Ca^+ exchanger (Mercuri *et al.*, 1993; McBain *et al.*, 1994; Keele *et al.*, 1997). In the hippocampus the CAN current is mediated by Group I mGluRs because the selective agonist DHPG produces a current identical to that evoked by ACPD and this effect involves a Ca^{2+}-dependent and G-protein-dependent process (Congar *et al.*, 1997). In neurons of the basolateral amygdala, the metabotropic-activated Na^+/Ca^{2+} exchanger is elicited by DHPG, which may play a role in epilepsy, increasing transmission following kindling (Keele *et al.*, 1997).

Activation of Group I mGluRs can also modulate currents through N-type, L-type and other voltage-dependent calcium channels [Sayer *et al.* (1992); Sahara and Westbrook (1993); Swartz and Bean (1992); Swartz *et al.* (1993); for review see Stefani *et al.* (1996)]. Quisqualate inhibits N-type Ca^{2+} channels in hippocampus and cortex, where it is mediated by G-protein and does not involve protein kinases (Lester and Jahr, 1990; Sayer *et al.*, 1992; Swartz and Bean, 1992), but it facilitates L-type channel function in the granule cells of the cerebellum via a G-protein mechanism not sensitive to pertussin toxin (PTX) (Chavis *et al.*, 1995). In cerebellar granule cells, activation of $mGluR_1$ triggers a functional coupling between ryandine receptors and L-type Ca^{2+} channels that leads to facilitation of the L-type Ca^{2+} channel and could be important in regulating a phenomenon of synaptic plasticity like long-term depression (LTD) (Chavis *et al.*, 1996). In fronto-parietal cortical neurons, inhibition of N-type Ca^{2+} channels produced by specific Groups I and II mGluRs agonists is reduced by MCPG, suggesting that both these mGluR groups participate in modulating Ca^{2+} channels in cortical neurons (Choi and Lovinger, 1996). However, a differential sensitivity to PTX can distinguish the two groups of mGluR. Inhibition of Ca^{2+} channels by Group II mGluRs seems to involve a PTX-sensitive G-protein whereas Group I mGluRs use both a PTX-sensitive and PTX-insensitive G-protein. These results suggest that mGluRs inhibiting Ca^{2+} channels in cortical neurons might be separated on the basis of the G protein involved (Choi and Lovinger, 1996). Moreover, Group I in contrast to Group II mGluRs can use several distinct signal transduction pathways to inhibit Ca^{2+} channels, both Ca^{2+} intracellular-independent and -dependent mechanisms (McCool *et al.*, 1998).

In the $mGluR_1$-rich cerebellum, ACPD increases excitation and firing rate of Purkinje cells both *in vivo* or in slices. MCPG and 4CPG both block the agonist-induced excitatory responses (Lingenhöhl *et al.*, 1993; Batchelor *et al.*, 1994). Two Group I mGluR antagonists, 4C3HPG and 4CPG, selectively depress ACPD-induced excitation of thalamic neurons in the anesthetized rat (Eaton *et al.*, 1993a; Salt and Eaton, 1995). ACPD also causes depolarization of neonatal rat motoneurons which is blocked by MCPG, 4C3HPG or 4CPG (Birse *et al.*, 1993), but not by 2*S*,1′*S*,2′*S*-2-methyl-2-(carboxycyclopropyl)-glycine (MCCG) or *S*-2-amino-2-methyl-4-phosphonobutanoate (MAP4), respectively, Groups II and III antagonists (Jane *et al.*, 1994).

Recent studies have shown that selective activation of Group I mGluRs with DHPG increases postsynaptic membrane excitability in hippocampus (Davies *et al.*, 1995), cortex (Mannaioni *et al.*, 1996; Libri *et al.*, 1997), striatum (Pisani *et al.*, 1997), amygdala (Keele *et al.*, 1997), subthalamic nucleus (Abbott *et al.*, 1997), hypothalamic supraoptic nucleus (Schrader and Tasker, 1997) and in motoneurons of the spinal cord (Ugolini *et al.*, 1997).

Although the profiles of agonist and antagonist pharmacology indicate that Group I mGluRs mediate postsynaptic depolarizations in a number of brain areas, the lack of subgroup-specific agents has prevented a determination of the actual subtype involved. Some indication of the roles of the two Group I subtypes comes from experiments where mice lacking specific mGluRs were generated. In CA1 neurons of $mGluR_1$-deficient mice, ACPD produced excitatory effects similar to normal (Aiba *et al.*, 1994a; Conquet *et al.*, 1994), whereas $mGluR_5$-deficient mice lacked the normal neuronal depolarization in response to ACPD (Lu *et al.*, 1997). Administration of $mGluR_5$ antisense deoxynucleotides injected into the hippocampal CA1 gave similar results (Dorri *et al.*, 1997). These results suggest that $mGluR_5$ mediates excitatory effects in pyramidal CA1 neurons where $mGluR_1$ is not expressed (Luján *et al.*, 1996), but they do not preclude a role for $mGluR_1$ in other regions. To test whether $mGluR_1$ would compensate for the absence of

$mGluR_5$ one should examine depolarization responses induced by mGluR agonists either in the $mGluR_5$-deficient mice or in animals injected with $mGluR_5$ antisense in brain areas where both receptors are present (e.g. dentate gyrus, hippocampus CA3).

Recent studies using cells expressing $mGluR_1$ or $mGluR_5$ only have found separate functions for the two Group I mGluR subtypes. While either receptor triggers the release of Ca^{2+} from intracellular stores through the IP_3 pathway, glutamate stimulation produces a single peak of intracellular Ca^{2+} mobilization in the cells transfected with $mGluR_1$, but Ca^{2+} oscillations in the $mGluR_5$ transfected cells. These oscillations are also seen in astrocytes expressing $mGluR_5$ and are PKC-dependent because they are blocked by the selective inhibitor H-7 (Kawabata *et al.*, 1996; Nakahara *et al.*, 1997; Nakanishi *et al.*, 1998). Interestingly, Ca^{2+} oscillations are found in CA1 hippocampal interneurons in response to glutamate stimulation and they are prevented completely by MCPG but only partially by co-administration of the iGluR antagonists AP5 and 6-cyano-7-nitro-quinoxaline-2,3-dione (CNQX) (Carmant *et al.*, 1997).

4.2. Modulation of Synaptic Transmission

4.2.1. *Presynaptic Inhibition*

Synaptic transmission is influenced by mGluRs via modulation of postsynaptic receptors, as described above, but also by modulation of transmitter release from presynaptic terminals. Activation of presynaptic mGluRs cause a widespread reduction of glutamatergic transmission in the CNS. This action is determined almost exclusively by presynaptic Group II and Group III mGluRs [Baskys and Malenka (1991); Desai and Conn (1991); Pook *et al.* (1992); Burke and Hablitz (1994); Glaum and Miller (1994) for review]. Reduction of glutamatergic transmission attributed to Group I mGluRs has been observed only in the hippocampus, at the level of the synapses between Shaffer collaterals and CA1 pyramidal cells. In this region inhibition of EPSPs is induced by DHPG or quisqualate and is accompanied by an increase in paired-pulse facilitation, a common and reliable test of presynaptic mechanisms (Gereau and Conn, 1995b; Manzoni and Bockaert, 1995). $MGluR_5$ probably mediates this effect because it is not blocked by 4CPG (an $mGluR_1$ preferential antagonist) (Manzoni and Bockaert, 1995) and because there is immunochemical evidence for the presynaptic expression of $mGluR_5$ in CA1 neurons (Romano *et al.*, 1995).

Interestingly, a recent report demonstrated that the DHPG-induced inhibition of EPSPs in CA1 is facilitated by activation of NMDA receptors (Harvey *et al.*, 1996). According to these authors this mechanism in CA1 may have important implications for synaptic plasticity where both mGluRs and NMDA receptors are involved.

4.2.2. *Modulation of GABA*

A third function of mGluRs in the CNS is to regulate inhibitory synaptic transmission mediated by the amino acid neurotransmitter GABA. Activation of mGluRs reduces GABAergic synaptic transmission in the hippocampus (Liu *et al.*, 1993; Jouvenceau *et al.*, 1995), the striatum (Calabresi *et al.*, 1992; Stefani *et al.*, 1994), the thalamus (Salt and Eaton, 1995), the olfactory bulb (Hayashi *et al.*, 1993), and the nucleus of the tractus solitarius (Glaum and Miller, 1993). The identity of the mGluR Group responsible for this effect is not certain, but evidence for a presynaptic activation of Group II or Group III receptors is emerging.

In the hippocampus, GABAergic interneurons can be activated by mGluRs either pre- or postsynaptically (Desai *et al.*, 1994; McBain *et al.*, 1994; Jouvenceau *et al.*, 1995; Poncer *et al.*, 1995; Doherty and Dingledine, 1998). In the CA3 region activation of Group I mGluRs, presumably located on the somato-dendritic membrane of GABA interneurons, enhances excitability. In contrast, Group II mGluRs are located on inhibitory terminals and reduce GABA release (Poncer *et al.*, 1995). In the CA1 region, Group I mGluRs are involved in modulating transmission from GABAergic interneurons onto pyramidal cells. Analysis of spontaneous inhibitory postsynaptic currents (IPSCs) suggests that these receptors are localized presynaptically (Gereau and Conn, 1995b). Activation of Group I mGluRs on GABA inhibitory neurons in the hippocampus can contribute to the generation of hyperexcitability connected with epilepsy (Doherty and Dingledine, 1998) and may have an important role in synaptic plasticity, as shown in mice lacking $mGluR_1$ [Bordi *et al.* (1997) see later].

In the rat frontal cortex Group I mGluRs can enhance GABA-mediated synaptic inhibition through activation of inhibitory interneurons and, as in CA1, these receptors seem to be located presynaptically (Chu and Hablitz, 1998).

4.2.3. *Modulation of Other Neurotransmitters*

Recent work has focused on the interaction of mGluRs with other neurotransmitter systems. It is now becoming evident that mGluRs regulate different neurotransmitters in a number of brain structures.

Activation of rat dentate gyrus neurons with ACPD or the specific Group I mGluR agonist DHPG increases NPY mRNA levels in granule cells and interneurons and this effect is antagonized by MCPG and 4CPG (Schwarzer and Sperk, 1998). These results are important in light of the recent evidence of a possible role of NPY in epilepsy (Schwarzer *et al.*, 1998).

In the hippocampus DHPG is also able to attenuate the inhibitory effects of adenosine A1 receptor activation and this attenuation occurs via a PKC-dependent mechanism. This interaction may be relevant to the pathology that occurs after hypoxia, where adenosine is an endogenous protective substance (de Mendonça and Ribeiro, 1997; Budd and Nicholls, 1998).

In cultures of astrocytes, $mGluR_5$ is associated with the regulation of β-adrenergic receptor function. The agonist DHPG, but not agonists for Group II or III mGluRs, potentiates cyclic AMP accumulation induced by β-adrenergic stimulation. This effect is independent of intracellular Ca^{2+} or the PKC pathway (Balázs *et al.*, 1998), but can contribute to the opening of Ca^{2+} channels and modulate neuronal activity by a feedback process to neurons (Verkhratsky and Kettenmann, 1996; Balázs *et al.*, 1998).

Recent work showed that mGluRs modulate dopamine (DA) neurons in various ways. ACPD produces an increase of the spontaneous firing rate and a depolarization of rat DA mesencephalic cells (Mercuri *et al.*, 1993). This excitation is attributed in part to an inward current that is antagonized by the Group I mGluR antagonist 4C3HPG. In the ventral midbrain, ACPD and DHPG cause a decrease in the EPSP's amplitude and depolarization of DA neurons (Wigmore and Lacey, 1998). ACPD mediates excitation and inhibition of substantia nigra DA neurons as well, and this action is blocked by Group I mGluR antagonist 4CPG (Meltzer *et al.*, 1997). Moreover, electrical stimulation of ventral tegmental DA neurons evokes a slow excitatory postsynaptic current (EPSC) which is mediated by mGluRs, particularly by Group I mGluRs because it is blocked by MCPG (Shen and Johnson, 1997). In primary cultures of striatal neurons, Group I mGluR agonists potentiate the cAMP formation induced by activation of D_1-like dopamine receptors. This potentiation is blocked by 4CPG and also by PKC inhibitors (Paolillo *et al.*, 1998).

A role of Group I mGluRs in modulating DA system function was shown also by the observation that intrastriatal injection of ACPD or DHPG caused a contralateral rotational behavior, a response that is DA-dependent (Sacaan *et al.*, 1991, 1992; Kearney *et al.*, 1997). When infused into the nucleus accumbens, ACPD increases locomotor activity in rats and MCPG blocks this effect. Blockade of DA receptors with haloperidol reduces (in a dose-dependent manner) the ACPD-induced locomotor activation (Attarian and Amalric, 1997), suggesting that the increase in locomotor activity is dependent on DA. A recent study has shown that MCPG injected into the nucleus accumbens also interferes with amphetamine-induced locomotion, and suggested that the mGluRs located postsynaptically to DA terminals mediate this action (Kim and Vezina, 1998a).

All these results strongly suggest a possible involvement of Group I mGluRs in Parkinson's Disease or Huntington's Chorea by modulating the DA system [Sacaan *et al.* (1992); see later].

4.2.4. *Modulation of Ionotropic GluRs*

Activation of mGluRs has been shown to modulate *N*-methyl-D-aspartate (NMDA) and (*S*)-α-amino-3-hydroxy-5-methyl-4-isoxazolepropionic acid (AMPA) receptor-mediated membrane currents in a number of brain areas and cell types. Potentiation of NMDA responses by ACPD was reported in the CA1 region of the hippocampus (Aniksztejn *et al.*, 1992; Harvey and Collingridge, 1993), cerebellum (Kinney and Slater, 1993), neocortex (Rahman and Neuman, 1996; Mannaioni *et al.*, 1996), visual cortex (Wang and Daw, 1996), striatum (Pisani *et al.*, 1997), and spinal cord (Cerne and Randic, 1992; Jones and Headley, 1995; Ugolini *et al.*, 1997). In some studies, however, ACPD attenuates NMDA responses (Colwell and Levine, 1994; Yu *et al.*, 1997) and this discrepancy can be explained by the NMDA receptor composition in different cell types (Shen *et al.*, 1995).

ACPD also potentiates AMPA responses in spinal cord (Cerne and Randic, 1992; Bleakman *et al.*, 1992; Jones and Headley, 1995; Bond and Lodge, 1995; Ugolini *et al.*, 1997) and visual cortex (Wang and Daw, 1996), but not in the hippocampus (Aniksztejn *et al.*, 1992; Harvey and Collingridge, 1993). Spinal cord depolarizations induced by kainate are increased by ACPD in some reports (Bleakman *et al.*, 1992; Jones and Headley, 1995) but not in others (Cerne and Randic, 1992; Ugolini *et al.*, 1997). Figure 1 illustrates the facilitation of NMDA or AMPA responses that is induced by ACPD in spinal cord motoneurons. The specific agonist DHPG produces effects similar to those obtained with ACPD in the hippocampus (Fitzjohn *et al.*, 1996), striatal slices (Pisani *et al.*, 1997) and spinal cord (Jones and Headley, 1995; Ugolini *et al.*, 1997).

The potentiation of excitatory responses is explained by an mGluR-mediated membrane depolarization that increases cell excitability (Jones and Headley, 1995; Bond and Lodge, 1995). Inhibition of K^+ currents (I_m or $I_{K\ leak}$) are implicated in these mGluR-induced depolarizations (Charpak *et al.*, 1990; Gerber and Gähwiler, 1994), resulting in an increase in cell input resistance.

PKC, which is triggered by activation of Group I mGluRs, has been proposed to mediate the potentiation of iGluR responses. In oocytes a specific PKC antagonist blocks the mGluR-induced enhancement of the NMDA response (Kelso *et al.*, 1992). In the CA1 region of the hippocampus, potentiation of the NMDA effect induced by ACPD was blocked by PKC antagonists in one study (Aniksztejn *et al.*, 1992), but not in another (Harvey and Collingridge, 1993). In the striatum, the PKC blockers staurosporine or calphostin C are effective in preventing DHPG-mediated potentiation of the NMDA-induced depolarization and the PKC activator phorbol-12,13-diacetate (PDAc) mimicks the enhancement of the NMDA responses (Pisani *et al.*, 1997). In spinal cord motoneurons, the potentiation of responses elicited by both NMDA and AMPA is blocked by the two PKC blockers, staurosporine or chelerythrine chloride [Ugolini *et al.* (1997) see Fig. 1], suggesting the involvement of a PKC-dependent mechanism in the mGluR-induced potentiation in the spinal cord.

PKC phosphorylates NMDA and AMPA receptors (Roche *et al.*, 1994). The activation by mGluRs of PKC might therefore modulate the phosphorylation state of these two ionotropic receptors, resulting in a potentiation of the response [see Michaelis (1998)]. This mechanism could also explain how mGluR potentiation of NMDA and AMPA re-

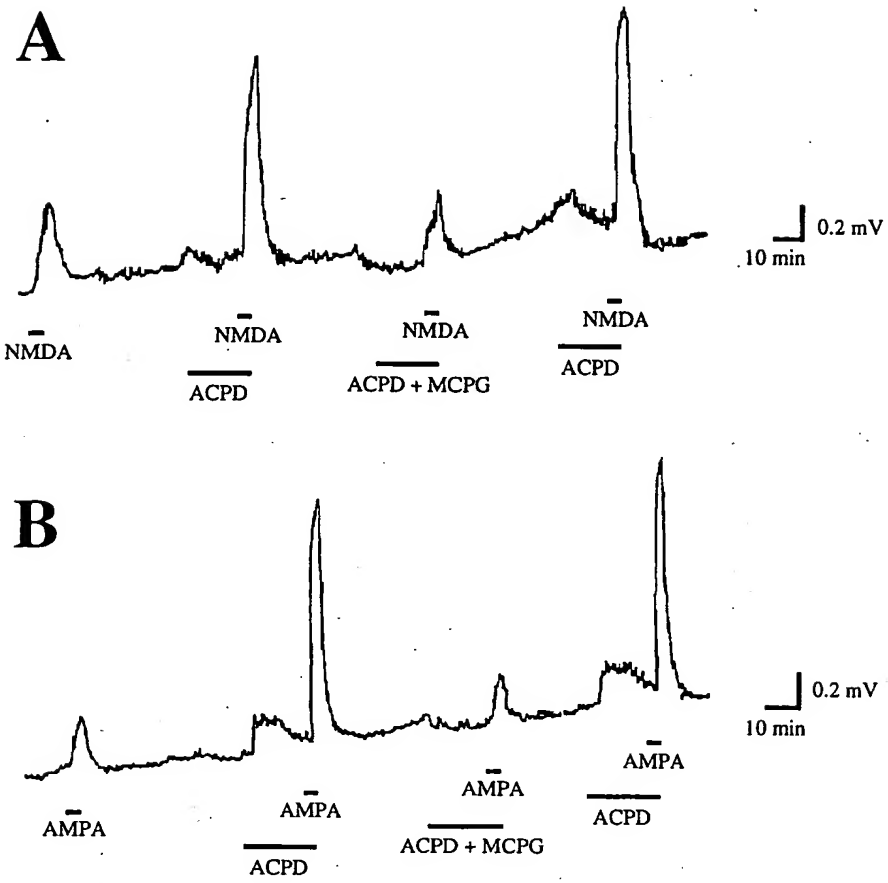

Fig. 1. The mGluR agonist ACPD facilitates the depolarization of motoneurons induced by NMDA or AMPA. This facilitation is blocked by the Group I mGluR antagonist MCPG. Top trace (A) is a representative recording from one experiment in which NMDA (10 μM, 4 min) potentiation caused by perfusion of ACPD (10 μM, 20 min) is blocked when ACPD is perfused together with MCPG (500 μM). In the bottom trace (B) an individual trace is taken from one experiment in which MCPG (500 μM) antagonizes the ACPD-induced potentiation of AMPA (0.1 μM, 4 min) responses [reproduced from Ugolini *et al.* (1997)].

sponses could be involved (or participate in) some forms of plasticity like long-term potentiation (LTP) or nociception [Harvey and Collingridge (1993); Corsi *et al.* (1997); see below].

The specific $mGluR_5$ agonist CHPG is also able to potentiate NMDA responses in the hippocampus (Doherty *et al.*, 1997) and NMDA or AMPA responses in spinal cord motoneurons (Ugolini and Bordi, unpublished observations), suggesting a role for $mGluR_5$ in this action either alone or in combination with $mGluR_1$ (Fig. 2). In the spinal cord, however, there is no evidence for an involvement of PKC, in contrast to what it is seen when the NMDA or AMPA responses are potentiated by ACPD. Both $mGluR_5$ and $mGluR_1$ may thus act to enhance iGluR responses but the two types of mGluRs may have different intracellular mechanisms of action. Different functions for the two types of Group I mGluRs has also been suggested by recent studies with cells transfected with $mGluR_1$ and $mGluR_5$ [see Nakanishi *et al.* (1998)].

4.3. Long-Term Regulation of Synaptic Efficacy

Group I mGluRs have been implicated in different forms of synaptic plasticity, such as LTP and LTD, and in memory formation (Bliss and Collingridge, 1993; Riedel and Reymann, 1996). LTP and LTD are persistent changes in synaptic efficacy induced by tetanic afferent stimulation and are considered models of the cellular mechanisms underlying learning and memory (Bliss and Lømo, 1973; Bear and Malenka, 1994).

4.3.1. *LTP and Memory*

Facilitating effects of the mGluR agonist ACPD in LTP potentiation have been shown in hippocampal slices. Pre-treatment with the mGluR agonist causes increased LTP following tetanus compared to untreated controls (Otani and Ben-Ari, 1991; McGuinness *et al.*, 1991). ACPD can also induce LTP in absence of electrical stimulation. This LTP induction depends on an intact connection between

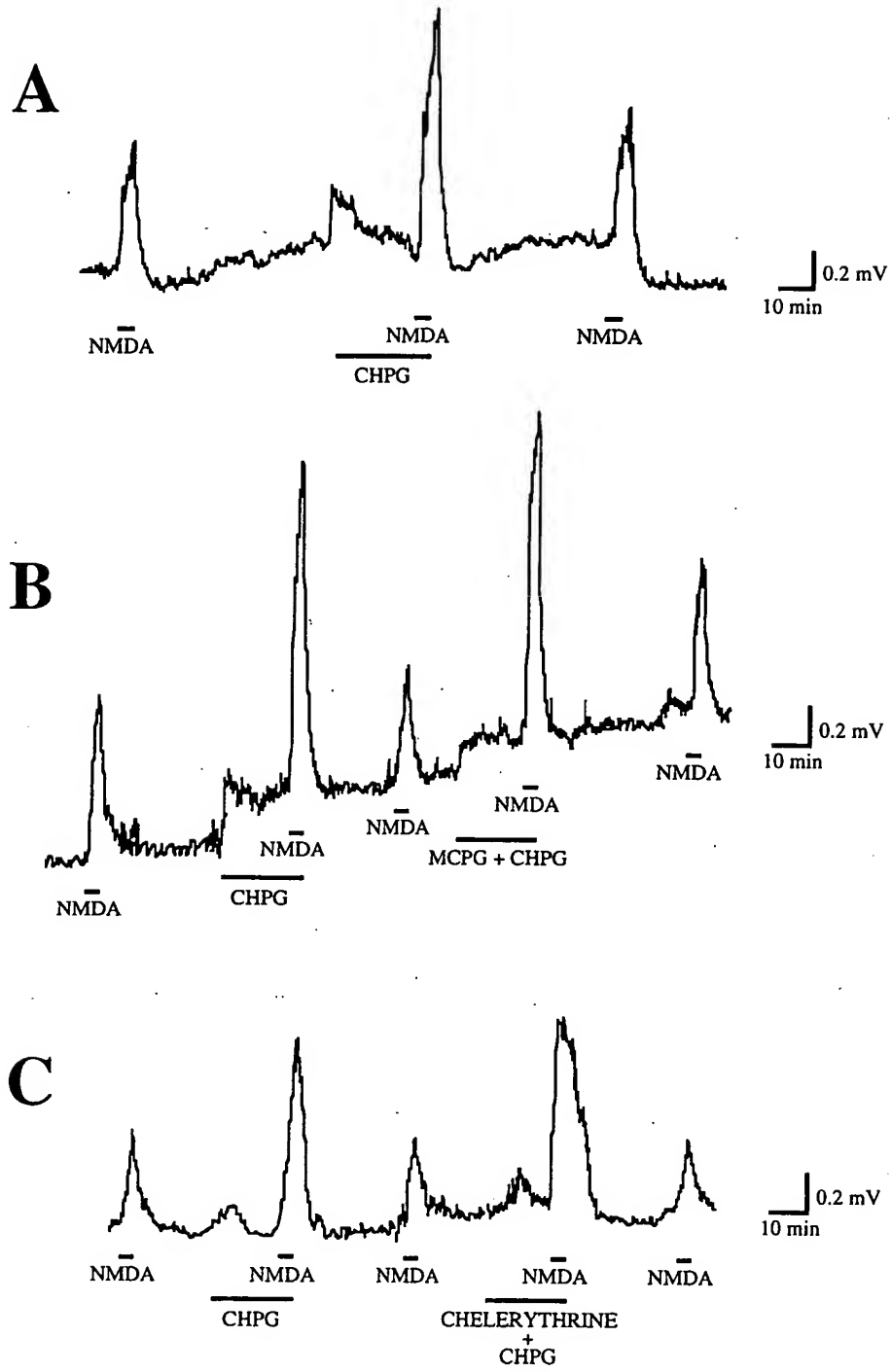

Fig. 2. The $mGluR_5$ agonist CHPG enhances the depolarization of motoneurons induced by NMDA. This facilitation is neither blocked by the Group I mGluR antagonist MCPG nor by the PKC inhibitor chelerythrine chloride. Each trace is taken from an individual experiment. Periods of drug perfusion are indicated by bars for NMDA (10 μM, 4 min) and CHPG (1 mM, 20 min). Chelerythrine chloride (3 μM) or MCPG (1 mM) are co-applied with CHPG.

the CA3 and CA1 regions of the hippocampus (Bortolotto and Collingridge, 1993, 1995; Breakwell *et al.*, 1996). Since ACPD exerts its facilitating action through a PKC-dependent pathway (Anwyl, 1991; Otani *et al.*, 1993), a mechanism proposed to explain the involvement of mGluRs in LTP is by modulation of NMDA receptors via PKC. This view holds that NMDA is sufficient to generate LTP (Ben-Ari and Aniksztejn, 1995). A different view suggests that mGluRs trigger directly LTP via activation of PKC in parallel with induction involving NMDA receptors (Watkins and Collingridge, 1994).

It has been difficult to distinguish between these hypotheses using the available mGluR antagonists. MCPG can inhibit both tetanus-induced and ACPD-induced LTP in the hippocampus CA1 (Bashir *et al.*, 1993). However, MCPG blocked LTP only in 'naive slices', but not in slices that had already been stimulated tetanically (Bortolotto *et al.*, 1994). The authors proposed that Group I mGluRs activate a molecular switch that, once stimulated, stays on for a long time and need not be activated again. This switch is PKC-mediated, since its activation is blocked by PKC inhibitors, but it does not require co-activation of NMDA receptors, and can be reset by low frequency stimulation that depotentiates LTP and re-establishes the need for mGluR-activation for LTP in non-naïve slices (Bortolotto *et al.*, 1994).

The effects of MCPG on LTP have been quite variable, however. While some reports confirmed the original blocking effect exerted by MCPG in the hippocampus (Sergueeva *et al.*, 1993; O'Connor *et al.*, 1994; Little *et al.*, 1995) or in the medial frontal cortex (Vickery *et al.*, 1997), other studies failed to find any effect of MCPG in inhibiting tetanus-induced or ACPD-induced LTP in the hippocampal (Chinestra *et al.*, 1993; Manzoni *et al.*, 1994; Selig *et al.*, 1995; Thomas and O'Dell, 1995) or in visual cortical slices (Hensch and Stryker, 1996; Huber *et al.*, 1998). Part of these conflicting results have been explained by the different conditions in which the slice is placed in the recording chamber (Bortolotto *et al.*, 1995; Ben-Ari and Aniksztejn, 1995; Breakwell *et al.*, 1996) or by the different developmental stage of the animals. Izumi and Zorumski (1994) found that MCPG given 5 minutes after tetanization was effective in inhibiting LTP in hippocampal slices taken from PND15 or 30 but not from PND60 rats.

Another factor that may explain different findings is the tetanization strength and the resulting intracellular response. Since it has been proposed that intracellular Ca^{2+} concentration is a critical factor for LTP induction (Malenka *et al.*, 1988, 1992), a recent study using Ca^{2+} imaging analysis suggests that Group I mGluRs involvement in LTP is confined to certain types of potentiation, which are induced by weak tetanization and require the release of Ca^{2+} from intracellular stores. The stronger the potentiation, the less are the mGluR antagonists able to inhibit LTP induction (Wang *et al.*, 1995; Wilsch *et al.*, 1998).

In adult rats, MCPG attenuates LTP in hippocampus dentate gyrus in anesthetized animals in one study (Richter-Levin *et al.*, 1994), but is completely ineffective in other studies (Bordi and Ugolini, 1995; Martin and Morris, 1997). Since the mGluR antagonist readily blocks LTP induction in freely behaving animals (Riedel *et al.*, 1994, 1995; Riedel and Reymann, 1996), it is possible that the state of anesthesia may interact with the drug action or that the weaker tetanization parameters necessary to induce a stable LTP in freely-moving rats may unmask the role of mGluRs in LTP (Martin and Morris, 1997).

Studies of mice lacking $mGluR_1$ confirm the involvement of Group I mGluRs in LTP induction, although different results have been reported. In one study $mGluR_1$ −/− mice had normal LTP in the CA1 or dentate gyrus areas, both NMDA receptor-dependent pathways, but reduced LTP in the mossy fiber CA3 area, which involves an NMDA receptor-independent pathway (Conquet *et al.*, 1994). The opposite result was found in a study using a different set of $mGluR_1$ knock-out mice (Aiba *et al.*, 1994a; Hsia *et al.*, 1995).

The question of LTP in $mGluR_1$-deficient animals was recently addressed by measuring LTP in the intact hippocampus of anesthetized mice. In these animals, LTP was reduced in the perforant path-dentate gyrus pathway (Bordi, 1996). A possible explanation of this result is that dentate gyrus neurons receive more inhibitory synaptic drive *in vivo* than in slice preparation where many inhibitory axon collaterals are lost (Buckmaster and Schwartzkroin, 1995). Decreasing the level of feedback inhibition by activation of $GABA_B$ receptors on GABA interneurons made it possible to induce normal LTP in $mGluR_1$ −/− mice [Bordi *et al.*, 1997; Fig. 3(A)]. A possible scenario is depicted in Fig. 3(B). According to this view glutamate controls GABA inhibition via $mGluR_1$ situated postsynaptically on the interneuron. $MGluR_1$ would thus have an indirect role in synaptic plasticity by regulating GABA inhibition.

Interestingly, a very similar mechanism has been described for a form of synaptic modulation exerted by $mGluR_2$ in the olfactory bulb. Here, activation of the $mGluR_2$-rich granule cells suppresses inhibitory GABA transmission to mitral cells allowing the formation of a specific olfactory memory (Hayashi *et al.*, 1993; Kaba *et al.*, 1994).

Mice lacking $mGluR_5$ show reduced LTP in the regions of the hippocampus that are known to be NMDA receptor-dependent, but they have a normal LTP in the mossy fiber synapses of the CA3 region (Lu *et al.*, 1997). Thus, $mGluR_5$ plays an important regulatory role in LTP in NMDA-dependent pathways in the hippocampus.

Treatments that interfere with LTP are usually also studied in cognitive tests (Morris *et al.*, 1986). To investigate whether reduced LTP resulted in an impairment in learning and memory, $mGluR_5$ mutant mice were tested in two different spatial learning tasks, both known to depend on an intact hippocampus, the Morris water maze (Morris, 1984) and the contextual fear conditioning test (Phillips and LeDoux, 1992). In both tasks, the performance of $mGluR_5$-deficient mice was significantly different than that of their wild-type littermates (Lu *et al.*, 1997). Interestingly, $mGluR_1$ mutant mice were also

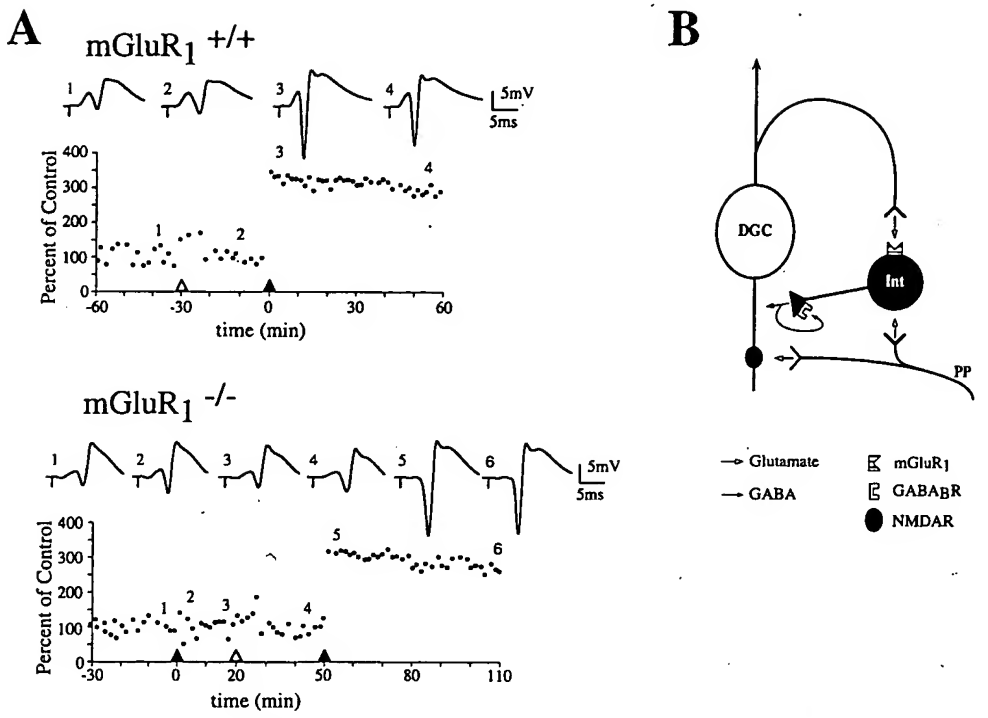

Fig. 3. (A Effects of $mGluR_1$ +/+ mice and $mGluR_1$ −/− on perforant path-dentate gyrus LTP. Consistent LTP was induced in wild-type animals whereas $mGluR_1$ −/− animals showed a reduced LTP of population spike amplitude compared to control. Baclofen injection did not modify the ability to evoke LTP in wild-type animals, but allowed a normal induction of LTP in mutant −/− mice. Top traces are representative EPSPs taken from one experiment each at the time indicated on the graph. Each point is the average of three evoked potentials. ▲, When the tetanus was induced (three trains 10 sec apart, 400 Hz, eight 0.4 msec impulses in each train). △, Start of the baclofen injection (10 mg kg^{-1} ml^{-1}, i.p.). (B) Schematic diagram of the basic dentate gyrus circuit with proposed localization of $mGluR_1$. The GABA-releasing interneuron (Int) can be activated by synapses from the glutamatergic perforant path (PP) or via a recurrent collateral from the dentate gyrus granule cell (DGC). When GABA is released from the interneuron it acts on presynaptic $GABA_B$ receptors [reproduced from Bordi *et al.* (1997)].

impaired in the same behavioral tasks (Conquet *et al.*, 1994; Aiba *et al.*, 1994a). Taken together these results strongly implicate Group I mGluRs in learning and memory function. However, since the mice are congenitally lacking $mGluR_1$ or $mGluR_5$, it is possible that these two receptors are only required during development to establish a plastic state, and may not be needed for the expression of learning and memory *per se*.

This argument leads to a review of the behavioral studies that tested animals in learning and memory tasks under pharmacological treatment to see if Group I mGluR antagonists also interfere with learning and memory. In fact, more consistent results of the effects of MCPG on behavior were obtained than on tests of LTP. Using different behavioral paradigms, a number of laboratories showed an impairment of the learning performance when MCPG was injected intraventricularly in rats. These include inhibition of water maze learning (Richter-Levin *et al.*, 1994; Bordi *et al.*, 1996) and of Y-maze with footshock reinforcement (Riedel *et al.*, 1994; Balschun and Wetzel, 1998). Retention deficits have also been reported in passive avoidance learning in young chicks [Holscher (1994); Rickard and Ng (1995); see Riedel (1996) for review]. Using a more potent Group I antagonist, AIDA, Nielsen *et al.* (1997) found blockade of hippocampus-dependent contextual fear conditioning, but not hippocampus-independent cue conditioning. In contrast, context-dependent fear conditioning was not altered by MCPG (Bordi *et al.*, 1996). Similarly, intra-hippocampal injections of MCPG did not affect working memory in rats, but AIDA dose-dependently increased the number of errors in the three panel runway setup (Ohno and Watanabe, 1996, 1998). Co-application of MCPG and a NMDA receptor antagonist aggravates impairment in the working memory task, while infusion of a partial agonist at the glycine site, D-cycloserine, reduced the errors induced by AIDA. These findings suggest an interactive regulation of memory processes by mGluR- and NMDA receptor-mediated mechanisms (Ohno and Watanabe, 1996, 1998).

4.3.2. *LTD*

Together with LTP, LTD in the cerebellum or in the hippocampus is an important example of cellular mechanism of long-lasting synaptic plasticity.

There is clear pharmacological evidence that Group I mGluRs are involved in the induction of LTD at parallel fiber-Purkinje cell synapses in the cerebellum (Daniel *et al.*, 1992; Linden and Connor, 1993; Hartell, 1994). The antagonist MCPG also blocks the induction of homosynaptic LTD in the hippocampus (Bolshakov and Siegelbaum, 1994; O'Mara *et al.*, 1995) but does not always do so (Selig *et al.*, 1995; Oliet *et al.*, 1997). MCPG is effective in blocking LTD induced by low-frequency stimulation in the visual cortex in some studies (Kato, 1993; Haruta *et al.*, 1994; Hensch and Stryker, 1996), but a recent report fails to reproduce the same results (Huber *et al.*, 1998). A possible explanation of the discrepancies found both in the hippocampus and in the visual cortex is that there are two forms of LTD, one presynaptic and MCPG-sensitive, the other postsynaptic and NMDA receptor-dependent (Oliet *et al.*, 1997; Nicoll *et al.*, 1998).

Activation of Group I mGluRs with the selective agonist DHPG or with the $mGluR_5$ specific agonist CHPG induces LTD in CA1 hippocampus slices in Mg^{2+}-free medium or with GABA-mediated inhibition blocked. Reduction of DHPG-induced LTD in Mg^{2+}-free medium is achieved by MCPG or by application of the NMDA receptor antagonist (*R*)-2-amino-5-phosphonopentanoate (AP5) (Palmer *et al.*, 1997). Application of ACPD in CA1 slices of immature rats causes LTD and this effect is also blocked by NMDA receptor antagonists (Overstreet *et al.*, 1997). Together, these results indicate that mGluRs and NMDA receptor-dependent forms of LTD may not be completely independent processes (Palmer *et al.*, 1997).

A study using freely-moving animals found that MCPG and 4CPG inhibited LTD induction in the hippocampus while Group II mGluR antagonists modulate LTD maintenance (Manahan-Vaughan, 1997).

Mice lacking $mGluR_1$ show reduced LTD in cerebellar Purkinje cells (Aiba *et al.*, 1994b; Conquet *et al.*, 1994). This electrophysiological phenomenon is accompanied by impaired eyeblink conditioning (Aiba *et al.*, 1994b) and severe motor coordination deficits, probably the result of cerebellar dysfunction. There are not, however, gross abnormalities of the basic bioelectric properties or of excitatory and inhibitory synaptic responses in these cells (Conquet *et al.*, 1994). The results from $mGluR_1$-deficient mice imply a role for these receptors in cerebellar LTD, as it was suggested by pharmacological experiments (Daniel *et al.*, 1992; Linden and Connor, 1993; Hartell, 1994) or by studies in which antibodies directed against the N-terminal extracellular segments of $mGluR_1$ blocked LTD induction in cultured Purkinje neurons (Shigemoto *et al.*, 1994). The other Group I mGluR, $mGluR_5$, does not compensate for the lack of LTD response in $mGluR_1$-deficient mice. In addition, mice lacking $mGluR_5$ do not exhibit motor deficits and they have a normal LTD (Lu *et al.*, 1997).

5. GROUP I mGLURs IN PATHOLOGICAL CONDITIONS

Glutamate is a major neurotransmitter that mediates synaptic excitation at the majority of CNS synapses and it is therefore involved in many important brain functions. Because of its widespread presence, glutamate has been implicated in a variety of CNS disorders. Overstimulation of glutamate receptors results in the death of neurons, a phenomenon called excitotoxicity that has been linked to several pathological states in the CNS, such as brain ischemia, hypoxia and traumatic brain injury. If this excessive glutamatergic activation is blocked by competitive or non-competitive glutamate receptor antagonists it is possible to reduce the hypoxic-ischemic brain damage (Rothman and Olney, 1986).

Excitotoxicity has also been related to epilepsy and may have a role in the pathogenesis of chronic neurodegenerative disorders such as Huntington's disease or Alzheimer's disease (Greenamyre and Young, 1989; Albin and Greenamyre, 1992). Whether the neurotoxic actions of glutamate are the primary cause of these diseases or a final common pathway to neuronal death in many neurological disorders is still a matter of numerous debates (Greenamyre and Porter, 1994; Kornbuber and Wiltfang, 1998). However, pharmacological agents that reduce glutamate receptor activation might provide a valuable therapeutic approach for neuroprotection of acute and chronic neurodegenerative disorders.

Modifying glutamatergic transmission with drugs acting selectively at Group I mGluRs can have important potential benefits. By developing drugs capable of inhibiting discrete populations of glutamatergic receptors it may be possible to bypass the profound side-effects that have limited the clinical use of iGluR antagonists (Olney *et al.*, 1989; Olney, 1994). Moreover, the ability of mGluRs to modulate the response of other neurotransmitters may also be crucial in the management of neurological and psychiatric illnesses.

In the following section the involvement of mGluRs belonging to Group I in pathophysiological processes will be reviewed.

5.1. Role of Group I mGluRs in Nociception

There is considerable evidence for the involvement of the excitatory amino acids, glutamate and aspartate, in transmission of both acute and chronic pain (Besson and Chaouch, 1987; Willis and Westlund, 1997; Dickenson *et al.*, 1997). A large number of peripheral sensory fibers contain glutamate, including C-fibers, and *ca* 80% of substance P-containing fibers also contain glutamate (Battaglia and Rustioni, 1988).

In the spinal cord, the response to brief acute mechanical or thermal stimuli appears to involve AMPA receptor activation (Aanonsen *et al.*, 1990). When the stimulus is maintained and/or its frequency or intensity is increased, however, NMDA receptors become activated, resulting in a potentiation of the response that underlies many forms of central sensitization (Dickenson, 1995). Sensitization

is an increase in response to stimulation and has been studied experimentally in the spinal cord using the 'wind-up' phenomenon (Woolf, 1983; Woolf and Wall, 1986), an increase in the number of spikes generated by a neuron after each successive stimulus during a pulse train [see Baranauskas and Nistri (1998) for review]. The wind-up is suggested to be a central mechanism for hyperalgesia (Mendell and Wall, 1965). Glutamate or NMDA reproduce the phenomenon of wind-up (King *et al.*, 1988), whereas NMDA antagonists can prevent it (Dickenson and Sullivan, 1987; Davies and Lodge, 1987).

Recent evidence suggests the involvement of mGluRs in nociceptive transmission, in accord with immunohistochemical distribution studies showing the presence of Group I mGluRs in layers I and II of the dorsal horn (Vidnyánszky *et al.*, 1994; Valerio *et al.*, 1997b). The potential importance of these receptors was suggested by their role in another sensitization phenomenon, LTP in the hippocampus, and by the facilitation induced by ACPD of AMPA and NMDA responses in dorsal horn neurons of the spinal cord [Bleakman *et al.* (1992); Cerne and Randic (1992); see Fig. 1].

Like NMDA receptor antagonists, the mGluR antagonist MCPG shows a significant inhibition of wind-up (Boxall *et al.*, 1996). Moreover, ACPD enhances wind-up of dorsal horn neurons and this effects is blocked by 4C3HPG, confirming the involvement of Group I mGluRs (Budai and Larson, 1998). Single shock electrical stimulation of the spinal cord dorsal root, sufficient to recruit both A- and C-fibers, is also used to study *in vitro* the response to acute noxious stimulation (Thompson *et al.*, 1992). Unlike the NMDA receptor antagonist AP5, MCPG is able to attenuate the late prolonged component of ventral root potentials (Boxall *et al.*, 1996). The late phase, mostly attributed to C-fiber activation, is defined as 'peptidergic' because it is also affected by neurokinin receptor antagonists (Thompson *et al.*, 1992, 1993) and might therefore involve second messenger systems. The early, monosynaptic component of the response, dependent on AMPA and kainate receptors, is not affected by MCPG or 4CPG (Boxall *et al.*, 1996; Corsi *et al.*, 1997). Figure 4 depicts the effects of MCPG on ventral root potentials after single shock stimulus of the dorsal root and after wind-up evoked by repetitive stimulation.

Excitation of dorsal horn cells induced by the Group I selective agonist DHPG is much greater than that evoked by Groups II and III agonists, suggesting a functional role for Group I mGluRs in this region (Young *et al.*, 1997). Activation of dorsal horn neurons is also produced by cutaneous application of the C-fiber chemical irritant mustard oil that brings about central sensitization of these neurons to afferent input, a process analogous to wind-up. The sensitization induced by mustard oil is inhibited by ionophoretic application of the selective Group I antagonist 4C3HPG (Young *et al.*, 1994, 1995), consistent with the observation that mGluRs are required in the inflammation induced by carrageenan (Neugebauer *et al.*, 1994).

These results suggest that, in addition to NMDA receptors, Group I mGluRs are important in the generation of the spinal cord nociceptive response. Since PKC inhibitors, as well as Ca^{2+}/calmodulin-dependent kinase II inhibitors, also attenuate nociceptive responses, it has been suggested that PKC and possibly Ca^{2+}/calmodulin kinase II play a role in sensitized nociception in the dorsal horn and that Group I mGluRs may be the synaptic mediators involved in triggering these signal transduction pathways. The activation of PKC by mGluRs could play this role via NMDA phosphorylation and enhancement (Young *et al.*, 1997).

Responses of thalamic neurons to noxious thermal somatosensory stimuli are also reduced by local ionophoretic application of Group I mGluR antagonists (Eaton *et al.*, 1993a,b). The effect is selective in that non-noxious vibrissal stimulation is not antagonized (Eaton *et al.*, 1993b). A recent study confirmed these findings using the selective $mGluR_1$ antagonist LY367385, demonstrating for the first time the specific contribution of this subclass of receptors in nociceptive responses (Salt and Turner, 1998). This result is in good agreement with the evidence of the prominent expression of $mGluR_1$ in the thalamus (Masu *et al.*, 1991; Shigemoto *et al.*, 1992; Fotuhi *et al.*, 1993).

Interestingly, as in the thalamus, synaptic responses evoked by innocuous vibrissal stimuli are not affected by MCPG in the rat somatosensory cortex, suggesting that Group I mGluRs in the cortex are also not involved in simple sensory transmission of mechanical stimuli (Cahusac, 1994). Instead, the action of mGluR antagonists seems to be selective for noxious stimuli.

Behavioral studies using the hot-plate model to study the nociceptive reflex show that 4CPG and MCPG injected intracerebroventricularly in mice induce a dose-related increase in paw-licking latency, although NMDA receptor antagonists seem to be more efficacious (Corsi *et al.*, 1997). Similar results were achieved using the more potent mGluR antagonist AIDA (Moroni *et al.*, 1997). Subcutaneous injections of formalin to the plantar surface of the rat hindpaw is a widely used animal model of persistent pain (Coderre *et al.*, 1990). The formalin test produces two phases: an immediate acute nociceptive phase up to 5 min post-injection followed by a prolonged tonic nociceptive response lasting 20–60 min. NMDA receptor antagonists reduce this late phase of nociceptive responses (Coderre and Melzack, 1992; Yamamoto and Yaksh, 1992). Similarly, rats pretreated with the mGluR antagonists 4CPG or 4C3HPG injected intrathecally have reduced nociceptive scores in the second phase of the formalin test, while the agonists DHPG or ACPD enhance these nociceptive responses in a dose-dependent manner (Fisher and Coderre, 1996a). If the antagonists 4C3HPG or MCPG are injected prior to the agonist, the enhancement of formalin-induced nociception is attenuated. Interestingly, the same blocking effect of mGluR-induced enhancement of formalin response can be achieved with the NMDA antagonist AP5, demonstrating the interaction between mGluRs and NMDA in this type of sustained pain (Fisher and Coderre, 1996a).

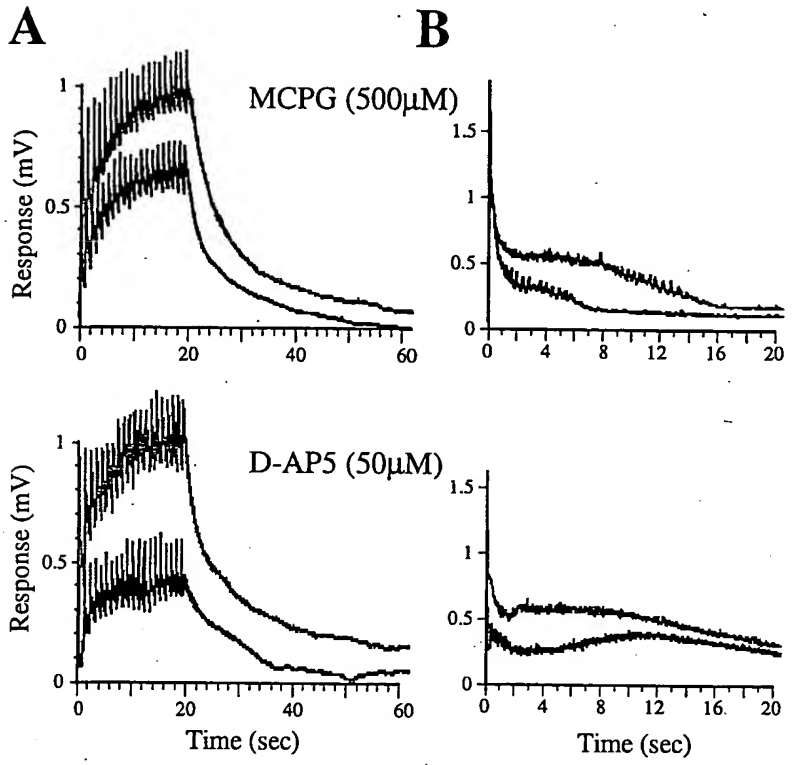

Fig. 4. Effects of D-AP5 (A) or MCPG (B) on high-intensity, single shock electrical stimulation (50 mV, 1 msec) of the dorsal root, and cumulative depolarization ('wind-up') of the ventral root evoked by 20 sec of 1 Hz repetitive electrical stimulation of the L_4/L_5 dorsal root. Traces represent different experiments. D-AP5 (50 μM) or MCPG (500 μM) are perfused for 20 min. They are able to reduce the amplitude of the wind-up or the amplitude of the late phase of the single shock evoked by dorsal root stimulation. Control traces for each experiment are depicted in gray. [reproduced from Corsi *et al.* (1997)].

Injection of DHPG or ACPD induces spontaneous nociceptive behavior which is blocked by Group I mGluR antagonists (Fisher and Coderre, 1996b). To investigate the relative contribution of mGluR1 or mGluR5 in the DHPG-induced responses, antibodies selective for the two receptor subtypes were injected intrathecally in rats. Both antibodies reduced the DHPG-induced nociceptive behavior (Fundytus *et al.*, 1998). Furthermore, both antibodies significantly attenuated hypersensitivity following chronic constriction injury (CCI) of the sciatic nerve but neither was effective in reducing nociceptive responses to acute heat or chemical stimuli (Fundytus *et al.*, 1998), supporting the notion that Group I mGluRs are primarily important in chronic, not acute, pain (Young *et al.*, 1997). Similar results were found using the CCI model with the Group I mGluR antagonist 4CPG used to attenuate chronic nociceptive behaviors (Fisher *et al.*, 1998).

Morphine is commonly used for the management of pain, although in a limited manner due to the development of tolerance and dependence after chronic use. Recent work has demonstrated that NMDA receptor antagonists attenuate the development of tolerance and dependence if co-administered with morphine (Trujillo and Akil, 1991). A study by Fundytus and Coderre (1994) has shown that mGluRs activation, too, is involved in the development of opioid dependence with chronic morphine use, possibly through changes in intracellular messengers such as PI hydrolysis and DAG. Chronic antagonism of Group I mGluRs may act to compensate the increase in PI hydrolysis that is elevated by activation of μ-opioids particularly during withdrawal (Fundytus and Coderre, 1994; Fundytus *et al.*, 1997). Thus, treatments with Group I mGluRs, as well as with agonists of the other mGluR groups (Fundytus and Coderre, 1997), can be very effective in decreasing the incidence of opioid dependence.

In summary, blockade of Group I mGluRs, possibly both $mGluR_1$ and $mGluR_5$, may be a promising new route for treatment of pain, particularly chronic pain disorders (Young *et al.*, 1994, 1997; Neugebauer *et al.*, 1994; Fisher *et al.*, 1998), with minimal effects on normal sensory perception.

5.2. Role of Group I mGluRs in Epilepsy

Glutamate plays a crucial role in epileptogenesis. Overstimulation of iGluRs leads to seizures and excitotoxic injury throughout the CNS and in par-

ticular in the hippocampus, a vulnerable region to injury after seizures (Meldrum, 1994; Bradford, 1995). Glutamate antagonists selective for either NMDA or non-NMDA receptors are potent anticonvulsants in several different models of epilepsy (Patel *et al.*, 1990; Chapman *et al.*, 1991).

The mGluRs are currently under intense investigation to understand their role in epileptogenesis. Early reports showed that ACPD injected in rats or mice induces limbic seizures followed by selective neuronal degeneration (Sacaan and Schoepp, 1992; McDonald *et al.*, 1993; Tizzano *et al.*, 1993). Later studies extended these findings to the specific Group I agonist DHPG. DHPG-induced limbic seizures in mice (Tizzano *et al.*, 1995) and rats (Camón *et al.*, 1998) are not prevented by NMDA or AMPA/kainate receptor antagonists (Tizzano *et al.*, 1995). Both ACPD and DHPG have been suggested to exert their action by a common mechanism, most likely involving Ca^{2+} mobilization subsequent to PI-linked mGluR activation. L-2-amino-3-phosphonopropanoic acid (L-AP3) and dantrolene, inhibitors of mGluR-mediated intracellular calcium mobilization, prevent or attenuate the ACPD or DHPG-induced seizures in mice (Tizzano *et al.*, 1993, 1995).

In the audiogenic-induced convulsion model, the Group I mGluR antagonist 4C3HPG has an anticonvulsant action in mice (Thomsen *et al.*, 1994; Dalby and Thomsen, 1996). Similar suppression effects by 4C3HPG are found in rats that are genetically prone to epilepsy (Tang *et al.*, 1997). Although 4C3HPG is also an agonist for Group II mGluRs, various types of evidence, including the failure by the selective Group II agonist L-CGG-I to induce seizures, suggest that the acute convulsant action is predominantly mediated by antagonism of Group I receptors (Tang *et al.*, 1997).

Recordings of epileptic activities made *in vitro* in hippocampal or neocortical slices confirm the contribution of Group I mGluRs in the production of seizure discharges. Spontaneous epileptiform bursts in guinea pig hippocampal neurons elicited by exposure to the GABA receptor antagonist picrotoxin can be blocked by MCPG (Merlin *et al.*, 1995) or transformed into persistent prolonged discharges by the agonist DHPG (Merlin and Wong, 1997). Group I mGluRs may have a role in initiating the epileptogenesis process, which also requires active protein synthesis (Merlin *et al.*, 1998). In rat neocortical neurons, the GABA antagonist bicuculline induces epileptiform discharges that are suppressed by MCPG, although this antagonist fails to attenuate the ACPD-induced increase of epileptiform activity (Burke and Hablitz, 1995).

Exposure to 4-aminopyridine (4-AP), a blocker of voltage-gated K^+ channels, results in the generation of spontaneous discharges in brain slices that resembles interictal spiking and ictal epileptiform bursts (Rutecki *et al.*, 1987). MCPG selectively prevents the development of these events in the basolateral amygdala, without affecting the maintenance of the ictal discharges or the interictal spiking (Arvanov *et al.*, 1995). The mGluRs appear to be important in the transition from normal neuronal functioning to epileptiform bursting. Whether this effect is mediated by Group I or Group II mGluRs is not yet clear, because MCPG is an antagonist for both groups and in the basolateral amygdala both mGluR1 and mGluR2 are expressed (Ohishi *et al.*, 1993; Shigemoto *et al.*, 1992). However, an action via Group I is more plausible since it is in agreement with the findings obtained both *in vivo* and *in vitro* showing Group I agonist-induced epileptic responses.

A popular model of epilepsy is electrical kindling, a phenomenon in which repeated application of low-intensity stimulation to amygdala or pyriform cortex causes gradual seizure development culminating in generalized motor seizures (Goddard *et al.*, 1969). Kindling, too, is blocked by injection of NMDA receptor antagonists (Croucher *et al.*, 1988; McNamara, 1988). There is accumulating evidence for a crucial role of presynaptic Groups II and III mGluR in this model (Attwell *et al.*, 1995; Suzuki *et al.*, 1996; Neugebauer *et al.*, 1997), but an involvement of postsynaptic Group I antagonists is not excluded (Suzuki *et al.*, 1996). Change in $mGluR_1$ and $mGluR_5$ mRNAs is seen in the hippocampus of amygdala-kindled rats (Akbar *et al.*, 1996), and alterations of both Groups I and II mGluRs-mediated responses are found in amygdala neurons of kindled animals. Upregulation of Group I may contribute to the transition to epileptiform bursting in kindled cells (Holmes *et al.*, 1996). Activation of Group I mGluRs should be effective in modulating epileptic activity considering the exaggerated Ca^{2+} entry into kindled slices (Heinemann and Hamon, 1986). Blocking intracellular Ca^{2+} via Group I mGluR antagonism may interrupt the increased excitatory response of the epileptic neuron (Bradford, 1995), but this hypothesis awaits future studies and more specific mGluR agents.

5.3. Role of Group I mGluRs in Neurodegeneration

5.3.1. *Brain Ischemia*

Since glutamate plays a key role in ischemic brain damage, drugs that decrease the accumulation of glutamate or block its postsynaptic effects are associated with the amelioration of ischemic injury and should be regarded as potential therapeutic agents for stroke (Simon *et al.*, 1984; Rothman and Olney, 1986). NMDA receptors in particular have attracted the attention of researchers because they gate an ion channel permeable to Ca^{2+} and glutamate-induced neurotoxicity is mainly dependent on the intracellular accumulation of Ca^{2+} (Choi, 1988, 1995). Recent evidence has demonstrated that mGluRs, too, may play an important role in excitotoxicity [Nicoletti *et al.* (1996) for a review].

Quisqualate, DHPG or *t*-ADA amplify the exitotoxic neuronal degeneration induced by NMDA in cultured murine cortical cells (Bruno *et al.*, 1995a; Strasser *et al.*, 1998), suggesting that Group I mGluRs enhance NMDA receptor-mediated neuronal toxicity. The relief of Mg^{2+} blockade of NMDA channels by PKC has been proposed to be the principal process by which activation of Group I mGluRs amplifies NMDA toxicity (Bruno *et al.*, 1995a).

A neuroprotective effect against NMDA-mediated damage has been observed both by blocking Group I mGluRs (Buisson and Choi, 1995; Orlando *et al.*, 1995; Strasser *et al.*, 1998) and by activating Groups II and III mGluRs (Bruno *et al.*, 1994, 1995b; Buisson *et al.*, 1996). These results are in agreement with earlier experimental evidence of mixed effects using the non-selective mGluR agonist ACPD. This compound protects cultured neurons against excitotoxic degeneration and ischemic damage *in vivo* (Koh *et al.*, 1991; Chiamulera *et al.*, 1992; Siliprandi *et al.*, 1992; Pizzi *et al.*, 1993), but also produces neurotoxic effects when infused into the striatum or the hippocampus (Sacaan *et al.*, 1991; McDonald and Schoepp, 1992; Schoepp *et al.*, 1995). The neuroprotective action of ACPD is probably mediated by activation of presynaptic Groups II or III mGluRs (Bruno *et al.*, 1995b), whereas neuronal toxicity is mediated by Group I mGluRs.

Neurons in hippocampal CA1, a region known to be highly vulnerable to cerebral ischemia (Pulsinelli, 1985), are protected by MCPG from a hypoxic-hypoglycimic injury measured in slices electrophysiologically (Opitz *et al.*, 1994). A follow-up study using a variety of selective mGluR agents has shown that in this *in vitro* model of hypoxia, activation of Group I mGluR antagonism is beneficial if it happens before or during the insult (Opitz *et al.*, 1995). MCPG also attenuates the hypoxia-induced suppression of excitatory synaptic transmission in dentate gyrus neurons *in vitro* (Doherty and Dingledine, 1997).

A widely used model of global ischemia, a type of injury that typically occurs following cardiac arrest in humans, is the transient or permanent forebrain ischemia in gerbils produced by an occlusion of the carotid arteries (Araki *et al.*, 1989). The antagonist 4C3HPG protects CA1 pyramidal neurons when applied 20 min before permanent occlusion of the carotid arteries (Henrich-Noack *et al.*, 1998). As previously mentioned, 4C3HPG is also an agonist for Group II mGluRs, therefore the neuroprotective action could be due to activation of these receptors, or to a synergistic effect of both blocking Group I mGluRs and activating Group II mGluRs, as suggested by the authors (Henrich-Noack *et al.*, 1998). A role for Group II mGluRs in the gerbil model of global ischemia was partially confirmed with the specific $mGluR_2$ agonist (1*S*,2*S*,5*R*,6*S*)-2-aminobicyclo[3.1.0]hexane-2,6-dicarboxylate (LY354740) (Bond *et al.*, 1998). In this study damage of CA1 cells induced by transient occlusion of the carotid arteries was reduced by LY354740. By increasing the severity of the ischemic insults, however, the neuroprotective effects were greatly reduced or disappeared.

Increased glutamate activation has been also implicated in another acute neurodegenerative disease, posttraumatic injury (Hayes *et al.*, 1988; Faden *et al.*, 1989). Pharmacological blockade of Group I mGluRs reduces neurological deficits produced by traumatic brain injury (Gong *et al.*, 1995), whereas activation of these receptors with DHPG exacerbates posttraumatic neuronal death in an *in vitro* model of cortical trauma (Mukhin *et al.*, 1996, 1997). In addition, an $mGluR_1$, but not $mGluR_5$, antisense oligodeoxynucleotide is neuroprotective in this experimental model.

Oxidative stress represents an important pathway leading to neuronal degeneration which can interact with excessive glutamate activation to cause damage to brain tissue, including stroke, hypoxia, and trauma (Coyle and Puttfarcken, 1993). Recent data have shown that activation of Group I mGluRs in a hippocampal cell line generates a cellular response that is protective to oxidative stress caused by cysteine-deprivation or glucose starvation (Sagara and Schubert, 1998). In line with these results, $mGluR_5$ activation of cultured cerebellar granule cells also protects against apoptotic death (Copani *et al.*, 1995, 1998). The development of apoptosis was accelerated after treatment with either $mGluR_5$ antisense oligonucleotides or with the Group I mGluR antagonist MCPG. Interestingly, the functions of $mGluR_5$ in astrocytes support a role for these receptors in repair processes of injured CNS tissue (Balázs *et al.*, 1997). Programmed cell death or apoptosis can also occur in response to ischemia, or trauma, situations in which most cells die by necrosis as a result of acute injury. If injured cells do not die immediately, they may die by apoptosis (Raff *et al.*, 1993for a review). Group I mGluRs, particularly $mGluR_5$, may contribute to the development of delayed death.

In summary, it appears that antagonism of Group I mGluRs, and particularly of $mGluR_1$, might be protective following brain ischemia and other forms of acute neuronal degenerative diseases like hypoxia/hypoglycemia (Opitz *et al.*; 1995) or traumatic brain injury (Mukhin *et al.*, 1996). Although lack of selectivity or brain penetration of the available compounds make it difficult to draw definite conclusions, it is already promising that blockade of mGluRs are effective in reducing neuronal damage after global ischemia, where NMDA receptor antagonists fail to do so (Buchan *et al.*, 1991; Rothman and Olney, 1995).

5.3.2. *Huntington's and Parkinson's Diseases*

Recently excitotoxicity has been proposed as participating in the pathogenesis of chronic neurodegenerative disorders such as Huntington's disease or Parkinson's disease (Albin and Greenamyre, 1992; Greenamyre and Porter, 1994; Blandini *et al.*, 1996). Consistent with this hypothesis, NMDA antagonists can attenuate the 1-methyl-4-phenyl-1,2,3,6-tetrahydropyridine (MPTP)-induced destruction of nigrostriatal neurons, a well known experimental model of Parkinson's disease (Turski *et al.*, 1991), and the NMDA receptor agonist, quinolinic acid, when injected into the striatum, causes lesions resembling the neuropathological features of Huntington's disease (Beal *et al.*, 1986).

The mGluR agonist ACPD injected in the striatum produces excitotoxicity (Sacaan *et al.*, 1991) and in the quinolinic acid model, the mixed Group I mGluR antagonist–Group II agonist 4C3HPG shows a protective action, similar to that produced by NMDA antagonists (Orlando *et al.*, 1995). In Parkinson's disease the degeneration of the dopaminergic neuronal system that projects from the

substantia nigra to the striatum is thought to lead to symptoms of the disease [Chase *et al.* (1998) for a review]. In the striatum, Sacaan *et al.* (1992) have demonstrated a functional interaction between DA and mGluRs. When ACPD was injected into the rat striatum, it induced extrapyramidal motor activation that was dependent on an intact DA system. Kearney *et al.* (1997) confirmed these results with the selective Group I agonist DHPG. Injections of ACPD or DHPG also activate the subthalamic nucleus, which provides excitatory input to the basal ganglia and influences locomotion and control of voluntary movements (Abbott *et al.*, 1997). Since overactivity of this nucleus is a major feature of Parkinson's disease (Albin *et al.*, 1989), Group I mGluR antagonists may provide a treatment for Parkinson's disease (Kearney *et al.*, 1997).

In the nucleus accumbens, an area in ventral striatum implicated in the limbic–motor interface [see Amalric *et al.* (1994) for a review], Group I mGluRs play an important role in the regulation of locomotor activity by interacting with dopaminergic neurotransmission (Attarian and Amalric, 1997; Kim and Vezina, 1997, 1998a). Recent findings have extended the contribution of Group I mGluRs in the nucleus accumbens to amphetamine-induced locomotion, suggesting a possible role for these receptors in the expression of sensitization behaviors induced by psychostimulant drugs (Kim and Vezina, 1998a,b).

Although research concerning the involvement of mGluRs in extrapyramidal motor disorders is still in its infancy, this beginning is surely very encouraging and in the next few years we can expect a great deal of progress in this area.

5.3.3. *Alzheimer's Disease*

The glutamatergic hypothesis of dementia was proposed in the late 1980s (Greenamyre *et al.*, 1988). According to this view, excitotoxicity participates in the pathogenesis of Alzheimer's disease (Greenamyre and Young, 1989; Choi, 1992). Interestingly, the β amyloid protein that accumulates in Alzheimer's disease can potentiate excitotoxic degeneration (Mattson *et al.*, 1992).

Stimulation of $mGluR_{1a}$ in human embryonic kidney (HEK) 293 cells accelerates the breakdown of the amyloid precursor protein (APP) into non-amyloidogenic soluble forms of APPs, thus reducing β amyloid formation (Lee *et al.*, 1995). A similar effect is seen when cultured hippocampal neurons are stimulated with glutamate, quisqualate, or *trans*-ACPD. The effect is blocked by a PKC inhibitor and is mGluR-selective because iGluR agonists do not affect APPs degradation.

Agonists of Group I mGluRs might therefore represent a new class of therapeutic agents for Alzheimer's disease (Lee *et al.*, 1996). Furthermore, the involvement of Group I mGluRs in synaptic plasticity, such as LTP and learning and memory (see earlier), could lead to the development of specific agents that might modulate hippocampal functions to enhance cognitive functions in patients afflicted by dementia. Drugs acting on mGluRs might also show better results in clinical trials or exhibit fewer side-effects than agents which block or modulate NMDA receptors [see Kornbuber and Wiltfang (1998) for a review].

5.4. Role of Group I mGluRs in Psychiatry Disorders

There are a number of clinical and animal laboratory reports suggesting an involvement of glutamate in psychiatric disorders. Indeed, glutamatergic abnormalities have been associated with schizophrenia (Bunney *et al.*, 1995; Olney and Farber, 1995) and mood disorders (Trullas and Skolnick, 1990; Skolnick *et al.*, 1996).

Recent evidence has demonstrated that treatment with the antidepressant imipramine can modify the sensitivity of Group I mGluRs, as measured by population spikes recorded in the CA1 region of the rat hippocampus (Pilc *et al.*, 1998). Modification of Group I mGluRs may thus play a role in the mechanism of action of certain antidepressants.

The mGluRs can represent an alternative, non-dopaminergic therapy for the treatment of schizophrenia, as suggested by Moghaddam and Adams (1998) who found that a Group II specific mGluR agonist inhibiting glutamate release by modulating presynaptic sites, reversed the behavioral disruptions in the phenyclidine model of schizophrenia.

Future studies will show whether Group I postsynaptic mGluR antagonists also play a role in relieving schizophrenic symptoms. In general, mGluRs may provide important pharmacological therapeutic targets for psychiatric disorders in which glutamatergic neurotransmission is abnormally regulated. The metabotropic receptors have a clear advantage over the iGluRs which are ubiquitous and mediate fast synaptic transmission throughout the CNS (Moghaddam and Adams, 1998).

6. CONCLUSIONS

Our understanding of the functions of mGluRs in the brain has progressed in recent years at an exceptional pace. The study of mGluRs may be the fastest growing area of all neurotransmitter receptors. In particular, Group I mGluRs have been extensively investigated at the molecular, cellular, and behavioral level leading us to an appreciation of their great importance in the CNS.

Both $mGluR_1$ and $mGluR_5$ have been linked to a variety of brain disorders, including epilepsy, pain, ischemia and chronic neurodegenerative disorders. The role of Group I mGluRs in modulating glutamatergic neurotransmission and their selective presence in the CNS may provide a potential important therapeutic approach in many CNS disorders. iGluR treatment, on the other hand, had demonstrated in clinical trials to be associated with multiple side-effects possibly due to their ubiquity throughout the CNS and their fast excitatory properties.

Progress in developing drugs specific for the different mGluR classes requires, however, more selective and potent antagonists and agonists. With more compounds available, the next few years

should witness major advances in this area, adding to our understanding of mGluR functions in the brain and in the discovery of new agents for the treatment of neurological and psychiatric disorders.

Acknowledgements—The authors thank Professor E. Frank (Neurobiology, University of Pittsburgh, USA) and Dr M. Corsi for critical reading of earlier versions of the manuscript.

REFERENCES

Aanonsen, L. M., Lei, S. and Wilcox, G. L. (1990) Excitatory amino acid receptors and nociceptive neurotransmission in rat spinal cord. *Pain* **41**, 309–321.

Abbott, A., Wigmore, M. A. and Lacey, M. G. (1997) Excitation of rat subthalamic nucleus neurones in vitro by activation of a group I metabotropic glutamate receptor. *Brain Res.* **766**, 162–167.

Abe, T., Sugihara, H., Nawa, H., Shigemoto, R., Mizuno, N. and Nakanishi, S. (1992) Molecular characterization of a novel metabotropic glutamate receptor mGluR5 coupled to inositol phosphate/Ca2+ signal transduction. *J. Biol. Chem.* **267**, 13361–13368.

Aiba, A., Chen, C., Herrup, K., Rosenmund, C., Stevens, C. F. and Tonegawa, S. (1994a) Reduced hippocampal long-term potentiation and context-specific deficit in associative learning in mGluR1 mutant mice. *Cell* **79**, 365–375.

Aiba, A., Kano, M., Chen, C., Stanton, M. E., Fox, G. D., Herrup, K., Zwingman, T. A. and Tonegawa, S. (1994b) Deficient cerebellar long-term depression and impaired motor learning in mGluR1 mutant mice. *Cell* **79**, 377–388.

Akbar, M. T., Rattray, M., Powell, J. F. and Meldrum, B. S. (1996) Altered expression of group I metabotropic glutamate receptors in the hippocampus of amygdala-kindled rats. *Brain Res. Mol Brain Res.* **43**, 105–116.

Albin, R. L. and Greenamyre, J. T. (1992) Alternative excitotoxic hypotheses. *Neurology* **42**, 733–738.

Albin, R. L., Young, A. B. and Penney, J. B. (1989) The functional anatomy of basal ganglia disorders. *Trends Neurosci.* **12**, 366–375.

Amalric, M., Ouagazzal, A., Baunez, C. and Nieoullon, A. (1994) Functional interactions between glutamate and dopamine in the rat striatum. *Neurochem. Int.* **25**, 123–131.

Anikstejn, L., Otani, S. and Ben-Ari, Y. (1992) Quisqualate metabotropic receptors modulate NMDA currents and facilitate induction of long-term potentiation through protein kinase C. *Eur. J. Neurosci.* **4**, 500–504.

Annoura, H., Fukunaga, A., Uesugi, M., Tatsuoka, T. and Horikawa, Y. (1996) A novel class of antagonists for metabotropic glutamate receptors, 7-(hydroxyimino)-cyclopropa[b]chromen-1a-carboxylates. *Bioorg. Med. Chem. Lett.* **6**, 763–766.

Anwyl, R. (1991) The role of the metabotropic receptor in synaptic plasticity. *Trends Pharmac. Sci.* **12**, 324–326.

Araki, T., Kato, H. and Kogure, K. (1989) Selective neuronal vulnerability following transient cerebral ischemia in the gerbil: distribution and time course. *Acta Neurol. Scand.* **80**, 548–553.

Aramori, I. and Nakanishi, S. (1992) Signal transduction and pharmacological characteristics of a metabotropic glutamate receptor, mGluR1, in transfected CHO cells. *Neuron* **8**, 757–765.

Arvanov, V. L., Holmes, K. H., Keele, N. B. and Shinnick-Gallagher, P. (1995) The functional role of metabotropic glutamate receptors in epileptiform activity induced by 4-aminopyridine in the rat amygdala slice. *Brain Res.* **669**, 140–144.

Attarian, S. and Amalric, M. (1997) Microinfusion of the metabotropic glutamate receptor agonist 1S,3R-1-aminocyclopentane-1,3-dicarboxylic acid into the nucleus accumbens induces dopamine-dependent locomotor activation in the rat. *Eur. J. Neurosci.* **9**, 809–816.

Attwell, P. J., Kaura, S., Sigala, G., Bradford, H. F., Croucher, M. J., Jane, D. E. and Watkins, J. C. (1995) Blockade of both epileptogenesis and glutamate release by (1S,3S)-ACPD, a presynaptic glutamate receptor agonist. *Brain Res.* **698**, 155–162.

Balázs, R., Miller, S., Romano, C., de Vries, A., Chun, Y. and Cotman, C. W. (1997) Metabotropic glutamate receptor mGluR5 in astrocytes: pharmacological properties and agonist regulation. *J. Neurochem.* **69**, 151–163.

Balázs, R., Miller, S., Chun, Y., O'Toole, J. and Cotman, C. W. (1998) Metabotropic glutamate receptor agonists potentiate cyclic AMP formation induced by forskolin or beta-adrenergic receptor activation in cerebral cortical astrocytes in culture. *J. Neurochem.* **70**, 2446–2458.

Balschun, D. and Wetzel, W. (1998) Inhibition of group I metabotropic glutamate receptors blocks spatial learning in rats. *Neurosci. Lett.* **249**, 41–44.

Baranauskas, G. and Nistri, A. (1998) Sensitization of pain pathways in the spinal cord: cellular mechanisms. *Progr. Neurobiol.* **54**, 349–365.

Bashir, Z. I., Bortolotto, Z. A., Davies, C. H., Berretta, N., Irving, A. J., Seal, A. J., Henley, J. M., Jane, D. E., Watkins, J. C. and Collingridge, G. L. (1993) Induction of LTP in the hippocampus needs synaptic activation of glutamate metabotropic receptors. *Nature* **363**, 347–350.

Baskys, A. and Malenka, R. C. (1991) Agonists at metabotropic glutamate receptors presynaptically inhibit EPSCs in neonatal rat hippocampus. *J. Physiol. (Lond.)* **444**, 687–701.

Batchelor, A. M., Madge, D. J. and Garthwaite, J. (1994) Synaptic activation of metabotropic glutamate receptors in the parallel fibre-Purkinje cell pathway in rat cerebellar slices. *Neuroscience* **63**, 911–915.

Batchelor, A. M., Knopfel, T., Gasparini, F. and Garthwaite, J. (1997) Pharmacological characterization of synaptic transmission through mGluRs in rat cerebellar slices. *Neuropharmacology* **36**, 401–403.

Battaglia, G. and Rustioni, A. (1988) Coexistence of glutamate and substance P in dorsal root ganglion neurons of the rat and monkey. *J. Comp. Neurol.* **277**, 302–312.

Baude, A., Nusser, Z., Roberts, J. D., Mulvihill, E., McIlhinney, R. A. and Somogyi, P. (1993) The metabotropic glutamate receptor (mGluR1 alpha) is concentrated at perisynaptic membrane of neuronal subpopulations as detected by immunogold reaction. *Neuron* **11**, 771–787.

Beal, M. F., Kowall, N. W., Ellison, D. W., Mazurek, M. F., Swartz, K. J. and Martin, J. B. (1986) Replication of the neurochemical characteristics of Huntington's disease by quinolinic acid. *Nature* **321**, 168–171.

Bear, M. F. and Malenka, R. C. (1994) Synaptic plasticity: LTP and LTD. *Curr. Opin. Neurobiol.* **4**, 389–399.

Ben-Ari, Y. and Aniksztejn, L. (1995) Role of glutamate metabotropic receptors in long-term potentiation in the hippocampus. *Semin. Neurosci.* **7**, 127–135.

Besson, J. M. and Chaouch, A. (1987) Peripheral and spinal mechanisms of nociception. *Physiol. Rev.* **67**, 67–186.

Birse, E. F., Eaton, S. A., Jane, D. E., Jones, P. L., Porter, R. H., Pook, P. C., Sunter, D. C., Udvarhelyi, P. M., Wharton, B. and Roberts, P. J. *et al.* (1993) Phenylglycine derivatives as new pharmacological tools for investigating the role of metabotropic glutamate receptors in the central nervous system. *Neuroscience* **52**, 481–488.

Blandini, F., Porter, R. H. and Greenamyre, J. T. (1996) Glutamate and Parkinson's disease. *Mol. Neurobiol.* **12**, 73–94.

Bleakman, D., Rusin, K. I., Chard, P. S., Glaum, S. R. and Miller, R. J. (1992) Metabotropic glutamate receptors potentiate ionotropic glutamate responses in the rat dorsal horn. *Mol. Pharmac.* **42**, 192–196.

Bliss, T. V. and Lømo, T. (1973) Long-lasting potentiation of synaptic transmission in the dentate area of the anaesthetized rabbit following stimulation of the perforant path. *J. Physiol. (Lond.)* **232**, 331–356.

Bliss, T. V. P. and Collingridge, G. L. (1993) A synaptic model of memory: long-term potentiation in the hippocampus. *Nature* **361**, 31–39.

Blümcke, I., Behle, K., Malitschek, B., Kuhn, R., Knopfel, T., Wolf, H. K. and Wiestler, O. D. (1996) Immunohistochemical distribution of metabotropic glutamate receptor subtypes mGluR1b, mGluR2/3, mGluR4a and mGluR5 in human hippocampus. *Brain Res.* **736**, 217–226.

Bolshakov, V. Y. and Siegelbaum, S. A. (1994) Postsynaptic induction and presynaptic expression of hippocampal long-term depression. *Science* **264**, 1148–1152.

Bond, A. and Lodge, D. (1995) Pharmacology of metabotropic glutamate receptor-mediated enhancement of responses to excitatory and inhibitory amino acids on rat spinal neurones in vivo. *Neuropharmacology* **34**, 1015–1023.

Bond, A., O'Neill, M. J., Hicks, C. A., Monn, J. A. and Lodge, D. (1998) Neuroprotective effects of a systemically active group II metabotropic glutamate receptor agonist LY354740 in a gerbil model of global ischaemia. *Neuroreport* **9**, 1191–1193.

Bordi, F. (1996) Reduced long-term potentiation in the dentate gyrus of mGlu1 receptor-mutant mice in vivo. *Eur. J. Pharmac.* **301**, R15–R16.

Bordi, F. and Ugolini, A. (1995) Antagonists of the metabotropic glutamate receptor do not prevent induction of long-term potentiation in the dentate gyrus of rats. *Eur. J. Pharmac.* **273**, 291–294.

Bordi, F., Marcon, C., Chiamulera, C. and Reggiani, A. (1996) Effects of the metabotropic glutamate receptor antagonist MCPG on spatial and context-specific learning. *Neuropharmacology* **35**, 1557–1565.

Bordi, F., Reggiani, A. and Conquet, F. (1997) Regulation of synaptic plasticity by mGluR1 studied in vivo in mGluR1 mutant mice. *Brain Res.* **761**, 121–126.

Bortolotto, Z. A. and Collingridge, G. L. (1993) Characterisation of LTP induced by the activation of glutamate metabotropic receptors in area CA1 of the hippocampus. *Neuropharmacology* **32**, 1–9.

Bortolotto, Z. A. and Collingridge, G. L. (1995) On the mechanism of long-term potentiation induced by (1S,3R)-1-aminocyclopentane-1,3-dicarboxylic acid (ACPD) in rat hippocampal slices. *Neuropharmacology* **34**, 1003–1014.

Bortolotto, Z. A., Bashir, Z. I., Davies, C. H. and Collingridge, G. L. (1994) A molecular switch activated by metabotropic glutamate receptors regulates induction of long-term potentiation. *Nature* **368**, 740–743.

Bortolotto, Z. A., Bashir, Z. I., Davies, C. H., Taira, T., Kaila, K. and Collingridge, G. L. (1995) Studies on the role of metabotropic glutamate receptors in long-term potentiation: some methodological considerations. *J. Neurosci. Meth.* **59**, 19–24.

Boxall, S. J., Thompson, S. W., Dray, A., Dickenson, A. H. and Urban, L. (1996) Metabotropic glutamate receptor activation contributes to nociceptive reflex activity in the rat spinal cord in vitro. *Neuroscience* **74**, 13–20.

Brabet, I., Mary, S., Bockaert, J. and Pin, J. P. (1995) Phenylglycine derivatives discriminate between mGluR1- and mGluR5-mediated responses. *Neuropharmacology* **34**, 895–903.

Bradford, H. F. (1995) Glutamate, GABA and epilepsy. *Progr. Neurobiol.* **47**, 477–511.

Breakwell, N. A., Rowan, M. J. and Anwyl, R. (1996) Metabotropic glutamate receptor dependent EPSP and EPSP-spike potentiation in area CA1 of the submerged rat hippocampal slice. *J. Neurophysiol.* **76**, 3126–3135.

Bruno, V., Copani, A., Battaglia, G., Raffaele, R., Shinozaki, H. and Nicoletti, F. (1994) Protective effect of the metabotropic glutamate receptor agonist, DCG-IV, against excitotoxic neuronal death. *Eur. J. Pharmac.* **256**, 109–112.

Bruno, V., Battaglia, G., Copani, A., Giffard, R. G., Raciti, G., Raffaele, R., Shinozaki, H. and Nicoletti, F. (1995a) Activation of class II or III metabotropic glutamate receptors protects cultured cortical neurons against excitotoxic degeneration. *Eur. J. Neurosci.* **7**, 1906–1913.

Bruno, V., Copani, A., Knopfel, T., Kuhn, R., Casabona, G., Dell'Albani, P., Condorelli, D. F. and Nicoletti, F. (1995b) Activation of metabotropic glutamate receptors coupled to inositol phospholipid hydrolysis amplifies NMDA-induced neuronal degeneration in cultured cortical cells. *Neuropharmacology* **34**, 1089–1098.

Buchan, A., Li, H. and Pulsinelli, W. A. (1991) The N-methyl-D-aspartate antagonist, MK-801, fails to protect against neuronal damage caused by transient, severe forebrain ischemia in adult rats. *J. Neurosci.* **11**, 1049–1056.

Buckmaster, P. S. and Schwartzkroin, P. A. (1995) Interneurons and inhibition in the dentate gyrus of the rat in vivo. *J. Neurosci.* **15**, 774–789.

Budai, D. and Larson, A. A. (1998) The involvement of metabotropic glutamate receptors in sensory transmission in dorsal horn of the rat spinal cord. *Neuroscience* **83**, 571–580.

Budd, D. C. and Nicholls, D. G. (1998) Arachidonic acid potentiates the duration of the metabotropic, protein kinase C-mediated, suppression of the inhibitory adenosine A1 receptor pathway in glutamatergic nerve terminals from rat cerebral cortex [In Process Citation]. *Neurosci. Lett.* **244**, 133–136.

Buisson, A. and Choi, D. W. (1995) The inhibitory mGluR agonist, S-4-carboxy-3-hydroxy-phenylglycine selectively attenuates NMDA neurotoxicity and oxygen-glucose deprivation-induced neuronal death. *Neuropharmacology* **34**, 1081–1087.

Buisson, A., Yu, S. P. and Choi, D. W. (1996) DCG-IV selectively attenuates rapidly triggered NMDA-induced neurotoxicity in cortical neurons. *Eur J. Neurosci.* **8**, 138–143.

Bunney, B. G., Bunney, W. E. and Carlsson, A. (1995) Schizophrenia and Glutamate. In: *Psychopharmacology: The Fourth Generation of Progress*, pp. 1205–1214. Eds. F. E. Bloom and D. J. Kupfer. Raven Press, New York.

Burke, J. P. and Hablitz, J. J. (1994) Presynaptic depression of synaptic transmission mediated by activation of metabotropic glutamate receptors in rat neocortex. *J. Neurosci.* **14**, 5120–5130.

Burke, J. P. and Hablitz, J. J. (1995) Modulation of epileptiform activity by metabotropic glutamate receptors in immature rat neocortex. *J. Neurophysiol.* **73**, 205–217.

Burke, J. P. and Hablitz, J. J. (1996) G-protein activation by metabotropic glutamate receptors reduces spike frequency adaptation in neocortical neurons. *Neuroscience* **75**, 123–131.

Cahusac, P. M. (1994) Cortical layer-specific effects of the metabotropic glutamate receptor agonist 1S,3R-ACPD in rat primary somatosensory cortex in vivo. *Eur J. Neurosci.* **6**, 1505–1511.

Calabresi, P., Mercuri, N. B. and Bernardi, G. (1992) Activation of quisqualate metabotropic receptors reduces glutamate and GABA-mediated synaptic potentials in the rat striatum. *Neurosci. Lett.* **139**, 41–44.

Camòn, L., Vives, P., de Vera, N. and Martinez, E. (1998) Seizures and neuronal damage induced in the rat by activation of group I metabotropic glutamate receptors with their selective agonist 3,5-dihydroxyphenylglycine. *J. Neurosci. Res* **51**, 339–348.

Carmant, L., Woodhall, G., Ouardouz, M., Robitaille, R. and Lacaille, J. C. (1997) Interneuron-specific Ca2+ responses linked to metabotropic and ionotropic glutamate receptors in rat hippocampal slices. *Eur. J. Neurosci.* **9**, 1625–1635.

Cerne, R. and Randic, M. (1992) Modulation of AMPA and NMDA responses in rat spinal dorsal horn neurons by trans-1-aminocyclopentane-1,3-dicarboxylic acid. *Neurosci. Lett.* **144**, 180–184.

Chapman, A. G., Smith, S. E. and Meldrum, B. S. (1991) The anticonvulsant effect of the non-NMDA antagonists, NBQX and GYKI 52466, in mice. *Epilepsy Res.* **9**, 92–96.

Charpak, S., Gahwiler, B. H., Do, K. Q. and Knopfel, T. (1990) Potassium conductances in hippocampal neurons blocked by excitatory amino-acid transmitters. *Nature* **347**, 765–767.

Chase, T. N., Oh, J. D. and Blanchet, P. J. (1998) Neostriatal mechanisms in Parkinson's disease. *Neurology* **51**, S30–S35.

Chavis, P., Fagni, L., Bockaert, J. and Lansman, J. B. (1995) Modulation of calcium channels by metabotropic glutamate receptors in cerebellar granule cells. *Neuropharmacology* **34**, 929–937.

Chavis, P., Fagni, L., Lansman, J. B. and Bockaert, J. (1996) Functional coupling between ryanodine receptors and L-type calcium channels in neurons. *Nature* **382**, 719–722.

Chiamulera, C., Albertini, P., Valerio, E. and Reggiani, A. (1992) Activation of metabotropic receptors has a neuroprotective effect in a rodent model of focal ischaemia. *Eur. J. Pharmac.* **216**, 335–336.

Chinestra, P., Aniksztejn, L., Diabira, D. and Ben-Ari, Y. (1993) (RS)-alpha-methyl-4-carboxyphenylglycine neither prevents induction of LTP nor antagonizes metabotropic glutamate receptors in CA1 hippocampal neurons. *J. Neurophysiol.* **70**, 2684–2689.

Choi, D. W. (1988) Calcium-mediated neurotoxicity: relationship to specific channel types and role in ischemic damage. *Trends Neurosci.* **11**, 465–469.

Choi, D. W. (1992) Bench to bedside: the glutamate connection. *Science* **258**, 241–243.

Choi, D. W. (1995) Calcium: still center-stage in hypoxic-ischemic neuronal death. *Trends Neurosci.* **18**, 58–60.

Choi, S. and Lovinger, D. M. (1996) Metabotropic glutamate receptor modulation of voltage-gated Ca2+ channels involves multiple receptor subtypes in cortical neurons. *J. Neurosci.* **16**, 36–45.

Chu, Z. and Hablitz, J. J. (1998) Activation of group I mGluRs increases spontaneous IPSC frequency in rat frontal cortex. *J. Neurophysiol.* **80**, 621–627.

Clark, B. P., Baker, S. R., Goldsworthy, J., Harris, J. R. and Kingston, A. E. (1997) (+)-2-Methyl-4-carboxyphenylglycine (LY367385) selectively antagonises glutamate mGluR1 receptors. *Bioorg. Med. Chem. Lett.* **7**, 2777–2780.

Coderre, T. J. and Melzack, R. (1992) The contribution of excitatory amino acids to central sensitization and persistent nociception after formalin-induced tissue injury. *J. Neurosci.* **12**, 3665–3670.

Coderre, T. J., Vaccarino, A. L. and Melzack, R. (1990) Central nervous system plasticity in the tonic pain response to subcutaneous formalin injection. *Brain Res.* **535**, 155–158.

Colwell, C. S. and Levine, M. S. (1994) Metabotropic glutamate receptors modulate N-methyl-D-aspartate receptor function in neostriatal neurons. *Neuroscience* **61**, 497–507.

Congar, P., Leinekugel, X., Ben-Ari, Y. and Crépel, V. (1997) A long-lasting calcium-activated nonselective cationic current is generated by synaptic stimulation or exogenous activation of group I metabotropic glutamate receptors in CA1 pyramidal neurons. *J. Neurosci.* **17**, 5366–5379.

Conn, P. J. and Pin, J. P. (1997) Pharmacology and functions of metabotropic glutamate receptors. *A. Rev. Pharmac. Toxic.* **37**, 205–237.

Conquet, F., Bashir, Z. I., Davies, C. H., Daniel, H., Ferraguti, F., Bordi, F., Franz-Bacon, K., Reggiani, A., Matarese, V., Condé, F., Collingridge, G. L., Crépel, F. (1994) Motor deficit and impairment of synaptic plasticity in mice lacking mGluR1. *Nature* **372**, 237–243.

Copani, A., Bruno, V. M., Barresi, V., Battaglia, G., Condorelli, D. F. and Nicoletti, F. (1995) Activation of metabotropic glutamate receptors prevents neuronal apoptosis in culture. *J. Neurochem.* **64**, 101–108.

Copani, A., Casabona, G., Bruno, V., Caruso, A., Condorelli, D. F., Messina, A., Di Giorgi Gerevini, V., Pin, J. P., Kuhn, R., Knopfel, T., Nicoletti, F. (1998) The metabotropic glutamate receptor mGlu5 controls the onset of developmental apoptosis in cultured cerebellar neurons [In Process Citation]. *Eur J. Neurosci.* **10**, 2173–2184.

Corsi, M., Ugolini, A., Quartaroli, M., Chiamulera, C., Corti, C., Maraia, G., Conquet, F. and Ferraguti, F. (1997) Phospholipase C-coupled metabotropic glutamate receptors modulate nociceptive transmission. In: *Metabotropic Glutamate Receptors and Brain Functions*, pp. 37–48. Eds. F. Moroni, F. Nicoletti and D. E. Pellegrini-Giampietro. Portland Press, London.

Coyle, J. T. and Puttfarcken, P. (1993) Oxidative stress, glutamate, and neurodegenerative disorders. *Science* **262**, 689–695.

Crépel, V., Aniksztejn, L., Ben-Ari, Y. and Hammond, C. (1994) Glutamate metabotropic receptors increase a Ca(2+)-activated nonspecific cationic current in CA1 hippocampal neurons. *J. Neurophysiol.* **72**, 1561–1569.

Croucher, M. J., Bradford, H. F., Sunter, D. C. and Watkins, J. C. (1988) Inhibition of the development of electrical kindling of the prepyriform cortex by daily focal injections of excitatory amino acid antagonists. *Eur. J. Pharmac.* **152**, 29–38.

Dalby, N. O. and Thomsen, C. (1996) Modulation of seizure activity in mice by metabotropic glutamate receptor ligands. *J. Pharmac. exp. Ther.* **276**, 516–522.

Daniel, H., Hemart, N., Jaillard, D. and Crépel, F. (1992) Coactivation of metabotropic glutamate receptors and of voltage-gated calcium channels induces long-term depression in cerebellar Purkinje cells in vitro. *Exp. Brain Res.* **90**, 327–331.

Davies, C. H., Clarke, V. R., Jane, D. E. and Collingridge, G. L. (1995) Pharmacology of postsynaptic metabotropic glutamate receptors in rat hippocampal CA1 pyramidal neurones. *Br. J. Pharmac.* **116**, 1859–1869.

Davies, S. N. and Lodge, D. (1987) Evidence for involvement of N-methylaspartate receptors in 'wind-up' of class 2 neurones in the dorsal horn of the rat. *Brain Res.* **424**, 402–406.

Desai, M. A. and Conn, P. J. (1991) Excitatory effects of ACPD receptor activation in the hippocampus are mediated by direct effects on pyramidal cells and blockade of synaptic inhibition. *J. Neurophysiol.* **66**, 40–52.

Desai, M. A., Smith, T. S. and Conn, P. J. (1992) Multiple metabotropic glutamate receptors regulate hippocampal function. *Synapse* **12**, 206–213.

Desai, M. A., McBain, C. J., Kauer, J. A. and Conn, P. J. (1994) Metabotropic glutamate receptor-induced disinhibition is mediated by reduced transmission at excitatory synapses onto interneurons and inhibitory synapses onto pyramidal cells. *Neurosci. Lett.* **181**, 78–82.

Dickenson, A. H. (1995) Central acute pain mechanisms. *Ann. Med.* **27**, 223–227.

Dickenson, A. H. and Sullivan, A. F. (1987) Evidence for a role of the NMDA receptor in the frequency dependent potentiation of deep rat dorsal horn nociceptive neurones following C fibre stimulation. *Neuropharmacology* **26**, 1235–1238.

Dickenson, A. H., Chapman, V. and Green, G. M. (1997) The pharmacology of excitatory and inhibitory amino acid-mediated events in the transmission and modulation of pain in the spinal cord. *Gen. Pharmac.* **28**, 633–638.

Doherty, J. and Dingledine, R. (1997) Regulation of excitatory input to inhibitory interneurons of the dentate gyrus during hypoxia. *J. Neurophysiol.* **77**, 393–404.

Doherty, J. and Dingledine, R. (1998) Differential regulation of synaptic inputs to dentate hilar border interneurons by metabotropic glutamate receptors. *J. Neurophysiol.* **79**, 2903–2910.

Doherty, A. J., Palmer, M. J., Henley, J. M., Collingridge, G. L. and Jane, D. E. (1997) (RS)-2-Chloro-5-hydroxyphenylglycine (CHPG) activates mGlu5, but no mGlu1, receptors expressed in CHO cells and potentiates NMDA responses in the hippocampus. *Neuropharmacology* **36**, 265–267.

Dorri, F., Hampson, D. R., Baskys, A. and Wojtowicz, J. M. (1997) Down-regulation of mGluR5 by antisense deoxynucleotides alters pharmacological responses to applications of ACPD in the rat hippocampus. *Exp. Neurol.* **147**, 48–54.

Eaton, S. A., Birse, E. F., Wharton, B., Sunter, D. C., Udvarhelyi, P. M., Watkins, J. C. and Salt, T. E. (1993a) Mediation of thalamic sensory responses in vivo by ACPD-activated excitatory amino acid receptors. *Eur J. Neurosci.* **5**, 186–189.

Eaton, S. A., Jane, D. E., Jones, P. L., Porter, R. H., Pook, P. C., Sunter, D. C., Udvarhelyi, P. M., Roberts, P. J., Salt, T. E. and Watkins, J. C. (1993b) Competitive antagonism at metabotropic glutamate receptors by (S)-4-carboxyphenylglycine and (RS)-alpha-methyl-4-carboxyphenylglycine. *Eur. J. Pharmac.* **244**, 195–197.

Faden, A. I., Demediuk, P., Panter, S. S. and Vink, R. (1989) The role of excitatory amino acids and NMDA receptors in traumatic brain injury. *Science* **244**, 798–800.

Fisher, K. and Coderre, T. J. (1996a) Comparison of nociceptive effects produced by intrathecal administration of mGluR agonists. *Neuroreport* **7**, 2743–2747.

Fisher, K. and Coderre, T. J. (1996b) The contribution of metabotropic glutamate receptors (mGluRs) to formalin-induced nociception. *Pain* **68**, 255–263.

Fisher, K., Fundytus, M. E., Cahill, C. M. and Coderre, T. J. (1998) Intrathecal administration of the mGluR compound, (S)-4CPG, attenuates hyperalgesia and allodynia associated with sciatic nerve constriction injury in rats. *Pain* **77**, 59–66.

Fitzjohn, S. M., Irving, A. J., Palmer, M. J., Harvey, J., Lodge, D. and Collingridge, G. L. (1996) Activation of group I mGluRs potentiates NMDA responses in rat hippocampal slices [published erratum appears in Neurosci. Lett. 1996 Mar 29;207(2):142]. *Neurosci. Lett.* **203**, 211–213.

Fotuhi, M., Sharp, A. H., Glatt, C. E., Hwang, P. M., von Krosigk, M., Snyder, S. H. and Dawson, T. M. (1993) Differential localization of phosphoinositide-linked metabotropic glutamate receptor (mGluR1) and the inositol 1,4,5-trisphosphate receptor in rat brain. *J. Neurosci.* **13**, 2001–2012.

Fundytus, M. E. and Coderre, T. J. (1994) Effect of activity at metabotropic, as well as ionotropic (NMDA), glutamate receptors on morphine dependence. *Br. J. Pharmac.* **113**, 1215–1220.

Fundytus, M. E. and Coderre, T. J. (1997) Attenuation of precipitated morphine withdrawal symptoms by acute i.c.v. administration of a group II mGluR agonist. *Br. J. Pharmac.* **121**, 511–514.

Fundytus, M. E., Ritchie, J. and Coderre, T. J. (1997) Attenuation of morphine withdrawal symptoms by subtype-selective metabotropic glutamate receptor antagonists. *Br. J. Pharmac.* **120**, 1015–1020.

Fundytus, M. E., Fisher, K., Dray, A., Henry, J. L. and Coderre, T. J. (1998) In vivo antinociceptive activity of anti-rat mGluR1 and mGluR5 antibodies in rats. *Neuroreport* **9**, 731–735.

Gerber, U. and Gähwiler, B. H. (1994) Modulation of Ionic Currents by Metabotropic Glutamate Receptors in the CNS. In: *The Metabotropic Glutamate Receptors*, pp. 125–146. Eds. P. J. Conn and J. Patel. Humana Press, Totowa, NJ.

Gereau, R. W. t. and Conn, P. J. (1995a) Multiple presynaptic metabotropic glutamate receptors modulate excitatory and inhibitory synaptic transmission in hippocampal area CA1. *J. Neurosci.* **15**, 6879–6889.

Gereau, R. W. t. and Conn, P. J. (1995b) Roles of specific metabotropic glutamate receptor subtypes in regulation of hippocampal CA1 pyramidal cell excitability. *J. Neurophysiol.* **74**, 122–129.

Glaum, S. R. and Miller, R. J. (1992) Metabotropic glutamate receptors mediate excitatory transmission in the nucleus of the solitary tract. *J. Neurosci.* **12**, 2251–2258.

Glaum, S. R. and Miller, R. J. (1993) Activation of metabotropic glutamate receptors produces reciprocal regulation of ionotropic glutamate and GABA responses in the nucleus of the tractus solitarius of the rat. *J. Neurosci.* **13**, 1636–1641.

Glaum, S. R. and Miller, R. J. (1994) Acute regulation of synaptic transmission by metabotropic glutamate receptors. In: *The Metabotropic Glutamate Receptors*, pp. 147–172. Eds. P. J. Conn and J. Patel. Humana Press, Totowa, NJ.

Goddard, G. V., McIntyre, D. C. and Leech, C. K. (1969) A permanent change in brain function resulting from daily electrical stimulation. *Exp. Neurol.* **25**, 295–330.

Gong, Q. Z., Delahunty, T. M., Hamm, R. J. and Lyeth, B. G. (1995) Metabotropic glutamate antagonist, MCPG, treatment of traumatic brain injury in rats. *Brain Res.* **700**, 299–302.

Greenamyre, J. T. and Porter, R. H. (1994) Anatomy and physiology of glutamate in the CNS. *Neurology* **44**, S7–S13.

Greenamyre, J. T. and Young, A. B. (1989) Excitatory amino acids and Alzheimer's disease. *Neurobiol. Aging* **10**, 593–602.

Greenamyre, J. T., Maragos, W. F., Albin, R. L., Penney, J. B. and Young, A. B. (1988) Glutamate transmission and toxicity in Alzheimer's disease. *Progr. Neuropsychopharmac. Biol. Psychiat.* **12**, 421–430.

Guérineau, N. C., Bossu, J. L., Gahwiler, B. H. and Gerber, U. (1995) Activation of a nonselective cationic conductance by metabotropic glutamatergic and muscarinic agonists in CA3 pyramidal neurons of the rat hippocampus. *J. Neurosci.* **15**, 4395–4407.

Hampson, D. R., Theriault, E., Huang, X. P., Kristensen, P., Pickering, D. S., Franck, J. E. and Mulvihill, E. R. (1994) Characterization of two alternatively spliced forms of a metabotropic glutamate receptor in the central nervous system of the rat. *Neuroscience* **60**, 325–336.

Hartell, N. A. (1994) Induction of cerebellar long-term depression requires activation of glutamate metabotropic receptors. *Neuroreport* **5**, 913–916.

Haruta, H., Kamishita, T., Hicks, T. P., Takahashi, M. P. and Tsumoto, T. (1994) Induction of LTD but not LTP through metabotropic glutamate receptors in visual cortex. *Neuroreport* **5**, 1829–1832.

Harvey, J. and Collingridge, G. L. (1993) Signal transduction pathways involved in the acute potentiation of NMDA responses by 1S,3R-ACPD in rat hippocampal slices. *Br. J. Pharmac.* **109**, 1085–1090.

Harvey, J., Palmer, M. J., Irving, A. J., Clarke, V. R. and Collingridge, G. L. (1996) NMDA receptor dependence of mGlu-mediated depression of synaptic transmission in the CA1 region of the rat hippocampus. *Br. J. Pharmac.* **119**, 1239–1247.

Hayashi, Y., Momiyama, A., Takahashi, T., Ohishi, H., Ogawa-Meguro, R., Shigemoto, R., Mizuno, N. and Nakanishi, S. (1993) Role of a metabotropic glutamate receptor in synaptic modulation in the accessory olfactory bulb. *Nature* **366**, 687–690.

Hayashi, Y., Sekiyama, N., Nakanishi, S., Jane, D. E., Sunter, D. C., Birse, E. F., Udvarhelyi, P. M. and Watkins, J. C. (1994) Analysis of agonist and antagonist activities of phenylglycine derivatives for different cloned metabotropic glutamate receptor subtypes. *J. Neurosci.* **14**, 3370–3377.

Hayes, R. L., Jenkins, L. W., Lyeth, B. G., Balster, R. L., Robinson, S. E., Clifton, G. L., Stubbins, J. F. and Young, H. F. (1988) Pretreatment with phencyclidine, an N-methyl-D-aspartate antagonist, attenuates long-term behavioral deficits in the rat produced by traumatic brain injury. *J. Neurotrauma* **5**, 259–274.

Heinemann, U. and Hamon, B. (1986) Calcium and epileptogenesis. *Exp. Brain Res.* **65**, 1–10.

Henrich-Noack, P., Hatton, C. D. and Reymann, K. G. (1998) The mGlu receptor ligand (S)-4C3HPG protects neurons after global ischaemia in gerbils. *Neuroreport* **9**, 985–988.

Hensch, T. K. and Stryker, M. P. (1996) Ocular dominance plasticity under metabotropic glutamate receptor blockade. *Science* **272**, 554–557.

Hollmann, M. and Heinemann, S. (1994) Cloned glutamate receptors. *A. Rev. Neurosci.* **17**, 31–108.

Holmes, K. H., Keele, N. B. and Shinnick-Gallagher, P. (1996) Loss of mGluR-mediated hyperpolarizations and increase in mGluR depolarizations in basolateral amygdala neurons in kindling-induced epilepsy. *J. Neurophysiol.* **76**, 2808–2812.

Holscher, C. (1994) Inhibitors of metabotropic glutamate receptors produce amnestic effects in chicks. *Neuroreport* **5**, 1037–1040.

Houamed, K. M., Kuijper, J. L., Gilbert, T. L., Haldeman, B. A., O'Hara, P. J., Mulvihill, E. R., Almers, W. and Hagen, F. S. (1991) Cloning, expression, and gene structure of a G protein-coupled glutamate receptor from rat brain. *Science* **252**, 1318–1321.

Hsia, A. Y., Salin, P. A., Castillo, P. E., Aiba, A., Abeliovich, A., Tonegawa, S. and Nicoll, R. A. (1995) Evidence against a role for metabotropic glutamate receptors in mossy fiber LTP: the use of mutant mice and pharmacological antagonists. *Neuropharmacology* **34**, 1567–1572.

Huber, K. M., Sawtell, N. B. and Bear, M. F. (1998) Effects of the metabotropic glutamate receptor antagonist MCPG on phosphoinositide turnover and synaptic plasticity in visual cortex. *J. Neurosci.* **18**, 1–9.

Irving, A. J., Schofield, J. G., Watkins, J. C., Sunter, D. C. and Collingridge, G. L. (1990) 1S,3R-ACPD stimulates and L-AP3 blocks Ca2+ mobilization in rat cerebellar neurons. *Eur. J. Pharmac.* **186**, 363–365.

Ito, I., Kohda, A., Tanabe, S., Hirose, E., Hayashi, M., Mitsunaga, S. and Sugiyama, H. (1992) 3,5-Dihydroxyphenylglycine: a potent agonist of metabotropic glutamate receptors. *Neuroreport* **3**, 1013–1016.

Izumi, Y. and Zorumski, C. F. (1994) Developmental changes in the effects of metabotropic glutamate receptor antagonists on CA1 long-term potentiation in rat hippocampal slices. *Neurosci. Lett.* **176**, 89–92.

Jane, D. E., Jones, P. L., Pook, P. C., Salt, T. E., Sunter, D. C. and Watkins, J. C. (1993) Stereospecific antagonism by (+)-alpha-methyl-4-carboxyphenylglycine (MCPG) of (1S,3R)-ACPD-induced effects in neonatal rat motoneurones and rat thalamic neurones. *Neuropharmacology* **32**, 725–727.

Jane, D. E., Jones, P. L., Pook, P. C., Tse, H. W. and Watkins, J. C. (1994) Actions of two new antagonists showing selectivity for different sub-types of metabotropic glutamate receptor in the neonatal rat spinal cord. *Br. J. Pharmac.* **112**, 809–816.

Joly, C., Gomeza, J., Brabet, I., Curry, K., Bockaert, J. and Pin, J. P. (1995) Molecular, functional, and pharmacological characterization of the metabotropic glutamate receptor type 5 splice variants: comparison with mGluR1. *J. Neurosci.* **15**, 3970–3981.

Jones, M. W. and Headley, P. M. (1995) Interactions between metabotropic and ionotropic glutamate receptor agonists in the rat spinal cord in vivo. *Neuropharmacology* **34**, 1025–1031.

Jones, P. L. S. J., Birse, E. F., Jane, D. E., Jones, A. W., Mewett, K. N., Pook, P. C.-K., Udvarhelyi, P. M., Wharton, B. and Watkins, J. C. (1993) Agonist and antagonist actions of the phenylglycine derivatives at depolarization-mediating (1S,3R)-ACPD receptors in neonatal rat motoneurones. *Br. J. Pharmac.* **108**, 86P.

Jouvenceau, A., Dutar, P. and Billard, J. M. (1995) Presynaptic depression of inhibitory postsynaptic potentials by metabotropic glutamate receptors in rat hippocampal CA1 pyramidal cells. *Eur. J. Pharmac.* **281**, 131–139.

Kaba, H., Hayashi, Y., Higuchi, T. and Nakanishi, S. (1994) Induction of an olfactory memory by the activation of a metabotropic glutamate receptor. *Science* **265**, 262–264.

Kato, N. (1993) Dependence of long-term depression on postsynaptic metabotropic glutamate receptors in visual cortex. *Proc. natl Acad. Sci. USA* **90**, 3650–3654.

Kawabata, S., Tsutsumi, R., Kohara, A., Yamaguchi, T., Nakanishi, S. and Okada, M. (1996) Control of calcium oscillations by phosphorylation of metabotropic glutamate receptors. *Nature* **383**, 89–92.

Kearney, J. A., Frey, K. A. and Albin, R. L. (1997) Metabotropic glutamate agonist-induced rotation: a pharmacological, FOS immunohistochemical, and [14C]-2-deoxyglucose autoradiographic study. *J. Neurosci.* **17**, 4415–4425.

Keele, N. B., Arvanov, V. L. and Shinnick-Gallagher, P. (1997) Quisqualate-preferring metabotropic glutamate receptor activates Na(+)-Ca2+ exchange in rat basolateral amygdala neurones. *J. Physiol. (Lond.)* **499**, 87–104.

Kelso, S. R., Nelson, T. E. and Leonard, J. P. (1992) Protein kinase C-mediated enhancement of NMDA currents by metabotropic glutamate receptors in Xenopus oocytes. *J. Physiol. (Lond.)* **449**, 705–718.

Kim, J. H. and Vezina, P. (1997) Activation of metabotropic glutamate receptors in the rat nucleus accumbens increases locomotor activity in a dopamine-dependent manner. *J. Pharmac. exp. Ther.* **283**, 962–968.

Kim, J. H. and Vezina, P. (1998a) The metabotropic glutamate receptor antagonist (RS)-MCPG produces hyperlocomotion in amphetamine pre-exposed rats. *Neuropharmacology* **37**, 189–197.

Kim, J. H. and Vezina, P. (1998b) Metabotropic glutamate receptors are necessary for sensitization by amphetamine. *Neuroreport* **9**, 403–406.

King, A. E., Thompson, S. W., Urban, L. and Woolf, C. J. (1988) The responses recorded in vitro of deep dorsal horn neurons to direct and orthodromic stimulation in the young rat spinal cord. *Neuroscience* **27**, 231–242.

Kinney, G. A. and Slater, N. T. (1993) Potentiation of NMDA receptor-mediated transmission in turtle cerebellar granule cells by activation of metabotropic glutamate receptors. *J. Neurophysiol.* **69**, 585–594.

Koh, J. Y., Palmer, E. and Cotman, C. W. (1991) Activation of the metabotropic glutamate receptor attenuates N-methyl-D-aspartate neurotoxicity in cortical cultures. *Proc. natl Acad. Sci. U.S.A.* **88**, 9431–9435.

Kornbuber, J. and Wiltfang, J. (1998) The role of glutamate in dementia. *J. Neural Transm. Suppl.* **53**, 277–287.

Lee, R. K., Wurtman, R. J., Cox, A. J. and Nitsch, R. M. (1995) Amyloid precursor protein processing is stimulated by metabotropic glutamate receptors. *Proc. natl Acad. Sci. U.S.A.* **92**, 8083–8087.

Lee, R. K., Jimenez, J., Cox, A. J. and Wurtman, R. J. (1996) Metabotropic glutamate receptors regulate APP processing in hippocampal neurons and cortical astrocytes derived from fetal rats. *Ann. N.Y. Acad. Sci.* **777**, 338–343.

Lester, R. A. and Jahr, C. E. (1990) Quisqualate receptor-mediated depression of calcium currents in hippocampal neurons. *Neuron* **4**, 741–749.

Libri, V., Constanti, A., Zibetti, M. and Postlethwaite, M. (1997) Metabotropic glutamate receptor subtypes mediating slow inward tail current (IADP) induction and inhibition of synaptic transmission in olfactory cortical neurones. *Br. J. Pharmac.* **120**, 1083–1095.

Linden, D. J. and Connor, J. A. (1993) Cellular mechanisms of long-term depression in the cerebellum. *Curr. Opin. Neurobiol.* **3**, 401–406.

Lingenhöhl, K., Olpe, H. R., Bendali, N. and Knopfel, T. (1993) Phenylglycine derivatives antagonize the excitatory response to Purkinje cells to 1S,3R-ACPD: an in vivo and in vitro study. *Neurosci. Res.* **18**, 229–234.

Little, Z., Grover, L. M. and Teyler, T. J. (1995) Metabotropic glutamate receptor antagonist, (R,S)-alpha-methyl-4-carboxyphenylglycine, blocks two distinct forms of long-term potentiation in area CA1 of rat hippocampus. *Neurosci. Lett.* **201**, 73–76.

Liu, Y. B., Disterhoft, J. F. and Slater, N. T. (1993) Activation of metabotropic glutamate receptors induces long-term depression of GABAergic inhibition in hippocampus. *J. Neurophysiol.* **69**, 1000–1004.

Lu, Y. M., Jia, Z., Janus, C., Henderson, J. T., Gerlai, R., Wojtowicz, J. M. and Roder, J. C. (1997) Mice lacking metabotropic glutamate receptor 5 show impaired learning and reduced CA1 long-term potentiation (LTP) but normal CA3 LTP. *J. Neurosci.* **17**, 5196–5205.

Luján, R., Nusser, Z., Roberts, J. D., Shigemoto, R. and Somogyi, P. (1996) Perisynaptic location of metabotropic glutamate receptors mGluR1 and mGluR5 on dendrites and dendritic spines in the rat hippocampus. *Eur J. Neurosci.* **8**, 1488–1500.

Lüthi, A., Gahwiler, B. H. and Gerber, U. (1997) 1S, 3R-ACPD induces a region of negative slope conductance in the steady-state current-voltage relationship of hippocampal pyramidal cells. *J. Neurophysiol.* **77**, 221–228.

Malenka, R. C., Kauer, J. A., Zucker, R. S. and Nicoll, R. A. (1988) Postsynaptic calcium is sufficient for potentiation of hippocampal synaptic transmission. *Science* **242**, 81–84.

Malenka, R. C., Lancaster, B. and Zucker, R. S. (1992) Temporal limits on the rise in postsynaptic calcium required for the induction of long-term potentiation. *Neuron* **9**, 121–128.

Manahan-Vaughan, D. (1997) Group 1 and 2 metabotropic glutamate receptors play differential roles in hippocampal long-term depression and long-term potentiation in freely moving rats. *J. Neurosci.* **17**, 3303–3311.

Mannaioni, G., Carla, V. and Moroni, F. (1996) Pharmacological characterization of metabotropic glutamate receptors potentiating NMDA responses in mouse cortical wedge preparations. *Br. J. Pharmac.* **118**, 1530–1536.

Manzoni, O. and Bockaert, J. (1995) Metabotropic glutamate receptors inhibiting excitatory synapses in the CA1 area of rat hippocampus. *Eur. J. Neurosci.* **7**, 2518–2523.

Manzoni, O. J., Weisskopf, M. G. and Nicoll, R. A. (1994) MCPG antagonizes metabotropic glutamate receptors but not long-term potentiation in the hippocampus. *Eur. J. Neurosci.* **6**, 1050–1054.

Martin, L. J., Blackstone, C. D., Huganir, R. L. and Price, D. L. (1992) Cellular localization of a metabotropic glutamate receptor in rat brain. *Neuron* **9**, 259–270.

Martin, S. J. and Morris, R. G. (1997) (R,S)-alpha-methyl-4-carboxyphenylglycine (MCPG) fails to block long-term potentiation under urethane anaesthesia in vivo. *Neuropharmacology* **36**, 1339–1354.

Masu, M., Tanabe, Y., Tsuchida, K., Shigemoto, R. and Nakanishi, S. (1991) Sequence and expression of a metabotropic glutamate receptor. *Nature* **349**, 760–765.

Mattson, M. P., Cheng, B., Davis, D., Bryant, K., Lieberburg, I. and Rydel, R. E. (1992) beta-Amyloid peptides destabilize calcium homeostasis and render human cortical neurons vulnerable to excitotoxicity. *J. Neurosci.* **12**, 376–389.

Mayer, M. L. and Miller, R. J. (1990) Excitatory amino acid receptors, second messengers and regulation of intracellular Ca2+ in mammalian neurons. *Trends Pharmac. Sci.* **11**, 254–260.

McBain, C. J., DiChiara, T. J. and Kauer, J. A. (1994) Activation of metabotropic glutamate receptors differentially affects two classes of hippocampal interneurons and potentiates excitatory synaptic transmission. *J. Neurosci.* **14**, 4433–4445.

McCool, B. A., Pin, J. P., Harpold, M. M., Brust, P. F., Stauderman, K. A. and Lovinger, D. M. (1998) Rat group I metabotropic glutamate receptors inhibit neuronal Ca2+ channels via multiple signal transduction pathways in HEK 293 cells. *J. Neurophysiol.* **79**, 379–391.

McCormick, D. A. and von Krosigk, M. (1992) Corticothalamic activation modulates thalamic firing through glutamate "metabotropic" receptors. *Proc. natl Acad. Sci. U.S.A.* **89**, 2774–2778.

McDonald, J. W. and Schoepp, D. D. (1992) The metabotropic excitatory amino acid receptor agonist 1S,3R-ACPD selectively potentiates N-methyl-D-aspartate-induced brain injury. *Eur. J. Pharmac.* **215**, 353–354.

McDonald, J. W., Fix, A. S., Tizzano, J. P. and Schoepp, D. D. (1993) Seizures and brain injury in neonatal rats induced by 1S,3R-ACPD, a metabotropic glutamate receptor agonist. *J. Neurosci.* **13**, 4445–4455.

McGuinness, N., Anwyl, R. and Rowan, M. (1991) Trans-ACPD enhances long-term potentiation in the hippocampus. *Eur. J. Pharmac.* **197**, 231–232.

McNamara, J. O. (1988) Pursuit of the mechanisms of kindling. *Trends Neurosci.* **11**, 33–36.

Meldrum, B. S. (1994) The role of glutamate in epilepsy and other CNS disorders. *Neurology* **44**, S14–S23.

Meltzer, L. T., Serpa, K. A. and Christoffersen, C. L. (1997) Metabotropic glutamate receptor-mediated inhibition and excitation of substantia nigra dopamine neurons. *Synapse* **26**, 184–193.

Mendell, L. M. and Wall, P. D. (1965) Response of single dorsal horn cells to peripheral cutaneous unmyelynated fibers. *Nature* **206**, 97–99.

de Mendonça, A. and Ribeiro, J. A. (1997) Contribution of metabotropic glutamate receptors to the depression of excitatory postsynaptic potentials during hypoxia. *Neuroreport* **8**, 3667–3671.

Mercuri, N. B., Stratta, F., Calabresi, P., Bonci, A. and Bernardi, G. (1993) Activation of metabotropic glutamate receptors induces an inward current in rat dopamine mesencephalic neurons. *Neuroscience* **56**, 399–407.

Merlin, L. R. and Wong, R. K. (1997) Role of group I metabotropic glutamate receptors in the patterning of epileptiform activities in vitro. *J. Neurophysiol.* **78**, 539–544.

Merlin, L. R., Taylor, G. W. and Wong, R. K. (1995) Role of metabotropic glutamate receptor subtypes in the patterning of epileptiform activities in vitro. *J. Neurophysiol.* **74**, 896–900.

Merlin, L. R., Bergold, P. J. and Wong, R. K. (1998) Requirement of protein synthesis for group I mGluR-mediated induction of epileptiform discharges. *J. Neurophysiol.* **80**, 989–993.

Michaelis, E. K. (1998) Molecular biology of glutamate receptors in the central nervous system and their role in excitotoxicity, oxidative stress and aging. *Progr. Neurobiol.* **54**, 369–415.

Moghaddam, B. and Adams, B. W. (1998) Reversal of phencyclidine effects by a group II metabotropic glutamate receptor agonist in rats [see comments]. *Science* **281**, 1349–1352.

Monaghan, D. T., Bridges, R. J. and Cotman, C. W. (1989) The excitatory amino acid receptors: their classes, pharmacology, and distinct properties in the function of the central nervous system. *A. Rev. Pharmac. Toxic.* **29**, 365–402.

Moroni, F., Lombardi, G., Thomsen, C., Leonardi, P., Attucci, S., Peruginelli, F., Torregrossa, S. A., Pellegrini-Giampietro, D. E., Luneia, R. and Pellicciari, R. (1997) Pharmacological characterization of 1-aminoindan-1,5-dicarboxylic acid, a potent mGluR1 antagonist. *J. Pharmac. exp. Ther.* **281**, 721–729.

Morris, R. G., Anderson, E., Lynch, G. S. and Baudry, M. (1986) Selective impairment of learning and blockade of long-term potentiation by an N-methyl-D-aspartate receptor antagonist, AP5. *Nature* **319**, 774–776.

Morris, R. G. M. (1984) Developments of a water-maze procedure for studying spatial learning in the rat. *J. Neurosci. Meth.* **11**, 47–60.

Mukhin, A., Fan, L. and Faden, A. I. (1996) Activation of metabotropic glutamate receptor subtype mGluR1 contributes to post-traumatic neuronal injury. *J. Neurosci.* **16**, 6012–6020.

Mukhin, A. G., Ivanova, S. A. and Faden, A. I. (1997) mGluR modulation of post-traumatic neuronal death: role of NMDA receptors. *Neuroreport* **8**, 2561–2566.

Nakahara, K., Okada, M. and Nakanishi, S. (1997) The metabotropic glutamate receptor mGluR5 induces calcium oscillations in cultured astrocytes via protein kinase C phosphorylation. *J. Neurochem.* **69**, 1467–1475.

Nakanishi, S. (1994) Metabotropic glutamate receptors: synaptic transmission, modulation, and plasticity. *Neuron* **13**, 1031–1037.

Nakanishi, S. and Masu, M. (1994) Molecular diversity and functions of glutamate receptors. *A. Rev. Biophys. Biomolec. Struct.* **23**, 319–348.

Nakanishi, S., Masu, M., Bessho, Y., Nakajima, Y., Hayashi, Y. and Shigemoto, R. (1994) Molecular diversity of glutamate receptors and their physiological functions. *Exs* **71**, 71–80.

Nakanishi, S., Nakajima, Y., Masu, M., Ueda, Y., Nakahara, K., Watanabe, D., Yamaguchi, S., Kawabata, S. and Okada, M. (1998) Glutamate receptors: brain function and signal transduction. *Brain Res. Brain Res. Rev.* **26**, 230–235.

Neugebauer, V., Lucke, T. and Schaible, H. G. (1994) Requirement of metabotropic glutamate receptors for the generation of inflammation-evoked hyperexcitability in rat spinal cord neurons. *Eur. J. Neurosci.* **6**, 1179–1186.

Neugebauer, V., Keele, N. B. and Shinnick-Gallagher, P. (1997) Epileptogenesis in vivo enhances the sensitivity of inhibitory presynaptic metabotropic glutamate receptors in basolateral amygdala neurons in vitro. *J. Neurosci.* **17**, 983–995.

Nicoletti, F., Wroblewski, J. T., Novelli, A., Alho, H., Guidotti, A. and Costa, E. (1986) The activation of inositol phospholipid metabolism as a signal-transducing system for excitatory amino acids in primary cultures of cerebellar granule cells. *J. Neurosci.* **6**, 1905–1911.

Nicoletti, F., Bruno, V., Copani, A., Casabona, G. and Knopfel, T. (1996) Metabotropic glutamate receptors: a new target for the therapy of neurodegenerative disorders? *Trends Neurosci.* **19**, 267–271.

Nicoll, R. A., Oliet, S. H. R. and Malenka, R. C. (1998) NMDA receptor-dependent and metabotropic glutamate receptor-dependent forms of long-term depression coexist in CA1 hippocampal pyramidal cells. *Neurobiol. Learn Mem.* **70**, 62–72.

Nielsen, K. S., Macphail, E. M. and Riedel, G. (1997) Class I mGlu receptor antagonist 1-aminoindan-1,5-dicarboxylic acid blocks contextual but not cue conditioning in rats. *Eur. J. Pharmac.* **326**, 105–108.

Nusser, Z., Mulvihill, E., Streit, P. and Somogyi, P. (1994) Subsynaptic segregation of metabotropic and ionotropic glutamate receptors as revealed by immunogold localization. *Neuroscience* **61**, 421–427.

Nusser, Z., Roberts, J. D., Baude, A., Richards, J. G., Sieghart, W. and Somogyi, P. (1995) Immunocytochemical localization of the alpha 1 and beta 2/3 subunits of the GABAA receptor in relation to specific GABAergic synapses in the dentate gyrus. *Eur. J. Neurosci.* **7**, 630–646.

O'Connor, J. J., Rowan, M. J. and Anwyl, R. (1994) Long-lasting enhancement of NMDA receptor-mediated synaptic transmission by metabotropic glutamate receptor activation. *Nature* **367**, 557–559.

Ohishi, H., Shigemoto, R., Nakanishi, S. and Mizuno, N. (1993) Distribution of the messenger RNA for a metabotropic glutamate receptor, mGluR2, in the central nervous system of the rat. *Neuroscience* **53**, 1009–1018.

Ohno, M. and Watanabe, S. (1996) Concurrent blockade of hippocampal metabotropic glutamate and N-methyl-D-aspartate receptors disrupts working memory in the rat. *Neuroscience* **70**, 303–311.

Ohno, M. and Watanabe, S. (1998) Enhanced N-methyl-D-aspartate function reverses working memory failure induced by blockade of group I metabotropic glutamate receptors in the rat hippocampus. *Neurosci. Lett.* **240**, 37–40.

Oliet, S. H., Malenka, R. C. and Nicoll, R. A. (1997) Two distinct forms of long-term depression coexist in CA1 hippocampal pyramidal cells. *Neuron* **18**, 969–982.

Olney, J. W. (1994) Neurotoxicity of NMDA receptor antagonists: an overview. *Psychopharmac. Bull.* **30**, 533–540.

Olney, J. W. and Farber, N. B. (1995) Glutamate receptor dysfunction and schizophrenia. *Arch. Gen. Psychiat.* **52**, 998–1007.

Olney, J. W., Labruyere, J. and Price, M. T. (1989) Pathological changes induced in cerebrocortical neurons by phencyclidine and related drugs [see comments]. *Science* **244**, 1360–1362.

O'Mara, S. M., Rowan, M. J. and Anwyl, R. (1995) Metabotropic glutamate receptor-induced homosynaptic long-term depression and depotentiation in the dentate gyrus of the rat hippocampus in vitro. *Neuropharmacology* **34**, 983–989.

Opitz, T., Richter, P. and Reymann, K. G. (1994) The metabotropic glutamate receptor antagonist (+)-alpha-methyl-4-carboxyphenylglycine protects hippocampal CA1 neurons of the rat from in vitro hypoxia/hypoglycemia. *Neuropharmacology* **33**, 715–717.

Opitz, T., Richter, P., Carter, A. J., Kozikowski, A. P., Shinozaki, H. and Reymann, K. G. (1995) Metabotropic glutamate receptor subtypes differentially influence neuronal recovery from in vitro hypoxia/hypoglycemia in rat hippocampal slices. *Neuroscience* **68**, 989–1001.

Orlando, L. R., Standaert, D. G., Penney, J. B., Jr. and Young, A. B. (1995) Metabotropic receptors in excitotoxicity: (S)-4-carboxy-3-hydroxyphenylglycine ((S)-4C3HPG) protects against rat striatal quinolinic acid lesions. *Neurosci. Lett.* **202**, 109–112.

Otani, S. and Ben-Ari, Y. (1991) Metabotropic receptor-mediated long-term potentiation in rat hippocampal slices. *Eur. J. Pharmac.* **205**, 325–326.

Otani, S., Ben-Ari, Y. and Roisin-Lallemand, M. P. (1993) Metabotropic receptor stimulation coupled to weak tetanus leads to long-term potentiation and a rapid elevation of cytosolic protein kinase C activity. *Brain Res.* **613**, 1–9.

Overstreet, L. S., Pasternak, J. F., Colley, P. A., Slater, N. T. and Trommer, B. L. (1997) Metabotropic glutamate receptor mediated long-term depression in developing hippocampus. *Neuropharmacology* **36**, 831–844.

Palmer, E., Monaghan, D. T. and Cotman, C. W. (1989) Trans-ACPD, a selective agonist of the phosphoinositide-coupled excitatory amino acid receptor. *Eur. J. Pharmac.* **166**, 585–587.

Palmer, M. J., Irving, A. J., Seabrook, G. R., Jane, D. E. and Collingridge, G. L. (1997) The group I mGlu receptor agonist DHPG induces a novel form of LTD in the CA1 region of the hippocampus. *Neuropharmacology* **36**, 1517–1532.

Paolillo, M., Montecucco, A., Zanassi, P. and Schinelli, S. (1998) Potentiation of dopamine-induced cAMP formation by group I metabotropic glutamate receptors via protein kinase C in cultured striatal neurons [In Process Citation]. *Eur. J. Neurosci.* **10**, 1937–1945.

Patel, S., Chapman, A. G., Graham, J. L., Meldrum, B. S. and Frey, P. (1990) Anticonvulsant activity of the NMDA antagonists, D(-)4-(3-phosphonopropyl) piperazine-2-carboxylic acid (D-CPP) and D(-)(E)-4-(3-phosphonoprop-2-enyl) piperazine-2-carboxylic acid (D-CPPene) in a rodent and a primate model of reflex epilepsy. *Epilepsy Res.* **7**, 3–10.

Pellicciari, R., Luneia, R., Costantino, G., Marinozzi, M., Natalini, B., Jakobsen, P., Kanstrup, A., Lombardi, G., Moroni, F. and Thomsen, C. (1995) 1-Aminoindan-1,5-dicarboxylic acid: a novel antagonist at phospholipase C-linked metabotropic glutamate receptors. *J. Med. Chem.* **38**, 3717–3719.

Pellicciari, R., Raimondo, M., Marinozzi, M., Natalini, B., Costantino, G. and Thomsen, C. (1996) (S)-(+)-2-(3'-carboxybicyclo[1.1.1]pentyl)-glycine, a structurally new group I metabotropic glutamate receptor antagonist. *J. Med. Chem.* **39**, 2874–2876.

Phillips, R. G. and LeDoux, J. E. (1992) Differential contribution of amygdala and hippocampus to cued and contextual fear conditioning. *Behav. Neurosci.* **106**, 274–285.

Pilc, A., Branski, P., Palucha, A., Tokarski, K. and Bijak, M. (1998) Antidepressant treatment influences group I of glutamate metabotropic receptors in slices from hippocampal CA1 region. *Eur. J. Pharmac.* **349**, 83–87.

Pin, J.-P. and Duvoisin, R. (1995) The metabotropic glutamate receptors: structure and functions. *Neuropharmacology* **34**, 1–26.

Pisani, A., Calabresi, P., Centonze, D. and Bernardi, G. (1997) Enhancement of NMDA responses by group I metabotropic glutamate receptor activation in striatal neurones. *Br. J. Pharmac.* **120**, 1007–1014.

Pizzi, M., Fallacara, C., Arrighi, V., Memo, M. and Spano, P. F. (1993) Attenuation of excitatory amino acid toxicity by metabotropic glutamate receptor agonists and aniracetam in primary cultures of cerebellar granule cells. *J. Neurochem.* **61**, 683–689.

Poncer, J. C., Shinozaki, H. and Miles, R. (1995) Dual modulation of synaptic inhibition by distinct metabotropic glutamate receptors in the rat hippocampus. *J. Physiol. (Lond.)* **485**, 121–134.

Pook, P. C.-K., Sunter, D. C., Udvarhelyi, P. M. and Watkins, J. C. (1992) Evidence for presynaptic depression of monosynaptic excitation in neonatal rat motoneurones by (1S,3S)- and (1S,3R)-ACPD. *Exp. Physiol.* **77**, 529–532.

Pulsinelli, W. A. (1985) Selective neuronal vulnerability: morphological and molecular characteristics. *Progr. Brain Res.* **63**, 29–37.

Raff, M. C., Barres, B. A., Burne, J. F., Coles, H. S., Ishizaki, Y. and Jacobson, M. D. (1993) Programmed cell death and the control of cell survival: lessons from the nervous system. *Science* **262**, 695–700.

Rahman, S. and Neuman, R. S. (1996) Characterization of metabotropic glutamate receptor-mediated facilitation of N-methyl-D-aspartate depolarization of neocortical neurones. *Br. J. Pharmac.* **117**, 675–683.

Richter-Levin, G., Errington, M. L., Maegawa, H. and Bliss, T. V. (1994) Activation of metabotropic glutamate receptors is necessary for long-term potentiation in the dentate gyrus and for spatial learning. *Neuropharmacology* **33**, 853–857.

Rickard, N. S. and Ng, K. T. (1995) Blockade of metabotropic glutamate receptors prevents long-term memory consolidation. *Brain Res. Bull* **36**, 355–359.

Riedel, G. (1996) Function of metabotropic glutamate receptors in learning and memory. *Trends Neurosci.* **19**, 219–224.

Riedel, G. and Reymann, K. G. (1996) Metabotropic glutamate receptors in hippocampal long-term potentiation and learning and memory. *Acta Physiol. Scand.* **157**, 1–19.

Riedel, G., Wetzel, W. and Reymann, K. G. (1994) (R,S)-alpha-methyl-4-carboxyphenylglycine (MCPG) blocks spatial learning in rats and long-term potentiation in the dentate gyrus in vivo. *Neurosci. Lett.* **167**, 141–144.

Riedel, G., Casabona, G. and Reymann, K. G. (1995) Inhibition of long-term potentiation in the dentate gyrus of freely moving rats by the metabotropic glutamate receptor antagonist MCPG. *J. Neurosci.* **15**, 87–98.

Roberts, P. J. (1995) Pharmacological tools for the investigation of metabotropic glutamate receptors (mGluRs): phenylglycine derivatives and other selective antagonists—an update. *Neuropharmacology* **34**, 813–819.

Roche, K. W., Tingley, W. G. and Huganir, R. L. (1994) Glutamate receptor phosphorylation and synaptic plasticity. *Curr. Opin. Neurobiol.* **4**, 383–388.

Romano, C., Sesma, M. A., McDonald, C. T., O'Malley, K., Van den Pol, A. N. and Olney, J. W. (1995) Distribution of metabotropic glutamate receptor mGluR5 immunoreactivity in rat brain. *J. Comp. Neurol.* **355**, 455–469.

Rothman, S. M. and Olney, J. W. (1986) Glutamate and the pathophysiology of hypoxic–ischemic brain damage. *Ann. Neurol.* **19**, 105–111.

Rothman, S. M. and Olney, J. W. (1995) Excitotoxicity and the NMDA receptor—still lethal after eight years. *Trends Neurosci.* **18**, 57–58.

Rutecki, P. A., Lebeda, F. J. and Johnston, D. (1987) 4-Aminopyridine produces epileptiform activity in hippocampus and enhances synaptic excitation and inhibition. *J. Neurophysiol.* **57**, 1911–1924.

Sacaan, A. I. and Schoepp, D. D. (1992) Activation of hippocampal metabotropic excitatory amino acid receptors leads to seizures and neuronal damage. *Neurosci. Lett.* **139**, 77–82.

Sacaan, A. I., Monn, J. A. and Schoepp, D. D. (1991) Intrastriatal injection of a selective metabotropic excitatory amino acid receptor agonist induces contralateral turning in the rat. *J. Pharmac. exp. Ther.* **259**, 1366–1370.

Sacaan, A. I., Bymaster, F. P. and Schoepp, D. D. (1992) Metabotropic glutamate receptor activation produces extrapyramidal motor system activation that is mediated by striatal dopamine. *J. Neurochem.* **59**, 245–251.

Sagara, Y. and Schubert, D. (1998) The activation of metabotropic glutamate receptors protects nerve cells from oxidative stress. *J. Neurosci.* **18**, 6662–6671.

Sahara, Y. and Westbrook, G. L. (1993) Modulation of calcium currents by a metabotropic glutamate receptor involves fast and slow kinetic components in cultured hippocampal neurons. *J. Neurosci.* **13**, 3041–3050.

Salt, T. E. and Eaton, S. A. (1995) Modulation of sensory neurone excitatory and inhibitory responses in the ventrobasal thalamus by activation of metabotropic excitatory amino acid receptors. *Neuropharmacology* **34**, 1043–1051.

Salt, T. E. and Turner, J. P. (1998) Reduction of sensory and metabotropic glutamate receptor responses in the thalamus by the novel metabotropic glutamate receptor-1-selective antagonist S-2-methyl-4-carboxy-phenylglycine. *Neuroscience* **85**, 655–658.

Sayer, R. J., Schwindt, P. C. and Crill, W. E. (1992) Metabotropic glutamate receptor-mediated suppression of L-type calcium current in acutely isolated neocortical neurons. *J. Neurophysiol.* **68**, 833–842.

Schoepp, D., Bockaert, J. and Sladeczek, F. (1990) Pharmacological and functional characteristics of metabotropic excitatory amino acid receptors. *Trends Pharmac. Sci.* **11**, 508–515.

Schoepp, D. D., Goldsworthy, J., Johnson, B. G., Salhoff, C. R. and Baker, S. R. (1994) 3,5-Dihydroxyphenylglycine is a highly selective agonist for phosphoinositide-linked metabotropic glutamate receptors in the rat hippocampus. *J. Neurochem.* **63**, 769–772.

Schoepp, D. D., Tizzano, J. P., Wright, R. A. and Fix, A. S. (1995) Reversible and irreversible neuronal injury induced by intrahippocampal infusion of the mGluR agonist 1S,3R-ACPD in the rat. *Neurodegeneration* **4**, 71–80.

Schrader, L. A. and Tasker, J. G. (1997) Modulation of multiple potassium currents by metabotropic glutamate receptors in neurons of the hypothalamic supraoptic nucleus. *J. Neurophysiol.* **78**, 3428–3437.

Schwarzer, C. and Sperk, G. (1998) Glutamate-stimulated neuropeptide Y mRNA expression in the rat dentate gyrus: a prominent role of metabotropic glutamate receptors. *Hippocampus* **8**, 274–288.

Schwarzer, C., Kofler, N. and Sperk, G. (1998) Up-regulation of neuropeptide Y-Y2 receptors in an animal model of temporal lobe epilepsy. *Molec. Pharmac.* **53**, 6–13.

Selig, D. K., Lee, H. K., Bear, M. F. and Malenka, R. C. (1995) Reexamination of the effects of MCPG on hippocampal LTP, LTD, and depotentiation. *J. Neurophysiol.* **74**, 1075–1082.

Sergueeva, O. A., Fedorov, N. B. and Reymann, K. G. (1993) An antagonist of glutamate metabotropic receptors, (RS)-alpha-methyl-4-carboxyphenylglycine, prevents the LTP-related increase in postsynaptic AMPA sensitivity in hippocampal slices. *Neuropharmacology* **32**, 933–935.

Shen, H., Gorter, J. A., Aronica, E., Zheng, X., Zhang, L., Bennett, M. V. and Zukin, R. S. (1995) Potentiation of NMDA responses by metabotropic receptor activation depends on NMDA receptor subunit composition. In: *Society for Neuroscience Abstracts*, Vol. 21 Part I, p. 77.

Shen, K. Z. and Johnson, S. W. (1997) A slow excitatory postsynaptic current mediated by G-protein-coupled metabotropic glutamate receptors in rat ventral tegmental dopamine neurons. *Eur. J. Neurosci.* **9**, 48–54.

Shigemoto, R., Nakanishi, S. and Mizuno, N. (1992) Distribution of the mRNA for a metabotropic glutamate receptor (mGluR1) in the central nervous system: an in situ hybridization study in adult and developing rat. *J. comp. Neurol.* **322**, 121–135.

Shigemoto, R., Nomura, S., Ohishi, H., Sugihara, H., Nakanishi, S. and Mizuno, N. (1993) Immunohistochemical localization of a metabotropic glutamate receptor, mGluR5, in the rat brain. *Neurosci. Lett.* **163**, 53–57.

Shigemoto, R., Abe, T., Nomura, S., Nakanishi, S. and Hirano, T. (1994) Antibodies inactivating mGluR1 metabotropic glutamate receptor block long-term depression in cultured Purkinje cells. *Neuron* **12**, 1245–1255.

Siliprandi, R., Lipartiti, M., Fadda, E., Sautter, J. and Manev, H. (1992) Activation of the glutamate metabotropic receptor protects retina against N-methyl-D-aspartate toxicity. *Eur. J. Pharmac.* **219**, 173–174.

Simon, R. P., Swan, J. H., Griffiths, T. and Meldrum, B. S. (1984) Blockade of N-methyl-D-aspartate receptors may protect against ischemic damage in the brain. *Science* **226**, 850–852.

Skolnick, P., Layer, R. T., Popik, P., Nowak, G., Paul, I. A. and Trullas, R. (1996) Adaptation of N-methyl-D-aspartate (NMDA) receptors following antidepressant treatment: implications for the pharmacotherapy of depression. *Pharmacopsychiatry* **29**, 23–26.

Sladeczek, F., Pin, J. P., Recasens, M., Bockaert, J. and Weiss, S. (1985) Glutamate stimulates inositol phosphate formation in striatal neurones. *Nature* **317**, 717–719.

Stefani, A., Pisani, A., Mercuri, N. B., Bernardi, G. and Calabresi, P. (1994) Activation of metabotropic glutamate receptors inhibits calcium currents and GABA-mediated synaptic potentials in striatal neurons. *J. Neurosci.* **14**, 6734–6743.

Stefani, A., Pisani, A., Mercuri, N. B. and Calabresi, P. (1996) The modulation of calcium currents by the activation of mGluRs. Functional implications. *Molec. Neurobiol.* **13**, 81–95.

Strasser, U., Lobner, D., Behrens, M. M., Canzoniero, L. M. and Choi, D. W. (1998) Antagonists for group I mGluRs attenuate

excitotoxic neuronal death in cortical cultures [In Process Citation]. *Eur. J. Neurosci.* **10**, 2848–2855.

Sugiyama, H., Ito, I. and Hirono, C. (1987) A new type of glutamate receptor linked to inositol phospholipid metabolism. *Nature* **325**, 531–533.

Suzuki, K., Mori, N., Kittaka, H., Iwata, Y., Yamada, Y., Osonoe, K. and Niwa, S. (1996) Anticonvulsant action of metabotropic glutamate receptor agonists in kindled amygdala of rats. *Neurosci. Lett.* **204**, 41–44.

Swartz, K. J. and Bean, B. P. (1992) Inhibition of calcium channels in rat CA3 pyramidal neurons by a metabotropic glutamate receptor. *J. Neurosci.* **12**, 4358–4371.

Swartz, K. J., Merritt, A., Bean, B. P. and Lovinger, D. M. (1993) Protein kinase C modulates glutamate receptor inhibition of Ca2+ channels and synaptic transmission. *Nature* **361**, 165–168.

Tanabe, Y., Masu, M., Ishii, T., Shigemoto, R. and Nakanishi, S. (1992) A family of metabotropic glutamate receptors. *Neuron* **8**, 169–179.

Tang, E., Yip, P. K., Chapman, A. G., Jane, D. E. and Meldrum, B. S. (1997) Prolonged anticonvulsant action of glutamate metabotropic receptor agonists in inferior colliculus of genetically epilepsy-prone rats. *Eur. J. Pharmac.* **327**, 109–115.

Thomas, M. J. and O'Dell, T. J. (1995) The molecular switch hypothesis fails to explain the inconsistent effects of the metabotropic glutamate receptor antagonist MCPG on long-term potentiation. *Brain Res.* **695**, 45–52.

Thompson, S. W., Gerber, G., Sivilotti, L. G. and Woolf, C. J. (1992) Long duration ventral root potentials in the neonatal rat spinal cord in vitro; the effects of ionotropic and metabotropic excitatory amino acid receptor antagonists. *Brain Res.* **595**, 87–97.

Thompson, S. W., Woolf, C. J. and Sivilotti, L. G. (1993) Small-caliber afferent inputs produce a heterosynaptic facilitation of the synaptic responses evoked by primary afferent A-fibers in the neonatal rat spinal cord in vitro. *J. Neurophysiol.* **69**, 2116–2128.

Thomsen, C., Klitgaard, H., Sheardown, M., Jackson, H. C., Eskesen, K., Jacobsen, P., Treppendahl, S. and Suzdak, P. D. (1994) (S)-4-carboxy-3-hydroxyphenylglycine, an antagonist of metabotropic glutamate receptor (mGluR) 1a and an agonist of mGluR2, protects against audiogenic seizures in DBA/2 mice. *J. Neurochem.* **62**, 2492–2495.

Tizzano, J. P., Griffey, K. I., Johnson, J. A., Fix, A. S., Helton, D. R. and Schoepp, D. D. (1993) Intracerebral 1S,3R-1-aminocyclopentane-1,3-dicarboxylic acid (1S,3R-ACPD) produces limbic seizures that are not blocked by ionotropic glutamate receptor antagonists. *Neurosci. Lett.* **162**, 12–16.

Tizzano, J. P., Griffey, K. I. and Schoepp, D. D. (1995) Induction or protection of limbic seizures in mice by mGluR subtype selective agonists. *Neuropharmacology* **34**, 1063–1067.

Toms, N. J., Jane, D. E., Tse, H. W. and Roberts, P. J. (1995) Characterization of metabotropic glutamate receptor-stimulated phosphoinositide hydrolysis in rat cultured cerebellar granule cells. *Br. J. Pharmac.* **116**, 2824–2827.

Trujillo, K. A. and Akil, H. (1991) Inhibition of morphine tolerance and dependence by the NMDA receptor antagonist MK-801. *Science* **251**, 85–87.

Trullas, R. and Sholnick, P. (1990) Functional antagonists at the NMDA receptor complex exhibit antidepressant actions. *Eur. J. Pharmac.* **185**, 1–10.

Turski, L., Bressler, K., Rettig, K. J., Loschmann, P. A. and Wachtel, H. (1991) Protection of substantia nigra from MPP+ neurotoxicity by N-methyl-D-aspartate antagonists [see comments]. *Nature* **349**, 414–418.

Ugolini, A., Corsi, M. and Bordi, F. (1997) Potentiation of NMDA and AMPA responses by group 1 mGluR in spinal cord motoneurons. *Neuropharmacology* **36**, 1047–1055.

Valerio, A., Paterlini, M., Boifava, M., Memo, M. and Spano, P. (1997a) Metabotropic glutamate receptor mRNA expression in rat spinal cord. *Neuroreport* **8**, 2695–2699.

Valerio, A., Rizzonelli, P., Paterlini, M., Moretto, G., Knopfel, T., Kuhn, R., Memo, M. and Spano, P. (1997b) mGluR5 metabotropic glutamate receptor distribution in rat and human spinal cord: a developmental study. *Neurosci. Res.* **28**, 49–57.

Verkhratsky, A. and Kettenmann, H. (1996) Calcium signalling in glial cells. *Trends Neurosci.* **19**, 346–352.

Vickery, R. M., Morris, S. H. and Bindman, L. J. (1997) Metabotropic glutamate receptors are involved in long-term potentiation in isolated slices of rat medial frontal cortex. *J. Neurophysiol.* **78**, 3039–3046.

Vidnyánszky, Z., Hámori, J., Négyessy, L., Rüegg, D., Knöpfel, T., Kuhn, R. and Görcs, T. J. (1994) Cellular and subcellular localization of the mGluR1a metabotropic glutamate receptor in rat spinal cord. *NeuroReport* **6**, 209–213.

Wang, X. F. and Daw, N. W. (1996) Metabotropic glutamate receptors potentiate responses to NMDA and AMPA from layer V cells in rat visual cortex. *J. Neurophysiol.* **76**, 808–815.

Wang, Y., Rowan, M. J. and Anwyl, R. (1995) (RS)-alpha-Methyl-4-carboxyphenylglycine inhibits long-term potentiation only following the application of low frequency stimulation in the rat dentate gyrus in vitro. *Neurosci. Lett.* **197**, 207–210.

Watkins, J. and Collingridge, G. (1994) Phenylglycine derivatives as antagonists of metabotropic glutamate receptors. *Trends Pharmac. Sci.* **15**, 333–342.

Wigmore, M. A. and Lacey, M. G. (1998) Metabotropic glutamate receptors depress glutamate-mediated synaptic input to rat midbrain dopamine neurones in vitro. *Br. J. Pharmac.* **123**, 667–674.

Willis, W. D. and Westlund, K. N. (1997) Neuroanatomy of the pain system and of the pathways that modulate pain. *J. Clin. Neurophysiol.* **14**, 2–31.

Wilsch, V. W., Behnisch, T., Jager, T., Reymann, K. G. and Balschun, D. (1998) When are class I metabotropic glutamate receptors necessary for long-term potentiation? *J. Neurosci.* **18**, 6071–6080.

Womble, M. D. and Moises, H. C. (1994) Metabotropic glutamate receptor agonist ACPD inhibits some, but not all, muscarinic-sensitive K+ conductances in basolateral amygdaloid neurons. *Synapse* **17**, 69–75.

Woolf, C. J. (1983) Evidence for a central component of post-injury pain hypersensitivity. *Nature* **306**, 686–688.

Woolf, C. J. and Wall, P. D. (1986) Relative effectiveness of C primary afferent fibers of different origins in evoking a prolonged facilitation of the flexor reflex in the rat. *J. Neurosci.* **6**, 1433–1442.

Yamamoto, T. and Yaksh, T. L. (1992) Comparison of the antinociceptive effects of pre- and posttreatment with intrathecal morphine and MK801, an NMDA antagonist, on the formalin test in the rat. *Anesthesiology* **77**, 757–763.

Young, M. R., Fleetwood-Walker, S. M., Mitchell, R. and Munro, F. E. (1994) Evidence for a role of metabotropic glutamate receptors in sustained nociceptive inputs to rat dorsal horn neurons. *Neuropharmacology* **33**, 141–144.

Young, M. R., Fleetwood-Walker, S. M., Mitchell, R. and Dickinson, T. (1995) The involvement of metabotropic glutamate receptors and their intracellular signalling pathways in sustained nociceptive transmission in rat dorsal horn neurons. *Neuropharmacology* **34**, 1033–1041.

Young, M. R., Fleetwood-Walker, S. M., Dickinson, T., Blackburn-Munro, G., Sparrow, H., Birch, P. J. and Bountra, C. (1997) Behavioural and electrophysiological evidence supporting a role for group I metabotropic glutamate receptors in the mediation of nociceptive inputs to the rat spinal cord. *Brain Res.* **777**, 161–169.

Yu, S. P., Sensi, S. L., Canzoniero, L. M., Buisson, A. and Choi, D. W. (1997) Membrane-delimited modulation of NMDA currents by metabotropic glutamate receptor subtypes 1/5 in cultured mouse cortical neurons. *J. Physiol. (Lond.)* **499**, 721–732.

EXHIBIT I

THE JOURNAL OF BIOLOGICAL CHEMISTRY
Vol. 271, No. 45, Issue of November 8, pp. 28612–28616, 1996
Printed in U.S.A.

Metabotropic Glutamate Receptor 5 Is a Disulfide-linked Dimer*

(Received for publication, August 16, 1996)

Carmelo Romano‡§¶, Wan-Lin Yang§, and Karen L. O'Malley§

From the Departments of ‡Ophthalmology and Visual Sciences and §Anatomy and Neurobiology, Washington University School of Medicine, St. Louis, Missouri 63110

The sequences of the metabotropic glutamate receptors (mGluRs) show little homology with other members of the G protein-coupled receptor family and exhibit several distinctive features, including a large N-terminal extracellular domain with 17 cysteines in conserved positions. Here we demonstrate that mGluR5, as well as other mGluRs, behave as species approximately twice as large as expected from their sequence, but reducing conditions cause a decrease to the predicted molecular mass. Co-immunoprecipitation experiments using wild type and epitope-tagged receptors demonstrate that this is due to specific, disulfide-dependent dimerization of the receptor. The intermolecular disulfide that mediates dimerization occurs in the extracellular domain, within about 17 kDa from the N terminus.

Glutamate is the primary neurotransmitter for excitatory neurotransmission in the vertebrate central nervous system and as such is responsible for a broad range of physiological and pathophysiological roles. These include transmission in sensory pathways, higher brain functions such as learning and memory, and cytotoxicity and neuronal death.

Two classes of receptors for glutamate are present on neural cells: the ionotropic glutamate receptors (iGluRs)[1] and the metabotropic glutamate receptors (mGluRs). The iGluRs are ligand-gated cation channels, and they mediate rapid synaptic transmission. The iGluRs include the *N*-methyl-D-aspartate, α-amino-3-hydroxy-5-methyl-4-isoxazole propionic acid, and kainic acid families of receptors. At least eight mGluRs have been molecularly characterized, and these activate effectors via interactions with heterotrimeric G proteins (1). Thus, the mGluRs are important for neuromodulatory functions, although mGluRs clearly mediate transmission at the retinal photoreceptor-depolarizing bipolar cell synapse (2–4) and at certain thalamic sensory neurons (5).

Although the mGluRs possess seven transmembrane domains, there are important differences between these receptors and other G protein-coupled receptors. There is no primary sequence similarity between the mGluRs and the rhodopsin-like receptors (4). The recently described Ca^{2+}-sensing receptors are homologous to the mGluRs (6, 7); so together the Ca^{2+} and glutamate receptors appear to constitute a unique subgroup of this supergene family. Receptor domains responsible for signal transduction also appear different. For example, the third intracellular loop is important for determining the specificity of G protein coupling in most G protein-coupled receptors examined, whereas the C-terminal end of the second intracellular loop is critical in the mGluRs (8–10). Moreover, all mGluRs have a very large N-terminal extracellular domain (about 65 kDa in mGluR5), constituting about one-half of the protein, whereas most G protein-coupled receptors do not. The glutamate binding domain is believed to lie in this extracellular region (11, 12), not within the bundle of membrane-spanning domains, as is typical of the rhodopsin-like receptors.

Another unique structural feature is that there are 21 conserved cysteine residues in all the mGluRs (13). Nineteen of these are in the N-terminal domain and extracellular loops. Nine of the cysteines are at the C-terminal portion of the extracellular domain, and this region has been compared with similar cysteine-rich domains of receptor tyrosine kinases (12). Although the function of these cysteines is unknown, the strict conservation of position implies that the function is a shared and important one for this family of receptors.

Although native iGluRs are thought to function as heteromeric pentamers (14–16), the mGluRs, by analogy with other G protein-coupled receptors, have been assumed to be monomeric (1, 4, 17). However, this has not been directly demonstrated. Using biochemical and molecular techniques, here we demonstrate that mGluRs are not monomeric but are instead covalently linked dimers, bound by disulfide bonds between conserved cysteines in the N-terminal extracellular domain.

EXPERIMENTAL PROCEDURES

Antibodies, Western blots, and Immunoprecipitates—Antibodies to wild type (wt) mGluR5 were affinity-purified antipeptide antibodies raised against an immunogen that contained the C-terminal 13 amino acids as described (18). Antibodies to wt mGluR1a were affinity-purified antipeptide antibodies raised against an immunogen that contained the sequence of residues 1116–1130 (*i.e.* EFVYEREGNTEEDEL) of the rat mGluR1a (19). Both monoclonal and polyclonal anti-hemagglutinin (HA) antibodies were obtained from Babco (Berkeley, CA); the polyclonal antibody was used for immunoprecipitation, the monoclonal antibody for Western blots and immunocytochemistry. Antibodies to mGluR2–3 and mGluR4 were the generous gift of Dr. Thomas Knoepfel (CIBA, Basel, Switzerland). Preparation of brain tissue, electrophoresis (on 6 or 7.5% polyacrylamide gels), and transfers onto polyvinylidene difluoride membranes (Immobilon P; Millipore, Waters, MA) were as described (18). For preparation of membranes from transfected cells, cells were washed once in PBS, then subjected to one freeze-thaw cycle. They were scraped into lysis buffer (2 mM HEPES and 2 mM EDTA, pH 7.4, containing protease inhibitors) and homogenized in a glass homogenizer with a motorized Teflon pestle. The nuclear pellet (1000 × *g*, 5 min) was discarded, and membranes were harvested after pelletting (35,000 × *g*, 30 min). For immunoprecipitations, membranes were homogenized in PBS containing 0.5 or 1% SDS. The SDS extract was diluted 5- or 10-fold into PBS containing 0.5% dodecyl maltoside to sequester free SDS into mixed micelles, thereby permitting immunoprecipitation. Antireceptor antibody was added, and

* This work was supported in part by National Institutes of Health Grants AG11355, EY02687, EY09370, an unrestricted grant from Research to Prevent Blindness, and the McDonnell Center for Cellular and Molecular Neuroscience. The costs of publication of this article were defrayed in part by the payment of page charges. This article must therefore be hereby marked "*advertisement*" in accordance with 18 U.S.C. Section 1734 solely to indicate this fact.

¶ To whom correspondence should be addressed: Dept. of Ophthalmology and Visual Sciences, Washington University School of Medicine, 660 South Euclid Ave., St. Louis, MO 63110. Tel.: 314-362-2676; Fax: 314-362-3638; E-mail: romano@am.seer.wustl.edu.

[1] The abbreviations used are: iGluR, ionotropic glutamate receptor; mGluR, metabotropic glutamate receptor; wt, wild type; HA, hemagglutinin; tHA, truncated HA; PBS, phosphate-buffered saline; DTT, dithiothreitol; PBP, periplasmic binding protein.

the mixture was incubated at 4 °C overnight. Protein A-Sepharose (Sigma) was added, and the incubation continued for 2 h at room temperature on a rocking table. The protein A pellets were washed three times with PBS before elution with sample buffer and electrophoresis. The sample buffer always contained 2% SDS and, when indicated, 20 mM dithiothreitol (DTT). Samples were heated at 60 °C for 3 min before electrophoresis.

Receptors and Cells—The cDNA fragments containing the full-length mGluR5 or mGluR1a coding sequences were ligated into pcDNA1neo (Invitrogen) downstream of the cytomegalovirus promoter (18). The HA-tagged mGluR5 mutant was constructed using recombinant polymerase chain reaction (20) with two sets of primer pairs. The first set (5′-CATGACGACCTTCGCAGAGAT-3′, nucleotides 3482 to 3501, GenBank accession number D10891; and 5′-ATCCTCTCCCAAATATGACACTTATCCATATGATGTTCCAGATTATGCT-3′, nucleotides 3720–3741 followed by the HA epitope in bold) and the second (5′-**TATCCATATGATGTTCCAGATTATGCTTGAGCCACT**-GGAAACTTCCCT-3′, representing the HA epitope in bold followed by nucleotides 3781–3801; and 5′-CACACACGGTGGAGACATGAGCGGCCGCTAAA, nucleotides 3897–3918 followed by a *Not*I restriction site) were used to amplify DNA fragments of 286 or 164 base pairs from wt-mGluR5. Both fragments were used as templates in another round of polymerase chain reactions using the two flanking primers, and the resulting fragments were then used to replace wt sequences in mGluR5. tHA was constructed using HA-tagged mGluR5 as a template together with primer sets fusing sequences within the first intracellular domain in frame with those of the HA-tagged C terminus. The 5′-primer set included 5′-GAAGTCAGCTGTTGTTGG-3′ (identical to nucleotides 1843–1860) as well as 5′-CGAGTCCACCGAGTCTCTAGACTTGACCACCGGAGT-3′ (complementary to nucleotides 2083–2097 and 3685–3668). The 3′-primer set consisted of the complement of the latter primer together with the *Not*I restriction site-containing primer described above. First and second round polymerase chain reaction was performed as described. The final product was digested with *Bst*EII and *Not*I and then subcloned into wt-mGluR5 cut with the same enzymes. The resulting plasmid was termed tHA. Both the HA-tagged mGluR5 and tHA were confirmed by sequencing.

HEK cells at 80% confluency were transfected with 15 μg of plasmid DNA using LipofectAMINE (Life Technologies, Inc). Forty-eight hours later membranes were prepared and immunoprecipitated with the indicated antibodies as described above. Immunohistochemical analysis of cotransfected cells was done on Lab-Tek chambered glass slides. Primary antibodies included the HA monoclonal antibody and anti-wt-mGluR5, followed by fluorescein isothiocyanate-labeled goat anti-mouse and CY3-labeled goat anti-rabbit (Jackson ImmunoResearch Labs, Inc.) secondary antibodies, respectively.

RESULTS

Metabotropic Glutamate Receptors Migrate at about Twice Their Predicted Molecular Mass under Nonreducing Conditions—To examine the possible structural or conformational roles of the conserved cysteines in mGluRs, the electrophoretic mobility of mGluR5 (from rat cortical membranes) was examined under reducing and nonreducing conditions in SDS gels (Fig. 1*A*). In the presence of the reducing agent DTT or 2-mercaptoethanol (not shown), mGluR5 migrated at an apparent molecular mass of ~148 kDa. Deglycosylation with peptide *N*-glycosidase F reduced this to ~130 kDa (not shown), consistent with the size predicted from the primary sequence. However, in the absence of reducing agent, mGluR5 migrated at an apparent molecular mass of ~260 kDa (Fig. 1*A*). Because samples were prepared in the presence of the denaturing detergent, 2% SDS, most noncovalent interactions should have been eliminated.

One interpretation of this result is that mGluR5 is covalently attached by intermolecular disulfide bonds to another component of the membrane, but other possibilities must be considered. A different electrophoretic mobility in the presence of reducing agents may reflect an altered conformation due to cleavage of intramolecular disulfide bonds. However, such bonds usually promote compact structures that on reduction increase the Stokes radius and, hence, increase the apparent molecular mass of the protein. Another possibility is that spurious disulfide bonds may form between free sulfhydryls during SDS denaturation of the protein, leading to artifactual covalent association of mGluR5 with another protein. To test this, membranes were treated with iodoacetate to alkylate free sulfhydryls and then solubilized with SDS (Fig. 1*A*, *right lane*). The receptor still behaved as a high molecular mass species, indicating that the disulfide bonds responsible for holding this species together were present prior to solubilization, as part of the native structure (Fig. 1*A*).

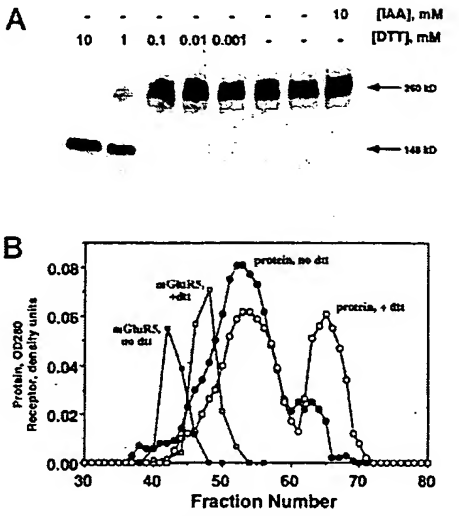

FIG. 1. **mGluRs have a high apparent molecular mass under nonreducing conditions.** *A*, Western blot analysis of rat cortical membranes (25 μg of protein/lane) using an antibody directed to the C terminus of wild type mGluR5. DTT caused the receptor to shift to a lower apparent molecular mass. Pretreatment of the membranes with iodoacetate (*IAA*) did not alter the apparent molecular mass. *B*, Sephacryl S-400 column chromatography of SDS-solubilized rat brain membranes in the presence or absence of DTT indicate that mGluR5 migrates as a lower molecular mass species in the presence of DTT. Protein was measured spectroscopically (*OD280*), and mGluR5 was detected by assaying every other fraction by Western blotting. Column dimensions, 75 × 1.5 cm.

To verify this reduction-dependent alteration in molecular mass by an independent technique, Sephacryl S-400 gel filtration chromatography in the presence of SDS was used. For this experiment cortical membranes (2 mg of protein) were dissolved in PBS containing 1% SDS (±10 mM DTT), which also served as column buffer. Reduction led to a large decrease in apparent molecular mass of the receptor (Fig. 1*B*). Taken together, these results indicate that mGluR5 is covalently attached via disulfide bonds to another component(s) of the membrane.

This molecular mass shift was not unique to mGluR5. Under nonreducing conditions mGluR1a (another group 1 mGluR), mGluR2–3 (a Group 2 mGluR) and mGluR4 (a Group 3 mGluR) all migrated as species about twice as large as expected, with reduction causing a shift to the appropriate molecular mass (data not shown).

Metabotropic Glutamate Receptors Are Dimers under Nonreducing Conditions—What is the nature of the molecule to which mGluR5 is attached? The receptor may be bound by disulfide bridges to a distinct molecule; therefore, the high molecular mass species would be heteromeric, or alternatively, the receptor may be a homodimer.

When mGluR5 was expressed in HEK cells, it migrated as the high molecular mass form in nonreducing gels (not shown); this indicated that either the receptor forms homodimers, or that HEK cells endogenously express the mGluR5-associated protein. To determine which of these hypotheses is correct,

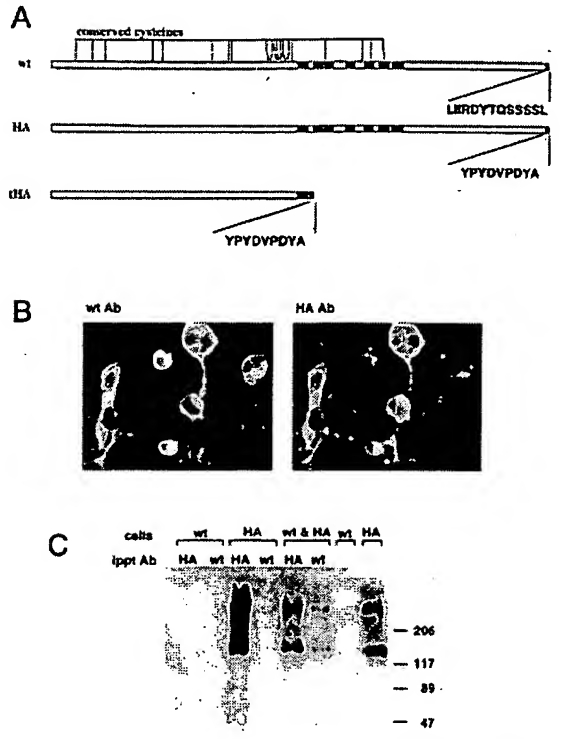

FIG. 2. **Co-immunoprecipitation of wt and epitope-tagged receptors.** *A*, schematic representations of wt, HA-tagged, and tHA mGluR5 receptors. Putative transmembrane domains are shown in *black*, and positions of the 21 conserved cysteine residues are indicated. The amino acid sequences of wt and HA epitopes present at the C termini of the receptors are shown. *B*, HEK 293 cells co-transfected with both HA-tagged and wt mGluR5, labeled with antibodies (*Ab*) to wt (*left panel*) or HA-tagged (*right panel*) mGluR5. The same population of cells are labeled. *C*, mGluRs form dimers. Membranes from cells expressing HA-mGluR5, wt-mGluR5, or both were treated with SDS and immunoprecipitated with HA polyclonal or wt antibodies (*ippt Ab*). Precipitated products were reduced using 20 mM DTT and resolved on a 6% SDS-polyacrylamide gel. Separated products were transferred to a polyvinylidene difluoride membrane and probed with anti-HA monoclonal antibody followed by enhanced chemiluminescence. Molecular mass markers are shown on the *right*. Antibody to the wt receptor immunoprecipitated HA receptor from cotransfected cells, indicating that heterodimerization occurred.

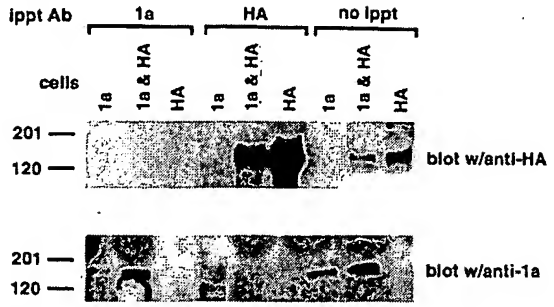

FIG. 3. **mGluR1a and mGluR5 do not form heterodimers.** Membranes from cells expressing wt-mGluR1a (*1a*), HA-mGluR5 (*HA*), or both (*1a & HA*), were treated with SDS and immunoprecipitated with anti-mGluR1a (*1a*) or anti-HA (*HA*) polyclonal antibodies. Precipitated products were reduced using 20 mM DTT and resolved on a 6% SDS-polyacrylamide gel. Separated products were transferred to a polyvinylidene difluoride membrane, and the blots probed with anti-HA monoclonal (*top blot*) or anti-mGluR1a polyclonal (*bottom blot*) antibodies followed by enhanced chemiluminescence. Molecular mass markers are shown on the *left* (201 and 120 kDa). Antibody to the mGluR1a precipitated mGluR1a, but not HA-mGluR5, and anti-HA immunoprecipitated HA-mGluR5, but not mGluR1a. Aliquots of each cell extract (no immunoprecipitation) are in the *right three lanes* on each gel. *ippt AB*, immunoprecipitation antibody.

cross-immunoprecipitation experiments were performed. A plasmid encoding an mGluR5 epitope tagged at the C terminus was constructed. Because the antibody we have used to recognize wt mGluR5 is directed toward the C terminus (18), the nucleotides coding for the wt C terminus were removed and replaced by the sequence encoding the HA epitope (Fig. 2A; Ref. 21). After expression in HEK cells, HA-mGluR5 also behaved as a high molecular mass species in nonreducing gels, indicating that alteration of the C terminus did not disrupt formation of the disulfide-bound complex (not shown). If the receptors form covalent homodimers, some of the wt-mGluR5 and HA-mGluR5 may be expected to be found in the same dimer when both receptors are expressed in the same cell. If, however, each receptor is bound to an unidentified, distinct molecule to form the high molecular mass form, no wt-mGluR5-HA-mGluR5 heterodimers should be found.

Transient transfection of HEK cells with both plasmids led to uptake and expression of both receptors in the same individual cells (Fig. 2*B*). Membranes prepared from the cotransfected cells were solubilized in 0.5% SDS to disrupt noncovalent interactions between proteins. As expected, anti-wt did not immunoprecipitate any HA-tagged proteins from cells expressing only HA-mGluR5 (Fig. 2*C*), nor did anti-HA bring down wt-mGluR5 (data not shown). However, HA-mGluR5 was immunoprecipitated from extracts of cotransfected cells by either anti-HA or anti-wt antibody (Fig. 2*C*). Moreover, wt-mGluR5 was also immunoprecipitated from these extracts when either antibody was used (not shown). Thus, these data indicate that mGluR5 polypeptides form dimers.

To determine the specificity of dimer formation, we performed an analogous experiment in which wild type mGluR1a was cotransfected with HA-mGluR5. If the assembly of mGluR dimers is specific, mGluR1a and HA-mGluR5 should not form heterodimers. As shown in Fig. 3, antibody selective for mGluR1a did not immunoprecipitate any HA-containing bands from cells transfected with mGluR1a, mGluR1a and HA-mGluR5, or HA-mGluR5 (Fig. 3, *top gel, left three lanes*), but it did immunoprecipitate mGluR1 from cells transfected with mGluR1a or mGluR1a and HA-mGluR5 (Fig. 3, *bottom gel, left two lanes*). Similarly, the antibody selective for HA did not immunoprecipitate any mGluR1a from cells transfected with mGluR1a, mGluR1a and HA-mGluR5, or HA-mGluR5, but it did immunoprecipitate HA-mGluR5 from cells transfected with HA-mGluR5 or HA-mGluR5 and mGluR1a. Thus, despite the 60% amino acid identity between mGluR1a and mGluR5, (22), they do not heterodimerize. These data indicate that there is great specificity in the assembly of the metabotropic receptor dimers.

Metabotropic Glutamate Receptors Are Linked via Their N-terminal Extracellular Domains—To localize which part of mGluR5 was involved in dimer formation, two types of experiments were performed.

In the first set of experiments, a mutant receptor, truncated after the first transmembrane domain and tagged with the HA epitope at the C terminus, was constructed (tHA; Fig. 2*A*). When this mutant receptor was expressed in HEK cells and immunoprecipitated with anti-HA, it migrated during electrophoresis as a dimer (160 kDa) under nonreducing conditions and as a monomer (doublet of 80–90 kDa) under reducing conditions (Fig. 4*A*). Therefore, the locus for disulfide-mediated dimerization is in the N-terminal half of the receptor, most of which is extracellular.

When the tHA receptor was co-expressed with wt-mGluR5 and then immunoprecipitated with antibody to HA, an additional HA-containing band (220 kDa) was observed on the

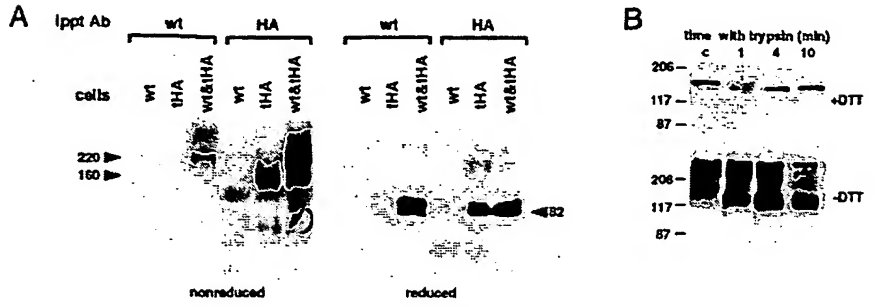

FIG. 4. **The disulfide bond responsible for dimerization is in the N-terminal region of mGluR5.** *A*, Western blot analysis of immunoprecipitates (*ippt Ab*) from SDS-solubilized membranes prepared from cells expressing wt, tHA, or both, using monoclonal anti-HA to visualize the immunoreactive bands. Antibody to the wt receptor did not immunoprecipitate any HA-positive bands from cells expressing only wt or tHA receptors but did precipitate the 220-kDa band present in co-transfected cells. Antibody to HA immunoprecipitated the 160-kDa band from tHA-expressing cells and both 220- and 160-kDa proteins from co-transfected cells. On reducing gels, all immunoprecipitated bands behaved as monomers. *B*, intact HEK cells expressing wt mGluR5 were treated with trypsin (standard 0.05% trypsin and 0.53 mM EDTA in Hank's balanced salt solution from Life Technologies, Inc.) for the times indicated, and then membranes were prepared and electrophoresed under reduced and nonreduced conditions. Trypsin treatment led to a ~17-kDa decrease in the apparent molecular mass of the monomer (reduced, *top*), and a loss of dimerization (nonreduced, *bottom*).

nonreduced gels, suggesting the formation of heterodimers between truncated-HA and wt receptors (Fig. 4*A*). In agreement with this interpretation, antibody to the wt receptor immunoprecipitated the 220-kDa heterodimer, but not the 160-kDa tHA homodimer, from cotransfected cells. The wt antibody did not precipitate any HA-containing species from cells transfected with only the wt or tHA mutant. Taken together, these results indicate that the truncated receptor forms both homodimers and heterodimers.

In the second experiment addressing location of the disulfide bond(s), intact HEK cells expressing the wt receptor were incubated with trypsin for various periods. We reasoned that proteolytic removal of all or part of the extracellular domain would generate a receptor fragment that does not dimerize, and from the size of this fragment we could infer the approximate location of the relevant cysteine(s). Since the wt antibody is directed toward the C terminus, all the proteolysis products observed will necessarily have intact C termini and loss of some length of the N terminus. Treatment with trypsin removed only a small fragment from the N terminus of the receptor, decreasing the apparent molecular mass by about 17 kDa (Fig. 4*B*, *+DTT*). This very limited digestion suggests that access of the protease to potential cleavage sites was restricted by steric factors due to the secondary structure of the extracellular domain. However, even very short periods of proteolysis removed the site of dimerization, since the proteolyzed receptor migrated at the monomer molecular mass under nonreducing conditions (Fig. 4*B*, *−DTT*). These results indicate that the cysteine(s) responsible for disulfide bond formation are in the N-terminal 17 kDa of mGluR5.

DISCUSSION

The experiments described here clearly show that mGluR5 normally exists as a dimer on the plasma membrane. Dimerization is mediated via a cysteine or cysteines located within 17 kDa from the N terminus in the extracellular domain. Since heterodimers between mGluR5 and mGluR1a do not form, but the truncated mGluR5 containing only the extracellular region and one transmembrane domain does dimerize, the information providing the specificity of mGluR5 dimerization also resides in the N-terminal region of the molecule. Because mGluR1a, 2–3 and 4 also migrate as dimeric species, we propose that dimerization may be a general property of the mGluR family.

Several authors who have examined mGluRs using Western blot analysis have noted the presence of high molecular mass aggregated forms of the receptors (23, 24), even in the presence of reducing agents. In the most extreme cases these aggregates are so large that the receptor polypeptides do not enter the gel. This aggregation may reflect strong interactions among the denatured, highly hydrophobic, multiple transmembrane domains in mGluRs. In our hands, aggregation is avoided by heating samples minimally before electrophoresis (60 °C, 3 min) and by using only SDS or dodecyl maltoside as solubilizing detergents. We believe the dimer we describe is the native form of the receptor and not an artifact because: 1) it is a discrete band with a characteristic and appropriate molecular mass and not a smear, as aggregates usually are; 2) it can be converted to the monomer by reducing agents, whereas mGluR aggregates cannot; 3) even under conditions that minimize aggregation, as described above, we never observed any monomer except when samples were reduced (or proteolyzed as in Fig. 3*B*), suggesting that all the receptor is initially present in the membrane as dimer; and 4) the truncated mutant (tHA), which contains only a single transmembrane domain and, hence, should exhibit little tendency to aggregate, also migrated as a dimer (Fig. 3*A*).

To date, there is no evidence that other G protein-coupled receptors exist as covalent dimers. The α1-adrenergic receptor of the rat ventricle behaves as a 77-kDa species in the presence or absence of DTT (25). Similarly, the electrophoretic mobility of the neuromedin B receptor is unaffected by DTT (26). A cholecystokinin receptor and an opioid receptor apparently increase in molecular mass when treated with DTT (27, 28), suggesting that disulfide bonds are maintaining compact conformations of these polypeptides. It is unlikely, therefore, that covalent, disulfide-dependent dimerization is a universal feature of G protein-coupled receptors. This structural feature may be unique to the mGluRs and perhaps the related Ca^{2+}-sensing receptors (6, 7). It is worth noting that the Ca^{2+}-sensing receptors do have the conserved cysteines characteristic of this subgroup.

The N-terminal extracellular domain of the mGluRs is related to the bacterial periplasmic binding proteins (PBPs) (12), as are extracellular domains of some iGluRs (12, 29). PBPs constitute a family of proteins involved in high affinity transport of amino acids, sugars, and other nutrients into bacteria. Three-dimensional crystal structures reported for several PBPs have indicated that these proteins are composed of two distinct globular domains with a ligand binding cleft between them (30, 31). Recently, O'Hara *et al.* (12) proposed a three-dimensional model of the structure of mGluR1a based on PBP structural information. Their alignment permitted them to

make several successful predictions concerning the glutamate binding site of the receptor, lending credence to the structural comparison. Our results indicate that the cysteine responsible for dimerization of mGluR5 is in the N-terminal 17 kDa. Within this region, there are four cysteines, all but one of which is conserved among the mGluRs. Based on the alignment of mGluRs and PBPs suggested by O'Hara *et al.* (12), it is conceivable that two of these cysteines are involved in intramolecular disulfides, leaving the remaining cysteine(s) available for intermolecular interactions.

Receptors with intracellular tyrosine kinase domains dimerize on ligand binding, and this is critical for signal transduction (32–34). Our evidence suggests that the cysteines responsible for mGluR dimerization are not those present in the cysteine-rich tyrosine kinase receptor-like domain (12). Dimerization of tyrosine kinase receptors brings the monomeric receptors into close proximity, allowing each member of the pair to phosphorylate the other, thereby providing the binding sites necessary for initiating assembly of the signal-transducing apparatus on the intracellular face of the membrane. These active tyrosine kinase receptor dimers are linked noncovalently, whereas mGluR dimers are covalently bound.

Earlier studies of adrenergic receptors emphasized the role of two disulfide-linked, conserved cysteine residues in the first and second extracellular loops. For example, in the mammalian β_2-adrenergic receptor maintenance of this extracellular disulfide bridge is important for high affinity agonist binding and function (35, 36). In contrast, DTT had no effect on binding of ligands to muscarinic receptors (37) or prostaglandin E_2 receptors (38) but potentiated binding to and functioning of H1 histamine receptors (39–42). Therefore, one cannot predict *a priori* what effect reducing conditions will have on receptor functioning. We have preliminary results indicating that maintenance of extracellular disulfides of mGluR5 are critically important for maintenance of signal transduction through this receptor.[2] Consistent with this result, Vignes *et al.* (43) showed that inositol phosphate production stimulated by glutamate in synaptoneurosomes was blocked by DTT, whereas that stimulated by carbachol was not. It is interesting that *N*-methyl-D-aspartate receptors are influenced oppositely by redox state: extracellular reduction leads to potentiation of receptor function, not inhibition (44–46). Perhaps ambient redox conditions lead to a complementary and coordinate regulation of iGluRs and mGluRs.

Acknowledgments—We thank U. Khosla, P. Gehlbach, S. Smout, S. Harmon, and M. Moffat for assistance at different phases of this work, Prof. S. Nakanishi for the mGluR5 and mGluR1a clones, and Peter Lukasiewicz and David Harris for comments on the manuscript.

REFERENCES

1. Pin, J.-P., and Duvoisin, R. (1995) *Neuropharmacology* **34**, 1–26
2. Ishii, T., Moriyoshi, K., Sugihara, H., Sakurada, K., Kadotani, H., Yokoi, M., Akazawa, C., Shigemoto, R., Mizuno, N., Masu, M., and Nakanishi, S. (1993) *J. Biol. Chem.* **268**, 2836–2843
3. Nomura, A., Shigemoto, R., Nakamura, Y., Okamoto, N., Mizuno, N., and Nakanishi, S. (1994) *Cell* **77**, 361–369
4. Nakanishi, S. (1994) *Neuron* **13**, 1031–1037
5. Eaton, S. A., Birse, E. F., Wharton, B., Sunter, D. C., Udvarhelyi, P. M., Watkins, J. C., and Salt, T. E. (1993) *Eur. J. Neurosci.* **5**, 186–189
6. Brown, E. M., Gamba, G., Riccardi, D., Lombardi, M., Butters, R., Kifor, O., Sun, A., Hediger, M. A., Lytton, J., and Hebert, S. C. (1993) *Nature* **366**, 575–580
7. Ruat, M., Molliver, M. E., Snowman, A. M., and Snyder, S. H. (1995) *Proc. Natl. Acad. Sci. U. S. A.* **92**, 3161–3165
8. Pin, J. P., Joly, C., Heinemann, S. F., and Bockaert, J. (1994) *EMBO J.* **13**, 342–348
9. Pin, J. P., Gomeza, J., Joly, C., and Bockaert, J. (1995) *Biochem. Soc. Trans.* **23**, 91–96
10. Gomeza, J., Joly, C., Kuhn, R., Knopfel, T., Bockaert, J., and Pin, J. P. (1996) *J. Biol. Chem.* **271**, 2199–2205
11. Takahashi, K., Tsuchida, K., Tanabe, Y., Masu, M., and Nakanishi, S. (1993) *J. Biol. Chem.* **268**, 19341–19345
12. O'Hara, P. J., Sheppard, P. O., Thqgersen, H., Venezia, D., Haldeman, B. A., McGrane, V., Houamed, K. M., Thomsen, C., Gilbert, T. L., and Mulvihill, E. R. (1993) *Neuron* **11**, 41–52
13. Tanabe, Y., Masu, M., Ishii, T., Shigemoto, R., and Nakanishi, S. (1992) *Neuron* **8**, 169–179
14. Wenthold, R. J., Yokotani, N., Doi, K., and Wada, K. (1992) *J. Biol. Chem.* **267**, 501–507
15. Hollmann, M., and Heinemann, S. (1994) *Annu. Rev. Neurosci.* **17**, 31–108
16. Wisden, W., and Seeburg, P. H. (1993) *Curr. Opin. Neurobiol.* **3**, 291–298
17. Nakanishi, S. (1992) *Science* **258**, 597–603
18. Romano, C., Sesma, M. A., Macdonald, C., O'Malley, K., van den Pol, A. N., and Olney, J. W. (1995) *J. Comp. Neurol.* **355**, 455–469
19. Masu, M., Tanabe, Y., Tsuchida, K., Shigemoto, R., and Nakanishi, S. (1991) *Nature* **349**, 760–765
20. Higuchi, R. (1990) in *PCR Protocols: A Guide to Methods and Applications* (Innis, M. A, Gelfand, D. H., Sninsky, J. J., and White, T. J, eds) pp. 177–183, Academic Press, San Diego, CA
21. Kolodzei, P. A., and Young, R. A. (1991) *Methods Enzymol.* **194**, 508–519
22. Abe, T., Sugihara, H., Nawa, H., Shigemoto, R., Mizuno, N., and Nakanishi, S. (1992) *J. Biol. Chem.* **267**, 13361–13368
23. Baude, A., Nusser, Z., Roberts, J. D., Mulvihill, E., McIlhinney, R. A., and Somogyi, P. (1993) *Neuron* **11**, 771–787
24. Petralia, R. S., Wang, Y.-X., Niedzielski, A. S., and Wenthold, R. J. (1996) *Neuroscience* **71**, 949–976
25. Terman, B. I., and Insel, P. A. (1986) *J. Biol. Chem.* **261**, 5603–5609
26. Kusui, T., Benya, R. V., Battey, J. F., and Jensen, R. T. (1994) *Biochemistry* **33**, 12968–12980
27. Bone, E. A., and Rosenzweig, S. A. (1988) *Peptides* **9**, 373–381
28. Gioannini, T. L., Liu, Y. F., Park, Y. H., Hiller, J. M., and Simon, E. J. (1989) *J. Mol. Recog.* **2**, 44–48
29. Stern-Bach, Y., Bettler, B., Hartley, M., Sheppard, P. O., O'Hara, P. J., and Heinemann, S. F. (1994) *Neuron* **13**, 1345–1357
30. Quiocho, F. A. (1990) *Phil. Trans. R. Soc. Lond.* **326**, 341–351
31. Adams, M. D., and Oxender, D. L. (1989) *J. Biol. Chem.* **264**, 15739–15742
32. Heldin, C. H., Ernlund, A., Rorsman, C., and Ronnstrand, L. (1989) *J. Biol. Chem.* **264**, 8905–8912
33. Qian, X., LeVea, C. M., Freeman, J. K., Dougall, W. C., and Greene, M. I. (1994) *Proc. Natl. Acad. Sci. U. S. A.* **91**, 1500–1504
34. Earp, H. S., Dawson, T. L., Li, X., and Yu, H. (1995) *Breast Cancer Res. Treat.* **35**, 115–132
35. Dohlman, H. G., Caron, M. G., DeBlasi, A., Frielle, T., and Lefkowitz, R. J. (1990) *Biochemistry* **29**, 2335–2342
36. Noda, K., Saad, Y., Graham, R. M., and Karnik, S. S. (1994) *J. Biol. Chem.* **269**, 6743–6752
37. Wei, J. W., and Sulakhe, P. V. (1980) *Naunyn Schmiedebergs Arch. Pharmacol.* **314**, 51–59
38. Michalak, M., Wandler, E. L., Strynadka, K., Catena, R., Liu, H. J., and Olley, P. M. (1992) *Biochim. Biophys. Acta* **1111**, 247–255
39. Carman-Krzan, M. (1984) *Agents Actions* **14**, 561–565
40. Dickenson, J. M., and Hill, S. J. (1994) *Biochem. Pharmacol.* **48**, 1721–1728
41. Donaldson, J., and Hill, S. J. (1986) *Br. J. Pharmacol.* **87**, 191–199
42. Donaldson, J., and Hill, S. J. (1987) *Br. J. Pharmacol.* **90**, 263–271
43. Vignes, M., Guiramand, J., Sassetti, I., and Recasens, M. (1992) *Neurochem. Int.* **21**, 229–235
44. Tang, L. H., and Aizenman, E. (1993) *J. Physiol. (Lond.)* **465**, 303–323
45. Reynolds, I. J., Rush, E. A., and Aizenman, E. (1990) *Br. J. Pharmacol.* **101**, 178–182
46. Sucher, N. J., Wong, L. A., and Lipton, S. A. (1990) *Neuroreport* **1**, 29–32

[2] C. Romano, I. Saito, and K. L. O'Malley, unpublished observation.

THE JOURNAL OF BIOLOGICAL CHEMISTRY
Vol. 268, No. 26, Issue of September 15, pp. 19341-19345, 1993
Printed in U.S.A.

Role of the Large Extracellular Domain of Metabotropic Glutamate Receptors in Agonist Selectivity Determination*

(Received for publication, May 3, 1993, and in revised form, June 2, 1993

Katsu Takahashi, Kunihiro Tsuchida‡, Yasuto Tanabe, Masayuki Masu, and Shigetada Nakanishi§
From the Institute for Immunology, Kyoto University Faculty of Medicine, Kyoto 606, Japan

Metabotropic glutamate receptors consist of at least six different subtypes termed mGluR1–mGluR6. They belong to the family of G protein-coupled receptors and commonly possess an unusually large extracellular domain preceding the seven transmembrane segments. mGluR1 and mGluR2 show similar affinities for L-glutamate but distinct patterns in their responsiveness to quisqualate and *trans*-1-amino-1,3-cyclopentanedicarboxylate (tACPD). To assign structural determinants for the different agonist selectivities, we constructed a series of chimeric receptors at the extracellular domains of mGluR1 and mGluR2 and determined their agonist selectivities by measuring their electrophysiological responses to L-glutamate, quisqualate, and tACPD in *Xenopus* oocytes. Replacement of the extracellular domain up to about one-half of the amino-terminal extracellular domain of mGluR1 with the corresponding portion of mGluR2 generated a pattern of the agonist selectivity characteristic of mGluR2. The acquirement of this property in agonist selectivity was further indicated by the selective responses of these chimeric receptors to an mGluR2-specific agonist, (2*S*,1′*R*,2′*R*,3′*R*)-2-(2,3-dicarboxycyclopropyl)glycine. This investigation demonstrates that the extracellular domain of mGluR is critical in determining agonist selectivity and that the mode of determination of agonist selectivity of mGluR is different from that of other G protein-coupled receptors for small molecule transmitters.

Glutamate neurotransmission plays an important role in neuronal plasticity and neurotoxicity in the central nervous system (Choi and Rothman, 1990; Bliss and Collingridge, 1993). The diverse functions of glutamate neurotransmission are mediated by a variety of glutamate receptors that can be classified into two distinct groups termed ionotropic and metabotropic receptors (mGluRs)[1] on the basis of electrophysiological, pharmacological, and molecular studies (Nakanishi, 1992). Recent molecular studies have indicated that mGluRs consist of at least six different subtypes termed mGluR1–mGluR6 (Masu *et al.*, 1991; Houamed *et al.*, 1991; Tanabe *et al.*, 1992; Abe *et al.*, 1992; Nakajima *et al.*, 1993). The six mGluRs show a high degree of sequence homology within this receptor family but share no sequence similarity to conventional G protein-coupled receptors and possess a large extracellular domain preceding the seven putative transmembrane segments (Masu *et al.*, 1991; Nakanishi, 1992). Thus, mGluRs form a novel family of G protein-coupled receptors. The six mGluR subtypes can be subdivided into three subgroups according to their sequence homology, signal transduction, and agonist selectivities (Nakanishi, 1992). mGluR1 and mGluR5 are coupled to inositol trisphosphates (IP_3)/Ca^{2+} signal transduction and show a strong agonist selectivity to quisqualate (Masu *et al.*, 1991; Aramori and Nakanishi, 1992; Abe *et al.*, 1992). The other four mGluR subtypes are linked to the inhibitory cyclic AMP cascade, but the agonist selectivities of mGluR2/mGluR3 and mGluR4/mGluR6 are totally different from each other. The former subtypes potently react with *trans*-1-amino-1,3-cyclopentanedicarboxylate (tACPD), whereas the latter subtypes effectively interact with L-2-amino-4-phosphonobutyrate (Tanabe *et al.*, 1992; Tanabe *et al.*, 1993; Nakajima *et al.*, 1993). Although the physiological roles of the mGluR family largely remain to be clarified, the individual mGluR subtypes seem to have their own functions in glutamate neurotransmission in a variety of neuronal cells (Nakanishi, 1992; Schoepp and Conn, 1993; Nakajima *et al.*, 1993).

G protein-coupled receptors interacting with small molecule ligands such as adrenaline and acetylcholine possess small extracellular amino-terminal domains and interact with the corresponding ligands in their transmembrane pockets (Frielle *et al.*, 1988; Kobilka *et al.*, 1988; Kubo *et al.*, 1988). In contrast, the binding of large glycohormones such as thyrotropin and lutropin-choriogonadotropin occurs by interaction with the large extracellular domains of these glycohormone receptors (Xie *et al.*, 1990; Nagayama *et al.*, 1991). mGluRs differ in their structural characteristics from either type of the G protein-coupled receptors. These receptors, though interacting with the small molecule glutamate, possess an unusually large extracellular amino-terminal domain consisting of 550–570 amino acid residues. This structural feature raises an interesting question concerning the ligand-binding domains of the mGluR family. To address this question, we designed the utilization of the difference in the agonist selectivity and signal transduction between mGluR1 and mGluR2. We constructed a series of chimeric receptors between these two receptor subtypes and determined the agonist selectivities of the resultant chimeric receptors expressed in *Xenopus* oocytes. The results presented here indicate that the extracellular domain preceding the seven transmembrane segments

* This work was supported in part by research grants from the Ministry of Education, Science and Culture of Japan, the Ministry of Health and Welfare, the Yamanouchi Foundation for Research on Metabolic Disorders, and the Inamori Foundation. The costs of publication of this article were defrayed in part by the payment of page charges. This article must therefore be hereby marked "*advertisement*" in accordance with 18 U.S.C. Section 1734 solely to indicate this fact.

‡ Present address: the Salk Institute for Biological Studies, San Diego, CA 92138-9216.

§ To whom correspondence should be addressed. Inst. for Immunology, Kyoto University Faculty of Medicine, Yoshida, Sakyo-ku, Kyoto 606, Japan.

[1] The abbreviations used are: mGluR, metabotropic glutamate receptor; tACPD, *trans*-1-amino-1,3-cyclopentanedicarboxylate; DCG-IV, (2*S*,1′*R*, 2′*R*,3′*R*)-2-(2,3-dicarboxycyclopropyl)glycine; IP_3, inositol trisphosphates.

of mGluR serves as a determinant that confers the agonist selectivity of this receptor family.

EXPERIMENTAL PROCEDURES

Materials—*In vitro* mutagenesis kit was purchased from Bio-Rad. The cDNA for the bovine homologue of $G_{\alpha 11}$ (also termed $G_{L2\alpha}$) (Strathmann and Simon, 1990; Nakamura *et al.*, 1991) and (2*S*,1′*R*,2′*R*,3′*R*)-2-(2,3-dicarboxycyclopropyl)glycine (previously referred to as DCG-1/4 and renamed DCG-IV) were kindly provided by Drs. T. Nukada (University of Tokyo) and Y. Ohfune (Suntory Institute), respectively. Other reagents were obtained as described (Masu *et al.*, 1991; Hayashi *et al.*, 1992; Abe *et al.*, 1992). cDNAs for rat mGluR1α and mGluR2 were prepared as reported previously (Masu *et al.*, 1991; Tanabe *et al.*, 1992).

Construction of Chimeric Receptor cDNAs—Six restriction sites (*Cla*I, *Nde*I, *Afl*II, *Mlu*I, *Bgl*II and *Eco*RV; see Fig. 1) at equivalent positions in the cDNAs covering the extracellular amino-terminal domains of rat mGluR1 (Masu *et al.*, 1991) and mGluR2 (Tanabe *et al.*, 1992) were used to construct chimeric receptor cDNAs; the *Nde*I site preexisted in the mGluR2 cDNA, while the others were introduced by site-directed mutagenesis (Kunkel, 1987; Kakizuka *et al.*, 1990; Yokota *et al.*, 1992) using the *in vitro* mutagenesis kit. These sites were chosen because they are unique in both cDNA sequences covering their extracellular domains and the chimeric formations cause no insertion, deletion, or substitution in the amino acid sequences of mGluR1 and mGluR2. The authenticity of the various chimeric receptor cDNAs constructed was confirmed by sequence determination in combination with restriction enzyme analysis.

Electrophysiological Measurements of Chimeric Receptors in Xenopus Oocytes—Preparations of oocytes and *in vitro* cRNA synthesis were carried out as described previously (Masu *et al.*, 1991). Electrophysiological measurements were performed by two microelectrode techniques under voltage clamp at −60 mV. To potentiate the electrophysiological response in *Xenopus* oocytes, the cRNA for the bovine homologue of $G_{\alpha 11}$ (20 ng) (Strathmann and Simon, 1990; Nakamura *et al.*, 1991) was co-injected with each chimeric receptor cRNA (25 ng) (Nakamura *et al.*, 1992). The oocytes were incubated at 19°C for 2–6 days. For electrophysiological measurements, oocytes were perfused by a constant stream of a standard solution (95 mM NaCl, 2 mM KCl, 2 mM $CaCl_2$, 1 mM $MgCl_2$, 5 mM HEPES pH 7.5), and drugs tested were applied by switching the flow, except that bath application was used to make high concentrations of quisqualate (≥1 mM), tACPD (≥1 mM), and 100 μM DCG-IV; these chemicals were adjusted to neutral pH before bath application. Dose-response curves for L-glutamate, quisqualate, and tACPD were determined by measuring peak currents after serial application of various concentrations of these compounds.

Statistical Analysis—Theoretical curves for determination of ED_{50} were drawn according to the equation $I = I_{max}/(1 + (ED_{50}/A)^n)$, where I represents the current response; I_{max}, the maximum response (=100%) of the respective agonist; A, the concentration of agonist; n, the Hill coefficient.

RESULTS

Construction and Expression of Chimeric Receptors—Our previous studies indicated that mGluR1 expressed in *Xenopus* oocytes is capable of inducing electrophysiological responses to ligand application through the activation of the oocyte IP_3/Ca^{2+} signal transduction (Masu *et al.*, 1991). In contrast, no such response was evoked for mGluR2 in *Xenopus* oocytes, because this receptor subtype is linked to the inhibitory cyclic AMP cascade (Tanabe *et al.*, 1992). The two receptor subtypes also showed distinct properties in their agonist selectivities. mGluR1 responds effectively to quisqualate but less so to tACPD, whereas mGluR2 reacts potently with tACPD but not appreciably with quisqualate (Masu *et al.*, 1991; Tanabe *et al.*, 1992; Aramori and Nakanishi, 1992). To investigate whether the extracellular amino-terminal domain of mGluR is involved in determining the agonist selectivity of mGluR, we first constructed a chimeric receptor in which the extracellular domain of mGluR1 was almost entirely replaced with the corresponding region of mGluR2 (TQ6 in Fig. 1). Because this chimeric receptor retained the cytoplasmic region that is

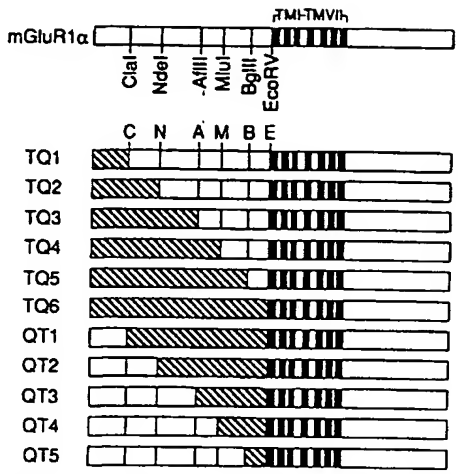

FIG. 1. **Schematic structures of chimeric receptors exchanged between the extracellular domains of rat mGluR1 and mGluR2.** *Hatched boxes* represent the amino acid sequences derived from mGluR2, and other portions are those derived from mGluR1; *solid boxes* depict the seven putative transmembrane segments (TMI–TMVII). The TQ series of the chimeric receptors were constructed by exchanging the mGluR1 and mGluR2 sequences at the restriction sites corresponding to the following amino acid positions of the mGluR1 sequence: TQ1 (118–120), TQ2 (225–227), TQ3 (355–356), TQ4 (429–431), TQ5 (521–522), and TQ6 (590–591). Chimeras in the QT series were mirror images of those of the TQ series. Six restriction sites used for the chimeric formations are indicated under the structure of mGluR1α and these sites are used for the definition of the segment boundaries (sites C, N, A, M, B, and E) discussed in the text as indicated above the TQ1 chimeric receptor.

responsible for coupling to IP_3/Ca^{2+} signal transduction, it was expected that the TQ6 receptor is capable of inducing an electrophysiological response to L-glutamate application when expressed in *Xenopus* oocytes. Our preliminary experiment indicated that TQ6 not only responded to L-glutamate but also, like mGluR2, showed a more preferred response to tACPD than to quisqualate. We thus constructed a series of chimeric receptors between mGluR1 and mGluR2 by sequentially replacing cDNA restriction fragments at the corresponding restriction sites situated in the extracellular domains of these two mGluR subtypes. A total of 11 chimeric receptors thus constructed consisted of two series of reciprocal receptors, termed TQ and QT series, as illustrated in Fig. 1. In the TQ series, the extracellular amino-terminal sequences of mGluR1 were substituted for the homologous regions of mGluR2 in the direction from the amino terminus to the carboxyl terminus. Chimeras in the QT series were mirror images of those in the TQ series in that the extracellular sequences of mGluR1 were replaced with the corresponding regions of mGluR2 in the reverse direction. The cRNAs for the native and chimeric receptors were synthesized *in vitro* and were injected into *Xenopus* oocytes to test for electrophysiological responses to L-glutamate or various agonists. We coinjected the cRNA for a bovine G protein, $G_{\alpha 11}$ (Strathmann and Simon, 1990; Nakamura *et al.*, 1991), that was reported to potentiate electrophysiological responses (Nakamura *et al.*, 1992) and thus yielded more reliable data. We also confirmed that oocytes injected with distilled water or with mGluR2 mRNA showed no oscillatory responses resulting from the activation of oocyte IP_3/Ca^{2+} signal transduction after application of L-glutamate or other agonists.

Measurements of Electrophysiological Responses—mGluR1 evoked a maximal electrophysiological response to application of 100 μM L-glutamate when expressed in *Xenopus* oocytes

(Masu *et al.*, 1991). However, in some chimeric formations, no obvious or very little electrophysiological responses were induced by application of 100 μM L-glutamate. To address whether various chimeric receptors were functionally expressed in *Xenopus* oocytes, we first measured the electrophysiological responses of the individual chimeric receptors after the addition of high concentrations (10 mM each) of L-glutamate, tACPD, and quisqualate. The result of this analysis is presented in Fig. 2, and several characteristic features of a series of chimeric receptors are summarized as follows.

All but TQ1 in the TQ series of chimeric receptors and only QT5 among the QT series of receptors showed appreciable electrophysiological currents in response to L-glutamate application. No other chimeric receptors (TQ1 and QT1–QT4) showed measurable responses to any of the three agonists. The failure of these receptors in responding to a high concentration of L-glutamate may be due to insufficient synthesis, inappropriate membrane incorporation, or some molecular incompatibility to maintain L-glutamate binding. These mechanisms, however, remain to be clarified. Among the positively responding chimeric receptors, TQ6 evoked a response that was comparable with that of mGluR1, whereas the five other chimeric receptors were reduced in their maximal responses to application of L-glutamate by about one-third that of the native mGluR1.

At a high concentration of quisqualate and tACPD, the native mGluR1 responded efficiently to quisqualate and less so with tACPD as compared with L-glutamate. QT5, which retains a large extracellular portion of mGluR1, responded equally well to quisqualate but lost the ability to interact with tACPD. In contrast, the reactivity with tACPD and quisqualate was reversed in the TQ3–TQ6 chimeric receptors, and these receptors responded relatively well to tACPD but failed to interact with quisqualate. TQ2 differed from either type of the above chimeric receptors and showed the potency to interact with all three agonists to a similar extent. These results strongly suggest that the extracellular domain preceding the seven transmembrane segments of mGluR is responsible for determining the agonist selectivity of this receptor.

Dose-Response Analyses—To confirm the above findings, we determined dose-response curves of the positively responding chimeric receptors by applying various concentrations of L-glutamate, quisqualate, and tACPD. The results are presented in Fig. 3 and Table I and can be summarized as follows.

The native mGluR1 showed a rank order of agonist potency with quisqualate > L-glutamate > tACPD as reported previously (Masu *et al.*, 1991). Half-maximal effective doses (ED_{50}) of the respective agonists were 7×10^{-7}, 1×10^{-5}, 2.4×10^{-4} M. All chimeric receptors examined were reduced in their ED_{50} values for L-glutamate by one order or more of magnitude when compared with the native mGluR1. However, in QT5 where a large extracellular domain is composed of the mGluR1 structure, the characteristics of mGluR1 of interacting with quisqualate more efficiently than with L-glutamate was maintained, though the reactivity with tACPD, unlike mGluR1, was totally lost in this chimeric formation.

In a series of the TQ3–TQ6 chimeric receptors, quisqualate was found to be inactive in inducing electrophysiological

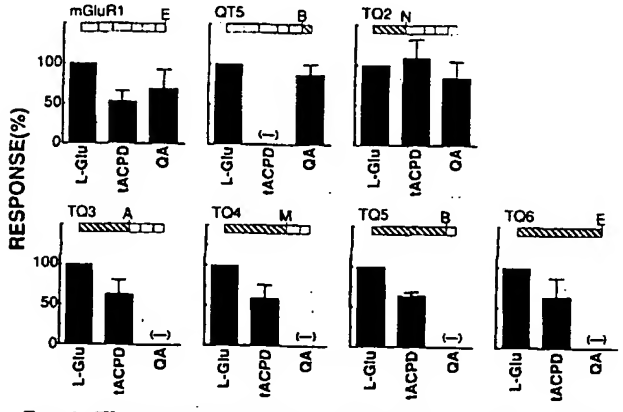

FIG. 2. **Electrophysiological responses of the native mGluR1 and various chimeric receptors after application of L-glutamate, tACPD, and quisqualate.** *Xenopus* oocytes were injected with cRNA for the native mGluR1α or the indicated chimeric receptor together with G_{o11} cRNA, and after 2–6 days of incubation, the electrophysiological responses to application of L-glutamate (*L-Glu*), tACPD, and quisqualate (*QA*) (a final concentration of 10 mM each) were measured as described under "Experimental Procedures." Responses are expressed as percentages of the response elicited by application of 10 mM glutamate for the respective receptor; (−), no response. Average responses of mGluR1 and TQ6 were about 550 nA, whereas those of other receptors were about 170 nA. Data represent the means ± S.E. of at least three experiments. The extracellular structures of different chimeric receptors are indicated *above* the respective data; *open boxes* and *hatched boxes* are derived from mGluR1 and mGluR2, respectively.

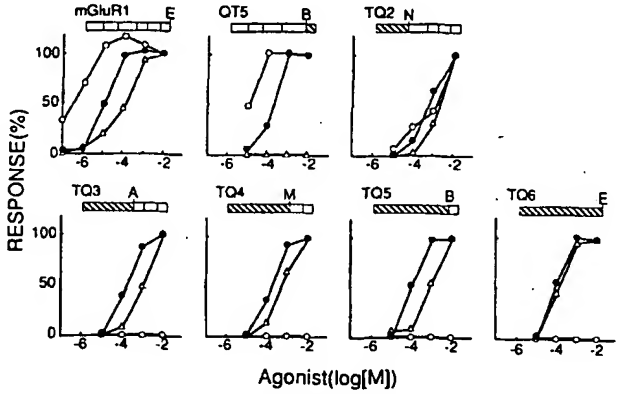

FIG. 3. **Dose-response curves of the native mGluR1 and various chimeric receptors for L-glutamate, quisqualate, and tACPD.** Current responses to serial application of indicated concentrations of L-glutamate (●), quisqualate (○), and tACPD (△) were recorded electrophysiologically 2–6 days after incubation of oocytes injected with the cRNA for mGluR1 or an indicated chimeric receptor together with G_{o11} cRNA. Responses are expressed as percentages of that elicited with 10 mM of the respective agonist. Data represent the means of the responses obtained from at least three experiments. For other explanations, see Fig. 2.

TABLE I

ED_{50} values of the native mGluR1 and various chimeric receptors for three agonists

ED_{50} values were obtained from the data shown in Fig. 3 as described under "Experimental Procedures" and are given as the means ± S.E. of at least three experiments; (−), not measurable. ED_{50} values of three agonists for TQ2 and those of tACPD for TQ3, TQ4, and TQ5 were calculated under the assumption that their responses reach maximal levels at 10 mM of these compounds.

Receptor	ED_{50}		
	L-Glutamate	tACPD	Quisqualate
		μM	
TQ2	520 ± 210 (n = 5)	1200 ± 190 (n = 3)	650 ± 240 (n = 4)
TQ3	160 ± 35 (n = 3)	1300 ± 700 (n = 4)	(−)
TQ4	160 ± 39 (n = 5)	650 ± 210 (n = 4)	(−)
TQ5	110 ± 12 (n = 4)	870 ± 29 (n = 4)	(−)
TQ6	100 ± 12 (n = 4)	110 ± 9.5 (n = 3)	(−)
QT5	180 ± 65 (n = 4)	(−)	30 ± 22 (n = 3)
mGluR1	10 ± 1.8 (n = 4)	240 ± 130 (n = 6)	0.70 ± 0.39 (n = 3)

response up to the concentration of 10 mM. In contrast, tACPD efficiently evoked responses in these chimeric receptors. Furthermore, in TQ6 in which the extracellular domain of mGluR1 was almost entirely replaced with the corresponding domain of mGluR2, the agonist potencies of tACPD and L-glutamate were virtually identical with each other. This agonist selectivity of TQ6 was very similar to that reported for the native mGluR2 as assessed by measuring agonist-mediated inhibition of forskolin-stimulated cyclic AMP formation in mGluR2-expressing Chinese hamster ovary cells (Tanabe *et al.*, 1992).

TQ2 responded to all three agonists comparably but less efficiently. This receptor thus differed from any of the above chimeric receptors and seemed to represent an intermediate form between the QT5 type and the TQ3–TQ6 type of chimeric receptors in terms of its agonist selectivity.

The above results, taken altogether, strongly indicated that about one-half of the amino-terminal extracellular domain (up to site A) is critical in determining the agonist selectivity of mGluR.

Responsiveness to Dicarboxycyclopropyl Glycine—In the above experiments, a distinct pattern in responsiveness to quisqualate and tACPD allowed the assignment of a structural determinant of the agonist selectivity at the extracellular amino-terminal domain of mGluR. However, the above result also showed that the native mGluR1 is capable of reacting with tACPD comparably with or more effectively than the TQ3–TQ6 chimeric receptors (Table I). It thus remained possible, though very unlikely, that the TQ3–TQ6 chimeric receptors could maintain a fundamental property characteristic of mGluR1 but could selectively lose a binding site specific for quisqualate. To exclude this possibility, we designed different experiments with the aid of a new glutamate analogue DCG-IV. DCG-IV was developed by Ohfune *et al.* (1993), who modified the 3′ carbon of 2-(carboxycyclopropyl)glycine that was identified as a selective agonist for the mGluR family (Hayashi *et al.*, 1992). An agonist selectivity of DCG-IV was analyzed by examining its effect on signal transduction of different mGluR subtypes expressed in Chinese hamster ovary cells, and this analysis indicated that DCG-IV is a very specific agonist for mGluR2 with no reactivity with mGluR1.[2]

We used this compound to distinguish whether the incorporation of the mGluR2 sequence in the chimeric receptors generates the ligand-selective property characteristic of mGluR2 or alternatively still retains the property of mGluR1. The result of this analysis is presented in Fig. 4. Although this experiment was carried out at a single concentration of DCG-IV (100 μM) because of its availability, it is clear from this analysis that the TQ3–TQ6 chimeric receptors acquire the reactivity with DCG-IV, whereas QT5, like the native mGluR1, shows no reactivity with this compound. This analysis thus explicitly demonstrated that about one-half of the amino-terminal extracellular domain is a critical determinant that confers an agonist selectivity of mGluR2. Interestingly, DCG-IV was not reactive with the TQ2 chimeric receptor, indicating that the amino-terminal sequence up to site N is not sufficient to exchange a different agonist selectivity between mGluR1 and mGluR2.

DISCUSSION

The mGluR family consisting of at least six different subtypes shows common structural architectures comprised of an unusually large extracellular domain preceding the seven transmembrane segments. mGluR1 and mGluR2 show similar affinities for L-glutamate but distinctive reactivities with quisqualate and tACPD. In this investigation, we attempted to assign structural determinants responsible for the different agonist selectivities between mGluR1 and mGluR2 by construction and expression of a series of chimeric receptors between these two receptor subtypes. Many chimeric receptors constructed responded to L-glutamate but lowered high-affinity responsiveness to L-glutamate by more than one order in magnitude. However, there was a distinct pattern in the reactivities with quisqualate and tACPD among the different series of chimeric receptors. Replacement of the amino-terminal portion up to site A of mGluR1 with the corresponding portion of mGluR2 in the TQ series of chimeric receptors (TQ3–TQ6) showed the reactivity with tACPD but not with quisqualate. In contrast, the QT5 receptor, in which the large amino-terminal portion was retained with the mGluR1 sequence, reacted with quisqualate more efficiently than L-glutamate but lost the ability to interact with tACPD. Thus, although the native mGluR1 showed the ability to respond to tACPD, the effective responsiveness to tACPD in the TQ3–TQ6 receptors was interpreted to indicate that incorporation of at least about one-half of the amino-terminal portion of mGluR2 generates the agonist selectivity characteristic of this receptor subtype. This interpretation was confirmed by the reactivity of these receptors and not the native mGluR1 or QT5 with DCG-IV, which is a specific agonist for mGluR2. Thus, the present investigation demonstrated that about one-half of the amino-terminal portion is critical in determining the agonist selectivity of mGluR.

It is curious that many of the QT series of chimeric receptors are nonfunctional despite the fact that most of the reciprocal TQ series of chimeric receptors are actively expressed in *Xenopus* oocytes. Similar functional defects were observed for some of the chimeric formations in other G protein-coupled receptors (Kobilka *et al.*, 1988; Nagayama *et al.*, 1991; Yokota *et al.*, 1992). This defect hampered the assignment of more limited domains important for agonist selectivity of mGluR. Because TQ2 and TQ3 differed only in the sequence between site N and site A but showed distinctive patterns in the responses to DCG-IV and other agonists, we constructed an additional chimeric receptor in which the sequence from site N to site A of mGluR1 was substituted by the corresponding region of mGluR2. However, the resultant chimeric receptor failed to respond to any of the agonists (data not shown). In our separate experiments, we raised

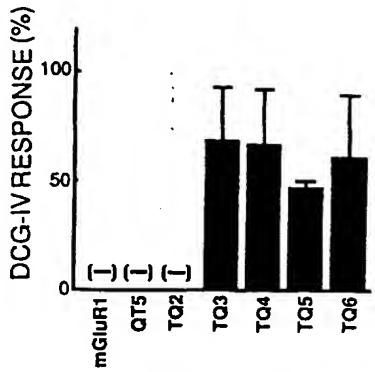

FIG. 4. **Responses of the native mGluR1 and various chimeric receptors to DCG-IV application.** Electrophysiological responses in *Xenopus* oocytes applied with 100 μM DCG-IV are expressed as percentages of those elicited by 100 μM L-glutamate; (−), no response. Data represent the means ± S.E. of at least three experiments.

[2] Y. Hayashi and S. Nakanishi, unpublished observation.

antibodies against limited portions of the extracellular domain along the sequence of mGluR1. Among these antibodies, we found that an antibody raised against a restricted portion (amino acid residues 177–341 of mGluR1) covering the sequence from site C to site A is capable of inhibiting the glutamate-stimulated phosphatidylinositol hydrolysis of mGluR1 expressed in Chinese hamster ovary cells. This finding thus strongly supported our conclusion that the amino-terminal portion of the extracellular domain of mGluR is critical in evoking the characteristic response of this receptor.

The structural basis for ligand binding and selectivity of G protein-coupled receptors has been studied in different members of this receptor family. In the G protein-coupled receptors for small molecule ligands such as catecholamines and acetylcholine, several transmembrane domains are important for determining the agonist and antagonist selectivities by forming a ligand binding pocket (Frielle *et al.*, 1988; Kobilka *et al.*, 1988; Kubo *et al.*, 1988). In the receptors for glycohormones such as lutropin-choriogonadotropin and thyrotropin, the large extracellular domains are responsible for binding these hormones and for conferring a high affinity (Xie *et al.*, 1990; Nagayama *et al.*, 1991), although the transmembrane segments are also partly involved in the recognition of these hormones (Ji and Ji, 1991a, 1991b). In the receptors for small peptides, both transmembrane segments and extracellular domains serve as determinants for the high-affinity interaction with these ligands (Yokota *et al.*, 1992; Perez *et al.*, 1993). Thus, mGluR seems to differ from any of the above modes of agonist selectivity determination of the G protein-coupled receptors.

The simple explanation for the involvement of the extracellular domain in the agonist selectivity is that the extracellular domain of mGluR represents a glutamate binding site that recognizes different agonists and thus confers agonist selectivity. In this case, the binding of an agonist to the extracellular domain could induce a conformational change that is transmitted across membrane-spanning domains and then activates a G protein at the cytoplasmic side. Alternatively, the membrane-spanning domains of mGluR may be more directly involved in signal transmission of ligand binding. In the case of the thrombin receptors, it has been reported that thrombin cleaves an amino-terminal extension of this receptor and creates a new amino terminus that is tethered to the binding pocket of the receptor and thus activates this receptor (Vu *et al.*, 1991). Analogous to the thrombin receptor, glutamate binding to the extracellular domain may generate a new conformation that allows the amino-terminal portion to interact with a binding pocket situated within the membrane-spanning domains. In this investigation, however, it remained to be determined whether the amino-terminal extracellular domain indeed serves as a glutamate-binding site. Therefore, a different possibility is that a primary glutamate-binding site is situated within the transmembrane segments, but this interaction is strengthened by a cooperative action of the amino-terminal extracellular domain. To address the question of whether the transmembrane segments of mGluR1 are capable of binding L-glutamate, we made a new receptor that deleted a large amino-terminal portion (residues 62–590) of mGluR1 and examined the ability of this deleted receptor to respond to agonists in *Xenopus* oocytes. However, we failed to detect any responses, and all three possibilities described above remain to be determined.

In conclusion, mGluR is unique in its mechanism responsible for determining agonist selectivity, reflecting a peculiar amino-terminal structure of this receptor family. This uniqueness raises an interesting question regarding whether mGluR is a representative that uses common and combined ligand-binding mechanisms observed for other G protein-coupled receptors or is an evolutionary specialization in the family of the G protein-coupled receptors.

Acknowledgments—We thank Drs. Y. Ohfune and T. Nukada for kind gifts of DCG-IV and bovine G_{o11} cDNA, respectively.

REFERENCES

Abe, T., Sugihara, H., Nawa, H., Shigemoto, R., Mizuno, N., and Nakanishi, S. (1992) *J. Biol. Chem.* **267**, 13361–13368
Aramori, I., and Nakanishi, S. (1992) *Neuron* **8**, 757–765
Bliss, T. V. P., and Collingridge, G. L. (1993) *Nature* **361**, 31–39
Choi, D. W., and Rothman, S. M. (1990) *Annu. Rev. Neurosci.* **13**, 171–182
Frielle, T., Daniel, K. W., Caron, M. G., and Lefkowitz, R. J. (1988) *Proc. Natl. Acad. Sci. U. S. A.* **85**, 9494–9498
Hayashi, Y., Tanabe, Y., Aramori, I., Masu, M., Shimamoto, K., Ohfune, Y., and Nakanishi, S. (1992) *Br. J. Pharmacol.* **107**, 539–543
Houamed, K. M., Kuijper, J. L., Gilbert, T. L., Haldeman, B. A., O'Hara, P. J., Mulvihill, E. R., Almers, W., and Hagen, F. S. (1991) *Science* **252**, 1318–1321
Ji, I., and Ji, T. H. (1991a) *J. Biol. Chem.* **266**, 13076–13079
Ji, I., and Ji, T. H. (1991b) *J. Biol. Chem.* **266**, 14953–14957
Kakizuka, A., Ingi, T., Murai, T., and Nakanishi, S. (1990) *J. Biol. Chem.* **265**, 10102–10108
Kobilka, B. K., Kobilka, T. S., Daniel, K., Regan, J. W., Caron, M. G., and Lefkowitz, R. J. (1988) *Science* **240**, 1310–1316
Kubo, T., Bujo H., Akiba, I., Nakai, J., Mishina, M., and Numa, S. (1988) *FEBS Lett.* **241**, 119–125
Kunkel, T. A., Roberts, J. D., and Zakour, R. A. (1987) *Methods Enzymol.* **154**, 367–382
Masu, M., Tanabe, Y., Tsuchida, K., Shigemoto, R., and Nakanishi, S. (1991) *Nature* **349**, 760–765
Nagayama, Y., Wadsworth, H. L., Chazenbalk, G. D., Russo, D., Seto, P., and Rapoport, B. (1991) *Proc. Natl. Acad. Sci. U. S. A.* **88**, 902–905
Nakajima, Y., Iwakabe, H., Akazawa, C., Nawa, H., Shigemoto, R., Mizuno, N., and Nakanishi, S. (1993) *J. Biol. Chem.* **268**, 11868–11873
Nakamura, F., Ogata, K., Shiozaki, K., Kameyama, K., Ohara, K., Haga, T., and Nukada, T. (1991) *J. Biol. Chem.* **266**, 12676–12681
Nakamura, K., Nukada, T., Hirose, E., Haga, T., and Sugiyama, H. (1992) *Neurosci. Res. Suppl.* **17**, S85
Nakanishi, S. (1992) *Science* **258**, 597–603
Ohfune, Y., Shimamoto, K., Ishida, M., and Shinozaki, H. (1993) *Bioorg. & Med. Chem. Lett.* **3**, 15–18
Perez, H. D., Holmes, R., Vilander, L. R., Adams, R. R., Manzana, W., Jolley, D., and Andrews, W. H. (1993) *J. Biol. Chem.* **268**, 2292–2295
Schoepp, D. D., and Conn, P. J. (1993) *Trends Pharmacol. Sci.* **14**, 13–20
Strathmann, M., and Simon, M. I. (1990) *Proc. Natl. Acad. Sci. U. S. A.* **87**, 9113–9117
Tanabe, Y., Masu, M., Ishi, T., Shigemoto, R., and Nakanishi, S. (1992) *Neuron* **8**, 169–179
Tanabe, Y., Nomura, A., Masu, M., Shigemoto, R., Mizuno, N., and Nakanishi, S. (1993) *J. Neurosci.* **13**, 1372–1378
Vu, T.-K. H., Hung, D. T., Wheaton, V. I., and Coughlin, S. R. (1991) *Cell* **64**, 1057–1068
Xie, Y.-B., Wang, H., and Segaloff, D. L. (1990) *J. Biol. Chem.* **265**, 21411–21414
Yokota, Y., Akazawa, C., Ohkubo, H., and Nakanishi, S. (1992) *EMBO J.* **11**, 3585–3591

Research News

Novel allosteric antagonists shed light on $mglu_5$ receptors and CNS disorders

Will P.J.M. Spooren, Fabrizio Gasparini, Thomas E. Salt and Rainer Kuhn

Although multiple metabotropic glutamate (mglu) receptor subtypes were cloned in the early 1990s, progress in the characterization of these receptors has been slow because of difficulties in obtaining subtype-selective ligands. However, in the past few years exciting progress has been made on the $mglu_5$ receptor subtype following the identification of selective non-amino-acid-like ligands that implicate the $mglu_5$ receptor as a potentially important therapeutic target, particularly for the treatment of pain and anxiety.

To date, eight subtypes of metabotropic glutamate (mglu) receptors have been cloned and classified into three groups on the basis of sequence similarities, and pharmacological and biochemical properties: Group I mglu receptors ($mglu_1$ and $mglu_5$), Group II mglu receptors ($mglu_2$ and $mglu_3$) and Group III mglu receptors ($mglu_4$, $mglu_6$, $mglu_7$ and $mglu_8$)[1].

Although Group I mglu receptors are highly related, both $mglu_1$ and $mglu_5$ receptors have a distinct expression pattern in the brain, which clearly suggests differential roles in nervous system function (Table 1)[2,3]. $mglu_5$ receptors are found most abundantly throughout the cerebral cortex, hippocampus, basal ganglia and some parts of the spinal cord (Fig. 1). Recently, subtype-selective ligands for the $mglu_5$ receptor were discovered and their effects in animal models of various nervous system disorders characterized.

Table 1. Distribution of $mglu_1$ and $mglu_5$ receptors in the rat brain[a,b]

Rat brain region	$mglu_1$	$mglu_5$
Cortex	+	++(+)
Caudate-putamen	+	+++
Nucleus accumbens	+	+++
Olfactory tubercle	+	+++
Globus pallidus	++	++
Substantia nigra	+	+
Subthalamic nucleus	++	+
Hippocampus		
CA1	+	+++
CA3	+	+++
dentate gyrus	++	+++
Cerebellum (Purkinje cell layer)	+++	-
Spinal cord		
lamina I–III	+	+++
lamina IV–V	+	+

[a]Abbreviation: mglu, metabotropic glutamate.
[b]Symbols: -, no detectable expression; +, low expression; ++, moderate expression; +++, high expression. Adapted and modified from Refs 2 and 3.

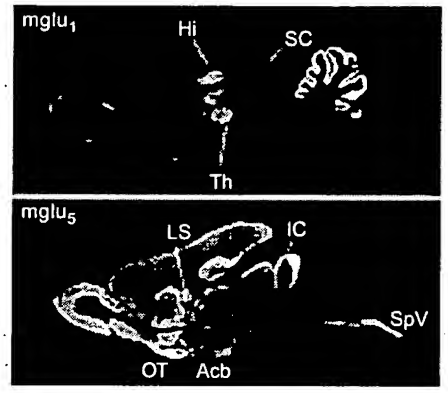

Fig. 1. Metabotropic glutamate Group I ($mglu_1$ and $mglu_5$) receptor-like immunoreactivity in rat brain parasagittal sections. Abbreviations: Acb, nucleus accumbens; Hi, hippocampus; IC, inferior colliculus; LS, lateral septal nucleus; OT, olfactory tubercle; SC, superior colliculus; SpV, spinal trigeminal nuclei; Th, thalamus. Reproduced, with permission, from Ref. 3.

Non-amino-acid-like $mglu_5$ receptor antagonists

A large number of mglu receptor ligands have been described and can be classified into two groups according to their mode of inhibition[4]. The vast majority of compounds are amino acid derivatives that interact competitively at the glutamate-binding site located in the large extracellular N-terminal domain. Particularly for Group I receptors, selective competitive antagonists are very scarce, have low potency and do not show subtype selectivity. The most potent compound is currently LY393675 (Fig. 2), a nonselective antagonist with IC_{50} values of 0.48 and 0.35 μM at $mglu_5$ and $mglu_1$ receptors, respectively[4]. More recently, LY344545 (Fig. 2) has been described as a selective competitive antagonist at the $mglu_5$ receptor with a selectivity factor of seven for $mglu_5$ over $mglu_1$ receptors. However, LY344545 has low potency (IC_{50} = 5.5 μM) and also antagonizes Group II receptors in a similar potency range[5]. Despite these significant advances, potent and subtype-selective competitive ligands have not been identified. Moreover, amino-acid-derived ligands generally show poor blood–brain barrier penetration, thus limiting their use.

Recently, novel mglu receptor antagonists were identified using functional assays by screening compound libraries for non-amino-acid-like substances. The first subtype-selective $mglu_5$ receptor antagonists reported were SIB1757 and SIB1893 (Fig. 2) with IC_{50} values of 3.7 and 3.5 μM, respectively, in the inositol phosphate (IP) accumulation assay[6]. Shortly after, 2-methyl-6-(phenylethynyl)-pyridine (MPEP) was described[7], a 100-fold more potent antagonist derived from chemical variation of SIB1893. At human $mglu_{5a}$ receptors, expressed in recombinant cells, and rat $mglu_5$ receptors in neonatal cortical slices, MPEP inhibited quisqualate-stimulated IP production with IC_{50} values of 36 nM and 17.9 nM, respectively, but had no significant agonist or antagonist activities at cells expressing other metabotropic or ionotropic glutamate receptor subtypes at concentrations up to 10 μM (Ref. 7). However, at high concentrations (i.e. 20 μM and 200 μM, respectively) 1000–10 000-fold above its IC_{50}, MPEP inhibited NMDA receptor activity by 22.6% and 64.9% in electrophysiological recordings of rat cultured primary cortical neurones[8]. Details of the mechanism and site of action of these new antagonists are provided in Box 1. Furthermore, extracellular recordings in the hippocampus showed that responses to iontophoretic application of the selective Group I mglu receptor agonist (*R,S*)-2,5-dihydroxyphenylglycine (DHPG) but not AMPA were inhibited by MPEP (either iontophoretically or intravenously)[7]; similarly, iontophoretic application of

 0165-6147/01/$ - see front matter PII: S0165-6147(00)01694-1

MPEP reduced neuronal responses in the thalamus to the selective $mglu_5$ receptor agonist (*R,S*)-2-chloro-5-hydroxyphenylglycine (CHPG) compared with those responses to NMDA (Ref. 11), indicating that MPEP is also a selective $mglu_5$ receptor antagonist *in vivo* (Box 2).

Physiology of $mglu_5$ receptors

Activation of Group I receptors can elicit a variety of postsynaptic effects on central neurones such as depolarization via a reduction of K^+ conductance or an increase in inward cation current[1]. This typically causes increases in neural firing and potentiation of synaptic inputs. Presynaptic effects of Group I receptor activation have also been demonstrated[1]. The development of selective $mglu_1$ and $mglu_5$ receptor antagonists now enables the investigation of some of these actions mediated by $mglu_1$ and/or $mglu_5$ receptors specifically. Interestingly, in the subthalamic nucleus *in vitro*, the depolarizing effect via reduction of K^+ conductance of Group I receptor activation is attributable solely to $mglu_5$ receptors, even though both $mglu_1$ and $mglu_5$ receptors are present[10]. The converse appears to be the case in the thalamus *in vitro*, where similar effects appear to be mediated specifically via $mglu_1$ receptors even though $mglu_5$ receptors are known to be present[9]. This indicates very specific membrane effects that are dependent on the brain region, which might be very important both functionally and pharmacologically. It is noteworthy that such mglu receptor activation by exogenous agonists *in vitro* is not necessarily accompanied by obvious excitatory synaptic events[10], possibly reflecting that conditions in slices are not optimal to reveal physiological release of glutamate onto such receptors[9,10]. In this respect, it is interesting that in the thalamus *in vivo*, activation of either $mglu_1$ or $mglu_5$ receptors can have an excitatory effect, and that both receptors appear to possess synaptic roles[11].

Specific modulation of NMDA responses by $mglu_5$ receptor activation occurs in several brain areas[11–13]. Together with the probable specific colocalization of receptors in synaptic and peri-synaptic areas, this offers a highly selective method of $mglu_5$ receptor potentiation of NMDA-receptor-mediated synaptic activity. However, *in vivo* (where neuronal membranes are not voltage clamped) there could also be a modulation of synaptic responses as a result of the effects of $mglu_5$ receptor activation on membrane resistance and potential, and this will be less selective[11,14,15]. Thus, there might be at least two ways in which $mglu_5$ and/or $mglu_1$ receptors could potentiate synaptic responses, and it might be that these have a different functional relevance, perhaps in terms of time-course or in synaptic plasticity[16]. Interestingly, $mglu_1$-receptor-mediated potentiation of ionotropic responses might involve protein kinase C, whereas the apparently similar effect of $mglu_5$ receptors might not[15]. The newly available antagonists should play a significant role as tools in further in-depth investigations.

Box 1. Allosteric mglu receptor antagonists

Metabotropic glutamate (mglu) receptors are members of the family III of G-protein-coupled receptors (GPCRs), which is characterized by a large N-terminal extracellular region and includes the Ca^{2+}-sensing receptor, $GABA_B$ receptors and some vomeronasal receptors. Homology modelling to bacterial periplasmic binding proteins[a], chimeric receptor analysis[b,c], and X-ray crystallography of a soluble extracellular region of the $mglu_1$ receptor in complex with glutamate[d] have shown that the extracellular region is responsible for ligand binding. The mglu receptor family therefore differs from the classical rhodopsin-type GPCRs, where the ligand-binding site occurs within the seven transmembrane (7TM) domain.

The discovery of novel mglu receptor antagonists[e–g] that are structurally unrelated to amino acids triggered the hypothesis that such compounds might act at novel receptor sites through allosteric mechanisms. Indeed, a detailed study by Pagano *et al.*[h] showed that 2-methyl-6-(phenylethynyl)-pyridine (MPEP) is a noncompetitive antagonist

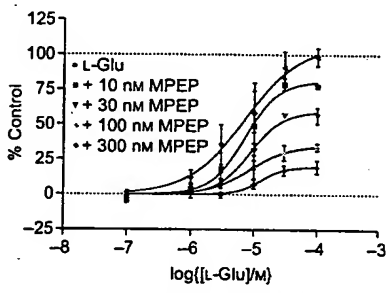

Fig. 1. Noncompetitive inhibition of glutamate (L-Glu)-stimulated inositol phosphate (IP) production with increasing concentrations of 2-methyl-6-(phenylethynyl)-pyridine (MPEP) in human metabotropic glutamate type 5a ($mglu_{5a}$)-receptor-expressing cells. Data are expressed as percentage of IP production over basal level and are mean ± SEM of three experiments performed in triplicates. Reproduced, with permission, from Ref. h.

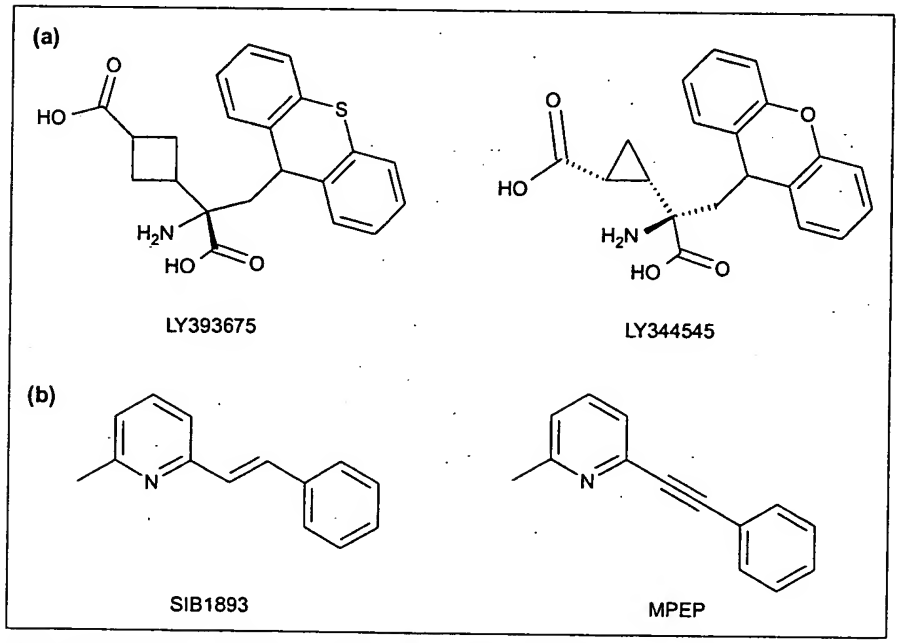

Fig. 2. Structures of Group I metabotropic glutamate (mglu) receptor antagonists. (a) LY393675 is a nonselective $mglu_1$ and $mglu_5$ receptor antagonist whereas LY344545 is a selective $mglu_5$ receptor antagonist. (b) SIB1893 and MPEP [2-methyl-6-(phenylethynyl)-pyridine] are recently developed noncompetitive and selective $mglu_5$ receptor antagonists.

In vivo effects of $mglu_5$ receptor antagonists

The available selective and brain-penetrable $mglu_5$ receptor antagonists (see above) have been applied in various nervous system disease models.

Pain and analgesia

Pharmacological and *in vivo* electrophysiological studies suggest a role for Group I mglu receptors in nociceptive processes[1,17], and the possible role(s) of $mglu_5$ receptors are highlighted in Box 2 (see also Table 2).

Anxiety and depression

Given the expression of $mglu_5$ receptors in limbic forebrain regions, a role in psychiatric conditions such as anxiety and depression was hypothesized and tested in validated animal models. In the so-called conditioned response tests

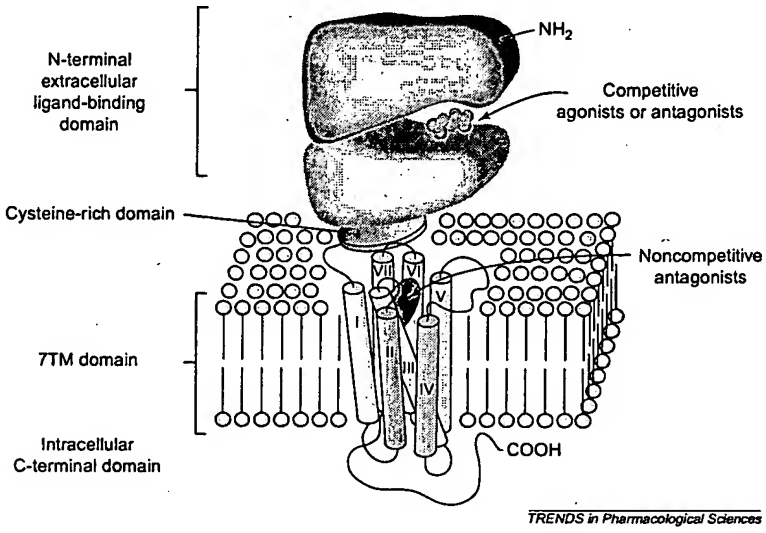

Fig. II. A monomeric form of the metabotropic glutamate type 5 ($mglu_5$) receptor, depicting the binding site of noncompetitive antagonists in the seven-transmembrane (7TM) domain and of competitive agonists or antagonists in the large N-terminal extracellular domain.

(Fig. I) that inhibits $mglu_5$ receptor function without affecting binding of glutamate to the extracellular region. MPEP also inhibited to a large extent constitutive receptor activity in cells overexpressing $mglu_5$ receptors, which suggests that MPEP acts as an inverse agonist.

Consistent with these functional data, high-affinity binding of [^{3}H]M-MPEP (a tritiated analogue of MPEP) to chimeric receptors and point mutants of $mglu_5$ receptors specifically required the amino acid residues Pro655 and Ser658 in TMIII and Ala810 in TMVII. Recently described non-amino-acid-like antagonists that are structurally unrelated to MPEP and are selective for $mglu_1$ receptors[i,j] or $mglu_1$ and $mglu_5$ receptors[k] share this mechanism and site of action in the 7TM domain.

Several important implications can be derived from these findings. (1) Novel regulators of family III GPCRs can act as competitive ligands at the extracellular agonist-binding site or as allosteric ligands in the 7TM domain (Fig. II). (2) The amino acid sequence of the allosteric binding site in the 7TM domain seems to be less conserved and to tolerate large structural variations, which will greatly facilitate the discovery of subtype-selective antagonists for other family III GPCRs. (3) It is not known how noncompetitive antagonists inhibit receptor activity but it can be assumed that activation of family III GPCRs requires a series of conformational changes in the extracellular ligand binding domain that are transmitted to the 7TM domain. Binding of noncompetitive antagonists in the 7TM domain can specifically affect conformational changes of the 7TM domain and thus have no direct effect on the occupation of the agonist binding site.

References

a O'Hara, P.J. *et al.* (1993) The ligand-binding domain in metabotropic glutamate receptors is related to bacterial periplasmic binding proteins. *Neuron* 11, 41–52

b Takahashi, K. *et al.* (1993) Role of the large extracellular domain of metabotropic glutamate receptors in agonist selectivity determination. *J. Biol. Chem.* 268, 19341–19345

c Tones, M.A. *et al.* (1995) The agonist selectivity of a class III metabotropic glutamate receptor, human mGluR4a, is determined by the N-terminal extracellular domain. *NeuroReport* 7, 117–120

d Kunishima, N. *et al.* (2000) Structural basis of glutamate recognition by a dimeric metabotropic glutamate receptor. *Nature* 407, 971–977

e Annoura, H. *et al.* (1996) A novel class of antagonists for metabotropic glutamate receptors, 7-(hydroxyimino)-cyclopropa[*b*]chromen-1a-carboxylates. *Bioorg. Med. Chem. Lett.* 6, 763–766

f Varney, M.A. *et al.* (1999) SIB-1757 and SIB-1893: selective, noncompetitive antagonists of metabotropic glutamate receptor type 5. *J. Pharmacol. Exp. Ther.* 290, 170–181

g Gasparini, F. *et al.* (1999) 2-Methyl-6-(phenylethynyl)-pyridine (MPEP), a potent, selective and systemically active mGlu5 receptor antagonist. *Neuropharmacology* 38, 1493–1503

h Pagano, A. *et al.* (2000) The noncompetitive antagonists 2-methyl-6-(phenylethynyl)pyridine and 7-hydroxyiminocyclopropan [*b*]chromen-1α-carboxylic acid ethyl ester interact with overlapping binding pockets in the transmembrane region of group I metabotropic glutamate receptors. *J. Biol. Chem.* 275, 33750–33758

i Litschig, S. *et al.* (1999) CPCCOEt, a noncompetitive metabotropic glutamate receptor 1 antagonist, inhibits receptor signaling without affecting glutamate binding. *Mol. Pharmacol.* 55, 453–461

j Carroll, F.Y. *et al.* (2000) Pharmacological characterization of BAY36-7620, a novel antagonist selective for mGluR1 receptors. *Soc. Neurosci.* 26, 618.4, 1649

k van Wagenen, B.C. *et al.* (2000) Structure–activity relationship studies of NPS2390: a potent and selective group I metabotropic glutamate receptor antagonist. *Soc. Neurosci.* 26, 618.3, 1649

Box 2. Role of $mglu_5$ receptors in pain and analgesia

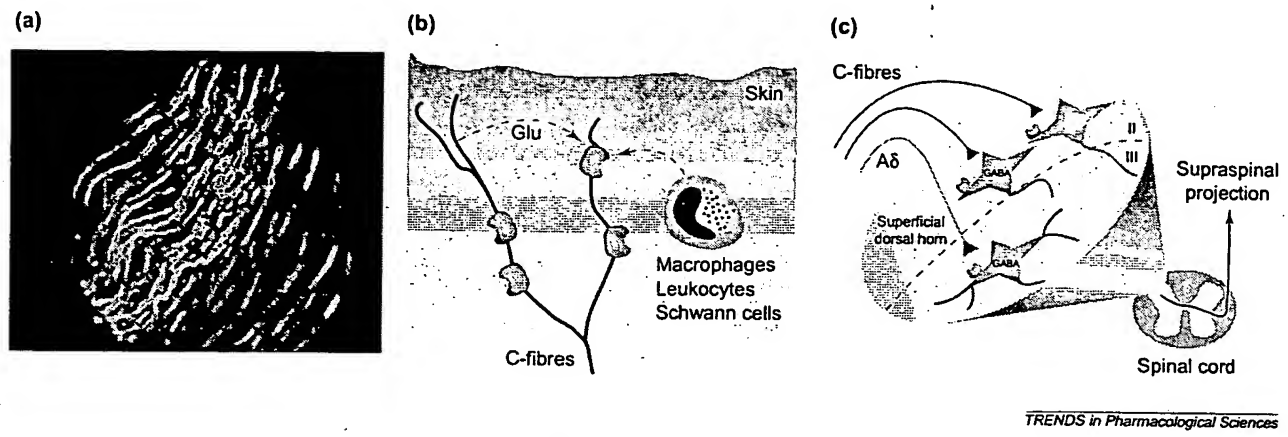

Fig. I. (a) Immunohistochemical staining of a rat skin section with a rabbit polyclonal antibody recognizing the metabotropic glutamate type 5 ($mglu_5$) receptor. Green fluorescence represents neuronal tubulin, and red fluorescence represents $mglu_5$ receptor staining, respectively. Reproduced, with permission, from Ref. h. (b) Possible activation of $mglu_5$ receptors on C-fibres by glutamate released from afferents or other cells in the skin following, for example, injury or inflammation. (c) Activation of dorsal horn GABA-containing and non-GABA-containing (possibly excitatory) neurones by C and Aδ afferents terminating in laminae II and III (Ref. c). $mglu_5$ receptors are represented by blue elements. Note that other glutamate receptors have been omitted for clarity.

Metabotropic glutamate type 5 ($mglu_5$) receptor protein and/or mRNA have been localized at several levels of the somatosensory neuraxis from the peripheral endings of nociceptive C-fibre afferents[a] (Fig. Ia), dorsal root ganglia[b] and superficial dorsal horn neurones[b–e] to the thalamus and cerebral cortex[f,g]. This suggests an intimate involvement of $mglu_5$ receptors in nociceptive processes. Recent studies using 2-methyl-6-(phenylethynyl)-pyridine (MPEP) and SIB1757 show that blockade of peripheral $mglu_5$ receptors can reverse inflammation-induced mechanical hyperalgesia[a,h] and neuropathy-induced thermal hyperalgesia[i]. By contrast, neuropathy-induced tactile allodynia and mechanical hyperalgesia appear unaffected[h,i]. This indicates that peripheral $mglu_5$ receptors are activated in certain hyperalgesic states, presumably by glutamate released from either primary afferents or other non-neural cells[j–l] (Fig. Ib). Given the peripheral location of $mglu_5$ receptors, it might be expected that these would also be found on central terminations of C-fibres, but this does not appear to be the case[c]. The role of spinal $mglu_5$ receptors is less clear, and a complicating factor might be the localization of this receptor on a variety of pre- and postsynaptic elements of either GABA- or non-GABA-containing neurones in the superficial dorsal horn[b,c] (Fig. Ic). Spinal application of $mglu_5$ receptor antagonists might therefore produce variable effects that might depend partly on the relative distribution of drugs and physiological factors such as which neural circuits are in play in a given behavioural state. Thus, there is data that suggest little involvement of spinal cord mglu receptors in either acute or chronic nociception[h], but also evidence that spinal $mglu_5$ receptors might have a role in thermal hyperalgesia[i] or acute nociception[m]. In the rat, there is less clear functional neuronal segregation between thermal and mechanical nociception supraspinally in the thalamus, but $mglu_5$ receptors are present in the thalamus[g], and direct application into the thalamus of MPEP selectively reduces acute thermal nociceptive responses of ventrobasal thalamic neurones[n] (Fig. II). These receptors might be an important target of systemic drugs because intravenous MPEP reduces such responses, but it is likely that $mglu_5$ receptors in other brain areas (e.g. the cerebral cortex and spinal cord) also contribute to these effects in the intact animal[o]. Taken together, it is apparent that $mglu_5$ receptors provide a novel target for intervention in pain processes, and it is likely that $mglu_5$ receptor antagonism might be particularly valuable in specific pain types (e.g. inflammatory pain)[a,h]. However, it should be remembered that other glutamate receptors, particularly $mglu_1$ receptors, have also been implicated in peripheral and central pain processes[n,p,q].

prominent anxiolytic-like activity of MPEP was seen in both the Vogel test and the four-plate test[18,19]. Acquisition as well as expression of fear was shown to be inhibited by MPEP in the fear-potentiated startle test[20]. Interestingly, acquisition but not expression of conditioned fear was also prevented by direct injection of MPEP into the lateral amygdala, directly linking $mglu_5$ receptors in the amygdala to fear conditioning[21]. In the Geller-Seifter test the effects of MPEP were inconclusive because treatment with MPEP, up to a dose of 100 mg kg^{-1}, tended to increase the number of punished responses as well as the number of received shocks, but neither effect reached statistical significance[22].

In the so-called unconditioned response tests MPEP exhibited anxiolytic-like activity in models of social anxiety (social exploration test), novelty-induced anxiety (marble burying test), anxiety in an approach-avoidance conflict (elevated plus maze) and finally in a model of anticipatory anxiety (stress-induced hyperthermia)[22]. Together, these and other findings, including testing of closely related derivatives of MPEP (W.P.J.M. Spooren, unpublished), indicate that $mglu_5$ receptor antagonists have a very broad and potent anxiolytic-like activity in rodent models of anxiety (Table 2), with low potential to induce sedation or psychotomimetic effects[22], although the

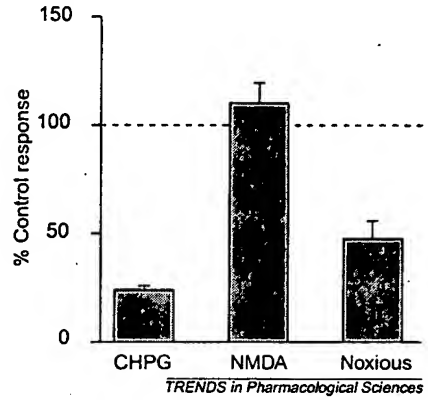

Fig. II. Reduction by iontophoretically applied 2-methyl-6-(phenylethynyl)-pyridine (MPEP) of responses of single thalamic neurones to iontophoretic application of the agonists (*R,S*)-2-chloro-5-hydroxyphenylglycine (CHPG) and NMDA, and to noxious thermal stimulation (Ref. n). Values are mean ± SEM ($n = 6$) percentages of the control responses recorded before MPEP application. Note that MPEP reduced CHPG and noxious responses but not NMDA responses.

References

a Walker, K. *et al.* (2001) mGlu5 receptors and nociceptive function II. mGlu5 receptors functionally expressed on peripheral sensory neurones mediate inflammatory hyperalgesia. *Neuropharmacology* 40, 10–19

b Valerio, A. *et al.* (1997) mGluR5 metabotropic glutamate receptor distribution in rat and human spinal cord: a developmental study. *Neurosci. Res.* 28, 49–57

c Jia, H. *et al.* (1999) Metabotropic glutamate receptors in superficial laminae of the rat dorsal horn. *J. Comp. Neurol.* 410, 627–642

d Berthele, A. *et al.* (1999) Distribution and developmental changes in metabotropic glutamate receptor messenger RNA expression in the rat lumbar spinal cord. *Dev. Brain Res.* 112, 39–53

e Vidnyanszky, Z. *et al.* (1994) Cellular and subcellular localization of the mGluR5a metabotropic glutamate receptor in rat spinal cord. *NeuroReport* 6, 209–213

f Romano, C. *et al.* (1996) Enhanced early developmental expression of the metabotropic glutamate receptor mGluR5 in rat brain: protein, mRNA splice variants, and regional distribution. *J. Comp. Neurol.* 367, 403–412

g Neto, F.L. *et al.* (2000) Differential distribution of metabotropic glutamate receptor subtype mRNAs in the thalamus of the rat. *Brain Res.* 854, 93–105

h Walker, K. *et al.* (2001) Metabotropic glutamate receptor subtype 5 (mGlu5) and nociceptive function. I. Selective blockade of mGlu5 receptors in models of acute, persistent and chronic pain. *Neuropharmacology* 40, 1–9

i Dogrul, A. *et al.* (2000) Peripheral and spinal antihyperalgesic activity of SIB-1757, a metabotropic glutamate receptor (mGLUR(5)) antagonist, in experimental neuropathic pain in rats. *Neurosci. Lett.* 292, 115–118

j De Groot, J. *et al.* (2000) Peripheral glutamate release in the hindpaw following low and high intensity sciatic stimulation. *NeuroReport* 11, 497–502

k Lawand, N.B. *et al.* (2000) Amino acid release into the knee joint: key role in nociception and inflammation. *Pain* 86, 69–74

l Parpura, V. *et al.* (1995) Neuroligand-evoked calcium-dependent release of excitatory amino acids from Schwann cells. *J. Neurosci.* 15, 5831–5839

m Bordi, F. and Ugolini, A. (2000) Involvement of mGluR(5) on acute nociceptive transmission. *Brain Res.* 871, 223–233

n Salt, T.E. and Binns, K.E. (2000) Contributions of mGlu1 and mGlu5 receptors to interactions with *N*-methyl-D-aspartate receptor-mediated responses and nociceptive sensory responses of rat thalamic neurons. *Neuroscience* 100, 375–380

o Binns, K.E. and Salt, T.E. (2001) Actions of the systemically active metabotropic glutamate antagonist MPEP on sensory responses of thalamic neurones. *Neuropharmacology* 40, 639–644

p Hargett, G.L. *et al.* (2000) Presynaptic control of primary afferents by mGluR1α receptors. *Soc. Neurosci.* 26, 949

q Young, M.R. *et al.* (1998) Antisense ablation of type I metabotropic glutamate receptor mGluR1 inhibits spinal nociceptive transmission. *J. Neurosci.* 18, 10180–10188

scope of potential CNS effects needs to be explored much further. Finally, although MPEP was inactive in the swim test (Table 2), MPEP shortened the immobility time in the tail suspension test[18]. These data suggest that MPEP might also have antidepressant-like activity, which remains to be further investigated.

Epilepsy

The role of distinct mglu receptor subtypes in epilepsy is at present not clear. However, intracerebroventricular application of CHPG in mice was shown to induce clonic seizures that were suppressed by MPEP or SIB1893 (Ref. 23). Both compounds also suppressed sound-induced seizures in DBA-2 mice and clonic seizures in the *lethargic* mouse[23]. Together, these data indicate that $mglu_5$ receptor antagonists exhibit anticonvulsant activity, which clearly needs further characterization in additional studies.

Neuroprotection

It has been shown that noncompetitive $mglu_5$ receptor antagonists exhibit neuroprotection against excitotoxic-induced degeneration *in vitro* and *in vivo*, as well as against β-amyloid-induced toxicity *in vitro*[8,24,25]. However, the role of $mglu_5$ receptors in neuroprotection is controversial in view of the varying concentrations of MPEP applied in different models. Given the relatively good selectivity of MPEP (Ref. 7) effects observed at concentrations close to the IC_{50} at $mglu_5$ receptors (e.g. partial inhibition of β-amyloid-induced toxicity and excitotoxicity induced by a short pulse of NMDA)[24] are indeed likely to reflect specific action at $mglu_5$ receptors whereas neuroprotection achieved at very high concentrations of MPEP (20 μM and 200 μM, 1000–10 000-fold above its IC_{50}, respectively) might instead reflect a combined action of MPEP at $mglu_5$ and additional receptors, such as NMDA receptors[8,25].

Parkinson's disease

The expression of $mglu_5$ receptors in the striatum and subthalamic nucleus suggests that antagonists might reduce the overactive glutamate-mediated pathways in the basal ganglia in Parkinson's disease. $mglu_5$ receptors have been implicated as major players in the excitatory drive to the subthalamic nucleus from glutamatergic afferents[10]. Indeed, in the unilateral 6-hydroxydopamine (6-OHDA) rat rotation model of Parkinson's disease, (acute) MPEP increased the number of net rotations (Table 2). However, the effect was marginal and consisted of an ipsilateral bias in spontaneous turning rather than a clear turning response[26]. In additional studies it was shown that MPEP inhibited dopamine-mediated rotations. The underlying mechanism of these findings is at present unclear. However, the interaction of MPEP with dopamine clearly awaits further elucidation in additional studies using distinct models of Parkinson's disease as well as applying a much wider dose range of MPEP.

Interestingly, in a conditioned reaction-time task in the rat, chronic but not acute treatment with MPEP significantly and gradually reduced the motor deficits induced by bilateral lesions of the nigrostriatal pathway

Table 2. Effects of the $mglu_5$ receptor anatagonist MPEP in animal models of distinct nervous system disorders[a,b]

Indication and model	Species	Tested dose range (mg kg^{-1})[c]	Effective dose range (mg kg^{-1})	Route of administration	Refs
Pain					
Tail flick	Rat	10–100	–	p.o.	27
FCA-induced mechanical hyperalgesia	Rat	10–100 0.03–0.3 µmole	30–100 0.03–0.3 µmole	p.o. i.pl.	27,28
Carageenin-induced mechanical hyperalgesia	Rat	3–100	30–100	p.o.	27
Neuropathic hyperalgesia	Rat	10–100	–	p.o.	27,28
Anxiety					
EPM	Rat	0.1–30	0.1–10 and 10–30	p.o.	18,19,22
Social exploration	Rat	0.003–10	0.3–1	p.o.	22
SIH	Mouse	1.5–30	15–30	p.o.	22
Marble burying	Mouse	1.5–30	7.5–30	p.o.	22
Vogel conflict	Rat	0.3–10	1–10	i.p.	18,19
Geller-Seifter	Rat	10–100	–	p.o.	22
Four-plate test	Mouse	3–30	30	i.p.	18,19
Fear potentiated startle:	Rat				20
acquisition		0.3–30	3–30	p.o.	
expression		0.3–30	30	p.o.	
Depression					
Swim test	Rat	0.1–30	–	i.p.	18
Tail suspension	Mouse	0.1–20	1–20	i.p.	18
Parkinson's disease					
6-OHDA model	Rat	7.5–30	30	p.o.	26
Side-effects					
PPI	Rat	1–10	–	p.o.	22
Rotarod	Rat	7.5 –300	–	p.o.	26
Spontaneous locomotor activity:	Mouse				22
horizontal activity		0.01–100	–	p.o.	
vertical activity		0.01–100	100 (↓)	p.o.	

[a]Abbreviations: EPM, elevated plus-maze; FCA, Freund's complete adjuvant; i.p., intra-peritoneal; i.pl., intra-plantar; mglu, metabotropic glutamate; MPEP, 2-methyl-6-(phenylethynyl)-pyridine; 6-OHDA, 6-hydroxydopamine; p.o., oral; PPI, prepulse inhibition; SIH, stress-induced hyperthermia.
[b]Symbols: –, no effect; ↓ decrease.
[c]Dose is given as mg kg^{-1} except for FCA-induced mechanical hyperalgesia.

(M. Amalric *et al.*, unpublished). Comparable results were obtained with chronic L-3,4-dihydroxyphenylalanine (L-DOPA) treatment. Subsequent studies in the unilateral 6-OHDA rat rotation model confirmed sensitization to MPEP following a sub-chronic (7 days) application resulting in a (limited) rotational response rather than an ipsilateral bias in spontaneous turning (W.P.J.M. Spooren *et al.*, unpublished). Furthermore, MPEP was found to counteract haloperidol-induced muscle rigidity and akinesia (A. Pilc *et al.*, unpublished). Accordingly, it appears that $mglu_5$ receptor antagonists have minor motor stimulating properties in models of Parkinson's disease but might improve rigidity and bradykinesia and thus provide an interesting new approach for the symptomatic treatment of Parkinson's disease.

Concluding remarks

The identification of the first subtype-selective $mglu_5$ receptor antagonists has fostered important progress in the understanding of the role of $mglu_5$ receptors in neurological and behavioural disorders. On the basis of published studies, a clear indication for the potential therapeutic use of $mglu_5$ receptor antagonists seems to be in chronic pain that arises from inflammatory conditions. Furthermore, additional potential indications are anxiety, epilepsy and chronic neurodegenerative diseases such as Parkinson's disease. Other potential applications such as asthma and bowel disorders, which involve peripherally expressed $mglu_5$ receptors, are only beginning to emerge and await further exploration. The next few years will witness major advances in the development of noncompetitive antagonists for $mglu_5$ receptors as well as other mglu receptors, and will bring further understanding in the role of these receptors in (patho)physiological processes.

Acknowledgements

We would like to thank M. Amalric (CNRS, Marseille) for critical reading of the manuscript, R. Shigemoto (National Institue for Physiological Sciences, Okazaki) and J. Winter (Novartis Institute for Medical Sciences, London) for kindly permitting the reproduction of immunohistochemical stainings of $mglu_1$ and $mglu_5$ receptors, and M. Amalric and A. Pilc (Institute of Pharmacology, Krakow) for communication of unpublished data.

References

1 Conn, J. and Pin, J.P. (1997) Pharmacology and functions of metabotropic glutamate receptors. *Annu. Rev. Pharmacol. Toxicol.* 37, 205–237
2 Martin, L.J. *et al.* (1992) Cellular localization of a metabotropic glutamate receptor in rat brain. *Neuron* 9, 259–270
3 Shigemoto, R. and Mizuno, N. (2000) Metabotropic glutamate receptors – immunocytochemical and *in situ* hybridization analysis. In *Handbook of Chemical Neuroanatomy: Metabotropic Glutamate Receptors: Immunocytochemical and* in situ *Hybridization Analyses* (Vol. 18) (Ottersen, O.P. and Storm-Mathisen, J., eds), pp. 63–98, Elsevier
4 Schoepp, D.D. *et al.* (1999) Pharmacological agents acting at subtypes of metabotropic glutamate receptors. *Neuropharmacology* 38, 1431–1476
5 Doherty, A.J. *et al.* (2000) A novel, competitive mGlu(5) receptor antagonist (LY344545) blocks DHPG-induced potentiation of NMDA responses but not the induction of LTP in rat hippocampal slices. *Br. J. Pharmacol.* 131, 239–244
6 Varney, M. *et al.* (1999) SIB-1757 and SIB-1893: selective, noncompetitive antagonists of metabotropic glutamate receptor type 5 (mGluR5). *J. Pharmacol. Exp. Ther.* 290, 170–181
7 Gasparini, F. *et al.* (1999) 2-Methyl-6-(phenylethynyl)-pyridine (MPEP), a potent, selective and systemically active mGlu5 receptor antagonist. *Neuropharmacology* 38, 1493–1504
8 O'Leary, D.M. *et al.* (2000) Selective mGluR5 antagonists MPEP and SIB-1893 decrease NMDA or glutamate-mediated neuronal toxicity through actions that reflect NMDA receptor antagonism. *Br. J. Pharmacol.* 131, 1429–1437
9 Turner, J.P. and Salt, T.E. (2000) Synaptic activation of the group I metabotropic glutamate receptor mGlu1 on the thalamocortical neurons of the rat dorsal lateral geniculate nucleus *in vitro*. *Neuroscience* 100, 493–505
10 Awad, H. *et al.* (2000) Activation of metabotropic glutamate receptor 5 has direct excitatory effects and potentiates NMDA receptor currents in neurons of the subthalamic nucleus. *J. Neurosci.* 20, 7871–7879
11 Salt, T.E. and Binns, K.E. (2000) Contributions of mGlu1 and mGlu5 receptors to interactions with N-methyl-D-aspartate receptor-mediated responses and nociceptive sensory responses of rat thalamic neurons. *Neuroscience* 100, 375–380

12 Doherty, A.J. *et al.* (1997) (RS)-2-chloro-5-hydroxyphenylglycine (CHPG) activates mGlu5, but not mGlu1, receptors expressed in CHO cells and potentiates NMDA responses in the hippocampus. *Neuropharmacology* 36, 265–267
13 Alagarsamy, S. *et al.* (1999) Activation of NMDA receptors reverses desensitization of mGluR5 in native and recombinant systems. *Nat. Neurosci.* 2, 234–240
14 Bond, A. and Lodge, D. (1995) Pharmacology of metabotropic glutamate receptor-mediated enhancement of responses to excitatory and inhibitory amino acids on rat spinal neurones *in vivo*. *Neuropharmacology* 34, 1015–1023
15 Ugolini, A. *et al.* (1999) Potentiation of NMDA and AMPA responses by the specific mGluR5 agonist CHPG in spinal cord motoneurons. *Neuropharmacology* 38, 1569–1576
16 Jia, Z. *et al.* (1998) Selective abolition of the NMDA component of long-term potentiation in mice lacking mGluR5. *Learn. Mem.* 5, 331–343
17 Salt, T.E. and Eaton, S.A. (1994) The function of metabotropic excitatory amino acid receptors in synaptic transmission in the thalamus: studies with novel phenylglycine antagonists. *Neurochem. Int.* 24, 451–458
18 Tatarczynska, E. *et al.* (2001) Potential anxiolytic and antidepressant-like effects of MPEP, a potent, selective and systemically active mGlu5 receptor antagonist. *Br. J. Pharmacol.* 132, 1423–1430
19 Klodzinska, A. *et al.* (2000) Anxiolytic-like effects of group I metabotropic antagonist 2-methyl-6-(phenylethynyl)-pyridine (MPEP) in rats. *Pol. J. Pharmacol.* 52, 463–466
20 Schultz, B. *et al.* The metabotropic glutamate receptor antagonist 2-methyl-6-(phenylethynyl)-pyridine (MPEP) blocks fear conditioning in rats. *Neuropharmacology* (in press)
21 Fendt, M. *et al.* (2000) Injections of the metabotropic glutamate receptor antagonist MPEP into the lateral amygdala prevent acquisition of conditioned fear in rats. *Soc. Neurosci.* 26, 200
22 Spooren, W.P.J.M. *et al.* (2000) Anxiolytic-like effects of the prototypical metabotropic glutamate receptor 5 ($mGlu_5$) antagonist 2-methyl-6-(phenylethynyl)-pyridine (MPEP) in rodents. *J. Pharmacol. Exp. Ther.* 295, 1267–1275
23 Chapman, A.G. *et al.* (2000) Anticonvulsant activity of two metabotropic glutamate group I antagonists selective for the mGlu5 receptor: 2-methyl-6-(phenylethynyl)-pyridine (MPEP), and (E)-6-methyl-2-styryl-pyridine (SIB 1893). *Neuropharmacology* 39, 1567–1574
24 Bruno, V. *et al.* (2000) Selective blockade of metabotropic glutamate receptor subtype 5 is neuroprotective. *Neuropharmacology* 39, 2223–2230
25 Movsesyan, V. *et al.* (2001) mGluR5 antagonists 2-methyl-6-(phenylethynyl)-pyridine and (E)-2-methyl-6-(2-phenylethenyl)-pyridine reduce traumatic neuronal injury *in vitro* and *in vivo* by antagonizing N-methyl-D-aspartate receptors. *J. Pharmacol. Exp. Ther.* 296, 41–47
26 Spooren, W.P.J.M. *et al.* (2000) Effects of the prototypical mGlu(5) receptor antagonist 2-methyl-6-(phenylethynyl)-pyridine on rotarod, locomotor activity and rotational responses in unilateral 6-OHDA-lesioned rats. *Eur. J. Pharmacol.* 406, 403–410
27 Walker, K. *et al.* (2001) Metabotropic glutamate receptor subtype 5 (mGlu5) and nociceptive function. I. Selective blockade of mGlu5 receptors in models of acute, persistent and chronic pain. *Neuropharmacology* 40, 1–9
28 Walker, K. *et al.* (2001) mGlu5 receptors and nociceptive function II. mGlu5 receptors functionally expressed on peripheral sensory neurones mediate inflammatory hyperalgesia. *Neuropharmacology* 40, 10–19

Chemical name

LY344545: (1*R*,2*S*)-2-[(*R*)-1-amino-1-carboxy-2-(9*H*-thioxanthen-9-yl)-ethyl]-cyclopropanecarboxylic acid
LY393675: 3-(*S*)-1-amino-1-carboxy-2-(9*H*-thioxanthen-9-yl)-ethyl]-cyclobutanecarboxylic acid
SIB1757: 6-methyl-2-(phenylazo)-3-pyridinol
SIB1893: (*E*)-2-methyl-6-(2-phenylethenyl)pyridine

Will P.J.M. Spooren*
Fabrizio Gasparini
Rainer Kuhn
Novartis Pharma AG, Nervous System Research, CH-4002 Basel, Switzerland.
*e-mail: willibrordus.spooren@pharma.novartis.com
Thomas E. Salt
Institute of Ophthalmology, University College London, London, UK EC1V 9EL.

Meeting Report

Histamine receptors are finally 'coming out'

Rob Leurs, Takehiko Watanabe and Henk Timmerman

The International Sendai Histamine Symposium *Histamine Research in the New Millennium* was held in Sendai, Japan on 22–25 November 2000.

The *Histamine Research in the New Millennium Symposium*, which covered various aspects of the histamine-mediated system, was one of the most exciting meetings in this field in past years, and was enjoyed by 300 attendants from 25 countries. Important information on histamine H_1 and H_2 receptors was reported, but the main reason for this enthusiasm was the wealth of new information on several new histamine receptors (Table 1).

Cloning and characterization of the H_3 receptor

Following the cloning of the human histamine H_3 receptor by Lovenberg *et al.* in 1999 (Ref. 1), the field of histamine receptors has gained considerable interest. At the meeting Tim Lovenberg (R.W. Johnson Pharmaceutical Research Institute, San Diego, CA, USA) briefly reviewed the cloning of the human and rat H_3 receptor cDNAs as part of their ongoing effort to identify orphan G-protein-coupled receptors. The two receptors exhibit a 97% homology in the transmembrane (TM) domains[1,2], but surprisingly they display a significant difference in affinity for some H_3 receptor ligands (e.g. thioperamide shows a tenfold preference for the rat receptor). Cloning of the mouse H_3 receptor allowed Lovenberg and co-workers to generate H_3 receptor knockout mice. These animals are viable and fertile, but less 'active' at all times. The mice are currently undergoing further testing and will provide interesting new model systems to learn more about the (patho)physiological role of the H_3 receptor.

Investigations by the groups of Rob Leurs (Leiden/Amsterdam Center for Drug Research, Amsterdam, The Netherlands) and Jean-Charles Schwartz (INSERM, Paris, France) revealed that Thr119 and Ala122 are fully responsible for the observed relative low affinity of thioperamide, iodophenpropit and ciproxyfan at the human H_3 receptor. The same two groups also reported on the high level of constitutive activity of the human and rat H_3 receptor, resulting in a reclassification of a variety of H_3 receptor antagonists. Burimamide, originally found to be an H_3 receptor antagonist[3], surprisingly acts as an agonist at the recombinant H_3 receptor, whereas compounds such as thioperamide, clobenpropit and ciproxyfan behave as inverse agonists. The constitutive activity

  PII: S0165-6147(00)01691-6

EXHIBIT L

THE JOURNAL OF BIOLOGICAL CHEMISTRY
Vol. 273, No. 21, Issue of May 22, pp. 13089–13096, 1998
Printed in U.S.A.

Expression and Purification of the Extracellular Ligand Binding Region of Metabotropic Glutamate Receptor Subtype 1*

(Received for publication, September 15, 1997, and in revised form, February 20, 1998)

Tomoyuki Okamoto‡§, Naohiro Sekiyama‡, Mieko Otsu‡¶, Yoshimi Shimada‡, Atsushi Sato‡, Shigetada Nakanishi‖, and Hisato Jingami‡**

From the ‡Department of Molecular Biology, Biomolecular Engineering Research Institute, 6-2-3 Furuedai, Suita, Osaka 565, Japan and the ‖Department of Biological Sciences, Kyoto University Faculty of Medicine, Yoshida, Sakyo-Ku, Kyoto 606, Japan

Each metabotropic glutamate receptor possesses a large extracellular domain that consists of a sequence homologous to the bacterial periplasmic binding proteins and a cysteine-rich region. Previous experiments have proposed that the extracellular domain is responsible for ligand binding. However, it is currently unknown whether the extracellular ligand binding site can bind ligands without other domains of the receptor. We began by obtaining a sufficient amount of receptor protein on a baculovirus expression system. In addition to the transfer vector that encodes the entire coding region, transfer vectors that encode portions of the extracellular domain were designed. Here, we report a soluble metabotropic glutamate receptor that encodes only the extracellular domain and retains a ligand binding characteristic similar to that of the full-length receptor. The soluble receptor secreted into culture medium showed a dimerized form. Furthermore, we have succeeded in purifying it to homogeneity. Dose-response curves of agonists for the purified soluble receptor were examined. The effective concentration for half-maximal inhibition (IC_{50}) of quisqualate for the soluble receptor was 3.8×10^{-8} M, which was comparable to that for the full-length receptor. The rank order of inhibition of the agonists was quisqualate ≫ ibotenate ≥ L-glutamate ≈ (1*S*,3*R*)-1-aminocyclopentane-1,3-dicarboxylic acid. These data demonstrate that a ligand binding event in metabotropic glutamate receptors can be dissociated from the membrane domain.

Glutamate receptors are divided into two distinct classes: ionotropic glutamate receptors (iGluRs)[1] and metabotropic glutamate receptors (mGluRs) (1, 2). The iGluRs consist of *N*-methyl-D-aspartate receptors and non-*N*-methyl-D-aspartate receptors. Non-*N*-methyl-D-aspartate receptors are further subdivided into two groups: α-amino-3-hydroxy-5-methyl-4-isoxazolepropionic acid receptors and kainate receptors. iGluRs are ligand-gated ion channels that transduce glutamate binding into cation influx. mGluRs that have been discovered most recently comprise eight subtypes, which are divided into three groups according to agonist selectivity, coupling to different effector systems, and sequence homology (3–6). Group I includes mGluR1 and mGluR5, which are coupled to inositol phospholipid metabolism. Group II (mGluR2 and mGluR3) and group III (mGluR4, mGluR6, mGluR7, and mGluR8) are negatively coupled to adenylate cyclase activity. Functional analyses of these mGluRs are now avidly being performed. The evidence is accumulating that mGluRs modulate excitatory synaptic transmission (7) through various neural transduction pathways, such as regulation of neurotransmitter release (8), influences on ion channel activity (9), and modulation of synaptic plasticity (10).

mGluRs have a remarkably large extracellular domain that has no homology with the other G protein-coupled receptors (GPCRs) except Ca^{2+}-sensing receptors (11). Previous experiments (12, 13) have proposed that the ligand binding site resides mainly in the extracellular domain. Thus, the mode of ligand binding of mGluRs is different from that of other GPCRs for small molecule transmitters, such as adrenaline and acetylcholine. Thus, it is a subject of great interest how extracellular signals are transmitted into cells and what roles other parts of the receptor protein perform in mGluRs. Recently, various data of mGluRs on the brain function have been obtained, and the more specific and stronger antagonists and agonists have been urgently requested both in neurobiology and clinical fields (6, 14). For designing the antagonists, the information on the three-dimensional structure of the receptor protein is very valuable. In order to determine a tertiary structure, a sufficient amount of pure receptor protein is needed. However, at present, it is extremely difficult to solubilize the receptor protein from membrane preparations. Therefore, we tried to produce a ligand binding region in a soluble form. If a ligand binding region can be produced independently of the membrane domain, it will be also a good tool for understanding activation mechanism of this intriguing receptor. In an α-amino-3-hydroxy-5-methyl-4-isoxazolepropionic acid receptor, one of glutamate-gated ion channels, Kuusinen *et al.* (15) have shown that an agonist binding site can be reconstituted by making a fusion protein of two discontinuous segments: one is proximal to the first transmembrane segment, and the other is located between the third and fourth transmembrane segments.

In the current study, we have expressed a mGluR subtype 1α (described as mGluR1 from now on) in insect cells on a baculovirus system. We have isolated an extracellular ligand bind-

* The costs of publication of this article were defrayed in part by the payment of page charges. This article must therefore be hereby marked "*advertisement*" in accordance with 18 U.S.C. Section 1734 solely to indicate this fact.

§ Present address: Kirin Brewery Co., Ltd., Central Laboratories for Key Technology, Kanazawa-Ku, Yokohama, Kanagawa 236, Japan.

¶ Present address: Tsukita Cell Axis Project, Japan Science and Technology Corp., Shimogyo-Ku, Kyoto 600, Japan.

** To whom correspondence should be addressed. Tel.: 81-6-872-8214; Fax: 81-6-872-8219.

[1] The abbreviations used are: iGluR, ionotropic glutamate receptor; mGluR, metabotropic glutamate receptor; GPCR, G protein-coupled receptor; ACPD, 1-aminocyclopentane-1,3-dicarboxylic acid; CHO, Chinese hamster ovary; PCR, polymerase chain reaction; PAGE, polyacrylamide gel electrophoresis; MAb, monoclonal antibody; AcNPV, *Autographa californica* nuclear polyhedrosis virus; Sf9 cells, *Spodoptera frugiperda* cells; Chaps, 3-[(3-cholamidopropyl)dimethylammonio]-1-propanesulfonic acid.

ing region that has a biochemical characteristic comparable to that of the full-length receptor. Purification and characterization of the soluble mGluR are presented. This is the first demonstration among GPCRs for small molecule transmitters that a ligand binding region is produced in a soluble form.

EXPERIMENTAL PROCEDURES

Materials—Quisqualic acid, (1*S*,3*R*)-1-aminocyclopentane-1,3-dicarboxylic acid (ACPD), (2*S*,1′*R*,2′*R*,3′*R*)-2-(2,3-dicarboxycyclopropyl)-glycine, L-2-amino-4-phosphonobutyrate, (*S*)-3,5-dihydroxyphenylglycine, (*R*,*S*)-1-aminoindan-1,5-dicarboxylic acid, (*S*)-α-methyl-4-carboxyphenylglycine, 7-(hydroxyimino)cyclopropa[b]chromen-1a-carboxylate ethyl ester, *N*-phenyl-7-(hydroxyimino)cyclopropa[b]chromen-1a-carboxamide, (*R*,*S*)-α-ethyl-4-carboxyphenylglycine, (*R*,*S*)-2-amino-4-(3-hydroxy-5-methylisoxazol-4-yl)butyric acid, (2*S*)-α-ethylglutamic acid, (*R*,*S*)-α-cyclopropyl-4-phosphonophenylglycine, and (*R*,*S*)-α-methylserine-*O*-phosphate were purchased from Tocris Cookson Inc. (St. Louis, MO). L-Glutamic acid was obtained from Wako Pure Chemical Industries Ltd. (Osaka, Japan). Ibotenic acid was purchased from Sigma. All other reagents were of analytical grade.

Cell Culture—*Spodoptera frugiperda* cells (Sf9 cells) were propagated in a monolayer at 27 °C in TNM-FH (Grace's powder medium, 0.4% yeastolate, 0.4% lactalbumin hydrolysate, and 0.1% pluronic F-68 from Life Technologies, Inc.), supplemented with 10% fetal bovine serum (Irvine Science, Santa Ana, CA) or in suspension at 27 °C in IPL-41 (Life Technologies, Inc.) supplemented with 10% fetal bovine serum, 0.3% tryptose phosphate (Life Technologies, Inc.). 100 units/ml of penicillin, 100 μg/ml streptomycin, and 25 ng/ml amphotericin B were used. *Trichoplusia ni* BTI-TN-5B1–4 (High Five cells) were cultured in a monolayer at 27 °C in Express Five serum-free medium (Life Technologies, Inc.) supplemented with 18 mM L-glutamine. Chinese hamster ovary (CHO) cells permanently expressing mGluR1 (16) were cultured in a monolayer at 37 °C, 5% CO_2 in Dulbecco's modified Eagle medium (Nissui) lacking L-glutamine, ribonucleosides, and deoxyribonucleosides and supplemented with 2 mM L-glutamine, 1% L-proline, and 10% dialyzed fetal bovine serum (Life Technologies, Inc.). Penicillin (100 units/ml) and streptomycin (100 μg/ml) were used.

Construction of Transfer Vectors for Expression of mGluRs in Insect Cells—A *Sac*II fragment that contains the full coding region of mGluR1 was excised from pmGR1 (3) and was ligated into *Sac*II-digested pBluscriptII SK(+) (Stratagene, La Jolla, CA). A *Not*I-*Xba*I fragment of the intermediate construct was ligated into *Xba*I-*Not*I-digested pVL1392 (PharMingen, San Diego, CA) to generate pmGluR102.

pmGluR104 was made as follows. pmGR1 was used as a template of polymerase chain reaction (PCR) to amplify a sequence (nucleotides 3276–3597) according to the numbering of the sequence by Masu *et al.* (3). Primer TO3 (5′-CCAGGAGGAGTCCATC-3′) and primer TO4 (5′-CAGTGCTCTAGATCACTAGTGATGGTGATGGTGATGCAGGGTGGAAGAGCTTTGC-3′) were used. TO4 contains six consecutive histidine codons and an *Xba*I site. A 310-base pair *Cla*I-*Xba*I fragment of the PCR product was ligated with a 3.3-kilobase pair *Not*I-*Cla*I fragment of pmGR1 and a 9.6-kilobase pair *Xba*I-*Not*I-digested pVL1392 vector.

pmGluR103 was made as follows. PCR was done using pmGR1 as a template to amplify a sequence (nucleotides 1239–1506) with primers TO1 (5′-CATCAATGCCATCTATGCCATGGC-3′) and TO2 (5′-CAGTGCTCTAGATCACTAGTGATGGTGATGGTGATGTTCATGCCAGGTCCCCACG-3′). Six histidine codons and an *Xba*I site were included in TO2. The PCR product was digested with *Nco*I and *Xba*I and was cloned into the *Xba*I-*Nco*I-digested fragment of pmGluR102.

pmGluR107 was made as follows. PCR was done with primers GN327361U (5′-AGCGGCCGCCACCGCGGTGGACCGCGTCTTCGCCACAAT-3′) and G394419FL (5′-TTTGTCATCGTCGTCCTTGTAGTCGGGCAAAATGGACATCTCCAAAAA-3′) using pmGluR104 as a template. Another PCR was performed with primers GF421442U (5′-GACTACAAGGACGACGATGACAAAAGGATGCCTGACAGAAAAGTATTG-3′) and G700730EL (5′-TCTGATGAATTCGATGCTCTGTTCGAGAGCCAC-3′). The PCR products were mixed, and a second PCR was performed with primers GN327361U and G700730EL. The PCR product was cut by *Not*I and *Eco*RI and ligated into *Not*I-*Eco*RI-digested pmGluR104. The resultant plasmid contains the sequence corresponding to DYKDDDDK after Pro20.

pmGluR108 was constructed from pmGluR104. A fragment (nucleotides 1687–1776) was made with primers HJ104 (5′-AGAGCCTGTGACCTGGGGTGGTGG-3′) and MO101 (5′-TCTAGATTACTAGTGATGGTGATGGTGATGGCTAGCTTCTATGTCACTCCACTCAAGATA-3′). Another fragment (nucleotides 1783–1911) was made with primers MO102 (5′-GCTAGCCATCACCATCACCATCACTAGTAATCTAGAATAGCCATCGCCTTTTCTTGCCTG-3′) and HJ107 (5′-ACCAGCCAGAATGATATAGCAGAG-3′). A second PCR was done with primers HJ104 and HJ107, and its product was digested with *Sac*I and ligated into *Sac*I-linearized pmGluR104. The resultant plasmid contains Ala-Ser-His_6 termination codons after Glu^{592}. All of the above PCR products were entirely sequenced.

Generation of Recombinant Baculoviruses for mGluRs—Recombinant baculoviruses encoding full-length and truncated cDNAs were produced in Sf9 cells with the transfer vectors. Briefly, Sf9 cells (1×10^5) were transfected with 0.1 μg of BaculoGold linear DNA (PharMingen) and 1.0 μg of each plasmid using a liposome transfection kit (Life Technologies, Inc.). The viruses were harvested after 6 days. For the expression assay, 2.5×10^6 Sf9 or High Five cells were infected with each baculovirus. 72 h after infection, cells were harvested, and membranes were prepared as below. In the case of the cells infected with baculoviruses for mGluR103, mGluR107, and mGluR108, culture medium was collected and centrifuged at $800 \times g$ for 10 min and filtered. Membranes were solubilized on ice for 30 min in lysis buffer (40 mM Hepes, pH 7.5, 150 mM NaCl, 1 mM EDTA, 1 mM EGTA, and 1.0% Chaps) containing protease inhibitor mixtures (1 mM phenylmethylsulfonyl fluoride, and 10 μg/ml each of leupeptin, aprotinin, pepstatin A, benzamidine, and trypsin inhibitor), and were centrifuged at 12,000 × *g* for 20 min. Aliquots of the supernatants and medium were analyzed by immunoblotting.

The plaque-purified recombinant viruses containing the full-length cDNAs for mGluR were used to infect Sf9 cells (1×10^9) at a multiplicity of infection of 1. The purified recombinant viruses containing truncated cDNAs for mGluR, mGluR103, mGluR107, and mGluR108 were used to infect High Five cells (1×10^8-2×10^8). Cells were harvested at approximately 72 h post infection. Culture medium was prepared as described above for smaller cultures. Membranes were prepared as described below.

Membrane Preparation—Membranes were obtained by nitrogen cavitation. Briefly, CHO cells or Sf9 cells were suspended in Buffer A (20 mM Tris-HCl, pH 7.5, 1 mM EDTA, and protease inhibitor mixtures), placed in a pressure chamber (Parr bomb) and pressurized to 800 p.s.i. with nitrogen gas for 30 min on ice. The mixture was collected by pressure release and centrifuged at $800 \times g$. The supernatant was then centrifuged at $100{,}000 \times g$ for 30 min to pellet down the membranes. The membranes were divided into aliquots, frozen in liquid nitrogen, and stored at −80 °C until use.

Western Blot Analyses—Cell membranes and culture medium were separated by SDS-polyacrylamide gel electrophoresis (PAGE) and electroblotted onto a nitrocellulose membrane (Schleicher & Schuell). The membrane was then blocked for 1 h in TBST (10 mM Tris-HCl, pH 8.0, 150 mM NaCl, and 0.05% Tween 20) with 1% bovine serum albumin and incubated overnight at room temperature with a 1:5000 dilution of anti-mGluR1 monoclonal antibody (MAb) mG1Na-1 and a 1:5000 dilution of polyclonal antibody A52 in TBST. After being washed, the membrane was incubated with a goat anti-mouse IgG or a goat anti-rabbit IgG conjugated with alkaline phosphatase. Color development was done by a commercial detection kit (Promega). A MAb mG1Na-1 was made by Dr. Akio Neki as follows. The spleen cells from Balb/c mice immunized with glutathione *S*-transferase (GST)-fused mGluR1 peptide (amino acid residues 104–154) were fused with X63-Ag8.653 cells as described (17). The character of MAb mG1Na-1 was verified using CHO cells, which produce mGluR1, in comparison with polyclonal antibodies G18 and A12 (18). Polyclonal antibody A52 was raised against an mGluR1α C-terminal peptide (amino acid residues 859–1199) (19).

Immunoaffinity Column Chromatography Using MAb mG1Na-1—About 2 liters of supernatant of hybridoma mG1Na-1 cells was concentrated to 30 ml using XM50 (Millipore Corp., Bedford, MA). After addition of 150 ml of PBSSC (8 mM Na_2HPO_4, pH 7.3, 1.5 mM KH_2PO_4, 136.9 mM NaCl, and 3.6 mM KCl) and concentration again to 45 ml, the concentrate was applied onto a HiTrap protein G column (Amersham Pharmacia Biotech). The bound material was eluted with 0.1 M glycine-HCl, pH 2.7. Peak fractions were pooled and dialyzed against PBSSC at 4 °C. MAb mG1Na-1 (11.2 mg) was coupled with 1 ml of HiTrap NHS-activated column (Amersham Pharmacia Biotech) in Buffer L (200 mM $NaHCO_3$, pH 8.3, and 500 mM NaCl) at 4 °C overnight. The column was washed several times alternately with Buffer W1 (0.5 M ethanolamine, pH 8.3, and 500 mM NaCl) and Buffer W2 (100 mM acetate, pH 4.0, and 500 mM NaCl). After neutralization with 100 mM Hepes, pH 7.5, the supernatant of High Five cells prepared below was loaded.

Ligand Binding Assay—Membrane fractions (20–100 μg) of baculoviruses-infected cells were incubated with [^{3}H]quisqualate (20 nM) in a total volume of 200 μl of Buffer B (40 mM Hepes, pH 7.5, and 2.5 mM $CaCl_2$) for 1 h at room temperature. The reaction mixture was aspirated

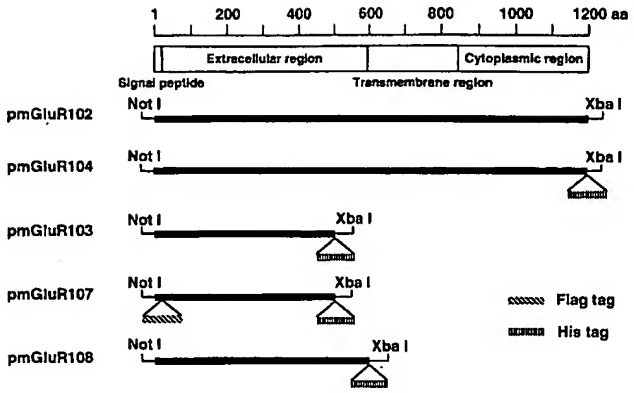

FIG. 1. **Schematic representation of various recombinant baculovirus transfer vectors for mGluR1 in insect cells.** A His tag consists of six consecutive histidine codons. A Flag tag encodes flag epitope.

onto GF/C filter (Millipore Corp.). After being washed with Buffer B, the filters were briefly dried and counted by the scintillation counter. Nonspecific binding was determined in the presence of 1 mM L-glutamate. For soluble mGluRs secreted into culture medium, a new binding assay was established using nickel conjugated beads as described below. The concentrated medium (100–200 μl) or purified soluble receptor mGluR108 (1 μg) was mixed with Ni^{2+}-NTA conjugated beads (Qiagen Inc., Chatsworth, CA) at 4 °C for 15 h. After several washings with Buffer B, [^{3}H]quisqualate was added with and without ligands. After being shaken for 1 h at room temperature, the reaction mixture was washed with Buffer B several times and filtered through GF/C filters. The remaining radioactivity was counted. Because aspirates through GF/C filters did not show any significant signal by immunoblotting, the entrapment of His-tagged receptor protein by Ni^{2+}-beads seemed to be complete.

Purification of the Soluble mGluR—A conditioned medium of soluble mGluR1-producing High Five cells was concentrated to 10–50-fold by XM50. After being dialyzed against Buffer C (10 mM Hepes, pH 7.5, and 200 mM NaCl), the dialyzate was centrifuged at 100,000 × *g* for 30 min and loaded onto an immunoaffinity column, which was conjugated with MAb mG1Na-1 as described above. The column was washed with 30 ml of Buffer C, and the bound material was eluted with 500 mM NaCl containing 500 mM sodium thiocyanate and 10 mM Hepes, pH 7.5. Aliquots of the eluate were analyzed by SDS-PAGE followed by immunoblotting. Positively stained fractions were pooled and analyzed by ligand binding assay. Then the pooled fraction was dialyzed against 10 mM Hepes, pH 7.5, containing 200 mM NaCl and 10% glycerol, and the dialyzate was loaded onto a HiLoad 16/60 Superdex 200 (Amersham Pharmacia Biotech) by high performance liquid chromatography (Waters 626 LC). The flow rate was 0.5 ml/min, and fractions of 2.5 ml each were collected.

RESULTS

Fig. 1 shows a schematic drawing of the transfer vectors used in the baculovirus infection experiments. pmGluR102 and pmGluR104 encode the membrane-bound forms of mGluR1. pmGluR103, pmGluR107, and pmGluR108 are designed to produce the truncated forms of mGluR1, which are expected to be secreted into the culture medium.

Recombinant baculoviruses for the expression of full-length mGluR1 were prepared and used to infect Sf9 insect cells in monolayer cultures. Immunoblotting analysis of expressed mGluR1 is shown in Fig. 2*A*. Both the polyclonal antibody A52, which was raised against a C-terminal peptide of mGluR1, and the MAb mG1Na-1 yielded a 155-kDa band in the membrane preparation from Sf9 cells infected with recombinant viruses but not in the control membrane preparation from Sf9 cells infected with wild-type virus, *Autographa californica* nuclear polyhedrosis virus (AcNPV). mGluR1 expressed in CHO cells showed a more slowly migrating band. This size difference may reflect less extensive glycosylation in the insect cells. A ligand binding assay was performed using membrane fractions of Sf9 cells infected with their respective recombinant viruses. ^{3}H-Labeled quisqualate specifically bound the membranes, and the binding was displaced by unlabeled glutamate (Fig. 2*B*). The control membranes prepared in parallel from wild-type virus (AcNPV)-infected cells did not show any specific binding. Both levels of expression of the receptor protein and the ligand binding ability seemed not to show a significant difference between the cells infected with recombinant viruses for mGluR102 and for mGluR104. The inhibition of [^{3}H]quisqualate binding with several agonists was examined as shown in Fig. 2*C*. The effective concentration for half-maximal inhibition (IC_{50}) of quisqualate was 3.0×10^{-8} M, which is comparable to the effective concentration for half-maximal response (EC_{50}) in inducing the stimulation of phosphatidylinositol hydrolysis in CHO cells permanently expressing mGluR1 (16). The rank order of inhibition was quisqualate ≫ L-glutamate ≈ ibotenate ≥ (1*S*,3*R*)-ACPD. Ohashi *et al.* (20) have obtained comparable data using the membrane fractions of Sf9 cells infected with recombinant baculovirus for the human full-length mGluR1. They reported that ^{3}H-labeled quisqualate binds the receptor in a saturable manner, with a K_d value of 5.26×10^{-8} M. Their IC_{50} value, 2×10^{-8} M, of quisqualate for the human full-length mGluR1 agrees with ours.

Next, we tried to dissect the ligand binding region of mGluR1. We infected High Five cells with recombinant viruses for mGluR103, mGluR107, and mGluR108, which were expected to produce the extracellular portions of mGluR1. Fig. 3 shows the Western blotting analyses of culture medium of cells infected with the recombinant baculoviruses. mGluR103 and mGluR107 produced a 66-kDa band, and mGluR108 produced a 74-kDa band under the reducing conditions. The level of expression of mGluR108 was much higher than those of mGluR103 and mGluR107. Under the nonreducing conditions, both bands shifted to the bands of approximately twice the size of the bands observed under the reducing conditions, suggesting a dimer formation. A minor faster migrating band observed in mGluR108 under the nonreducing conditions seemed to be a monomer. The 74-kDa band under the reducing conditions looked broad and may reflect heterogeneities of the glycosylation pattern. mGluR107, which differs from mGluR103 only in the flag tag sequence added to the N-terminal end, did not show any obvious band under the nonreducing conditions. Although the cause of the anomalous electrophoresis of the mGluR107 protein was not clear, it suggested an aggregated or an unfolded protein formation, which may be brought about by the disruption of the tertiary structure due to the peptide tag.

To study ligand binding properties of soluble receptors, we developed a new binding assay using Ni^{2+}-conjugated beads, which can trap the histidine tag added to the soluble mGluRs. Concentrated culture medium (100–200 μl) was incubated with Ni^{2+}-conjugated beads. Although mGluR103 and mGluR107 showed no appreciable binding, mGluR108 did reveal a significant binding ability. This binding was inhibited in the presence of 1 mM L-glutamate. Neither concentrated control culture medium nor separately prepared His-tagged soluble receptor (soluble low density lipoprotein receptor; data not shown) showed any significant binding. We examined the agonist selectivity of mGluR108 as shown in Fig. 4. Inhibition of labeled quisqualate binding by several agonists was analyzed. The rank order of inhibition was quisqualate ≫ L-glutamate ≈ (1*S*,3*R*)-ACPD ≈ ibotenate. (2*S*,1′*R*,2′*R*,3′*R*)-2-(2,3-Dicarboxycyclopropyl)-glycine and (1*S*,3*S*)-ACPD inhibited the quisqualate binding by 37 and 56% at 1×10^{-4} M, respectively; however, L-2-amino-4-phosphonobutyrate, which is a group III-specific agonist, hardly inhibited it (data not shown). The iGluR ago-

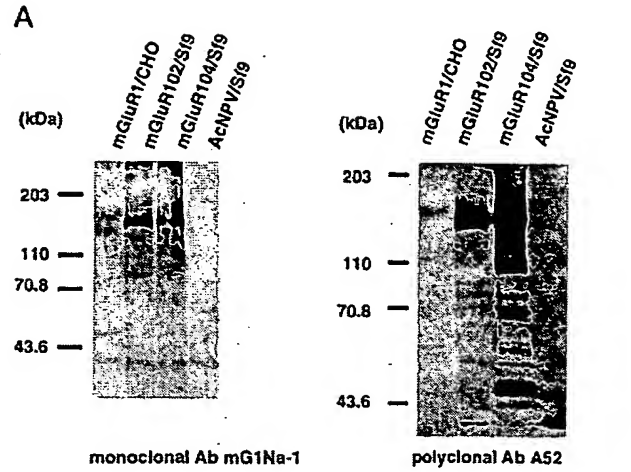

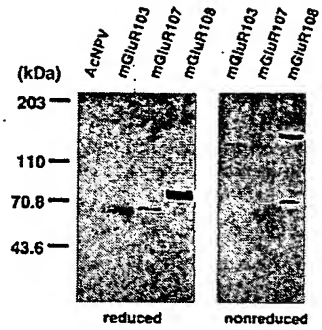

FIG. 3. **Immunoblotting analyses of the secreted soluble mGluRs.** 20 μl of culture medium of High Five cells infected with each baculovirus for mGluR103, mGluR107, and mGluR108 were loaded on 7.5% SDS-polyacrylamide gels under the reducing conditions with 2% β-mercaptoethanol and under the nonreducing conditions. Proteins were transferred onto nitrocellulose membranes and probed with MAb mG1Na-1, as described in the legend to Fig. 2*A*.

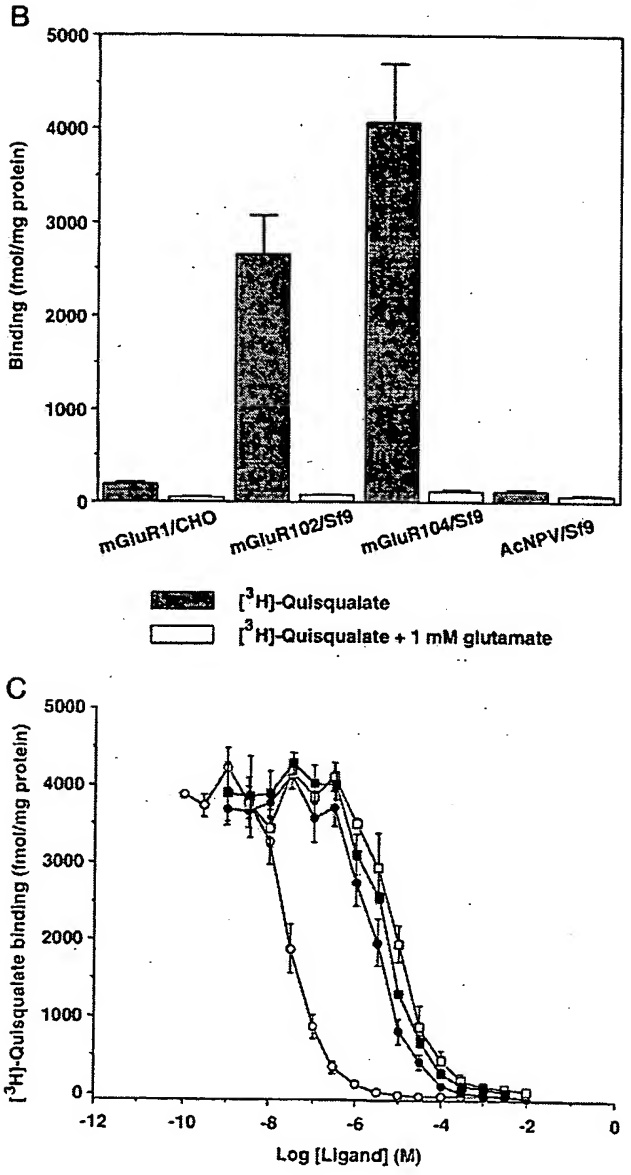

FIG. 2. **Biochemical and pharmacological characterization of full-length mGluR1 in insect cells infected with recombinant baculoviruses.** *A*, expression of full-length mGluR1 in insect cells was examined by immunoblotting. Membrane fraction (60 μg) of CHO cells producing mGluR1 and membrane fractions (30 μg) of Sf9 cells infected with recombinant viruses for mGluR102, mGluR104, and wild-type virus (AcNPV) were loaded onto a 7.5% SDS-polyacrylamide gel. Proteins were transferred onto a nitrocellulose membrane and probed with mGluR1-specific MAb mG1Na-1 and polyclonal antibody A52. Immunostained proteins were visualized by a goat anti-mouse IgG or a goat anti-rabbit IgG coupled to alkaline phosphatase as described under "Experimental Procedures." Marker proteins are myosin heavy chain (203 kDa), phosphorylase B (110 kDa), bovine serum albumin (70.8 kDa), and ovalbumin (43.6 kDa). *B*, ligand binding of full-length mGluRs was measured. Membrane fractions (100 μg) of Sf9 cells infected with recombinant viruses for mGluR102, mGluR104, and wild-type virus (AcNPV) and of CHO cells producing mGluR1 were incubated in a binding buffer (40 mM Hepes, pH 7.5, and 2.5 mM $CaCl_2$) with [^{3}H]quisqualate (20 nM) at room temperature for 1 h. The reaction mixtures were aspirated onto GF/C filters, and the material remaining on the filters were counted with a scintillation counter. Nonspecific binding was determined with 1 mM L-glutamate. Each binding was performed in triplicate and is shown as mean ± S.D. A representative of two experiments is shown. *C*, dose-response curves of various agonists in inhibiting [^{3}H]quisqualate binding to full-length mGluR104 were determined. Indicated concentrations of quisqualate (*open circles*), L-glutamate (*closed circles*), (1*S*,3*R*)-ACPD (*open squares*), and ibotenate (*closed squares*), each with the addition of [^{3}H]quisqualate (20 nM), were incubated with 100 μg of membrane fraction of Sf9 cells infected with recombinant virus for mGluR104 prepared as described under "Experimental Procedures." Binding counts obtained without any agonist were 7507 ± 624 dpm. Each *point* shows the mean ± S.E. of three experiments done in triplicate.

nists *N*-methyl-D-aspartate, α-amino-3-hydroxy-5-methyl-4-isoxazolepropionic acid, and kainate did not show any significant inhibition at 1×10^{-4} M (data not shown). These binding characteristics clearly indicate that the expressed soluble receptor, mGluR108, is capable of binding ligands in the same manner as the native group I mGluR.

Because newer ligands have recently been used in physiological and pharmacological experiments on mGluRs, we examined their reactivities with the soluble mGluR108. Fig. 5*A* shows the dose-response curves of the newer ligands. (*S*)-3,5-Dihydroxyphenylglycine, which is a group I-specific agonist (21–23) and (*R,S*)-1-aminoindan-1,5-dicarboxylic acid, which is a group I-specific antagonist (24), inhibited the [^{3}H]quisqualate binding at IC_{50} values of 0.23×10^{-4} and 0.50×10^{-4} M, respectively. (*S*)-α-Methyl-4-carboxyphenylglycine, which is a nonselective group I/group II antagonist (25, 26, 23), also inhibited the quisqualate binding at an IC_{50} value of 1.2×10^{-4} M. 7-(Hydroxyimino)cyclopropa[b]chromen-1a-carboxylate ethyl ester and *N*-phenyl-7-(hydroxyimino)cyclopropa[b-]chromen-1a-carboxamide, which are structurally novel group I antagonists (27), did not show any inhibition. Results of other

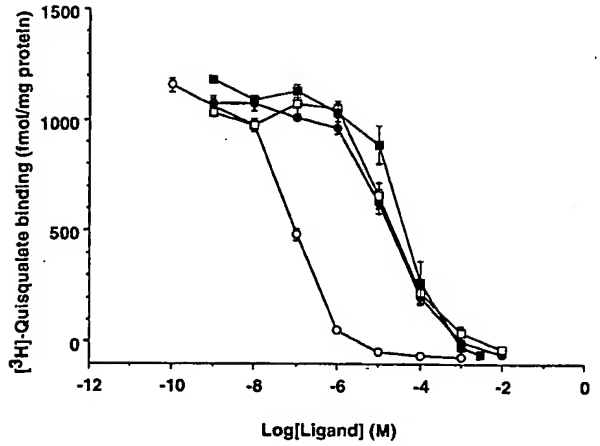

FIG. 4. **Dose-response curves of various agonists in inhibiting [^{3}H]quisqualate binding to the soluble mGluR108 secreted into culture medium.** The supernatant of High Five cells infected with recombinant virus for mGluR108 was concentrated 40-fold. 200 μl of it was incubated with Ni^{2+}-conjugated beads. Then, the indicated concentrations of quisqualate (*open circles*), L-glutamate (*closed circles*), (1*S*,3*R*)-ACPD (*open squares*), and ibotenate (*closed squares*), together with [^{3}H]quisqualate, were added into the reaction mixture. Ligand binding was assayed as described under "Experimental Procedures." Binding counts obtained without any agonist were 9268 ± 1387 dpm. Each *point* shows the mean ± S.E. of two experiments done in triplicate.

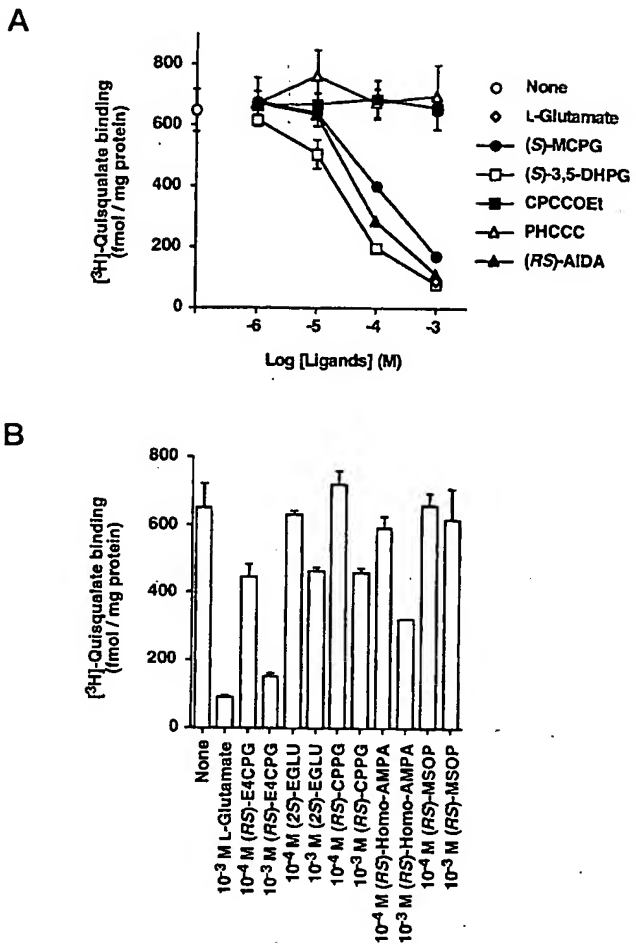

FIG. 5. **Dose-response curves and effects of newer ligands on inhibiting [^{3}H]quisqualate binding to the soluble mGluR 108 secreted into culture medium.** *A*, concentrated culture medium of High Five cells infected with the recombinant virus for mGluR108 were prepared and used for inhibition of the [^{3}H]quisqualate binding as described in Fig. 4. The indicated concentrations of (*S*)-α-methyl-4-carboxyphenylglycine (*MCPG*), (*S*)-3,5-dihydroxyphenylglycine (*DHPG*), 7-(hydroxyimino)cyclopropa-[b]chromen-1a-carboxylate ethyl ester (*CPCCOEt*), *N*-phenyl-7-(hydroxy-imino)cyclopropa[b]chromen-1a-carboxamide (*PHCCC*), (*R*,*S*)-1-aminoindan-1,5-dicarboxylic acid (*AIDA*), and L-glutamate were added in the reaction mixtures. Binding counts without any ligand were 2133 ± 229 dpm. The values indicated are means ± S.D. of tripricate determinations. A representative of two experiments is shown. *B*, effects of various ligands on the inhibition of [^{3}H]quisqualate binding are shown. The ligands analyzed are (*R*,*S*)-α-ethyl-4-carboxyphenylglycine (*E4CPG*), (2*S*)-α-ethylglutamic acid (*EGLU*), (*R*,*S*)-α-cyclopropyl-4-phosphonophenylglycine (*CPPG*), (*R*,*S*)-2-amino-4-(3-hydroxy-5-methylisoxazol-4-yl)butyric acid (*Homo-AMPA*), and (*R*,*S*)-α-methylserine-*O*-phosphate (*MSOP*). Each ligand was incubated in the reaction mixture together with [^{3}H]quisqualate. Basal levels were 2133 ± 229 dpm. A representative of two experiments is shown.

ligands are shown in Fig. 5*B*. (*R*,*S*)-α-Ethyl-4-carboxyphenylglycine (23, 28) showed an inhibition of 37% at 1×10^{-4} M. (*R*,*S*)-2-Amino-4-(3-hydroxy-5-methylisoxazol-4-yl)butyric acid, which is an mGluR subtype 6-specific agonist (29), showed a slight inhibition of 10% at 1×10^{-4} M. Other compounds, including (2*S*)-α-ethylglutamic acid, (*R*,*S*)-α-cyclopropyl-4-phosphonophenylglycine, and (*R*,*S*)-α-methylserine-*O*-phosphate, which are classified as group II or group III antagonists, did not show significant inhibition.

Next, we started the purification of the soluble receptor mGluR108 from the culture medium. Approximately 2.5 liters of the culture medium was concentrated, dialyzed, and loaded on an immunoaffinity column as described under "Experimental Procedures." After being washed with the binding buffer, the bound material was eluted. Aliquots of the flow-through and the eluates were analyzed by silver staining (Fig. 6*A*) and immunoblotting (Fig. 6*B*). Fractions that were positively stained by the immunoblot completely agreed with the ligand binding activity, and these fractions were pooled and purified by size exclusion column chromatography (Superdex 200) as shown in Fig. 7. A single peak was obtained. Peak fractions were collected and analyzed by SDS-PAGE under reducing and nonreducing conditions, followed by silver staining. On the basis of the result of an overloaded gel electrophoresis of the purified soluble receptor protein, we estimated that the purity of our final material is 99% (data not shown). Calibration with the molecular size markers showed the eluting position of the soluble mGluR108 to be around 190 kDa. The purified material is definitely larger than a monomer and seems to be a dimer or a larger oligomer.

Fig. 8 shows dose-response curves of group I mGluR agonists for the purified mGluR108. IC_{50} value of quisqualate, 3.8×10^{-8} M, was close to that for the full-length receptor, mGluR104, as described in Fig. 2*C*. The rank order of inhibition of the agonists was quisqualate ≫ ibotenate ≥ L-glutamate ≈ (1*S*,3*R*)-ACPD. The IC_{50} values of L-glutamate and (1*S*,3*R*)-ACPD for the purified receptor seems to be 2–5 times as large as those for the full-length receptor. The rank order of the inhibition is reversed between L-glutamate and ibotenate. Although the significance of this small difference is unknown, it may reflect the difference between the crude membrane preparation and the purified receptor protein.

DISCUSSION

mGluRs have occupied a unique place in the sense that they have a very large extracellular domain and no amino acid sequence homology in the transmembrane helix with the other conventional GPCRs. Takahashi *et al.* (12) have made chimeric receptors between mGluR1 and mGluR2 and have shown that the large extracellular domain plays a crucial role in determining agonist selectivity. O'Hara *et al.* (13) have discovered the homology between the N-terminal extracellular region (residues 1–496) (which we tentatively call region I) and the bac-

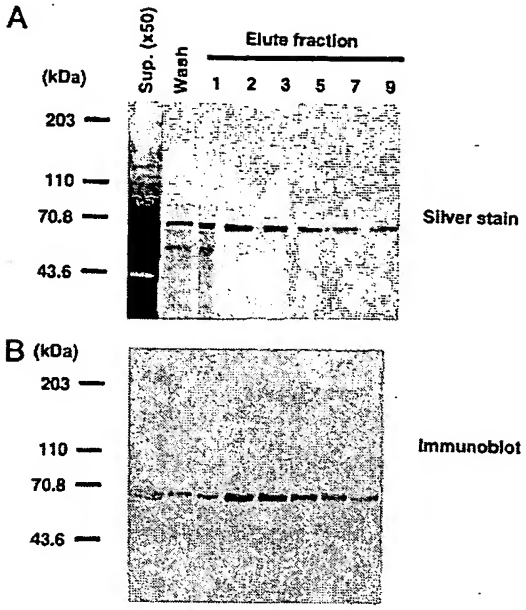

FIG. 6. **Immunoaffinity chromatography of the soluble mGluR108.** Culture medium (2.5 liters) of High Five cells infected with recombinant virus for mGluR108 was concentrated 50-fold and dialyzed against Buffer C. The dialyzate was loaded on a HiTrap Affinity column (1 ml) that had been coupled with mGluR1-specific MAb mG1Na-1 and equilibrated with Buffer C. The column was washed with 30 ml of Buffer C, and the bound material was eluted with 500 mM NaCl containing 500 mM sodium thiocyanate and 10 mM Hepes, pH 7.5. *A*, indicated aliquots of the eluate were subjected to 7.5% SDS-PAGE and silver stained. *B*, identical samples were analyzed by Western blot with MAb mG1Na-1 as described in the legend to Fig. 2A.

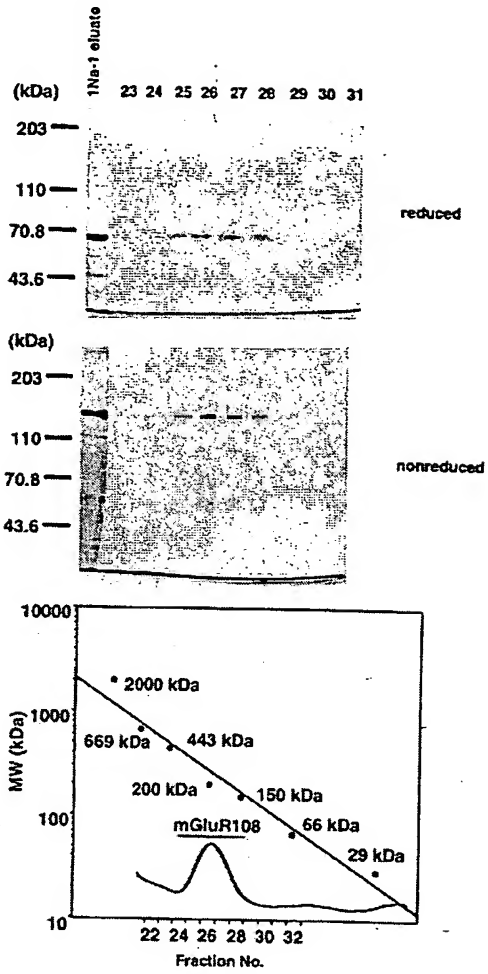

FIG. 7. **Gel filtration chromatography of the soluble mGluR108.** Soluble mGluR108 (64 μg) from the immunoaffinity column (Fig. 6) was loaded onto a HiLoad 16/60 Superdex 200 gel filtration column (Amersham Pharmacia Biotech). The column was equilibrated and eluted with 10 mM Hepes, pH 7.5, containing 200 mM NaCl and 10% glycerol. 2.5 ml of each fraction was collected. The molecular masses of the marker proteins were blue dextran (>2000 kDa), bovine thyroglobulin (669 kDa), horse spleen apoferritin (443 kDa), sweet potato β-amylase (200 kDa), yeast alcohol dehydrogenase (150 kDa), bovine serum albumin (66 kDa), and bovine erythrocytes carbonic anhydrase (29 kDa). Aliquots (20 μl) of the indicated gel filtration fractions were subjected to 7.5% SDS-PAGE under the reducing conditions with 2% β-mercaptoethanol and under the nonreducing conditions, followed by silver staining.

terial amino acid-binding proteins. They have constructed the molecular model of the glutamate binding site. The model has led them to point out the two critical amino acid residues, substitutions of which abolished [^{3}H]glutamate binding. In the extracellular domain of mGluR, there is also a short stretch of the cysteine-rich sequence (region II) just proximal to the membrane-spanning domain. However, the ligand binding site has not yet been isolated as a soluble molecule. In this investigation, we have succeeded in producing a soluble metabotropic glutamate receptor without the membrane-anchored domain and have provided compelling evidence that the soluble receptor consisting of the extracellular regions I and II is sufficient for conferring the affinity and selectivity of ligand binding characteristic of the mGluR.

Extensive studies of structure-function relationships have been done in GPCRs, and different modes of agonist binding are known (30, 31). Monoamines and other small ligands, such as catecholamine and acetylcholine, are bound to the pockets formed within the transmembrane segments. In the receptors for neuropeptides or chemokines, a major binding site is located in the N-terminal segments of the receptors, with some contribution of the extracellular loops or the outer portions around the transmembrane segments. In receptors for large glycoprotein hormones, such as luteinizing hormone and thyrotropin, a large extracellular domain is responsible for high affinity ligand binding (32–35), but a low affinity site is located in the extracellular loops in luteinizing hormone receptor (36, 37). Although the role(s) of the extracellular loops and transmembrane segments of mGluR remains to be determined in the present study, it should be pointed that the soluble form of mGluR1 has a ligand affinity and specificity comparable to those of the full-size mGluR1. Thus, our results indicate that the ligand binding event is really dissociable from transmembrane signaling in this receptor system. Pharmacological analyses with the conventional agonists and the newer ligands suggest that the soluble mGluR would be a reliable method for binding studies of future ligands that are expected to be developed.

We have made and analyzed several truncated forms of soluble mGluR1, which encode parts of the extracellular domain of mGluR1. The IC_{50} value of quisqualate for mGluR108 is remarkably similar to those of the full-length membrane-anchored form of the receptor. The agonist selectivity examined also constitutes a typical feature of mGluR1. These results indicate that the secreted extracellular domain forms a correct conformation for ligand binding. The soluble form of mGluR1 shows a dimerized form. A similar dimerization has been reported for several members of the conventional GPCRs, and this dimerization is ascribed to the molecular association in the transmembrane domains of these receptors (38, 39). In addi-

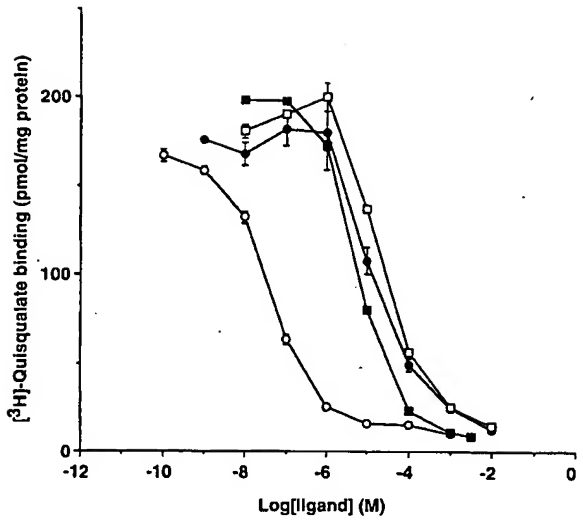

FIG. 8. **Dose-response curves of various agonists in inhibiting [^{3}H]quisqualate binding to the purified soluble mGluR108.** Purified mGluR108 (1 μg) from a gel exclusion chromatography (Superdex 200) as described in the legend to Fig. 7. was mixed with Ni^{2+}-conjugated beads. Then, the indicated concentrations of quisqualate (*open circles*), L-glutamate (*closed circles*), (1*S*,3*R*)-ACPD (*open squares*) and ibotenate (*closed squares*), each with the addition of [^{3}H]quisqualate, were incubated in the reaction mixture. Ligand binding was assayed as described under "Experimental Procedures." Binding counts obtained without any agonist were 2967 ± 69 dpm. Each *point* shows the mean ± S.E. of three experiments done in triplicate.

tion, Romano *et al.* (40) have reported that the truncated form of mGluR5 containing the first transmembrane segment forms a dimer. They demonstrated that an N-terminal 17-kDa region is required for dimerization. Our observation that mGluR103 dimerized is consistent with theirs. However, the truncated forms of the receptor, mGluR103 and mGluR107, which contain only region I, do not express well, and they show no significant ligand binding. Furthermore, mGluR108, which contains both region I and region II, expresses well and binds the ligand. This cysteine-rich region II of mGluR may thus impose a structural constraint on the receptor protein. A less likely possibility is that the ligand binding site might be composed of the two regions. In this context, the $GABA_B$ receptor (41), although belonging to the mGluR family with a large extracellular domain and a low but significant sequence homology to region I of mGluR, does not possess a region homologous to the cysteine-rich region II of mGluR. Furthermore, such a cysteine-rich region is absent in bacterial periplasmic amino acid-binding proteins. Thus, the real role of the cysteine-rich region II of mGluR remains an open question.

The bacterial periplasmic binding proteins serve as initial receptors of active transport for a variety of amino acids, sugars, peptides, oxyanions, and other nutrients. Although the binding proteins have different sizes (20–60 kDa) and share little sequence homology, they all fold a similar two-lobed tertiary structure. Atomic structures of the binding proteins have been analyzed by Quiocho and co-workers (42) and other groups (43) using crystallography. On the basis of the comparison between ligand-bound and ligand-free forms, the "Venus flytrap" model has been proposed (44): the ligand binds preferentially to one lobe of the open, ligand-unloaded form. A bending motion at the hinge region between the two lobes in turn causes the other lobe to participate in binding and completely entrap the ligand. The closed, ligand-loaded form of the binding protein then interacts with membrane-bound components, thereby initiating nutrient translocation or flagella motion. Therefore, it should give us insights into the receptor activation mechanism of mGluR to reveal the three-dimensional structure of the mammalian glutamate receptor and determine whether a domain movement similar to that of the bacterial binding protein is produced upon ligand binding in mGluR. We speculate that glutamate induces a conformational change of the preexisting dimer or oligomer of glutamate receptor and triggers the signal transmission to the cytoplasmic signaling domain through the cysteine-rich region and the seven-transmembrane domain. The soluble form of mGluR1 produced in a sufficient amount will make it possible to conduct the biophysical analysis of mGluR1.

Acknowledgments—We thank Drs. Yutaka Takeuchi and Hidemi Higashi-Matsumoto for helpful discussions and Drs. Akio Neki, Hitoshi Ohishi, and Ryuichi Shigemoto and Prof. Noboru Mizuno for various antibodies. We are very grateful to Dr. Yoshiro Shimura for continuous encouragement.

REFERENCES

1. Nakanishi, S., and Masu, M. (1994) *Annu. Rev. Biophys. Biomol. Struct.* **23**, 319–348
2. Hollmann, M., and Heinemann, S. (1994) *Annu. Rev. Neurosci.* **17**, 31–108
3. Masu, M., Tanabe, Y., Tsuchida, K., Shigemoto, R., and Nakanishi, S. (1991) *Nature* **349**, 760–765
4. Tanabe, Y., Masu, M., Ishii, T., Shigemoto, R., and Nakanishi, S. (1992) *Neuron* **8**, 169–179
5. Nakanishi, S. (1992) *Science* **258**, 597–603
6. Conn, P. J., and Pin, J.-P. (1997) *Ann. Rev. Pharmacol. Toxicol.* **37**, 205–237
7. Hayashi, Y., Momiyama, A., Takahashi, T., Ohishi, H., Ogawa-Meguro, R., Shigemoto, R., Mizuno, N., and Nakanishi, S. (1993) *Nature* **366**, 687–690
8. Herrero, I., Miras-Portugal, M. T., and Sanchez-Prieto, J. (1992) *Nature* **360**, 163–166
9. Ikeda, S. R., Lovinger, D. M., McCool, B. A., and Lewis, D. L. (1995) *Neuron* **14**, 1029–1038
10. Bashir, Z. I., Bortolotto, Z. A., Davies, C. H., Berretta, N., Irving, A. J., Seal, A. J., Henley, J. M., Jane, D. E., Watkins, J. C., and Collingridge, G. L. (1993) *Nature* **363**, 347–350
11. Brown, E. M., Gamba, G., Riccardi, D., Lombardi, M., Butters, R., Kifor, O., Sun, A., Hediger, M. A., Lytton, J., and Hebert, S. C. (1993) *Nature* **366**, 575–580
12. Takahashi, K., Tsuchida, K., Tanabe, Y., Masu, M., and Nakanishi, S. (1993) *J. Biol. Chem.* **268**, 19341–19345
13. O'Hara, P. J., Sheppard, P. O., Thogersen, H., Venezia, D., Haldeman, B. A., McGrane, V., Houamed, K. M., Thomsen, C., Gilbert, T. L., and Mulvihill, E. R. (1993) *Neuron* **11**, 41–52
14. Watkins, J. C., Krogsgaard-Larsen, P., and Honoré, T. (1990) *Trends Pharmacol. Sci.* **11**, 25–33
15. Kuusinen, A., Arvola, M., and Keinänen, K. (1995) *EMBO J.* **14**, 6327–6332
16. Aramori, I., and Nakanishi, S. (1992) *Neuron* **8**, 757–765
17. Neki, A., Ohishi, H., Kaneko, T., Shigemoto, R., Nakanishi, S., and Mizuno, N. (1996) *Neurosci. Lett.* **202**, 197–200
18. Shigemoto, R., Abe, T., Nomura, S., Nakanishi, S., and Hirano, T. (1994) *Neuron* **12**, 1245–1255
19. Shigemoto, R., Kinoshita, A., Wada, E., Nomura, S., Ohishi, H., Takada, M., Flor, P. J., Neki, A., Abe, T., Nakanishi, S., and Mizuno, N. (1997) *J. Neurosci.* **17**, 7503–7522
20. Ohashi, H., Higashi-Matsumoto, H., Maruyama, T., and Takeuchi, Y. (1997) *Soc. Neurosci. Abstr.* **23**, 2023
21. Ito, I., Kohda, A., Tanabe, S., Hirose, E., Hayashi, M., Mitsunaga, S., and Sugiyama, H. (1992) *Neuroreport* **3**, 1013–1016
22. Schoepp, D. D., Goldsworthy, J., Johnson, B. G., Salhoff, C. R., and Baker, S. R. (1994) *J. Neurochem.* **63**, 769–772
23. Sekiyama, N., Hayashi, Y., Nakanishi, S., Jane, D. E., Tse, H.-W., Birse, E. F., and Watkins, J. C. (1996) *Br. J. Pharmacol.* **117**, 1493–1503
24. Pellicciari, R., Luneia, R., Constantino, G., Marinozzi, M., Natalini, B., Jakobsen, P., Kanstrup, A., Lombardi, G., Moroni, F., and Thomsen, C. (1995) *J. Med. Chem.* **38**, 3717–3719
25. Jane, D. E., Jones, P. L., Pook, P. C.-K., Salt, T. E., Sunter, D. C., and Watkins, J. C. (1993) *Neuropharmacology* **32**, 725–727
26. Hayashi, Y., Sekiyama, N., Nakanishi, S., Jane, D. E., Sunter, D. C., Birse, E. F., Udvarhelyi, P. M., and Watkins, J. C. (1994) *J. Neurosci.* **14**, 3370–3377
27. Annoura, H., Fukunaga, A., Uesugi, M., Tatsuoka, T., and Horikawa, Y. (1996) *Bioorg. Med. Chem. Lett.* **6**, 763–766
28. Bedingfield, J. S., Kemp, M. C., Jane, D. E., Tse, H.-W., Roberts, P. J., and Watkins, J. C. (1995) *Br. J. Pharmacol.* **116**, 3323–3329
29. Bräuner-Osborne, H., Sløk, F. A., Skjærbæk, N., Ebert, B., Sekiyama, N., Nakanishi, S., and Krogsgaard-Larsen, P. (1996) *J. Med. Chem.* **39**, 3188–3194
30. Strader, C. D., Fong, T. M., Tota, M. R., Underwood, D., and Dixon, R. A. (1994) *Annu. Rev. Biochem.* **63**, 101–132
31. Coughlin, S. R. (1994) *Curr. Opin. Cell Biol.* **6**, 191–197
32. Tsai-Morris, C. H., Buczko, E., Wang, W., and Dufau, M. L. (1990) *J. Biol. Chem.* **265**, 19385–19388
33. Xie, Y. B., Wang, H., and Segaloff, D. L. (1990) *J. Biol. Chem.* **265**,

21411–21414
34. Braun, T., Schofield, P. R., and Sprengel, R. (1991) *EMBO J.* 10, 1885–1890
35. Nagayama, Y., Wadsworth, H. L., Chazenbalk, G. D., Russo, D., Seto, P., and Rapoport, B. (1991) *Proc. Natl. Acad. Sci. U. S. A.* 88, 902–905
36. Fernandez, L. M., and Puett, D. (1996) *J. Biol. Chem.* 271, 925–930
37. Ryu, K. S., Gilchrist, R. L., Ji, I., Kim, S. J., and Ji, T. H. (1996) *J. Biol. Chem.* 271, 7301–7304
38. Hebert, T. E., Moffett, S., Morello, J. P., Loisel, T. P., Bichet, D. G., Barret, C., and Bouvier, M. (1996) *J. Biol. Chem.* 271, 16384–16392
39. Maggio, R., Vogel, Z., and Wess, J. (1993) *Proc. Natl. Acad. Sci. U. S. A.* 90, 3103–3107
40. Romano, C., Yang, W. L., and O'Malley, K. L. (1996) *J. Biol. Chem.* 271, 28612–28616
41. Kaupmann, K., Huggel, K., Heid, J., Flor, P. J., Bischoff, S., Mickel, S. J., McMaster, G., Angst, C., Bittiger, H., Froestl, W., and Bettler, B. (1997) *Nature* 386, 239–246
42. Sack, J. S., Trakhanov, S. D., Tsigannik, I. H., and Quiocho, F. A. (1989) *J. Mol. Biol.* 206, 193–207
43. Adams, M. D., and Oxender, D. L. (1989) *J. Biol. Chem.* 264, 15739–15742
44. Quiocho, F. A. (1990) *Philos. Trans. R. Soc. Lond. B Biol. Sci.* 326, 341–351

THE JOURNAL OF BIOLOGICAL CHEMISTRY

Vol. 275, No. 36, Issue of September 8, pp. 28144–28151, 2000
Printed in U.S.A.

Cryptic Dimer Interface and Domain Organization of the Extracellular Region of Metabotropic Glutamate Receptor Subtype 1*

Received for publication, April 14, 2000, and in revised form, June 27, 2000
Published, JBC Papers in Press, June 28, 2000, DOI 10.1074/jbc.M003226200

Yuji Tsuji‡§, Yoshimi Shimada‡§, Tomoko Takeshita¶, Naoko Kajimura‖, Sayuri Nomura¶, Naohiro Sekiyama‡, Jun Otomo¶, Jiro Usukura, Shigetada Nakanishi‡‡, and Hisato Jingami‡§§**

*From the Departments of ‡Molecular Biology and ‖Structural Biology, Biomolecular Engineering Research Institute, 6-2-3 Furuedai, Suita-City, Osaka 565-0874, the ¶Advanced Research Laboratory, Hitachi, Ltd., Hatoyama, Saitama 350-0395, the **Department of Anatomy, Nagoya University School of Medicine, Showa-Ku, Nagoya 466-8550, and the ‡‡Department of Biological Sciences, Kyoto University Faculty of Medicine, Sakyo-Ku, Kyoto 606-8501, Japan*

Previously, we produced the whole extracellular region of metabotropic glutamate receptor subtype 1 (mGluR1) in a soluble form. The soluble receptor retained a ligand affinity comparable with that of the full-length membrane-bound receptor and formed a disulfide-linked dimer. Here, we have identified a cysteine residue responsible for the intermolecular disulfide bond and determined domain organization of the extracellular region of mGluR1. A mutant, C140A, was a monomer under nonreduced conditions by SDS-polyacrylamide gel electrophoresis; however, C140A was eluted at the position similar to that of mGluR113, the wild type soluble receptor, by size exclusion column chromatography. Furthermore, C140A bound a ligand, [^{3}H]quisqualate, with an affinity similar to that obtained by mGluR113. Oocytes injected with RNA for full-length mGluR1 containing C140A mutation showed responses to ligands at magnitudes similar to those with wild type full-length RNA. Thus, elimination of the disulfide linkage did not perturb the dimer formation and ligand signaling, suggesting that cryptic dimer interface(s) possibly exist in mGluR1. Limited proteolysis of the whole extracellular fragment (residue 33–592) revealed two trypsin-sensitive sites, after the residues Arg^{139} and Arg^{521}. A 15-kDa NH_2-terminal proteolytic fragment (residue 33–139) was associated with the downstream part after the digestion. Arg^{521} was located before a cysteine-rich stretch preceding the transmembrane region. A new shorter soluble receptor (residue 33–522) lacking the cysteine-rich region was designed based on the protease-sensitive boundary. The purified receptor protein gave a K_d value of 58.1 ± 0.84 nM, which is compatible to a reported value of the full-length receptor. The B_{max} value was 7.06 ± 0.82 nmol/mg of protein. These results indicated that the ligand-binding specificity of mGluR1 is confined to the NH_2-terminal 490-amino acid region of the mature protein.

L-Glutamate is a major neurotransmitter of excitatory synapses in mammalian brains. Metabotropic glutamate receptors (mGluRs)[1] are thought to modulate synaptic neurotransmission (1). Eight subtypes of mGluRs and the calcium sensing receptor (CaR) (2) share amino acid sequence homology. mGluRs possess seven transmembrane segments and are considered to be G protein-coupled receptors (GPCRs). mGluRs contain a large extracellular region (~600 amino acids) in contrast to ordinary GPCRs. The NH_2-terminal extracellular regions have amino acid sequence similarity (3) to that of leucine/isoleucine/valine-binding protein (LIVBP) (4), one of the bacterial periplasmic binding proteins. The LIVBP-like region is followed by a cysteine-rich region that precedes the first transmembrane segment. LIVBP-like regions are also found in the $GABA_B$ receptor (5), the putative pheromone receptor (6, 7). The cysteine-rich region is not shared by the bacterial binding proteins and the $GABA_B$ receptor. These receptor proteins, which contain a large extracellular region similar to that of mGluR, have been designated as family 3 GPCR (8). Thus, structural resemblance among the family 3 receptors has been predicted.

Previously, we were able to express the whole extracellular region of mGluR1 in a soluble form (9). The receptor protein secreted into the culture medium retained the ligand binding affinity and selectivity comparable with those of the full-length membrane bound receptor. Interestingly, the soluble receptor of mGluR1 was a cysteine-linked dimer. Dimer or oligomer forms of other subtypes of mGluRs, mGluR5 (10) and mGluR4 (11), or of CaR (12, 13) have been also reported. However, the precise mechanism of ligand binding to the mGluR is unknown. It is still unclear whether glutamate binds to mGluRs in an analogous way to the venus flytrap model proposed in the bacterial binding proteins (14), whereby the ligand bound to one lobe is trapped to another lobe by the bending motion of the hinge region. Role(s) of dimerization of mGluR1 in ligand binding and signal transmission remain to be elucidated.

The significance of dimerization in signal transduction of single-span transmembrane receptors for growth factors or cytokines has been studied extensively (15). The main focus is on whether structural details of extracellular regions have an influence on intracellular signaling (16, 17). For GPCRs, het-

* The costs of publication of this article were defrayed in part by the payment of page charges. This article must therefore be hereby marked "*advertisement*" in accordance with 18 U.S.C. Section 1734 solely to indicate this fact.

§ Both authors contributed equally to this work.

§§ To whom correspondence should be addressed. Tel.: 81-6-6872-8214; Fax: 81-6-6872-8219; E-mail: jingami@beri.co.jp.

[1] The abbreviations used are: mGluR, metabotropic glutamate receptor; CaR, calcium sensing receptor; GPCR, G protein-coupled receptor; LIVBP, leucine/isoleucine/valine-binding protein; EGS, ethylene glycol bis(succinimidylsuccinate); CAPS, *N*-cyclohexyl-3-aminopropanesulfonic acid; PMSF, phenylmethylsulfonyl fluoride; PCR, polymerase chain reaction; PAGE, polyacrylamide gel electrophoresis; mAb, monoclonal antibody; PEG, polyethylene glycol; DTT, dithiothreitol; LBD, ligand binding domain; CRD, cysteine-rich domain; bp, base pair(s); kbp, kilobase pair(s); $GABA_B$, γ-aminobutyric acid B.

ero- or homodimer formation has been reported in a few cases such as some subtypes of dopamine receptors (18), β_2-adrenergic receptor (19), and muscarinic acetylcholine receptors (20). Domain swapping among transmembrane segments has been proposed to be a causative factor in self-association of adrenergic receptors (21). Technical difficulties have been accompanied with those studies because of seven hydrophobic transmembrane segments. However, more convincing evidence has recently emerged of dimer formation in GPCRs. A heterodimeric opioid receptor dimer with an affinity and ligand selectivity different from those of the homodimer has been reported (22). Dimerization in the intracellular region is also reported to be essential for functional expression of the $GABA_B$ heterodimer receptor (23–25). These results suggest a possibility that dimerization of GPCR is not a rare phenomenon but rather a common occurrence.

In this study, with the advantage of purified dimerized material, we have determined a cysteine residue responsible for the intermolecular disulfide bonding by amino acid point mutation. Effects of disruption of the disulfide bond on ligand binding and signaling were examined. The existence of a cryptic dimer interface in mGluR is discussed. In order to delineate ligand binding core of mGluR1, we furthermore defined the domain organization of the extracellular region by proteolysis experiments. The new recombinant virus, designed according to the protease-sensitive boundary, produced the shorter soluble receptor lacking the cysteine-rich region. We have determined a ligand-binding constant and a maximal binding value of this soluble receptor that consists solely of the LIVBP-like domain in comparison with that of the soluble receptor encompassing the whole extracellular domain.

EXPERIMENTAL PROCEDURES

Materials—L-Quisqualic acid was purchased from Tocris Cookson Ltd. (Langford Bristol, United Kingdom). L-Glutamic acid monosodium salt was purchased from Nakalai tesque, Inc. (Kyoto, Japan). Linear gradient polyacrylamide gels were Multigel, obtained from Daiichi Pure Chemicals (Tokyo, Japan). Ethylene glycol bis(succinimidylsuccinate) (EGS) was obtained from Pierce. *N*-cyclohexyl-3-aminopropanesulfonic acid (CAPS) and phenylmethylsulfonyl fluoride (PMSF) were purchased from Wako Pure Chemical Industries (Osaka, Japan). Type XI trypsin, diphenyl carbamyl chloride-treated, from bovine pancreas, was obtained from Sigma Aldrich. All other reagents were of analytical grade.

Cell Culture and Isolation of Recombinant Viruses—*Spodoptera frugiperda* (Sf9) cells were propagated in a monolayer at 27 °C in TNM-FH (Grace's powder medium, 0.3% yeastolate, 0.3% lactalbumin hydrolyzate, 0.1% pluronic F-68; Life Technologies, Inc.), supplemented with 10% (v/v) heat-inactivated fetal bovine serum (Life Technologies, Inc.) or in suspension at 27 °C in IPL-41 (Life Technologies, Inc.) supplemented with 10% (v/v) heat-inactivated fetal bovine serum, 0.3% tryptose phosphate (Life Technologies, Inc.), and 0.1% pluronic F-68. 100 units/ml penicillin, 100 μg/ml streptomycin, and 250 ng/ml amphotericin B were used. *Trichoplusia ni* BTI-TN-5B1–4 (High Five) cells were cultured in a monolayer at 27 °C in Express Five™ serum-free medium (Life Technologies, Inc.) supplemented with 18 mM L-glutamine. Recombinant baculoviruses were generated by co-transfecting Sf9 insect cells with 1 μg of plasmid DNA and 0.1 μg of BaculoGold baculovirus DNA (PharMingen) with Lipofectin reagent (Life Technologies, Inc.). After 6 days of incubation, the supernatant was harvested. The virus in the supernatant was titrated, and individual plaques were isolated. Virus stocks were prepared in monolayer or suspension cultures of Sf9 cells. Baculovirus infection was performed as described previously (9). Briefly, after being infected with baculoviruses for soluble receptors, High Five cells were incubated for 4 or 5 days.

Construction of Transfer Vectors for Expression of mGluRs in Insect Cells—Both transfer vectors, pVLmGluR113 and pVLmGluR114, were constructed from pmGluR108 (9). pVLmGluR113 was made as follows. A set of complementary oligonucleotides, HJ110 (5′-CACAGGCTGTGAGCCCATTCCTGTCCGTTATCTTGAGTGGAGTGACATAGAATAGTGAT-3′) and HJ111 (5′-CTAGATCACTATTCTATGTCACTCCACTCAAGATAACGGACAGGAATGGGCTCACAGCCTGTGAGCT-3′), were annealed and cloned into the *SacI*/*Xba*I-digested fragment of pmGluR108. pVLmGluR114 was made as follows. Polymerase chain reaction (PCR) was done with primers TO1 (5′-CATCAATGCCATCTATGCCATGGC-3′) and HJ112 (5′-TCTAGATTACTAAGATCGTACCATTCCGCTTTTGTTC-3′) using pmGluR108 as a template. TO1 contains an *Nco*I site. HJ112 contains an *Xba*I site. The PCR product was digested with *Nco*I and *Xba*I and was cloned into the *NcoI*/*Xba*I-digested fragment of pmGluR108. Transfer verctors for mutant receptors were made as follows. Mutants in the wild type background are denoted with the number of the residue and amino acid substituted. A *Bgl*II-*Xba*I fragment was cut out of pVLmGluR114 and ligated into *Bam*HI/*Xba*I-digested pKF19k (Takara). With this plasmid as a template, PCR was performed with selection primer and each of primers C67A (5′-GATCTCCCCAGCCTTCCTTTCG-3′), C109A (5′-AGAGTGCCAGGCGGAGTCCCGG-3′) and C140A (5′-ATCAGGCAGGGCTCGGTTCAGC-3′). Following the protocol of Mutan-Super Express Km kit (Takara), the plasmids pKFC67A, pKFC109A, and pKF140A, which contain the mutated sequences, were obtained. 391-bp *Not*I-*Eco*RI fragments of pKFC67A and pKFC109A and a 390-bp *Eco*RI-*Aat*I fragment were ligated into the *NotI*/*Eco*RI-digested pVLmGluR113 and *Eco*RI/*Aat*I-digested pVLmGluR113, yielding pVLmGluR113C67A, pVLmGluR113C109A, and pVLmGluR113C140A. All the PCR products were fully sequenced. These transfer vectors were used for transfection to insect cells with BaculoGold baculovirus DNA.

Immunoblotting—Essentially the same as described previously (9). Culture medium was separated by SDS-polyacrylamide gel electrophoresis (PAGE) and electroblotted onto a nitrocellulose membrane (Schleicher & Schuell). mGluRs were identified by using the monoclonal antibody (mAb) mG1Na-1 (9, 26, 27) and anti-(mouse IgG)-conjugated alkaline phosphatase (Promega). Color development was done by a commercial detection kit (Promega).

Native PAGE—Samples were analyzed by 2–15% or 4–20% linear gradient polyacrylamide gels not containing SDS in the gel matrix. SDS was not included in either the running buffer or the sample buffer. Gels were silver-stained. Molecular weight standards were from Daiichi Pure Chemicals.

Purification of the Soluble Receptors—A conditioned medium of receptor-producing High Five cells was concentrated to 10–50 fold in the presence of protease inhibitor mixtures (1 mM PMSF, 5 μg/ml leupeptin, 10 μg/ml benzamidine, 10 μg/ml trypsin inhibitor, and 1 μg/ml aprotinin) and washed by 40 mM 2-[4-(2-hydroxyethyl)-1-piperazinyl]ethanesulfonic acid (Hepes) (pH 7.5) containing 10% glycerol, 1 M NaCl, and the protease inhibitor mixtures. Concentrated material was centrifuged at 15, 000 rpm for 20 min, filtrated by a 0.22-μm filter, and loaded on an immunoaffinity column, which was conjugated with mAb mG1Na-1 as described previously (9). The column was washed by 30 ml of 10 mM Hepes, pH 7.5, containing 200 mM NaCl, and the bound material was eluted with 100 mM CAPS, pH 11, containing 200 mM NaCl. Eluate was neutralized with 2 M Hepes, pH 7.5. Aliquots of the eluate were analyzed by SDS-PAGE followed by immunoblotting. Positively stained fractions were pooled and analyzed by ligand binding assay. The pooled fraction was then further purified by ion exchange column chromatography. After being diluted five times with 10 mM Hepes, pH 7.5, the sample was applied on Resource Q (Amersham Pharmacia Biotech) fitted to ÄKTA Explorer 10S (Amersham Pharmacia Biotech) equilibrated with 10 mM Hepes, pH 7.5, and eluted by NaCl at a gradient from 0 to 1.2 M. In order to compare the gel filtration pattern of mGluR113 with that of its cysteine mutant, aliquots of the immunoaffinity column eluate were loaded on a HiLoad 16/60 Superdex 200pg (Amersham Pharmacia Biotech) equilibrated with 10 mM Hepes, pH 7.5, containing 200 mM NaCl and 10% glycerol, by high performance liquid chromatography (Waters 626LC). The flow rate was 0.5 ml/min, and fractions of 5 ml each were collected.

Ligand Binding—Ligand binding was performed with the polyethylene glycol (PEG) precipitation method as described previously (28). Briefly, 20 or 40 nM [^{3}H]quisqualate (323 GBq/mmol) (a gift from Banyu Tsukuba Research Institute) and soluble receptor samples were mixed in 150 μl of a binding buffer (40 mM Hepes, pH 7.5, containing 2.5 mM $CaCl_2$) at 4 °C for 1 h. After the binding reaction, 6-kDa PEG was added to the sample at the concentration of 15% with 3 mg/ml of γ globulin. Precipitated material was washed twice with 1 ml of 8% 6-kDa PEG and dissolved in 1 ml of water. After addition of 14 ml of Scintisol EX-H (Wako Pure Chemical Industries), the radioactivity was counted in the scintillation counter. Binding data was analyzed by the software of Prism II (Graphpad Software, San Diego, CA). Saturation binding curves were fitted to a one-site binding model, and K_d and B_{max} values were calculated.

Expression of mGluRs in Oocytes and Electrophysiology—A 777-bp *Sac*II-*Aat*I fragment of pKFC140A, a 3.2-kbp *Aat*I-*Sac*II fragment of

pmGR1 (29), and a 3.7-kbp *Sac*II-*Sac*II fragment of pmGR1 were ligated. The resulting plasmid, pmGR1C140A, and pmGR1 were used as templates for *in vitro* transcription to yield complementary RNA (cRNAs). The plasmid DNA was linearized by *Not*I, and capped cRNA was synthesized with MEGAscript T7 kit (Ambion, Austin, TX). *Xenopus laevis* oocytes were prepared according to the standard procedure. The follicular cell layer was removed by treatment with Ca^{2+}-free ND solution (96 mM NaCl, 2 mM KCl, 1 mM $CaCl_2$, 1 mM $MgCl_2$, and 5 mM Hepes, pH 7.6) containing 100 μg/100 ml of collagenase-B (Yakuruto, Tokyo, Japan) for 1.5 h at 18 °C. The oocytes were then injected with 10 ng of cRNAs. The injected oocytes were incubated in ND solution for 1–2 days. A two-electrode voltage clamp system was used to measure glutamate- and quisqualate-induced chloride ion currents. The membrane potential was held at −60 mV in all measurements. All currents were filtered at 1 kHz, and data were stored and analyzed using MacLab system (Bio-Research-Center, Nagoya, Japan). All measurements were conducted at room temperature.

Cross-linking Procedure—The cross-linker, EGS, was dissolved at 20 mM in dimethyl sulfoxide and diluted into the protein solution to give the final concentration of 1 mM. The reaction proceeding at 25 °C for 30 min was stopped by the addition of Tris-HCl buffer from a 1 M stock solution at pH 7.5, and a further incubation was conducted at 25 °C for 15 min. The cross-linked material was analyzed by 4–20% SDS-PAGE and silver-stained (Wako Pure Chemical Industries).

Trypsin Digestion and Protein Sequencing—Purified protein was digested in 10 mM Hepes, pH 7.5, with different concentrations of trypsin. Reaction was stopped with 0.01 mM PMSF and sample buffer. Aliquot was not heated and was subjected to SDS-PAGE. The gel was electroblotted onto a polyvinylidene difluoride membrane (Trans-Blot transfer medium, Bio-Rad), stained with Coomassie Brilliant Blue R250 (PAGE Blue83, Daiichi Pure Chemicals), and destained with 20% methanol. The protein bands were excised and subjected to automated Edman degradation by an Applied Biosystems Procise model 492 protein sequencer.

Low Angle Rotary Shadowing—The purified mGluRs in 50 mM Hepes, pH 7.5, was equilibrated with glycerol (up to 50% (v/v)). Final concentration of the protein was 50 μg/ml each. 50 μl of the sample was sprayed onto mica surface cleaved freshly by using a painter's airbrush (Olympus model SP-B, f 0.18 mm). Then, the sample on the mica was rapidly brought into a freeze-etching device equipped with a large turbo pump (FR 7000, Hitachi, Mito, Japan), dried for 10 min (room temperature) in vacuum (1×10^{-6} pascals), and then cooled down to −100 °C. Subsequently, specimens were rotary shadowed with platinum by an electron gun positioned at an angle of 2.5° to the mica surface and followed by carbon evaporation. Shadowed films were removed from the mica by slowly soaking the mica into water, mounted on copper grids and examined under a Jeol 100CX electron microscope (Jeol Co., Ltd., Tokyo).

RESULTS

Fig. 1 shows a schematic view of the transfer vectors, pVLmGluR113, pVLmGluR113C67A, pVLmGluR113C109A, pVLmGluR113C140A, and pVLmGluR114, used for making the recombinant viruses for mGluR113, mGluR113C67A, mGluR113C109A, mGluR113C140A, and mGluR114. pVLmGluR113 encodes complementary DNA (cDNA) corresponding to the region Met^1–Glu^{592} of the primary amino acid sequence of mGluR1. pVLmGluR114 encodes cDNA corresponding to the region Met^1–Ser^{522}. pmGluR108 that was used in our previous study (9) encoded the amino acid region identical with that of pVLmGluR113 and six histidine codons at its COOH terminus. In this study, a His tag sequence of pmGluR108 was omitted in pVLmGluR113. Recombinant viruses for the receptors were prepared as described under "Experimental Procedures."

mGluR113 encodes the whole extracellular region of mGluR1. Amino acid mutation was introduced at the first three consecutive cysteine residues (Cys^{67}, Cys^{109}, and Cys^{140}). The mutant receptor proteins were designated C67A, C109A, and C140A. Concentrated culture medium of insect cells infected with the recombinant viruses for cysteine mutants as well as for mGluR113 was subjected to SDS-PAGE and analyzed by immunoblotting (Fig. 2*A*). In the presence of 20 mM DTT (*left panel*), the three mutants were detected as approximate

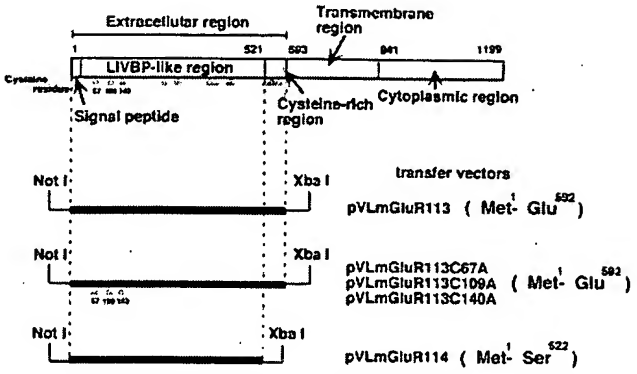

FIG. 1. **Schematic diagram of the expression construct of the transfer vectors in insect cells.** Full-length wild type mGluR1 was presented as a diagram according to its primary amino acid sequence deduced from mGluR1cDNA (29). The numerical positions of amino acid residues of mGluR1 are indicated. Functional regions are *boxed*. Inserts of transfer vectors, pVLmGluR113 and pVLmGluR114, used in this study are presented according to the primary sequence of mGluR1. *Open triangles* indicate cysteine residues within the extracellular region of mGluR1. pVLmGluR113 encodes cDNA corresponding to the entire extracellular region consisting of a signal sequence, an LIVBP-like region, and a cysteine-rich region. mGluR113C67A, mGluR113C109A, and mGluR113C140A are cysteine to alanine mutants at residues 67, 109, and 140, respectively. pVLmGluR114 is devoid of the sequence corresponding to COOH-terminal 70 amino acids out of pVLmGluR113. *Not*I-*Xba*I fragments were ligated into pVL1392.

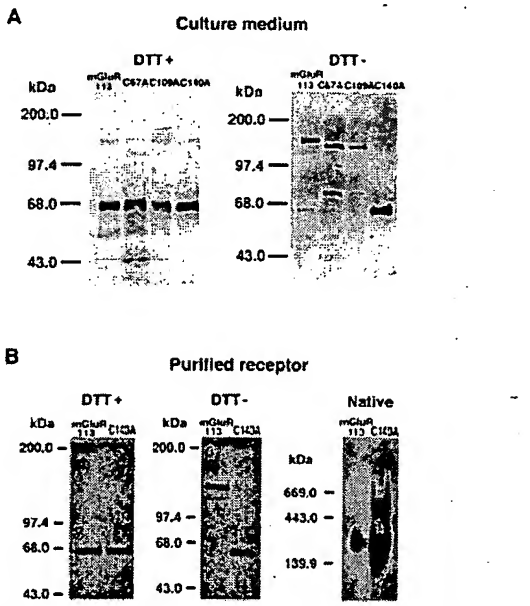

FIG. 2. **Effect of cysteine to alanine point mutation on dimerization.** *A*, immunoblotting of culture medium of insect cells infected with the recombinant viruses for mGluR113, C67A, C109A, and C140A. Samples were run either in the presence of 20 mM dithiothreitol (*DTT+*) or under nonreduced conditions (*DTT−*) on a 7.5% SDS-polyacrylamide gel. Marker proteins are myosin heavy chain (200.0 kDa), phosphorylase B (97.4 kDa), bovine serum albumin (68.0 kDa), and ovalbumin (43.0 kDa). *B*, analysis of purified mGluR113 and C140A by SDS-PAGE and native-PAGE. Purified mGluR113 and C140A (125 ng, respectively) from the immunoaffinity columns were run either in the presence of 20 mM DTT (*DTT+*) or under nonreduced conditions (*DTT−*) on 7.5% SDS-polyacrylamide gels. Purified mGluR113 (250 ng) and C140A (750 ng) from the immunoaffinity columns were run on 2–15% native-polyacrylamide gels (*Native*). Gels were silver-stained.

65-kDa bands. Under nonreduced conditions (*right panel*), C67A and C109A was electrophoresed at around 130-kDa bands; however, C140A was electrophoresed much faster with a position corresponding to the monomer band. The sizes of

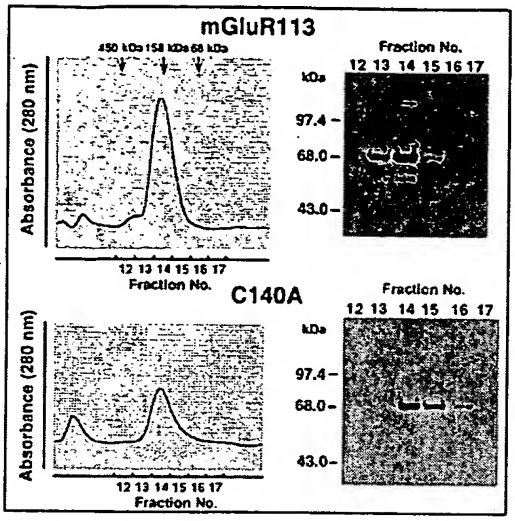

FIG. 3. **Size exclusion column chromatography of mGluR113 and C140A.** 100 μg of mGluR113 and C140A from the immunoaffinity columns were loaded onto Hiload 16/60 Superdex gel filtration columns (Amersham Pharmacia Biotech). The columns were equilibrated and eluted with 10 mM Hepes, pH 7.5, containing 200 mM NaCl and 10% glycerol. 5 ml of each fraction was collected. Aliquots (50 μl) of the indicated gel filtration fractions were subjected to 7.5% SDS-PAGE under reduced conditions with 20 mM DTT, followed by immunoblotting. The *vertical arrows* indicate the positions of the marker proteins. The molecular masses of the marker proteins were horse spleen ferritin (450 kDa), rabbit muscle aldolase (158 kDa), and bovine serum albumin (68 kDa).

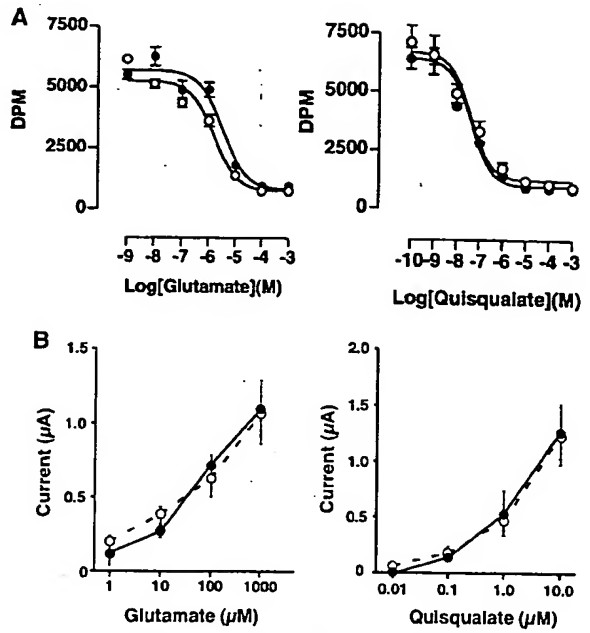

FIG. 4. **Dose-response curves of glutamate and quisqualate in inhibiting [^{3}H]quisqualate binding to the purified mGluR113 and C140A (*A*) and electrophysiology of oocytes injected with RNAs for the mutant mGluR1 containing Ala^{140} mutation and for wild type mGluR1 (*B*).** *A*, indicated concentrations of quisqualate (*right panel*) and glutamate (*left panel*) with 40 nM [^{3}H]quisqualate were incubated with C140A (1.5 μg) and mGluR113 (0.5 μg) from the immunoaffinity column. *Closed circles* indicate C140A. *Open circles* indicate mGluR113. Each point shows the mean ± S.E. of a representative one of three experiments done in triplicate. The displacement curves were obtained by sigmoidal fitting with Prism II (Graphpad Software, San Diego, CA). *B*, *X. laevis* oocytes were injected with 10 ng of *in vitro* transcribed cRNA as described under "Experimental Procedures." 24–48 h after the injection, holding potential was set at −60 mV and current was measured with stimulation of ligands, glutamate (*left panel*) and quisqualate (*right panel*). Each point shows mean ± S.E. of a representative one of two experiments done in quadruplicate. *Closed circles* indicate mGluR1 containing Ala^{140} mutation. *Open circles* indicate wild type mGluR1.

C67A and C109A appeared significantly different from that of mGluR113, suggesting a conformational change. These results clearly showed that alanine mutation at Cys^{140} eliminated the intermolecular disulfide bonding.

Next we compared ligand binding capacities between C140A and mGluR113. As concentrated culture medium of insect cells infected with the viruses for C140A showed ligand binding capacity comparable to that of mGluR113 (data not shown), we next purified C140A by an immunoaffinity column as described under "Experimental Procedures." Although the purified C140A sample showed a band equal to that of mGluR113 under reduced conditions (Fig. 2*B*, *left panel*), C140A migrated much faster than mGluR113 under nonreduced conditions (*center panel*). Surprisingly, this mutated receptor migrated as a dimer on native-polyacrylamide gels as did mGluR113 (*right panel*). We also observed a small amount of larger oligomers of C140A. These data indicated that mutation at Cys^{140} eliminated disulfide bonding in the extracellular portion of mGluR1, but the extracellular portion of the C140A receptor folded in a manner that maintained noncovalent dimerization of the receptor molecule. To reinforce this result, C140A was subjected to gel filtration column chromatography in parallel with mGluR113 (Fig. 3). Calibration with molecular size markers showed the eluting position of mGluR113 to be around 185 kDa and that of C140A to be around 150 kDa. Both receptors were definitely larger than a monomer and seemed to be a dimer or a larger oligomer.

The ligand binding ability of C140A was quantitatively examined by comparing the inhibition of [^{3}H]quisqualate binding to the purified C140A and mGluR113 with unlabeled glutamate and quisqualate (Fig. 4*A*). Both receptors did not make a great difference in dose-response curves of unlabeled glutamate and quisqualate. These data indicated that there was no great difference between mGluR113 and C140A in affinities to glutamate and quisqualate. We next examined the importance of the disulfide linkage in signal transmission of mGluR1 using the oocyte expression system (Fig. 4*B*). A messenger RNA (mRNA), which encodes a full-length of mGluR1 whose Cys^{140} was mutated to alanine, was created. Oocytes injected with the mutated mGluR1mRNA as well as the wild type mGluR1-mRNA were stimulated with ligands, glutamate and quisqualate. The magnitude of the chloride currents induced by both ligands of oocytes injected with mutant RNA increased dose-dependently. At each ligand concentration, the current response of mutant mGluR1 was comparable with that of wild type mGluR1. This result indicated that C140A mutation in a full-length receptor did not alter the affinity to the ligands or the ability to couple to intracellular signaling cascades.

Next, in order to understand the domain organization of the mGluR1 extracellular region, we determined the NH_2-terminal amino acid sequence of soluble receptor protein, mGluR113, that was generated by removal of a signal peptide and found that mGluR113 began with residue Ser^{33}. Proteinase digestion was then performed using the purified mGluR113 (Fig. 5, *A* and *B*). Limited proteolysis of mGluR113 by trypsin gave rise to at least five major bands. Each of these bands (designated as fragments 1–5) were excised from a polyvinylidene difluoride blot and sequenced at the NH_2-terminal end by Edman degradation. The NH_2-terminal amino acid sequence of the 15-kDa band (fragment 4) was identical with that of mGluR113. NH_2-terminal sequencing of the 50-kDa band (fragment 2) revealed that the digestion site was Arg^{139} before (C)^{140}LPDG. Thus, the

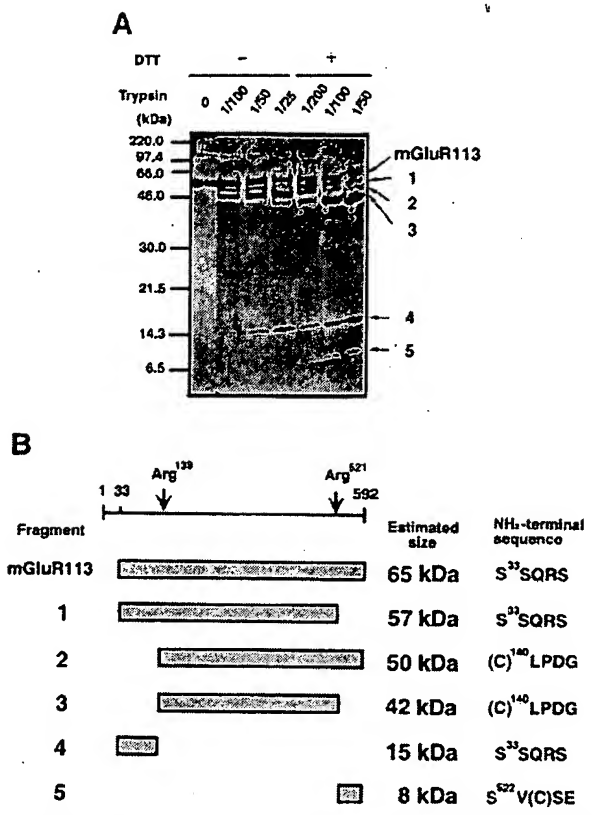

FIG. 5. **Trypsin digestion (*A*) and proteolytic cleavage mapping (*B*) of the soluble mGluR113.** *A*, 13.6 μg of immunoaffinity-purified mGluR113 was digested with the indicated ratio (w/w) of trypsin at 25 °C for 1 h, loaded on a 15–25% gradient gel and Coomassie-stained. Proteolytic fragments were labeled *1–5*. NH_2-terminal sequences of mGluR113 and the five tryptic fragments were determined as described under "Experimental Procedures." *B*, the five fragments, *1-5*, are located relative to the primary amino acid sequence of mGluR1. NH_2-terminal sequences of mGluR113 and the fragments are shown. The *vertical arrows* indicate the trypsin cleavage sites.

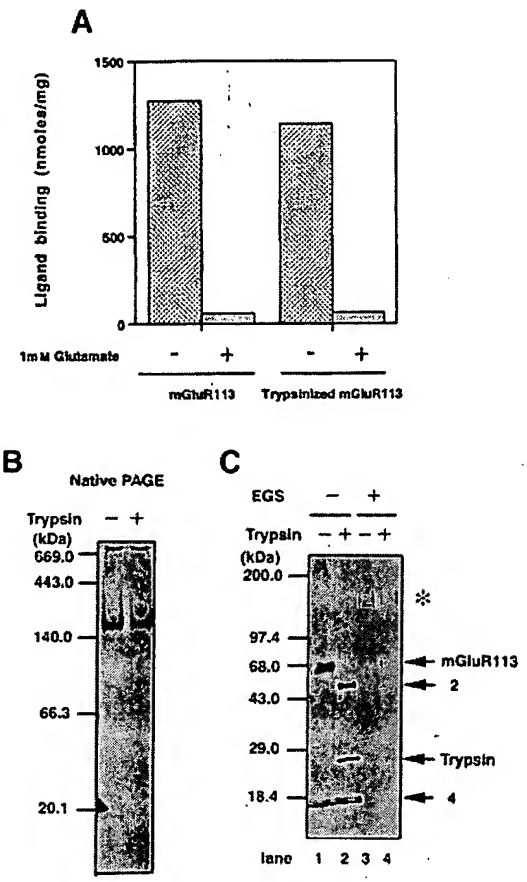

FIG. 6. **Ligand binding (*A*), native PAGE analysis (*B*), and chemical cross-linking (*C*) of trypsinized mGluR113.** *A*, 11.3 μg of mGluR113 purified with an immunoaffinity column was digested with 1.1 μg trypsin at 25 °C for 1 h. After addition of 1 mM PMSF for quench, aliquot containing 0.86 μg of trypsin-digested mGluR113 were incubated in the binding buffer (40 mM Hepes, pH 7.5, and 2.5 mM $CaCl_2$) with 20 nM [^{3}H]quisqualate at 4 °C for 1 h. Undigested mGluR113 was assayed as a control. Nonspecific binding was measured in the presence of 1 mM glutamate. *B*, trypsin-digested mGluR113 was analyzed by native PAGE. 0.75 μg of mGluR113 purified with an immunoaffinity column was digested with 0.075 μg of trypsin at 25 °C for 1 h. After addition of 1 mM PMSF and sample buffer without SDS, the digested sample was loaded onto a 4–20% native gradient gel and silver-stained. Control sample treated without trypsin was electrophoresed in parallel. *C*, cross-linking study of trypsinized mGluR113. Immunoaffinity-purified mGluR113 was digested with 10% (w/w) trypsin at 25 °C for 16 h (*lane 2*). Half of the reaction mixture was cross-linked with 1 mM EGS (*lane 4*). 0.75 μg of protein was loaded on each lane of a 4–20% SDS gradient gel under reduced conditions. The undigested samples without cross-linking (*lane 1*) and with cross-linking (*lane 3*) underwent with the same procedure in parallel. The *asterisk* indicates cross-linked material.

15-kDa fragment 4 was residues 33–139 and the 50-kDa fragment 2 was residues 140–592. The NH_2-terminal sequence of an 8-kDa band (fragment 5), which was faintly observed by limited digestion without DTT but was clearly visible in the lanes of samples digested in the presence of 1 mM DTT, disclosed the other trypsin-sensitive site, Arg^{521} before $S^{522}V(C)SE$. Thus, the 8-kDa fragment 5 was residues 522–592. A 42-kDa band (fragment 3) corresponded to residues 140–521. A 57-kDa band (fragment 1) was the intermediate that resulted from initial digestion at Arg^{521}. The site Arg^{521} seemed to be more accessible in the presence of DTT. Although mass spectroscopic analysis or amino acid content calculation is needed for strict identification of each band, we summarized our interpretation of the results (Fig. 5*B*) and proceeded to the next experiments.

We examined the ligand binding capacity of trypsinized mGluR113. Surprisingly, trypsin digestion, at up to a ratio of 1/10, which is larger than that used in Fig. 5, did not abolish ligand binding capacity of mGluR113, as shown in Fig. 6*A*. Trypsinized mGluR113 did show [^{3}H]quisqualate binding comparable to that of undigested mGluR113. In order to know whether or not the 15-kDa NH_2-terminal fragment (residue 33–139) is required for ligand binding, the trypsinized sample was loaded on a native polyacrylamide gel that did not contain SDS in the gel matrix (Fig. 6*B*). The trypsinized mGluR113 was electrophoresed at a very close position to that of the undigested mGluR113. To prove that the NH_2-terminal fragment is attached to the remaining fragment, we performed a cross-linking experiment (Fig. 6*C*). First, mGluR113 was digested by trypsin, and an aliquot of the reaction mixture was stored in SDS sample buffer. The remaining trypsinized mGluR113 was cross-linked with EGS and analyzed with the non-cross-linked sample by SDS-PAGE under the reduced condition. The proteolytic fragments, 2 and 4, were detected in *lane 2* of trypsinized sample. The cross-linked trypsinized mGluR113 (*lane 4*) was electrophoresed at a position (*asterisk*) similar to that of cross-linked undigested mGluR113 (*lane 3*). These results led us to conclude that the NH_2-terminal 15-kDa fragment was associated with the remaining fragment after trypsin cleavage at Arg-Cys bond after residue 139. Thus, on the basis of the trypsin-sensitive site, Arg^{521}, we designed a new construct, pVLmGluR114, which encodes cDNA corresponding to

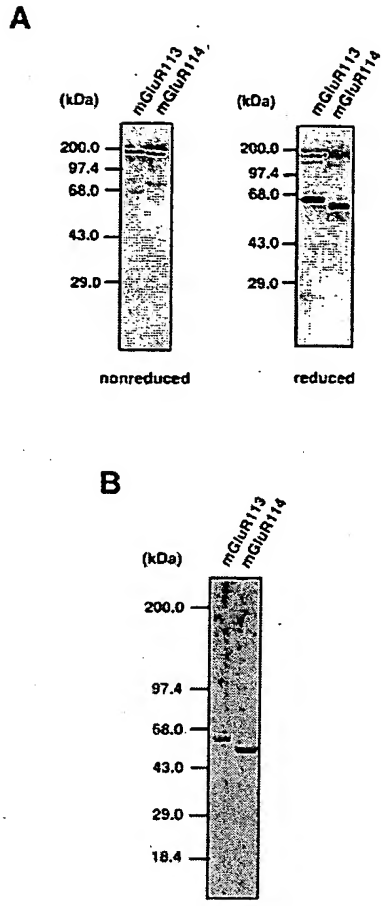

FIG. 7. **Immunoblotting analysis (*A*) and Coomassie staining of purified mGluR113 and mGluR114 (*B*).** *A*, 20 μl of culture medium of High Five cells infected with baculoviruses for mGluR113 and mGluR114 were loaded on 10% SDS-polyacrylamide gels under nonreduced conditions (*left panel*) and reduced conditions (*right panel*). Proteins were transferred onto the nitrocellulose membrane and probed with mAb mG1Na-1. *B*, mGluR113 (4 μg) and mGluR114 (6 μg) purified by Resource Q as described under "Experimental Procedures" were loaded on 10–20% SDS-polyacrylamide gels and Coomassie-stained.

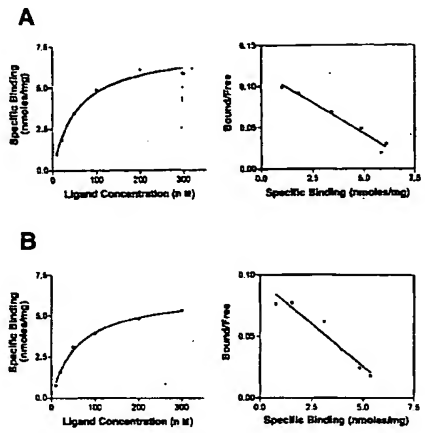

FIG. 8. **Saturation binding of [^{3}H]quisqualate to mGluR113 and mGluR114.** 0.5 μg of immunoaffinity-purified mGluR113 (*A*) and mGluR114 (*B*) were incubated in the binding buffer (40 mM Hepes containing 2.5 mM $CaCl_2$) with different ligand concentrations of [^{3}H]quisqualate at 4 °C for 1 h. Specific binding was determined by subtraction of nonspecific binding determined in the presence of 1 mM glutamate from total binding. The results were analyzed by Prism II for saturation kinetics (*left panels*) and for Scatchard analysis (*right panels*). A representative result from three independent experiments is shown. Each binding was performed in triplicate and is shown as the mean ± S.E. A non-linear regression analysis of mGluR113 revealed a K_d of 54.1 ± 5.82 nM and a B_{max} of 6.92 ± 0.73 nmol/mg of protein. mGluR114 showed a K_d of 58.1 ± 0.84 nM and a B_{max} of 7.06 ± 0.82 nmol/mg of protein. These K_d and B_{max} values are means ± S.E. (n = 3).

the region Met^1–Ser^{522}, as shown in Fig. 1.

Fig. 7*A* shows the immunoblot of the supernatant of the insect (High Five) cells infected with the recombinant viruses for the new shorter soluble receptor protein, mGluR114, as well as for mGluR113. mGluR114 and mGluR113 were detected by mAb mG1Na-1 as a 57-kDa band and a 65-kDa band under reduced conditions (*right panel*). Under nonreduced conditions (*left panel*), both soluble receptors seemed to be a dimer or oligomer. The levels of expression of the two soluble receptors looked compatible. This result is in contrast to our previous study (9), in which recombinant virus derived from pmGluR103 that encoded cDNA corresponding to the region Met^1–Glu^{492} of mGluR1 did not efficiently produce the soluble receptor protein, mGluR103. The COOH-terminal 30 amino acids of mGluR114 may be involved in a secondary structure and contribute to protein stability. Next, to purify mGluR114, the 40-fold concentrated medium was applied on an immunoaffinity column as described under "Experimental Procedures." Then we further purified the material by Resource Q column chromatography. Fig. 4*B* shows Coomassie staining of the purified material of mGluR114 and mGluR113. We also confirmed that the NH_2-terminal amino acid sequence of mGluR114 is identical with that of mGluR113 (data not shown).

Using purified mGluR114 as well as mGluR113, a ligand binding study was performed. mGluR114 and mGluR113 showed saturable binding as in Fig. 8 (*A* and *B*). The K_d value of mGluR114 for quisqualate, which lacks the cysteine-rich region, was 58.1 ± 0.84 nM, similar to the K_d value, 54.1 ± 5.82 nM, of mGluR113. These values are comparable to those reported using full-length membrane bound mGluR1 (30). Thus, the LIVBP-like region is sufficient enough to bind ligands. B_{max} values of mGluR 114 and mGluR 113 were 7.06 ± 0.82 nmol/mg of protein and 6.92 ± 0.73 nmol/mg of protein, respectively. *Right panels* are Scatchard plots of the data.

Next, we performed rotary shadowing of the soluble receptor proteins, mGluR114 and mGluR113 (Fig. 9). Both were globular proteins consisting of two similar components facing each other, consistent with the above finding that they were electrophoresed as dimers in the native gels. Remarkable difference in the shadowing image was not observed between mGluR114 and 113, implying that the LIVBP-like region can fold regardless of the presence or absence of the cysteine-rich region.

DISCUSSION

Previously, we have reported dimer formation of soluble forms of mGluR1 expressed in insect cells (9), in which the dimer was disulfide-linked. In this investigation we have made cysteine to alanine mutants and identified the cysteine residue responsible for the disulfide linkage. One of the mutants, C140A, was electrophoresed in the monomer position under nonreduced conditions by SDS-PAGE. Thus, we have demonstrated that Cys^{140} is the responsible residue for the disulfide bond. However, under the native state, namely without SDS in the gel matrix, C140A was electrophoresed at the position similar to that of mGluR113. C140A was also eluted at the position very close to that of mGluR113 by size exclusion chromatography. These data led us to conclude that the disulfide linkage at Cys^{140} does not play a predominant role in dimer formation of mGluR1. Interestingly, C140A retained the binding capacity to the ligand. Dose-response curves with ligands obtained by purified C140A showed affinities comparable to those of mGluR113. Furthermore, response to the ligands of

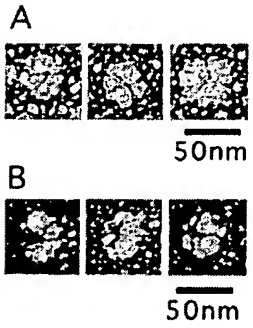

FIG. 9. **Rotary shadowing image of the soluble mGluRs.** Gallery of electron micrographs of soluble mGluR113 (*A*) and mGluR114 (*B*).

oocytes injected with RNA corresponding to a full-length form of mGluR1 containing Ala^{140} mutation was similar to that with RNA for the original intact mGluR1. Thus, the local environment around the ligand binding site and the signal transmission within the receptor molecule have not been interfered by disruption of the disulfide linkage. We speculate that a putative dimer interface is located apart from Cys^{140}.

mGluR1 contains 19 cysteine residues in the extracellular region and these residues are conserved among all eight mGluR subtypes and CaR. CaR contains Cys^{129} in addition to Cys^{131}, which exists at the corresponding residue of Cys^{140} of mGluR1. Recently Ray *et al.* (31) reported that the C129S/C131S double mutant of CaR was detected as monomer by SDS-PAGE, consistent with our results. On the other hand, the C129S/C131S mutant was not co-immunoprecipitated with wild type truncated mutant that contained the whole extracellular region and the first membrane segment of CaR. They speculated that the intermolecular disulfide bond in CaR plays predominant roles in dimer formation, which was in contrast to our result. Thus, roles and formation of the disulfide linkages between mGluR1 and CaR might not be exactly alike. Cysteine residues responsible for intermolecular disulfide dimer or oligomer formation of m3 muscarinic receptor, which is one of the classical GPCRs, have recently been reported (32). Interestingly, a mutant in which the two responsible cysteines located at the second and third extracellular loops were mutated to alanines lost the intermolecular disulfide linkage, but retained the capacity to form non-covalent receptor dimer or multimer.

In this study, we have also succeeded in outlining the domain structure of the extracellular region of mGluR1. A number of Arg and Lys residues are distributed in the extracellular region; nevertheless, trypsin digested mGluR113, which consists of the whole extracellular region of mGluR1, at the site of Arg^{521}. Thus, the extracellular region of mGluR1 was subdivided into two domains: an NH_2-terminal LIVBP-like region and a cysteine-rich region preceding the first transmembrane segment. We call the former part the ligand binding domain (LBD) and the latter the cysteine-rich domain (CRD) hereafter. Furthermore, five major fragments generated by partial tryptic digestion were assigned according to the two trypsin sites.

An extracellular fragment devoid of CRD, mGluR114, was expressed well and showed a K_d value of 58.1 ± 0.84 nM for its ligand, [^{3}H]quisqualate, which is close to that of mGluR113. Both of the soluble receptors, mGluR113 and mGluR 114, showed dimer under nonreduced conditions and monomer under reduced conditions. Thus, cysteine 140 responsible for the intermolecular disulfide bond resides within LBD. Because the trypsin-digested mGluR113 electrophoresed at a position similar to that of the undigested one under a native condition, nick introduced by trypsin treatment seems not to interfere with the dimer interface. Interestingly, trypsin-digested mGluR113 as well as mGluR114 (data not shown) retains ligand binding activity, suggesting that the digestion site, Arg^{139}, is exposed to the surface and resides in a flexible region. The NH_2-terminal 15-kDa fragment seems to be associated with the remaining part after trypsin digestion. Therefore, we did not make an expression construct that lacked the corresponding cDNA sequence. Thus, whether the 15-kDa fragment is required for ligand binding could not be determined. The 15-kDa region might have a role for folding LBD. We speculate that the ligand binding site forms a rather rigid structure.

Provided that two molecules of the ligand, quisqualate, bind to a dimer form of the soluble receptor, the stoichiometry of binding can be calculated to be approximately 39–44% based on the B_{max} values of mGluR113 and mGluR114 for the ligand. Only half of the material might retain binding capacity, or we may have been unable to measure maximal binding capacity because our PEG precipitation assay is not expected to resolve low affinity site, if any, with a K_d in the micromolar range. However, if we assume that cooperative binding is operated in the dimer form of the mGluR1 or the two binding sites possess different affinities, this value of stoichiometry would be meaningful. Interestingly, it has been reported that a purified 42-kDa ligand-binding fragment of GluR-D, an α-amino-3-hydroxy-5-methyl-4-isoxazolepropionic acid receptor, one of glutamate-gated ion channels, showed a B_{max} value of 6–12 nmol/mg, indicating 50% stoichiometry of the theoretical maximum (33).

Model buildings of part of the extracellular region of monomer mGluR1 were proposed on the basis of an atomic structure of a bacterial binding protein that resides in the periplasmic space (34, 3). If the dimerized form is the principal form of active mGluR1, a novel mechanism may be at work in ligand binding and signal transmission in mGluR. Although the cysteine residue(s) responsible for the intermolecular disulfide bonding has been determined, the precise mechanism of the dimer formation has not been explored, and the character of the dimer interface still remains to be elucidated. Whether or not dimer formation is critical for ligand binding and signal transmission in mGluRs is a topic that should be examined further. Because the cryptic dimer interface, which is different from that formed by the intermolecular disulfide bond in mGluR1, is sensitive to SDS detergent, electrostatic or hydrophobic interaction can be suspected to be a driving force for the dimer formation of mGluR1. Intriguingly, a stretch of 24 consecutive uncharged amino acids in the extracellular region of mGluR1 (residues 155–178) has been pointed out when the primary amino acid sequence was determined (29).

Whether or not CRD interacts with LBD or the transmembrane region is still unknown. The absence of large differences between the rotary shadowing imagings of mGluR113 and mGluR114 suggests that CRD appears not to perform major roles in dimer formation. Ligand binding within LBD may elicit conformational change of the seven transmembrane segments through CRD. If the structure of CRD is not flexible, magnitude and orientation of the conformational change occurred within LBD, if any, would transmit directly to the seven transmembrane helices. Alternatively, CRD may be a flexible stalk and remold itself upon ligand binding to LBD. Thus, elucidation of the structure and function of CRD is an intriguing challenge. Through structural analysis of the ligand binding core of GluR2, Armstrong *et al.* (35) pointed out a possible interacting site to the allosteric effector or of domain-domain contact through its hydrophobic character. CRD in mGluR might be involved in such an interaction, although we do not have any evidence.

In conclusion, Cys^{140} is responsible for the intermolecular

disulfide bond of the dimeric mGluR1. C140A mutant remained to be a dimer, suggesting exsistence of a cryptic dimer interface distinct from the disulfide bond. C140A would be a valuable tool for analysis of the dimer interface. The final answer for the enigmatic dimer interface can be expected to be obtained by the determination of the atomic structure of a soluble form mGluR1. Because of the nine cysteine residues in a 70-amino acid stretch, mGluR113 preparation might contain some misfolded material. Thus, mGluR114 complexed with ligands may be a good candidate for use in analysis of the tertiary structure of mGluR1.

Acknowledgments—We thank Dr. Yutaka Takeuchi at Banyu Pharmaceutical Inc. for [^{3}H]quisqualate and Dr. Kosuke Morikawa for discussion. We are grateful to Dr. Yoshiro Shimura for suggestions and encouragement.

REFERENCES

1. Nakanishi, S., and Masu, M. (1994) *Annu. Rev. Biophys. Biomol. Struct.* **23**, 319–348
2. Brown, E. M., Gamba, G., Riccardi, D., Lombardi, M., Butters, R., Kifor, O., Sun, A., Hediger, M. A., Lytton, J., and Hebert, S. C. (1993) *Nature* **366**, 575–580
3. O'Hara, P. J., Sheppard, P. O., Thøgersen, H., Venezia, D., Haldeman, B. A., McGrane, V., Houamed, K. M., Thomsen, C., Gilbert, T. L., and Mulvihill, E. R. (1993) *Neuron* **11**, 41–52
4. Sack, J. S., Saper, M. A., and Quiocho, F. A. (1989) *J. Mol. Biol.* **206**, 171–191
5. Kaupmann, K., Huggel, K., Heid, J., Flor, P. J., Bischoff, S., Mickel, S. J., McMaster, G., Angst, C., Bittiger, H., Froestl, W., and Bettler, B. (1997) *Nature* **386**, 239–246
6. Herrada, G., and Dulac, C. (1997) *Cell* **90**, 763–773
7. Matsunami, H., and Buck, L. B. (1997) *Cell* **90**, 775–784
8. Bockaert, J., and Pin, J. P. (1999) *EMBO J.* **18**, 1723–1729
9. Okamoto, T., Sekiyama, N., Otsu, M., Shimada, Y., Sato, A., Nakanishi, S., and Jingami, H. (1998) *J. Biol. Chem.* **273**, 13089–13096
10. Romano, C., Yang, W. L., and O'Malley, K. L. (1996) *J. Biol. Chem.* **271**, 28612–28616
11. Han, G., and Hampson, D. R. (1999) *J. Biol. Chem.* **274**, 10008–10013
12. Bai, M., Trivedi, S., and Brown, E. M. (1998) *J. Biol. Chem.* **273**, 23605–23610
13. Goldsmith, P. K., Fan, G. F., Ray, K., Shiloach, J., McPhie, P., Rogers, K. V., and Spiegel, A. M. (1999) *J. Biol. Chem.* **274**, 11303–11309
14. Quiocho, F. A. (1990) *Philos. Trans. R. Soc. Lond. B Biol. Sci.* **326**, 341–351
15. Weiss, A., and Schlessinger, J. (1998) *Cell* **94**, 277–280
16. Syed, R. S., Reid, S. W., Li, C., Cheetham, J. C., Aoki, K. H., Liu, B., Zhan, H., Osslund, T. D., Chirino, A. J., Zhang, J., Finer-Moore, J., Elliott, S., Sitney, K., Katz, B. A., Matthews, D. J., Wendoloski, J. J., Egrie, J., and Stroud, R. M. (1998) *Nature* **395**, 511–516
17. Livnah, O., Johnson, D. L., Stura, E. A., Farrell, F. X., Barbone, F. P., You, Y., Liu, K. D., Goldsmith, M. A., He, W., Krause, C. D., Pestka, S., Jolliffe, L. K., and Wilson, I. A. (1998) *Nat. Struct. Biol.* **5**, 993–1004
18. Ng, G. Y., O'Dowd, B. F., Lee, S. P., Chung, H. T., Brann, M. R., Seeman, P., and George, S. R. (1996) *Biochem. Biophys. Res. Commun.* **227**, 200–204
19. Hebert, T. E., Moffett, S., Morello, J. P., Loisel, T. P., Bichet, D. G., Barret, C., and Bouvier, M. (1996) *J. Biol. Chem.* **271**, 16384–16392
20. Maggio, R., Vogel, Z., and Wess, J. (1993) *Proc. Natl. Acad. Sci. U. S. A.* **90**, 3103–3107
21. Gouldson, P. R., Snell, C. R., Bywater, R. P., Higgs, C., and Reynolds, C. A. (1998) *Protein Eng.* **11**, 1181–1193
22. Jordan, B. A., and Devi, L. A. (1999) *Nature* **399**, 697–700
23. Jones, K. A., Borowsky, B., Tamm, J. A., Craig, D. A., Durkin, M. M., Dai, M., Yao, W. J., Johnson, M., Gunwaldsen, C., Huang, L. Y., Tang, C., Shen, Q., Salon, J. A., Morse, K., Laz, T., Smith, K. E., Nagarathnam, D., Noble, S. A., Branchek, T. A., and Gerald, C. (1998) *Nature* **396**, 674–679
24. White, J. H., Wise, A., Main, M. J., Green, A., Fraser, N. J., Disney, G. H., Barnes, A. A., Emson, P., Foord, S. M., and Marshall, F. H. (1998) *Nature* **396**, 679–682
25. Kaupmann, K., Malitschek, B., Schuler, V., Heid, J., Froestl, W., Beck, P., Mosbacher, J., Bischoff, S., Kulik, A., Shigemoto, R., Karschin, A., and Bettler, B. (1998) *Nature* **396**, 683–687
26. Neki, A., Ohishi, H., Kaneko, T., Shigemoto, R., Nakanishi, S., and Mizuno, N. (1996) *Neurosci. Lett.* **202**, 197–200
27. Shigemoto, R., Kinoshita, A., Wada, E., Nomura, S., Ohishi, H., Takada, M., Flor, P. J., Neki, A., Abe, T., Nakanishi, S., and Mizuno, N. (1997) *J. Neurosci.* **17**, 7503–7522
28. Miyazaki, J., Nakanishi, S., and Jingami, H. (1999) *Biochem. J.* **340**, 687–692
29. Masu, M., Tanabe, Y., Tsuchida, K., Shigemoto, R., and Nakanishi, S. (1991) *Nature* **349**, 760–765
30. Ohashi, H., Higashi-Matsumoto, H., Maruyama, T., and Takeuchi, Y. (1997) *Soc. Neurosci. Abstr.* **23**, 2023
31. Ray, K., Hauschild, B. C., Steinbach, P. J., Goldsmith, P. K., Hauache, O., and Spiegel, A. M. (1999) *J. Biol. Chem.* **274**, 27642–27650
32. Zeng, F. Y., and Wess, J. (1999) *J. Biol. Chem.* **274**, 19487–19497
33. Kuusinen, A., Arvola, M., and Keinänen, K. (1995) *EMBO J.* **14**, 6327–6332
34. Costantino, G., Maccharulo, A., and Pellicciari R. (1999) *J. Med. Chem.* **42**, 5390–5401
35. Armstrong, N., Sun, Y., Chen, G. Q., and Gouaux, E. (1998) *Nature* **395**, 913–917

Structural basis of glutamate recognition by a dimeric metabotropic glutamate receptor

Naoki Kunishima*‡, Yoshimi Shimada†, Yuji Tsuji†, Toshihiro Sato†, Masaki Yamamoto‡, Takashi Kumasaka‡, Shigetada Nakanishi§, Hisato Jingami† & Kosuke Morikawa*

*Departments of *Structural Biology and †Molecular Biology, Biomolecular Engineering Research Institute, 6-2-3 Furuedai, Suita, Osaka 565-0874, Japan*
‡ Structural Biophysics Laboratory, RIKEN Harima Institute, 1-1-1 Kouto, Mikazuki, Sayo, Hyogo 679-5148, Japan
§ Department of Biological Sciences, Kyoto University Faculty of Medicine, Yoshida, Sakyo-ku, Kyoto 606-8501, Japan

The metabotropic glutamate receptors (mGluRs) are key receptors in the modulation of excitatory synaptic transmission in the central nervous system. Here we have determined three different crystal structures of the extracellular ligand-binding region of mGluR1—in a complex with glutamate and in two unliganded forms. They all showed disulphide-linked homodimers, whose 'active' and 'resting' conformations are modulated through the dimeric interface by a packed α-helical structure. The bi-lobed protomer architectures flexibly change their domain arrangements to form an 'open' or 'closed' conformation. The structures imply that glutamate binding stabilizes both the 'active' dimer and the 'closed' protomer in dynamic equilibrium. Movements of the four domains in the dimer are likely to affect the separation of the transmembrane and intracellular regions, and thereby activate the receptor. This scheme in the initial receptor activation could be applied generally to G-protein-coupled neurotransmitter receptors that possess extracellular ligand-binding sites.

Glutamate is a principal excitatory neurotransmitter in the mammalian central nervous system and functions in long-term potentiation/depression, learning and memory. Glutamate receptors are membrane proteins, which mediate excitatory transmission on the cellular surface through initial binding of glutamate[1,2], and are categorized into ionotropic glutamate receptors (iGluRs) and metabotropic glutamate receptors (mGluRs). The mGluRs are coupled to G proteins and are thus distinct from the iGluRs which internally contain ligand-gated ion-channels. From a structural viewpoint, mGluRs belong to the seven-transmembrane protein family mostly shared by G-protein-coupled receptors, such as rhodopsin and the adrenergic receptor.

The eight subtypes of mGluRs are classified into three subgroups according to sequence similarity, agonist selectivity and effector system differences[3]: subgroup I (mGluR1 and -5), subgroup II (mGluR2 and -3) and subgroup III (mGluR4, -6, -7 and -8). They share sequence similarity with the calcium-sensing receptor[4] and the pheromone receptor[5,6] to form the mGluR family. The mGluR structure is divided into three regions: the extracellular region, the seven-spanning transmembrane region and the cytoplasmic region (Fig. 1a). The extracellular region is further divided into the ligand-binding region (LBR) and the cysteine-rich region. LBR has sequence similarity to the leucine/isoleucine/valine-binding protein (LIVBP), which is a bacterial periplasmic binding protein[7] (PBP), as well as to the extracellular regions of both iGluR[7] and the γ-aminobutyric acid $(GABA)_B$ receptor[8]. Both chimaeric receptor analysis[9] and homology model building[7,10] based on the crystal structure of LIVBP[11] have suggested that LBR is responsible for ligand binding. More directly, the extracellular regions of mGluR have been expressed in soluble forms, and have been shown to serve as ligand-binding sites and thus confer ligand-binding selectivity[12–14]. The mGluR family therefore differs in the ligand-binding mode from the classical rhodopsin-type G-protein-coupled receptors, which bind ligands in pockets in their transmembrane helices. To gain insight into the mechanism of how ligand binding induces a conformational change that is transmitted across the transmembrane region and into the intracellular region in the mGluR family proteins, we crystallized the LBR of mGluR1 (m1-LBR) and analysed it by X-ray crystallography. Here we report three crystal structures of m1-LBR with and without glutamate, and discuss their structural differences to deduce the implications of receptor activation.

General description of crystal structures

We determined the crystal structures of m1-LBR in two unliganded forms, called free forms I and II, and in a complex form with glutamate (Table 1). The asymmetric unit of all crystal forms contains two molecules of m1-LBR. These two protomers form a homodimer related by a non-crystallographic pseudo-twofold axis (Fig. 1b, c). The global conformations of the dimers substantially differ between the complex form and the free form I, whereas the free form II and the complex form share almost identical conformations, except for ligand binding.

The two protomers are covalently connected by an interprotomer disulphide bridge between Cys 140 of each monomer, which lie in a long disordered segment between the B helix and the D strand. This disulphide bridge has been confirmed by biochemical analyses of the protein with an alanine substitution at Cys 140 (ref. 15). Obviously, this disulphide bond cannot act as a structural scaffold because of its location within the disordered segment. Instead, it most probably functions as an interprotomer linker to increase the effective concentration of a dimeric form of mGluR1 on the cellular surface. Similar reports showing the formation of disulphide-linked dimers of mGluR5 (ref. 16) and the calcium receptor[14] further support the critical role of this residue, in addition to the conservation of the corresponding cysteines in the mGluR family (Fig. 2).

Each protomer consists of the amino-terminal and the carboxy-terminal domains, designated LB1 and LB2, respectively. Only the LB1 domain provides the dimer interfaces in all three crystal forms, and hence the LB1–LB2 relative orientations are independent of the dimer interface construction. These two domains, both with α/β topology, are connected by three short loops on one side of the molecule to form a 'clamshell'-like shape similar to that found in iGluR[17] or PBPs, such as LIVBP[11], lysine/arginine/ornithine-binding

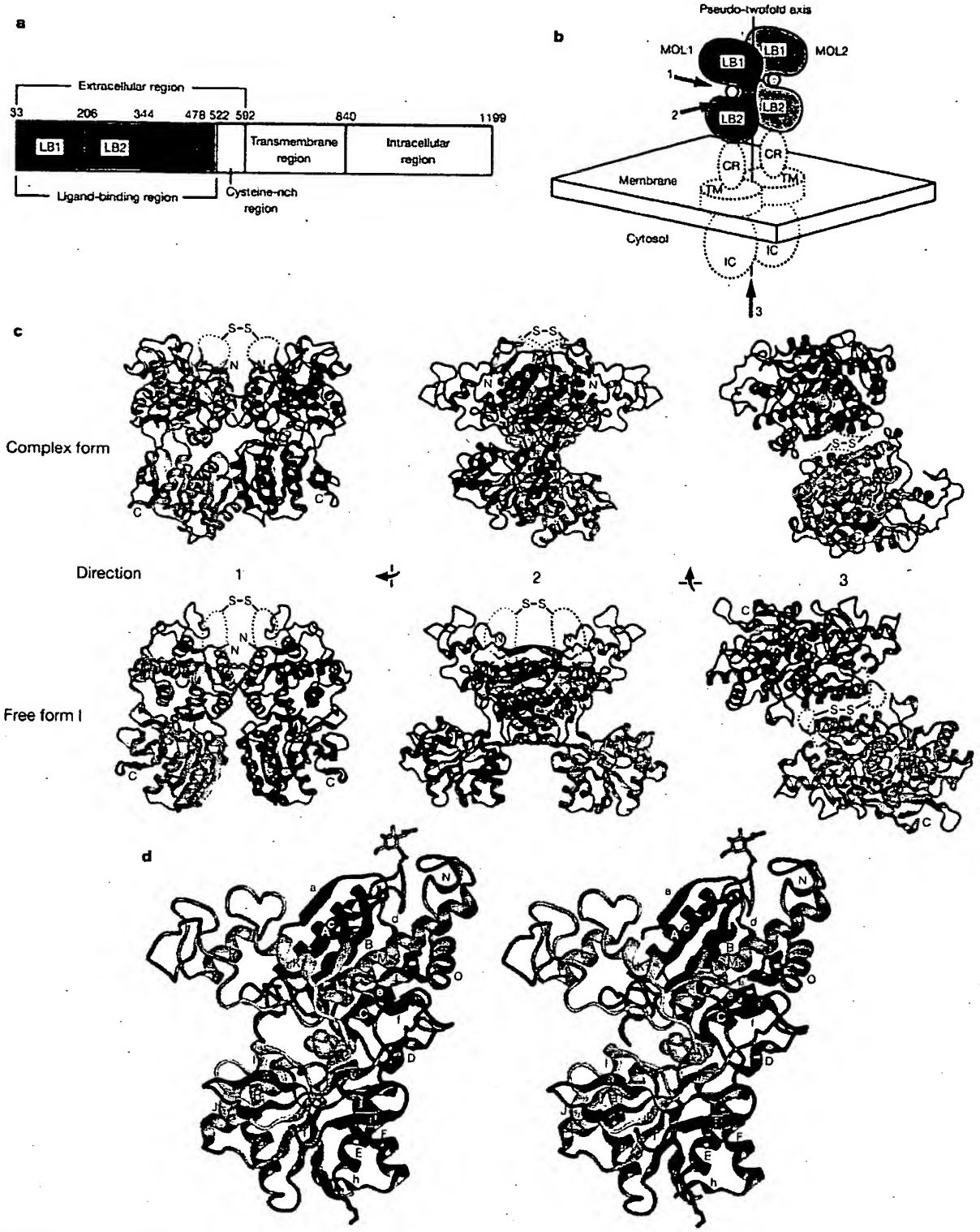

Figure 1 Crystal structures of mGluR1 in the liganded and unliganded states. **a**, Diagram of full-length mGluR1. Functional regions are boxed. The LB1 and LB2 domains, which constitute a ligand-binding region, are coloured blue and red, respectively. Numerical positions of amino-acid residues are indicated according to the primary amino-acid sequence[40]. Protein regions not determined in this study are indicated by open boxes. **b**, Drawing of the spatial arrangements of mGluR1 domains. The MOL1 and MOL2 molecules of the m1-LBR dimer are distinguished by dark and light colouring, respectively. The ligand, glutamate, is shown as yellow spheres. CR, cysteine-rich region; IC, intracellular region; TM, transmembrane region. **c**, Three orthogonal views of the dimer structures of the complex form and the free form I. The perspectives are indicated by arrows in **b**. Bound glutamate molecules are shown as yellow space-filling models. Disordered regions with a potential interprotomer disulphide bridge are indicated by dotted lines. The B helix, constituting the dimer interface between subunits, is coloured green. **d**, Stereoview of MOL1 of the complex form. The ribbon model, viewed from direction 2 in **c**, is coloured in a rainbow gradation from purple (N terminus) to red (C terminus). Helices and strands are indicated by upper and lower cases, respectively. Sugar moieties and a bound metal ion are depicted by green licorice models and a red sphere, respectively.

protein[18] (LAOBP), polyamine-binding protein[19,20] and glutamine-binding protein[21] (GlnBP). As predicted from sequence analysis[7], the main-chain folding of m1-LBR is similar to that of LIVBP; the r.m.s. deviations for the corresponding Cα atoms are about 1.8 Å for each domain.

Glutamate is bound in an interdomain crevice, as found in iGluR or PBPs. In common with these proteins, m1-LBR shows an open–closed conformation characterized by the different spatial arrangements between the LB1 and LB2 domains. We designate the relatively closed subunit of the m1-LBR dimer as MOL1 and the other as MOL2. The most characteristic feature of m1-LBR is the strikingly different dimer configurations, which are dependent on the dimer interface construction.

We found a bound metal ion in the loop region between the A helix and the C strand (Figs 1d, 2). From its hexavalent coordination and temperature factor, this metal is most likely to be Mg^{2+}, although Ca^{2+} cannot be ruled out. mGluR1 has been reported to bind di-/trivalent cations near the glutamate-binding site and function as a cation receptor[22]. However, the found metal-binding position appears to be far from the reported cation-binding site. As we added neither magnesium nor calcium during the purification and crystallization, the metal appears to bind to m1-LBR more tightly than the reported affinity[22]. Therefore, it may be a scaffold factor for the LB1 domain, rather than a second physiological ligand.

The B helix adjacent to the N terminus of the long disordered segment shows a notable conformational change between the free form I and the complex form. The residues 125–131 are disordered in the complex form, whereas in the free form I they are incorporated into the B helix to form a helical extension of about two turns on the C-terminal side (Fig. 2). The extended helical residues in the free form I interact with those in the counterpart of the m1-LBR dimer. The same residues in the free form II are disordered, like those in the complex form. These findings suggest that the elongation of the B helix is more directly coupled with the domain arrangements rather than with glutamate binding itself.

Ligand recognition

In the complex form, both MOL1 and MOL2 bind glutamate at

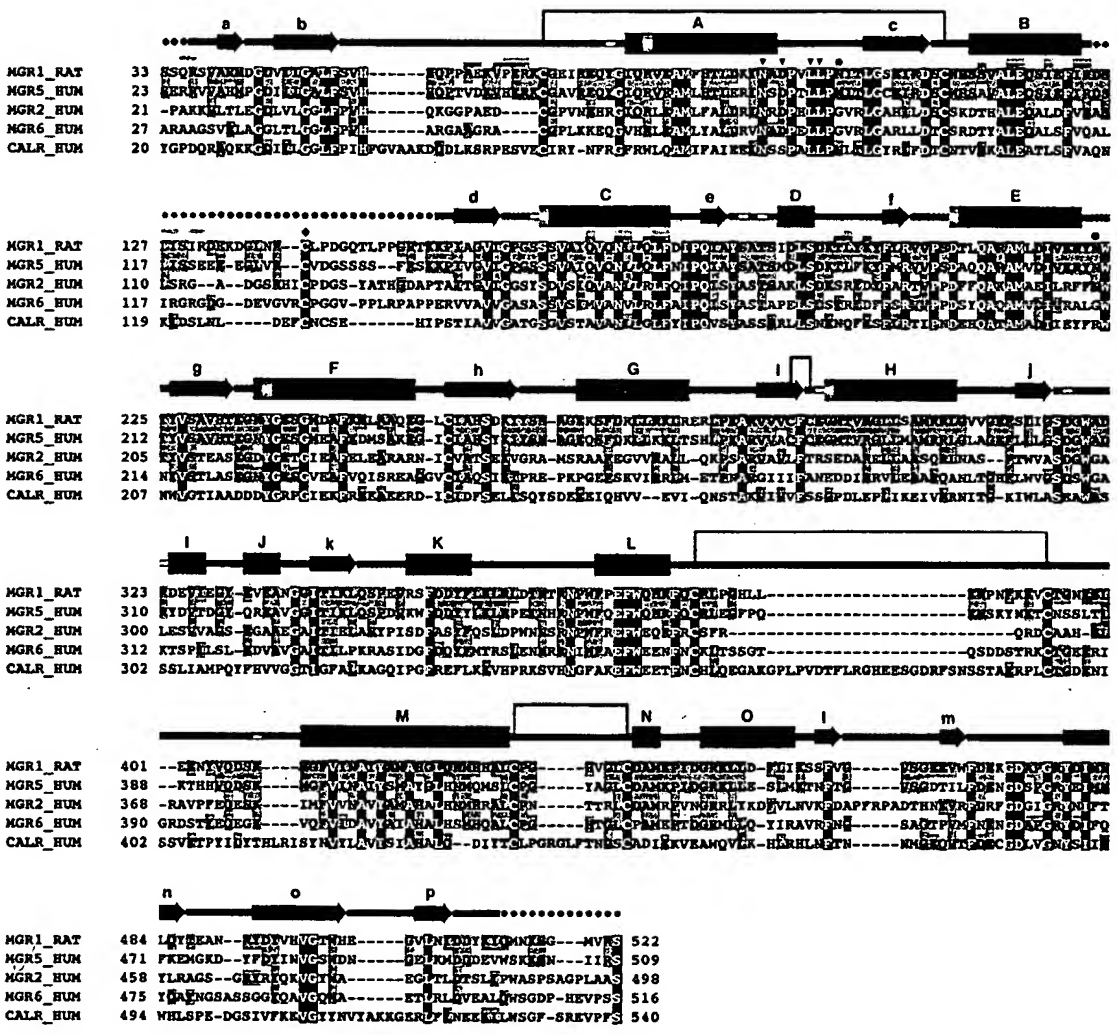

Figure 2 Secondary structure assignment (PROCHECK[37]) and multiple sequence alignments. Secondary structure in MOL1 of the complex form is displayed over the sequences: helices are shown as cylinders; strands as arrows, with the same labelling as in Fig. 1d; disordered residues are shown as dots. The LB1 and LB2 domains, the ligand-binding sites, and the additionally visible region in the free form I are coloured blue, red, yellow and green, respectively. Intraprotomer disulphide bridges are indicated by thin solid lines connecting cysteines. Residues of interest are highlighted beneath the secondary structure: cyan and magenta bars indicate residues involved in the dimer interfaces of the free form I and the complex form, respectively; arrowheads and filled circles indicate residues coordinating with the metal ion and glycosylated residues, respectively; filled diamond indicates the cysteine residue forming the interprotomer disulphide bridge. The sequences of selected mGluR family proteins, mGluR1, -2, -5 and -6 (refs 40–43) and the calcium receptor[44], are aligned together and shown with the shading highlighting conserved sequences.

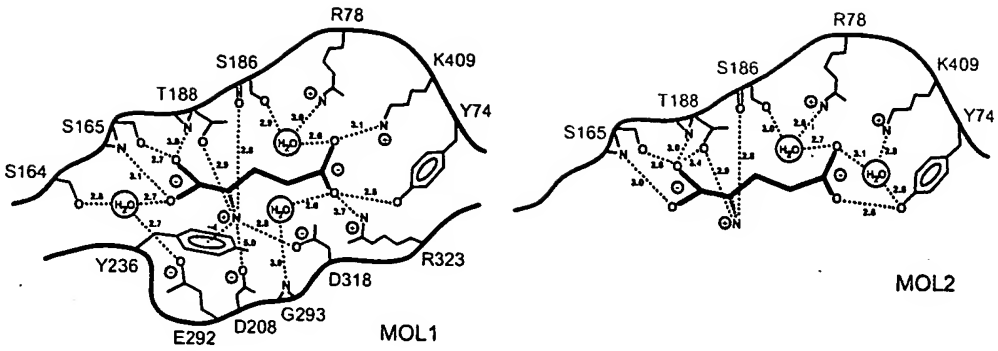

Figure 3 Representation of glutamate binding. Polar interactions of glutamate with MOL1 and MOL2 are denoted by dotted lines with distances. Domain colouring is as in Fig. 1b.

similar sites (Fig. 3). A large cleft formed by the bi-lobed architecture involves two interfaces that contact the glutamate: one lies in the LB1 domain (LB1 interface) and the other in the LB2 domain (LB2 interface). The structures of the LB1 interface are essentially identical between MOL1 and MOL2, except for the positions of a few bound water molecules. By contrast, the LB2 interface with the open conformation is not used for glutamate binding by MOL2. The similar averaged temperature factors of the two bound glutamates indicate essentially identical mobility between MOL1 and MOL2, suggesting a predominant role for the LB1 domain in anchoring the ligand.

The LB1 interfaces with a buried surface area of 168 Å^2 are dominated by direct hydrogen bonds, while water-mediated hydrogen bonds and salt bridges are predominant in the LB2 interface with a 135 Å^2 buried surface area. A cation–π interaction[23] between glutamate and Tyr 236 may contribute additionally to stabilizing the complex.

All of the potential ligand-binding residues identified by mutational analyses[7,24] are hydrogen bonded to glutamate in the LB1 interfaces. Our recent mutational analysis has confirmed that the hydrogen bond of Tyr 74 with glutamate is important for ligand binding (data not shown). Seven polar residues, which contribute to the ligand recognition, are conserved among all of the mGluR subtypes (Fig. 2). On the other hand, five polar residues are conserved only in subgroup I (mGluR1 and -5). These five residues may be related to the ligand preference of subgroup I. The two glutamate-binding schemes in the closed and open bi-lobed structure provide a structural basis for drug design.

Table 1 Statistics from the crystallographic analysis

Native data statistics*

Data set	Space group	Unit-cell dimensions (Å)	(deg)	Resolution (Å)	Completeness (%)	Multiplicty	R_{merge} (%)	$I/\sigma(I)$
Complex form	$P2_1$	a = 83.4 b = 95.2 c = 97.5	β = 114.9	2.2 (2.25–2.20)	98.9 (96.2)	3.26 (2.83)	4.5 (13.7)	17.5 (8.6)
Free form I	$P4_12_12$	a = 111.4 c = 293.7		3.7 (3.83–3.70)	99.9 (100.0)	6.08 (5.96)	14.6 (52.0)	11.6 (3.5)
Free form II	$P2_1$	a = 84.8 b = 94.5 c = 95.5	β = 113.2	4.0 (4.14–4.00)	89.1 (77.3)	2.55 (2.51)	18.1 (25.0)	5.4 (3.6)

MAD phasing from the K_2PtCl_4 derivative of the complex form (17.0–4.0 Å)†

Data set	Wavelength (Å)	Completeness (%)	R_{merge} (%)	Number of sites	Phasing power (acentric/centric) Isomorphous	Anomalous	Mean FOM
Edge	1.0720	99.4	4.3	6	3.25/2.48	1.65/-	0.442
Peak	1.0717	99.6	4.8	–	3.12/2.47	1.87/-	–
Remote	1.0200	99.5	4.6	–	–	1.82/-	–

Refinement statistics‡

	Complex form	Free form I	Free form II
Resolution range (Å)	17.0–2.2	12.0–3.7	20.0–4.0
R factor (%)	19.6 (65,274 reflections)	24.4 (18,693 reflections)	25.4 (10,016 reflections)
R_{free} (%)	22.7 (3,497 reflections)	28.7 (950 reflections)	32.8 (534 reflections)
Ramachandran (%)			
Favoured	89.1	89.3	85.4
Generous	0.4	0.5	0.4
Disallowed	0.0	0.0	0.0
R.m.s. deviations from ideality			
Bond lengths (Å)	0.006	0.013	0.014
Bond angles (deg)	1.2	1.7	1.8
B factor (Å^2)	0.80 (1.14)	1.48 (1.56)	1.08 (1.16)

*Values in parentheses indicate statistics for the highest resolution shells. $R_{merge} = \Sigma_j\Sigma_i|I_i\rangle - I_{ij}|/\Sigma_j\Sigma_i I_{ij}$, where $\langle I_i\rangle$ is the mean intensity of ith unique reflection, and I_{ij} is the intensity of its jth observation.
†Phasing power = $\langle F(H)\rangle/E$, where $\langle F(H)\rangle$ is the r.m.s. amplitude of the heavy atom structure factor and E is the residual lack of closure error. Mean figure of merit (FOM) = $\langle\Sigma P(\alpha)\exp(i\alpha)/\Sigma P(\alpha)\rangle$, where $P(\alpha)$ is the phase probability at the angle α.
‡The residues in disordered regions were eliminated from the model: S33–Q35 (MOL1), S33–S34 (MOL2), D125–K153 and Q513–S522 of the complex form; S33–S34, D132–K153 and Q513–S522 of the free form I; S33–Q35, D125–K153 and Q513–S522 of the free form II. R factor = $\Sigma_i|F(\text{obs})_i - F(\text{calc})_i|/\Sigma_i F(\text{obs})_i$, where F(obs) and F(calc) are the observed and calculated native structure factors, respectively. R_{free} = R factor calculated using 5% of total reflections, which were chosen randomly and omitted from the refinement. All observed reflections, except for those for the calculation of R_{free}, were used for the refinement. R.m.s. deviations of B factors were calculated for main-chain atoms and side-chain atoms (in parentheses).

Interdomain movement

The open–closed conformational change of m1-LBR can be described as a rotation about an axis roughly passing across the three connecting loops (Fig. 1c, d). The difference in LB1–LB2 interdomain orientations between MOL1 (closed conformer) and MOL2 (open conformer) in the complex form is 31°, which is smaller than the 52° in LAOBP[18] and 56° in GlnBP[21] (see Methods). We compared the determinants for interdomain movements, the ϕ and ψ backbone dihedral angles on the three connecting loops, between the two conformers. The largest changes were 47° in the ϕ angle at Gly 477 and 61° in the ψ angle at Arg 478 on the same loop. These values are comparable to the 52° change that occurs in the ψ angle at Ala 90 in LAOBP[18], whereas the other two loops show much smaller angle differences spread over many residues.

In contrast to the closed and open conformers in the complex form, the free form I contains two open conformers, similar to each other in the overall shapes but different in detail (Fig. 1c). The two closed conformers and the four open conformers, available in all three different crystal forms, allowed us to estimate the robustness of both conformers by comparing the interdomain orientations. The two closed conformers are identically orientated within an azimuth angle of 1°, whereas the four open conformers show a polymorphism of about 10°. This orientational restraint of the closed conformers seems to be derived from the direct contact between the LB1 and LB2 domains, which is shared by the surroundings of the ligand interfaces in the free form II and the complex form. This contact with a buried surface area of 477 Å^2 involves six polar and many non-polar interactions.

The free form II maintains the same dimer conformations as those of the complex form, even in the absence of ligand. This suggests that the interdomain orientation of the ligand-free m1-LBR exchanges in solution between the open and closed conformations. From a comparison of the unliganded and complex forms of the LAOBP crystal structures, it was proposed that the unliganded protein undergoes a dynamic change between an open and a closed conformation, and that the role of the ligand is to stabilize the closed conformation[18]. Furthermore, as reported for LAOBP, we could not find any evidence for a direct link between the ligand binding and the conformational change of the three connecting loops in m1-LBR. Together, we conclude that one role of glutamate may be to stabilize the closed conformation of the bi-lobed m1-LBR protomer in dynamic equilibrium.

Relocation of dimer interfaces

On the dimer interfaces, the two LB1 domains rotate by about 70° between the free form I and the complex form (Fig. 4a). The rotation axis is approximately perpendicular to these interfaces and passes through the vicinity of Ile 120 and Leu 174 (Fig. 4b, c). This rotation, which is uncoupled from the intraprotomer open–closed conformational change, solely determines the interprotomer orientations of the non-crystallographic symmetry (NCS) related LB1 domains. We designated the two distinct interprotomer orientations of the LB1 domains in the free form I and the complex form as the 'R' and 'A' conformations, respectively. A comparison between the free form II and the complex form revealed that the A conformation is fixed within an azimuth angle of 3°. A restraint comparable to this angle would be applied to the R conformation, because the buried surface areas of the two interfaces are similar: 906 Å^2 for the R conformation and 793 Å^2 for the A conformation. The central hydrophobic cores of the two distinct interfaces comprise residues Leu 116, Ile 120, Leu 127, Leu 174 and Leu 177, which are well conserved in the mGluR family (Figs 2, 4c).

The dimer interface related by NCS mainly consists of the B and C helices, including the extension of the B helix in the free form I (Fig. 4b). This helical extension appears to predominantly differentiate between the R and A conformations. The angles between the B and C helices of each LB1 domain are estimated to be 140° in the R conformer and 70° in the A conformer. The mode of helical packing in this interface appears to be different from that of the globin fold or the four-helix bundle[25], where the crossing angles are usually 20° or 50°. The packing in the dimer interface appears to be looser than that in the internal protein folding. This looseness may be favourable for the smooth conversion between the R and A conformations.

Multiple conformations of the LBR dimer

The entire conformations of the m1-LBR dimer in the three crystal forms can be defined as a combination of the intra and interprotomer conformations: open–open/R for the free form I and closed–open/A for both of the free form II and the complex form (Fig. 5). The latter, closed–open/A conformation is assumed to be

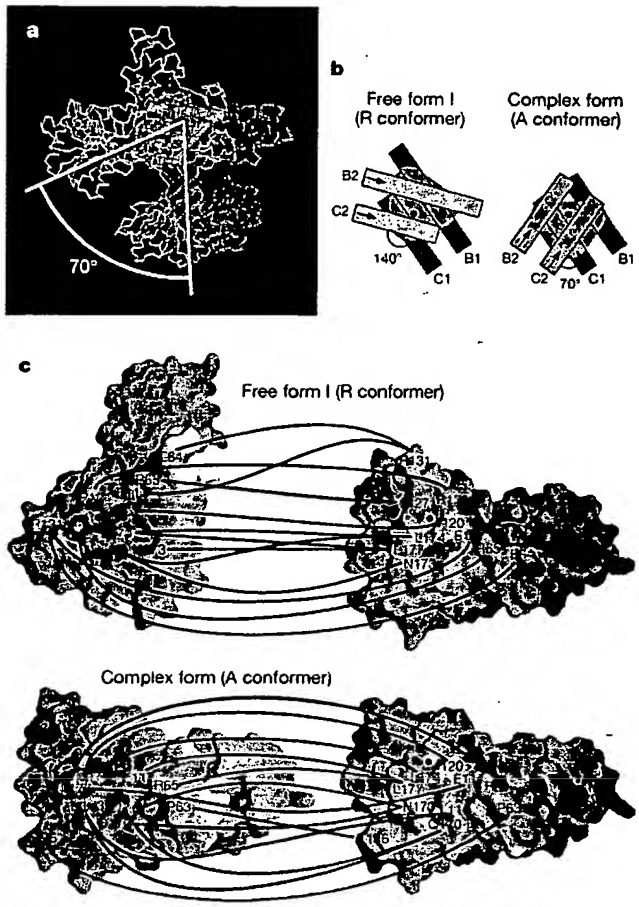

Figure 4 Relocation of dimer interfaces. **a**, Superposition of the free form I (green) and the complex form (red) after the alignment of the corresponding Cα atoms in the LB1 domains of MOL1. MOL1 and MOL2 are distinguished by dark and light colouring, respectively. The two molecules in the different states are viewed along the rotation axis of the dimer interfaces. The helices B and C, which mainly contribute to the dimeric interactions, are represented as ribbon diagrams in MOL2 with the same colouring as that of the subunits. **b**, Close-up view of the dimer interfaces. Perspective and colouring of the receptors are the same as those in **a**. Helices B and C are represented as rectangles with arrows that denote sequence directions. Dimer interfaces and their rotation axes are depicted as orange planes and filled circles, respectively. **c**, Open-book view of dimer interfaces. GRASP[45] models of the LB1 domains, viewed from the right side of **a**, are disassembled in the manner of an 'open book' to reveal the dimer interfaces. Hydrophobicity based on the reported hydropathy values[46] and buried surface area were mapped, respectively, onto the right MOL1 models and the left MOL2 models by gradation colouring. The blue and the yellow in MOL1 represent the hydrophilic and hydrophobic regions, respectively; the yellow and the red in MOL2 indicate the low and high values of buried surface area, respectively. Residue–residue interactions and rotation axes of the dimer interfaces are indicated.

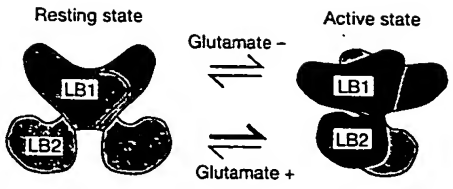

Conformation	open-open/R	closed-open/A
Crystal form	Free form I	Free form II and Complex form
LB2–LB2 spacing (Å)	63 (88)	36 (63)

Figure 5 Diagram of the two states of the m1-LBR in dynamic equilibrium. Open and closed conformations of m1-LBR are distinguished by light and dark colouring, respectively. LB2–LB2 spacings are shown between the centres of masses or C termini (in parentheses) of the two LB2 domains in each conformer.

trapped by crystal packing, because of the lack of connection between the asymmetric protomer combination and the interprotomer A conformation. This implies that unidentified conformations of m1-LBR with various combinations might be present in solution. We confirmed the feasibility of other putative conformers by model building (see Methods). This examination allowed us to construct four additional conformers of the m1-LBR dimers without steric clashes: closed–open/R, closed–closed/R, open–open/A and closed–closed/A.

If glutamate binding changes the equilibrium of such multiconformers and thereby activates the receptor, then the spatial arrangements of the two LB2 domains near the cellular membrane would be crucial for signal transduction (Figs 1b, 5). Thus, we estimated the spacings between the two LB2 domains in each of the six conformers (see Fig. 5 legend). Notably, in spite of the large variety of LB2–LB2 orientations, there are only two spacings with a roughly 26 Å difference determined exclusively by the interprotomer R–A conformations (Fig. 5). Notably, the crystal structures indicate that glutamate binding settles the A conformation, which should be defined as the 'active' state, and hence the R conformation should correspond to the 'resting' state. This notion implies that glutamate binding should be the determinant for the R–A conformational change, perhaps through a subtle structural change that occurs on binding. The limited resolutions of the ligand-free crystals prevent manifesting a clear structural basis for the stabilization mechanism, although a loop region (residues 59–67), including a conserved disulphide bridge, appears to have an important role, because of its proximity to both the glutamate-binding site and the extending region of the B helix.

Implications of receptor activation

The initial activation mode of mGluR1 is totally different from those postulated in the classical rhodopsin-type G-protein-coupled receptors including rhodopsin[26] and the adrenergic receptor[27]. It is intriguing to compare the activation mechanism of mGluR1 with cytokine–receptor recognition. Structural studies revealed that cytokine binding causes the assembly and/or the relocation of their extracellular domains of receptor molecules[28,29]. In activation of the dimeric erythropoietin receptor (EPOR), the conformational rearrangement of the extracellular region coupled with ligand binding induces the access of the transmembrane and cytoplasmic domains[30,31]. Similarly, the interdomain and interprotomer rearrangements of the m1-LBR dimer may cause the approach of two transmembrane regions linked to intracellular regions (Fig. 5), although we have to consider the cysteine-rich region with an unknown 3D structure (Fig. 1b). Alternatively, glutamate with a much smaller size and lower affinity does not use the induced-fit activation mechanism, and the ligand binding increases only the population of activated forms by stabilizing them among the several conformations that are in dynamic equilibrium.

The crystal structures of m1-LBR also suggest roles for the LBR homologous regions (LBR-HRs) of related receptors, such as the $GABA_B$ receptor and iGluR. The extracellular LBR-HRs of both receptors possess a short stretch of hydrophobic residues, corresponding to the C helix of the m1-LBR dimer interface, suggesting the conservation of the oligomerization interface among the three receptors. In the case of the $GABA_B$ receptor, a heterodimerization of two distinct subunits with homologous sequences is essential for receptor expression and activation[32–34]. Thus, a large variety of interdomain and intersubunit conformations of LBR-HR might be important for the $GABA_B$ receptor activation. Similarly, in the case of iGluR, which forms a multisubunit ion channel, LBR-HR at the N terminus of the receptor might regulate the function of the ion channel by using an additional extracellular interface for oligomerization.

In conclusion, we have shown that the dimeric ligand-binding region of mGluR adopts multiple conformations, where the activated domain arrangements of the dimer are in equilibrium with other states and are selectively stabilized by glutamate binding. Analogous multiple conformations in a multisubunit receptor, formed as a result of the relocations of both the interdomain and intersubunit interfaces, may be one of the fundamental principles of the activation mechanism of receptors that bind small ligands in extracellular regions. □

Methods

Crystallization and data collection

We expressed and purified the LBR of rat mGluR1 (residues 33–522) as described[15]. The complex form grew in hanging drops containing 20% PEG4000, 1 mM L-glutamate, 10 mg ml^{-1} m1-LBR and 200 mM HEPES-NaOH pH 7.5. Heavy atom derivatives were prepared by soaking crystals in 5 mM K_2PtCl_4 for 5 h or by expressing m1-LBR in a medium containing selenomethionine. The free form I was grown in 1.9 M ammonium sulphate solution, containing 10 mg ml^{-1} m1-LBR and 200 mM Tris-HCl pH 8.5, and the free form II in a 20% PEG4000 solution, containing 10 mg ml^{-1} m1-LBR, 100 mM ammonium sulphate and 100 mM Tris-HCl pH 7.5. We collected diffraction data with cryocooling at 100 K on undulator beamlines BL45XU (complex form) and BL24XU (free forms) at SPring-8, Hyogo, Japan. Cryosolvents were artificial mother liquor containing 20–30% glycerol. We processed all data with DENZO/SCALEPACK[35].

Structure determination

We used multiwavelength anomalous dispersion (MAD) for the phase determination of the platinum derivative of the complex form. MAD phasing from six platinum sites was performed with the program SHARP[36] at 4.0 Å resolution. Phase extension to higher resolution data was unsuccessful; however, an initial atomic model containing most of the secondary structure in m1-LBR could be built on the 4.0 Å resolution map, after phase improvement using the program DM[37]. In this process, we found 22 selenium sites in a difference Fourier map from the selenomethionine derivative. These selenium sites and the atomic coordinates of LIVBP (PDB code 2LIV) were effectively used as guides in the model building. Further phase improvement by molecular averaging and by phase combination with the partial model phases allowed us to build a model for the entire complex molecule. This model was refined with the program CNS[38] followed by manual rebuilding. We applied bulk-solvent correction, NCS restraints and anisotropic *B* factor corrections. The NCS restraints were released in the final two rounds of the refinement. During the refinement, a few bound HEPES molecules were found in regions sufficiently far from both the glutamate-binding site and the dimer interface. The final model contains 897 residues of a m1-LBR dimer, 2 L-glutamate molecules, 642 water molecules, 4 *N*-acetyl-glucosamine residues, 3 HEPES molecules and 2 metal ions. The model of Cys 289 had two conformers probably produced by radiation damage during data collection, as reported for acetylcholine esterase and lysozyme crystal structures[39].

The molecular replacement analysis with AMORE[37], using modified coordinates of the complex form as a search model, allowed the structure determination of the free form I crystal. The combination of molecular replacement phases with single isomorphous replacement phases from a Pt derivative provided the identical conformation. We refined the model using CNS with bulk-solvent correction, tight NCS restraints (300 kcal mol^{-1} $Å^{-2}$) except for the regions of crystal contact, and anisotropic *B*-factor corrections. In the free form I, bound sulphate ions were found in the moieties essentially identical to the HEPES sites in the complex form. The final model contains 912 amino-acid residues of an m1-LBR dimer, an *N*-acetyl-glucosamine residue and 4 sulphate ions. The structure of the free form II was solved by rigid-body refinement with CNS, using the coordinates of the complex form. For the calculation, we regarded the four domains in the m1-LBR dimer as four independent rigid bodies. Bulk-solvent correction and anisotropic *B*-factor corrections were applied. Finally, the model was refined with tight restraints. The current model contains 896 residues of an m1-LBR dimer. No obvious electron densities were observed around the glutamate-binding site of the free form II, after simulated annealing using CNS. $F_{obs} - F_{calc}$ simulated annealed omit maps for the free forms I and II

were calculated at 3.7 Å and 4.0 Å resolution, respectively, and both of them clearly revealed one by one all α-helices from A to O, confirming that the refined conformations are accurate. A stereochemical analysis of the refined model by PROCHECK[37] showed excellent geometry for all crystal forms (Table 1).

We calculated the orientation differences between two identical components and buried surface areas with the programs LSQKAB[37] and QUANTA98 (Molecular Simulations), respectively, as described[28]. Figures 1c, 1d and 4a were drawn in QUANTA98.

Received 1 June; accepted 30 August 2000.

1. Nakanishi, S. & Masu, M. Molecular diversity and functions of glutamate receptors. *Annu. Rev. Biophys. Biomol. Struct.* 23, 319–348 (1994).
2. Hollmann, M. & Heinemann, S. Cloned glutamate receptors. *Annu. Rev. Neurosci.* 17, 31–108 (1994).
3. Nakanishi, S. Molecular diversity of glutamate receptors and implications for brain function. *Science* 258, 597–603 (1992).
4. Brown, E. M. *et al.* Cloning and characterization of an extracellular Ca^{2+}-sensing receptor from bovine parathyroid. *Nature* 366, 575–580 (1993).
5. Herrada, G. & Dulac, C. A novel family of putative pheromone receptors in mammals with a topographically organized and sexually dimorphic distribution. *Cell* 90, 763–773 (1997).
6. Matsunami, H. & Buck, L. B. A multigene family encoding a diverse array of putative pheromone receptors in mammals. *Cell* 90, 775–784 (1997).
7. O'Hara, P. J. *et al.* The ligand-binding domain in metabotropic glutamate receptors is related to bacterial periplasmic binding proteins. *Neuron* 11, 41–52 (1993).
8. Kaupmann, K. *et al.* Expression cloning of $GABA_B$ receptors uncovers similarity to metabotropic glutamate receptors. *Nature* 386, 239–246 (1997).
9. Takahashi, K., Tsuchida, K., Tanabe, Y., Masu, M. & Nakanishi, S. Role of the large extracellular domain of metabotropic glutamate receptors in agonist selectivity determination. *J. Biol. Chem.* 268, 19341–19345 (1993).
10. Costantino, G., Macchiarulo A. & Pellicciari, R. Modeling of amino-terminal domains of group I metabotropic glutamate receptors: structural motifs affecting ligand selectivity. *J. Med. Chem.* 42, 5390–5401 (1999).
11. Sack, J. S., Saper, M. A. & Quiocho, F. A. Periplasmic binding protein structure and function. Refined X-ray structures of the leucine/isoleucine/valine-binding protein and its complex with leucine. *J. Mol. Biol.* 206, 171–191 (1989).
12. Okamoto, T. *et al.* Expression and purification of the extracellular ligand binding region of metabotropic glutamate receptor subtype 1. *J. Biol. Chem.* 273, 13089–13096 (1998).
13. Han, G. -M. & Hampson, D. R. Ligand binding to the amino-terminal domain of the mGluR4 subtype of metabotropic glutamate receptor. *J. Biol. Chem.* 274, 10008–10013 (1999).
14. Goldsmith, P. K. *et al.* Expression, purification, and biochemical characterization of the amino-terminal extracellular domain of the human calcium receptor. *J. Biol. Chem.* 274, 11303–11309 (1999).
15. Tsuji, Y. *et al.* Cryptic dimer interface and domain organization of the extracellular region of metabotropic glutamate receptor subtype 1. *J. Biol. Chem.* 275, 28144–28151 (2000)
16. Romano, C., Yang, W.-L. & O'Malley, K. L. Metabotropic glutamate receptor 5 is a disulphide-linked dimer. *J. Biol. Chem.* 271, 28612–28616 (1996).
17. Armstrong, N., Sun, Y., Chen, G.-Q. & Gouaux, E. Structure of a glutamate-receptor ligand-binding core in complex with kainate. *Nature* 395, 913–917 (1998).
18. Oh, B.-H. *et al.* Three-dimensional structures of the periplasmic lysine/arginine/ornithine-binding protein with and without a ligand. *J. Biol. Chem.* 268, 11348–11355 (1993).
19. Sugiyama, S. *et al.* Crystal structure of PotD, the primary receptor of the polyamine transport system in *Escherichia coli*. *J. Biol. Chem.* 271, 9519–9525 (1996).
20. Vassylyev, D. G., Tomitori, H., Kashiwagi, K., Morikawa, K. & Igarashi, K. Crystal structure and mutational analysis of the *Escherichia coli* putrescine receptor. *J. Biol. Chem.* 273, 17604–17609 (1998).
21. Sun, Y.-J., Rose, J., Wang, B.-C. & Hsiao, C.-D. The structure of glutamine-binding protein complexed with glutamine at 1.94 Å resolution: comparisons with other amino acid binding proteins. *J. Mol. Biol.* 278, 219–229 (1998).
22. Kubo, Y., Miyashita, T. & Murata, Y. Structural basis for a Ca^{2+}-sensing function of the metabotropic glutamate receptors. *Science* 279, 1722–1725 (1998).
23. Gallivan, J. P. & Dougherty, D. A. Cation–π interactions in structural biology. *Proc. Natl. Acad. Sci. USA* 96, 9459–9464 (1999).
24. Hampson, D. R. *et al.* Probing the ligand-binding domain of the mGluR4 subtype of metabotropic glutamate receptor. *J. Biol. Chem.* 274, 33488–33495 (1999).
25. Chothia, C., Levitt, M. & Richardson, D. Structure of proteins: packing of α-helices and pleated sheets. *Proc. Natl. Acad. Sci. USA* 74, 4130–4134 (1977).
26. Khorana, H. G. Rhodopsin, photoreceptor of the rod cell: an emerging pattern for structure and function. *J. Biol. Chem.* 267, 1–4 (1992).
27. Strader, C. D., Fong, T.-M., Tota, M. R., Underwood, D. & Dixon, R. A. F. Structure and function of G protein-coupled receptors. *Annu. Rev. Biochem.* 63, 101–132, (1994).
28. Aritomi, M. *et al.* Atomic structure of the GCSF-receptor complex showing a new cytokine-receptor recognition scheme. *Nature* 401, 713–717 (1999).
29. Deller, M. C. & Jones, E. Y. Cell surface receptors. *Curr. Opin. Struct. Biol.* 10, 213–219 (2000).
30. Livnah, O. *et al.* Crystallographic evidence for preformed dimers of erythropoietin receptor before ligand activation. *Science* 283, 987–990 (1999).
31. Remy, I., Wilson, I. A. & Minchnick, S. W. Erythropoietin receptor activation by a ligand-induced conformation change. *Science* 283, 990–993 (1999).
32. Jones, K. A. *et al.* $GABA_B$ receptors function as a heteromeric assembly of the subunits $GABA_BR1$ and $GABA_BR2$. *Nature* 396, 674–679 (1998).
33. White, J. H. *et al.* Heterodimerization is required for the formation of a functional $GABA_B$ receptor. *Nature* 396, 679–682 (1998).
34. Kaupmann, K. *et al.* $GABA_B$-receptor subtypes assemble into functional heteromeric complexes. *Nature* 396, 683–687 (1998).
35. Otwinowski, Z. & Minor, W. Processing of X-ray diffraction data collected in oscillation mode. *Methods Enzymol.* 276, 307–326 (1997).
36. de La Fortelle, E. & Bricogne, G. Maximum-likelihood heavy-atom parameter refinement for multiple isomorphous replacement and multiwavelength anomalous diffraction methods. *Methods Enzymol.* 276, 472–494 (1997).
37. Collaborative Computational Project, Number 4. The CCP4 Suite: programs for protein crystallography. *Acta Crystallogr. D* 50, 760–763 (1994).
38. Brünger, A. T. *et al.* Crystallography & NMR system: a new software suite for macromolecular structure determination. *Acta Crystallogr. D* 54, 905–921 (1998).
39. Weik, M. *et al.* Specific chemical and structural damage to proteins produced by synchrotron radiation. *Proc. Natl. Acad. Sci. USA* 97, 623–628 (2000).
40. Masu, M., Tanabe, Y., Tsuchida, K., Shigemoto, R. & Nakanishi, S. Sequence and expression of a metabotropic glutamate receptor. *Nature* 349, 760–765 (1991).
41. Flor, P. J. *et al.* Molecular cloning, functional expression and pharmacological characterization of the human metabotropic glutamate receptor type 2. *Eur. J. Neurosci.* 7, 622–629 (1995).
42. Minakami, R., Katsuki, F., Yamamoto, T., Nakamura, K. & Sugiyama, H. Molecular cloning and the functional expression of two isoforms of human metabotropic glutamate receptor subtype 5. *Biochem. Biophys. Res. Commun.* 199, 1136–1143 (1994).
43. Hashimoto, T. *et al.* The whole nucleotide sequence and chromosomal localization of the gene for human metabotropic glutamate receptor subtype 6. *Eur. J. Neurosci.* 9, 1226–1235 (1997).
44. Garrett, J. E. *et al.* Molecular cloning and functional expression of human parathyroid calcium receptor cDNAs. *J. Biol. Chem.* 270, 12919–12925 (1995).
45. Nicholls, A., Sharp, K. A. & Honig, B. Protein folding and association: insights from the interfacial and thermodynamic properties of hydrocarbons. *Proteins* 11, 281–296 (1991).
46. Kyte, J. & Doolittle, R. F. A simple method for displaying the hydropathic character of a protein. *J. Mol. Biol.* 157, 105–132 (1982).

Acknowledgements

We thank N. Yagi and Y. Katsuya for use of the facilities at SPring-8, Hyogo, Japan. We also thank T. Tomura and S. Yamamoto for technical assistance; H. Toh and T. Hiroike for their help in bioinformatic analyses; and Y. Shimura, H. Nakamura and A. Pähler for discussions and encouragement. This study is partly supported by a grant from the SPring-8 Joint Research Promotion Scheme of the Japan Science and Technology Corporation.

Correspondence and requests for materials should be addressed to K.M. (e-mail: morikawa@beri.co.jp) or H.J. (e-mail: jingami@beri.co.jp). Atomic coordinates have been deposited in the PDB under accession codes 1EWT for free form I, 1EWV for free form II, and 1EWK for the complex form.

Structural views of the ligand-binding cores of a metabotropic glutamate receptor complexed with an antagonist and both glutamate and Gd^{3+}

Daisuke Tsuchiya*, Naoki Kunishima*, Narutoshi Kamiya†, Hisato Jingami‡§, and Kosuke Morikawa*§

Departments of *Structural Biology, †Bioinformatics, and ‡Molecular Biology, Biomolecular Engineering Research Institute, 6-2-3 Furuedai, Suita, Osaka 565-0874, Japan

Communicated by Shigetada Nakanishi, Kyoto University, Kyoto, Japan, December 28, 2001 (received for review December 1, 2001)

Crystal structures of the extracellular ligand-binding region of the metabotropic glutamate receptor, complexed with an antagonist, (S)-(α)-methyl-4-carboxyphenylglycine, and with both glutamate and Gd^{3+} ion, have been determined by x-ray crystallographic analyses. The structure of the complex with the antagonist is similar to that of the unliganded resting dimer. The antagonist wedges the protomer to maintain an inactive open form. The glutamate/Gd^{3+} complex is an exact 2-fold symmetric dimer, where each bi-lobed protomer adopts the closed conformation. The surface of the C-terminal domain contains an acidic patch, whose negative charges are alleviated by the metal cation to stabilize the active dimeric structure. The structural comparison between the active and resting dimers suggests that glutamate binding tends to induce domain closing and a small shift of a helix in the dimer interface. Furthermore, an interprotomer contact including the acidic patch inhibited dimer formation by the two open protomers in the active state. These findings provide a structural basis to describe the link between ligand binding and the dimer interface.

Metabotropic glutamate receptors (mGluRs) are a class of G-protein coupled receptors that possess seven transmembrane regions and couple with a variety of second messenger systems, including the activation of phosphoinositide hydrolysis and the regulation of adenylyl cyclase. To date, eight subtypes are known, which are categorized into three groups according to sequence similarity, location in the nervous system, and responses to agonists/antagonists (1–3). mGluRs exert a number of effects on neural excitability and synaptic transmission at most glutamatergic synapses in the central nervous system, performing crucial roles in changing synaptic efficacy or plasticity.

We have recently reported the crystal structures of the extracellular ligand-binding region of the homodimeric mGluR subtype 1 (m1-LBR) in the complex with glutamate and in the two unliganded forms (4). These structures suggested that the "Active" and "Resting" conformations of m1-LBR are modulated through the dimer interface. The bi-lobed protomer is composed of two domains, LB1 and LB2, and flexibly changes the domain rearrangement to form the "open" or "closed" conformation. Glutamate binding increases the population of the "Active" conformer, designated as "closed–open/A," which adopts the "Active" type of the dimeric interface with each of the "closed" and "open" protomers. The ligand-free state exhibits two different structures, "closed–open/A" and "open–open/R" (the "Resting" dimer with two open protomers). These results suggested that the m1-LBR is in dynamic equilibrium, and that glutamate binding stabilizes both the "Active" dimer and the "closed" protomer.

To obtain clearer insights into the structural basis of receptor activation, we have determined the crystal structure of m1-LBR complexed with an antagonist, (*S*)-(α)-methyl-4-carboxyphenylglycine (*S*-MCPG) (5–7). Furthermore, we have solved the crystal structure in the presence of both the native agonist, L-glutamate, and gadolinium ions, because metal cations, including Gd^{3+}, modulate the signaling of mGluRs (8–11). Here we report the new structural basis of agonism and antagonism, which accounts for the receptor activation mechanism.

Materials and Methods

Structure Determination of the Antagonist-Bound Form. Overproduction and purification of the m1-LBR (residues 33–522) were done as described (12). Crystals of the complex with *S*-MCPG were obtained under the conditions used for the ligand-free form (0.2 M Tris·HCl, pH 8.5/1.9 M ammonium sulfate) (4) with 10 mM *S*-MCPG. The crystals belong to the space group $P4_12_12$, with unit cell dimensions of $a = b = 112.14$ Å and $c = 289.91$ Å. Intensity data were collected with the R-AXIS V image plate detector (Rigaku, Tokyo) at the BL24XU beamline ($\lambda = 0.8360$ Å) of SPring8 (Hyogo, Japan). The data were processed with MOSFLM (13) and were reduced with SCALA in CCP4 (14) with an R_{merge} of 0.086 within 20- to 3.3-Å resolution. Molecular replacement by using AMORE (15) was successful when the probe [Protein Data Bank ID code (PDB) 1EWK] was separated into two domains. Under the noncrystallographic symmetry (NCS) restraint between the two subunits, the structure was refined by the use of CNS (16) to provide final R_{cryst} and R_{free} values of 0.257 and 0.314, respectively (20- to 3.3-Å resolution). Other crystallographic statistics are shown in Table 1.

Structure Determination of the Glutamate/Gd^{3+}-Bound Form. The m1-LBR in complex with the agonist and the gadolinium ion was crystallized under the same conditions used for the glutamate-bound form of m1-LBR (0.2 M Hepes, pH 7.5/20% polyethylene glycol 4000/1 mM L-glutamate) (4), except for the presence of 0.5 mM $GdCl_3$. The crystal data [space group $P3_221$; $a = b = 145.3$ (Å), and $c = 76.75$ (Å)] are different from the previous data, suggesting that the gadolinium ions affect the crystal packing. The absorption edges (1.563 and 1.711 Å), measured at beamline BL40B2 at SPring8, correspond to the L_{II} and L_{III} edges of gadolinium [1.5612 and 1.7094 Å (17)], proving the presence of the element in the crystal. X-ray diffraction images were recorded on a Quantum 4R charge-coupled device detector (Area Detector Systems, Poway, CA) at the same beamline ($\lambda = 1.000$ Å). Because the crystal was too sensitive to find adequate conditions for cryoprotection, the diffraction data had to be collected at 298 K. Consequently, radiation damage was so serious that only partial data could be obtained with one crystal.

Abbreviations: mGluR, metabotropic glutamate receptor; mGluR1, mGluR subtype 1; m1-LBR, ligand-binding region of mGluR1; PDB, Protein Data Bank ID code; NCS, noncrystallographic symmetry; rmsd, rms deviation; *S*-MCPG, (*S*)-(α)-methyl-4-carboxyphenylglycine; *R*-MCPG, (*R*)-(α)-methyl-4-carboxyphenylglycine.

Data deposition: The atomic coordinates have been deposited in the Protein Data Bank, www.rcsb.org [PDB ID codes 1ISS (the S-MCPG-bound form) and 1ISR (the glutamate/Gd^{3+}-bound form].

§To whom reprint requests may be addressed. E-mail: jingami@beri.co.jp or morikawa@beri.co.jp.

The publication costs of this article were defrayed in part by page charge payment. This article must therefore be hereby marked "*advertisement*" in accordance with 18 U.S.C. §1734 solely to indicate this fact.

www.pnas.org/cgi/doi/10.1073/pnas.052708599

Table 1. Data collection and refinement statistics

	S-MCPG complex	Glutamate/Gd^{3+} complex
Data collection		
Wavelength, Å	0.8340	1.0000
Resolution limit, Å	3.3	4.0
R_{merge}	0.086 (0.493*)	0.10 (0.230†)
Completeness, %	97.8 (99.3*)	90.1 (75.6†)
$I/\sigma(I)$	8.5 (1.6*)	6.7 (2.9†)
Multiplicity	4.3 (4.7*)	5.0 (2.8†)
Refinement		
Resolution, Å	20–3.3	12–4.0
Number of reflections	26032	7182
R_{work}	0.257 (0.461‡)	0.237 (0.277§)
R_{free}¶	0.314 (0.445‡)	0.259 (0.332§)
Deviation from ideality		
Bond length, Å	0.009	0.003
Bond angle, °	1.3	0.9

*3.37–3.30 Å.
†4.20–4.00 Å.
‡3.33–3.30 Å.
§4.13–4.00 Å.
¶7% of the diffraction data.

The partial data of four crystals, indexed with MOSFLM (13), were combined and scaled [by using SCALA (14)] to obtain the complete data set, with an R_{merge} of 0.101 within a 20- to 4.0-Å resolution range. The application of AMORE (15) provided a clear solution of the molecular replacement by using the closed conformation of m1-LBR (chain A of PDB 1EWK) as a search model. Refinement by use of CNS (16) provided the converged structure with an R_{cryst} value of 0.237 and an R_{free} value of 0.259 for the 12- to 4.0-Å resolution data. Other crystallographic statistics are shown in Table 1.

Calculation of Interprotomer Nonbonded Energy. Models of the m1-LBR dimer with variable interdomain angles were constructed by using the coordinates of PDB 1EWK. The initial models, consisting of 14,180 atoms, including the ligand (glutamate) and the Mg^{2+} ion, were energy-minimized with PRESTO Ver. 3 (18) to alleviate unreasonable steric collision. The AMBER PARAM96 force field (19) was applied for the potential energy calculation, except for the ligand, for which the partial charge was calculated with MOPAC2000 (Fujitsu, Kawasaki, Japan) by using the AM1 Hamiltonian. The electrostatic interactions (dielectric constant 4.0) were exactly evaluated with no cutoff procedure.

Results and Discussion

Mechanism of Antagonism by *S*-MCPG. The crystal structure of m1-LBR in complex with *S*-MCPG contains two protomers in the asymmetric unit. The two NCS-related protomers, which form a dimeric structure, equivalently bind the antagonist (Fig. 1*B*) and, as a result, are well superimposed, with a rms deviation (rmsd) of 0.38 Å for 453 C_α atoms. The conformation of the protomer is the "open" form, in which the bound *S*-MCPG is accessible to the bulk solvent region. The two open protomers symmetrically dimerize with the "Resting" interface. Thus, this

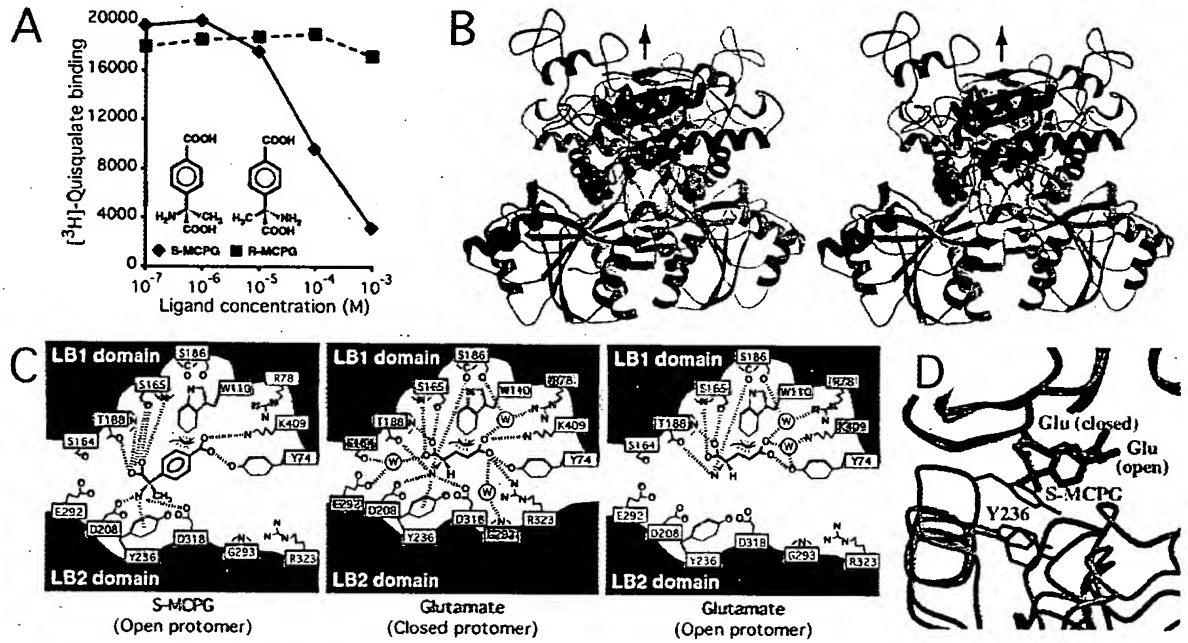

Fig. 1. (*A*) Dose–response curves of *S*-MCPG (filled diamonds) and *R*-MCPG (filled squares) in inhibiting [^{3}H]quisqualate binding to m1-LBR. Each reaction contained 0.75 μg of purified m1-LBR. The binding assay was done as described (12, 20). (*B*) Stereo-pair diagram of m1-LBR complexed with *S*-MCPG, viewed from the perpendicular direction to the dimer interface. The LB1 and LB2 domains are colored blue and red, respectively, except for the B (cyan), C (green), and F (yellow) helices. The two protomers in the dimeric m1-LBR are distinguished by saturated and light colors. The magenta Corey–Pauling–Koltun model represents the bound *S*-MCPG. These protomers are related by an NCS 2-fold axis (black arrow). (*C*) Schematic diagrams of the recognition of *S*-MCPG (*Left*) and glutamate, observed in both the closed (*Center*) and open (*Right*) protomers of the closed-open/A dimer (4). Yellow and green boxes represent residues forming direct and water-mediated interactions, respectively, with the corresponding ligand. The bound water molecule is depicted by the circled "W." The recognition of each ligand is established by polar interactions (broken lines) and van der Waals interactions (with W110). (*D*) Structures of the glutamate-bound form [closed–open/A (4); red for closed, blue for open] superimposed onto the *S*-MCPG complex (green) by their LB1 domains. The side chain of Y236 blocks the *S*-MCPG complex from closing. This figure was generated as if the front protomer (saturated color) in *B* were viewed from the left.

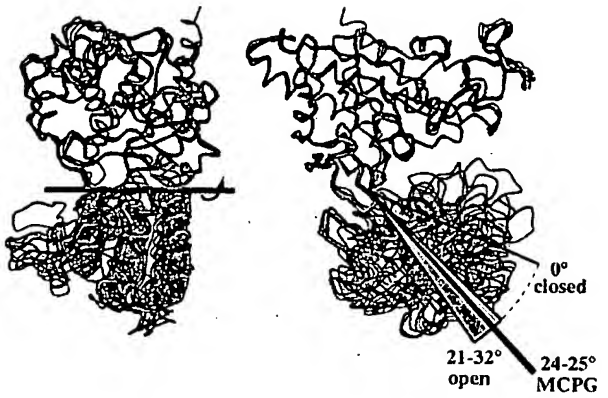

Fig. 2. Two orthogonal views of the six open protomers superimposed on the closed protomer (complexed with glutamate; black) by using the LB1 domains [blue, glutamate-bound form (closed-open/A); magenta, ligand-free form (closed-open/A); red and orange, ligand-free form (open-open/R); yellow and green, *S*-MCPG complex (open-open/R)]. Although the LB1 domains are well superimposed (rmsd 0.44–0.67 Å), the deviations including the LB2 domain increase to 2.9–4.3 Å. However, the application of a simple rotation around the cyan bar significantly reduced the deviation to ≤1.0 Å (Table 2).

Table 2. Superimposition of the m1-LBR protomers

Protomer	rmsd, Å*	Open angle, °†	rmsd after rotation, Å‡
Closed			
Closed–open/A (+glutamate)§	—	0	—
Closed–open/A (ligand-free)§	0.58	0.0	0.58
Closed–closed/A (+glutamate, + Gd^{3+})¶	0.38	0.0	0.38
Open			
Closed–open/A (+glutamate)‖	4.3	32	0.67
Closed–open/A (ligand-free)‖	3.7	26	1.0
Open–open/R (ligand-free)**	2.9	21	0.78
	4.0	29	0.91
Open–open/R (+S-MCPG)**	3.2	24	0.57
	3.4	25	0.73

*C_α atoms are superimposed on the closed protomer of the glutamate-bound closed–open/A structure.
†Rotation angle of the LB2 domain around the axis in Fig. 2.
‡Calculated with the structure after application of the "open angle" rotation.
§The closed protomer is used for the calculation.
¶The two closed protomers are related by crystallographic symmetry.
‖The open protomer is used for the calculation.
**These crystal structures contain a dimer (two protomers) in their asymmetric units.

symmetric dimer is defined as "open–open/R," which was observed in the ligand-free state (4). This antagonist-bound complex strongly supports the previous proposal that the open–open/R structure indeed corresponds to the "Resting" state of the ligand-binding region.

S-MCPG is bound into the interdomain cleft, where glutamate is found in the closed–open/A structure (4). On the side of the LB1 domain, the same residues involved in glutamate recognition (Y74, W110, S165, T188, and K409), except for S186, are used for *S*-MCPG recognition (Fig. 1*C*). The LB2 domain also participates in *S*-MCPG recognition with D208, Y236, and D318 (Fig. 1*C*), which similarly interact with glutamate (4), even in the different protomer conformations: open for the antagonist and closed for the agonist. Notably, these three residues cannot reach glutamate in the open conformation because of the large spacing between the two domains. Similarly, the open conformation separates R323 not only from glutamate but also from *S*-MCPG, whereas this side chain makes a salt bridge with the agonist in the closed protomer. This recognition scheme implies that the role of the antagonist is to wedge the open protomer conformation. In fact, the binding of *S*-MCPG restricts the open angle within a narrow range (24–25°), in contrast to the considerable polymorphism of the other open protomers, where open angles range from 21 to 32° (Fig. 2, Table 2). *S*-MCPG is longer by two carbon atoms than glutamate, and thus the antagonist collides with the LB2 domain, in particular at Y236, when the two domains approach each other (Fig. 1*D*). This structural feature of the open protomer wedged by this ligand may provide hints for the design of new antagonists.

[^{3}H]Quisqualate binding to m1-LBR is displaced by *S*-MCPG (20), whereas its stereoisomer, (*R*)-(α)-methyl-4-carboxyphenylglycine (*R*-MCPG), does not inhibit binding (Fig. 1*A*). *R*-MCPG can be placed on the binding site for *S*-MCPG without any steric collision. However, *R*-MCPG is unable to form the same polar interactions as *S*-MCPG (Fig. 1*C*) because of the different steric configuration of the α amino and α carboxyl groups around the chiral center, the C_α atom. Therefore, *R*-MCPG is unlikely to form a stable complex with the receptor.

4-Carboxyphenylglycine has been used as a lead compound for mGluR antagonist development (21, 22). Its derivative, *S*-MCPG, is a nonselective antagonist for group I and II receptors (5–7), whereas it has little or no activity with group III receptors (6, 22). All of the residues that directly recognize the antagonist are completely conserved among all of the groups, except for Y74. This

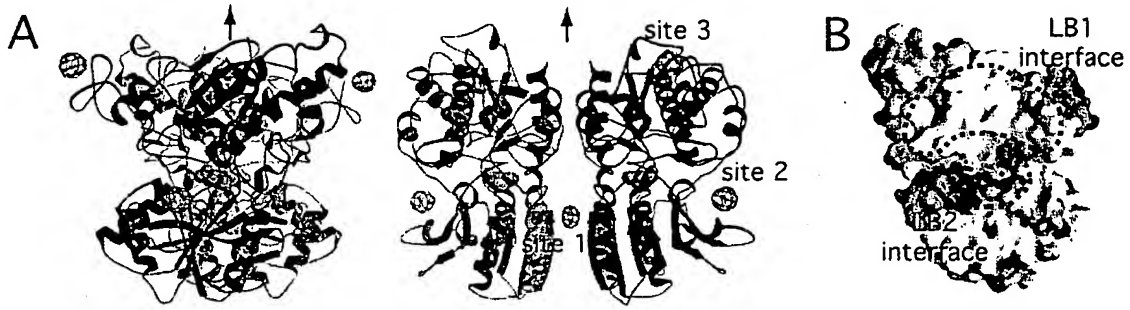

Fig. 3. (*A*) Structure of m1-LBR complexed with glutamate and Gd^{3+} ion, viewed from perpendicular (*Left*) and parallel (*Right*) directions to the dimer interface, with the anomalous difference Fourier map (green cages; contoured at 5σ). The coloring is the same as in Fig. 1*B*. The yellow Corey–Pauling–Koltun model represents the bound glutamate. As the asymmetric unit contains one protomer, its symmetry mate, related by a crystallographic 2-fold axis (black arrows), is drawn by light colors to represent the dimer structure. (*B*) GRASP (28) electrostatic surface representation (negative, red; neutral, white; positive, blue) of the two dimer interfaces, encircled by broken lines.

tyrosine residue is variable among mGluRs (Tyr in group I, Arg in group II, and Lys/Asn/Gln in group III). Therefore, these direct contacts are not sufficient to discriminate the group III receptors from the others. Instead, the discrimination may be accomplished by the other residues, which would not make direct interaction with *S*-MCPG but interact with it through water molecules. Otherwise, the residues specific to the group III receptors may cause steric inhibition of the *S*-MCPG binding.

Role of Gd^{3+} Ion in Receptor Activation. The structure of the m1-LBR protomer complexed with glutamate and the Gd^{3+} ion (Fig. 3*A*) is essentially the same as that of the closed conformation with glutamate (4). The rmsd value was calculated to be 0.38 Å by using the 449 C_α positions. The dimeric structure consists of the two protomers related by a crystallographic 2-fold axis. The dimer interface formed by the LB1 domains (LB1 interface; Fig. 3*B*) is also the same as that observed in the complex with glutamate. According to the conformational notation of the LB1 interface, which determines the R and A conformations (4), this dimer is defined as the A state. The conformation of the complex related by the exact 2-fold symmetry is different from the closed–open/A of the Gd^{3+}-free complex, where the two LB1 domains are related by the pseudo-2-fold symmetry, but the LB2 domains are asymmetric. Thus, the present structure can be defined as "closed–closed/A," which was not observed in the previous study.

An anomalous difference Fourier map clearly revealed three gadolinium sites bound to the protomer (Fig. 3*A*). Site 1 is located on the crystallographic 2-fold axis. Sites 2 and 3 are too distant from any protein atoms to affect interprotomer or interdomain interactions, and therefore neither appears to modulate receptor activation. This notion is in agreement with the fact that the residues interacting with Gd^{3+} at sites 2 or 3 are not conserved among mGluRs. In the vicinity of site 1, a new interprotomer interaction is found between the LB2 domains. This contact site is designated as the LB2 interface (Fig. 3*B*). The LB2 interface is markedly negative because of the cluster of four acidic residues, D191, E233, E238, and D242 (Fig. 4). Among them, E238 and D242 lie close enough to interact with the Gd^{3+} ion, which alleviates the electrostatic repulsion between the two protomers (Fig. 4*A*). Similar interactions of Gd^{3+} with acidic residues were observed in the other crystal structures (23–25). On the other hand, the closed–open/A dimer (4) also involves the LB2–LB2 contact, in the absence of the Gd^{3+} ion (Fig. 4*B*). In addition to the four acidic residues forming the acidic patch, K260 participates in the interprotomer LB2–LB2 contact in the closed–open/A structure. The amino group of K260 in the closed protomer is located at the position similar to the site 1 Gd^{3+} ion to form interprotomer salt bridges with E238 and D242 in the open protomer. The same basic side chain of the open protomer is also salt-bridged to the acidic side chain of D242 of the closed one but not to E238, because of the asymmetry.

These findings suggest a functional role of the Gd^{3+} ion at the LB2 interface. K260 is close enough to interact with the acidic patch, not only in the closed–open/A structure (Fig. 4*B*) but also in the closed–closed/A structure (Fig. 4*A*). Even in the absence of the cation, these two "Active" structures are possible under the environment where water molecules are accessible to the edge of the acidic patch. In fact, the closed–open/A structure without Gd^{3+} is stable enough to be crystallized (4). Once the Gd^{3+} binds at the center of the acidic patches, their repulsion is alleviated more efficiently than by K260 alone. As a result, only the closed–closed/A is selectively stabilized. Notably, the core residues in the interface are highly conserved among the mGluR sequences. In particular, two acidic residues, E233 and E238, are completely conserved among all subtypes. K260 is also invariant, except for subtype 7, with Arg at the same position. D242 is replaced with Glu in the other subtypes. The interactions formed by these conserved residues should be common in the mGluRs.

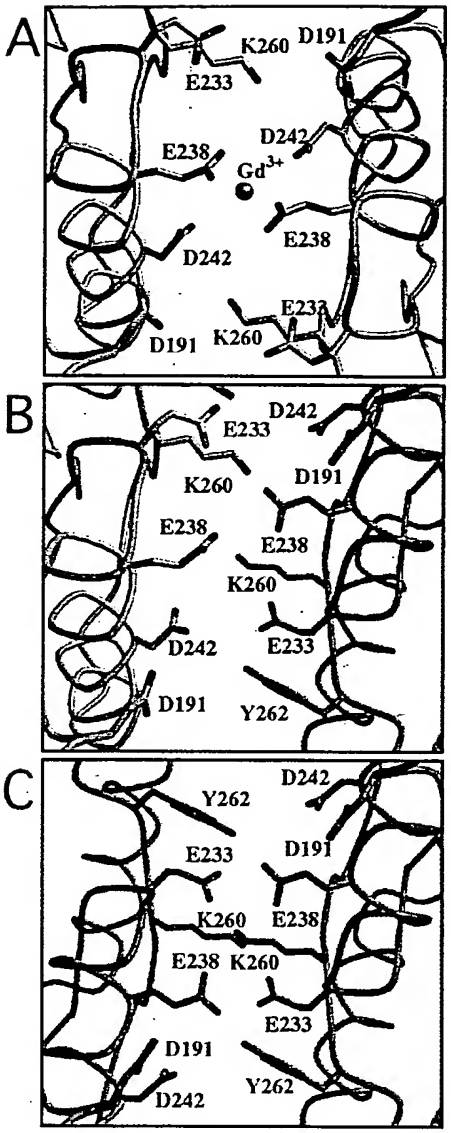

Fig. 4. Local structures of the LB2 interface of the complexes with glutamate and a Gd^{3+} ion in the closed–closed/A conformer (*A*), and with the glutamate in the closed–open/A (*B*). The interface of the hypothetical open–open/A model, of which both open angles are 30°, is shown in *C*. Yellow and green represent the closed and open protomers, respectively. The 2-fold axis of the dimer is directed perpendicularly to the paper through the center of each figure. The silver sphere in *A* denotes the site 1 Gd^{3+} ion.

Extracellular calcium ion at several millimolar concentrations was reported to potentiate phosphoinositide signaling by the receptor (9) and to directly activate it in the oocyte system (8). Recently, it was found that the persistent response by glutamate requires extracellular Ca^{2+} in mGluR1-transfected Chinese hamster ovary cells (10, 11). In this context, the selective stabilization of the closed–closed/A structure is induced not only by Gd^{3+} but also by Ca^{2+}, because these two metals have similar ionic radii (26) and a similar tendency of binding to carboxyl side chains. In the absence of glutamate, the Gd^{3+} ion is insufficient to crystallize the $P3_221$ form, suggesting that the

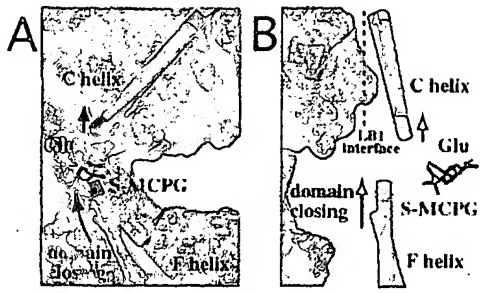

Fig. 5. Structures around the C helix at the LB1 interface. The C and F helices of the *S*-MCPG-bound open protomer (green) and of the glutamate-bound closed protomer (yellow) are drawn with the corresponding ligands (stick models). The blue and red ends of the helices indicate their N and C termini, respectively. The gray surface represents the open protomer forming the dimeric structure of the glutamate-bound closed–open/A. The LB1 interface is approximately parallel to *A*, and its orthogonal view is on *B*. Note that the small upward shift of the C helix is presumably caused by dipole–dipole repulsion between the C and F helices, of which the N termini approach each other on domain closing.

metal plays only a subsidiary role in the stabilization of the "Active" dimer. In fact, the receptor is activated by glutamate without extracellular metal cation. Consequently, the cation is unnecessary for the closed–open/A structure (4) and may not be absolutely essential even for the closed–closed/A structure because of the presence of K260. Therefore, it appears reasonable that prolonged receptor activation, but not its ignition, explains the physiological role of the metal ion (11). However, another interpretation is also possible: that the metal itself exhibits an agonistic function (8) by transient formation of the closed–closed/A structure.

Conformational Change of the LB1 Domain Induced by Ligand Binding. In the previous report, we proposed that receptor activation is modulated by the relocation of the LB1 interface (4). To explore how ligand binding affects the conversion between the A and R conformers, we compared the two crystal structures between the *S*-MCPG complex (open–open/R) and the glutamate one (closed–open/A). Neither the agonist nor the antagonist induces any global conformational change within the LB1 domain (rmsd 0.49 Å for 279 C_α atoms). Instead, a local conformational change was observed at the B helix (residues 112–123), in which the C terminus is extended by one turn (residues 124–127) in the antagonist-bound complex to expand the LB1 interface slightly (4). In addition, the C helix is apparently pushed away by ≈0.5 Å from the LB2 domain when glutamate is trapped in the closed protomer (Fig. 5), whereas the B helix exhibits a smaller deviation (≈0.2 Å). Even such small alteration in the relative positions of these two helices could modulate the LB1–LB1 contacts in some degree. It is intriguing that the N termini of almost all of the α-helices are directed onto the domain crevice, where glutamate is bound to alleviate the strong dipole–dipole repulsion, particularly between the C and F helices (residues 235–251) (Fig. 5). Although the movement of the C helix is nearly comparable to the average error of structure determination [0.5 Å; estimated from the Luzzati plot (27)] and the rmsd of the superimposition, the agonist may be able to induce the relocation of the LB1 interface through such a subtle perturbation, in coordination with the open–closed movement of the protomers.

Functional Role of the Dimer Interface in Dynamic Equilibrium. In addition to the conformational link between ligand binding and the relocation of the LB1 interface, other factors may be required to fully account for the activation mechanism, where the agonist simply increases the relative population of the

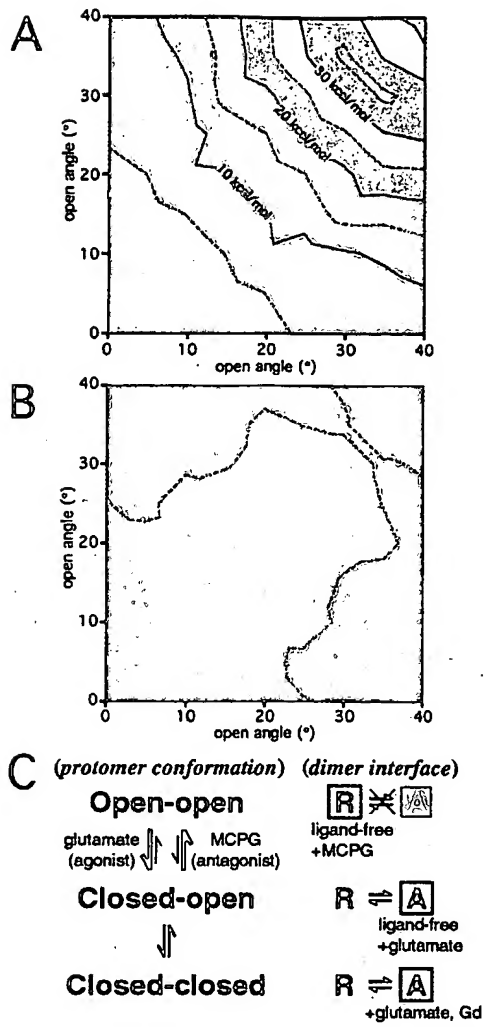

Fig. 6. Computed potential energy for the interprotomer nonbonded interactions. Relative electrostatic (*A*) and van der Waals (*B*) energies were plotted as a function of the open angles for the two protomers (horizontal and vertical axes). The potential energy difference is contoured at every 5 kcal/mol. The conformations with open angles (5°, 5° and 0°, 0°) exhibit the lowest energies for the electrostatic and van der Waals interactions, respectively. (*C*) An equilibrium model proposed for m1-LBR. The open boxes indicate the states for which structures have been determined by x-ray crystallographic analyses. The shaded A conformer in the open–open combination forms an energetically unfavorable structure, because of the electrostatic barrier of the LB2 interface.

"Active" conformer through dynamic equilibrium (4). The crystal structure of the complex with glutamate and Gd^{3+} revealed another dimer interface between the LB2 domains. Interprotomer interactions at the LB2 interface significantly differ between the closed–closed (Fig. 4*A*) and closed–open (Fig. 4*B*) dimers, when the LB1–LB1 contact is the A state. Therefore, the LB2 interface is capable of sensing the protomer conformation, which seems to be modulated by ligand binding.

To elucidate the functional role of the LB2 interface, we built a hypothetical dimeric model in which the open angles of the two protomers are varied independently. To investigate the effects of the open angles on the dimer formation, the interprotomer nonbonded interaction energy was theoretically computed. Nine protomer models with various open angles (0–40° with 5° intervals)

were constructed by using the structure of the closed protomer in the closed–open/A state (PDB 1EWK, corresponding to 0°). Larger open angles caused steric collisions between the two regions, ranging through residues 475–478 and 501–503, respectively. These protomers were combined to build 45 hypothetical A-conformer dimers by using the glutamate-bound closed–open/A structure (PDB 1EWK). The potential energies of the electrostatic (Fig. 6*A*) and van der Waals (Fig. 6*B*) interactions formed between the two protomers are shown in Fig. 6. The open–open/A state extensively exhibits higher electrostatic energy, by ≈30 kcal/mol, than the closed–closed/A and closed–open/A states, although solvation energy should be also taken into consideration. The hypothetical open–open/A model (Fig. 4*C*) suggests that the interprotomer LB2–LB2 contact, involving E233, E238, and K260, generates strong electrostatic repulsion. On the other hand, the interprotomer van der Waals energy is relatively constant. Actually, the invariable LB1–LB1 contact mainly contributes to the interprotomer van der Waals interaction. Therefore, the open–open/A state yields an electrostatically unfavorable dimer interface, which could exclude only the open–open/A state from the components in the dynamic equilibrium of m1-LBR.

This exclusion of the open–open/A state suggests another activation mechanism, where the extracellular region of mGluR adopts various conformations in the dynamic equilibrium (Fig. 6*C*). On agonist binding to mGluR, the population of the open–open dimer decreases, because the agonist induces domain closure. Because of the exclusion of the open–open/A structure, only the R conformer is allowed in the open–open combination. Under these conditions, glutamate binding decreases the open–open/R population and thereby increases the relative population of A conformers in the equilibrium of the five components. On the other hand, *S*-MCPG, as an antagonist, fixes the open protomers so that the dimeric receptor is forced into the open–open/R state alone. Thus, the LB2 interface appears to play a regulatory role in eliminating the open–open/A state, whereas the LB1 interface contributes to dimerizing the two protomers and determining the receptor activation state. This receptor may be modulated by the equilibrium shift, which is directed by the ligand (agonist or antagonist) and by the structural changes on the LB1 interface, where the structures of the two helices are supposed to change on ligand binding.

We are grateful to Dr. S. Nakanishi (Kyoto University) for critical reading of the manuscript and discussions. We also thank Drs. Y. Tsuji and Y. Shimada (Biomolecular Engineering Research Institute) for the m1-LBR preparation and the MCPG-binding experiment, Drs. Y. Katsuya (SPring8 Service), K. Miura, and N. Yagi (Japan Synchrotron Radiation Research Institute) for assistance with synchrotron x-ray experiments, and Dr. D. Sunter (Tocris Cookson, Ltd.) for *R*-MCPG. We are grateful to Drs. Y. Shimura and H. Toh (Biomolecular Engineering Research Institute) for discussions.

1. Masu, M., Tanabe, Y., Tsuchida, K., Shigemoto, R. & Nakanishi, S. (1991) *Nature (London)* **349**, 760–765.
2. Nakanishi, S. & Masu, M. (1994) *Annu. Rev. Biophys. Biomol. Struct.* **23**, 319–348.
3. Hollmann, M. & Heinemann, S. (1994) *Annu. Rev. Neurosci.* **17**, 31–108.
4. Kunishima, N., Shimada, Y., Tsuji, Y., Sato, T., Yamamoto, M., Kumasaka, T., Nakanishi, S., Jingami, H. & Morikawa, K. (2000) *Nature (London)* **407**, 971–977.
5. Jane, D. E., Jones, P. L., Pook, P. C.-K., Salt, T. E., Sunter, D. C. & Watkins, J. C. (1993) *Neurophamacology* **32**, 725–727.
6. Hayashi, Y., Sekiyama, N., Nakanishi, S., Jane, D. E., Sunter, D. C., Birse, E. F., Udvarhelyi, P. M. & Watkins, J. C. (1994) *J. Neurosci.* **14**, 3370–3377.
7. Sekiyama, N., Hayashi, Y., Nakanishi, S., Jane, D. E., Tse, H.-W., Birse, E. F. & Watkins, J. C. (1996) *Br. J. Pharmacol.* **117**, 1493–1503.
8. Kubo, Y., Miyashita, T. & Murata, Y. (1998) *Science* **279**, 1722–1725.
9. Saunders, R., Nahorski, S. R. & Challiss, R. A. (1998) *Neuropharmacology* **37**, 273–276.
10. Miyashita, T. & Kubo, Y. (2000) *Recept. Channels* **7**, 25–40.
11. Nash, M. S., Saunders, R., Young, K. W., Challiss, R. A. & Nahorski, S. R. (2001) *J. Biol. Chem.* **276**, 19286–19293.
12. Tsuji, Y., Shimada, Y., Takeshita, T., Kajimura, N., Nomura, S., Sekiyama, N., Otomo, J., Usukura, J., Nakanishi, S. & Jingami, H. (2000) *J. Biol. Chem.* **275**, 28144–28151.
13. Leslie, A. (1991) in *Crystal Computing V*, eds. Moras, D., Podjarny, A. D. & Thierry, J. C. (Oxford Univ. Press, Oxford), pp. 27–38.
14. Collaborative Computational Project Number 4 (1994) *Acta Crystallogr. D* **50**, 760–763.
15. Navaza, J. (1994) *Acta Crystallogr. A* **50**, 157–163.
16. Brünger, A. T., Adams, P. D., Clore, G. M., DeLano, W. L., Gros, P., Grosse-Kunstleve, R. W., Jiang, J. S., Kuszewski, J., Nilges, M., Pannu, N. S., *et al.* (1998) *Acta Crystallogr. D* **54**, 905–921.
17. Koch, B., MacGillavry, C. H., Milledge, H. J., Koopmans, K., Rieck, G. D. & Bacon, G. E. (1985) in *International Tables for X-Ray Crystallography*, eds. MacGillavry, C. H. & Rieck, G. D. (Reidel, Dordrecht, The Netherlands), Vol. III, pp. 157–200.
18. Morikami, K., Nakai, T., Kidera, A., Saito, M. & Nakamura, H. (1992) *Comput. Chem.* **16**, 243–248.
19. Kollman, P. A., Dixon, R. W., Cornell, W. D., Chipot, C. & Pohorille, A. (1997) in *Computer Simulations of Biological Systems*, ed. van Gunsteren, W. F. (ESCOM, Leiden, The Netherlands).
20. Okamoto, T., Sekiyama, N., Otsu, M., Shimada, Y., Sato, A., Nakanishi, S. & Jingami, H. (1998) *J. Biol. Chem.* **273**, 13089–13906.
21. Watkins, J. & Collingridge, G. (1994) *Trends Pharmacol. Sci.* **15**, 333–342.
22. Schoepp, D. D., Jane, D. E. & Monn, J. A. (1999) *Neuropharmacology* **38**, 1431–1476.
23. Gabelli, S. B., Bianchet, M. A., Bessman, M. J. & Amzel, L. M. (2001) *Nat. Struct. Biol.* **8**, 467–472.
24. Bone, R., Springer, J. P. & Atack, J. R. (1992) *Proc. Natl. Acad. Sci. USA* **89**, 10031–10035.
25. Gaudet, R., Bohm, A. & Sigler, P. B. (1996) *Cell* **87**, 577–588.
26. Lide, D. R., ed. (1994) *CRC Handbook of Chemistry and Physics* (CRC, Boca Raton, FL).
27. Luzzati, P. V. (1952) *Acta Crystallogr.* **5**, 802–810.
28. Nicholls, A. & Honig, B. J. (1991) *J. Comput. Chem.* **12**, 435–445.

THE JOURNAL OF BIOLOGICAL CHEMISTRY

Vol. 279, No. 34, Issue of August 20, pp. 35526–35534, 2004
Printed in U.S.A.

Negative Cooperativity of Glutamate Binding in the Dimeric Metabotropic Glutamate Receptor Subtype 1*

Received for publication, April 30, 2004, and in revised form, June 15, 2004
Published, JBC Papers in Press, June 15, 2004, DOI 10.1074/jbc.M404831200

Yoshikazu Suzuki‡, Eiko Moriyoshi‡, Daisuke Tsuchiya§, and Hisato Jingami‡¶

From the Departments of ‡Molecular Biology and §Structural Biology, Biomolecular Engineering Research Institute, 6-2-3 Furuedai, Suita, Osaka 565-0874, Japan

Metabotropic glutamate receptor (mGluR) subtype 1 is a Class III G-protein-coupled receptor that is mainly expressed on the post-synaptic membrane of neuronal cells. The receptor has a large N-terminal extracellular ligand binding domain that forms a homodimer, however, the intersubunit communication of ligand binding in the dimer remains unknown. Here, using the intrinsic tryptophan fluorescence change as a probe for ligand binding events, we examined whether allosteric properties exist in the dimeric ligand binding domain of the receptor. The indole ring of the tryptophan 110, which resides on the upper surface of the ligand binding pocket, sensed the ligand binding events. From saturation binding curves, we have determined the apparent dissociation constants ($K_{0.5}$) of representative agonists and antagonists for this receptor (3.8, 0.46, 40, and 0.89 μM for glutamate, quisqualate, (*S*)-α-methyl-4-carboxyphenylglycine ((*S*)-MCPG), and (+)-2-methyl-4-carboxyphenylglycine (LY367385), respectively). Calcium ions functioned as a positive modulator for agonist but not for antagonist binding ($K_{0.5}$ values were 1.3, 0.21, 59, and 1.2 μM for glutamate, quisqualate, (*S*)-MCPG, and LY367385, respectively, in the presence of 2.0 mM calcium ion). Moreover, a Hill analysis of the saturation binding curves revealed the strong negative cooperativity of glutamate binding between each subunit in the dimeric ligand binding domain. As far as we know, this is the first direct evidence that the dimeric ligand binding domain of mGluR exhibits intersubunit cooperativity of ligand binding.

Glutamate is a major neurotransmitter in the excitatory synapses of the central nervous system, and two types of glutamate receptors are expressed in nerve cells: one is an ionotropic glutamate receptor, and the other is a metabotropic glutamate receptor (mGluR).[1] The former is a glutamate-gated ion channel, which induces a synaptic potential upon glutamate binding, whereas the latter is a G-protein-coupled receptor (GPCR), which induces various cellular responses to glutamate stimulation, *e.g.* inositol triphosphate production and the subsequent elevation of intracellular calcium, or a cytoplasmic cyclic AMP concentration change caused by the modulation of adenylyl cyclase activity. Because these cellular responses modulate the degree of synaptic neurotransmission, mGluRs are believed to be involved in higher order neuronal activities such as memory, learning, and so on (1, 2).

The mGluR belongs to the Class III GPCR and forms a subfamily consisting of eight subtypes (mGluR1–8) (3–6). One outstanding feature of the receptor is the large extracellular ligand binding domain (LBD), which is characteristic of the Class III GPCRs. The mGluR1 LBD consists of ~520 amino acids and forms a clamshell-like bilobate domain (LB1 and LB2) (7, 8). Our previous biochemical and crystallographic studies demonstrated that the LBD forms a homodimer by not only an intersubunit disulfide bond but also hydrophobic interactions (7–10). In the crystal structures, one protomer of the dimeric LBD adopts two different conformations: an open conformation and a closed conformation. A symmetric structure with both protomers in the open conformation is observed in the absence of glutamate, whereas the structure of the glutamate binding state is asymmetric, because one protomer adopts the closed conformation and the other adopts the open conformation. Interestingly, even in the absence of glutamate, the asymmetric open-closed conformation is observed, implying that the open and closed conformations of the protomer are in equilibrium in an aqueous solution without ligands. Glutamate binding promotes the closing motion of the ligand binding pocket, so the closed conformation should be stabilized. Thus, the glutamate-bound open conformation observed in the crystal structure is a fascinating puzzle. One attractive explanation for this is an allosteric property in the dimeric LBD: the closed conformation in one protomer would negatively affect the binding mode of the other protomer. However, such an allosteric effect on ligand binding has not been demonstrated yet for this receptor.

Some allosteric properties have been previously reported for several receptors. Extensive biochemical and crystallographic studies have been performed on the bacterial dimeric aspartate receptor, and the mechanism of negative cooperativity on aspartate binding has been elucidated on the basis of the structure (11–14). Allosteric properties are also inferred in several GPCRs (15, 16), however, in these cases, the observed cooperativity seems to result from oligomerization of receptors on the membrane surface. Thus, the allosteric properties in terms of subunit-subunit communication are more obscure in the GPCRs than those in the bacterial aspartate receptor. Recently, dimer formation by GPCRs has been detected, and ligand selectivity appears to be broader than previously expected (17–20). It was also reported that, in the heterodimeric γ-aminobutyric acid type B receptor, the GB2 subunit and its association with the GB1 subunit control the agonist affinity in GB1 subunit (21). Therefore, the cooperativity in dimeric GPCRs has become a current issue. In this context, our mGluR

* This study was supported by a grant from the New Energy and Industrial Technology Development Organization (NEDO). The costs of publication of this article were defrayed in part by the payment of page charges. This article must therefore be hereby marked "*advertisement*" in accordance with 18 U.S.C. Section 1734 solely to indicate this fact.

¶ To whom correspondence should be addressed. Tel.: 81-6-6872-8214; Fax: 81-6-6872-8210; E-mail: jingami@beri.or.jp.

[1] The abbreviations used are: mGluR, metabotropic glutamate receptor; mGluR1, mGluR subtype 1; GPCR, G-protein-coupled receptor; LBD, ligand binding domain; MCPG, α-methyl-4-carboxyphenylglycine; LY367385, (+)-2-methyl-4-carboxyphenylglycine; PEG, polyethylene glycol.

system provides a unique opportunity to decipher the cooperativity in the ligand binding event of Class III GPCR using a purified pre-formed dimer.

To investigate whether allostery functions in ligand binding, it is essential to analyze a saturation ligand binding curve with a wide range of ligand concentrations from sub-nanomolar to millimolar. ^{3}H-Labeled quisqualate, which is an agonist specific for mGluR1 and -5, is widely used in the ligand binding assay. However, this conventional assay cannot yield a saturation binding curve because of the upper limit of the applicable ligand concentration.

Because the fluorescence emitted from tryptophan is sensitive to the environment surrounding the indole group, the intrinsic tryptophan fluorescence can be a good probe to sense ligand binding events (22–25). In the present study, we found that the fluorescence spectrum of the intrinsic tryptophans of purified mGluR1 LBD changed upon ligand binding. The system led us to obtain saturation binding curves by titration of the tryptophan fluorescence with glutamate, a native ligand, and other non-native ligands, such as quisqualate, (*S*)-α-methyl-4-carboxyphenylglycine ((*S*)-MCPG), and (+)-2-methyl-4-carboxyphenylglycine (LY367385). These binding curves allowed us to determine the apparent binding constants of these ligands and to demonstrate the positive effect of calcium ions on agonist binding. Furthermore, Hill analyses of the titration curves revealed that negative cooperativity of glutamate binding exists between each protomer of the dimeric mGluR1 LBD.

EXPERIMENTAL PROCEDURES

Materials—L-Quisqualate, (*S*)-MCPG, and LY367385 were purchased from Tocris (UK). (*R*)-MCPG was a gift from Dr. D. Shunter (Tocris). L-Glutamate was purchased from Nacalai Tesque (Japan). Oligonucleotide primers were obtained from Proligo (Japan). All other reagents used in the present study were of molecular or analytical grade.

Construction of an Expression Vector for the FLAG-tagged LBD and Its Mutant—To obtain a C-terminal FLAG-tagged mGluR1 LBD, we performed PCR with pmGluR104 (9) as the template. The forward primer for the PCR was designed at the N terminus of the LBD with a NotI site. The reverse primer was designed at the C terminus of the LBD (at the 1566th thymine in the mGluR1 cDNA) with the DNA sequence for the FLAG epitope (DYKDDDDK) and a stop codon followed by an XbaI site. After verification by DNA sequencing, the PCR product was cloned into the pFastBac DUAL vector (Invitrogen) using the NotI and XbaI sites. The I120A and T188A point mutations were introduced into the FLAG-tagged LBD gene by replacing the NotI/PshAI region of the wild type with the same fragment containing the mutation, which was excised from the plasmid previously used in the mutation experiments (26). The W110V mutation was introduced by site-directed mutagenesis using the QuikChange site-directed mutagenesis kit (Stratagene), with pmGluR103 (9) as the template. After sequence verification, the NotI/PshAI fragment of this mutant was exchanged for that of the wild type on the pFastBac DUAL vector.

Production of Baculoviruses for Protein Expression—Baculoviruses for protein expression were obtained by following the protocol of the Bac-To-Bac baculovirus expression system (Invitrogen). Briefly, the vector DNA was transformed into DH10Bac *Escherichia coli* cells (Invitrogen). Then, the recombinant bacmid DNA purified from the DH10Bac cells was transfected into Sf9 insect cells, using the Cellfectin reagent (Invitrogen). After an incubation for 72 h at 27 °C, the viruses were harvested from the cell culture medium. Then, the recombinant viruses were amplified by re-infecting Sf9 cells to enhance the viral titer. Finally, we checked the viral titer by a plaque formation assay using an immobilized monolayer culture of Sf9 cells.

Protein Expression and Purification—The wild-type and mutant FLAG-tagged LBD proteins were expressed by inoculating the baculoviruses into HighFive cells as previously described (9, 10). Purification of the protein was done by taking advantage of the FLAG tag. The cell culture medium (~500 ml) into which the target protein was sufficiently secreted was collected 4–5 days after the inoculation. After the addition of protease inhibitors (10 μg/ml, 2 μg/ml, and 0.1 mM for leupeptin, pepstatin, and phenylmethylsulfonyl fluoride, respectively), the cells were pelleted by centrifugation at 6,700 × *g* for 15 min at 4 °C. Then, the supernatant was directly applied to ~1 ml of anti-FLAG M2-agarose (Sigma) packed in a disposable column (Bio-Rad). After the column was washed with a low salt buffer containing 10 mM Tris-HCl, pH 7.5, and 20 mM NaCl, the proteins bound to the beads were eluted by a high salt buffer containing the FLAG peptide at a concentration of 150 μg/ml, dissolved in 10 mM HEPES, pH 7.4, and 300 mM NaCl. The eluted fractions were collected, and the protein was concentrated and buffer-exchanged to the assay buffer (20 mM HEPES, pH 7.4, and 50 mM NaCl) using an Ultra-free centrifugation filter unit (Millipore). The protein concentration was determined by the absorbance at 280 nm with a molar extinction coefficient of 126,500 $M^{-1}cm^{-1}$ as a dimer, which was calculated from the number of tryptophans, tyrosines, and cystines in the protein (27). The molecular weight of the FLAG-tagged protein was 119,800 as calculated from the amino acid sequence, including the C-terminal FLAG tag.

Purification of the wild-type LBD of mGluR1 (non-tagged) was done as previously described by using an immunoaffinity column conjugated with monoclonal antibodies (mG1Na-1) (9). The molecular weight of the wild-type LBD was estimated to be 117,800 from the amino acid sequence.

Steady-state Fluorescence Measurement—Steady-state tryptophan fluorescence was measured by an F-4500 spectrofluorometer (Hitachi, Japan) with an excitation wavelength of 290 nm at 20 °C using a stirring cuvette. Protein concentration was 0.67 μM as the dimer. Measurements were performed in a buffer composed of 20 mM HEPES, pH 7.4, and 50 mM NaCl with or without 2.0 mM $CaCl_2$. Emission spectra from 300 to 400 nm were recorded. For the titration experiments, small aliquots of ligand (0.1–1.0% of total volume) were sequentially added to the cuvette, and the fluorescence intensity at 350 nm was recorded. Volume changes in the titration experiments were corrected before analyzing the data. To obtain the titration curves, we also used the peak values of the fluorescence spectra instead of the values at 350 nm, because the peak shift of the fluorescence spectrum would affect the calculated values of the Hill coefficients. Both calculations yielded similar Hill coefficient values, and, hence, in this report we used the values calculated from the fluorescence intensity at 350 nm.

Transient Kinetics Measurement—Transient kinetics of the intrinsic tryptophan fluorescence change were measured with an SX18 stopped-flow spectrophotometer (Applied Photophysics, UK) at 20 °C. The excitation wavelength was 290 nm, and the emission was monitored with a 335-nm longpass optical filter. The protein and ligand were dissolved in a buffer consisting of 20 mM HEPES, pH 7.4, and 50 mM NaCl. Measurements were done with a fixed protein concentration of 0.84 μM (value after mixing).

Ligand Binding Assay—The ^{3}H-labeled ligand binding assay was performed using the polyethylene glycol (PEG) precipitation method (10) as previously described with minor modifications. Briefly, 20 nM ^{3}H-labeled quisqualate or glutamate (Amersham Biosciences) and the protein solution (1 μg of protein) were mixed in 150 μl of binding buffer composed of 40 mM HEPES, pH 7.4, and 2.5 mM $CaCl_2$ at 4 °C for 1 h. Then, 6-kDa PEG was added to the sample to a final concentration of 15% with 3 mg/ml of γ-globulin. After vortexing and centrifugation, the precipitated material was washed twice with 1 ml of the binding buffer containing 8% of 6-kDa PEG, and then it was dissolved in 1 ml of water. After the addition of 14 ml of Clearsol II (Nacalai Tesque), the radioactivity was measured using a scintillation counter.

Data Analysis of the Titration Experiments—Titration curves for glutamate and quisqualate binding were made by plotting the values of $(F - F_0)/\Delta F_{max}$ against the ligand concentrations, where F and F_0 are the fluorescence intensities in the presence and absence of ligand, respectively, and ΔF_{max} is the maximum value of the fluorescence change in the titration experiment. For the titration curves of (*S*)-MCPG and LY367385 binding, the values of $(F_0 - F)/\Delta F_{max}$ were used because the intrinsic tryptophan fluorescence decreased upon the addition of these antagonists. The titration curves were fitted to the following equation by the KaleidaGraph software (Synergy), $\Delta F/\Delta F_{max} = S^{n_H}/(K_{app} + S^{n_H})$, where ΔF equals $F - F_0$ or $F_0 - F$, S is the concentration of the ligand, K_{app} is the apparent dissociation constant, and n_H is the Hill coefficient. Hill coefficients were also calculated from the Hill plot, which yielded values similar to those derived from the curve fitting. With respect to K_{app}, we also obtained similar values from the half-maximal value of the titration curves. This value is denoted as $K_{0.5}$ in the text, and we used it to estimate the affinity of the ligand in this report.

RESULTS

To elucidate intersubunit allostery in the dimeric ligand binding domain of mGluR1, we worked out a plan to utilize the

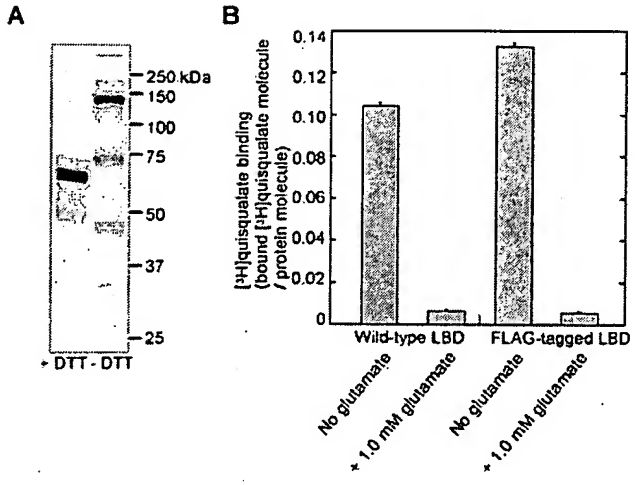

FIG. 1. **Purification and ligand binding activity of the FLAG-tagged mGluR1 LBD.** *A*, silver-stained polyacrylamide gel of the FLAG-tagged mGluR1 LBD, purified with the anti-FLAG M2-agarose gel. Samples were run in the presence (*left*, *+DTT*) and absence (*right*, *−DTT*) of 20 mM DTT on a 9% SDS-PAGE gel. The interprotomer disulfide bond was formed under the non-reduced condition (*−DTT*), resulting in an upward shift of the target band. *B*, ligand binding ability of the FLAG-tagged LBD. The amount of the bound [^{3}H]quisqualate in equilibrium with 20 nM [^{3}H]quisqualate was measured in the presence and absence of 1.0 mM non-labeled glutamate. The difference between the two *bars* represents the specific binding of [^{3}H]quisqualate. Each binding experiment was performed in triplicate, and each *bar* is shown as mean ± S.D.

intrinsic tryptophan fluorescence signal to detect a ligand binding event. For the first step, we constructed and purified the FLAG-tagged LBD of mGluR1 to test whether the intrinsic tryptophan fluorescence changes upon ligand binding.

Purification of the FLAG-tagged Ligand Binding Domain—Because the protein from the anti-FLAG-antibody-conjugated agarose gel was eluted with the FLAG peptide at a neutral pH instead of with an acidic or alkaline buffer, the protein damage was minimized. As analyzed by SDS-PAGE followed by silver staining, the purified FLAG-tagged LBD was observed as almost a single band (Fig. 1*A*). It was previously reported that under the non-reduced conditions the two protomers of the mGluR1 LBD are cross-linked to form a dimer through an interprotomer disulfide bond even under the denaturing conditions on an SDS-polyacrylamide gel (9, 10). Like the non-tagged wild-type LBD, the band of the FLAG-tagged LBD under the reduced conditions (Fig. 1*A*, *+DTT*) was shifted to a position corresponding to twice the molecular weight under the non-reduced conditions (Fig. 1*A*, *−DTT*), indicating that the FLAG-tagged protein maintained the ability to form an interprotomer disulfide bond as demonstrated for the non-tagged LBD (9).

Next, we investigated the ligand binding ability of the FLAG-tagged LBD using a ^{3}H-labeled quisqualate ([^{3}H]quisqualate) by the previously described PEG-precipitation method (10). The final concentration of [^{3}H]quisqualate was 20 nM. As shown in Fig. 1*B*, the FLAG-tagged LBD bound the [^{3}H]quisqualate at the same level as that of the non-tagged LBD. This indicates that the additional eight amino acids at the C terminus of the protein do not influence the ligand binding capacity. From these data, we concluded that the FLAG tag at the C terminus did not perturb the activities of the protein, and therefore, we utilized the FLAG-tagged LBD for the following experiments described below.

Intrinsic Tryptophan Fluorescence Changes of the FLAG-tagged LBD Induced by Ligand Binding—We examined whether the intrinsic tryptophan fluorescence changed upon

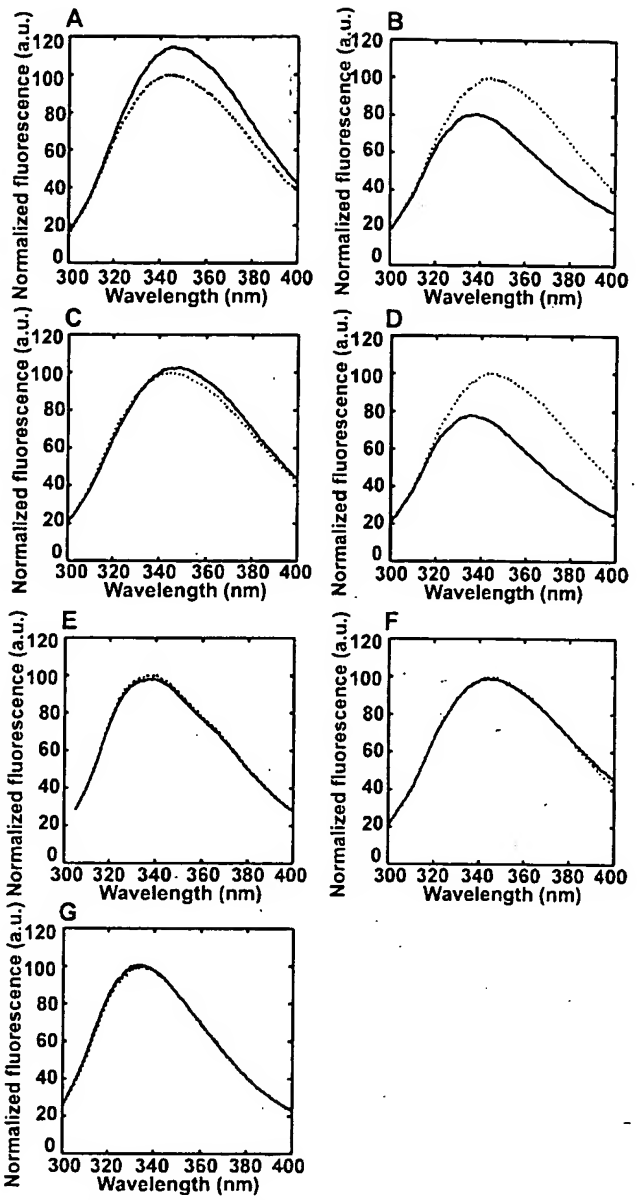

FIG. 2. **Intrinsic tryptophan fluorescence spectra of wild-type and mutant FLAG-tagged LBDs.** Steady-state fluorescence spectra of intrinsic tryptophan were measured by a fluorophotometer. The excitation wavelength was 290 nm. *A*, fluorescence spectra of wild-type FLAG-tagged LBD with and without 1.0 mM glutamate. *B*, fluorescence spectra of wild-type FLAG-tagged LBD with and without 0.1 mM (*S*)-MCPG. *C*, fluorescence spectra of wild type FLAG-tagged LBD with and without 0.1 mM quisqualate. *D*, fluorescence spectra of wild-type FLAG-tagged LBD with and without 0.1 mM LY367385. *E*, fluorescence spectra of T188A FLAG-tagged LBD with and without 1.0 mM glutamate. *F*, fluorescence spectra of wild-type FLAG-tagged LBD with and without 0.1 mM (*R*)-MCPG. *G*, fluorescence spectra of W110V FLAG-tagged LBD with and without 1.0 mM glutamate. In all spectra, the *solid* and *dotted lines* show the spectra with and without the denoted ligand, respectively. Conditions were 20 mM HEPES, pH 7.4, and 50 mM NaCl at 20 °C. The protein concentration was 0.67 μM.

the addition of ligand. In the absence of ligand, the intrinsic tryptophans of the FLAG-tagged LBD exhibited an emission spectrum with a peak at ~345 nm when excited at 290 nm (Fig. 2*A*, *dotted line*). Upon the addition of excess glutamate (1.0 mM final concentration), a native agonist for mGluR, the fluorescence spectrum changed in a manner such that the fluorescence intensity was enhanced by about 18% and the fluorescence maximum was slightly shifted by ~1 nm toward a longer wave-

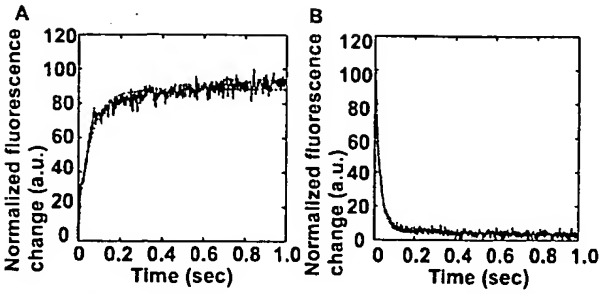

FIG. 3. **Transient kinetic measurements of glutamate and (*S*)-MCPG binding to the FLAG-tagged LBD.** Binding rate constants of glutamate and (*S*)-MCPG were measured with a stopped-flow apparatus in 20 mM HEPES, pH 7.4, and 50 mM NaCl. The protein concentration was 0.84 μM (value after mixing). *A*, transient tryptophan fluorescence change upon mixing with excess glutamate (0.5 mM after mixing). The *dotted line* shows a single exponential fitting curve. From the fitting curve, the observed rate constant was estimated to be 22.2 s^{-1}. *B*, transient tryptophan fluorescence change upon mixing with excess (*S*)-MCPG (0.5 mM after mixing). The *dotted line* shows a single exponential fitting curve. From the fitting curve, the observed rate constant was estimated to be 38.6 s^{-1}.

length (red shift). Upon the addition of excess quisqualate (100 μM at final concentration), a non-native strong agonist for group I mGluRs, the emission spectrum was enhanced, but amplitude of the spectral change was less than that observed for glutamate addition (Fig. 2*C*). This result probably reflects some environmental differences between the glutamate and quisqualate binding states around the tryptophans that contribute toward sensing the ligand binding. As a control for these observations, we measured the emission spectrum of the T188A mutant. It has been demonstrated that this mutation dramatically reduced the binding affinity of agonists and that no cellular responses were detected in HEK293 cells expressing the full-length mGluR1 carrying the same mutation (26). As shown in Fig. 2*E*, the emission spectrum of the mutant did not exhibit any noticeable change upon the addition of excess glutamate. Although we also examined the spectrum upon the addition of quisqualate, no effects were observed as well (data not shown). Therefore, the enhanced emission spectra observed for the wild-type FLAG-tagged LBD resulted from agonist binding to the protein.

Fig. 2*B* shows fluorescence spectra in the presence and absence of (*S*)-MCPG (100 μM final concentration), an antagonist for mGluR1. In contrast to the results with the agonists, the fluorescence intensity of the intrinsic tryptophans decreased and the fluorescence maxima shifted toward a shorter wavelength (blue shift) upon the addition of (*S*)-MCPG. These changes were opposite to those observed for agonist binding. A similar spectral change was observed upon the addition of an excess of LY367385 (100 μM final concentration), another antagonist (Fig. 2*D*), suggesting that, in the ligand binding states of the two antagonists, the environments around tryptophans involved in the fluorescence change were similar to each other. On the other hand, no spectral change was observed upon the addition of (*R*)-MCPG (Fig. 2*F*), a stereoisomer of (*S*)-MCPG that does not bind to the mGluR1 LBD (8). This result clearly indicates that the observed spectral changes are due to the binding of the antagonists.

We measured the rate constants of ligand binding to the LBD with a stopped-flow apparatus. As shown in Fig. 3*A*, the tryptophan fluorescence was abruptly enhanced upon mixing with glutamate (0.5 mM after mixing), and it almost reached a plateau within 1 s. The time course of the fluorescence intensity change was roughly fitted to a single exponential curve. From the fitting curve, the observed rate constant (k_{obs}) of glutamate binding to the LBD was estimated to be 22.2 s^{-1}. On the other hand, upon mixing with (*S*)-MCPG (0.5 mM after mixing), the intrinsic tryptophan fluorescence was suddenly quenched and completely reached a plateau within 1 s (Fig. 3*B*). The time course of the fluorescence change was fitted well to a single exponential curve, and the observed rate constant was estimated to be 38.6 s^{-1}. It should be noted that these rate constants of ligand binding are apparent rates measured only at the saturating concentration of ligands. They do not represent actual association rate constants of ligand.

TABLE I

Solvent-accessible area of tryptophan side chains in mGluR1 LBD

Solvent-accessible area of each tryptophan side chain in mGluR1 LBD was estimated by a program SURFACE (29) with a sphere probe whose radius was 1.4 Å. S_{open} is an average of three values for each tryptophan calculated from the two open conformations in 1ISS (PDB ID code) and one open conformation in 1EWK. S_{closed} is an average of two values calculated from one closed conformation in 1EWK and the other closed conformation in 1ISR. These values except for those in parentheses were calculated from atomic coordinates whose coordinates of bound ligands were excluded. The values in parentheses were calculated from the coordinates including the bound ligands.

	S_{open}	S_{closed}	$S_{open} - S_{closed}$
		$Å^2$	
Trp-110	74.7 (52.3)	46.1 (27.9)	28.6 (24.4)
Trp-224	72.1	66.2	5.9
Trp-320	0.9	0.8	0.1
Trp-367	8.2	10.0	−1.8
Trp-372	4.0	2.8	1.2
Trp-468	109.7	118.0	−8.3
Trp-500	4.9	4.2	0.7

Identification of the Tryptophan Residue Contributing to the Spectral Change of the Intrinsic Tryptophan Fluorescence—Tryptophan fluorescence in a protein is generally influenced by the surrounding environment. Water molecules, attacking the indole moiety of tryptophan, and polar side chains and peptide bonds in close proximity of the indole ring are major causes of tryptophan fluorescence quenching (28). There are seven tryptophan residues in one protomer (Trp-110, Trp-224, Trp-320, Trp-367, Trp-372, Trp-468, and Trp-500). To predict which tryptophan residue contributes to the observed spectral changes, we examined the environment around each tryptophan side chain using the atomic models.

We first considered solvent accessibility of each tryptophan. To quantify it, we calculated the solvent-accessible area of each of the tryptophan side chains (indole rings) for the two distinct conformations of the protomer, *i.e.* the open conformation and the closed conformation, by the program SURFACE (29) (Table I). Of the seven tryptophans, only the values for one tryptophan, Trp-110, which is located on the upper surface of the ligand binding pocket (Fig. 4), dramatically changed between the open and closed conformations: the solvent-accessible area markedly decreased in the closed conformation. In addition, the Trp-110 indole ring and the bound glutamate also contact with each other through a hydrophobic interaction (Fig. 4 and Ref. 8). These observations suggest that the closed conformation shields the Trp-110 indole ring from water attack, implying that the fluorescence intensity increases in the transition from the open to the closed conformations. We next examined the polar side chains and the peptide bonds around tryptophans. The side chain of Glu-502 approaches the side chain of Trp-468 in a structural transition from the closed conformation to the open conformation. However, Glu-502 is fully exposed to the solvent, and the temperature factors of its side chain in the crystal structures are extremely high (86–107 $Å^2$), indicating that it rotates freely in random orientations in solution. Thus it was unlikely that this side chain affects the fluorescence of Trp-468 through electrostatic interactions. On the other hand, the carboxyl group of Glu-292 side chain forms a

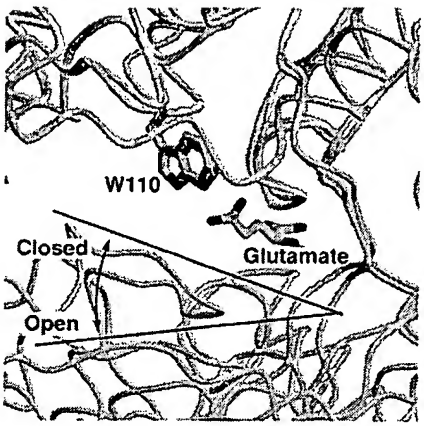

FIG. 4. **Structure around Trp-110.** The open conformation (*light blue*) of the protomer superimposes onto the glutamate-bound closed conformation (*ivory*) by their LB1 domains. The side chain of Trp-110 is colored *green* (the closed conformation) and *orange* (the open conformation). The glutamate in the closed conformation is colored *yellow*.

hydrogen bond with a nitrogen atom of the Trp-110 indole ring in the closed conformation. In addition, the carboxyl group of the bound glutamate is also located near the indole ring. Thus, these carboxyl groups might quench the emission from Trp-110 with the excited state electron transfer (28).

These considerations from crystal structures led us to predict that the observed fluorescence changes mainly resulted from environmental changes around Trp-110. To confirm this prediction, we altered the tryptophan residue to valine by site-directed mutagenesis and measured the fluorescence spectra of the W110V mutant in the presence and absence of glutamate. This mutant maintained the agonist binding ability as judged from the ligand binding assay (data not shown). Nonetheless, no changes were detected in the fluorescence spectrum upon the addition of a sufficient amount of glutamate (Fig. 2*G*). Therefore, we concluded that the observed spectral changes of the intrinsic tryptophan fluorescence upon ligand binding were due to environmental changes around the Trp-110 indole ring. The fluorescence spectra exhibited the enhanced intensity rather than decreased intensity upon the addition of glutamate (Fig. 2*A*). This fact suggests that the two carboxyl groups of Glu-292, and the bound glutamate in the closed conformation slightly affect, if any, the emission from Trp-110. In this case, the solvent effects would predominate over the effects of these carboxyl groups. Hence the main mechanism of the spectral changes on ligand binding is possibly due to the solvent quench of the Trp-110 fluorescence.

Titration of the Intrinsic Tryptophan Fluorescence with Ligands and Effects of Calcium Ions on Binding Affinity—Using the intrinsic tryptophan fluorescence change, we produced saturation binding curves by ligand titration and evaluated the apparent binding constants from the titration curves. We also examined the effects of calcium ions on the ligand binding affinity by carrying out titrations in the presence and absence of calcium ions. Fig. 5 (*A–D*) shows the titration curves for four different ligands. In the titration with glutamate without calcium ions, we estimated the apparent dissociation constant ($K_{0.5}$) of glutamate to be 3.8 μM from the half-maximal change of the titration curve (Fig. 5*A* and Table II). In the presence of 2.0 mM calcium ion, the curve was shifted leftward as compared with that in the absence of calcium ions (Fig. 5*A*). In this case, the apparent dissociation constant was estimated to be 1.3 μM, which was about 3-fold higher affinity than that without calcium ions. These results indicate that calcium ions act to increase the affinity of glutamate for the LBD. In the titration with quisqualate, the $K_{0.5}$ values were shifted to lower ones by about one order in comparison with those of glutamate (0.21 μM and 0.46 μM in the presence and absence of calcium ion, respectively), indicating that quisqualate binds to the LBD more tightly than glutamate (Fig. 5*C* and Table II). This was consistent with the previously reported pharmacological data, in which the relative binding affinities of these agonists were examined by inhibiting the binding of [^{3}H]quisqualate in the conventional ligand binding assay (9, 10). We further tested the positive effect of calcium ions by the ligand binding assay using [^{3}H]quisqualate and [^{3}H]glutamate (Table III). As expected, the amount of bound ligand in the absence of calcium ions was smaller than that in the presence of calcium ions in both cases.

We also carried out titration experiments for two antagonists, (*S*)-MCPG and LY367385 (Fig. 5, *B* and *D*). In the absence of calcium ions, the apparent dissociation constants were 40 and 0.89 μM, respectively, for (*S*)-MCPG and LY367385 (Table II). The higher affinity of LY367385 than (*S*)-MCPG was consistent with the previous pharmacological data (30–32). Interestingly, the positive effects of calcium ions observed for the agonist were not detected for these antagonists, suggesting that the positive effect of the calcium ions is specific for agonist binding.

Hill Analysis of Ligand Binding to the LBD—To investigate the allosteric properties of ligand binding, we analyzed the titration curves by a Hill analysis. It is well known that a Hill coefficient calculated from the slope of a Hill plot represents the cooperativity of ligand binding in oligomeric proteins. If the Hill coefficient is larger than 1, then the ligand binding has positive cooperativity, whereas the Hill coefficient smaller than 1 indicates negative cooperativity.

Typical Hill plots of the titration curves for glutamate and (*S*)-MCPG are shown in Fig. 6. With respect to glutamate binding, the Hill plots at low and high concentrations of the ligand below 1.0 μM and above 100 μM, respectively, showed no (or low) cooperativity as judged from the Hill coefficients, which were close to 1 (0.88 and 0.89, respectively). However, at ligand concentrations between 1.0 and 100 μM, the Hill plot exhibited strong negative cooperativity with a Hill coefficient of 0.48. This result is reasonable because the cooperativity of ligand binding generally does not appear at the upper and lower limits of the ligand concentration and emerges at the middle range of ligand concentrations. On the other hand, with respect to (*S*)-MCPG, the Hill plot showed one straight line over all ligand concentrations with a Hill coefficient of ~0.8, suggesting that the negative cooperativity observed for glutamate tends to disappear upon (*S*)-MCPG binding. The *inset* in Fig. 6 shows the Hill plots at the middle range of ligand concentrations (around $K_{0.5}$), where the averaged values of three independent experiments were plotted. The Hill coefficients calculated from the plots of the *inset* were 0.55 and 0.83 for glutamate and (*S*)-MCPG, respectively. Taking the errors denoted in the graph into account, these Hill coefficient values were convincing enough to conclude that negative cooperativity was present. Similarly, we calculated the Hill coefficients for other ligands in the presence and absence of calcium ions. These values are summarized in Table IV. For quisqualate, the Hill coefficient was close to 1, indicating the lack of cooperativity between each protomer on quisqualate binding. For LY367385, the Hill coefficient was also close to 1. Calcium ions seemed to slightly affect the Hill coefficient of glutamate binding, because it changed from 0.55 to 0.70. Among the four different ligands examined, only the Hill coefficient for glutamate showed remarkable negative cooperativity.

Reduced Cooperativity in the I120A Mutant—The negative cooperativity in mGluR1 LBD indicates that the conformational change of one subunit is transmitted into the other

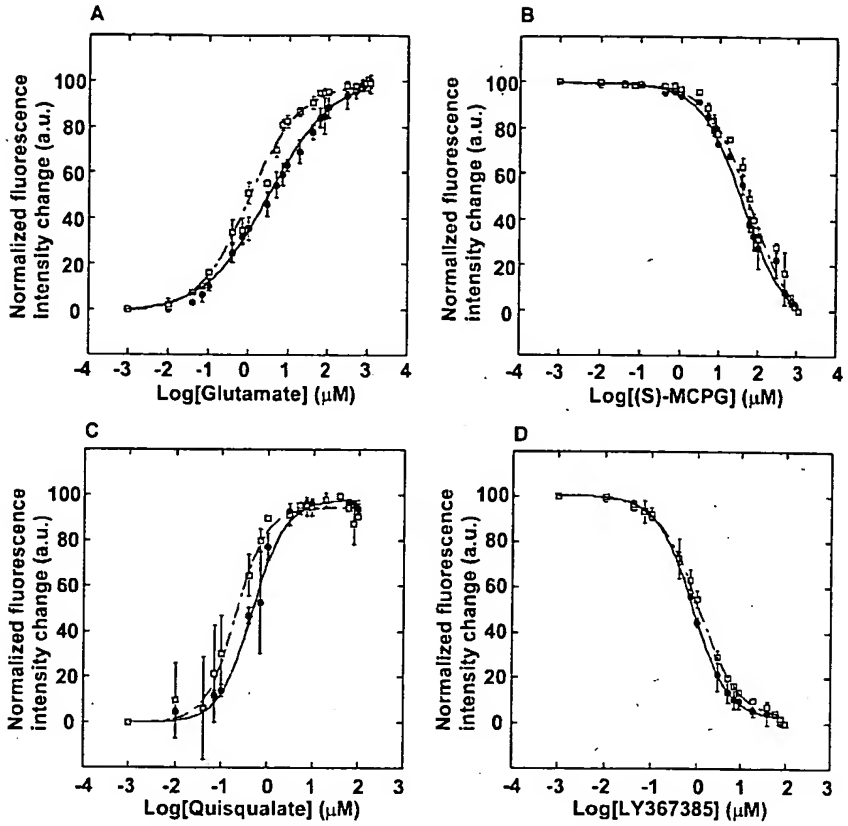

FIG. 5. **Titration curves of the intrinsic tryptophan fluorescence change with ligand binding.** Titration curves with (*open squares*) and without (*closed circles*) calcium ion were generated by monitoring the fluorescence intensity at 350 nm with sequential additions of a small aliquot of ligand solution as described under "Experimental Procedures." *A*, titration curves for glutamate binding; *B*, titration curves for (*S*)-MCPG binding; *C*, titration curves for quisqualate binding; *D*, titration curves for LY367385 binding. Data were fitted by a hyperbola as described under "Experimental Procedures" with the Hill coefficients shown in Table IV.

TABLE II
Apparent dissociation constant ($K_{0.5}$) of ligands for the FLAG-tagged mGluR1 LBD

These values were calculated from the half maximum of the titration curves shown in Fig. 5.

Ligand	Wild type		I120A, 0 mM Ca^{2+}
	0 mM Ca^{2+}	2.0 mM Ca^{2+}	
		μM	
Glutamate	3.8	1.3	16
Quisqualate	0.46	0.21	ND[a]
(*S*)-MCPG	40	59	39
LY367385	0.89	1.2	ND

[a] ND, not determined.

TABLE III
Calcium effect on ligand binding activity

These values were obtained from ligand binding assay using the PEG precipitation method. The final concentration of the ^3H-labeled ligand in the assay mixture was 20 nM. Each assay mixture contained 1 μg of protein. These were averaged values obtained from at least three independent experiments (mean ± S.D.). Units of the values are expressed as bound ligand molecule per one protein molecule.

Ligand	Bound ligands	
	0 mM Ca^{2+}	2 .0 mM Ca^{2+}
[^3H]quisqualate	0.057 ± 0.003	0.17 ± 0.002
[^3H]glutamate	0.029 ± 0.002	0.092 ± 0.004

through the dimer interface. Thus, we carried out the same experiments using a purified FLAG-tagged I120A LBD, which has a mutation in the subunit interface. This mutation led to the uncoupling of ligand binding and signal transduction induced by mGluR1 (26). This mutant still maintained the capacity of ligand biding as previously demonstrated (Fig. 7*A*). The intrinsic tryptophan fluorescence of this mutant was enhanced and reduced upon the addition of excess glutamate and (*S*)-MCPG, respectively, as observed for the wild type (Fig. 7*B*). We then obtained the titration curves for glutamate and (*S*)-MCPG binding (Fig. 7*C*). From the half-maximal value of the titration curve, we estimated the apparent dissociation constants ($K_{0.5}$) to be 16 and 39 μM for glutamate and (*S*)-MCPG, respectively (Table II). These results indicate that only the glutamate binding affinity is negatively affected by the mutation. We also obtained the Hill coefficient value from the titration curves. For glutamate binding, the Hill coefficient was calculated to be 0.80, whereas it was 0.83 for (*S*)-MCPG binding. In comparison with the wild type, the Hill coefficient for glutamate binding was significantly increased in this mutant, whereas the value for (*S*)-MCPG binding was similar to that of wild type. These results indicate that the negative cooperativity of glutamate binding observed for the wild type tends to disappear with the mutation. Hence, the negative cooperativity possibly operates through the hydrophobic subunit interface.

DISCUSSION

This study demonstrated that the intrinsic tryptophan fluorescence of the mGluR1 LBD changed upon ligand binding and that this intrinsic fluorescence yielded a saturation binding curve with an extensive range of ligand concentrations. Consequently, the Hill analysis revealed the negative cooperativity of glutamate binding between each protomer of the homodimeric mGluR LBD.

Relationship between the Structure and the Intrinsic Tryptophan Fluorescence Change of the mGluR1 LBD—Interestingly, the directions of the fluorescence change were opposite between agonist and antagonist binding, for not only the emission intensity but also the peak position of the emission spectrum (see Fig. 2 and summary in Fig. 8). With respect to the emission intensity, agonist binding enhanced the emission, whereas antagonist binding reduced it. Because the tryptophan fluorescence intensity change of the protein is attributed to the emission intensity of Trp-110, the opposite changes in the spectral

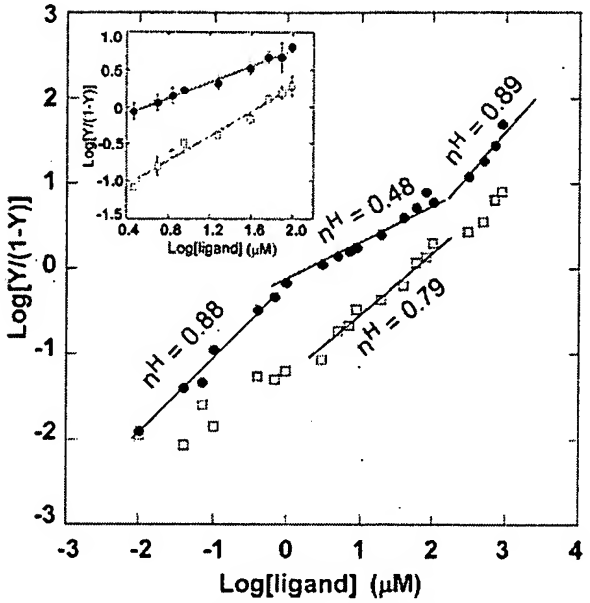

FIG. 6. **Hill plot for the titration curves of glutamate and (*S*)-MCPG binding.** Typical Hill plots derived from the titration curves are shown for glutamate (*closed circles*) and (*S*)-MCPG (*open squares*) binding. *Y* means the degree of saturation of the ligand binding sites with bound ligand. Thus, *Y* equals $|F - F_0|/\Delta F_{max}$, where *F* and F_0 are the fluorescence intensities in the presence and absence of ligand, respectively, and ΔF_{max} is the maximum of the fluorescence change in the titration experiment. n_H is the Hill coefficient estimated from the slope of the plot. The *inset* shows Hill plots at the middle range of ligand concentrations, with values representing the mean of at least three independent experiments.

TABLE IV
Hill coefficients calculated from titration curves measured by intrinsic tryptophan fluorescence change

These values were obtained from the slope in the middle section (around K_d of the ligand) of Hill plots of the titration curves shown in Figs. 5 and 7. These are mean values and standard deviations derived from at least three independent titration experiments (mean ± S.D.). Statistical significance of some pairs of these values was examined by the Student's *t* test.

Ligand	Wild type		I120A, 0 mM Ca^{2+}
	0 mM Ca^{2+}	2.0 mM Ca^{2+}	
	n_H		
Glutamate	0.55 ± 0.07[a,b]	0.70 ± 0.07[b]	0.80 ± 0.04[a]
Quisqualate	1.04 ± 0.06[a]	0.92 ± 0.05	ND[c]
(*S*)-MCPG	0.83 ± 0.09[a]	0.91 ± 0.03	0.83 ± 0.29
LY367385	1.06 ± 0.08	0.92 ± 0.07	ND

[a] The differences are statistically significant ($p < 0.05$).
[b] The *p* value was 0.058.
[c] ND, not determined.

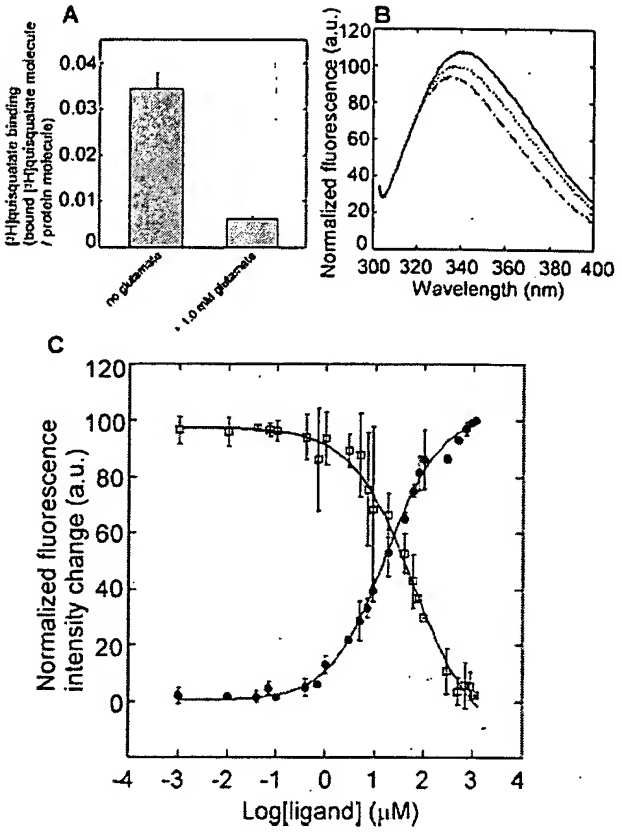

FIG. 7. **Characterization of the I120A mutant.** *A*, the ligand binding activity of the FLAG-tagged I120A LBD was measured by the PEG precipitation method with [^{3}H]quisqualate. 20 nM [^{3}H]quisqualate was used in the binding experiment. The difference between the two *bars* represents the specific binding of [^{3}H]quisqualate as shown in Fig. 1*B*. *B*, intrinsic tryptophan fluorescence spectra of the I120A LBD in the presence and absence of ligand. The *dotted line* is a fluorescence spectrum in the absence of ligand. *Solid* and *broken lines* show fluorescence spectra in the presence of 1.0 mM glutamate and 0.1 mM (*S*)-MCPG, respectively. *C*, titration curves for glutamate (*closed circles*) and (*S*)-MCPG (*open squares*) binding to the I120A LBD. Data were fitted by a hyperbola as described under "Experimental Procedures" with the Hill coefficients shown in Table IV. These data were generated using the averaged values of three independent experiments.

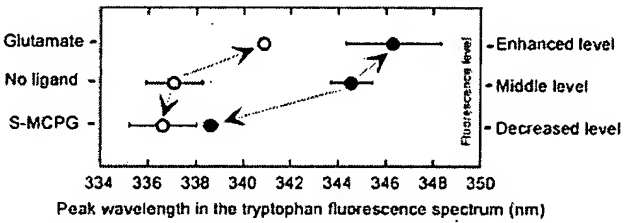

FIG. 8. **Correlation between the peak wavelength and the relative fluorescence level of the intrinsic tryptophan fluorescence spectrum.** Peak wavelength *versus* relative fluorescence level in the tryptophan fluorescence spectrum was plotted for the wild-type (*closed circles*) and I120A (*open circles*) FLAG-tagged LBDs. Each *point* in the *graph* is an averaged value, and the errors are derived from three independent fluorescence spectra. The *left* and *right ordinates* indicate ligand binding states and fluorescence intensity levels, respectively. The fluorescence intensities of the emission spectra in each ligand binding state are divided into three levels. It should be noted here that the *right ordinate* represents the direction of fluorescence change rather than the actual fluorescence intensity.

intensity between agonist and antagonist are reasonable for the following reasons. In the agonist-induced closed conformation, the solvent-accessible area decreases. As a result, the indole ring of Trp-110 would be protected from attacks by water molecules. This should lead to the observed enhanced emission upon agonist binding. By contrast, in the antagonist-induced open conformation, the water molecules could attack the indole ring more easily than in the closed conformation. This would result in the decreased emission.

With respect to the peak position of the emission spectrum, agonist binding yielded a spectrum with a slightly red-shifted peak, whereas antagonist binding provides a spectrum with a markedly blue-shifted peak (Fig. 8). These spectral shifts can be also explained by the emission intensity of Trp-110. The fluorescence spectrum of W110V was significantly blue-shifted with an emission maximum at ~335 nm (Fig. 2*G*). The blue-shifted spectrum induced by the lack of the Trp-110 indicates that the Trp-110 itself has a red-shifted fluorescence spectrum with a peak maximum longer than 335 nm. This is reasonable,

because the indole ring of Trp-110 is not buried inside the protein, but instead exposed to the solvent in the open conformation (7, 8, 25). If the red-shifted emission of Trp-110 is quenched upon antagonist binding, the total emission would be apparently blue-shifted. Indeed, the fluorescence spectrum was blue-shifted upon the addition of antagonist (Fig. 2, *B* and *D*), indicating that this consideration is valid. Based on this notion, we can correlate the position of the emission maximum with the conformational states of the protomer: A blue-shifted spectrum indicates an open cleft conformation, whereas a red-shifted spectrum indicates a closed conformation. In this context, the blue-shifted emission spectrum of the I120A mutant in the ligand-free state (Fig. 8) indicates that the ligand binding cleft of this mutant opens more easily than that of the wild type even in the absence of antagonist. This is consistent with the reduced affinity of glutamate in this mutant (Table II).

The opposite directions of the spectral changes between the agonist and antagonist binding states imply that, in the ligand-free state, the LBDs exist in a mixed population of the open and closed conformations. This observation suggests that, in the ligand-free state, the LBD protomers are in dynamic equilibrium between the two conformations. This notion is consistent with the activation model previously proposed by crystallographic studies (7, 8).

Positive Effect of Calcium Ions on Agonist Binding—From the titration curves based on the ligand-dependent fluorescence change, we evaluated the apparent dissociation constant for several ligands from the titration binding curves and found that calcium ions increased the affinity of agonists. This calcium effect was specific for agonists and was not observed for antagonists, indicating that calcium ions stabilize the closed conformation of the protomer. Positive effects of calcium ions on physiological mGluR activity have been reported. For example, extracellular calcium ions potentiate the phosphoinositide signaling generated by receptor activation (33), and extracellular calcium ions were required for a persistent response to glutamate stimulation (34). Thus, our finding may provide one of the molecular mechanisms for the positive effects of calcium ions described in these previous reports.

Negative Cooperativity of Glutamate Binding in the Dimeric Ligand Binding Domain—The Hill analysis of glutamate binding yielded the Hill coefficient, which was smaller than 1 (n_H = 0.55 without Ca^{2+}). Although one interpretation of the result is the negative cooperativity between the two binding sites in the dimer, an alternative interpretation is also possible: it is due to the presence of two independent non-interacting sites, which have different affinities for glutamate. However, this is not plausible, because glutamate does not bind to any other portion except each ligand binding cleft of the homodimer in the crystal structures even at the saturating concentration of glutamate (1 mM). Therefore, we concluded that the Hill coefficient of less than 1 was due to the negative cooperativity of glutamate binding. Contrary to glutamate, the negative cooperativity was completely abolished for the other agonist, quisqualate (n_H = 1.04 without Ca^{2+}). This might be due to the higher affinity of quisqualate for the receptor than glutamate. That is, the strong affinity of quisqualate may overcome the weak binding conformation of the protomer. As a result, quisqualate could also bind to the second protomer, and the ligand binding cleft of the second protomer would close. The notion that the negative cooperativity tends to disappear for a high affinity agonist is consistent with the observation that calcium ions, which raise the agonist affinity, slightly increased the Hill coefficient (Table IV). Thus, the possibility remains that calcium ions are partly involved in the cooperativity through affinity modulation.

For the I120A mutant, the negative cooperativity upon glutamate binding had a tendency to disappear in comparison with that of the wild type, because the Hill coefficient was closer to 1 with this mutation (n_H = 0.80 without Ca^{2+}). Ile-120 is located at the center of the dimer interface formed by the hydrophobic interaction between each LB1, and hence, it is likely that the cooperativity would come out by the interaction between each protomer through the hydrophobic dimer interface. It should be noted that this mutation reduced the affinity for glutamate, despite the relatively long distance between Ile-120 and the ligand binding site. The reduced affinity only for glutamate indicates that the closing motion of the protomer of this mutant would be restricted. This is consistent with the blue-shifted fluorescence spectrum of this mutant, which implies that the ligand binding cleft of this mutant prefers the open conformation as discussed above. The reduced affinity of I120A also suggests that the modulation of the hydrophobic dimer interface can indirectly affect the affinity of the ligand. Taken altogether, the conformational changes of one protomer induced by ligand binding, such as the closing motion of the ligand binding pocket, will modulate the interaction between the two protomers, resulting in suppression of the closing motion in the second protomer.

The fact that the negative cooperativity was obliterated in the I120A mutant reminds us of the behaviors of mutants of the bacterial homodimeric aspartate receptor, whose structures have been solved in the apo-form, one aspartate-bound dimer (one half-site occupied) and two aspartate-bound dimeric states (11, 12). Mutations at a single residue (serine 68), which is located in the subunit interface and within the aspartate binding pocket, altered the original negative cooperativity to non- or positive cooperativity (13). These results, together with our present mutation study, indicate that the cooperativity of ligand binding in a dimeric receptor would be maintained by a subtle balance of force in the dimer interface.

What is the role for the negative cooperativity in receptor functions? In general, negative cooperativity extends the ligand concentration range over which the protein can work (14). Thus one possible role for the negative cooperativity is to extend the glutamate concentration range to which the receptor can respond. This mechanism will be useful in the situations where continuous stimulation takes place at the synapse. Even in such a situation, the receptor will be able to respond, because the ligand binding sites of the receptors on the cell surface would not be completely saturated by glutamate. The other advantage for the negative cooperativity is a greater sensitivity for low ligand concentration (14). This effect would also work favorably at the glutamatergic synapse in neuronal activity.

Each protomer of the mGluR LBD seems to close easily at the hinge without structural constraints, and a closed protomer was actually observed in the ligand-free crystal. Nevertheless, the crystallization with glutamate disclosed the asymmetric open-closed conformation. This is probably due to the negative cooperativity of glutamate binding between each protomer. If a closed-closed conformation actually exists *in vivo*, then it might perform a distinct function from that of the open-closed conformation, although the closed-closed symmetric crystal structure has been obtained only with co-existence of glutamate and possibly non-physiological gadolinium ions. The rank order in the signal strength between the open-closed and closed-closed states has not been examined, however, the release of the negative cooperativity with aid of metal ions, such as calcium ions, might trigger the shift to the closed-closed form. If the negative cooperativity defines the proportion between the open-closed and closed-closed forms, and they differ in their signal strength or pathway, then the negative cooperativity

may discriminate between the associations with interacting proteins, including G proteins, in the cytoplasmic milieu and define the receptor destinies. In this context, an intriguing phenomenon is receptor desensitization. A receptor conformation with both ligand binding sites fully occupied by agonists might be a desensitization signal, and the frequency of desensitization events would be suppressed by the feature of the negative cooperativity. Further analysis will be needed to clarify these possibilities.

Acknowledgments—We are grateful to Dr. K. Morikawa (Biomolecular Engineering Research Institute) and Dr. S. Nakanishi (Kyoto University) for critical reading of the manuscript and discussions. We also thank Dr. K. Sutoh (University of Tokyo) for kindly sharing the stopped-flow apparatus.

REFERENCES

1. Nakanishi, S., and Masu, M. (1994) *Annu. Rev. Biophys. Biomol. Struct.* **23**, 319–348
2. Hollmann, M., and Heinemann, S. (1994) *Annu. Rev. Neurosci.* **17**, 31–108
3. Masu, M., Tanabe, Y., Tsuchida, K., Shigemoto, R., and Nakanishi, S. (1991) *Nature* **349**, 760–765
4. Tanabe, Y., Masu, M., Ishii, T., Shigemoto, R., and Nakanishi, S. (1992) *Neuron* **8**, 169–179
5. Conn, P. J., and Pin, J. P. (1997) *Annu. Rev. Pharmacol. Toxicol.* **37**, 205–237
6. Jingami, H., Nakanishi, S., and Morikawa, K. (2003) *Curr. Opin. Neurobiol.* **13**, 271–278
7. Kunishima, N., Shimada, Y., Tsuji, Y., Sato, T., Yamamoto, M., Kumasaka, T., Nakanishi, S., Jingami, H., and Morikawa, K. (2000) *Nature* **407**, 971–977
8. Tsuchiya, D., Kunishima, N., Kamiya, N., Jingami, H., and Morikawa, K. (2002) *Proc. Natl. Acad. Sci. U. S. A.* **99**, 2660–2665
9. Okamoto, T., Sekiyama, N., Otsu, M., Shimada, Y., Sato, A., Nakanishi, S., and Jingami, H. (1998) *J. Biol. Chem.* **273**, 13089–13096
10. Tsuji, Y., Shimada, Y., Takeshita, T., Kajimura, N., Nomura, S., Sekiyama, N., Otomo, J., Usukura, J., Nakanishi, S., and Jingami, H. (2000) *J. Biol. Chem.* **275**, 28144–28151
11. Milburn, M.V., Prive, G.G., Milligan, D.L., Scott, W.G., Yeh, J., Jancarik, J., Koshland, D. E., Jr., and Kim, S. H. (1991) *Science* **254**, 1342–1347
12. Yeh, J. I., Biemann, H. P., Prive, G. G., Pandit, J., Koshland, D. E., Jr., and Kim, S. H. (1996) *J. Mol. Biol.* **262**, 186–201
13. Kolodziej, A. F., Tan, T., and Koshland, D. E., Jr. (1996) *Biochemistry* **35**, 14782–14792
14. Koshland, D. E., Jr. (1996) *Curr. Opin. Struc. Biol.* **6**, 757–761
15. Limbird, L. E., and Lefkowitz, R. J. (1976) *J. Biol. Chem.* **251**, 5007–5014
16. Pizard, A., Marchetti, J., Allegrini, J., Alhenc-Gelas, F., and Rajerison, R. M. (1998) *J. Biol. Chem.* **273**, 1309–1315
17. Devi, L. A. (2001) *Trends Pharmacol. Sci.* **22**, 532–537
18. Franco, R., Canals, M., Marcellino, D., Ferre, S., Agnati, L., Mallol, J., Casado, V., Ciruela, F., Fuxe, K., Lluis, C., and Canela, E. L. (2003) *Trends Biochem. Sci.* **28**, 238–243
19. Bouvier, M. (2001) *Nat. Rev. Neurosci.* **2**, 274–286
20. Milligan, G. (2001) *J. Cell Sci.* **114**, 1265–1271
21. Liu, J., Maurel, D., Etzol, S., Brabet, I., Ansanay, H., Pin, J. P., and Rondard, P. (2004) *J. Biol. Chem.* **279**, 15824–15830
22. Verjovski-Almeida, S., and Silva, J. L. (1981) *J. Biol. Chem.* **256**, 2940–2944
23. Nelson, S. W., Iancu, C. V., Choe, J. Y., Honzatko, R. B., and Fromm, H. J. (2000) *Biochemistry* **39**, 11100–11106
24. Xu, Y., Johnson, J., Kohn, H., and Widger, W.R. (2003) *J. Biol. Chem.* **278**, 13719–13727
25. Lakowicz, J. R. (1999) *Principles of Fluorescence Spectroscopy, 2nd Ed.* Plenum Publishers, New York, pp. 452–486
26. Sato, T., Shimada, Y., Nagasawa, N., Nakanishi, S., and Jingami, H. (2003) *J. Biol. Chem.* **278**, 4314–4321
27. Gill, S. C., and von Hippel, P. H. (1989) *Anal. Biochem.* **182**, 319–326
28. Chen, Y., and Barkley, M. D. (1998) *Biochemistry* **37**, 9976–9982
29. Lee, B., and Richards, F. M. (1971) *J. Mol. Biol.* **55**, 379–400
30. Lin, F. F., Varney, M., Sacaan, A. I., Jachec, C., Daggett, L. P., Rao, S., Flor, P., Kuhn, R., Kerner, J. A., Standaert, D., Young, A. B., and Velicelebi, G. (1997) *Neuropharmacology* **36**, 917–931
31. Brabet, I., Mary, S., Bockaert, J., and Pin, J. P. (1995) *Neuropharmacology* **34**, 895–903
32. Schoepp, D. D., Jane, D. E., and Monn, J. A. (1999) *Neuropharmacology* **38**, 1431–1476
33. Saunders, R., Nahorski, S. R., and Challiss, R. A. (1998) *Neuropharmacology* **37**, 273–276
34. Nash, M. S., Saunders, R., Young, K. W., Challiss, R. A., and Nahorski, S. R. (2001) *J. Biol. Chem.* **276**, 19286–19293